2007 Annual Report

“Emergence of Adaptive Motor Function through Interaction among the Body, Brain and Environment - A Constructive Approach to the Understanding of Mobiligence - ”

Project Leader: Hajime Asama (The University of Tokyo)

March, 2008

Area No. 454
Under Grant-in-Aid for Scientific Research
on Priority Area
from the Japanese Ministry of Education, Culture, Sports, Science and Technology

Academic Year from 2005 to 2009

2007 Annual Report

“Emergence of Adaptive Motor Function through Interaction among the Body, Brain and Environment - A Constructive Approach to the Understanding of Mobiligence - ”

Project Leader: Hajime Asama (The University of Tokyo)

March, 2008

Area No. 454
Under Grant-in-Aid for Scientific Research
on Priority Area
from the Japanese Ministry of Education, Culture, Sports, Science and Technology

Academic Year from 2005 to 2009

Contents

Introduction of the *Mobiligence* Program

Emergence of Adaptive Motor Function through Interaction among the Body, Brain and Environment - A Constructive Approach to the Understanding of *Mobiligence* -

Hajime Asama
Director of the *Mobiligence* Program
The University of Tokyo

1. Introduction

The *Mobiligence* program is a five-year program started from 2005[1], which was accepted as a program of Scientific Research on Priority Areas of Grant-in-Aid Scientific Research from the Japanese Ministry of Education, Culture, Sports, Science and Technology (MEXT). In addition to the planned research groups which started in 2005, new two-years-research groups (applied research groups) will be selected and start from 2006. This paper presents the abstract of the program.

2. Objective of the *Mobiligence* Program

Human can behave adaptively even in diverse and complex environment. All the animals can perform various types of adaptive behaviors, such as a locomotive behavior in the form of swimming, flying walking, a manipulation behaviors such as reaching, capturing, grasping by using hands and arms, a social behavior to the other subjects, etc. Such adaptive behaviors are the intelligent sensory-motor functions, and most essential and indispensable ones for animals to survive.

It is known that the function of such adaptive behaviors is disturbed in patients with neurological disorders. Parkinson disease is a typical example of disorders on adaptive motor function, and autism or depression can also be considered as a disorder on social adaptive function.

Recently, due to aging or environmental change of society, the population of people who are suffering from these diseases is growing rapidly, and it is urgent to cope with this problem. However, the mechanisms for the generation of intelligent adaptive behaviors are not thoroughly understood. Such an adaptive function is considered to emerge from the interaction of the body, brain, and environment, which requires that a subject acts or moves. Base on the consideration, we call the intelligence for generating adaptive motor function *mobiligence*.

The present program is designed to investigate the mechanisms of *mobiligence* by closely collaborative research of biology and engineering. In the course of this collaborative program, the following processes will be carried out:

1. Biological and physiological examinations of animals;
2. Modeling of biological systems;
3. Construction and experiments on artificial systems by utilizing robotic technologies; and
4. Creation of a hypothesis and its verification.

The final goal of this program is to establish the common principle underlying the emergence of *mobiligence*.

3. Research Approach of the *Mobiligence* Program

In this program, the *mobiligence* mechanism is to be elucidated by the constructive and systematic approaches, through the collaboration of biologists and engineering scientists who developed biological models by integrating physiological data and kinetic modeling technologies as shown in figure 1. In other words, the *Mobiligence* Program is pursued by integrating biology and engineering, i.e., physiological analysis (biology), modeling and experiments on artificial systems (engineering), verification of models (biology), and discovery and application of principles (engineering).

In the following discussion, the focus is on three adaptive mechanisms:

1. Mechanism whereby animals adapt to recognize environmental changes;
2. Mechanism whereby animals adapt physically to environmental changes; and
3. Mechanism whereby animals adapt to society.

Research groups for each of the categories listed above are organized. The three groups conduct their respective research and clarify the universal, common principle underlying the mechanism of *mobiligence*. The Planned Research Team studies the following specific subjects: analysis of the environmental cognition and the adaptive mechanism in reaching movements; analysis of the physical adaptive mechanism in walking; and analysis of the adaptive mechanism observed in the social behaviors of insects. In addition, the Planned Research Team clarifies the common principle underlying *mobiligence* from a dynamic viewpoint. Furthermore, we study adaptive mechanisms relating to various objects by publicly inviting proposed topics and clarify the universal, common principle therein.

4. Research Activities till the *Mobiligence* Program

The *Mobiligence* program is highly motivated by the previous program on emergent systems, which was carried out from 1995 to 1997 and directed by Prof. Shinzo Kitamura of Kobe University. Although the system theory on emergent function formation was actively discussed in the program, the principle it couldn't be revealed enough how to design the emergent systems. After the program on emergent systems, a special interest group on System Principle on Emergence of *Mobiligence* and Its Engineering Realization was organized in the System and Information Division of the Society of Instrument and Control Engineers (SICE) in 2003, and the research activities have been continued.

We held a workshop sponsored by the Tohoku University Nation-wide Cooperative Research Program from 2001, and a workshop on the development of the emergence system of *mobiligence* and its control system under the sponsorship of the Nissan Science Foundation.

Before starting the *mobiligence* program, we planned and held organized sessions in international conferences and in lecture meetings of academic societies

- IFAC Intelligent Autonomous Vehicles (IAV)
- International Symposium on Distributed Autonomous Robotic Systems (DARS)
- International Symposium on Adaptive Motion of Animals and Machines (AMAM)
- IEEE/RSJ International Conference on Intelligent Robots and Systems (IROS)
- SICE Annual Conference
- SICE System and Information Division Annual Conference (SSI)
- SICE System Integration Division Annual Conference (SI)
- SICE Symposium on Decentralized Autonomous Systems

5. Expected Impact of the *Mobiligence* Program

Various types of adaptive motor function mechanisms performed by animals are expected to be elucidates. In the medical field, the results of our research will contribute to the discovery of a method to improve motor impairment and develop rehabilitation systems. In addition, in the engineering field, the results of our research will contribute to the derivation of the design principles of artificial intelligence systems. Furthermore, we will explore the new research field, *mobiligence*, establish a research organization that integrates biology and engineering, and implement programs to foster young engineering scientists and biologists to conduct collaborative and interdisciplinary research between biological and engineering research, respectively.

References

[1] http://www.arai.pe.u-tokyo.ac.jp/mobiligence/index_e.html

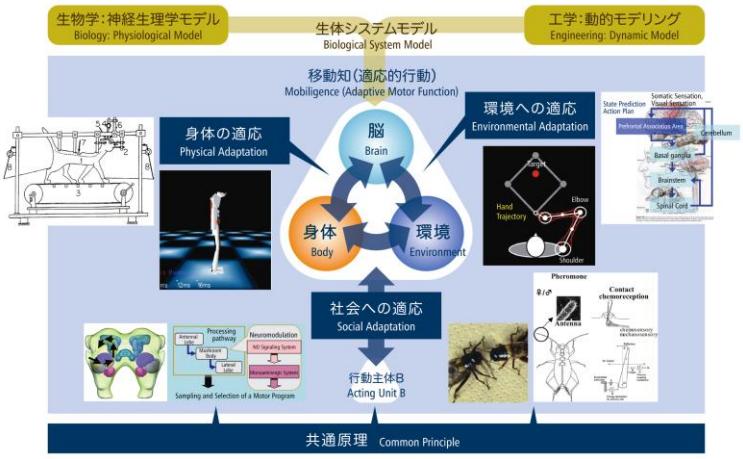

Fig. 1 Framework of the *Mobiligence* Program

Fig. 2 Expected Impact of the *Mobiligence* Program

Steering Committee Report on the *Mobiligence* Program

Hajime Asama*[1], Kazuo Tsuchiya*[2], Koji Ito*[3], Masafumi Yano*[4], Koichi Osuka*[5], Kaoru Takakusaki*[6], Ryohei Kanzaki*[1], Hitoshi Aonuma*[7], Akio Ishiguro*[8], Jun Ota*[1]

*[1]The University of Tokyo, *[2]Kyoto University, *[3]Tokyo Institute of Technology, *[4]Tohoku University, *[5]Kobe University, *[6]Asahikawa Medical College, *[7]Hokkaido University, *[8]Nagoya University

1. Missions

The missions of the steering committee are as follows:

- Establish goals for the *Mobiligence* Program
- Plan and coordinate research
- Evaluate research progress and consult
- Determine the procedures for the public invitation of proposed topics
- Organize symposia and research meetings for the purpose of developing related research
- Plan publicity of research results
- Encourage close collaboration among researchers, i.e., information exchange, mutual understanding, and communication
- Plan international research and lectures by members of academic societies and announce interim and ex post evaluations of progress
- Devise programs to encourage fused collaboration among biologists and engineering scientists and establish a research center and research organization

2. Summary of 2007 Activities of the Steering Committee

Research subjects were coordinated in each group to facilitate the fused collaboration between biologists and engineering scientists, which characterizes this program, and joint group meetings and open group meetings were organized to promote the inter-group collaboration effectively. Many events were organized as follows; a domestic symposium, an open symposium, a closed symposium, practice programs, tutorials, and seminars. The internal evaluation was performed twice. Many organized sessions are organized at international and domestic conferences. The homepage for publicity and the database to record the activities in the program were maintained and updated. Research report was edited and published. Junior Academy of the *mobiligence* program was established and their activities were supported.

3. Steering Committee Meetings and WGs

The following Steering Committee meetings and its WG meetings were held:

[1] 1st Steering Committee Meeting
July 20th, 2007, 13:00-16:30
at Awaji Yumebutai International Conference Center

[2] 2nd Steering Committee Meeting
Mar. 7th, 2008, 12:00-14:00
at Hotel Taikanso in Matsushima

[1] 1st WG Meeting
April 21st 13:30-22nd 12:00
at Makuhari Seminar House

[2] 2nd WG Meeting
May 31st, 2007, 14:00-18:00
at Hongo Campus of the Univ. of Tokyo

[3] 3th WG Meeting
July 31st 13:00-Aug. 1st 12:00
at Kirishima Hotel

[4] 4th WG Meeting
Aug. 19th, 2007, 13:00-14:30
at Intec Oyama Training Center

[5] 5th WG Meeting
Oct. 9th, 2007, 15:00-18:00
at Hongo Campus of the Univ. of Tokyo

[6] 6th WG Meeting
Jan. 17th, 2007, 16:00-18:30
at Hongo Campus of the Univ. of Tokyo

4. Organization of Symposia

4.1 International Workshop

The International Workshop on Mobiligence (Emergence of Adaptive Motor Function through Interaction among the Body, Brain, and Environment) was held in University of Padua, Italy on Apr. 5-6, 2007. 12 speakers made presentations including members of each group of mobiligence program.

4.2 International Symposium

The 2nd International Symposium on Mobiligence was held at Awaji Yumebutai Conference Center, Japan on July 18-20, 2007. Symposia organized by each group of the Mobiligence program were held on the first and second day of the symposium, which include 4 invited speeches and 21 oral presentations. The invited speakers are; Prof. Jean-Louis Deneubourg (Universit Libre de Bruxelles), Prof. Pietro G. Morasso (DIST, University of Genova, Italy), Prof. Kier G. Pearson (University of Alberta, Canada), and Prof. Kouhei Ohnishi (Keio University, Japan). The members of Mobiligence program presented the current research activities in their presentations. A night session was organized by Junior Academy of the *Mobiligence* program. On the third day, individual research outcome was presented in the poster session, and a panel discussion titled "From Motor and Perception to Intelligence" was organized in cooperation with ERATO Asada Synergistic Intelligence project. The panelists are; Prof. Minoru Asada(Chairman), Prof. Rolf Pfeifer, Prof. Toshio Inui, Prof. Kaoru Takakusaki. Total number of participants was 126.

4.3 Domestic Symposium

A symposium for internal evaluation was held in Hotel Taikanso in Matsushima, Japan, on Mar. 5-7, 2008. Oral and poster presentations on the research progress in 2007 of all the subjects in the *Mobiligence* program were made by each research leader and members. They were all reviewed by the review committee members and the steering committee members. A night session was also organized by Junior Academy of the *Mobiligence* program. Total number of participants was about 100.

5. Publicity

5.1 Organization of Special Issues of Journals

A special issue on Mobiligence was organized in the Journal of Robotics and Mechatronics Vol.19, No.4, in which 18 papers were included. It was published in August of 2007.

A special issue on "Understanding of Social Adaptation Function of Biological Systems and Technological Applications" was organized in the Japanese Journal of the Society of Instrument and Control Engineers Vol.46, No.12, in which 13 review papers were included. It was published in December of 2007.

5.2 Session Organization in Conferences

Sessions on Mobiligence were organized in the following international conferences:

- The 3rd International Symposium on Measurement, Analysis and Modeling of Human Functions (ISHF2007), Portugal, June (2007), 12 papers
- 2007 International Congress of Comparative Physiology and Biochemistry (ICCPB-Brazil 2007), Salvador, Brazil, Aug. (2007), 5papers
- SICE Annual Conference 2007 (International Conference on Instrumentation, Control and Information Technology), Takamatsu, Japan, Sep. (2007), 6 papers

Sessions on Mobiligence were organized in the following international conferences:

- 2007 JSME Robotics and Mechatronics Division Annual Conference, Akita, Japan, May 2007, 8 posters
- 17th Intelligent Systems Symposium, Nagoya, Japan, Aug. 2007, 5 papers
- 2007 RSJ Annual Conference, Chiba, Japan, Sep. 2007, 4 papers
- SICE System and Information Division Annual Conference, Tokyo, Japan, Nov. 2007, 5 papers
- SICE System Integration Division Annual Conference, Hiroshima, Japan, Dec. 2007, 10 papers
- SICE Decentralized Autonomous Systems Symposium, Suwa, Japan, Jan. 2008, 9 papers

5.3 Other Publicity Activities

The home page of the *Mobiligence* program was updated accordingly[1], database on research achievements[2] and activity records was maintained and presented on the web site.

The brochure of the *Mobiligence* program including subscribed research groups was published and distributed as well as call for proposals for the new subscribed research. The report, this volume, on the research activities of the *Mobiligence* program in 2007 was edited and published. The concept of the Mobiligence and current research outcome were broadcasted through an internet TV program, Netrush[3].

6. Organization of Tutorials and Seminars

To accelerate the fused collaboration and to foster young scientists and students who are doing *mobiligence* research, one forum, two workshops, 4 tutorials, and 9 seminars were arranged and held:

7. Review

Three foreign reviewers, who are, Prof. Sten Grillner (Karolinska Institute, Sweden), Prof. Rolf Pfeifer (University of Zurich, Switzerland), and Prof. Avis H. Cohen (University of Maryland, USA), and three domestic members of reviewers, who are Prof. Shinzo Kitamura (Kobe University), Prof. Shigemi Mori (National Institute for Physiological Sciences), and Prof. Ryoji Suzuki (Kanazawa Institute of Technology), participated in the international symposium mentioned above, and evaluated the organization of the Mobiligence program and current research outcome of each group. As the result of the review, the review committee reported that the new research area "Mobiligence" has been successfully established, and valuable research outcome has been obtained by the close collaborations of researchers in biology and robotics.

At the domestic symposium mentioned above, steering committee members in addition to the three domestic reviewers evaluated the research progress and grade of collaboration between biology and robotics. The review results are fedback to the research leaders toward successful research execution in future.

8. Activity Support for Junior Academy of the *Mobiligence* program

The steering committee supported the following activities of the Junior Academy of the *mobiligence* program:

[1] The 25th Annual Conference of the Robotics Society of Japan, The Opened Robotics Seminar for Young Researchers Network

[2] The 20th SICE Symposium on Decentralized Autonomous System, Tutorial by Junior Academy of the Mobiligence Project: Decentralized Autonomous Systems in Motor Control of Living-systems

[3] Creating Glossaries (ongoing project)

References

[1]http://www.robot.t.u-tokyo.ac.jp/mobiligence/index_e.html

[2]http://www.robot.t.u-tokyo.ac.jp/mobiligence/act/index.html

[3]http://www.netrush.jp/science_top.htm

Group A: Adaptation to Environment
Annual Report

Koji ITO

Tokyo Institute of Technology, Japan

1. RESEARCH PROJECT

The aim of Group A is 1) to clarify the intelligence mechanisms for creating appropriate hypotheses ("Mi-Nashi" information) based on the accumulated experiences under unpredictable environments, 2) to analyze the motor control mechanisms producing adaptive behaviors corresponding to dynamical environments, and 3) to construct mathematical models of the adaptive motor control composed of the brain, body and environment. In order to perform the above subjects, the project organizes the following subgroups.

Subgroup A01: Real time formation of constraint conditions for adaptive motor actions in dynamical environments.

Motor control system consists of <Body> with various action outputs and sensory inputs, <Brain> as the central controller, and <external environment>. The body includes large number of sensors and actuators, and connects the brain with the environment. The interaction between the body and environment imposes some constraints on the redundant degree of freedom in the total dynamical system. Then, the body and environment are the controlled object and builds up the external dynamics to the brain. Accordingly, it is essential in the motor control to self-adjust the dynamic relations among the brain, body and environment corresponding to the purpose of his/her action or movement under an infinite variety of environments. That is, in the dynamical system with the redundant degree of freedom composed of the brain, body and environment, it is the most important problem in the adaptation to environment to find some constraints ("Mi-Nashi" information) from the spatiotemporal contexts and to create the internal dynamics appropriate to the forthcoming environment.

Subgroup A02: Understanding of intra-cerebral mechanisms for the motor adaptation to unknown environments.

In order to create adaptive behaviors in various environments, it is necessary to integrate the redundant degrees of freedom in the brain, body and environment based on changing contexts of situation. Subgroup A02 aims to elucidate the brain mechanisms of the sensorimotor coordination corresponding to the dynamical environments by the experimental, constructive and systematic approaches.

Subgroup A03: Computational modeling and understanding of sonsorimotor integration.

Subgroup A03 aims to analyze the mechanisms of the environment cognition and motor constraint based on the perceptual dynamics of visual, auditory sensations, etc., and to construct the computational model of real time sensorimotor integrations.

2. RESEARCH GROUPS

- Planned Research Groups

1) M. Yano (Tohoku University)
2) K. Ito (Tokyo Institute of Technology)

- Subscribed Research Groups

3) S. Shioiri (Tohoku University)
4) T. Inamura (National Institute of Informatics)
5) Y. Koike (Tokyo Institute of Technology)
6) Y. Maeda (Yokohama National University)
7) T. Matsushima (Hokkaido University)
8) Y. Sawada (Tohoku Institute of Technology)
9) S. Ichikawa (Tokyo University of Science, Suwa)
10) A. Murata (Kinki University, School of Medicine)
11) J. Tani (Brain Science Institute, RIKEN)

3. RESEARCH RESULTS

(1) A voluntary movement is an action that the biological system makes for carrying out an aim with adapting unpredictable environments. The aim of the movement can be acquired by the system having "Mi-Nashi". As a higher constraint for resolving the ill-posedness in motor control, "Mi-Nashi" has to set practical constraints in various levels of control mechanisms in real time. Here, we focused attentions on the reaching movement and addressed the following two issues.

i) We examined **a**) kinematical and dynamic properties of the 3-DOF-arm movements generated by the autonomously-decentralized controller that calculates the "mobility measure" of each joint in real time for determining the instantaneous motion direction, and **b**) the adaptability of the proposed controller to a change of DOF of the body.

ii) The 2-joints-arm robot that we developed is driven by three pairs of antagonistic actuators, and is equipped with sensors for kinematical information of the arm robot and dynamical information of the actuators. For controlling this redundant arm robot, we developed the control system that can acquire the kinematical and dynamical information and can generate control commands in real time. By controlling the co-contraction level of the antagonistic actuators based on the sensor information, the control system could appropriately modulate the viscosity of the joints in real time depending on environmental conditions.

(2) In daily life, humans must compensate for the resultant force arising from interaction with the physical environment. It has been shown that humans can acquire a neural representation of the relation between motor command and movement, i.e. learn an internal model of the environment dynamics. For example, Shadmehr, Mussa-Ivaldi et al have analyzed various reaching movements under velocity-dependent force field (VF) where the hand receives the external load in proportion to the hand velocity. It is then shown that human compensates for the external load by the feedforward control based on the internal model. It is here called "internal model control". On the other hand, in manipulation tasks, such as opening a door, grasping a cup etc., the dynamic interaction between the human arm and external environment determines the stability of motion. Therefore, it has much importance to adjust the arm impedance corresponding to the environment dynamics change. Burdet et al demonstrated that the subject employed the strategy to raise the robustness to external fluctuations by the high arm impedance through the simultaneous activation of the agonist and antagonist muscles, which is called "impedance control".

We investigated motor adaptation of human arm movements to external dynamics. In the experiment, we examined whether humans can learn an internal model of a "mixed force field"(V+P) which is sum of a "velocity-dependent force"(V) and a "position-dependent force"(P). The experiment results showed that the subjects did not learn the internal model of V+P accurately and they compensated the loads by using impedance control. Our results suggest that humans use impedance control when internal models become inaccurate because of the complexity of external dynamics.

(3) The abilities of environment cognition and motor adaptation are based on internal models of the external world which are acquired through active sensorimotor learning process. In addition, the process is influenced by the context, i.e. the order of experience or internal state of learners. For instance, Osu et al. reported that a random training schedule with a preceding audiovisual cue has better effect for simultaneous learning of conflicting tasks compared with an alternating schedule. The preceding cue should be effective because it would remind the subjects the change of the task. However it still remains unclear why the random presentation contributes the simultaneous learning. We assumed this is because the alternating presentation condition gives no chance to repeat the same task successively. To be clear the validity of the assumption, we compared three training conditions; 1) alternating every one trial, 2) alternating every two trials, and 3) random presentation, respectively. As the result, it can be concluded that endowing the successive trials (alternating every two trials) have positive effect on the simultaneous learning compared with the switching condition (alternating every trial). Nevertheless, the random presentation training is superior to the other alternating schedules.

4. MEETING AND OTHERS

- Meeting of Group A

  Date: 13:30-17:00, 1 June, 2007.

  Place: Meeting room 303, Campus Innovation Center.

  Attendee: 20 members.

  Presenters: Prof. M. Yano (Tohoku University),
  Dr. J. Tani (RIKEN)

  Contents: Discussion on Anticipatory adaptation to environments.

- Joint meeting of Group A and B

  Date: December 14, 13:00 – December 15, 15:40, 2007.

  Place: Meeting room, Department of Computational Intelligence and Systems Science, Tokyo Institute of Technology.

  Attendee: 35 members of group A and B.

  Contents: Reports on 17 research results by group A members and the general discussions on adaptation to environments.

- Organized Session on the 3rd International Symposium on Measurement, Analysis and Modeling of Human Functions (ISHF2007).

  Date: June 14 –17, 2008

  Place: Faculty of Human Kinetics, Technical University of Lisbon, Cascais, Portugal

  Attendee: 50.

  # Invited lecture

  Koji Ito: Adaptive Motor Functions through Dynamic Interactions among the Body, Brain and Environment.

  # Organized Session: 11 Papers which are consisted of Group A members.

- Organized Session on "Mobiligence" in Division Symposium of Systems and Information (SICE-SSI2007)

  Date: November 16, 2007

  Place: National Olympics Memorial Youth Center

  OS: Learning and Adaptation to Environments in Arm Movements.

  Attendee: 16.

Voluntary Movements Controlled by "Mi-Nashi" Created in the Motor Cortices

Masafumi Yano, *Research Institute of Electrical Communication, Tohoku University*

1. Introduction

A voluntary movement is an action that the biological system makes for carrying out an aim with adapting unpredictable environments. The aim of the movement can be acquired by the system having "Mi-Nashi". As a higher constraint for resolving the ill-posedness in motor control, "Mi-Nashi" has to set practical constraints in various levels of control mechanisms in real time. Furthermore, for adapting unpredictable changes in conditions of the system and the environment, "Mi-Nashi" should emerge from the system itself depending on interactions between the system and the environment, and the system have to evaluate whether the emerged "Mi-Nashi" would be satisfied every moments. These are computational problems that the motor control system, i.e., the motor cortices, has to solve during the voluntary movement control in the real world. Here, we focused attentions on the reaching movement and addressed the following two issues: i) kinematical and dynamic properties of the 3-DOF-arm movements generated by the autonomously-decentralized controller that we proposed and the adaptability of the proposed controller to a change of DOF of the body; ii) development of the control system for the 2-joints-arm robot that is driven by three pairs of antagonistic actuators.

2. Reaching Model by Mobility Measure

Biological systems can achieve various goals in the real environment, by executing appropriate motions in real-time. However, a control scheme for the adaptive motions is not clear. We have focused on sensory information in the biological system during motion, since it would reflect real-time condition of the environment and a body of the system. By using the information, we defined a joint mobility measure, and proposed a reaching model in which motions are determined through a mobility based interactions among the joints [1].

2.1. Kinematic and dynamic smoothness

It is well known that biological motions tend to be smooth in kinematic (position and velocity) and dynamic (force and torque) spaces. In our model, each joint starts motion instantaneously to generate a given desired hand velocity, evaluates its kinematic and dynamic mobility using kinematic sensory information, and modulates the motion such that instantaneously more mobile joint works dominantly. It is expected that the motion could be moderate and smooth in kinematic and dynamic spaces. To test this, we calculate biologically smooth motions using a minimum torque change model [2], and compare kinematic and dynamic profiles generated by the MTCM and our model.

1) Calculation method: The desired hand velocity $\boldsymbol{v}_d$ is given as follows:

$$\boldsymbol{v}_d = G_t(\boldsymbol{x}_d - \boldsymbol{x}_h)t^2, \tag{1}$$

where, $\boldsymbol{x}_d$, $\boldsymbol{x}_h$, G_t are desired hand position, current hand position, and gain, respectively. MTCM states that reaching motions are planned so that cost function C_T as follows is optimized:

$$C_T = \int_0^{t_f} \dot{\boldsymbol{\tau}}^T \dot{\boldsymbol{\tau}} dt, \tag{2}$$

where, t_f is convergence time. In Eq. (1) and (2), we set G_t= 9.0 s^{-3}(constant) and modulate t_f, so that convergence times to a target in both models become identical.

2) Simulation results: First, as for the kinematic profiles, we compared hand trajectories in Fig.1 Ai, Bi, and confirmed that almost smooth and straight paths were obtained in both models. Next, as for the dynamic profiles, we compared patterns of the joint torque during motion in Fig.1 Aii, Bii and confirmed that the patterns generated by our model and MTCM were qualitatively similar. Specifically, the torque of the shoulder, elbow, and wrist were high in 0/90°, 45/225°, and 90/270°, in our model, respectively(Fig.1 Aii), indicating that kinematically mobile joint worked dominantly. This feature could be seen in MTCM as well(Fig.1 Bii). Patterns of the time derivative of the joint torque generated by our model and MTCM were also qualitatively similar as shown in Fig.1 Aiii, Biii. As a result, total costs, *i.e.*, C_T in Eq. (2), were comparable in 13/16 directions(data are not shown). On the other hand, in 3/16 directions, our model needed significantly larger costs than MTCM. In these directions, several mobility measures were at similar level and unrest, and instantaneously fluctuated.

These results suggested that a strategy to use a mobile joint dominantly, which involved in our model, was basically effective in generating smooth motions in kinematic and dynamic spaces. While in some directions, the smoothness in the dynamic space was not guaranteed. The present model does not concern with the smoothness in that space explicitly; it calculates the dynamic mobility using solely kinematic sensory information. Thus, our model could be improved by using explicitly dynamic sensory information, such as joint torque, for the mobility measure evaluation. This should be further studied in the future.

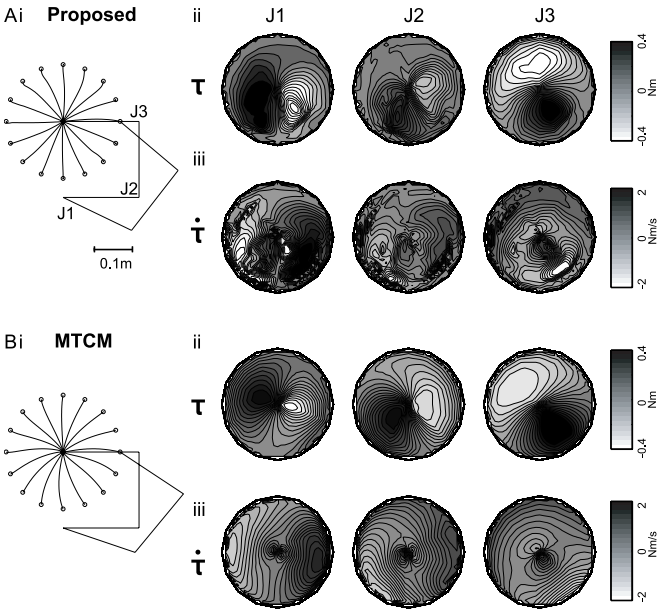

Fig. 1. Comparison of motion patterns generated by the proposed model and the minimum torque change model(MTCM) [2]. A: Hand trajectories and spacial patterns of joint torque and time derivative of joint torque generated by the proposed method. B: Corresponding results by MTCM.

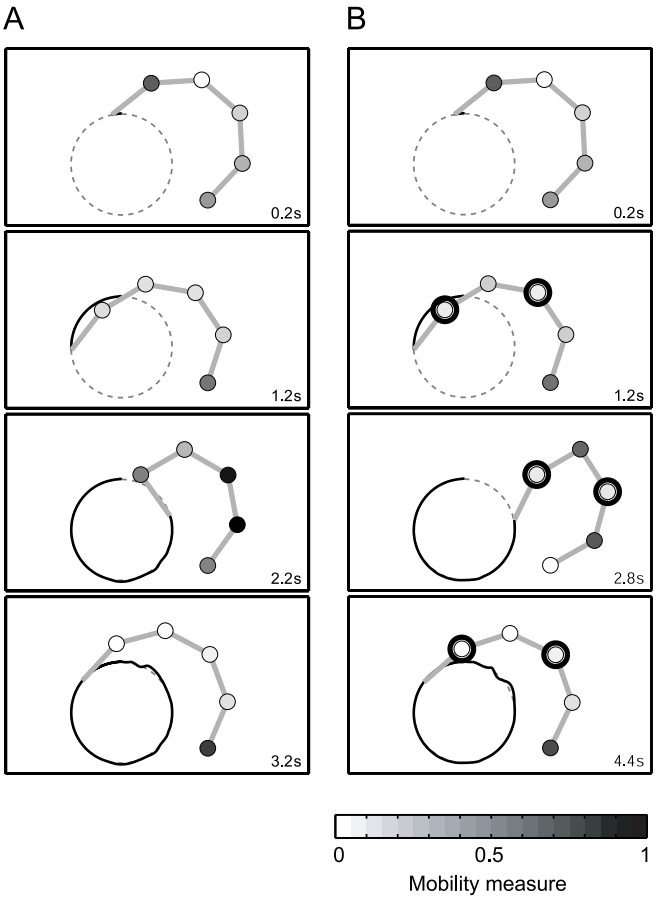

Fig. 2. Rotating movements by 5 dof arm. A: Normal condition. B: Perturbed condition, in which the viscosity of the two joints 3 and 5 were abruptly increased from 0.4 to 10 kg m^2/s during motion(shown by tick circles). Joint color shows which joint is instantaneously mobile. Black: mobile joint($k_i = 1$). White: immobile joint($k_i = 0$).

2.2. Adaptability to a change of DOF

In general, increasing the DOF of the body might contribute to carry out purposive motions in various environmental conditions, but it will simultaneously make hard for the controller to coordinate the DOF for generating an appropriate motion. So, from the computational point of view, it is critical whether the controller can adapt to an increase of DOF of the body. Since the proposed controller is modeled as functional modules for each joint that work competitively and cooperatively as an autonomously decentralized system, it is easy to adapt the original 3-joints-arm controller for an arm having more redundant joints. We developed the controller for 5-joints-arm and examined its performance.

Figure 2A shows a motion of the 5-joints-arm when the desired hand velocity $\boldsymbol{v}_d$ was given as a rotating velocity field and all the joints could normally work. The controller could generate the continuous circular motion of hand. During the motion, the mobility measures for each joint were calculated in real time and the dominant joints were appropriately switched according to configuration of the arm (Fig.2A). In the case of malfunction (i.e., the viscosity of the third and fifth joints from the base was suddenly increased during motion), the controller could also maintain the circular motion of hand. The mobility measures of the third and fifth joints were zero after their malfunction, implying that these joints could not contribute the motion generation. This caused the changes in the configuration of arm during the motion, and thus a pattern of the mobility measures of the other joints (the first, second and fourth ones) were dramatically changed (e.g., comparing the third panels of Fig.2A and B). Since these joints could still interact and autonomously coordinate each other through their mobility measures, the joint trajectories were remarkably different from those in normal condition but the hand trajectory could maintain the circular motion.

3. Developing the arm robot

Redundancy of the body and actuator enables the biological system to generate various motion patterns. By using the sensory information, the biological system can generate appropriate motions according to environmental conditions. The controller that we have proposed is designed to take full advantage of such characteristics of the biological body for generating adaptive motions. To examine the performance of the proposed controller in the real world, we designed and developed an arm robot that is driven by redundant actuators and equipped various sensors [3].

3.1. 2-Joints-6-Muscles Arm Robot

In general, joints of the biological system are driven by pairs of agonist and antagonist muscles. Agonist and antagonist muscles driving a single joint are called mono-articular muscles, and those driving two or more joints are called bi- or multi-articular muscles, respectively. With respect to the

A

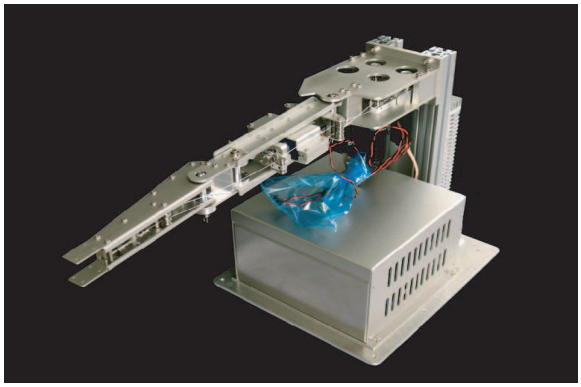

B

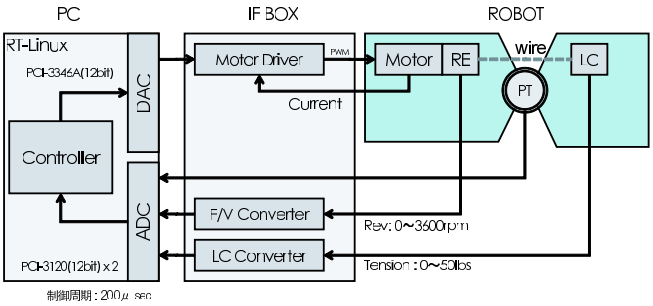

Fig. 3. A: Overview of the robot system with 2-joints-6-muscles. B: Block diagram of the control system.

arm, each joint-impedance of shoulder and elbow can be controlled by changing the co-contraction level of respective mono-articular muscles, whereas the bi-articular muscles for shoulder and elbow are thought to appropriately constrain or coordinately modulate their motions. For carrying out purposive motions, especially in unpredictably changing force field (e.g., in water stream), these characteristics of mono- and biarticular muscles are important [4] [5] and should be appropriately controlled by using various sensory information about kinematical states of the link and joint and dynamical state of muscles.

Based on these considerations, we developed a senor-rich, 2-joints-6-muscles arm robot, shown in Fig.3A The shoulder and elbow of the arm can move in the horizontal plane. The arm is equipped with three pairs of agonist and antagonist DC motors (i.e., two pairs are mono-articular ones for the shoulder and elbow joints and one pair is bi-articular one). Each motor torque is transmitted to respective link through a thin string. At the ends of strings, load cells are connected to sense the string tensions. For sensing the angular velocity of motor, the DC motors are equipped with rotary encoders. To obtain information about configuration of the arm, each joint is equipped with a potentiometer. PC/AT (Celeron, 2.93 GHz; OS, RT-Linux) is used as the control system and sampling time is 200 usec. Over view of the arm robot connecting with the control system is shown in Fig.3B.

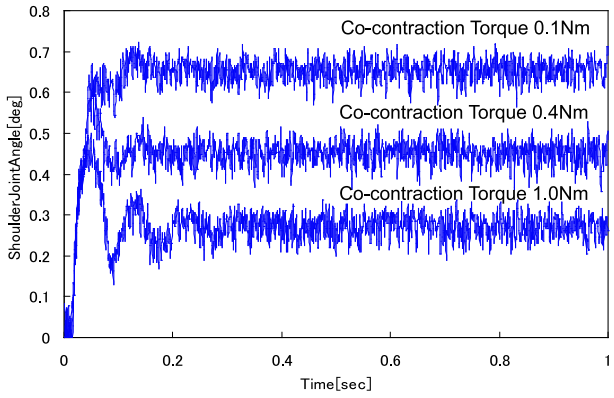

Fig. 4. Modulation of joint impedance due to co-contraction.

3.2. Impedance control by muscle co-contraction

When redundant muscles drive joints, joint impedance can be controlled by antagonistic muscle co-contraction, which is necessary for posture maintenance. This is a great advantage of this driving method, like human does. We have evaluated whether our developing robot system can control joint impedance by co-contraction. This time we have evaluated maintenance ability of shoulder joint control system driven by extensor and flexor motor.

The external force necessary for impedance measurement was applied by two-joint-muscle motor. The elbow joint was fixed at $135°$, and the shoulder joint angle was maintained at $0°$ by the antagonistic torque, which was generated joint by co-contraction of shoulder extensor and flexor motor. The maintenance ability was evaluated by measuring how shoulder joint angle was displaced when disturbance torque was applied by two-joint-muscle motor (Fig.4).

Fig.4 shows the time course of the shoulder angle joint, where disturbance torque was applied from 0 sec. It shows that the converged joint angle depends on the amplitude of antagonistic torque, which means that joint impedance can be controlled by antagonistic muscle co-contraction in our system.

3.3. Modulation of the co-contraction level according to perturbation

To develop a real-time controller for the co-contraction level, we investigated a posture control task in an unstable force field. Stretch-reflex mechanisms for each actuator would be useful for maintaining a posture if perturbations to the body are sparse in time. However, if the body is perturbed continuously form random directions, the co-contraction level of the agonist and antagonist muscles should be modulated to increase the joint-impedance. Furthermore, the system should adopt the latter strategy autonomously and appropriately according to need. For realizing such autonomous and appropriate control, we hypothesized a mechanism that would modulate the co-contraction level depending on the stretch-reflex's activity since high stretch-

reflex activity implies that there would be unpredictable but continuous perturbations.

For examining whether this mechanism would work well in the arm robot, we build the controller consisting of mechanisms of stretch-reflex and co-contraction modulation. For simplification, we only dealt with the mono-articular motors for the shoulder joints.

First, the stretch-reflex controller was developed as:

$$u_{pi} = \begin{cases} k_{pi}\dot{L}_{i\max}\dot{L}_i & \dot{L}_i \geq 0 \\ 0 & \dot{L}_i < 0 \end{cases}, \tag{3}$$

where, u_{pi}, k_{pi}, $\dot{L}_{i\max}$, $\dot{L}_i$ are an output activity of the stretch-reflex controller, a reflex gain, the maximum contraction velocity, and the current contraction velocity, respectively. From Eq. (3), u_{pi} increases when the muscle is extended passively by an external force.

Next, the co-contraction controller was developed as:

$$u_{ci} = f(\tau_c) \tag{4}$$

where, u_{ci}, τ_c are an output activity of the co-contraction controller, and the co-contraction torque of the joint. The function f is a transformation from the joint torque to the output activity. We determined $\dot{\tau}_c$ using the output activity of the stretch-reflex controller as follows:

$$\dot{\tau}_c = k_c \left(\int \sum_i u_{pi} dt - \epsilon \right). \tag{5}$$

where, ϵ is a threshold to evaluate whether the summed stretch-reflex activity $\int \sum_i u_{pi} dt$ is large. From Eq. (4), u_{ci} increases when the stretch-reflex controller is continuously activated.

Finally, using 式 (3), 式 (4), the total muscle activity was determined as

$$u_i = u_{pi} + u_{ci} \tag{6}$$

To test the adaptability of the controller (6), we studied the posture control task in an unstable force field. To generate the unstable force to the shoulder, we used the biarticular muscle(Fig.5 A). An initial configuration of the shoulder was set 20°. The other experimental setup was almost identical to the experiment in Section 3-2,

Just after the force was applied, the shoulder angle and angular velocity instantaneously fluctuated as shown in Fig.5B. This implies that the stretch-reflex controller solely worked. This fluctuation was gradually decreased, and eventually, the joint displacement became nearly zero level. The fluctuation decrease was accompanied by a simultaneous increase of the shoulder flexor and extensor activity as shown in Fig.5C. This result indicates that the co-contraction controller was added to the stretch-reflex controller. From these results, it was confirmed that the controller could maintain the arm posture appropriately in the unstable force field.

4. Conclusion

"Mobility measure" calculated from the kinematical information of the body can be considered as a constraint that is created in real time by the system itself during motion. Simulation results shown in Section 2-1 indicate that this constraint can contribute to generating appropriate motion patterns with regard to not only kinematical property but also dynamic one. The adaptability to the increase of DOF of the body shown in Section 2-2 is an essential characteristic of the proposed "autonomously-decentralized" controller. By using the developed 2-joints-arm robot shown in Section 3, we will test the performance of the proposed controller in the real world.

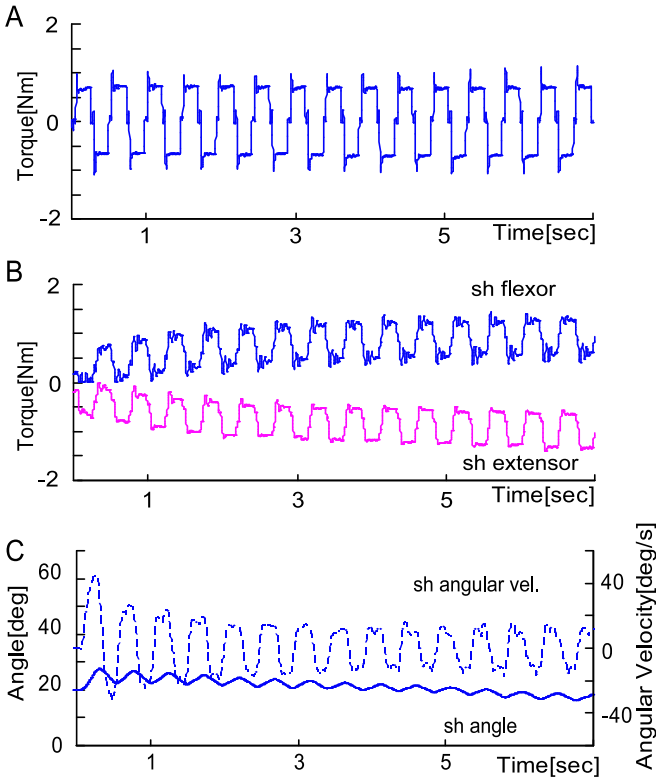

Fig. 5. Adaptation to unstable force field by co-contraction. A: Unstable force to the shoulder joint. B: Shoulder kinematics. C: Activation of the shoulder flexor and extensor.

References

[1] Yoshihara Y, Tomita N, Asano T, Makino Y, & Yano M (2007) Journal of Robotics and Mechatronics, 19, 4, 448-458

[2] Uno Y et al. (1989) Biol. Cybern., 61, 89-101

[3] Hagiwara R, Tomita N, Makino Y, & Yano M (2008) Proceedings of 20th SICE-DAS, 319-324 (in Japanese)

[4] D.W. Franklin et al. (2003) Journal of Neurophysiology, 90, 3270-3282

[5] Luc P.J.Selen et al. (2005) Biol. Cybern., 93, 373-381

Modeling of Intra-cerebral Mechanisms for Motor Adaptation to Unknown Environment

Toshiyuki Kondo (Tokyo University of Agriculture and Technology)
Koji Ito (Tokyo Institute of Technology)

I. INTRODUCTION

Even if we situated in unfamiliar environments with any kinematic and/or dynamic transformations, we can adapt to them in several trials-and-errors. As a consequence of the motor learning process, we can acquire a neural representation of the relation between motor command and the movement, i.e. *internal model* of the environment. However, it is still open question to explain the neural representation, i.e. how the internal models are represented in our brains.

For instance, we can instantly manipulate any objects by using any tools even though there are a number of combinational possibilities. In addition, we can select an appropriate internal model according to the contextual information of the environments. It implies that there is an intrinsic prediction and motor adaptation mechanisms in the motor area of our brain.

The A02 group aims to clarify the intra-cerebral mechanisms to recognize unfamiliar environments and to generate suitable motor commands, through psychophysical experiments and computational modeling of human arm-reaching movement learning.

In this report we explain about our recent research topics entitled "Decomposition of internal models in arm movements under mixed force fields" and "Simultaneous learning of mouse operation with conflicting visuomotor transformation."

II. DECOMPOSITION OF INTERNAL MODELS IN ARM MOVEMENTS UNDER MIXED FORCE FIELDS

To manipulate objects or to use tools, humans must compensate for the resultant forces arising form interaction with the physical environment. Recent studies have shown that humans can acquire a neural representation of the relation between motor command and movement, i.e. learn an internal model of the environment dynamics [1]. Then, we can compensate for the mechanical perturbation in a feedforward manner.

Humans can learn an enormous number of motor behaviors in different environments. Then, it is required to construct multiple internal representations of various dynamic environments, which can be recollected corresponding to each environment. Several previous studies have examined arm movement adaptation to multiple dynamic environments [2]. The concept of multiple models implies the ability to adapt to diverse perturbations with different contexts and to make efficient use of redundancy by performing the same task in different ways under different environments.

Now, when we carry a cup of water, we can recognize each dynamics of water and cup separately. That is, when we manipulate objects, it is possible to acquire a simple dynamics from complicated ones. This will be essential to use tools. In order to simulate these situations, we mixed two different force fields linearly. Then the present paper discusses whether humans can identify one side of dynamics from the mixed force field.

A. Experimental protocol

The experimental apparatus is shown in Fig.1. The manipulandum (x and y axes) was actuated by a couple of linear direct drive motors, which were controlled by the digital servo at the sampling rate 2 kHz and could generate various mechanical impedances against the grip grasped by the subject.

The subject was seated on the chair in front of the manipulandum and learned point-to-point arm movements to eight targets located radially from a central start position. The movement distance was 0.125 m. The subject was instructed to reach the target from the initial position within 300±50 ms. The hand, start and target positions were indicated on the screen. During the reaching movements, visual feedback of the hand position was suppressed and the entire hand pass was shown after the movements were terminated. One cycle consisted of 8 trials, including randomly ordered movements to all eight targets.

As shown in Fig.2, we used two types of force fields: (a) velocity-dependent force field (V) and (b) position- dependent force field (P). The velocity-dependent force field (V) is represented as follows.

$$\mathbf{F}=\begin{bmatrix}F_x\\F_y\end{bmatrix}=\begin{bmatrix}0 & -17.5\\17.5 & 0\end{bmatrix}\begin{bmatrix}\dot{x}\\\dot{y}\end{bmatrix}\ \text{[N]}, \qquad (1)$$

where $\boldsymbol{F}=[F_x, F_y]^T$ is the hand load and $[\dot{x}, \dot{y}]^T$ is the hand velocity. The subject's hand receives the external load in proportion to the hand velocity. The position- dependent force field (P) is represented as follows.

$$\mathbf{F}=\begin{bmatrix}F_x\\F_y\end{bmatrix}=\begin{bmatrix}0 & 77\\-77 & 0\end{bmatrix}\begin{bmatrix}dx\\dy\end{bmatrix}\ \text{[N]}, \qquad (2)$$

where $[dx, dy]^T$ is the hand position. The subject's hand receives the external load in proportion to the hand position.

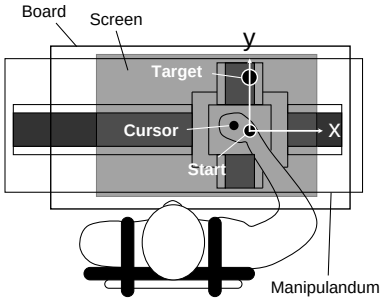

Fig.1 Experimental setup.

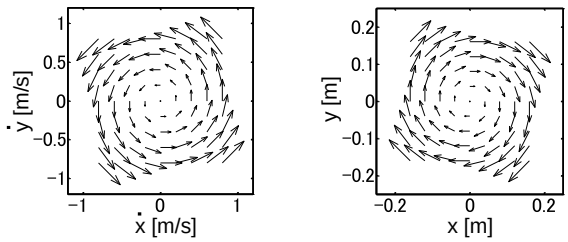

(a) V: Velocity-dependent F.F. (b) P: Position-dependent F.F.

Fig.2 Force fields (F.F.).

Fifteen students participated in the experiments. The experiments were performed over two consecutive days as shown in Table 1. The subjects were divided into three groups. On 1st day, all subjects started with free movement in the null field for practice (200 trials). Then, group1 learned the mixed force field V+P which is sum of V and P. Group2 learned the force field V and group3 learned the force field P. All groups performed 288 movements under each environment. On 2nd day, all groups performed 288 movements under the force field V.

Table.1 Experimental protocol.

Group	Subjects	**Day 1**	**Day 2**
Group 1	(N = 5)	Null → V+P	V
Group 2	(N = 5)	Null → P	V
Group 3	(N = 5)	Null → V	V
Trial number		(200) (288)	(288)

We quantified the adaptation of the reaching movements to the force field by calculating the error relative to a straight line joining the centers of the start and target circles. The absolute hand trajectory error was calculated as follows.

$$Error = \int_{t_s}^{t_f} |a(t)||\dot{b}(t)|\,dt \quad (3)$$

which represents the area between the actual path and the straight line. The start time is 20 ms before crossing a hand velocity threshold of 0.05 m/s. t_f is a time when a hand velocity crosses 0 m/s line first.

The EMG signal measured on the skin surface was A/D converted with the sampling frequency of 2 kHz. Activity was recorded from two muscles; *the biceps brachii* and *the triceps brachii*. After full-wave rectified, it was smoothed through the low-pass second-order Butterworth filters (cut-off frequency: 20 Hz).

B. Experimental result

Fig.3 shows the hand trajectories of typical subjects at the beginning of learning the force field V on Day 2. These trajectories are the first 3 sets of movements. The subject of group3 who learned the force field V on day 1 performed straight reaching movements toward eight targets. It indicates that the subject predicted the external dynamics by using the internal model of V acquired on day 1. On the other hand, the subject of group2 who learned the force field P on day 1 is not able to perform straight reaching movements. His hand trajectories are slipped out from the straight line toward the target, which demonstrates that the subject does not acquire the internal models of V to predict the novel dynamics. On the other hand, let's see the trajectories of the subject of group1 who learned the force field V+P on day 1. It is clear that the trajectories of group1 are straighter than those of group2. The subject of group1 can predict the novel dynamics better than group2. However, the straightness of trajectories is not perfect comparing with that of group3.

Fig.4 shows the absolute hand trajectory error for the force field V on day 2. The horizontal axis represents the trial number and the vertical axis represents the average in each group. The error bar represents a standard deviation (SD). Then, the errors of group 1 are smaller than those of group 2 in the initial learning phases. This indicates that group 1 could adapt quickly to the force field V because they had learned the force field V to some extent during previous learning of the mixed force field V+P. It suggests that they decomposed internal models of V+P. However, the learning curves of group 1 are upper than one of group 3, which means that the transfer of V+P learning is not perfect.

We analyzed EMG of two muscles during later period across all directions of movements. We calculated a scalar activation level for each muscle by averaging normalized EMG trace over the time interval between 250 ms and 500 ms after the onset of movement. The results are shown in Fig.5. The curves show the averaged EMG across subjects. The error bar represents a standard deviation (SD). EMG levels of all groups decrease with the progress of learning of the force field V. It is then seen that the subject can adapt the force field V gradually and shifts the control strategy to the feedforward control. It should be noted that group 1 lies between group 2 and 3 for two muscles.

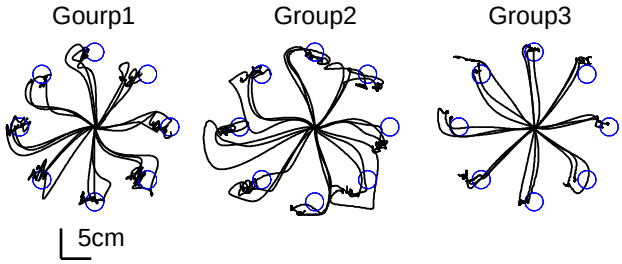

Fig.3 Hand paths at the beginning of learning for "V" (Day2).

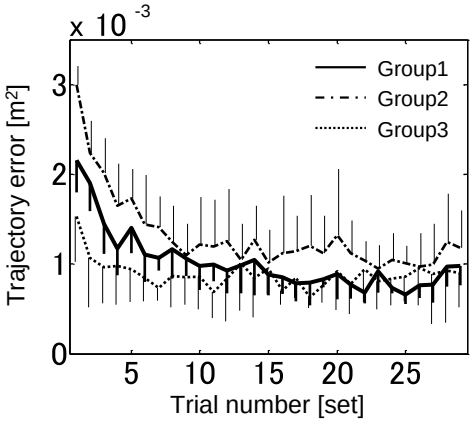

Fig.4 Learning curves of "V" (Day2).

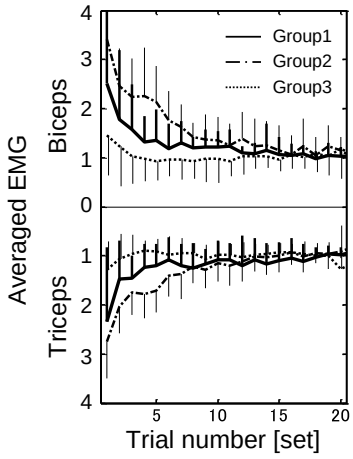

Fig.5 Averaged EMG during learning for "V" (Day2).

III. SIMULTANEOUS LEARNING OF MOUSE OPERATION WITH CONFLICTING VISUOMOTOR TRANSFORMATION

According to recent neurophysiology, it has been revealed that appropriate sensorimotor coordination can be stored in our brain as internal model [1]. The abilities of environment cognition and motor adaptation are based on the internal models of the external world which are acquired through active sensorimotor learning process. In addition, the process is influenced by the context, i.e. the order of experience or internal state of learners.

For instance, Osu et al. reported that a random training schedule with a preceding audiovisual cue has better effect for simultaneous learning of conflicting tasks compared with an alternating schedule. Here, the preceding visual cue should be effective because it would remind the subjects the change of the task. However it still remains unclear why the random presentation schedule contributes the simultaneous learning of the conflicting tasks.

In the study, we assumed this is because the alternating presentation condition gives no chance to repeat the same task successively. To be clear the validity of the assumption, we compared three training conditions; (1) alternating every one trial, (2) alternating every two trials, and (3) random presentation, respectively.

A. Experimental protocol

The experimental setup is illustrated in Fig.6. There is a computer mouse on a pen tablet (WACOM PTZ-631W). The subject is seated on a height adjustable high-back chair.

As shown in Fig.6, a mouse cursor and a target are visualized on a computer monitor (Hewlett-Packard, hp2035) that is placed in front of the subject (approx. 600mm). The target is a small green square (approx. 6.5mm each). At each trial, the target is displayed on the place that is randomly selected from 12 peripheral candidate positions (see Fig.6).

The procedure of a trial is as follows.

1) The subject returns the mouse device to an initial position indicated on the tablet. At this time, the background of the frontal monitor is filled with blue or red color in accordance with the successive task (**CW90**/**CCW90**). Then click the mouse button in any timing.

2) At the same time, a selected target is displayed on the monitor, and the measurement of the mouse operation is begun.

3) The subject operates the mouse device to reach the cursor into the target.

4) When the cursor arrives in the target, the trial is terminated with message; "Please return the mouse device to the home position."

5) Repeat the procedure until a series of trials is completed.

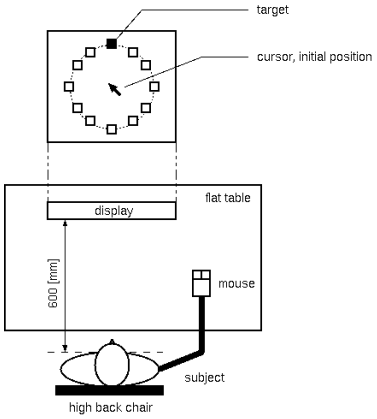

Fig.6: task.

In the following experiment, a series of 36 trials is called "set". Thus 12 candidates of target are randomly selected three times each in a set, however a consecutive representation of the same target is restricted.

Fig.7 shows the rotational transformation of a computer mouse operation used in the experiment. In the figure, the lower part indicates mouse device movements, and the upper side represents corresponding cursor movements. As can be seem, **NULL** means no transformation. On the contrary, **CW90** transformation corresponds to a clockwise 90 deg rotation, and **CCW90** is a counterclockwise 90 deg rotation, respectively.

Before starting the experiment, all subjects were asked to be accustomed to the task procedure under **NULL** condition. During the training, subjects were exposed to two types of rotational transformations (**CW90** or **CCW90**) under several training conditions. The training lasts 20 sets with 90 seconds interval.

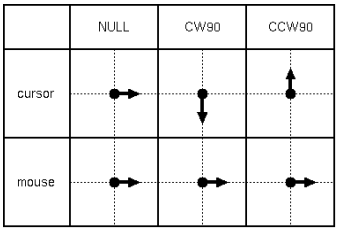

Fig.7: transformation.

Table.2: training conditions.

Group	*Subjects*	*Training conditions*
A1	N=3	Alternating every trial
A2	N=3	Alternating every two trials
B	N=3	Random

Nine subjects participated in this experiment with informed consent, but they know nothing about the purpose of the experiment. They were randomly assigned into the three groups; (1) Group A1: alternating every one trial, (2) Group A2: alternating every two trials, and (3) Group B: random presentation, respectively (Table. 2). After the training, the performance of each subject was tested by *post-hoc* random test (240 trials) so as to evaluate the effectiveness of the training conditions. In this experiment, all subjects were instructed to move the cursor quickly and draw as straightway as possible. To evaluate the effectiveness of motor learning based on these criteria, the reaching time and accumulated directional errors were measured in the experiments.

B. Experimental result

Fig.8 shows the performance indexes normalized with baseline performance (**NULL** condition) in the *post-hoc* random test. This result clarified that the subjects trained in random presentation condition still express significant advantage ($p<0.01$) compared with the subjects trained under alternating schedule conditions (A1 and A2).

In addition, we can see that the average performance of group A2 is superior to the result of group A1. It implies that endowing the chance of successive trials to a subject (i.e. alternating every two trials) has not a little positive effect on the simultaneous learning compared with the switching condition (i.e. alternating every trial).

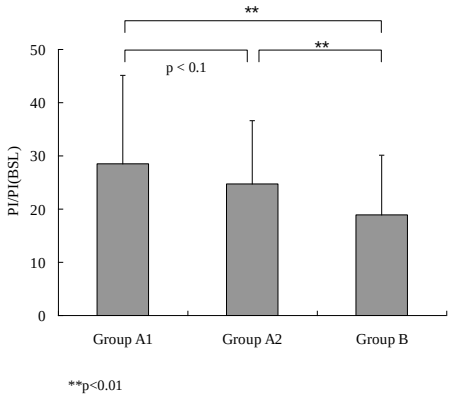

Fig.8: Performance Indexes (alternating 1, 2 v.s. random).

IV. CONCLUSION

In the paper, we shortly reported our recent research results; "Decomposition of internal models in arm movements under mixed force fields" and "Simultaneous learning of mouse operation with conflicting visuomotor transformation."

Next year, we continue to clarify the intra-cerebral mechanisms for recognizing unfamiliar environments and/or generating suitable motor commands, through psychophysical motor learning experiments and computational modeling of human arm-reaching movement.

REFERENCES

[1] K. Ito: Systems Theory of Embodied Motor Intelligence – Motor Learning and Control for Human-Robotics -, Kyoritsu Pub, 2005 (in Japanese).

[2] R.Shadmehr and S.P.Wise: The Computational Neurobiology of Reaching and Pointing, pp.379-446, The MIT press, 2005.

[3] R.Shadmehr and F.A.Mussa-Ivaldi: Adaptive representation of dynamics during learning of a motor task, ***J.Neuroscience***, Vol. 14, pp.3208-3223, 1994.

[4] H.Imamizu, S.Miyauchi, T.Sasaki, R.Takino, B.Puetz, T.Yoshioka. and M.Kawato: Human cerebellar activity reflecting an acquired internal model of a novel tool, ***Nature***, Vol. 403, pp.192-195, 2000.

[5] J.W.Krakauer, M.-F.Ghilardi, and C.Ghez: Independent learning of internal models for kinematic and dynamic control of reaching, ***Nature neuroscience***, Vol. 2, No. 11, pp.1026-1031, 1999.

[6] A.Karniel and F.A.Mussa-Ivaldi: Sequence, time, or state representation: how does the motor control system adapt to variable environments? ***Biological Cybernetics***, Vol. 89, No. 1, pp.10-21, 2003.

[7] R.Osu, H.Hirai, T.Yoshioka, and M.Kawato: Random presentation enables subjects to adapt to two opposing forces on the hand, ***Nature neuroscience***, Vol. 7, pp.111-112, 2004.

The Roles of Implicit and Explicit Processes in Vision

Satoshi Shioiri, Matsumiya Kazumichi, Kuriki, Ichiro, Hironori Nagata, Takuro Mano
Tohoku University

***Abstract*—We investigated the differences between processes of explicit and implicit learning related to visual perception with two different approaches. The first one is the investigation of facilitation effect by learning stimulus configuration in visual search experiments (contextual cueing effect). The second one is the investigation of a learning effect of visuo-motor task. Both of the experiments showed differences in explicit and implicit learning. The contextual cuing effect was less efficient in explicit learning than implicit learning when evaluated by visual search time. Larger effect of learning in tracking a visual target was found in implicit learning than in explicit learning. These results suggest that the learning and/or memory process without explicit knowledge of the repeats is different from the process with explicit learning.**

I. Introduction

When we perceive the world, we usually think we are aware what we are seeing. This feeling of visual awareness suggests that the visual system works with processes that are explicit to us. However, through the history of the visual science as well as other perception researches, it has been revealed that much of visual information is processed without consciousness (as has been suggested by counter-intuitive perception[1,2]). The human brain has processes that we are not aware. It is important and possible to differentiate conscious and unconscious processes to understand the brain functions, which in turn is important to develop interfaces to machines and/or education system suitable for the human brains. However, we have little knowledge of the role of consciousness in perception and also in action, which uses the results of the perceptual processes. Our approach for the issue is to investigate the differences in performance between the conditions, which we assume that the explicit and implicit processes concern due to some experimental manipulations.

II. Visual Serach and Contextual Cuing Effect

In the first experiment, we focus on a phenomenon called contextual cuing effect to investigate the differences in visual perception between conscious and unconscious processes. Contextual cuing effect is a type of unconscious or implicit learning of visual images. Although implicit processes for motor control have been investigated for decades[3, 4], those for perception and recognition is not much known. Contextual cuing effect is one of a few implicit learning effect known for visual perception[5, 6]. It is found when participants search a target among similar distracters repeatedly in a visual search task. In the original condition of the first report of contextual cueing[5], half of the displays (the location of the target and distracters) are unique to each trial, whereas the remaining displays are repeated throughout the experiment. There were twelve different repeated displays, where the locations, but not the identities, of the target and distracters are held. The contextual cuing effect is the fastening of the target detection time in the repeated displays. This is an example of implicit learning since most of the participants are unaware that any repetitions have occurred. When an recognition test of the displays is performed at the end of the search sessions, performance is at chance even for participants who report being consciously aware of the repetitions during.

The purpose of the present study is to investigate how implicit and explicit learning/memory of stimulus images differ in performing visual search tasks. We measured the reaction time and eye movements of participants when they were searching a target in repeated or new displays. Participants were told to search the target without being informed of the repetition of displays in the implicit condition. In the explicit condition, in contrast, participants were told to memorize the display so that they would be able to use the information to search the target in later trials in the session. Possible differences in the learning processes could cause differences between the two conditions in the degree of the shortening of reaction, in time course of the learning, and in eye movements properties.

A. Method

An example of search stimuli was shown in Fig.1 (the target was T among eleven Ls) but there are two repeating conditions. First eight blocks of a total of 32 blocks are for learning (learning phase) and the rest blocks are for search (search phase). There were implicit, explicit and new display conditions in a session. Each block consisted six explicit, six implicit and six new display trials. Differences among different stimulus conditions were in the learning phase.

The explicit stimulus display was presented for 1s or 3s after a uniform field with a red circle at the location of the target in the stimulus display (Fig. 2). The stimulus display replaced the field when participants initiated the trial by pressing a key. Participants were told to memorize the configuration (the location of the target and distracters) so that the knowledge was used to find target later in the search phase. We therefore assume that participants memorized the image configurations explicitly in this condition.

The implicit and new displays were presented after a uniform field with a green circle at the center of the display and participants simply searched the target when it was presented. These two displays

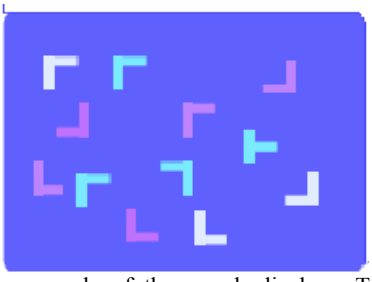

Fig 1. An example of the search displays. Target T was displayed among distracter Ls.

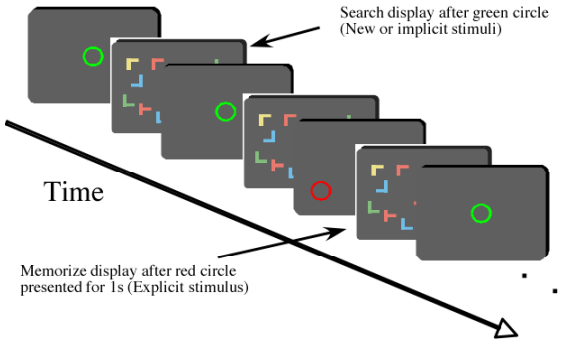

Fig.2 Sequence of trials in the learning phase. A pre-cue frame with a red (in the explicit display) or a green circle (implicit and new displays) was presented before each stimulus display.

were the same in the all three conditions. There was no difference among stimulus conditions in the search phase. Only a fixation point was displayed at the center of the display before the search display. At the end of a session, participants performed a recognition task. The recognition task consisted of 6 new and 12 repeated displays (explicit and implicit ones).

The eye movements were recorded with an eye tracker (Cambridge Research Ltd.) with a 50-Hz sampling rate. Twenty students from Tohoku University participate in the experiment. Ten of them participated in the 1s explicit presentation and the other ten did in the 3s presentation.

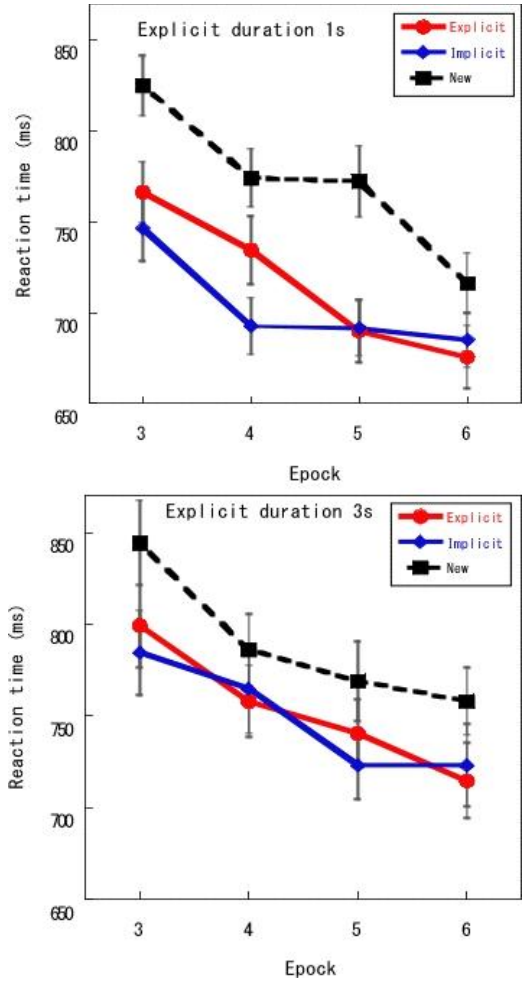

Fig. 3 Reaction time for each condition as a function of epoch. 1s (left) and 3s (right) presentation duration conditions for explicit display.

B. Results

Figure 4 shows reaction times averaged over participants as a function of epoch (which is a sum of four blocks) separately for 1 and 3 s conditions. First and the second epochs are in the learning phase, and the data from epochs 3 or later.

The results for the 1s presentation condition show that shortest reaction time was found in the implicit display, and the second shortest in the explicit display and the longest in the new display. The differences between the explicit and implicit conditions cannot be attributed to the difference in time for memorizing because the reaction time of epochs 1 and 2 for implicit display is shorter than 1 s, which was presentation time for explicit display. The results, therefore, suggests that explicit effort to memorize the display configuration is not as effective as simple repeats of searching displays at lease in the present experiment. When the presentation duration was 3 seconds, the performance was found to be similar between the explicit and implicit conditions, which was better than the new display condition. In other words, 3s for memorizing stimulus layouts is equivalent to the searching the target with less than 1 second of period.

The reaction time is different between the 1 and 3 seconds sessions in the new and implicit layouts. They can be attributed to the observers and stimulus variations because the conditions for these displays are the same. However, it is worth to note that the difference between the new and implicit display conditions (i.e., contextual cuing effect) are smaller in 3s session. This may suggests that the explicit effort to memorize display configuration may have suppressed the contextual cueing effect in the 3s explicit presentation condition.

Figure 4 shows the recognition rate in each condition. The performance is higher for explicit than for implicit displays. Although the recognition rate is not very high in general, the rate higher for the explicit display than that for implicit displays suggests that explicit learning contributes to the recognition memory more than implicit learning. The results of reaction time and recognition rate revealed that there are qualitative differences between the explicit and implicit learning.

Figure 5 shows the average fixation number per each search trial. The differences among different displays are consistent with the difference in reaction time for 1 s explicit display condtion. The smallest number was found for implicit, the second smallest for explicit and the largest for the new display. To reduce reaction time,

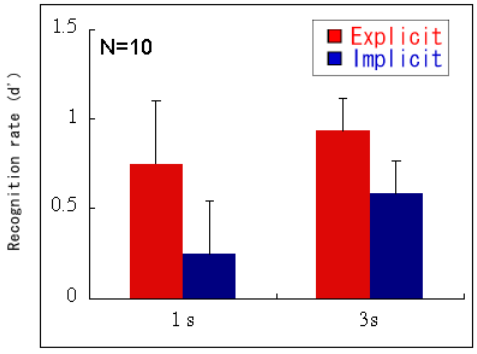

Fig. 4 Recognition rates for explicit and implicit.

reduction of fixation number has been reported[7, 8]. For 3s condition, however, fixation numbers are not consistent with the reaction time data. Number of fixations was smaller for the explicit display than for the implicit display, despite that the reaction time was similar. This suggests that fixation duration was longer for explicit display for 3s condition. Indeed, we found about 10 ms longer on average for

explicit layout than for implicit one. The similar performances in reaction time between the explicit and implicit displays are not based on a common factor. Again, qualitative difference between explicit and implicit learning was suggested.

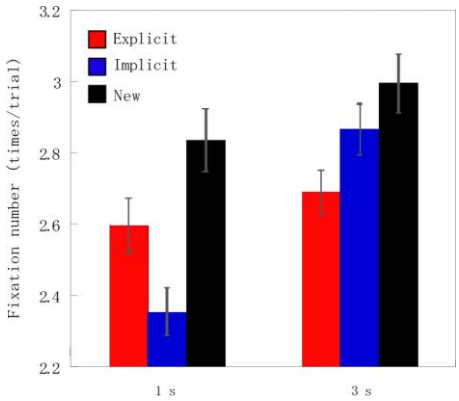

Fig. 5 Fixation numbers for each condition. Date from 1s and 3s are not the same,.

Results of reaction time and eye movements suggest that explicit and implicit processes work differently for memorizing spatial configuration of images. Most importantly, the memory through explicit effort to memorizing display configurations is not as efficient as implicit memory with repeating at least for visual search task For the recognition memory, in contrast, explicit effort seem to help recognition. The eye movements results suggest that the usage of the information learned is also between the explicit and implicit conditions. The fixation duration was longer in the explicit condition. This may be explained by the time required to access in the memory in the explicit condition, where explicit accesses to memory could play an important role.

III. TRACKING EXPERIMENT

In the second line of experiments, we focused on visuo-motor tasks to investigate the implicit and explicit learning related to perception and action. It has been shown that the participants can learn implicitly how to control a cursor on a screen even under manipulation of the relationship between the cursor and the mouse (or similar device) movements such as rotating the angle of cursor position around the center of the screen[7,8]. Some of the studies of visuo-motor learning found a difference between implicit and explicit learning during the recovering period from the manipulated condition to the normal condition[7]. When the visuo-motor condition becomes normal after manipulated, it takes for a while to adjust the movements to the normal again. At the time the condition changed to the normal, the control is not appropriate and the error increases, which is called aftereffect of the learning. The increase of the error can be regarded as an index of learning or adaptation effect since the participant learned or adapted more to the situation manipulated, the aftereffect is expected to be larger. In the condition of implicit learning, large and prolonged aftereffects were reported, comparing that in the explicit learning. The presence of a cognitive strategy may change the learning.

The purpose of the present experiments is to investigate the differences in aftereffect of learning between implicit and explicit conditions using a visuo-motor task. To investigate the effect of awareness, a manipulation was made in one of three types of time courses. In the continuous change condition, very small shift continuously embedded until the shift reached a given amount. In the gradual change condition, small shift embedded every cycle of the stimulus movement until the shift reached the given amount. In the sudden change, the given amount of shift was embedded at a time. The subjective report after the experiment showed that the participants were aware the embedment of the shift in the sudden change while not in the continuous condition, and there were individual differences in the gradual conditions. We compared the amount of the aftereffect among conditions.

We also investigated the effect of attention on explicit and implicit learning. Everyday experience provides impression that we pay attention to action with being aware what we are doing(e.g. writing) while not to action without awareness (e.g. walking). To investigate the effect of attention, we added a second task while participants were tracking the visual target. The target color changed every 500ms and the participants were asked to check the color of the target and to report the number of the target color of blue.

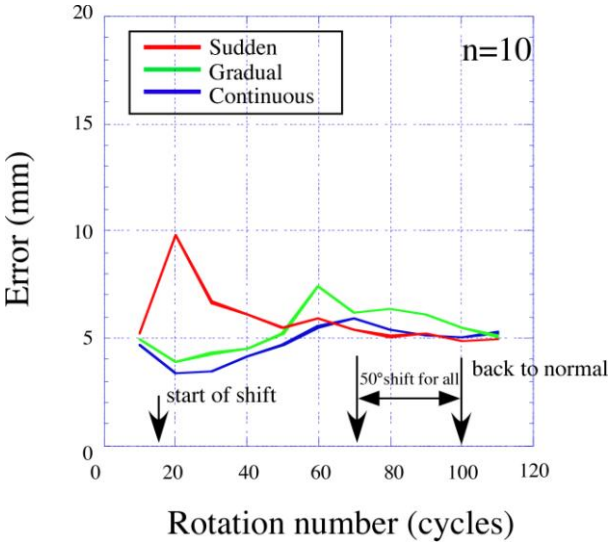

Fig. 6 Error in each condition as a function of time (number of target rotation)

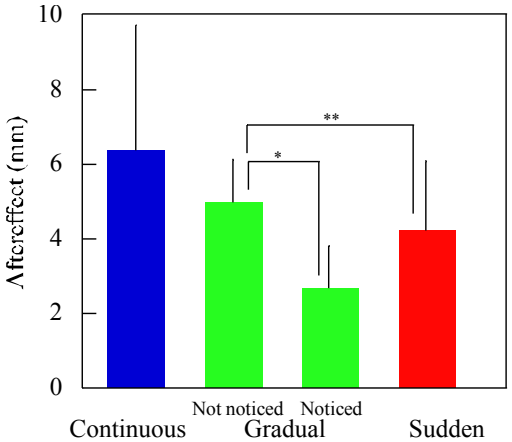

Fig. 7 Aftereffect in each condition. The results of gradual condition are divided into two groups: one is for participants who noticed the embedded shift and the other is for participants who did not.

A. *Effect of awareness*

Participants' task was to track a target on a display with a cursor that was controlled by the movements of a force feedback device (PHANToM Omni, SensAble). The target, a ring, moved on a display circularly in clockwise around the center of the display and the participants controlled the cursor of a small square to center it on

the target. The angle shift embeded was 50° in total while the shift was 1° every cycle in the continuous condition, 10° every 10 cycles in the gradual condition and 50° at a time in the sudden condition.

Figure 6 shows error as a function of time (cycles of target rotation). When the shift was embedded, error was found dependently on the amount of the shift (largest in the sudden condition). After the amount of the shift was became the same (after 70 cycles), errors in the three conditions were similar. Our interest is in the amount of the aftereffect, which can be evaluated by the difference in error between the performance in the final stage of adaptation and that right after the shift was removed. We defined the difference in error between the last ten cycles of shifted condition (between No.91 and No.100) and the cycle right after the removal of the shift (No.101). The amount of aftereffect is shown in Fig. 7. Aftereffect is the largest in the continuous condition and the smallest in the sudden condition. The results of gradual condition were divided into two groups. One is for participants who noticed the embedded shift of the cursor and the other is for participants who did not (3 noticed and 7 did not).

Figure 7 suggests that aftereffect is larger when participants notice the experimental manipulation than when they did not. If we assume that the amount of aftereffect reflects the amount of learning, repeating action without awareness is better than doing so with awareness.

B. Effect of attention

The first experiment suggested that awareness of the embedded shift on cursor movements influenced the degree of learning. It is likely that the participant who noticed the embedded shift paied attention to the visuomotor task more than who did not. Attention can be an important factor for learning process. We investigated the effect of attention on learning of tracking the target with an embedded shift using dual task experiment. To control the participants' attention, we asked them to check the color of the target ring and count how many times the ring was colored blue. We used more difficult tracking than that in the first experiment to have condition where adding the second task influence the performance if attention was attracted to it.

We repeated learning experiment of the tracking task with and without the second task using new participants. The aftereffect was compared between the conditions with and without counting how many times the target became blue. Figure10 shows the difference in aftereffect between with and without the counting task. Since there was individual differences in error rate of the counting task, we divided the participants into the high and low error rate groups. The high error rate group may not have paid attention to the second task much and may show little effect of the second task on the tracking. The results are consistent with the prediction in the sudden condition. The high error rate group showed little difference between the conditions with and without the second task. In contrast, no such difference between the high and low error rate groups in the continuous condition. Both groups showed similar amount of reduction in aftereffect due to the second task. These results suggest that attentional state influences learning with awareness. The effect of the second task in the continuous condition may be caused by the influence of task difficulty. When tracking becomes more difficult due to the second task, the difficulty may reduce the learning effect independently of the attentional state.

IV. Discussion

We compared explicit and implicit (or with and without awareness) learning of perceptual and behavioral tasks. Both of the experiments showed qualitative differences between explicit and implicit learning, suggesting contribution of different processes in the two cases. We are interested in how they differ and also in applying the knowledge to propose efficient learning systems in future. The results of the present experiments suggest two important differences. First, explicit process may use the memory that is explicitly accessible. Such memory can be time consuming although may flexible. The memory process that is used for implicit learning may be something that is more automatically accessed. This can be fast and useful for visual search in familiar places. Second, the explicit process may require attention to learn while the implicit process may not. The explicit process simply does the task as usual

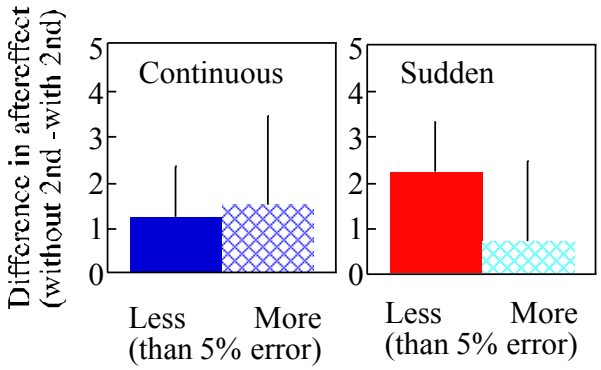

Fig. 8 Difference in aftereffect between the conditions with and without 2nd task.

and moving pattern may be adapted to new situation when coordinate manipulation was made. perhaps, the same process to control hands in everyday life works and learn the new visuomotor relationship that can be used without thinking. In contrast, controlling hands explicitly to make error, perhaps, uses top down control. If error is reduced by top down control, no adaptation or learning is necessary in the control system that works without awareness. This can reduce the learning effect and in turn the aftereffect. These two differences between explicit and implicit learning are, perhaps, important to understand how we adapt to unfamiliar situations. These findings are expected to help to invent appropriate strategies to learn things or adapt to new environment.

References

[1] S. Shioiri and P. Cavanagh, "ISI produces reverse apparent motion," Vision Res **30**(5), 757-768 (1990).

[2] S. Shioiri and K. Matsumiya, "High spatial frequency superiority of motion aftereffect," presented at the Vision Science SocietieS, Sarasota, FL, 2006.

[3] P. Mazzoni and J. W. Krakauer, "An implicit plan overrides an explicit strategy during visuomotor adaptation," J Neurosci **26**(14), 3642-3645 (2006).

[4] D. B. Willingham, "Becoming aware of motor skill," Trends Cogn Sci **5**(5), 181-182 (2001).

[5] M. M. Chun and Y. Jiang, "Contextual cueing: implicit learning and memory of visual context guides spatial attention," Cognit Psychol **36**(1), 28-71 (1998).

[6] M. M. Chun, "Contextual cueing of visual attention," Trends Cogn Sci **4**(5), 170-178 (2000).

[7] H. Imamizu, Y. Uno, and M. Kawato, "Internal representations of the motor apparatus: implications from generalization in visuomotor learning," J Exp Psychol Hum Percept Perform **21**(5), 1174-1198 (1995).

[8] J. W. Krakauer, Z. M. Pine, M. F. Ghilardi, and C. Ghez, "Learning of visuomotor transformations for vectorial planning of reaching trajectories," J Neurosci **20**(23), 8916-8924 (2000).

Novel Motion Pattern Synthesis based on Geometric Symbol Manipulation in Proto-symbol Space

Tetsunari Inamura

***Abstract*— In this paper, we propose a motion-pattern synthesis method in the proto-symbol space. The proto-symbol space is an outcome of our previous work, that uses abstracted phase space which can recognize/generate/abstract motion pattern by continuous hidden Markov models. Previously, an interpolation method was proposed, but several problems have been opened. In this paper, we newly introduce two kinds of target features: expected stay time and pose vector. Experiments in a virtual environment demonstrate the feasibility of the proposed method.**

I. Introduction

Inamura *et al.* proposed the mimesis model [1] for imitation learning by humanoid robots. In their model, a continuous hidden Markov model (CHMM) was used to recognize, abstract and generatie of motion patterns. Motion patterns were transformed into the locations of proto-symbols in a topological space, called the proto-symbol space [2]. Even unknown motion patterns was able to be modeled as a static point of a proto-symbol in the proto-symbol space. Novel motion patterns were generated by synthesizing known proto-symbols. Interpolation can be interpreted an internal dividing point between two proto-symbols, and recognition can be interpreted in a way that a given motion pattern is transformed into an internal dividing point.

There were, however, three problems with the former mimesis model. First problem was that the motion pattern generated by interpolating known proto-symbols generally became smaller compared with the original motion patterns associated with the proto-symbols.

Second problem was extrapolation could not be done. One of the target features for interpolating proto-symbols was the state transition probabilities of the CHMM. If we were to extrapolate them, the resultant probabilities would often be out of the range from 0 to 1. To synthesize a variety of motion patterns solely through the interpolation of finite motion patterns, a huge number of motion patterns must be used, and thus extrapolation of motion patterns is needed for synthesis of novel motion patterns.

Third problem was the number of states of each CHMM was assumed to be the same. In other words, it was not allowed to synthesize two motion patterns which had different motion durations.

The purpose of this research is to clear above problems.

T. Inamura is with National Institute of Informatics / Dept. of Informatics, The Graduate University for Advanced Studies, Japan inamura@nii.ac.jp

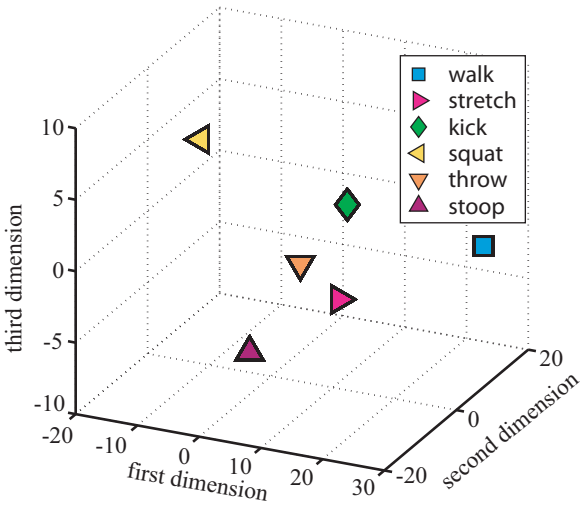

Fig. 1. An example of the proto-symbol space

II. Proto-symbol Space for Recognition and Generation of Unknown Motion Patterns

A. Construction of the proto-symbol space

The CHMM is one of the most famous tools for recognition of time series data, especially in speech recognition research. In this research, left-to-right model [3] is adopted. The CHMM consists of a set of parameter $\lambda = \{Q, \pi, A, B\}$, where $Q = \{q_1, \cdots, q_N\}$ is a finite set of states, $A = \{a_{ij}\}$ is a state transition probability matrix from q_i to q_j, and $B = \{b_i\}$ is a vector of output probabilities of $o[t]$, at q_i, corresponding to the joint angle vector $\theta[t]$ at a discrete time t. The CHMM can abstract and generate motion patterns, and it can also be used for generating time series data [2]. The π is the same for every CHMM because we assume that the Left-to-Right model is used for every CHMM; hence the set of $\mathscr{P} = \{a_{ij}, b_i\}$ determines the behavior of the stochastic process; $\mathscr{P}$ is called a proto-symbol. The proto-symbol space is a topological space that represents the relationship between continuous motion patterns as locations of proto-symbols. The location of the proto-symbols is assigned by a multi-dimensional scaling (MDS) [4] with the distance between CHMMs measured with the Kullback-Leibler divergence [5].

Figure 1 shows an example proto-symbol space constructed using six categories of motion patterns.

B. Problems

In the previous study on the proto-symbol space [2], motion patterns were created by interpolating of the locations of the proto-symbols. More specifically, to create a new proto-symbol $\hat{\mathscr{P}} = \{\hat{a}_{ij}, \hat{b}_i\}$ whose location is a dividing point between the location of $\mathscr{P}_1 = \{a_{ij}^{(1)}, b_i^{(1)}\}$ and the location of $\mathscr{P}_2 = \{a_{ij}^{(2)}, b_i^{(2)}\}$ with fraction $(1-\alpha) : \alpha$, the following equations were used.

$$\hat{a}_{ij} = \alpha a_{ij}^{(1)} + (1-\alpha) a_{ij}^{(2)} \tag{1}$$

$$\hat{b}_i = \sum_{m=1}^{M} \left[\alpha w_{im}^{(1)} \mathscr{N}(\mu_{im}^{(1)}, \Sigma_{im}^{(1)}) + (1-\alpha) w_{im}^{(2)} \mathscr{N}(\mu_{im}^{(2)}, \Sigma_{im}^{(2)}) \right], \tag{2}$$

where M is the number of Gausssian distributions at each node, and w_{im}, μ_{im}, and σ_{im} respectively indicate the mixing coefficient, mean vector and variance vector for the m-th Gaussian distribution at the i-th node. The mean of multiple stochastic generations from an HMM which uses $\{\hat{a}_{ij}, \hat{b}_i\}$ is calculated for motion generation[6].

Equation (1) shows that the state transition probabilities are directly interpolated; thus it cannot be used for extrapolation because negative probabilities may be generated.

In the previous method, the coefficients in Eq. (1) and Eq. (2) were always less than 1, and the joint angles were always less than the original angles. This kind of interpolation is not sufficient for flexible motion synthesis. It is desirable to keep and synthesize joint angle values in the interpolation process.

III. New Method for Synthesis of Proto-symbols

A. Introduction of expected duration

The main difficulty of the previous method for synthesis of proto-symbols is that the outcome did not satisfy the properties of the probability space. Additionally, the number of states for each CHMM is assumed to be the same. To overcome these difficulties, we propose a new method. There are two key aspects: One is that the state transition probabilities and the output probabilities are separately operated upon. The other is that the state transition matrices are calculated in a different domain, i.e., the time domain. Because we employ the left-to-right model, the expected duration s_i in a state q_i can be calculated as

$$s_i = \sum_{n=1}^{\infty} n(1-a_{ii}) a_{ii}^{n-1} = \frac{1}{1-a_{ii}}, \tag{3}$$

where a_{ii} indicates a probability that a self-transition occurs for q_i. By assuming that two CHMMs have the same the number of states, state-wise synthetic operations can be calculated, and the resulting expected stay period can then be transformed into a state transition probability.

B. Generalization of interpolation and extrapolation

The motion pattern synthesis algorithms are essentially the same as the previous one. The only difference is whether negative coefficients are used or not. Not only synthesis using dyadic proto-symbols but also synthesis using three or more points can be easily achieved. Thus, we can derive a general algorithm to synthesize m proto-symbols ($\mathscr{P}_1, \cdots, \mathscr{P}_m$). When mixing coefficients $c_1, \cdots, c_m$ to which negative values could be assigned are given, the expected duration in the state q_i is calculated as

$$\hat{a}_{ii} = \frac{\hat{s}_i - 1}{\hat{s}_i}, \tag{4}$$

where

$$\hat{s}_i = \sum_{j}^{N} c_j \frac{1}{1-a_{ii}^{(j)}}. \tag{5}$$

Regarding the output probability $\hat{b}$ of the synthesized proto-symbol, the mean vector $\hat{\mu}_i$ and the variance vector $\hat{\sigma}_i$ are calculated as

$$\hat{\mu}_i = \sum_{j}^{m} c_j \mu_i^{(j)}, \tag{6}$$

$$\hat{\sigma}_i = \sum_{j}^{m} c_j \sigma_i^{(j)}. \tag{7}$$

C. Synthesis of CHMMs that have different numbers of states

Above algorithms assume that the number of states for each CHMM is the same. We propose a following algorithm to synthesize CHMMs that have different numbers of states. Let the number of states of the j-th CHMM be n_j as shown in Fig.2. Let the number of states of a synthesized CHMM $\hat{n}$ as the maximum number among $n_1, \cdots, n_m$. We define *expected passage time* τ_i^j of the i-th state of the j-th CHMM as

$$\tau_i^j = \sum_{k}^{i-1} s_k^j \tag{8}$$

that means the time when the state transition arrives at the q_i. Next, we define that the expected stay period for each state in the synthesized CHMM as

$$\hat{s} = \frac{1}{(\hat{n}-2)\sum_{j}^{m} c_j} \left\{ \sum_{j}^{m} c_j \tau_{n_j}^j \right\}, \tag{9}$$

that is an interpolation/extrapolation of whole duration of the CHMM transition. Using $\hat{s}$, the expected passage time $\hat{\tau}_i$ of the synthesized CHMM is calculated by $\hat{\tau}_i = (i-1)\hat{s}$.

For each i-th state in the synthesized CHMM, the output probability $\hat{b}_i$ is calculated as follows:

*S*tep 1 Consider the phase of the expected passage time in a time domain of a specific CHMM to interpolate motion patterns that have different number of states. Let $\hat{\tau}_i^j$ be an expected passage time of the j-th CHMM, that corresponds to the expected passage time of the state q_i in the synthesized CHMM. The $\hat{\tau}_i^j$ is calculated as

$$\hat{\tau}_i^j = \hat{\tau}_i \frac{\tau_{n_j}}{\tau_{\hat{n}}}. \tag{10}$$

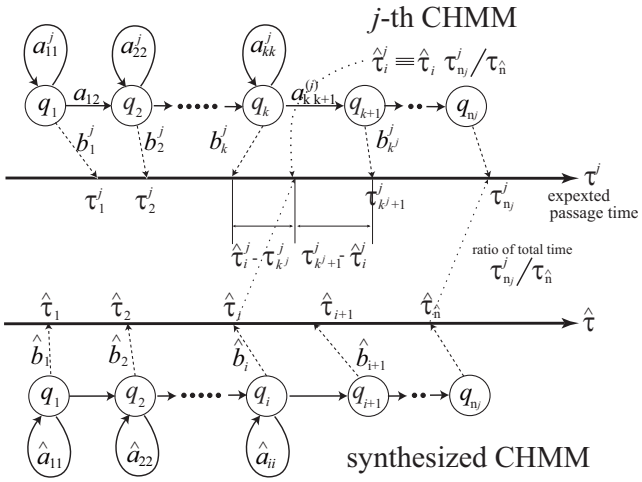

Fig. 2. Concept of expected passage time for interpolation between CHMMs that have different number of states

Selecting the nearest state whose expected passage time is smaller than the expected passage time of the state q_k, in the j-th CHMM as

$$k^j = \arg\min_k \left(\hat{\tau}_i^j - \tau_k^j \right), \tag{11}$$

where a condition $\hat{\tau}_i^j > \tau_k^j$ is assumed.

*S*tep 2 The output probability b_i^j in the state q_i for the j-th CHMM is interpolated by $b_{k^j}^j$ and $b_{k^j+1}^j$. The ratio for the interpolation is proportional to

$$\hat{\tau}_i^j - \tau_{k^j}^j : \tau_{k^j+1}^j - \hat{\tau}_i^j, \tag{12}$$

as shown in Fig.2. This interpolation is calculated as

$$b_i^j = \frac{\tau_{k^j+1}^j - \hat{\tau}_i^j}{\tau_{k^j+1}^j - \tau_{k^j}^j} b_{k^j}^j + \frac{\hat{\tau}_i^j - \tau_k^j}{\tau_{k^j+1}^j - \tau_{k^j}^j} b_{k^j+1}^j. \tag{13}$$

*S*tep 3 Finally, the output probability $\hat{b}_i$ of the synthesized CHMM is calculated as

$$\hat{b}_i = \sum_j^m c_j b_i^j. \tag{14}$$

IV. Experiments

The experimental motion patterns corresponded to time-series data of the joint angle vectors of a human and a simulated humanoid robot. The humanoid robot has 20 degrees of freedom (DOF): 3 for each shoulder, 1 for each elbow, 3 for each leg, 1 for each knee, and 2 for each ankle. All simulations were kinematic. Using a motion capturing system, we recorded two kinds of motion patterns (punching and squattting) with a sampling time of 33 [ms] for about 3 [s]. Figures 3 and 4 show representative recorded motion patterns. These two behaviors were used in the following experiments.

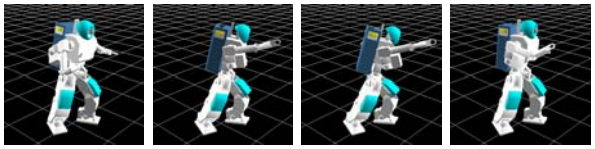

Fig. 3. Punching behavior as a known motion pattern

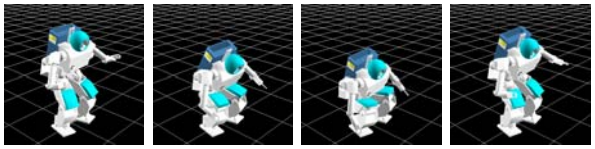

Fig. 4. Squat behavior as a known motion pattern

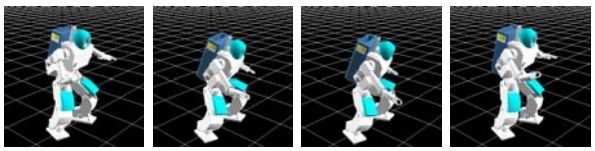

Fig. 5. Interpolation between squat and punch (mixing coefficient of each motion was 0.5)

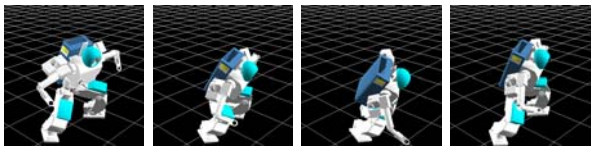

Fig. 6. Interpolation between squat and punch (mixing coefficient of each motion was 1.0)

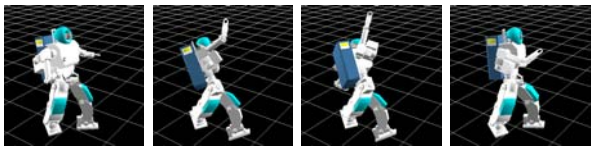

Fig. 7. Extrapolated motion pattern from squat to punch

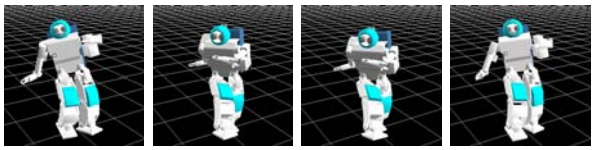

Fig. 8. Kicking behavior as a known motion pattern

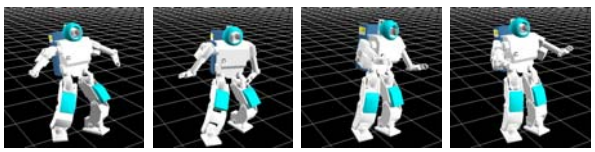

Fig. 9. Interpolated motion pattern with punching and kicking whose HMMs have different numbers of states

A. Interpolation experiment

Fig. 5 shows an interpolated motion patterns using the punching and squatting with $c_1 = 0.5, c_2 = 0.5$ in from Eq.(4) to Eq.(7) Fig. 6 shows a generated motion pattern by $c_1 = 1.0, c_2 = 1.0$ using the same two motion patterns. Both figures demonstrate that our interpolation method blends the behaviors as expected. Even though the mixing rates are the same for both cases, the behavior differ in how the synthesized behavior preserves the joint amplitude of each original behavior. This fact can be easily seen in Figure 10.

B. Extrapolation experiment

Fig.7 shows an extrapolated motion pattern using the punching and squatting behaviors with $c_1 = -1.0, c_2 = 1.5$.

Although the left knee stayed almost straight without any bending motion in the extrapolated motion pattern, it bent both in the original punching and squatting behaviors as shown in Fig.10. This motion is in the opposite direction to the squatting motion, which clearly demonstrates the effect of the extrapolation.

To show the effectiveness of our method quantitatively, Figure 10 plot the time-series pattern for the left knee joint.

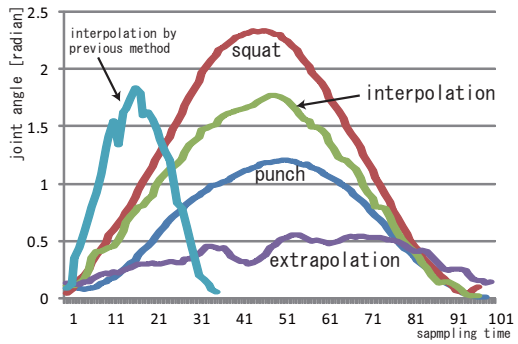

Fig. 10. The joint angle pattern of the left knee

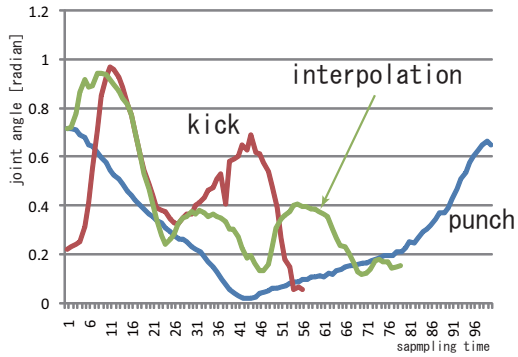

Fig. 11. The joint angle pattern of the pitch joint angle of the right leg in case that two CHMMS having different numbers of states were synthesized

C. Synthesis of CHMMs that have different numbers of states

To confirm the synthesis method described in section III-C, two CHMMs having different numbers of states were synthesized; Punching behavior that abstracted by a CHMM with 20 states, and kicking behavior that abstracted by a CHMM with 15 states. The durations of punching and kicking were 102 and 56, respectively. Fig. 9 shows a synthesized motion using punching (Fig.3) and kicking (Fig.8) with $c_1 = 1.0, c_2 = 1.0$. Fig. 11 shows the pitch joint angle of the right leg of the synthesized motion pattern. The duration of the interpolated motion was 78, that is an average between original durations. These results show the feasibility of our method.

V. Discussion and Conclusion

The feasibility of the proposed method utilizing the expected stay period is clearly shown in Fig. 10 for the duration of the generated motion patterns. Although the duration of the motion synthesized by the previous algorithm was quite shorter than the original motions, the duration of motions synthesized by the proposed algorithm were nearly equal to the original motions. In this study, the synthesis of joint angle vectors was done by the interpolating and extrapolating the mean vector and variance vector of the output probability of proto-symbols.

There are several interpolation methods for motion patterns [7][8][9], but the advantage of the mimesis model is that not only synthesis but also recognition is possible. Another advantage is that not only motion patterns but also multimodal sensorimotor patterns can be accepted. An application in which a robot can estimate novel sensor information based on the basic known motion patterns, is being planned as an advanced function for humanoid robots.

VI. Acknowledgments

The author wish to thank Associate Professor T. Shibata (NAIST, Japan) for the deep and effective discussion.

References

[1] Tetsunari Inamura, Yoshihiko Nakamura, Iwaki Toshima, and Hiroaki Tanie. Embodied symbol emergence based on mimesis theory. *International Journal of Robotics Research*, Vol. 23, No. 4, pp. 363–378, 2004.

[2] Tetsunari Inamura, Hiroaki Tanie, and Yoshihiko Nakamura. From stochastic motion generation and recognition to geometric symbol development and manipulation. In *International Conference on Humanoid Robots*, 2003. (CD-ROM).

[3] S.Young, D. Kershaw, J. Odell, D. Ollason, V. Valtchev, and P. Woodland. *The HTK Book*. Microsoft Corporation, 2000.

[4] Susan Schiffman. *Introduction to Multidimensional Scaling: Theory, Methods, and Applications*. Academic Press, 1981.

[5] Solomon Kullback. *Information Theory and Statistics*. Wiley, 1959.

[6] Tetsunari Inamura, Hiroaki Tanie, and Yoshihiko Nakamura. Keyframe compression and decompression for time series data based on the continuous hidden markov model. In *Proc. of Int'l Conf. on Intelligent Robots and Systems*, pp. 1487–1492, 2003.

[7] Kiyoshi Hoshino. Interpolation and extrapolation of repeated motions obtained with magnetic motion capture. *IEICE Trans. Fundamentals of Electronics, Communications and Computer Sciences*, Vol. E87-A, No. 9, pp. 2401–2407, 2004.

[8] Matthew Brand, Nuria Oliver, and Alex Pentland. Coupled hidden markov models for complex action recognition. In *Proceedings of the 1997 Conference on Computer Vision and Pattern Recognition (CVPR '97)*, pp. 994–999, 1997.

[9] Takumi Kobayashi and Nobuyuki Otsu. Action and Simultaneous Multiple-Person Identification Using Cubic Higher-order Local Auto-Correlation. In *Proc. of International Conference on Pattern Recognition*, pp. 741–744, 2004.

Unrealistic condition between visual and haptic stimuli in ball catching task

Yasuharu Koike

Abstract— **Humans show a variety of motor behavior which enables us to interact with many different objects under different environments. Considering the number of objects and environments which influence the dynamics of the arm, the corresponding motor control system must be capable of providing appropriate motor commands for the multitude of distinct contexts that are likely to be experienced.**

In the experiments, we showed a virtual ball moving vertically downward on a 50 inch plasma display with three different force timing from -60 msec to 60 msec at intervals of 60 msec. The ball catching was simulated by a force-feedback system, provided by the SPIDAR. The subject was asked to catch the virtual ball at an initial hand position. The hand position and Electromyographic (EMG) signals of flexor carpi radialis were recorded.

We found that subjects learned new environments in which the ball was falling by a different timing even though the visual information was same with the different height conditions. Moreover the timing at the different height was different for each height and it was indicated that the subject learned the different timing to the different acceleration environments.

I. INTRODUCTION

An internal model is a neural mechanism that mimics the dynamics of motor apparatus or environment [4]. Forward internal models can be acquired to predict sensory feedback from efference copies through motor learning. Inverse internal models can generate motor command to realize the goal of the task.

Recent researches focus on the issue of whether multiple internal models are learned and switched. Many disparate results were reported about consolidation hypothesis [1], [5]. In these study, subjects had to learn both visuomotor environment and dynamic motor command generation. Here we addressed this issue by investigation how only visuomotor environment is learned without changes of the visual environment and with changes of the haptic information. Catching a falling ball task was investigated in order to reveal

P & I Laboratory, Tokyo Institute of Technology, R2-15, 4259, Nagatsuta-cho, Midori-ku, Yokohama, 226-8503 koike@pi.titech.ac.jp

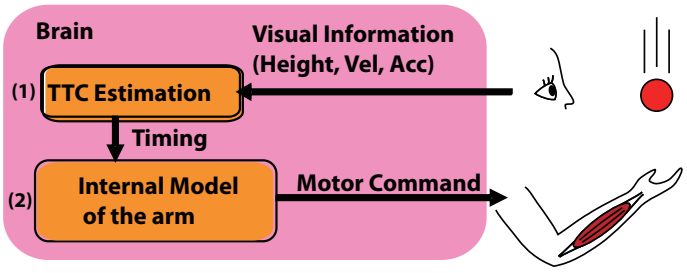

Fig. 1. Two hypotheses for learning this task

mechanisms that estimate time-to-contact (TTC) [2], [6], [7], [8]. Also, internal model of invariant gravity (1g) and zero-gravity (0g) were compared by using hitting moving object task [10], [11], [12]. In these studies, subject had to learn only visuomotor environment, because the hitting movement was same for different conditions. From our previous experiment [9], human can learn the different acceleration conditions and they can discriminate the different acceleration using visual or haptic information.

What happen, if visual and haptic stimuli are inconsistent? That is, haptic stimulus is given before or after the contact time in visual stimulus.

Almost of all experiments used the physically consistent conditions. So at the ball contact, the visual and haptic stimuli were displayed simultaneously. How do we detect the TTC by visual or haptic information? In this experiments, we showed a virtual ball moving vertically downward on a 50 inch plasma display with three different force timing from -60 msec to 60 msec at intervals of 60 msec. The ball catching was simulated by a force-feedback system. We found that subjects learned new environments in which the ball was falling by a different timing even though the visual information was same. These results suggest that humans can learn different timing by force feedback.

We can assume two hypotheses for explaining this phenomena in fig. 1. One is that the subject learned the different timing by using visual stimuli (1). They would become to estimate the different TTC with same

visual stimuli as they learned the different acceleration. The other one is that the subject learned the delay between the motor command and muscle tension (2). It is known that the delay between muscle activation and force exertion is about 100 msec, and the delay between motor cortex and muscle is about 20 msec. Usually, we don't aware of this delays during motor tasks. We probably learned this delay and send the motor command beforehand to compensate these delay.

In order to confirm these two hypotheses, we tried to same experiments with the different height conditions.

II. Experiment

A. Subjects

3 healthy subjects (3 men, 23 $\sim$ 29 years old) participated in the study. The subjects were right-handed, had normal vision or vision that was corrected for normal. Experiments were conformed to the Declaration of Helsinki on the use of human subjects in research.

Fig. 2. Experimental environment.

B. Visual and haptic display using virtual reality environment

Figure 2 shows a experimental environment. We use a haptic device "SPIDAR" which use four motors (Maxon DC motor, RE25) to strain by strings for applying the force to a hand [3]. Figure 3 shows system configuration. We also measure Electromyo-

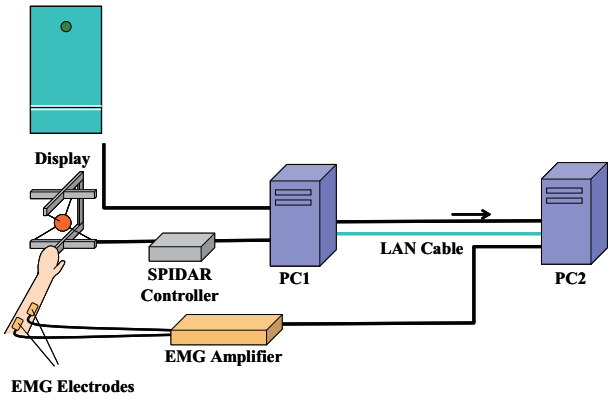

Fig. 3. system configuration

graphic (EMG) signals (Bagnoli-16 system Delsys inc.) for measuring a intention for catching, because EMG signals activate about 100 msec before exerting a force. Active electrode was put on palmaris longus and EMG signals was sampled at 2 kHz with 16bit. In order to show the visual stimuli to the subject, plasma display (PDP503-CMX, 50 inches, Pioneer) was used. Virtual ball was falling from 80 [cm] height with 0 [m/sec] initial velocity, was same color and size, and applied 4.9 [N] force to right hand for 1.1 sec for different perturbation conditions.

C. Experimental procedure

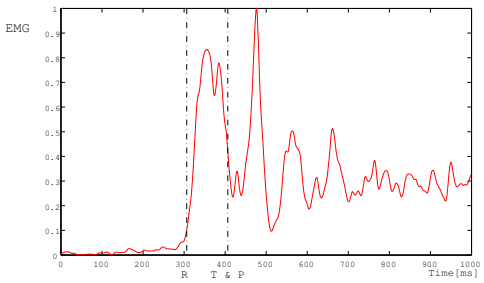

Fig. 4. Average onset timing of EMG signals as a function of repetition for each condition

Subjects were asked to catch the ball at the initial position. At the beginning of the trial, beep signal sounded and after a random delay ranging from 0.75 to 1.25 sec, the virtual ball was falling with 0 m/s initial velocity and 9.8 m/s^2 acceleration.

Subjects perfomed 3 different experiments. In each experiment, the force timing and the drop altitude was different, and the timing was selected from 3 conditions, -60, 0, 60 [msec] and the height was selected from 5 conditions, 70.0, 77.5, 82.5, 85.0, 100 [cm].

III. Results

Figure 4 shows the average rectified EMG signals and low-pass filtered EMG signals with 50 Hz cut off frequency. The time when the force was applied to the hand was shown as dotted vertical line (indicated "T and P"). In each delay condition, EMG activities became to increased 100 msec before applying the force (indicated "R").

Figure 5 shows the EMG onset at the different height conditions. The estimated acceleration was 9.65[m/sec^2] (solid line) , 16.60[m/sec^2] (dotted line) and 8.87[m/sec^2] (dashed line) for ± 0, -60 and $+60$ conditions respectively. The average acceleration for 3 subjects was 11.71, 18.70 and 8.56 for ± 0, -60 and $+60$ conditions respectively. The theoretical value of acceleration is 13.38[m/sec^2] and 7.49[m/sec^2] for -60 and $+60$ conditions.

Figure 6 shows the time difference between EMG onset and force onset. At the 85cm height conditions, the subjects learned the different timing and the difference were about 100 msec. In the condition ± 0, the time difference were almost 100 msec. In the condition -60 and 60 msec,the time difference were not equal comparing to the ± 0 condition.

IV. Discussion

Visual stimulus was followed the normal gravitational environment and only the timing of force was changed. In this condition, the subjects could learn the proper timing of catching task. From this result, the haptic information is also important for learning. Moreover the subject could adjust the timing of the EMG onset without perceive the delay visually.

The subjects learned the timing at the different height conditions. From this experimental results, the timing was different depending on the height and the estimated acceleration indicated that the subject learned the different acceleration environments.

V. ACKNOWLEDGMENTS

This work has been partially supported by a Grant-in-Aid for Scientific Research on Priority Areas "Emergence of Adaptive Motor Function through Interaction between Body, Brain and Environment"from the Japanese Ministry of Education, Culture, Sports, Science and Technology.

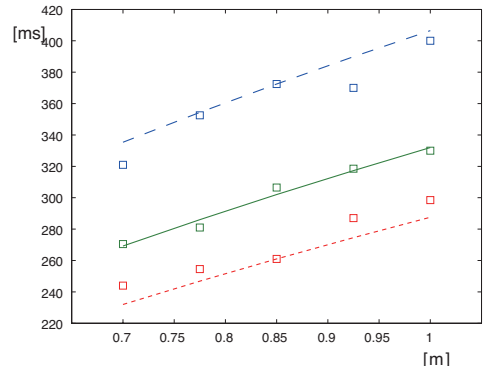

(a) subject A

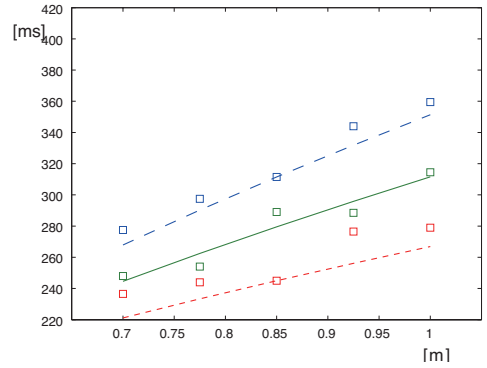

(b) subject B

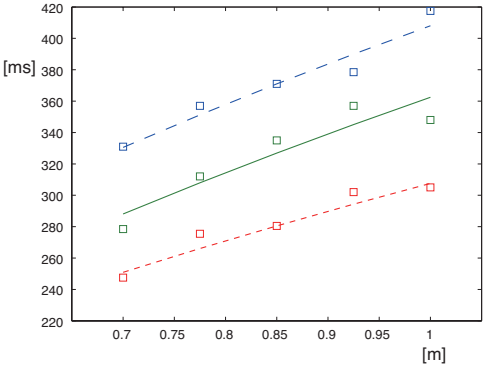

(c) subject C

Fig. 5. EMG onset timing for different height conditions

References

[1] G. Caithness, R. Osu, P. Bays, H. Chase, J. Klassen, M. Kawato, D.M. Wolpert, and J.R. Flanagan. Failure to consolidate the consolidation theory of learning for sensorimotor adaptation tasks. *J Neurosci*, 24(40):8662–71, 2004.

[2] G.J.K.Alderson, D.J.Sully, and H.G.Sully. An operational analysis of a one-handed catching task using high speed photography. *Journal of Motor Behavior*, 6:217–226, 1974.

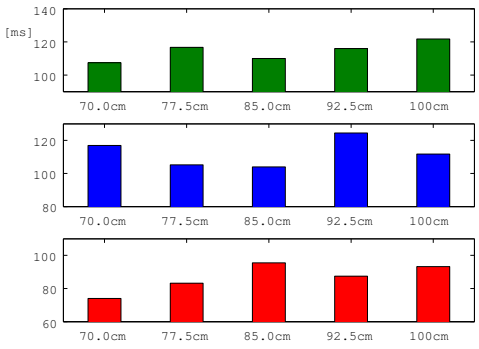

(a)

subject A

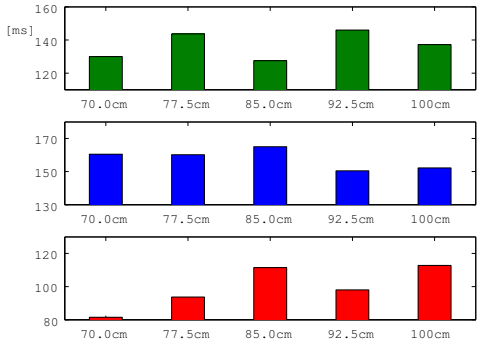

(b) subject B

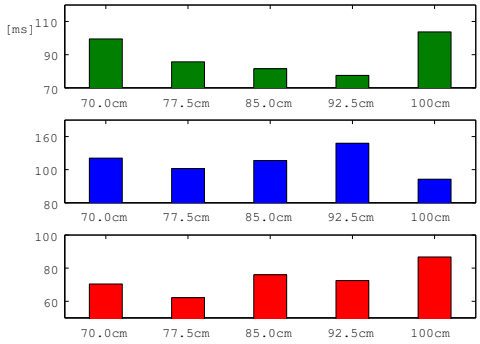

(c) subject C

Fig. 6. Time difference for different height condtions

[3] Masahiro Ishii and Makoto Sato. A 3d spatial interface device using tensed strings. *Presence*, 3:81–86, 1994.

[4] M. Kawato. Internal models for motor control and trajectory planning. *Curr Opin Neurobiol*, 9(6):718–27, 1999.

[5] J.W. Krakauer and R. Shadmehr. Consolidation of motor memory. *Trends Neurosci*, 29(1):58–64, 2006.

[6] F. Lacquaniti and C. Maioli. The role of preparation in tuning anticipatory and reflex responses during catching. *J Neurosci*, 9(1):134–148, 1989.

[7] Lee.D.N., Young.D.S., Reddish.P.E., Lough.S., and Clayton.T.M.H. Visual timing in hitting an acceleration ball. *Quarterly Journal of Experimental Psychology*, 35A:333–346, 1983.

[8] G.J. Savelsbergh, H.T. Whiting, A.M. Burden, and R.M. Bartlett. The role of predictive visual temporal information in the coordination of muscle activity in catching. *Exp Brain Res*, 89(1):223–228, 1992.

[9] Y.Koike, S.Hong, and D.Shin. Learning and switching between multiple nonzero-gravity environments for catching task. In *Neuroscience abstract*, 2005.

[10] M. Zago, G. Bosco, V. Maffei, M. Iosa, Y.P. Ivanenko, and F. Lacquaniti. Internal models of target motion: expected dynamics overrides measured kinematics in timing manual interceptions. *J Neurophysiol*, 91(4):1620–34, 2004.

[11] M. Zago, G. Bosco, V. Maffei, M. Iosa, Y.P. Ivanenko, and F. Lacquaniti. Fast adaptation of the internal model of gravity for manual interceptions: evidence for event-dependent learning. *J Neurophysiol*, 93(2):1055–68, 2005.

[12] M. Zago and F. Lacquaniti. Internal model of gravity for hand interception: parametric adaptation to zero-gravity visual targets on earth. *J Neurophysiol*, 94(2):1346–57, 2005.

Analysis of Human Skills in Manipulation with Interaction with Environment
—Modeling of Two-Fingered Pivoting Based on CPG—

Yusuke MAEDA and Hajime SUGIUCHI

***Abstract*— Two-fingered pivoting is a typical example of human dexterous manipulation interacting adaptively with the environment. In this paper, we construct a skill model of two-fingered pivoting manipulation based on CPG (Central Pattern Generator) with five neurons. The CPG drives a virtual hand, which consists of a wrist, a palm, a thumb and an index finger, rhythmically to achieve robust pivoting through the interaction with the environment. Its adaptability is demonstrated in dynamic simulation of box pivoting. The virtual hand successfully adapts to environmental changes such as sudden decrease of the friction coefficient of the floor.**

I. Introduction

It is known that rhythmical adaptive motions found in biped walking of humans and quadruped walking of other animals are generated by CPG (Central Pattern Generators). The activity of the CPG is easily entrained by external periodic signals, which enables CPG-based adaptive motion control by using sensory feedback from the environment. While the idea of the CPG has been applied primarily to the locomotion control of robots, the possibility that human multifingered manipulation is realized by the CPG is suggested [1].

However, previous studies applied CPG-based control only a few kinds of manipulation, such as crank rotation by a three-link manipulator [2] and cylinder rotation by a multifingered hand [3], [4]. Graspless manipulation [5], a method to manipulate an object by utilizing contacts between the object and the environment, requires motion control that adapts to environmental situation due to the existence of the contacts. Therefore CPG-based control is promising, but there have been no studies on CPG-based control of graspless manipulation.

In this study, we focus on pivoting [5], a typical graspless manipulation, and construct a CPG-based model for two-fingered pivoting skill.

II. Pivoting Task

In pivoting operation (Fig. 1), a vertex of the manipulated object is used as a pivot around which the object is rotated. The object is in one-point contact with the ground in pivoting and therefore the human operator does not have to support all the weight of it. Thus, pivoting is suitable for manipulation of heavy objects. Repeating small rotations around two vertices of the object by turns, the object can be moved to any locations.

Yusuke MAEDA and Hajime SUGIUCHI are with Division of Systems Research, Faculty of Engineering, Yokohama National University, 79-5 Tokiwadai, Hodogaya-ku, Yokohama 240-8501, Japan {maeda, sugi}@ynu.ac.jp

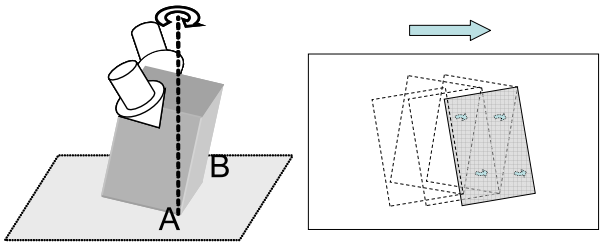

Fig. 1. Pivoting

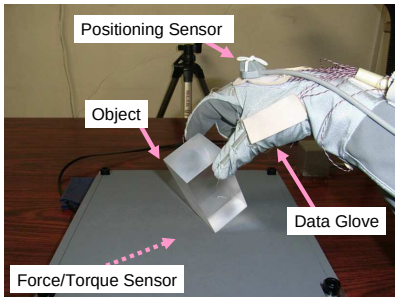

Fig. 2. Data Acquisition Setup

The pivoting operation can be analyzed into the following steps:

1) Raise the vertex B and make the object be in the point contact at the vertex A.
2) Rotate the object around the axis that passes through the vertex A.
3) Put the vertex B down and make the object be in the line contact at the edge AB.
4) Exchange the vertex A and B, and go to the step 1.

Smooth pivoting requires rhythmical and adaptive motion through the interaction with the environment.

The motion of the human hands in pivoting operation was measured by a data glove and other apparatus (Fig. 2) for reference in constructing a CPG-based pivoting model.

III. Hand Model

We use a hand model composed of a palm, an index finger and a thumb (Fig. 3, 4). For simplicity, we ignore kinematic constraint on the palm by the wrist. The index finger and the thumb are composed of three and five revolutionary joints, respectively.

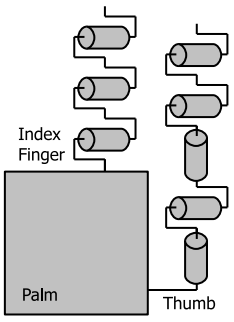

Fig. 3. Hand configuration

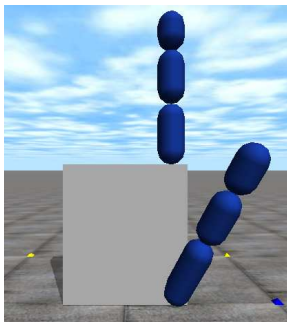

Fig. 4. Hand on simulator

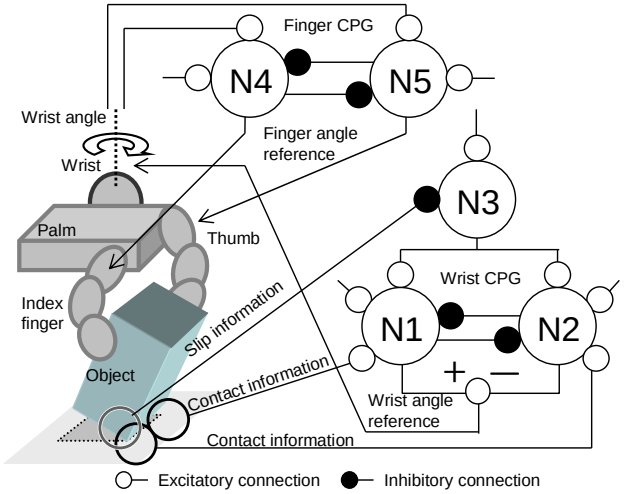

Fig. 5. Overview of hand control model

In order to simplify the motion of the hand model, we assume that the index finger and the thumb are in charge of the above step 1 and 3, and the wrist that moves the palm is in charge of step 2.

The control references of the fingers and the wrist are determined by the output of CPGs. The index finger and the thumb pinch the object and put it up and down. The wrist rotates the palm around a vertical axis, and its translational motion is passively determined in pivoting operation.

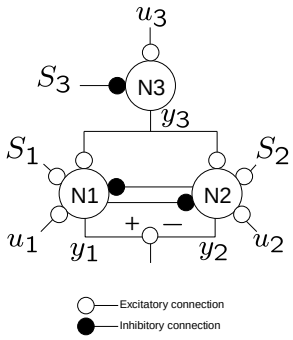

Fig. 6. Wrist CPG configuration

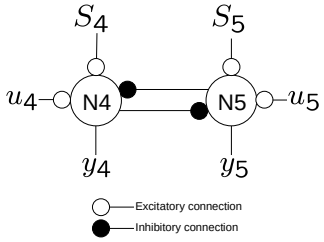

Fig. 7. Finger CPG configuration

IV. Design of CPG

A. CPG Model

We use Matsuoka's model [6] for neurons that compose CPGs. The dynamics of the i-th neuron is given by the following equations:

$$\frac{1}{T_{r_i}}\dot{x}_i + x_i = -\sum_{j=1}^{n} a_{ij}y_j - b_i z_i + u_i + S_i \tag{1}$$

$$\frac{1}{T_{a_i}}\dot{z}_i + z_i = y_i \tag{2}$$

$$y_i = \max(0, x_i), \tag{3}$$

where x_i is the internal state of the neuron, y_i is the output, z_i is the fatigue state, u_i is the external input, S_i is the feedback input, a_{ij} is a inhibitory connection coefficient from the j-th neuron to the i-th neuron, b_i is a fatigue coefficient, and T_{r_i} and T_{a_i} are time constants.

B. CPG Configuration and Its Adaptability

Successful pivoting requires good synchronization of the following:

- Rotation of the wrist.
- Lifting up and down of the object.
- Switching of the pivot vertex.

In this study, we control the hand model with CPGs in order to synchronize the above motions and tune the amplitude of pivoting step for adapting to the environmental situation.

We assume that the following information are available for motion control:

- Rotation angle of the wrist.
- Which vertex is grounded.
- Presence or absence of slippage at the pivot.

We use two CPGs for driving the hand model: wrist CPG for driving the palm, and finger CPG for driving the index finger and thumb (Fig. 5). These two CPGs have no direct signal connections, but they can mutually entrain through the interaction among the palm, the fingers and the environment. We design the CPGs so that their mutual entrainment enables pivoting of the object.

Wrist CPG

The wrist CPG consists of three neurons: N_1, N_2 and N_3 (Fig. 6). The reference of wrist angle, $\theta_{\mathrm{wrist,ref}}$, is determined from the outputs of N_1 and N_2 as follows:

$$\theta_{\mathrm{wrist,ref}} = p_1 y_1 - p_2 y_2 - \theta_0, \tag{4}$$

where θ_0, p_1, p_2 are constants. The external stimuli inputted to the neuron N_1 and N_2 are given by the following equation:

$$S_i = k_i s_i + s_V \quad (i = 1, 2), \tag{5}$$

where k_1 and k_2 are constants, and s_i is the following grounding signals:

$$\begin{cases} s_1 = 1 \text{ and } s_2 = 0 \\ \quad \text{when the index-finger-side vertex is grounded,} \\ s_1 = 0 \text{ and } s_2 = 1 \\ \quad \text{when the thumb-side vertex is grounded.} \end{cases} \tag{6}$$

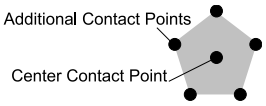

Fig. 8. Surface contact approximated by point contacts

TABLE I
NEURON PARAMETERS

Neuron	T_{r_i}[s]	T_{a_i}[s]	b_i	u_i
N_1	0.4	1.2	2.5	0.5
N_2	0.4	1.2	2.5	0.5
N_3	12	2.4	0.25	1.25
N_4	0.6	1.2	7	1
N_5	0.6	1.2	7	1

TABLE II
CONNECTION COEFFICIENTS (a_{ij})

a_{ij}	N_1	N_2	N_3	N_4	N_5
N_1	0.0	1.5	0.0	0.0	0.0
N_2	1.5	0.0	0.0	0.0	0.0
N_3	0.0	0.0	0.0	0.0	0.0
N_4	0.0	0.0	0.0	0.0	1.5
N_5	0.0	0.0	0.0	1.5	0.0

The CPG output is entrained to the timing of exchange of grounded vertices, which enables appropriate control of the rotation of the wrist.

The amplitudes of the outputs of N_1 and N_2 are dominated by s_V in (5), which is given by:

$$s_V = p_3 y_3, \tag{7}$$

where p_3 is a constant. The neuron N_3 is placed to tune the amplitudes of the neuron N_1 and N_2 according to the slippage at the grounded vertex in pivoting. The excitation of N_3 is controlled by the feedback input S_3 as follows:

$$S_3 = k_3 s_3, \tag{8}$$

where k_3 is a negative constant, and s_3 is a slippage signal; $s_3 = 1$ when slippage occurs and $s_3 = 0$ otherwise. When the friction coefficient of the floor is large enough to suppress slippage, N_3 is excited by the constant input u_3. On the other hand, when slippage occurs, inhibitory stimuli is inputted to N_3 and the output y_3 becomes small.

Because y_3 is used as excitatory input to N_1 and N_2, it affects the amplitudes of these neurons. When the slippage occurs, N_3 is inhibited according to the time of the slippage and the wrist motion becomes small. This helps to achieve stable pivoting on a slippery floor and adaptive pivoting to the changes of a friction coefficient of the floor.

Finger CPG

The angle of the wrist is inputted to the finger CPG neurons (Fig. 5). The exchange of the pivot vertices is realized by the entrainment to the input. The finger CPG consists of two neurons (Fig. 7). The output of N_4 is used to calculate the desired MP and PIP joints of the index finger. The output of N_5 is used to calculate the the desired CMC joint of the thumb. The mapping between the CPG outputs and the desired joint angles is determined by trial and error. The motion of the fingers causes lifting up and down of the object.

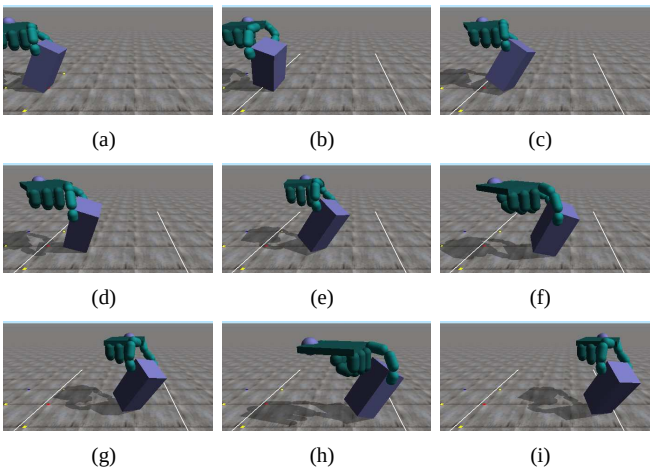

Fig. 9. Pivoting on simulator

As the wrist angle becomes large, the neuron driving the pivot-side finger is inhibited and that driving the opposite-side finger is excited as follows:

$$S_4 = k_4(\theta_{\text{wrist}} - \theta_0) \tag{9}$$
$$S_5 = -k_5(\theta_{\text{wrist}} - \theta_0), \tag{10}$$

where θ_{wrist} is the current wrist angle, and p_4 and p_5 are constants. The finger CPG causes finger motion according to the wrist angle, which leads to the exchange of pivot vertices. Then the exchange makes the wrist CPG to be entrained. Thus the synchronization between the finger CPG and the wrist CPG is achieved and pivoting is realized.

When the slippage occurs, the finger motion becomes small according to the entrainment to the wrist CPG. That helps to suppress the slippage.

V. SIMULATION OF PIVOTING

A. Simulation Conditions

We performed dynamic simulation of two-fingered pivoting using the above CPG-based model on an open source simulation engine, ODE (Open Dynamics Engine) [7]. ODE can deal with friction, but has no functionality to represent soft finger contacts (rotational frictional contacts). Thus we set pseudo contacts around the original contact point (Fig. 8).

The manipulated object is a cuboid of 310 [g] and its size is $50 \times 50 \times 100$ [mm]. Table I and II shows the parameters of neurons of the CPGs. Other parameters are: $p_1 = p_2 = 0.471$ [rad/s], $p_3 = 40$, $k_1 = k_2 = 8$, $k_3 = -80$, $p_4 = p_5 = 8$ [1/rad], $\theta_0 = 0.6$ [rad].

B. Simulation Results

We performed simulations of pivoting when the friction coefficient of the floor is constant. In this case, pivoting can be performed stably. Fig. 9 shows screenshots of the simulation when the friction coefficient is 0.5.

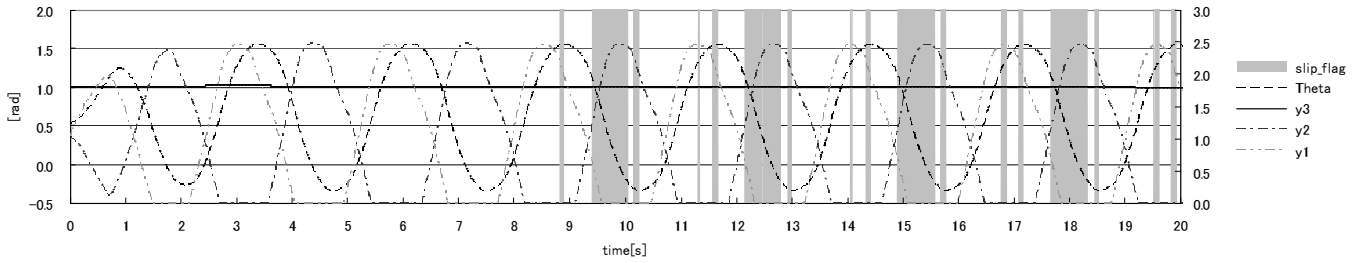

Fig. 10. Wrist joint angles and CPG output (without adaptability, Friction changes at 8 [s])

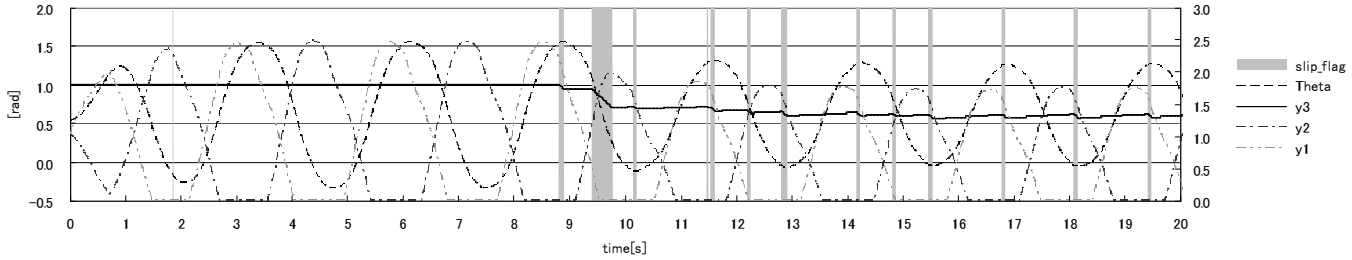

Fig. 11. Wrist joint angles and CPG output (with adaptability, Friction changes at 8 [s])

Next, we checked the adaptability of pivoting by causing sudden decrease of the friction coefficient during pivoting operation. Concretely, we decreased the friction coefficient from 0.5 to 0.01 at 8 [s] after the start of pivoting. For comparison, we constructed another CPG model without adaptation functionality as a control. It is almost identical to the proposed model but $k_3 = 0$, which disables the adaptability of the pivoting step in the proposed model.

The wrist angle, the outputs of the neurons of the wrist CPG, and the status of slippage in simulations are shown in Fig. 10 and Fig. 11. The shaded areas in the figures indicate that the slippage occurs. y_3 is around 1 both in the proposed and control model when the friction coefficient is large. However, after the sudden decrease of the friction coefficient, the excitation of N_3 is suppressed only in the proposed model.

The control model with $k_3 = 0$ continues to perform pivoting allowing slippage (Fig. 10). On the other hand, in the proposed model, y_3 is suppressed according to the slippage, which leads to small wrist motion. Because of this, slippage is suppressed.

y_3 becomes smaller as the slippage occurs, and the amplitude of θ_{wrist} becomes smaller until the S_3 and u_3 are balanced. After the balance, the slippage can be found only around the instants of the exchange of pivot vertices (Fig. 11). Thus, the CPGs worked as designed and achieved adaptive pivoting.

VI. Conclusion

In this paper, we modeled a skill of two-fingered pivoting with interactions with the environment by using CPGs. The constructed CPGs cause mutual entrainment and achieve rhythmical and stable pivoting motion in dynamic simulation. The CPG-based model also shows adaptability to the sudden decrease of the friction coefficient to suppress slippage.

References

[1] H. Taguchi, K. Hase, and T. Maeno, "Analysis of the motion pattern and the learning mechanism for manipulating objects by human fingers," *Trans. of Japan Soc. of Mechanical Engineers (Series C)*, vol. 68, no. 670, pp. 1647–1654, 2002, (in Japanese).

[2] T. Kondo, T. Somei, and K. Ito, "A predictive constraints selection model for periodic motion pattern generation," in *Proc. of IEEE/RSJ Int. Conf. on Intelligent Robots and Systems*, 2004, pp. 975–980.

[3] Y. Kurita, , J. Ueda, Y. Matsumoto, and T. Ogasawara, "CPG-based manipulation: Generation of rhythmic finger gaits from human observation," in *Proc. of 2004 IEEE Int. Conf. on Robotics and Automation*, 2004, pp. 1209–1214.

[4] Y. Kurita, K. Nagata, J. Ueda, Y. Matsumoto, and T. Ogasawara, "CPG-based manipulation: Adaptive switchings of grasping fingers by joint angle feedback," in *Proc. of 2005 IEEE Int. Conf. on Robotics and Automation*, 2005, pp. 2528–2533.

[5] Y. Aiyama, M. Inaba, and H. Inoue, "Pivoting: A new method of graspless manipulation of object by robot fingers," in *Proc. of IEEE/RSJ Int. Conf. on Intelligent Robots and Systems*, Yokohama, Japan, 1993, pp. 136–143.

[6] K. Matsuoka, "Sustained oscillations generated by mutual inhibiting neurons with adaptation," *Biological Cybernetics*, vol. 52, no. 6, pp. 367–376, 1985.

[7] "Open Dynamics Engine," http://www.ode.org/.

Violations of optimal foraging: risk, impulsiveness, and serotonin

Toshiya Matsushima, Animal Behavior and Intelligence, Department of Biology, Faculty of Science, Hokkaido University

***Abstract*—Do animals have mind? Do non-mammalian vertebrate animals in particular have mental processes similar to ours? The issue of "animal mind" has long been unchallenged simply because it was ill-defined. Recent progresses in behavioral studies in birds, however, revealed that they have cognitive process analogous to ours. In this study, we report a series of data obtained from experimental psychological studies using chicks of domestic chickens as subjects. In 2007, we obtained the following results; (1) Chicks consistently showed risk-aversion, when the profitability of food gain varied by a risk on the amount of reward. When the risk was brought about by a varying delay time (or proximity of reward), on the other hand, chicks showed risk-neutral / or even risk-prone choices, suggesting that the gain rate maximization is not the rule. Consequently, the overall gain was significantly reduced, indicating a clear violation of optimality. (2) Impulsiveness measured in the inter-temporal choice paradigm was subject to competitive foraging during early stage of life. When trained for association between color cues and rewards in highly competitive condition, the trained chicks showed significantly higher level of impulsiveness. The enhanced level of impulsiveness decreased the gain rate at the long term, thus another case for the violation of optimality. Systemic injection of SSRI (serotonin-selective reuptake inhibitor, fluvoxamine; 20mg/kgBW) caused the chicks to choose a larger and delayed reward, indicating that the SSRI suppressed impulsiveness. (3) Patch residence time, or time until the chick leaves a food patch with gradually decreasing gain rate (or, feeder of a diminishing return), was measured. The residence time had a large variance, that was nearly proportionate to the square of the mean, indicating that a Poisson process could underlie. Injection of SSRI at the same dose caused chicks to stay longer at the diminishing feeder, suggesting that common mechanisms (such as the sense of time, or time perception) is modulated by serotonin. These results suggest; (i) Foraging decision is based on multi-factorial evaluation function including amount, delay and risk of the reward. (ii) Chick behaviors in controlled laboratory conditions consistently violated the optimality, thus that the consequent gain was not maximized. (iii) Serotonergic system control the foraging decisions probably through modulation of time perception.**

I. Introduction

RECENT progress in behavioral studies of birds suggested that they have cognitive processes analogous to ours, humans. Pepperberg [1] reported that African Grey Parrots are able to manipulate vocal labeling for communication with human. Clayton [2] has studied food storing behaviors and assumed that blue jays (corvids in general) could have episodic-like memory. Furthermore, Emery [3] has suggested that jays organize their behaviors based on assumption of other individuals' cognitive process, indicative of "theory of mind" in birds. All these cases were successful in showing that the birds have cognitive processes similar to primates. Does it mean that the they have "mind" that is identical to ours?

This issue of the animal mind is however, terribly ill-defined, simply because many topics and concepts still remain highly ambiguous; without specifying human mind, for example, we are unable to precisely argue the "similarity" to ours. It is also highly controversial whether elementary brain processes in animals (and humans) mind process can be categorized in the same fashion. Purely materialistic approaches have limited applicability to the issue of mind.

In this report, I will introduce some of the experimental psychology of domestic chicks as subjects. The idea is that the ecological backgrounds of foraging choice can be related to the neural bases and cognitive processes. Through viewing the issue in both ecology and neuroscience, we will be prepared to discuss the issue of animal mind (or evolution of intelligence) with minimal assumptions.

Accompanying phenomenal convergence of dynamics, a given equation often yields a diverging spectrum of solutions. Neuroscience has been a powerful tool, because we could omit and disregards solutions that were physiologically unrealistic. Similarly, through filtering the possible solutions by ecological / evolutionary realisms, we will be given additional constraints, thus making our arguments on animal minds highly practical (less imaginary) than it used to be. The present series of study thus aims at the foundation of neuro-ecology.

II. Optimal Foraging Theory

Based on insect behaviors, Charnov [4] proposed two classical models for foraging behaviors based on foraging behaviors, both of which are quantitatively formulated and are highly sensitive to experimental verifications; they are, optimal diet menu model (or optimal prey menu model) and optimal patch use model (or optimal patch stay time model). Both of these two models are organized based on an assumption that rational decision makers adopt the optimization strategy, so that subjective gain rate (in the long term) should be maximized after each microscopic actions. In other words, the theory tried to formulate decisions that

Toshiya Matsushima, Department of Biology, Faculty of Science, Hokkaido University (corresponding author), phone & fax: +81-11-706-3523; e-mail:matusima@mail.sci.hokudai.ac.jp).

subsequently lead the animal to maximize the long-term gain. In both of these models, the point is how do animals have to do with the lost opportunity, the possible gain that was lost by making a choice. No one can take two exclusive options in foraging choices. One takes an option and gives up another. The question is whether the immediate one could give rise to a better consequence than the other, or the lost opportunity.

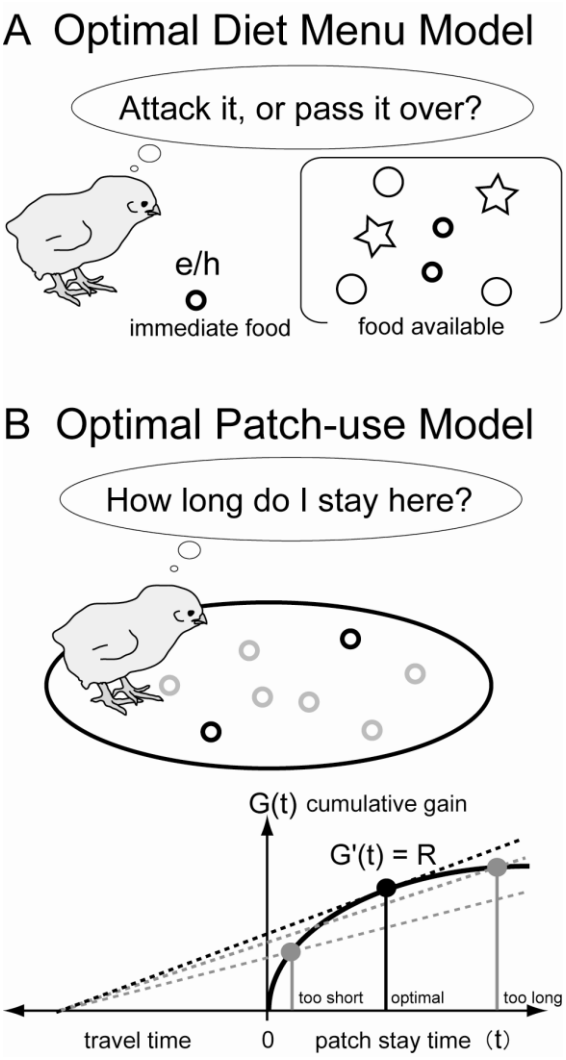

Let us assume a forager in an environment (space), in which food of several different types is randomly scattered. The omniscient forager (single individual in the environment) knows the gain and the handling time for each type of the food. However, the encounter is randomized, and the subject forager does not know what type of food the subject will encounter next, and when. Decision to attack it will give rise to a certain gain at the expense to the lost opportunity, in which the handling time was invested to further searching food, yielding a possibly better food item.

The situation the forager faces in natural condition is actually much more complicated. Food items are often scattered in a patchy fashion. In between food patches, the forager must move, searching for a new patch of food. The point is that the subject must invest locomotor work cost in a situation where no immediate food reward was available. Once the subject encountered a patch, it will stay there and start to collect the food items. Initially, the gain rate will be very high, because the patch is fresh and filled with a certain amount of food. Subsequently, however, the density of food items gradually decrease as the subject forage, making the gain rate (instantaneous gain rate) monotonically decreasing. What if the forager stayed until the patch is exhausted? Does this strategy optimal? The answer is definitely "no." Optimal forager must leave the patch on the way, much early before the food is exhausted. At certain point of time in the stay time, the lost opportunity (the gain available in the next patch) will exceed the immediate gain, making the move-out from the food patch an economically rational action, even though the patch still contains some food. The law of "diminishing return" hold true in animal economics as in ours.

Ecological and ethological studies in insects, birds and fish revealed that these two models are realistic, as they are powerful in predicting some of the foraging behaviors [5]. The molar properties of foraging behaviors follow general rules irrespective of the species, and the rule of long-term gain maximization hold true. What behavioral actions and cognitive processes at the molecular level are thus responsible? Are these molecular phenomena uniquely determined under the optimal strategy?

III. Choice Theory

Birds do not learn aerodynamics in order to fly. Similarly, economical decision makers do not need to learn economics in order to achieve the optimal foraging. The point is whether the action at its microscopic level leads to the long-term gain, what-so-ever the immediate consequence is.

It should be noted that the foragers face a binary choice, namely, choices between "small-but-immediate reward" (immediate food or the food available within reach) and "large-but-delayed food" (lost opportunity). In psychological framework for human behaviors, the former is assumed to be ***impulsive***, while the latter is ***self-control*** [6]. At least in human society, we have a social agreement that the self-control choice is a matured alternative and the impulsive choice is to be hatred violation of rules.

When viewed from the ecological standpoint, however, it does not hold true. Actually, in many situations, foraging animals show a strong level of impulsiveness in their choices, suggesting that the distance (as a spatial factor) or delay (a temporal factor) is a critical factor. Why?

Under natural condition, in contrast to our human society, the immediate food is available for a limited short period of time. The food item may move away, or captured by other conspecific individuals, thus making the value only short-term lasting. Definitely, the prey items are living organisms that must survive to reproduce, so that they develop counter-predatory strategy against the foragers. In such situation, the impulsive choice makers can maximize the

long-term gain rate. It is therefore possible to claim that the adaptive behaviors in choice situation are achieved when the level of impulsiveness is appropriately adjusted, instead of being highly self-controlled.

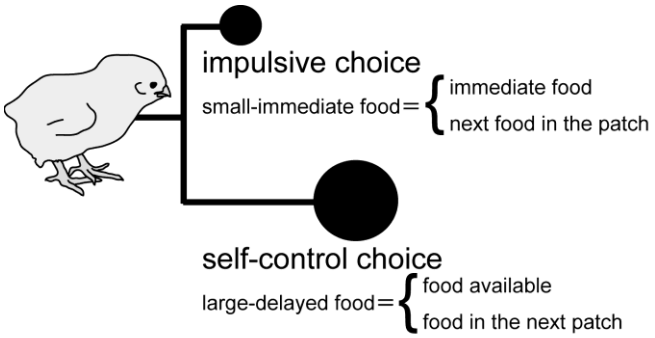

IV. Risk, Impulsiveness, and Serotonin

In 2007, we found the following three lines of cases that stand against the optimality, or its violation.

(1) Risk sensitive choices
(2) Factors controlling impulsiveness
(3) Optimal patch use

Risk-sensitivity depends on contexts

Two feeders were connected via a runway, and subject chick was allowed to gain food from either one of them. One feeder always supplied a certain amount of food (*k* pellets of millet), and another feeder supplied a varying amount (e.g., 0 or 10 pellets) at p=0.5. We measured the equilibrium *k* value, at which chick chose these two feeders equally. Irrespective of the initial *k* value (=1 or 9 on day 1), equilibrium *k* value turned out to converge at around 3 pellets, that was smaller than the expected gain (= 5 pellets) (see the figure below). Chicks avoided risky option. Consequently, the averaged gain rate was not maximized.

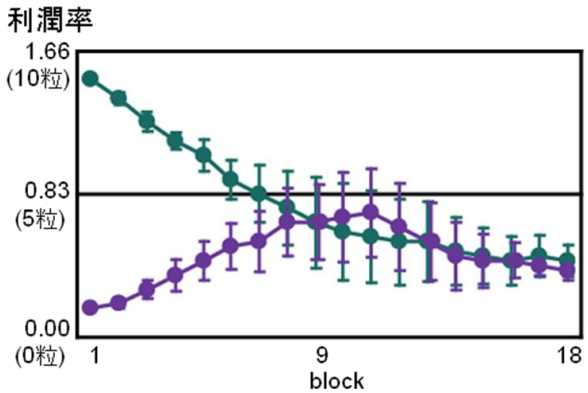

Instead, chicks might behave to avoid the worst case in which they gain no reward (i.e., feeder supplying 0 pellet of food). It is possible to assume that both of the optimality and the max-min principles govern the foraging choices [7].

Factors controlling impulsiveness

Chick loves big food. Chick also loves immediate food. When amount (big food) and proximity (immediate food) contradict, which one should be given a priority? No trivial solution exists. In the framework of psychology, the tendency to stress the proximity is referred to as "impulsive", while that to stress the amount is "self-control." Two factors were revealed in the control of impulsiveness; developmental and causal factors.

Effects of competitive foraging: Chicks must learn to associate between colored cues and the consequent food reward, and they do within a few days of training sessions. Chicks were grouped in three individuals and trained for 3 days (see below); in this condition, food reward supplied was shared by the 3 chicks, and the actor (the one who pecked the bead) was not necessarily rewarded.

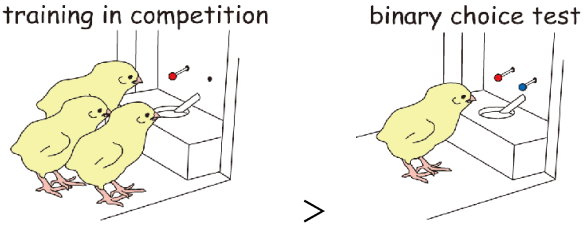

In control chicks (figure not shown), training was accomplished in isolation. Chicks of both groups were tested in isolation. Number of trials in which each chick chose large reward (6 pellets) was plotted against delay (or the time associated with the large reward) (see the graph below). As expected, the choice decreased as the delay increased. However, the dependence was much more skewed in competitive group than in the non-competitive chicks. Colored curves indicate the estimations based on generalized linear model after fitting to logistic function. The model including the factor of competitive/non-competitive yielded the smallest value of AIC, indicating that competitive foraging enhanced impulsive choice. [8]

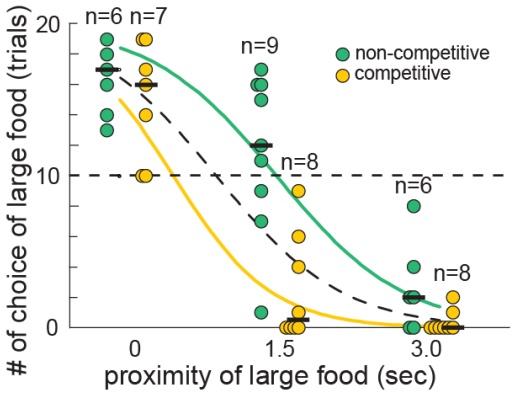

Effects of SSRI: involvement of serotonin: We have so far shown that the lesions to nucleus accumbens in the basal ganglia enhances impulsive choice [9,10]. This nucleus receives massive innervations of serotonergic and dopaminergic projections, similarly to most vertebrates. To

reveal the role of serotonin in the control of impulsiveness, we examined effects of systemic injection of SSRI (serotonin-selective reuptake inhibitor, fluvoxamine or FLV, 20 mg/kgBW) in our standard inter-temporal choice paradigm as described above. In choices between "6 pellets delivered after a 1.5 sec delay" and "1 pellet delivered immediately", number of trials in which 6 pellets food was chosen was plotted; each symbol denotes one individual. As shown in the graph below, the FLV chicks chose the delayed-but-large food significantly more frequently than the vehicle control, indicating that the impulsiveness was suppressed [11].

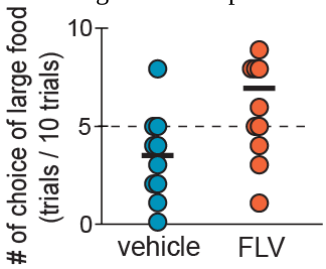

Optimal patch use and perception of time

We tried to reproduce the situation of optimal patch use in a laboratory condition. A feeder supplied food (one pellet of millet at a time), and the interval was computer-controlled so that the gain rate was gradually decreased in a pseudo-exponential manner. Subject chick approached to the feeder, stayed there gaining a series of millet grains, and finally left the feeder. The patch use time (or patch residence time) varied from trial to trial, and the variance was nearly proportionate to the square of the mean value. It is thus assumed that the distribution is best fit to the Poisson process, and the mean value gives rise to the inverse of leave probability, the major parameter of the decision. As predicted from the optimality theory, the mean use time depended on the degree of diminishing return, suggesting that the behavior was controlled pseudo-optimally. Furthermore, SSRI of the same dose significantly elongated the use time when compared with the vehicle control (data not shown), indicating that a common mechanism (probably through modulation of time perception) underlie the impulsive choice and the patch use [12].

V. Conclusion

1. Foraging choice follow evaluation function composed of multiple factors, such as amount, delay, cost and risk of anticipated food reward.
2. Chick behaviors in controlled laboratory conditions consistently violated the optimality, thus that the consequent gain was not maximized.
3. Serotonergic system modulates the time perception, thus that the foraging .decisions deviates from optimality.

References

[1] Pepperberg, I.M. The Alex Studies. Cambridge, Massachusetts: Harvard University Press, 1999.

[2] Clayton, N. & Dickinson, A. Episodic-like memory during cache recovery by scrub jays. Nature, 395, 272-274, 1998.

[3] Emery, H.J. & Clayton, N. Effects of experience and social context on prospective cashing strategies by scrub jays. Nature, 414, 443-446, 2001.

[4] Charnov, E.L. Optimal foraging: the marginal value theorem. Theoretical Population Biology, 9, 129-136, 1976.

[5] Stephens, D.W. & Krebs, J.R. Foraging Theory. Princeton, New Jersey: Princeton University Press. 1986.

[6] Mazur, J.E. Learning and memory (5th ed.). Prentice Hall. 2002.

[7] Kawamori, A., Nishii, E., Matsushima, T. Are chicks optimal foragers? Discounting food value by distance and risk. In: The 30th International Ethological Conference (IEC2007), August 15-23, Halifax, Canada

[8] Amita, H. and Matsushima, T., unpublished.

[9] Izawa, E.-I., Zachar, G., Yanagihara, S., and Matsushima, T. (2003) Localized lesion of caudal part of lobus parolfactorius caused impulsive choice in the domestic chick: evolutionarily conserved function of ventral striatum. *Journal of Neuroscience* 23: 1894-1902.

[10] Aoki, N., Suzuki, R., Izawa, E.-I., Csillag, A., and Matsushima, T. (2006) Localized lesions of the ventral striatum, but not the arcopallium, enhanced impulsiveness in the choice based on anticipated spatial proximity of food rewards. *Behavioural Brain Research*, 168: 1-12.

[11] Amita, H., Matsunami, S., and Matsushima, T., unpublished.

[12] Matsunami, S., and Matsushima, T., unpublished.

An Universal Relation between the Proactive Phase and Harmonicity in Hand Tracking
——The phase of proactivity is determined uniquely by the strength of the rhythmic component in the motion independent of the external stimuli——

Yasuji Sawada, Daisuke Uragami
Tohoku Institute of Technology
sawada@tohtech.ac.jp

1. Importance of Proactive Control

Predictive function of motion is extremely important for the humen and animals to respond in real time to constantly changing external world or to communicate smoothly with the member of the group. As the muscles of the humen and animals cannot move fast in the order of miliseconds as the modern robot does after receiving the signal, it is necessary for them to be equipped with a proactive control system which orders their motor system to act proactively to the external motion.

In fact, the evidence of proactive control was observed experimentally(1) in the visual tracking experiments, and it was proved experimentally that the amount of the positive phase shift is set in the human visual-motion system at the optimum value for which the "dynamical error" be minimized ;the error which the hand commits when an unexpected change in the target motion occurs. This finding, we believe, is one of the important principles for the MOBILIGENCE.

2. The remaining problems in the predictive function for the proactive control

A feedforward mechanism is indispensable for the predictive and proactive control. In the simplest model (1,2), we proposed that the observed experimental proactive behavior is approximately achieved by assuming that the feedforward term is the velocity of the target at δ seconds past time (a delay time in the brain necessary for the visual information processing), multiplied by a factor(proactive factor) which is slightly greater than unity.

The following points, however, remained unexplained by this simple model.

1. The origin of the proactive factor in the model was not understood.
2. The phase of the hand position is retarded with respect to the target in the low frequency region ($f<0.3$Hz) of one-dimensional hand tracking experiments, whereas it precedes even at the lower frequecy region in the model.
3. The hand position is observed to be retarded in a wider frequency region for the hand tracking experiments on a circles, while there is no difference between the one dimennsional motion and circular motion in the model.

These problems led us to be aware of the

following possible facts.

A. Visual system may not be able to measure the velocity of the target, when it is moving with a constant velocity?

B. Velocity information in vision may not be utilized for motional order, for a target moving slowly enough.?

C. In short, the mathematical expression for the speed recognition satisfying these questions is not presently available in spite of its importance.

3. The purpose of the present research

The purpose of the present research is to solve the problems described and to contribute to the understanding of sensory-motor system in brain (MOBILIGENCE) by finding a unversal relation in the complex tracking systems with a variety of modified stimuli.

Real world in which we incessantly respond to is much more complex compared to the hand tracking experiments. We intended in this experiments to make the experimental system more complex by adding colors and sounds, and to ask if there is a universal mechanism in the response to the variety of stimuli. Examples of the questions are following;

1. Is there any effects of different colors on the response characteristics in the tracking?
2. Is there any universality in the response characteristics among the results for the different colors?
3. Is there any effects in the response characteristics when the subject hears audio-stimuli during tracking.
4. Is there any universality in the results in the absence or in the presence of variety of audio-stimuli.

4. Experimentals

The subjects were asked to track a target by a mouse for 30sec which moves with a constant speed in a circle (6.5cm in diameter) on a PC board as accurate as possible. The position of the curser representing the hand of the subject is recorded every 20msec. and analysed. The power spectrum of the velocity and the distribution of the relative phase difference of the hand position with respect to the target position were averaged for 20 runs for each conditions as follows;

Experiment 1　with different colors;

1. colors of the target and the cursor; red, blue, black, white

2. speed of the target; 0.5Hz

Experiment 2　with audio-stimuli

1. short acoustic stimuli (800Hz and 10msec duration) when the target crosses either the horizontal line or vertical line.
2. The rotation frequency of the target ;0.1Hz, 0.2Hz, 0.3Hz, 0.4Hz, 0.5Hz, 0.6Hz

5. Results

5-1、Effect of colors

(5-1-1) An example of power spectra of the hand velocity (Fig.1)

(5-1-2) Strength of the rhythmic component (2f) (Fig.2)

(5-1-3) Mean value of the phase difference

(Fig.3)

(5-1-4) Correlation between the strength of the rhythmic component and the mean phase difference (Fig.4)

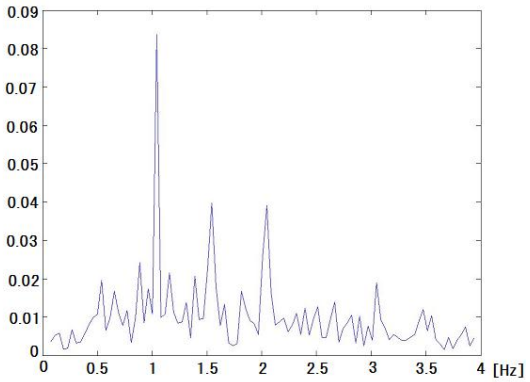

Fig.1. An example of the power spectum of the hand velocity

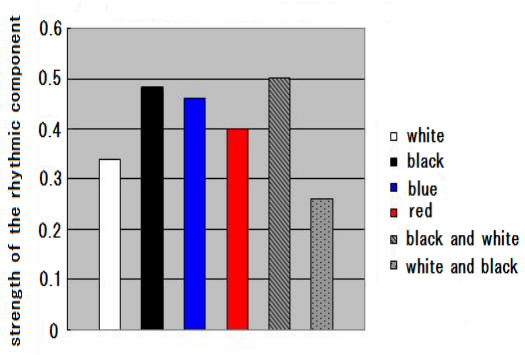

Fig.2. The strength of the rhythmic component for a variety of color combination for the target and the cursor

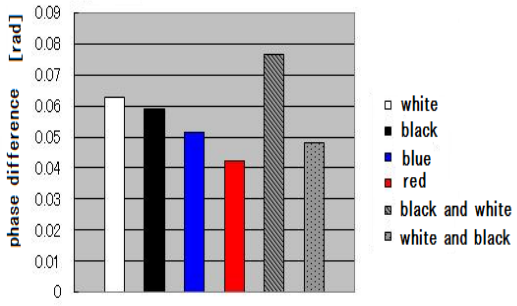

Fig.3 . The phase difference of the hand with respect to the target for a variety of color combination

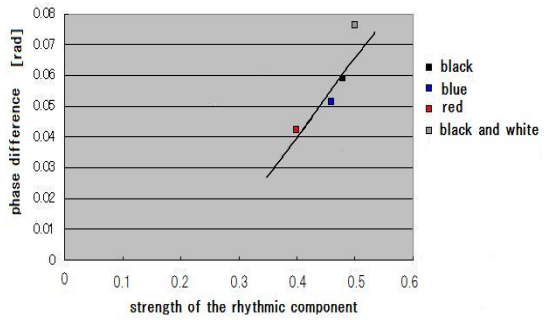

Fig.4. The correlation between the strength of the rhythmic component and the phase difference between the target and the cursor

5-2, Effect of audio-stimuli

(5-2-1)Power spectrum of the hand velocity without and with acoustic stimuli at horizontal cross-points (Fig.5)

(5-2-2)Correlation between the strength of the rhythmic component and the mean phase difference (Fig.6)

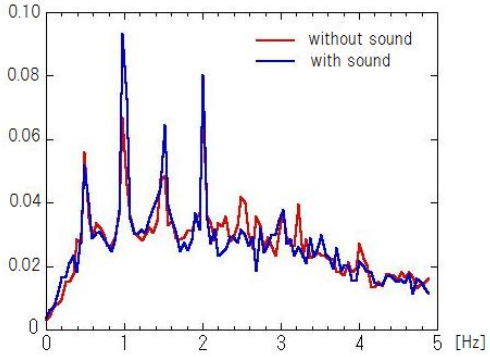

Fig.5, An example of the power spectrum with and without audio stimuli. Red curve is without stimuli and the blue line is with stimuli at the cross point with the horizontal line.

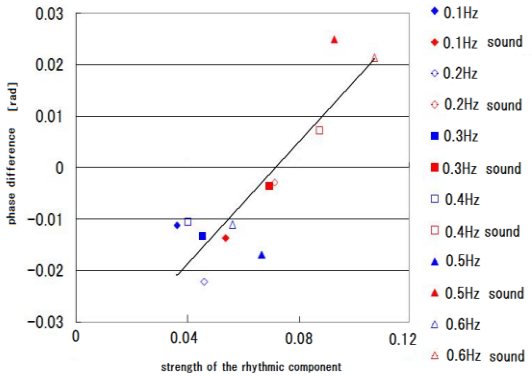

Fig.6. Correlation between the strength of the rhythmic component and the phase difference between the target and the cursor for a variety of acoustic stimuli pattern.

Summary of the experimental results

1.The rythmic component is self-created in the hand motion an the strength varies among the experiments with different stimuli.

2.An universal relation seems to exist between the relative phase difference and the strength of the rhythmic component of the hand velocity.

3. It seems that there is a critical value (about 6%～10% of the velocity of the target)of the amplitude of the rhythmic component in the hand motion only above which the control becomes proactive, independently of the speed, colors or acoustic stimuli in the tracking experiments.

6. Conclusion

1) Proactive control is an important component for MOBILIGENCE in order to respondto the constantly changing environments. We verified in this research that a certain strength of self-produced rhythmic component is necessary for measuring the rate of environmental change and predict future.

2) There is no case found in experiments where proactivity appeared without self-created rhythmic motion in hand

3) There seems to be a universal correlatioj between the relative phase and the amplitude of the rhythmic component in the hand velocity.

4) We have already reported in a past general mobiligence meeting that a similar relation exists between the quality of the communication(velocity correlation) and the rythmic component of the velocity in the mutual tracking experiments. At present we just comment that interestingly the critical value for good communication seems to be lower than 6%. We are going to verify this relation in the coming year.

5) We have clarified that the rhythmic component of certain strength is necessary for the proactive control. However, we have not clarified how the rhythmic component is created and how it is developed. It will also be studied in the coming year.

Reference

1） ”Human hand moves proactively to the external stimulus; An evolutional strategy for minimizing transient error”, F.Ishida and Y.Sawada, Physical Review Letters, 96, 168105(2004)

2)”Semi-analytical transient solution of a delayed differential equation and its application to the tracking motion in the sensory-motor system”, F.Ishida and Y.Sawada, Physical Review E 75, 9,12901(2007)

Classification abilities of Object Shape by A Finger and Perception of Movement at A Human Finger by Vibratory Stimulation

Sumiaki ICHIKAWA [*1] and Fumio HARA [*2]

*1 Tokyo University of Science, Suwa *2 Tokyo University of Science

1. Introductions

It is anatomically said that somatosensor consists of two parts; one is the cutaneous sensation of tactile sense and the other is the deep sensation of postural sense. In general, a body image such as postural sense will be vanished in keeping quiet on a bed rest, although, on slightly moving the body the body image will be got in very clear soon. To percept the object shape by hands, it also needs body movement such as grasping action by finger. These will give a suggestion that there are close relationship between the generation of somatosensor and the integration of cutaneous sensation and deep sensation.

To investigate a mechanism of somatosensor system in human body, physiology has been progressing to clarify the ascending pathway from cutaneous receptors or muscular receptors into the brain, on the other hand, it is difficult to recognize the information process in the neural system because it is very hard to observe the whole stimulus signals in living body. Investigations with robot body will give good results to clarify the mechanisms in the neural system because whole data in the robot body is able to be obtained easily.

We think that the quick perception and the quick response for the surrounding environment in neural system are the significant factors to behave flexible and adaptable ability in the real world. To clarify the mechanism of the flexible and adaptable behaviors, we focus on the tactile sensing of a finger, which needs to integrate numerous stimulus signals distributed on the finger skin, and we propose the rational method which reduces the amount of tactile information to classify the object shape and we investigate the classification ability of the method through the experiments with robot finger.

The proposed method is that focusing on a stimulated receptor on the finger skin which had been contacted with an object grasped by the finger, the statuses of the neighbor stimulations to the contacted receptor forms a specific pattern. In addition to that, the statistical feature of the frequency by the specific patterns also forms a specific pattern corresponding to the grasped object. Therefore, the statistical specific pattern can identify the shape of the object grasped by a finger. The proposed method has an advantageous character that enables drastic reduction of the amount of data obtained by the tactile sensors to discount the position information of the stimulus signal on the skin.

Firstly, this paper reports that validation of generalization in the proposed method applying to the classification of the object shapes grasped by the robot finger. Secondly, to draw a comparison between the proposed method in a robot finger and the nature in a human finger, the experiments to evaluate the classification ability with human finger were carried out. This paper reports about the results. Finally, to be grounded in the idea that the body image is generated through the integration with cutaneous sensation and deep sensation, an experiment for the perception of movement in a human finger was carried out. The experiment is stimulating a tendon of a finger by vibration excitement on back of the hand without actual movement of the finger. The experiment was carried out under certain contacting conditions of the finger and postural conditions of the arm. This paper reports the results.

2. Generalization capability on the perception of object shape

As a fundamental experiment, classification of round objects with various diameters was carried out by a robot finger. Target round objects have 6 diameters, ϕ = 50, 100, 150, 200, 250, 300. Here, these set were called '*fundamental 6 objects*'. Grasping experiments were carried out in 10 times in each object. Applying the statistical analysis to the obtained data in the experiments the characteristic pattern were extracted, which was corresponding to the contacting situations on the skin. Fig. 1 shows the result of the classification for the diameter size for the fundamental 6 objects. The classification accuracy counted with 4 characteristic patterns, that is, 4-dimensional feature space, was 81.7%. In the larger number of the dimension, the accuracy was improved more than. It was leading to 100% in the case of over 9 dimensions.

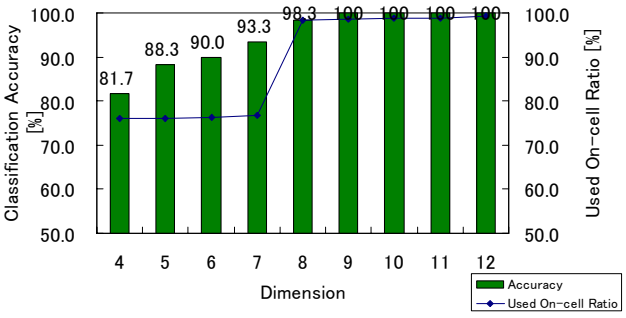

Fig. 1 classification of diameter size for fundamental 6 objects

In the next experiment, another 6 objects were arranged, which have 6 diameters, ϕ = 100, 110, 120, 130, 140, 150. At first, the classification for the new 6 objects was done to use the identical characteristic patterns in the case of the fundamental 6 object. Fig. 2 shows the results of the

classification accuracy. It was similarity in both cases that the accuracy was larger than 90% in larger dimension order, over 7th dimension. On the other hand, in the smaller dimension order, especially in the 4th and 5th dimension, the accuracy was in lower.

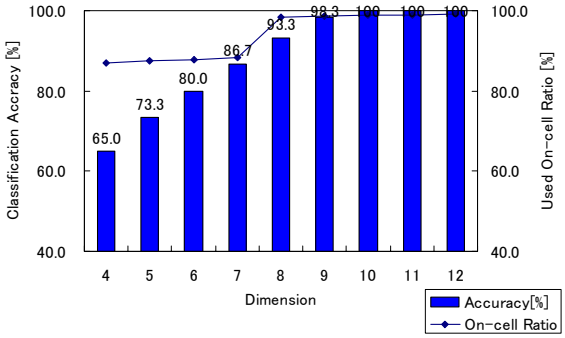

Fig. 2 Classification accuracy of diameter size using the characteristic patterns in the fundamental 6 objects

Next, the dimensional feature space was reconstructed from the new characteristic patterns to apply again the statistical analysis for the new 6 objects. The classification accuracy was shown in Fig. 3. These results were taken through the reevaluation with the new dimensional feature space. In Fig. 3, the both results with the previous feature space and with the new feature space were shown. This figure shows that in the case of new 6 objects the accuracy also higher even in the case of 4-dimensional feature space, because of reevaluation for the characteristic patterns. They show a certain trend that the generalization ability of a feature space is limited to low performance in the case of smaller dimensional feature space.

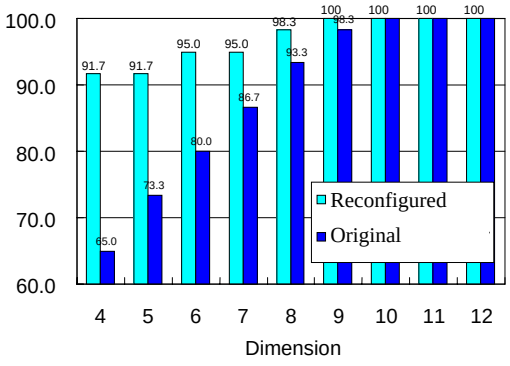

Fig. 3 Classification accuracy with reconfigured feature space

3. Classification ability in human finger

3.1. Experiment for classification of diameter size

6 objects, N1～N6, which has different diameter in each, were arranged. The objects were made of MC-nylon and have an identical weight each other. The specifications in the size of the object are shown in Table 1. The objects are grasped by the index finger.

Table 1 Specifications of round object

	diameter[mm]	differentia[mm]		weight[g]
N1	25.5	2		14.9
N2	27.5		3	14.8
N3	30.5	2		14.9
N4	32.5		3	14.9
N5	35.5	2		14.9
N6	37.5			14.9

The subjects were 10 persons, who tried to learn the 6 sizes of the round shape through their grasping for 1 minutes, in advance. The subjects, who shut their eyes, answered the size of an object which was handed on their finger in random order. The duration of the grasping and holding was in 1 second and in 5 seconds.

Table 2 shows the experimental results. To figure out a sum in raw the frequency is 10, which is the number of the subjects. In both cases of the smallest diameter N1 and the largest diameter N6, the percentages of correct answers were higher than that of the other cases. In the other cases the percentages of the correct anser were almost a half. Therefore, the whole percentage was around 60%. Almost all the incorrect answers were within the neighbors of the correct answers such as answer N2 or N4 in incorrect to the answer N3 in correct. The duration of grasping and holding had very small effect to raise the percentages.

Table 2 Classification of the diameter size

a) 1 second(Total: 62%)

ab1	N1	N2	N3	N4	N5	N6
N1	9	1				
N2	4	4	2			
N3	1	3	5	1		
N4			4	5	1	
N5				2	6	2
N6			1		1	8

b) 5 seconds (Total: 67%)

ab5	N1	N2	N3	N4	N5	N6
N1	9	1				
N2	6	4				
N3		3	5	2		
N4			3	7		
N5				1	7	2
N6					2	8

3.2. Classification of polygonal shape

The 11 target objects which have polygonal shape between 3rd and 24th were arranged with corresponding to the size of a human finger, which is corresponding to the case of using a robot finger. The subjects were 10 persons, who tried to learn the shapes of the 11 objects within 3 minutes, in advance. Note that, the cases between the 3rd polygonal shape S3 and the 6th that S6 have two grasping styles; one is a side of the polygon contacts to the middle phalanx joint of a finger, the other is a vertex of the polygon contacts to the middle phalanx joint.

The duration of the grasping and holding a target was 1 second in the case, and 5 seconds in the other case, as well as the case of classification experiments for the diameter size by human. The target objects were exposed on a finger of the subjects in random order. The results were that the percentage of correct answer in 1 second was 52% and that in 5 seconds was 47%. There was also little effect of the duration to the percentages. Instead, it was depraved in the case of long duration, because

indecision may be occurred in the persons. Table 3 shows the results of the case in 1 second.

Table 3 Classification ability for polygonal shape by human finger (Total: 52%)

ab1	S3-1	S3-2	S4-1	S4-2	S5-1	S5-2	S6-1	S6-2	S8	S10	S12	S15	S18	S20	S24
S3−1	10														
S3−2		10													
S4−1			8		2										
S4−2	1			9											
S5−1			1		2		6		1						
S5−2			1			7	2								
S6−1					1		7		2						
S6−2					2			4	4						
S8									6	4					
S10									2	4	2		1		1
S12										4	2	2	1	1	
S15										1	2	2	4	1	
S18										2	3	1	4		
S20												2	3	1	4
S24											1	2	1	4	2

Table 4 Classification ability for polygonal shape by robot finger with 10-dimensional feature space (Total: 79%)

	S3-1	S3-2	S4	S5-1	S5-2	S6	S8	S10	S12	S15	S18	S20	S24
S3−1	8						2						
S3−2		10											
S4			10										
S5−1				10									
S5−2					10								
S6						10							
S8							10						
S10							1	9					
S12							1	1	7	1			
S15								5		5			
S18							1	3		2	4		
S20							1	1			1	6	1
S24								2		3		1	4

Table 4 shows the results in the case of robot finger. The dimensional feature space consists of 10 dimensions. The trend to descend the classification ability was shown in larger polygonal number.

It was same trend between human and robot that the false recognition was prone to be raised in increasing the polygonal number. The recognition ability of robot finger using 10-dimensional feature space was 70%, which was higher ability, on the other hand, there was difference between human and robot in the distribution in false recognition for larger polygonal number; in the robot finger, the false were concentrated on several specific shape such as S-10, on the other hand, in the human finger, the false were concentrated on the neighbor shape of the correct shape. Additional investigation about the classification ability of the robot finger with lower dimensional feature space will be expected in the near future work.

4. Perception of movement in vibration stimulus on tendon

The investigation clarifying the characteristics of the integration for somatosensor information through perception of movement was carried out. We focused on a hand on a table. Conditions, such as postural condition of the wrist, contacting condition between the finger and the table, and movement condition of the finger, will be integrated, and they will affect the perception of movement. To investigate the somatosensor mechanism, we gave regulated conditions among the conditions and the subjects answered the feelings about the perception of movement in each regulated conditions.

Sensory input from the tendon was given by vibration stimulation on the tendon outside the back of hand, thus, the subjects can feel the perception of movement of their finger without actual movement.

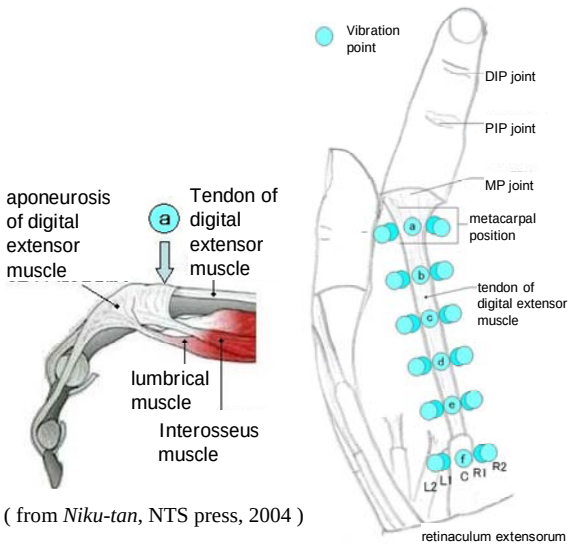

(from *Niku-tan*, NTS press, 2004)

a) Anatomical chart of finger b) Vibration position

Fig. 4 anatomical chart and vibration position

Fig. 4 shows anatomical chart about skeletons, muscles and tendons of the index finger of human. Circular points in the figure were the positions where the vibration stimulation was given. The vibration was 60 Hz in frequency for 10 seconds. The vibration was generated by commercially available electric toothbrush (*CREST Spinbrush Prowhite*). The subjects took in relax without muscle stress and close their eyes.

In the case of feeling the perception of movement it was in 2 seconds, or it was felt by 10 seconds at least. About the case of no feeling over 10 seconds, it was the case of '*none*' of the perception of movement. In the case of feeling the perception, the subjects answered the position among the joints on their finger, that is, *DIP, PIP or MP* joints, and answered the direction of the perception of movement, that is, *extension* or *bending*. As a preliminary experiment adding vibration stimulus on the tendon from back of the hand, the results was that the perception of movement was frequently come up on the column C. Therefore, in the following experiments the vibration positions were point 'a' and point 'c' on the column C to reduce the number of trials for the experiments.

4.1. Perception of movement with position of wrist

From viewpoint of the neurophysiology adding vibration stimulus on the tendon will be corresponding to that tensional force on a muscle was occurred to act the

muscle. To take into account the multiple conditions, such as the condition of muscles position and the condition of cutaneous contact on an object, the experimental conditions were arranged; that is, a hand was on a desk with or without contact of fingertip and contacting with arm or wrist; the position of a wrist was in bending or extension; a hand was at waist height or at shoulder height. The position conditions were illustrated in Fig. 5. Condition 6 and 7 were corresponding to the condition 3 and 4 except the height position.

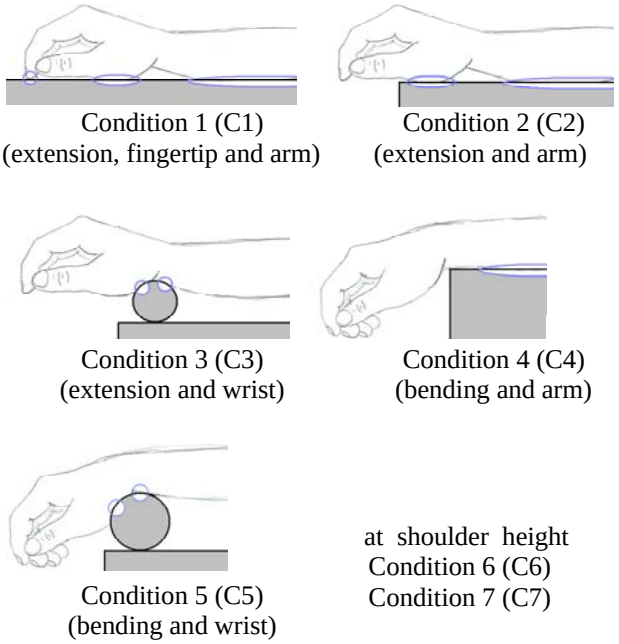

Fig. 5 Conditions of hand and wrist

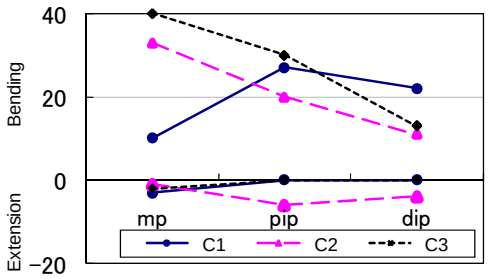

Fig. 6 perception of movement in contacting condition (Condition 1, 2, 3)

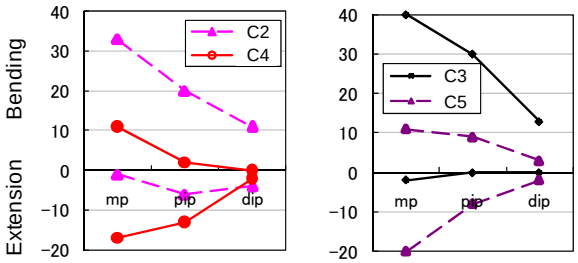

a) arm contacting (Condition 2, 4)

b) wrist contacting (Condition 3,5)

Fig. 7 Perception of movement in wrist condition

Fig. 6 and Fig. 7 show the frequency of the perception of movement, which is counted up about the direction of the movement in each joint and grouped with the same conditions. The subjects were 6 persons, who tried several experiments; the total number of trials was 60 times in a condition. The frequencies of *bending* were shown in the positive direction in the figure, on the other hand, the frequencies of *extension* were shown in the negative direction. The result showed a trend that the frequency at MP joint was larger than that of other joints. But, there was an exceptional case. In the condition 1 of Fig. 6 showed different trend at MP joint. Only in this case the frequency was small at MP joint. It will show the contacting condition of the fingertip influenced on the perception of movement.

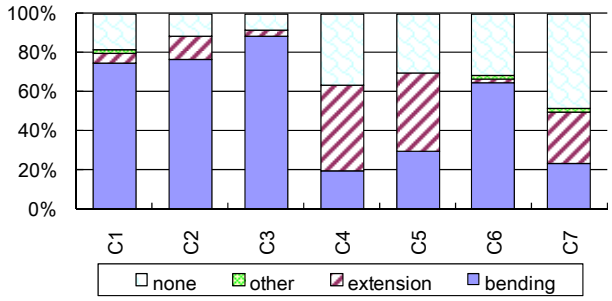

Fig. 8 the ratio of the direction in the perception of movement

Fig. 8 showed the ratio of the direction in the perception of movement in each condition. A bar was build up by frequency among '*bending*', '*extension*', '*other*' and '*none*', in bottom up order. The index 'other' includes the other cases except the '*bending*' and the '*extension*', although, it was few case. Especially in the case which the wrist was in *bending*, it showed that the frequency of a perception, which the finger had moved in *extension*, was high ratio.

5. Summaries

The generalization capability on the perception of object shapes by a robot finger was investigated. In the low dimensional feature space such as 4^{th} or 5^{th}, the generalization capability tends to be low, that is, the high-capability of the perception was strongly shown on the objects that were used in the statistical analysis to generate the dimensional feature space.

To investigate the classification accuracy of the object shapes by human perception by finger, it showed similarities in both cases that the classification capabilities was high within the smaller polygonal number of the polygonal shape, on the other hand, it showed the different trend in the false cases of the recognition.

To investigate the integration of somatosensors into the perception of movement, the experiments were carried out. As a result, it was obviously associated with the contact condition of the fingertip and the bending position of the wrist.

Representation of self and other in the parieto-premotor network

Murata A and Ishida H., Department of Physiology, Kinki University School of Medicine

Abstract— **It is well known that parietal cortex is very much concerned with self body representation by integrating visual and somatosensory input. Furthermore, it is claimed that other is represented in the brain with self. Mirror neuron is one example. These neurons represent image of other's behavior on own motor representation. This suggests shared representation of self body and other's body in the brain. In this report, we will show some of parietal bimodal neurons were concerned with other's body, not only self body. Then we also report the results of information analysis of spike frequency of single neurons of area AIP with collaboration of University of Electro-communication.**

I. Introduction

THE body is not separable from action control. Recently, it is claimed that the body representation is also important for the social cognitive function, like communication, imitation, and/or theory of mind. In the last year, we reported that neuronal mechanisms how the brain distinguish own body and other's[1]. On the other hand, self and other are encoded in the brain on the same neuronal bases. For example mirror neurons represent other's visual action on own motor representation[2]. The function of these neurons is considered to be related to action recognition. Existence of mirror neurons suggests that there are some mechanisms for recognition of other's body in the brain. In the imitation of other's action, the mechanisms of matching own body and other's body seems to be necessary. Accordingly, we suggest that the process of corporeal awareness share self and other. In this paper we will report neuronal activity that is related to both self and other bodily consciousness[3].

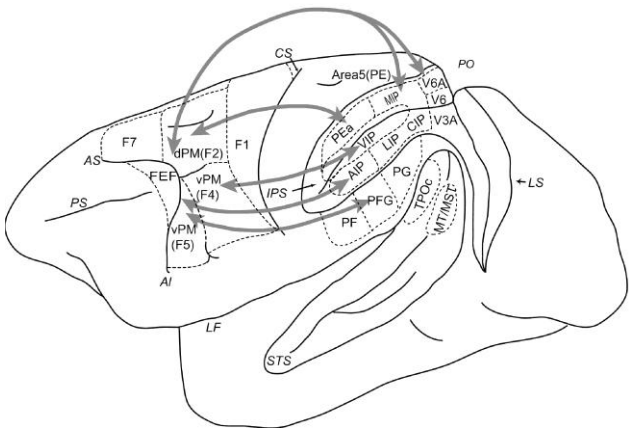

Fig.1 parito-premotor networks
(from IEICE technical Report Murata and Ishida 2006)

Furthermore, the system which is concerned to corporeal awareness share the network with motor control system[4]. Information analysis was adapted to investigate functional properties of each area which were involved in sensory motor control system. In this study, real neuronal spike data of the monkey area AIP was analyzed. The area concerned to precise distal hand movement that the analysis enabled to investigate the spike data in temporal sequence. The study has been done by collaboration with University of Electro-Communications[5, 6].

II. Representation of other's body in the brain

As we reported in the last year, the parietal cortex and premotor cortex are much involved in self body representation. For corporeal awareness, integration of visual-somatosensory is very important[7]. In the parietal association cortex, there are several areas where multimodal neurons are found, for example visual-tactile bimodal neurons. In these areas, properties of area VIP have been well studied[8]. The tactile receptive fields of the neurons are usually located on the face, head or sometimes limbs and the visual receptive fields are in locations congruent with the tactile receptive fields. In many cases, the visual receptive fields are located very close to the body, namely in the peripersonal space. These neurons may encode body parts centered frame of reference.

On the other hand, for the recognition of others action, imitation or communication, representation of other's body is necessary in one's own brain. For moment, it is not clear how the brain represent other's body. Decety et al. suggested that self body and other's body were represented in the shared brain network[1]. Further, it was reported a female subject for whom the observation of another person being touched was experienced as tactile stimulation on the equivalent part of own body[9].

We expect that other's body map in the brain may be influenced by own body map. We studied neuronal activity in area VIP whether these neurons are related to other's body representation[3, 10].

A. Materials and methods

Single neurons in the ventral intraparietal area were recorded from the left hemisphere of one Japanese monkey. The electrode was inserted from the convexity of the inferior parietal cortex, then went inside of the medial or lateral bank of the intraparietal sulcus, The border of VIP was functionally recognized on the basis of distribution of tactile and visual receptive fields (RFs). Neurons in area VIP showed tactile

RFs principally located on the face and visual RFs, limited to the peripersonal space, in register with the tactile ones.

Once a cell was isolated, we tested with a standard battery of tactile and visual stimuli. Somatosensory stimuli consisted of hair bending, touch of the skin, gentle pressure of the tissue, manipulation of the joint. Somatosensory RFs were plotted by repeated presentation of the most effective of these stimuli. Somatosensory responses were tested while the eyes were covered.

Visual stimuli consisted of three-dimensional real objects. Geometrical solids, food and various objects found at hand in the laboratory were used. No obvious differences were observed between these stimuli in determining neuronal responses. A quantitative study of preferences of neurons for different stimuli was not carried out in the present study, however.

In order to investigate the RFs of neurons, stimuli were moved by hand towards the animal from different angles and distance. The procedure was repeated again and again until the borders of the visual RFs were defined. Especially, we were very careful for the extension in the depth of the RFs.

After mapping of the tactile and visual RFs, an experimenter confronted with the monkey. To ensure that bimodal neurons also responded to stimuli within other's peripersonal space, visual stimuli were presented vicinity of the experimenter's body parts which is congruent with the RFs on the monkey's body.

Additionally, when the monkey observed visual stimuli near the experimenter's body parts, the experimenter kept regular distance 120cm from the monkey. The reason of this regulation was to exclude the possibility of a false interpretation that the neuronal response merely due to simple visual response within the visual RFs in the extrapersonal space. Since previous studies suggested that the extension in the depth of visual RFs in VIP was 5cm to 50cm from the surface of body: we set the distance between the monkey and experimenter more than twice of that.

B. Results

We recorded 115 VIP bimodal neurons from one left hemisphere of the monkey. We found that RFs of these neurons were distributed on the face (face tactile + visual neurons: N=91, 79%), or on the limbs (arm/ hand or legs tactile + visual neurons: N=24, 21%). RFs of almost all of these neurons tended to be spatially congruent in the both modalities. For example, a visual RF in the upper left quadrant was often accompanied by a tactile RF of very small part on the left forehead. In addition, the extension of visual RFs was within 50cm from the skin. Two of 115 neurons depths of visual RFs extended beyond the experimenter more than 1.5m then these were discarded.

Of the 113 bimodal neurons, 19(17%) responded to the visual stimuli presented near the experimenter's body parts. Remarkably, visual RFs surround the experimenter's body parts of these neurons corresponded with location of bimodal RFs on the monkey's body parts.

As shown in Fig.2, the neuron showed tactile RFs particularly on the right cheek of the monkey and visual RFs extended for a few dozen cm from the right cheek. Further, when the monkey observed visual stimuli moving toward the experimenter's left cheek, the neuron was particularly activated. This neuron neither responded when stimuli were presented toward the right side of experimenter's cheek nor any other his body parts.

Importantly, visual RFs on the experimenter's body lateralized in a manner of mirror image of visual-tactile RF on the monkey. As in the case of the neuron in Fig.1, the RF on the monkey was on the "right" cheek, then also on the experimenter's "left" side. As a result, 12 of 19 neurons (63%) showed this mirror symmetry correspondence of the RFs.

In addition to this type of RFs, we found other type of distribution of RFs. For example, bimodal RFs located within "left" side of monkey's cheek. The neuron was selectively activated when the monkey observed visual stimuli moving

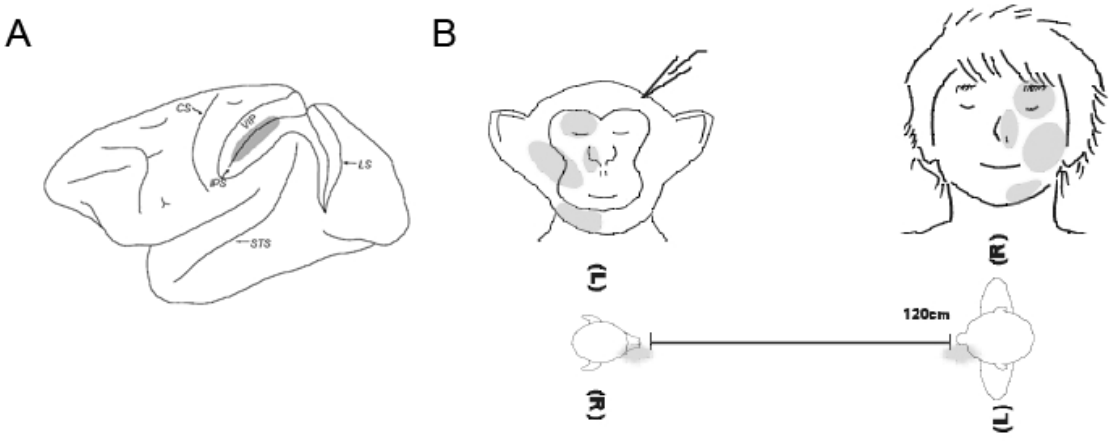

Fig.2 A. lateral view of the brain of the Japanese monkey IPS: intraparietal sullcus, LS: lunate sulacus, VIP: ventral intraparietal area is in the fundus of IPS.
B. One example of visual-tactile bimodal neuron which showed visual-tactile RF on the monkey's right face and visual RF on the experimenter's left face.

toward the experimenter's "left" cheek. In contrast with mirror symmetry correspondence, despite the experimenter confronted with the monkey, location of RFs matched anatomically with the same side of the body each other (left to left cheek). Of 19 neurons, two neurons have this kind of an anatomical correspondence. Of 19 neurons, 5 showed more extended overlap of RFs in the body parts on the monkey and experimenter, not like a regional correspondence described before. For example, RFs of 2 neurons were located on the mandiblae of monkey. On the other hand, the neuron was activated when the monkey observed visual stimuli toward the experimenter's "bilateral" cheek (correspondence of the face and the face). Furthermore, the rest of 3 neurons have RFs onto the monkey's contralateral face, arm, hand and bilateral legs then the neuron was activated when stimuli presented near the one of those body parts of experimenter.

To ensure that visual RFs just anchored on the experimenter's peripersonal space, visual stimuli were moved between the monkey and experimenter (back and forth from in front of the monkey's body to that of the experimenter). As a result neurons only responded when stimuli were within approximately 50cm from the monkey and experimenter's body surface respectively. The neurons did not respond in the intermediate space between the monkey and experimenter. Importantly, the activity was modified only by the position of stimuli, but not by the direction of the movement. These neurons responded both in cases that the stimuli moved from the monkey to the experimenter and vice versa.

To elucidate further reliability of visual RFs on the experimenter's body, we investigated the neuronal responses when the experimenter shifted the sitting position toward the left or right side of the monkey maintaining 1.2m distance. As a result, RFs of these neurons were always on the same body parts. In similar way, when stimuli were presented in the intermediate space between both bodies, the neurons did not respond.

Taken together, activities of these VIP bimodal neurons were independent of position of the experimenter (the other) and may be represented self and others body parts independently from egocentric spatial position.

These results suggest that coding of other's body parts is in the same area that codes own body parts, and a map of self body parts is referred for recognition of other's body. In the humanoid robots, it is a big issue how the system recognizes other's body. In the imitation learning, the system should superimpose other's body onto one's own. Our data will provide important idea for matching system between one's own body and other's.

III. INFORMATION ANALYSIS FOR HAND MANIPULATION RELATED ACTIVITY OF AIP NEURONS

In a previous study, information analysis has been applied to neuronal activity of face neurons in inferior temporal cortex. The study revealed that the neurons encoded global information of the face in early phase of processing and then fine information of the face was conveyed later[11]. Of course this information analysis could be adopted in other all spike data. For example, if it will be applied to the spike data in motor control system, it might be possible to reveal dynamics of intra and/or inter areas in temporal sequence.

In this year, information analysis was applied to actual spike data by collaboration with Sakaguchi's group in University of Electro-Communications[5, 6]. The data was recorded from monkey parietal area AIP that was well known to be related to precise control of distal hand movement. In the recording session, the monkeys were required to manipulate an object with guidance of LED spot (hand manipulation task). The monkey was asked to fixate on the object and then reach and grasp it. The neurons in this area were classified into 5 types according activity for motor component and visual stimuli. Visual-motor neurons showed less activity during manipulation in the dark than in the light. Visual dominant neurons were not active during manipulation in the dark. Motor dominant neurons did not show any difference of activity in the dark and the light. The neurons with visual input were also subdivided into object type which showed visual response to the objects, and non-object type which did not show[12]. The activity of these neurons also changed with 6 different objects, plate, ring, cube, cylinder, cone and sphere.

The information analysis was applied to spike data of these hand manipulation neurons. Mutual information (MI) was calculated between spike frequency of single neurons and various combinations among 6objects. Analysis for each type of neurons was done separately. The calculation was performed with a following function in each 50 ms during task trials.

$$I(S;R) = H(S) - H(S \mid R) = \sum_{s} -p(s)\log p(s) - \langle \sum_{s} -p(s \mid r)\log p(s \mid r) \rangle_{r} \quad (1)$$

In this function, *H* indicates entropy. *S* and R are sets of the objects and number of spikes, respectively. The conditional entropy $H(S \mid R)$ is the uncertainty about *S* after observing spikes. In this study, the analyzed spikes were of the neurons which were strongly responded to the one of the 6 objects in order to see variance with the combination of the objects. Then relationship between the timing of peak and the task phase (i.e., fixation of the object, reaching , and grasping) was examined in each types of neurons[6].

As the results, in some of visual-motor neurons object type, MI showed peak value in the fixation period with rough categorization of the objects while in reaching or grasping phase with finer clustering of the object[6]. In motor dominant neurons, MI showed peak value in the phase of preshaping before grasping the object[5]. AIP neurons conveyed different information in the different phase, and timing of peak was different dependent on type of neurons. This suggests that MI changes with temporal sequence in the task because AIP neurons received visual and/or motor information from other areas in the different phase of the hand manipulation task.

As in the following figure, AIP has strong connection with F5 in the ventral premotor cortex. The previous study suggested that AIP received visual information about 3D objects and this information was sent to F5, then appropriate motor pattern was selected in F5, while the copy of this motor information returned to AIP in which matching with visual information occurred. It is important to analyze spike data in this network using MI, since the analysis may reveal stream of information in the temporal sequence. This is not only useful to reveal dynamics in the cortical motor control system, but also functional model of mirror neuron system and body recognition system. Because motor control system are shared with these systems.

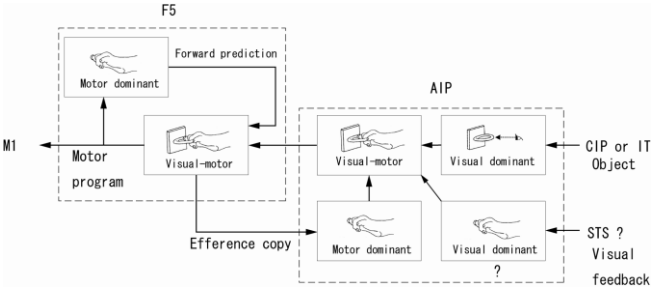

ACKNOWLEDGMENT

The MI analysis mainly has been done by Mr. Takashi Shimizu and Dr. Fumihiko Ishida with leadership of Prof. Yutaka Sakaguchi in University of Electro-Communications. We gratefully acknowledge the collaboration.

REFERENCES

[1]Decety, J. and Sommerville, J.A., Shared representations between self and other: a social cognitive neuroscience view. Trends Cogn Sci, 2003. **7**(12): p. 527-33.

[2]Rizzolatti, G., Fadiga, L., Gallese, V., and Fogassi, L., Premotor cortex and the recognition of motor actions. Brain Res Cogn Brain Res, 1996. **3**(2): p. 131-41.

[3]Ishida, H. and Murata, A. Representation of others□f body parts by visuo-tactile bimodal neuron in area VIP. in *2nd International symposium on the Mobiligence in Awaji 2007*. 2007. Awaji.

[4]Murata, A. and Ishida, H., Representaion of bodily self in the multimodal parieto-premotor network, in *Representaion and brain*, S. Funahashi, Editor. 2007, Springer: Tokyo, Berlin, Heidelberg, New York. p. 151-176.

[5]Shimizu, T., Ishida, F., Murata, A., and Sakaguchi, Y. Information analysis of monkey AIP neurons during hand manipulation task. in *Neuro2007*. 2007. 横浜.

[6]Shimizu, T., Ishida, F., Murata, A., and Sakaguchi, Y., Information analysis of monkey AIP neurons during hand manipulation task. Thecnical report of IEICE, 2007. **107**(157): p. 1-6.

[7]Jeannerod, M., The mechanism of self-recognition in humans. Behav Brain Res, 2003. **142**(1-2): p. 1-15.

[8]Colby, C.L., Duhamel, J.R., and Goldberg, M.E., Ventral intraparietal area of the macaque: anatomic location and visual response properties. J Neurophysiol, 1993. **69**(3): p. 902-14.

[9]Blakemore, S.J., Bristow, D., Bird, G., Frith, C., and Ward, J., Somatosensory activations during the observation of touch and a case of vision-touch synaesthesia. Brain, 2005. **128**(Pt 7): p. 1571-83.

[10]石田裕昭 村田哲, サル頭頂葉の視覚－触覚バイモーダルニューロンによる他者感覚. 第１９回自律分散システム・シンポジウム資料, 2007: p. 1-4.

[11]Sugase, Y., Yamane, S., Ueno, S., and Kawano, K., Global and fine information coded by single neurons in the temporal visual cortex. Nature, 1999. **400**(6747): p. 869-73.

[12]Murata, A., Gallese, V., Luppino, G., Kaseda, M., and Sakata, H., Selectivity for the shape, size, and orientation of objects for grasping in neurons of monkey parietal area AIP. J Neurophysiol, 2000. **83**(5): p. 2580-601.

Constructive Approach to Understanding the Active Learning Process of Adaptation within a Given Task Environment

Hiroaki Arie, Shigeki Sugano
Science & Engineering, Waseda University

Jun Tani
RIKEN Brain Science Institute

I. Introduction

We humans learn our behavior skills through repetitions of own behavior experiences. We learn to manipulate object, to use tools and to navigate to desired location.

The compositionality is an essential issue in considering human skilled behaviors. If the mission of a particular robot is just to repeat the same goal-directed behavior, all the things to do for the robot is to acquire a single motor scheme to generate the target behavior. However, it will be not the case if robots or humans are required to adapt to various goals under diverse situations. In this case, the motor schemes should be organized in a compositional manner such that compositions of various motor schemes can generate diverse actions adaptively corresponding to required goals. For example, an attempt of drinking a cup of water might be decomposed into multiple motor schemes such as reaching to a cup, grasping the cup and moving the cup toward own mouth. Each motor scheme can be utilized as a component for other goal-directed actions as like reaching to a cup can do for the goal of clearing it away.

This idea of decomposition of whole behaviors into sequences of reusable primitives are originally considered by [1] as the motor schemata theory. However, when we think about the behavior primitives, they should not be treated as concrete objects. Instead, each behavior primitive should be acquired as enough "elastic" such that it can be utilized flexibly in various situations. For example, a behavior primitive of grasping an object should be utilized enough adaptively to variations of the object positions as well as their shapes. This requires generalization in learning of the skills. In addition, the context-dependent aspects in generating motor act sequences are important, which was metaphorically termed as "kinetic melody" by [2]. For example, exact motor trajectories of grasping a cup should be affected by next motor act to follow them as well as the entire goals of whether to drink a cup of water or to clean off the cup. The whole motor behaviors should be generated fluently by capturing the context-dependent nature of intended action goals. Then, the essential question here is that how this sort of "organic" compositionality can be achieved through learning processes.

In the brain science perspective, we speculate that such "organic" compositional structures responsible for generating skilled behaviors might be acquired in inferior parietal lobe (IPL) through the repeated sensory-motor experiences. Our ideas have been inspired by [3] who suggested that the world models are firstly stored in parietal cortex and then they are consolidated into cerebellum. Conventionally, parietal cortex has been viewed as a core cite to associate and integrate the multi-modality of the sensory inputs [4], [5]. However, the neuropsychological studies investigating various apraxia cases, including ideomotor apraxia and ideational apraxia [6], [7], have suggested that IPL should be also an essential site to represent a class of behavior skills, especially related to object manipulations. We speculate that this region might function as internal models by having certain anticipatory mechanisms for coming sensory inputs as related to motor acts. Furthermore, it has been speculated that IPL might function both for generating and recognizing the goal-directed behaviors [8] by having dense interactions with cells in ventral premotor (PMv) which are known as mirror neurons [9].

Our group have investiagted how the "organic" compositionality can be attained in modeling of IPL and PMv interactions for several years. One of our original neural network models is so-called the recurrent neural network with parametric biases (RNNPB)[10], [11]. In this modeling, a recurrent neural network (RNN) learns various forward models of motor-related sensory inputs sequences as parameterized by the parametric biases (PBs). This means that the forward dynamics of the RNN can be modulated by values of the PBs that function as bifurcation parameters of the dynamics.

The PBs can be used to encode the goal information

both for behavior generation by means of prediction and its recognition by postdiction. Once the goal is set by means of setting a specific value for the PBs, the forward model autonomously generates prediction of the sensory inputs sequence reaching to the goal. In this model, we assume that the PB is manipulated in PMv and that the forward model predicts sensory inputs sequences in IPL. The prediction of the sensory image includes that of proprioception regarding to posutures of limbs. We assume that this prediction for the time-development for the posture might be sent to M1 as well as cerebellum where exact motor commands to achieve the posture changes might be obtained by inverse models.

The goals or intentions by others can be recognized by making match between the sensory sequence imaginary generated by the forward model and the observed actual one [10], [12]. The PB value of minimizing the error in this match is inversely computed through iterative search. The PB value obtained by this postdiction scheme represents the goal or the intention for the observed behavior.

Recent years we reported further extensions of our models. We have shown that on-going behavior can be adapted to the contextual changes in the environment in real time by simultaneously conducting the prediction and the postdiction interacively for modulating the PB value dynamically [13]. We also found that different goal-directed behaviors can be embedded in a single continuous-time recurrent neural network with utilizing its initial sensitivity characteristics of which mechanism seems to be much simpler than the parameter bifurcation mechanism of the PB [14]. Furthermore, we found that the forward model can be scaled significantly by self-organizing level structures with having different time-constant dynamics in the networks [15]. Our robotics experiments showed that behavior primitives are self-organized in the lower level dynamics with fast time-constant and combinational manipulations of them are learned in the higher one with slower time constsnt. The analysis of these experiments indicated that the composition mechanism attained in the level-structured dynamics is “organic” in a sense that it captures generalization through learning of various sensory-motor experiences as well as contextual natures of the goal-directed skilled behaviors.

Another new challenge of this year was to introduce the exploration-based learning paradigm to acquisitions of behavior skills, which turns to be the main focus in the following sections in the current report. It is widely assumed that basel gangulia (BG) plays importat roles for the exploration-based learning [16]. Although BG seems to involve deeply with the on-line learning mechanisms assumed in reinforcemnt learning scheme, it is not well known that whether the skills consolidated after long time period still stay in BG or they are transformed to other cortex areas. From the reviews of neuropsychological studies [6], [7], [2], [17], it is natural to consider that behavior skills especially for manipulating objects and tools are initially acquired in BG through the on-line exploration and then they are consolidated in IPL after the long run through incremental off-line learning during sleep. It is furthermore assumed that the behavior skills might be consolidated in IPL with association of their goal information, presumably represented in PMv, as have been discussed previously. Based on these assumptions on human brain mechanisms, the current report introduces our novel models that could explain how exploration-based experiences can be transformed to structured skills through the memory consolidation processes.

Before closing this introduction section, we briefly describe our motivation to build physical robot platforms for our experiments. Main reason to conduct robot experiments is to show that the proposed model can work in more realistic setting compared to simulation ones. Although the real physical experiments have limitations in searching for adequate parameter values through iterative experiments, the fact that the robot actually works inversely would prove that the proposed model is robust enough to function with only limited amounts of the parameter adjustments. In order to conduct the long time exploration-based learning experiments with a physical robot, there was necessity to build a durable robot. Therefore, we built a novel robot with a tendon-based actuation mechanism which can afford elasticity at each joint of the robot. The following sections will describe, our brain-inspired model for the exploration-based learning of goal-directed behavior skills, its implementation in neural network models and their early stage experiments both in simulations and with our developed real robot.

II. Biological model

This section describes more details of our biological brain model. The model basically consisits of two parts (see Figure1). One part is PMv-IPL-M1 network that works as a mirror system both to generate and recognize goal-directed skilled behaviors. The cases with supervised training of this network have been

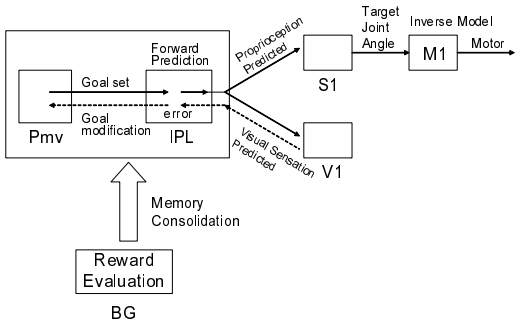

Fig. 1. brain model

reported in [12], [13], [14]. In the generation pathway, PMv provides the goal information to the forward model assumed in IPL by means of setting its internal state (it could correspond to PB or context state in RNN implementation). The prediction of proprioception inputs are sent to primary sensor (S1) and its conversion to target joint angles are further sent to M1 as well as cerebellum to compute corresponding motor commands. At the same time, the prediction of visual sensation is computed in IPL and it is compared with the real visual sensation in early vision area including v1. If the error is generated, the error is fed-back to PMv to modify the internal state in direction of minimising error. In this way, the goals of current behaviors can be adapted to contextual changes in environment [13].

The other part is BG that evaluates the cumulative reward of on-going behavior trials. In our model, it is assumed that BG memorizes only sensory-motor sequence patterns with good cumulative rewards in its short-term memory. The memorized patterns are later transfered to PMv-IPL network as teaching patterns to train the network in off-line. It is expected that multiple behavior schemes of gaining the higher cumulative rewards will be consolidated in PMv-IPL network through the iterative trials of the robot.

Currently, this whole model is still under construction The current report describes parts of this global picture, namely BG-IPL interactions and IPL-M1 interactions.k For the study of BG-IPL interactions, we investigate a reinforcement learning scheme which realize the memory consolidation of well-rewarded behavior patterns in simulations. For the study of IPL-M1 interactions, we examine how the forward model in IPL and the inverse model in M1 or cerebellum can function cooperatively though their learning.

III. Architecture

We utilized two neural networks as shown in figure 2. One is a Continuous Time Recurrent Nenral Network (CTRNN) which receives joint angles of the robot arm and sends target rotational velocity of each joints for lower network. The lower network, which is Recurrent Neural Network (RNN), recieves target signals and calculates joint torque which realize the target joint motion. Then a random noise signal, that is needed for reinforcement learning of top network, is added to the output of the lower network.

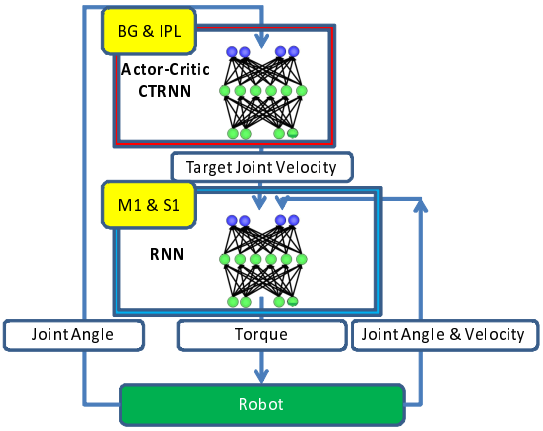

Fig. 2. implementation

A. BG-IPL Model

We utilized the actor critic method which is one of the temporal difference (TD) family of reinforcement learning methods. The model is consists of two parts called actor and critic. In this model, an actor plays the role of IPL whose output decieds the behavior of a robot, and a critic, which is corresponding to a part of BG. We implemented an actor and a critic into one CTRNN to share the context loop which plays an important role in state recognition.

In reinforcement learning, CTRNN has to learn a new sequence generated in each trial, which is inherently incremental learning. We use a database, which is corresponding to BG, to store sequences and the CTRNN is trained using these sequences. A sequence, stored in the database, is selected by the total reward of the trial. The maximal total reward in passed trials is stored and the total reward of a new trial is compared to it. If the total reward of a new trial is greater than a certain rate of a passed maximal one, then the new sequence is stored in the database.

B. IPL-M1S1 Model

As M1/S1 model, we utilized Recurrent Neural Network which is able to learn temporal sequence pattern. The RNN received current joint angle and rotational velocity, that represent the state of the robot arm, and target joint rotational velociy. And the output of the RNN is joint torque which realize the target signal given by the top network. The motion trajectory duaring search behavior of reinforcement learning is used for the training data for this network.

IV. Experiment with Real Robot

To test the proposed model, we applied it to the task of reaching for an object with real robot(figure 3). In this task, the distance between the tip of the robot hand and the red ball is measured by the camera which is settled on the ceiling. The robot can get more reward as the hand comes closer to the red ball. The connection weight of both networks are initialized with random value, therefore these networks have to be trained simultaneously. Specifically, the top network has to learn the motion trajectory through the repetitive trial of the reinforcement learning and the bottom network has to learn the way to control the motion of the robot arm by controling the joint torque. The time cource of the total reward through learning is shown in figure 4. In this case, the robot get relatively-large reward in the early phase because the hand and the ball were very close at the initial condition. When the ball moves and get away from the hand at the middle phase, the reward curve gose down. However, the reward curve gose up again when there are more learning iterations because the top network acquires the appropriate motion trajectory and the bottom network learns how to control the joint.

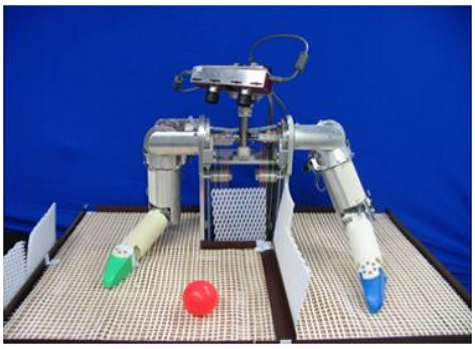

Fig. 3. robot experiment

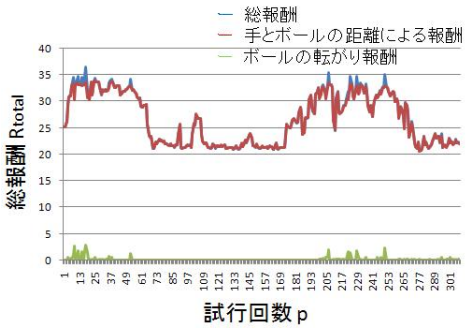

Fig. 4. reward curve

References

[1] M.A. Arbib. Perceptual structures and distributed motor control. In *Handbook of Physiology: The Nervous System, II. Motor Control*, pages 1448–1480. Cambridge, MA: MIT Press, 1981.

[2] Luria A.R. *The Working Brain*. Penguin Books Ltd., 1973.

[3] M. Ito. Bases and implications of learning in the cerebellum - adaptive control and internal model mechanism. *Progress in Brain Research*, 148:95–109, 2005.

[4] C.L. Colby, J. Duhamel, and M.E.Goldberg. Ventral intraparietal area of the macaque: anatomic location and visual response properties. *Journal of Neurophysiology*, 69:902–914, 1993.

[5] H. Sakata, M. Taira, A. Murata, and S. Mine. Neural mechanisms of visual guidance of hand action in the parietal cortex of the monkey. *Cereb Cortex*, 5:429–438, 1995.

[6] H. Liepmann. Apraxie. *Erg ges Med*, 1:516–543, 1920.

[7] K.M. Heilman. Ideational apraxia - a re-definition. *Brain*, 96:861–864, 1973.

[8] L. Fogassi, P.F. Ferrari, B. Gesierich B, S. Rozzi, F. Chersi F., and G. Rizzolatti. Parietal lobe: from action organization to intention understanding. *Science*, 308:662–667, 2005.

[9] G. Rizzolatti, L. Fadiga, V. Galless, and L. Fogassi. Premotor cortex and the recognition of motor actions. *Cognitive Brain Research*, 3:131–141, 1996.

[10] J. Tani and M. Ito. Self-organization of behavioral primitives as multiple attractor dynamics: a robot experiment. *IEEE Trans. on Sys. Man and Cybern. Part A*, 33(4):481–488, 2003.

[11] J. Tani, M. Ito, and Y. Sugita. Self-organization of distributedly represented multiple behavior schemata in a mirror system: reviews of robot experiments using RNNPB. *Neural Networks*, 17:1273–1289, 2004.

[12] M. Ito and J. Tani. On-line imitative interaction with a humanoid robot using a dynamic neural network model of a mirror system. *Adaptive Behavior*, 12(2):93–114, 2004.

[13] M. Ito, K. Noda, Y. Hoshino, and J. Tani. Dynamic and interactive generation of object handling behaviors by a small humanoid robot using a dynamic neural network model. *Neural Networks*, 19:323–337, 2006.

[14] R. Nishimoto. *Learning to Generate Combinatorial Action Sequences Utilizing the Initial Sensitivity of Deterministic Dynamical Systems*. PhD thesis, PhD thesis, Graduate School of Arts and Sciences, University of Tokyo, 2007.

[15] R. Paine and J. Tani. How hierarchical control self-organizes in artificial adaptive systems. *Adaptive Behavior*, 13(3):211–225, 2005.

[16] K. Doya, K. Samejima, K. Katagiri, and M. Kawato. Multiple model-based reinforcement learning. *Neural Computation*, 14:1347–1369, 2002.

[17] N. Geschwind and E.A. Kaplan. Human cerebral disconnection syndromes. *Neurology*, 12:675–685, 1962.

Group B: Research Report

Kazuo Tsuchiya
Dept. of Aeronautics and Astronautics, Graduate School of Engineering, Kyoto University

I. Research Brief

Animals generate locomotion adaptive to various environments by cooperatively manipulating their complicated and redundant musculoskeletal systems. So far, biomechanical studies have investigated the mechanical and dynamical characteristics of animal behaviors. On the other hand, neurophysiological studies have examined neural activities and evaluated their functional roles. They individually conduct their studies. However, animal skillful behaviors emerge through dynamical interactions between brain, nervous system, and musculoskeletal system. Group B consists of biologists who study exercise physiology and engineers who study biomechanics and conducts cooperative research aiming to elucidate how the mechanisms of selection and realtime generation of motion patterns adapt themselves to environmental variations. In particular, they construct neuromusculoskeletal models founded on anatomically based whole-body musculoskeletal system and mathematical model of locomotor nervous system based on neurophysiological findings and clarify the nervous system mechanism that generates adaptive behaviors by simulating locomotion based on the constructed models and comparing simulation results with physiological experimental results. This group wants to open a new research field called 'System Biomechanics' that integrates biomechanics and neurophysiology.

II. Research Organization

This research group consists of planned and subscribed research groups. The research subject of each group is as follows:

Planned research gourps

- B01-01 Neuronal mechanisms of generating and selection of adaptive behaviors (Kaoru Takakusaki, Asahikawa Medical College)
- B01-02 Exploration of the principle mechanism of generating adaptive locomotion on the basis of neurophysiological findings (Naomichi Ogihara, Kyoto University)
- B01-03 Realization of adaptive locomotion based on dynamic interaction among the body, brain, and environment (Koh Hosoda, Osaka University)

Subscribed research groups

- B01-11 Modulation of motor behavior by motivational and autonomic nervous systems (Yoshimasa Koyama, Fukushima University)
- B01-12 Study on brain adaptation in rat-machine fusion systems (Takafumi Suzuki, The University of Tokyo)
- B01-13 Detecting with BMI methods how body movements are involved in neural coding in the brain (Yoshio Sakurai, Kyoto University)
- B01-14 Multi-disciplinary investigations of adaptive of human bipedal (Takashi Hanakawa, National Center of Neurology and Psychiatry)

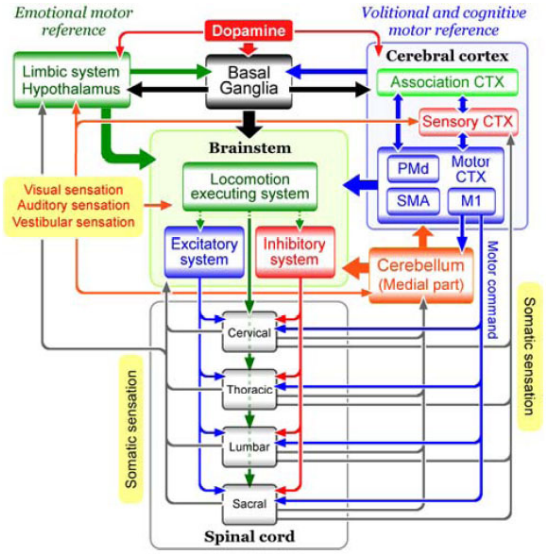

Fig. 1. Multi-tiered organization of CNS for locomotor behaviors

- B01-15 Neural mechanisms of integration of the locomotor and respiratry control systems in the emergence of motor behaviors (Kiyoji Matsuyama, Sapporo Medical University)
- B01-16 Environmental adaptation of the multipedal gait modeled by complex-valued neural networks (Ikuko Nishikawa, Ritsumeikan University)
- B01-17 Function of spinal cord for controlling volitional movement (Kazuhiko Seki, National Institute for Physiological Sciences)

III. Research Achievement

This report shows the representative studies of this group. Further details are shown in the report of each subgroup.

A. Multi-tiered Organization of the CNS for the Control of Posture and Locomotion in Mammals (B01-01 Kaoru Takakusaki, Asahikawa Medical College)

For these 3 years, our research has been aimed at elucidating the mechanisms of integration of postural and locomotor synergies. Important findings are as follows; 1) there are functional organizations in the cortical motor-related areas in relation to the control of posture and locomotion, 2) basic and functional architectures of the basal ganglia-brainstem pathways and those of the limbic-brainstem pathways in the integrating posture and locomotion have been identified, 3) role of cerebellar control of posture and locomotion has been elucidated by selective deletions of input and output systems using gene-targeted mutant mice. On the basic of these findings we suggest that neuronal architectures of integrating posture and locomotion are organized in "multi-tiered" manner so that adaptive locomotor control can be achieved (Fig. 1).

Fig. 2. Measurement of locomotor kinematics and kinetics in Japanese monkey. Japanese monkey walking bipedally on a treadmill in which a force plate can be embedded and reconstruction of whole-body kinematics of the Japanese monkey using a model matching method.

B. Gait analysis of Japanese monkeys using the musculoskeletal model (B01-02 Naomichi Ogihara, Kyoto University)

We are currently working on three-dimensional kinematic and kinetic analyses of locomotion in the Japanese monkey. Particularly, we focus on the following two projects this year.

1) Adaptive changes in bipedal locomotion with increase in walking velocity: Japanese monkeys walking bipedally on a treadmill at 3, 4, and 5 km/h was filmed using 4 high-speed cameras and locomotion was analyzed. The whole-body kinematics of a Japanese monkey walking on a treadmill was reconstructed using an anatomically based musculoskeletal model constructed last year (with 20 segments and 41 joint degrees of freedom) and the model-based matching technique (Fig. 2). It was found that the hip and knee joints were relatively more flexed and dorsiflexed, respectively, with increasing waking velocity and their ranges of joint motion increased, indicating that gait pattern is adaptively altered depending on intended walking velocity; the velocity was not controlled by simple tuning of step frequency of the locomotor rhythm generated by a neuronal network. The comparison of the vertical ground reaction force profile showed that the peak vertical force is also altered and it gets larger if the velocity is higher.

2) Ground reaction force of quadrupedal walking: Ground reaction force (GRF) profiles of quadrupedal walking in Japanese monkeys were analyzed and the functional significance of the diagonal sequence walking pattern was considered. Three Japanese monkeys walked on a wooden walkway at a self-selected speed, and three components of the GRF vector were measured using a force platform. Our measurements revealed that 1) the vertical GRF reached its maximum value when the ipsilateral hand and foot are in contact with the ground; 2) the propelling force generated by hand was largely countered by the breaking force generated by the ipsilateral foot and hence the forelimbs fundamentally generate net breaking force while the hindlimbs generate net propelling force; and 3) the transverse GRF are basically generated by the hindlimbs. We are now trying to figure out if such biomechanical characteristics of the quadrupedal walking in primates could be related to the energetic efficiency as well as the selection of the diagonal sequence walking pattern using the constructed numerical simulator.

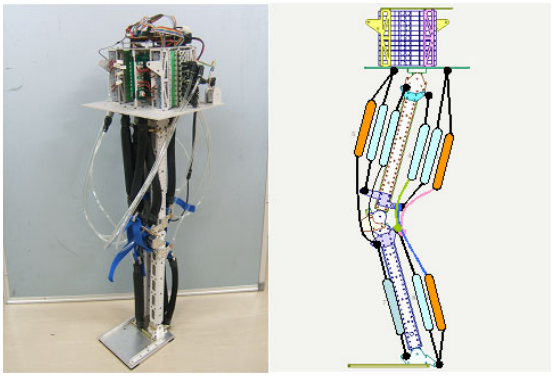

Fig. 3. Biped robot equipped with biarticular muscles

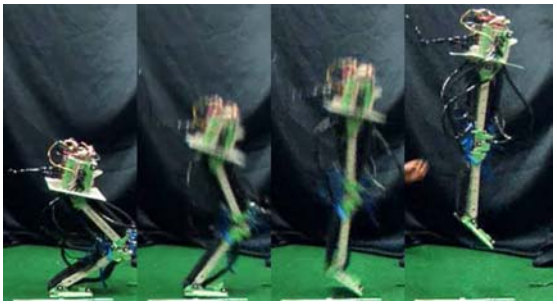

Fig. 4. Jumping experiment from standstill

C. Development of a biped robot equipped with biarticular muscles and experiments of its dynamic locomotion (B01-03 Koh Hosoda, Osaka University)

An animal has complicated structure consisting of many bones connected with muscles and ligaments that works antagonistically and/or synergistically. Especially, biarticular muscles that drive not only one joint but also multi joints play an important role for realizing synergistic motion of the joints. Moreover, redundancy provided from such complicated mechanism effectively contributes to the hierarchical system consisting of a lower layer devoted to rhythm generation and a higher layer devoted to purposive behavior. On the other hand, existing legged robots are driven by electric motors placed at their joints. It is hard for such a mechanism to realize animal-like compliant motion. In this study, we develop a biped robot driven by artificial pneumatic muscles, and clarify the contribution of the joint elasticity on the adaptive locomotion. Until now, we have demonstrated that the tonus controller can regulated the locomotion speed. In 2007, we develop a biped robot equipped with biarticular muscles, and conduct fundamental experiments on dynamic locomotion such as jumping and running to demonstrate the contribution of compliance (Figs. 3 and 4). The robot consists of a body, a thigh, a shank and a foot. Three joints are driven by 6 (3 pairs) monoarticular and 3 biarticular McKibben artificial pneumatic muscles. These muscles are controlled based on the information observed by pressure sensors equipped in the artificial muscles and gyro sensor on the body. We conducted (1) jumping experiment from standstill, (2) landing experiment, and (3) bouncing experiment to investigate the role of the biarticular muscles.

Multi-tiered Organization of the CNS for the Control of Posture and Locomotion in Mammals

Kaoru TAKAKUSAKI, Futoshi MORI, Katsumi NAKAJIMA, Dai YANAGIHARA, Taizo NAKAZATO, Kenji YOSHIMI, Masahiko INASE ,Shigeru KITAZAWA.

***Abstract* – Postural alteration always precedes the onset and the execution of motor behaviors. Postural control consists of 1) the adjustment of postural muscle tone, 2) postural reflexes and 3) the postural equilibrium. Fundamental neural mechanisms of controlling postural reflexes and postural muscle tone are located in the brainstem and spinal cord. However, in the unpredictable circumstance, real-time postural control requires the operation of neuronal networks in the central nervous system and active acquisition of sensory information from both the internal and external circumstances. The neuronal networks are multi-tiredly organized by the linkage between the forebrain structures (the cerebral cortex, the basal ganglia, the limbic system) and the hindbrain structures (the brainstem, the cerebellum and the spinal cord). Sensory information arising from the mechanoreceptors, propriocepters, visual, auditory and vestibular organs are particularly important as feedback signals for compensation of movements and feedforward signals for anticipatory postural preparation. In this annual report, we consider the mechanisms of postural control which can be accomplished by multi-tiredly organized neural networks that enable sensorimotor integration for the execution of variety of locomotor behaviors on the basis of our findings so far.**

I. Introduction

The cognitive and bodily functions of all animals are required to adapt to the external conditions. An adaptive capability will be achieved mostly through the motor behavior that depends on factors such as the intention and the emotional state of an individual. Sensory signals have dual roles. One is to generate cognitive cortical processing for working memory that can be used for guide future behavior. The other may be to affect the emotional states of the animal.

Locomotion has been considered as a type of emotional motor behaviors triggered by signals from the limbic and hypothalamic system to the brainstem [1] (Fig.1A). However, stepping movements with very accurate foot placement resemble the forelimb reaching movements of higher primates [2]-[3] (Fig.1B). Locomotion therefore also requires visuomotor cognitive processes which are controlled by loops involving the cerebral cortex, basal ganglia and cerebellum [4]. Whether the locomotion is either volitional or emotional, it is accompanied by movement processes that are automatically controlled by the brainstem and spinal cord [5] (Fig.1C). The automatic process includes activation of sequences of programs that are designed for the basic motor repertoires such as eye movements, swallowing, locomotion and posture [6].

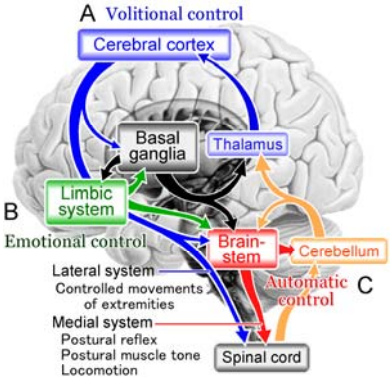

Figure 1 Framework of locomotor control

A. Projections from the cerebral cortex contribute to volitional aspects of locomotion. B. Projections from the limbic-hypothalamus to the brainstem contribute to emotional aspects. C. The brainstem and spinal cord play automatic aspects of locomotor movements. The cerebral cortex and the brainstem receive efferents from both the basal ganglia and the cerebellum.

The present studies achieved by Group B01 in this Research Program have been designed to understand how multi-tiered plural neuronal networks in the central nervous system (CNS) contribute to the postural control during loco- motion. For this purpose, electrophysiological studies combined with molecular biology and genetic approaches have been employed in several different types of experimental animal models.

II. Cortical Motor Areas Subserving Adaptive Bipedal Walking of the Monkey

Appropriate brain-body interaction is required to execute bipedal walking. One of the most critical questions in the motor control is how the cerebral cortex contributes to control of walking with biped. We have recently developed bipedally -walking animal models; Japanese monkey, *m. fuscat*a can be operant-trained to walk bipedally on the surface of a moving treadmill [7].

Using this model, we first tried to elucidate the whether the Monkey could acquire adaptive bipedal (Bp) walking capability, which required to walk on slanted surface and to avoid obstacles. Kinematic analysis demonstrated that the Bp walking monkey was able to adapt his posture and limb movements to these tasks. The alteration of was similar to that observed in human walking.

Then we tried to identify cortical areas involved in the acquisition of Bp walking capability using above tasks. For this, glucose metabolism of cerebral cortex was measured by positron emission tomography (PET) neuroimaging technique. Next, muscimol ($GABA_A$-receptor antagonist) was injected into the cortical areas which were identified by the PET neuroimaging so that alternation of Bp walking could be examined after inactivation of neurons in these areas.

K. TAKAKUSAKI is with the Department of Physiology, Division of Neural Function, Asahikawa Medical College, Asahikawa, Japan
F. MORI is with the Department of Veterinary Physiology, Yamaguchi University, Yamaguchi, Japan
K. NAKAJIMA and M. INASA are with the Department of Physiology, Kinki University School of Medicine, Sayama, Japan
D. YANAGIHARA is the Department of Life Science, Graduate School of Arts and Science, University of Toyo, Tokyo, Japan
T. NAKAZATO, K. YOSHIMI and S. KITAZAWA are with the Department of Physiology, School of Medicine, Juntendo University, Tokyo, Japan

As shown in Fig.2, PET study revealed the involvement of motor-related areas such as the primary motor cortex (M1), the supplementary motor area (SMA) and the dorsal premotor cortex (PMd). Glucose metabolism was more increased in the M1 during uphill than downhill walking. On the other hand, glucose metabolism was higher in the SMA in the obstacle avoidance task than the M1 and the PMd.

Muscimol injection into ankle and knee regions of the M1 did not obviously impaired upright standing. However foot-drop like impairment was observed during Bp walking; the monkey did not adequately pull up (or flex) contralateral hoot during swing phase. The monkey no more cleared obstacles and displayed stumbled walking. Injections of muscimol into bilateral SMA (hip and knee regions) resulted in severe locomotor instability with postural disturbance which was characterized by hypotonia and truncal sway. When muscimol was injected into the PMd, the monkey had a difficulty in initiation of locomotion even reward were visually presented.

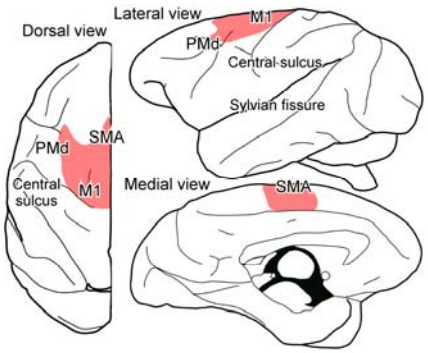

Figure 2 Cortical motor areas involved in bipedal locomotion identified by PET imaging study

See text for detail explanations. Abbreviations; M1; primary motor cortex, SMA; Supplementary motor area, PMd; dorsal premotor cortex.

An increase in glucose metabolism identified by the PET neuroimaging is considered to reflect increased presynaptic inputs. Bp walking in slanted treadmill tasks and obstacle avoiding tasks require much sensory information from proprioceptive, exteroceptive, visual and vestibular organs. These tasks may therefore require increased synaptic signals within these motor cortices and those from sensory and association cortices. An increase in inputs from subcortical structures including the basal ganglia, the cerebellum and the brainstem via thalamus may also contribute to this finding. Because inactivation of the M1, SMA and PMd resulted in motor deficits specific to each area, each motor cortical area has its own role in the elaboration of Bp locomotion.

III. Firing Properties of Cortical Motor Area Neurons In Bipedal Walking Monkey

Then the next question as to cortical control of Bp walking is "How are postural and locomotor synergies organized within motor related cortical areas?" To answer this question, firing properties of the motor cortical areas were examined along with recording electromyographic (EMG) activities of limb and trunk muscles during quadrupedal (Qp) and Bp locomotion in the Monkey.

EMG recordings during Qp and BP locomotion are shown in Fig.3A. Fore- and hindlimb muscles were activated in relation to step cycles during Qp locomotion. Transition of locomotor pattern from Qp to Bp, activities of forelimb muscles were attenuated but those of hindlimb muscles are enhanced in conjunction with elevation of tonic EMG activities of truncal muscles.

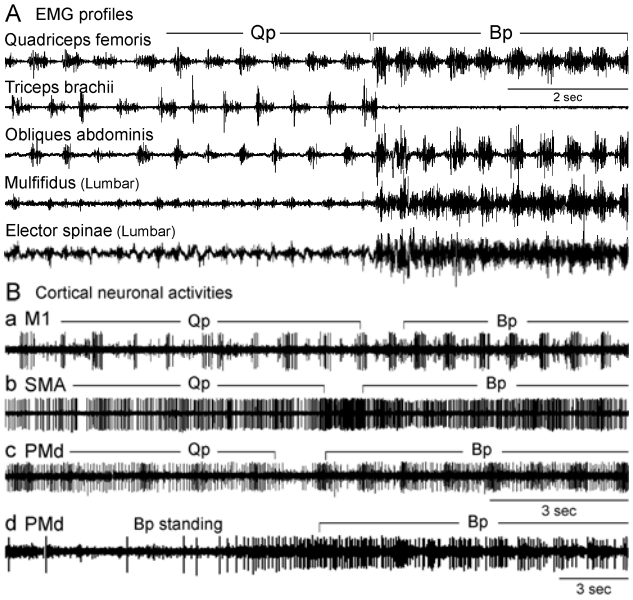

Figure 3 Muscle contraction and cortical neuronal activities during quadrupedal and bipedal locomotion

A. Electromyographic activities of hindlimb (quadriceps femoris) and forelimb (triceps brachii), abdominal (obliques abdominis) and back muscles (multifidus and elector spinae) during quadrupedal (Qp) and bipedal (Bp) locomotion. B. Firing properties of single cortical neurons during Qp and Bp locomotion in primary motor cortex (a. M1), supplementary motor area (b. SMA) and dorsal premotor cortex (c, d. PMd).

Figure 3B shows representative firing patterns of cortical neurons. Majority of M1 neurons phasically discharged during Qp and Bp locomotion (Fig.3Ba). On the other hand, more than half of SMA neurons displayed tonic or phasic-tonic firing during Qp locomotion. During Bp locomotion, most neurons exhibited tonic firing (Fig.3Bb). In the PMd, 40-50% neurons exhibited phasic-tonic firing (Fig.3Bc). Small but significant proportion of PMd neurons started to discharge before onset of locomotion (Fig.3Bd).

Findings described in the sections II and III suggest that the M1 is coupled with limb movements of locomotor steps, the SMA contributes to the postural control of limb and trunk, and the PMd is involved in the initiation of locomotor behaviors in addition to both processes. It should be noted that firing rates of most neurons are higher in Bp than Qp locomotion, indicating that alterations of musculoskeletal architecture accompany the changes in the operation of the CNS.

IV. Contribution of the Basal Ganglia to the Regulation of Locomotion

The basal ganglia control volitional and emotional motor process of movements via projections to the cerebral cortex and to the limbic system, respectively. Moreover, efferents from the basal ganglia control basic postural and locomotor

mechanisms via projections to the brainstem (Fig.1). Then role of the basal ganglia projections to the brainstem postural and locomotor systems was studied by recording intracellular activities of spinal motoneurons in decerebrate cats. Electrical stimulation applied to the midbrain locomotor region (MLR) generated rhythmic membrane oscillations in motoneurons (so-called fictive locomotion; Fig.4A). Stimulation of the substantia nigra reticulata (SNr), one of basal ganglia output nuclei, did not alter the excitability of motoneurons. However, the rhythmic membrane oscillations were replaced by tonic firing during SNr stimulation in both extensor and flexor motoneurons. Hyperpolarizing phases of oscillations were greatly reduced in size.

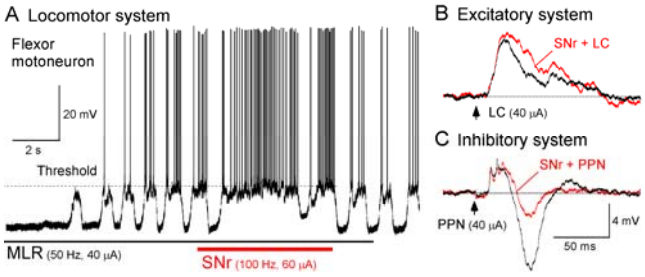

Figure 4 Effects from the basal ganglia to the brainstem in the control of locomotion and postural muscle tone

A. An MLR-induced fictive locomotion in a hindlimb flexor motoneuron was blocked during SNr stimulation where membrane potential was kept at the depolarizing state. B. EPSPs evoked by LC stimulation (3 pulses, 40 μA, 5 ms intervals) was enhanced by SNr stimulation (100 Hz, 60 μA). C. IPSPs evoked from PPN (3 pulses, 40 μA, 5 ms intervals) was greatly reduced in size by the SNr stimulation. Upward arrows indicate the onset of the stimuli.

Descending pathways arising from the pedunculopontine tegmental nucleus (PPN) and the locus coeruleus (LC) are identified as muscle tone inhibitory and excitatory systems, respectively [8]. Short train pulses of stimuli applied to the LC and the PPN induced EPSPs and IPSPs respectively. Conditioning SNr stimulation greatly reduced the amplitude of the PPN-induced IPSPs but slightly enhanced the LC-induced EPSPs (Fig. 4B, 4C), indicating that basal ganglia efferents suppress muscle tone inhibitory system but enhance muscle tone excitatory system. These results suggest that an increase in the basal ganglia output to the brainstem terminate locomotion by decreasing the activity of central pattern generators and by increasing muscle tone of both extensor and flexor muscles, which increases stiffness of limb joints.

V. Real-Time Measurements of Striatal Dopamine Signal using Wireless Voltammetry

Output from the basal ganglia is regulated by dopaminergic tone in the striatum. Because the activity of the midbrain dopamine (DA) neuron is critical to not only motor control but also cognition and sociality, there is a need to develop new techniques for measuring DA in relation to the alteration of animal behaviors. Here we show wireless in vivo voltammetry technique for rapid measurement of DA in the brain of freely behaving rats utilizing radio waves [9].

This system consisted of a potentiostat and transmitter system that was mounted on the back of the rat, and a receiver and analysis system. In vivo experiment was performed at least 1 week after the recording electrode with a carbon fiber of a diameter of 7 μm, was implanted in the rat striatum. Then changes in the striatal DA signals in relation to the social interaction were measured in a resident-intruder test (Fig.5A).

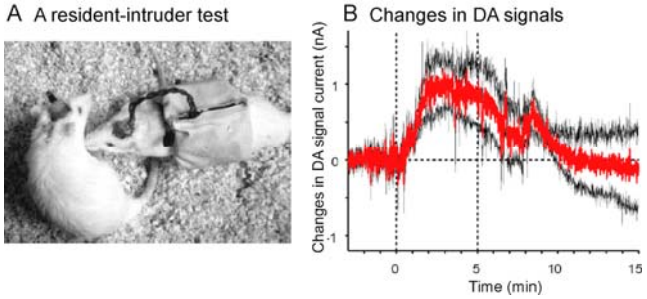

Figure 5 Changes in dopamine signal current during a resident–intruder test

A. The standard model (Kagohashi et al., 2008) placed on the back of the rat during the resident–intruder test. B. An intruder rat was introduced into the home cage of the resident rat at time zero and removed at 5 min (vertical broken lines). The red trace shows the mean dopamine signal current in the resident rat. Black lines show the standard error of the mean. The second peak around 9 min was contributed by a single rat and possibly reflects an artifact due to an abrupt movement of the rat. These experiments were performed 13–280 days after operations.

During a resident–intruder test, dopamine signal current in a resident rat increased upon introduction of an intruder rat. These results suggest that alternation of striatal DA content contribute to the social or cognitive interaction of self and others. This advantage enabled us to detect rapid increase in the dopamine current that occurred within 2 min in the resident animal after introduction of an intruder. Moreover the present wireless system is useful for a long-term measurement of dopamine in behaving rats. Next stage is to examine changes in striatal DA current in relation to the adaptable locomotor behaviors depending on the context.

VI. Cerebellar Control of Posture and Locomotion

Clinical studies of patients with cerebellar atrophy and ataxia describe that the cerebellar ataxic gait is typically characterized by significant increment of the stride length and discoordination of stepping movements [10]. Kinematic analysis of locomotion in mice with spontaneous and targeted mutations is possible to demonstrate qualitative changes in intralimb and interlimb coordination patterns and permit the identification of the specific genes and/or proteins on the ataxic gait. δ2 glutamate receptor (GluR δ2) is selectively expressed in cerebellar Purkinje cells (Fig.6A), and plays key role in long-term depression at the parallel fiber-Purkinje cell synapses, normal developments of the parallel fiber-Purkinje cell synapses as well as the climbing fiber-Purkinje cell synapses, and motor coordination. On the other hand, the spinocerebellar ataxia (SCA) type 3 transgenic mice have severe cerebellar atrophy including Purkinje cells (Fig.6Cc).

In this investigation, we compared the hindlimb kinematics of ho15J and wild-type mice during walking on a treadmill.

The kinematic differences between wild-type and ho15J were most pronounced during the swing phase (Fig.6B, D). These hypermetric hindlimb movements are mainly caused by the increased knee and ankle flexions. The SCA type 3 tg mice have more severe hypermetric hindlimb movements and deficits in balance control during locomotion (Fig.6E).

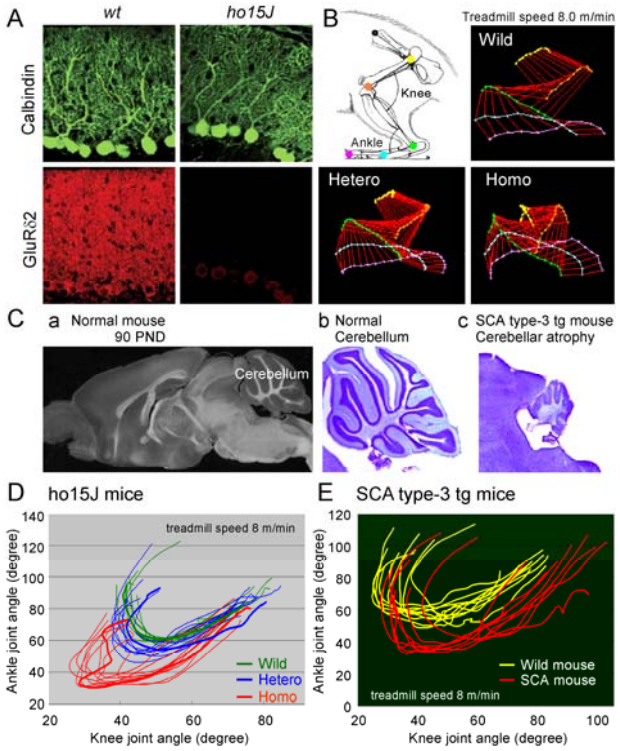

Figure 6 Impairment of locomotion in cerebellar deficiency mice

A. GluR δ2 is expressed in cerebellar Purkinje cells in wild type (wt) but is not expressed in ho 15J mice in the synaptic layer of parallel fibers, although calbindin was expressed in both mice, B. Kinematic analysis of hindlimb movements in wild-type and hetero- and homo-types 15J mice on treadmill locomotion with a speed of 8.0 m/min. C. (a). Parasagittal section of normal mice at 90 postnatal days (PND). Parasagittal sections in normal (b) and SCA type-3 tg mice (c). Severe cerebellar atrophy is observed in the latter. D and E. Relationship between ankle and knee joints during locomotion in ho 15J mice (D) and SCA type-3 tg mice (E). The kinematic difference between wild-type and ho15J was pronounced during the swing phase. These hypermetric movements are caused by the increased knee and ankle flexions.

It was observed that both mice did not adequately extend their knee and ankle joints during stance phase and displayed hyperflexion of hindlimb during swing phase. Because of the failure in the cerebellar information processing in both mice, cerebellar output to the cerebrum and the brainstem would be reduced, resulting in disturbance of posture and locomotion.

VII. Role of Muscle Tone Control Systems in the Modulation of Spinal Cord Reflex Pathways

Because basic muscle tone control systems exist in the brainstem and spinal cord, the cerebral cortex, the basal ganglia, the limbic-hypothalamic system and the cerebellum control muscle tone via the brainstem.

We have identified muscle tone inhibitory system (Fig.7). The inhibitory system arises from cholinergic neurons in the PPN, which consecutively excite pontine reticular formation neurons, medullary reticulospinal neurons and spinal inhibitory interneurons. This system induces postsynaptic inhibitory effects upon α- and γ-motoneurons innervating extensor and flexor muscles. Also interneurons mediating reciprocal Ia inhibition, Ib inhibition, recurrent (Renshaw) inhibition and flexion reflexes are largely suppressed by this system. Because this system induces primary afferent depolarization in sensory afferents from muscles and skin, primary afferents can be presynaptically inhibited. Motoneurons, interneurons and primary afferents are possibly inhibited by the identical category of spinal interneurons (an arrow in Fig.7) that are characterized by receiving inhibition from volleys in flexion reflex afferents (FRA). The interneuron may partly include Ib interneurons. Recent our findings suggest that the muscle tone inhibitory system; 1) reduce the amount of sensory signals, 2) inhibit the activity of spinal interneuronal networks, such as the locomotor central pattern generators (CPG) and 3) reduce the excitability of motoneurons, a final common path.

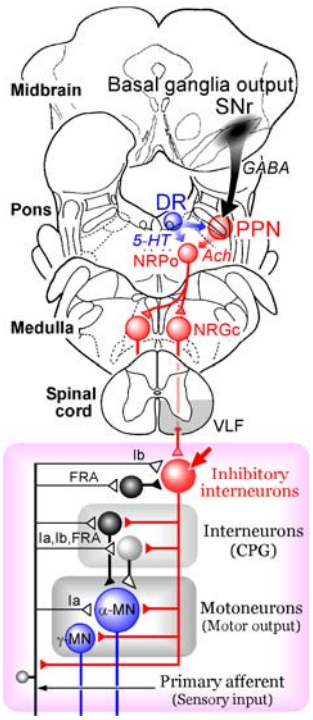

Figure 7
Muscle tone inhibitory system

Muscle tone inhibitory system is denoted by red color. Activation of this system would inhibit sensory afferents, interneurons mediating reflex pathways and motoneurons, resulting in general suppression of movements. This system receives excitatory inputs from the cerebral cortex, the limbic system and the cerebellum at the level of the pons and the medulla. The PPN receives inhibitory GABAergic input from the basal ganglia via the substantia nigra pars reticulata (SNr). Serotonergic projections from the raphe nuclei to the PPN and the pontine reticular formation inhibit this system.

Abbreviations; GABA; γ-amino butyric acid, DR; the dorsal raphe nucleus, Ach; acetylcholine, 5HT; serotonin, NRPo; the nucleus reticularis pontis oralis, NRGc; the nucleus reticularis gigantocellularris, VLF; ventrolateral funiculus, Ia and Ib, group Ia and Ib afferents, MN; motoneurons, CPG; central pattern generators.

Consequently muscle tone can be generally maintained by the excitability of spinal reflex arcs. The muscle tone inhibitory system receives excitatory inputs from the cerebral cortex (possibly the SMA and the PMd), the limbic-hypothalamic system and the cerebellum. Output from the basal ganglia inhibits the activity of the inhibitory system via GABAergic projections from the substantia nigra pars reticulata (SNr) to the PPN. Moreover the inhibitory system has reciprocal inhibitory interactions between the muscle tone excitatory systems such as the coerulospinal, the raphe spinal, vestibulospinal and excitatory reticulospinal systems [11]. As a result, dysfunction of these projection systems may elicit abnormal levels in postural muscle tone [12].

VIII. Multi-Tiered Organization of the CNS for the Control of Posture and Locomotion

On the basis of all findings, we try to draw out possible multi-tiered organization of neural networks involved in the control of locomotion and postural muscle tone.

1. Lower Level Tier for Basic Locomotor Systems

The lower level tire consists of the brainstem and spinal cord where basic locomotor systems are located as schematically illustrated in Fig.8. Fundamentally spinal cord motor system is composed of various spinal reflex arcs. Spinal interneuron is a major site for integration of sensory signals and descending commands from the cerebral cortex and the brainstem. For evoking locomotion, three major systems descend from the midbrain and the pons. These are; 1) the locomotor executing (reticulospinal) system arising from the MLR, 2) the muscle tone inhibitory (inhibitory reticulospinal) system arising from the PPN, and 3) the muscle tone excitatory system including the raphespinal, the coerulospinal, the vestibulospinal and the excitatory reticulospinal tracts.

Signals from the MLR may recruit these descending systems [11]. The locomotor executing system activates spinal interneuronal networks, resulting in locomotor rhythm genera- tion and locomotor pattern formation [13]-[14]. Therefore, integration of descending locomotor signals and sensory afferents may elicit locomotion. Because muscle tone control systems affect the activities of motoneurons and interneurons in reflex pathways, these systems may modulate locomotor rhythm and pattern in addition to the level of muscle tone.

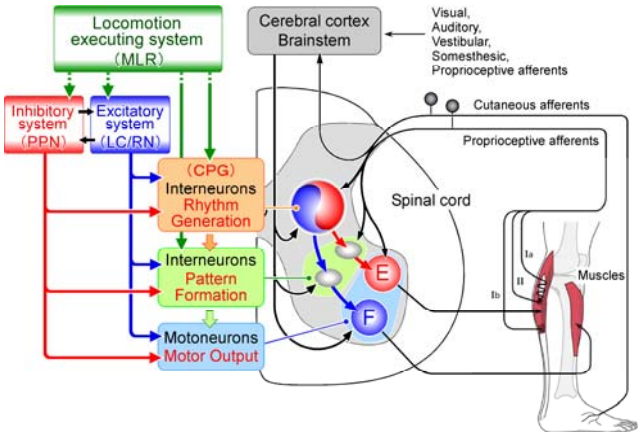

Figure 8 The basic locomotor systems in the brainstem and spinal cord
See text for detail explanations.

2. Middle Level Tier for Regulating Posture and Locomotion

The middle level consists of the cerebral cortex, the limbic –hypothalamic system, the basal ganglia and the cerebellum which project to the brainstem (Fig.9). Findings obtained from several lines of studies in section II and III suggest that each motor cortical area has its own role in the elaboration of Bp locomotion. Neuroanatomically, axons from the M1 mostly project to the spinal cord and those from the SMA and the PMd largely project to the brainstem [15]. It is therefore possible to consider that the M1 is coupled with limb movements of locomotor steps through the corticospinal tract. The SMA contributes to the postural control of both limb and trunk via cortico-reticular projections. The PMd is involved in the initiation of locomotor behaviors in addition to above both processes.

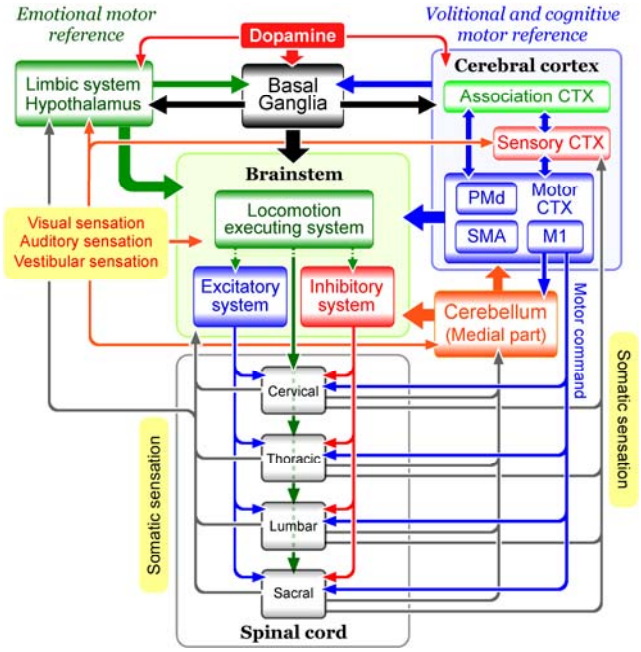

Figure 9 Multi-tiered organization of CNS for locomotor behaviors
See text for detail explanations

Basal ganglia controls postural muscle tone and locomotion via projections to the brainstem [11]. Findings in section IV suggest that GABAergic SNr projections to the brainstem 1) suppressed the activity of muscle tone inhibitory system, 2) enhanced the activity of muscle tone excitatory system and 3) attenuated rhythmic locomotor activity. Presumably, the basal ganglia control locomotion by simultaneously modulating the activity of rhythm generating system, or locomotion executing system, and muscle tone control systems (Fig.9). Accordingly, an increase in basal ganglia output may induce hypertonia of both extensor and flexor muscles, resulting in increasing stiffness of limb joints to quit movements. We postulate that “inhibition and disinhibition of motor systems” by the basal ganglia are basic mechanisms of the basal ganglia control of locomotion as well as eye movements and hand movements [6], [16]. It is a great achievement that real-time recording of DA signals using wireless voltammetry technique has been succeeded as described in Section V. Because basal ganglia output is greatly affected by the nigrostriatal DA neurons, and their deficiency causes Parkinsonian symptoms, there is a need to elucidate how the DA system modulates locomotor behaviors depending on the context.

In Section VI, mice with deficiencies in cerebellar function displayed hypermetric hindlimb movements and deficits in (postural) balance control during locomotion. The cerebellar

Purkinje cells receive abundant sensory inputs from spinal cord and special sensory systems, and efferent copy from the cerebral cortex via mossy-fibers and parallel fibers (Fig.9). Because parallel fiber-Purkinje cell synapses do not normally operate in ho15J mice due to deficiency in GluR δ2, the input from the parallel fibers are critical to maintain normometric limb movements and postural equilibrium. Severity of these functions observed in the spinocerebellar ataxia type 3 transgenic mice can be interpreted as cerebellar dysfunction due to severe cerebellar atrophy (Fig.6Cc) in which not only input - output systems but also Purkinje cells are largely damaged.

One of plausible mechanisms of cerebellar ataxia is due to hypotonia [10]. Because cerebellar output to the brainstem reticular formation contributes to the activation of both α- and γ-motoneurons via the vestibulospinal and excitatory reticulospinal systems [11], a reduction of cerebellar output may not adequately activate muscle tone excitatory systems. Less capability in utilizing sensory information (feedback signals) in the cerebellum may contribute to the deficiency of the above process. On the other hand, dysmetria is also caused by the deficiency of the lateral part of the cerebellar hemisphere where fibers arising project to the cortical motor areas via the thalamus. A deficiency of this projection system may be also involved in the dysmetria and hypotonia.

3. Higher Level Tier for Expression of Locomotor Behaviors

The higher level may consist of structures involved in the initiation, integration and selection of locomotor behaviors. As described in "Introduction", emotional stimuli whatsoever elicit emotional motor behaviors which are characterized by stereotyped movement patterns such as increasing muscle tone and/or running associating with "fight and flight reactions" [1]. On the other hand, goal-directed locomotor activity requires non-limbic systems. Stepping with very accurate foot placement as in the case of overcoming obstacles requires a precise visuomotor gait modification [3]. Loops involving the cerebral cortex with the basal ganglia and the cerebellum can assist such accurate cognitive operations (cognitive loops) [4]. For this process, visual sensation is particularly critical. These loops are involved in the generation of a *"volitional and cognitive motor reference"*. Although memories of volitional behavior require activity of the non-limbic sensorimotor system, unconscious and motivational limbic influences, such as *"emotional motor references"*, are also needed to enact any motor plans. So that the limbic system can influence the sensorimotor system, an integrated "*gating function*" has to be operated between the limbic system and non-limbic structures [5].

Here we refer to a "gating mechanism at the level of the midbrain". The midbrain receives excitatory inputs from the cerebral cortex and the limbic system, and inhibitory inputs from the basal ganglia (Figs.1 and 9). The basal ganglia also have neuronal loops with both the motor cortical areas and the limbic structures. Accordingly, emotional signals from the limbic-hypothalamus as well as volitional signals from the cerebral cortex could be modulated by basal ganglia output to the brainstem. Consequently, basal ganglia efferents to both the forebrain and the midbrain may have a role in the selection of volitionally-initiated and emotionally-triggered behavior so that an animal could elicit a variety of locomotor behaviors, depending on the behavioral context. The preference of the forebrain structures (cerebral cortex versus limbic system) is critical to the selection of context-dependent motor behaviors.

Rational gating mechanisms could exist in the forebrain. Doral premotor cortex, of which function is identified in this study, might be one of constituents of the gating mechanisms. Nonetheless it has not been elucidated how rational and emotional behaviors are selected between the limbic system and prefrontal cortex depending on the information of past memory and real-time working memory [17].

REFERENCES

[1] H. M. Sinnamon, "Preoptic and hypothalamic neurons and initiation of locomotion in the anesthetized rat", Prog. Neurobiol., vol. 41, pp. 323-344, 1993.

[2] T. Drew, S.Prentice, B. Schepens, "Cortical and brainstem control of locomotion", Prog. Brain Res. 143, vol. pp. 251-261, 2004.

[3] A.P. Georgopoulos, S. Grillner, "Visuomotor coordination in reaching and locomotion", Science, vol. 245, pp. 1209-1210, 1989.

[4] F.A. Middleton, P.L. Strick, "Basal ganglia and cerebellar loops: motor and cognitive circuits", Brain Res. Rev., vol. 31, pp. 236–250, 2000.

[5] K. Takakusaki, "Forebrain control of locomotor behaviors", Brain Res. Rev., vol. 57, pp. 192-198, 2008.

[6] O. Hikosaka, Y. Takikawa, R. Kawgoe, "Role of the basal ganglia in the control of purposive saccadic eye movements", Physiol. Rev. vol. 80, pp. 954–978, 2000.

[7] F. Mori, K. Nakajima, A. Tachibana, C. Takasu, M. Mori, T. Tsujimoto, H. Tsukada and S. Mori, "Reactive and anticipatory control of posture and bipedal locomotion in a nonhuman primate", Prog. Brain Res., vol. 143, pp. 191-198, 2004.

[8] K. Takakusaki, K. Saitoh, S. Nonaka, T. Okumura, N. Miyokawa, Y. Koyama, "Neurobiological basis of state-dependent control of motor behavior", Sleep Biol. Rhyth., vol. 4, pp. 87-104, 2006.

[9] M. Kagohashia, T. Nakazato, K. Yoshimia, S. Moizumia, N. Hattori, S. Kitazawa, "Wireless voltammetry recording in unanesthetised behaving rats", Neurosci. Res., vol. 60, pp. 120-127, 2008.

[10] S. M. Morton, A. J. Bastian, "Mechanisms of cerebellar gait ataxia", Cerebellum, vol. 6, pp. 79-86, 2007.

[11] K. Takakusaki, K. Saitoh, H. Harada, M. Kashiwayanagi, "Role of basal ganglia - brainstem pathways in the control of motor behaviors", Neurosci. Res., vol. 50, pp. 137-151, 2004.

[12] K. Takakusaki, K. Saitoh, M. Kashiwayanagi, "The pedunculopontine nucleus and the basal ganglia in locomotion", In: Bezard, E. (Ed), Recent Breakthroughs in Basal Ganglia Research, Nova Science Publishing Co. New York, USA, pp. 109-121, 2006.

[13] S. Rossignol, R. Dubuc, J-P. Gossard, "Dynamic sensorimotor interactions in locomotion", Physiol. Rev., vol. 86, pp. 89-154, 2006.

[14] D.A. McCrea, I.A. Rybak, "Organization of mammalian locomotor rhythm and pattern generation", Brain Res. Rev. vol. 57, pp. 134-146, 2008.

[15] K. Keizer, H.J.G.M. Kuypers, "Distribution of corticospinal neurons with collaterals to the lower brain stem reticular formation in monkey (Macaca fascicularis)", Exp. Brain Res., vol. 74, 311-318, 1989.

[16] A. Numbu, "Globus pallidus internal segment", Prog. Brain Res., vol. 161, pp. 135-150, 2007.

[17] S. Grillner, A.P. Georgopoulos, L.M. Jordan, "Selection and initiation of motor behavior". In: Stein, P.S.G., Grillner, S., Selverson, A.I., Stuart, D.G. (Eds.), Neurons, Networks, and Motor Behavior, MIT Press, Boston, pp. 3-19, 1997.

System Biomechanics of locomotion in the Japanese monkey: Exploration of principal mechanism for generating adaptive locomotion based on a neuro-musculoskeletal model

Naomichi Ogihara, Shinya Aoi, Yasuhiro Sugimoto, Masato Nakatsukasa, and Kazuo Tsuchiya

I. INTRODUCTION

Animals are capable of generating locomotion adaptive to diverse environments by coordinately controlling complex musculoskeletal systems. Mechanisms underlying the emergence of such intelligent adaptive behavior have conventionally been attributed to the sophisticated control mechanism of a biological sensorimotor nervous system. However, the suggestion has recently been made that animals achieve such adaptive yet efficient locomotion by exploiting intrinsic designs and properties of the musculoskeletal structures acquired through evolutionary history. A fundamental limitation may thus exist in attempts to clarify how the nervous system adaptively functions during locomotion based solely on neurophysiological studies; towards elucidating the mechanisms, the mechanisms of information processing emerging from appropriate dynamic interactions among the neuro-control system, musculoskeletal system and environment must be thoroughly investigated.

For this reason, our group has been biomechanically analyzing adaptive locomotor phenomena observed in actual bipedal/quadrupedal locomotion in the Japanese monkey (*Macaca fuscata*) using an anatomical whole-body musculoskeletal model. Furthermore, we try to construct a biologically plausible computer simulation of Japanese monkey locomotion by integrating physiological findings from the locomotor nervous system and the anatomy and biomechanics of the musculoskeletal system, with the aim of illuminating the dynamic principles underlying the emergence of adaptive locomotion in animals. Herein we report current progress in our system biomechanics study of bipedal/quadrupedal locomotion in the Japanese monkey, i.e., three-dimensional gait analysis and forward dynamic simulation based on the anatomically based whole-body musculoskeletal model.

II. GAIT ANALYSIS USING MUSCULOSKELETAL MODEL

Locomotion is an elaborate physical phenomenon generated by dynamic interactions between a complex chain of musculoskeletal elements and the changing outside world. To understand the mechanism underlying the generation of adaptive locomotion, actual locomotion must be thoroughly investigated from the outset. Therefore, we are currently working on three-dimensional kinematic and kinetic analyses of locomotion in the Japanese monkey. Particularly, we focus on the following two projects this year.

2.1 Adaptive changes of bipedal locomotion with increase in walking velocity

Japanese monkeys walking bipedally on a treadmill at 3, 4, and 5 km/h was filmed using 4 high-speed cameras (Nac Image Technology, HotShot 1280) and locomotion was analyzed. Frame rate and shutter speed are set to 125 frame/sec and 1/250 sec, respectively. The treadmill (Maruyasu Kikai, MMX300-FG-140) was specially designed so that a force platform (Kyowa Dengyo, EFP-S-1.5KNSA13) can be embedded, and we synchronously measured vertical component of ground reaction force acting on right foot during bipedal walking. From the motion images, well-recorded bipedal sequences were manually digitized frame-by-frame using three-dimensional motion analysis software and the coordinates of markers were calculated (Figure 1A). A total of 18 reflexive markers (9 on one side) were digitized at: 1) head of 5th metatarsal; 2) lateral malleolus of fibula; 3) lateral epicondyle of femur; 4) greater trochanter; 5) acromion; 6) lateral epicondyle of humerus; 7) styloid process of ulna; 8) head of 5th metacarpal; and 9) eyeball. If our anatomically-based whole-body musculoskeletal model of Japanese monkey constructed last year (with 20 segments and 41 joint degrees of freedom) could be matched to the temporal history of digitized marker coordinates, all body skeletal motion could be reconstructed as in video fluoroscopy. For this, the musculoskeletal model was firstly scaled to the size of the monkey in the video based on segment lengths, and the joint angles were adjusted frame-by-frame to minimize the sum of distances between corresponding markers while minimizing deviations of joint angles from the anatomically natural position (midpoints of the ranges of joint rotations). The

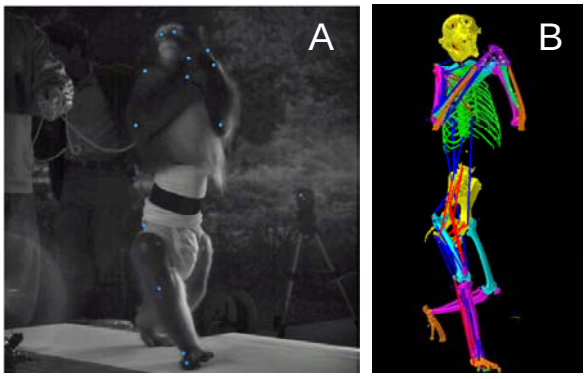

Fig. 1. Measurement of locomotor kinematics and kinetics in Japanese monkey. A) Japanese monkey walking bipedally on a treadmill in which a force plate can be embedded. B) Reconstruction of whole-body kinematics of the Japanese monkey using a model matching method.

N. Ogihara and M. Nakatsukasa are with Laboratory of Physical Anthropology, Graduate School of Science, Kyoto University, Kitashirakawa-oiwakecho, Sakyo, Kyoto 606-8502, Japan (e-mail: {ogihara, nakatsuk}@anthro.zool.kyoto-u.ac.jp).

S. Aoi, Y. Sugimoto, and K. Tsuchiya are with Department of Aeronautics and Astronautics, Graduate School of Engineering, Kyoto University, Yoshida-honmachi, Sakyo, Kyoto 606-8501, Japan (e-mail: {shinya_aoi, yas, tsuchiya}@kuaero.kyoto-u.ac.jp).

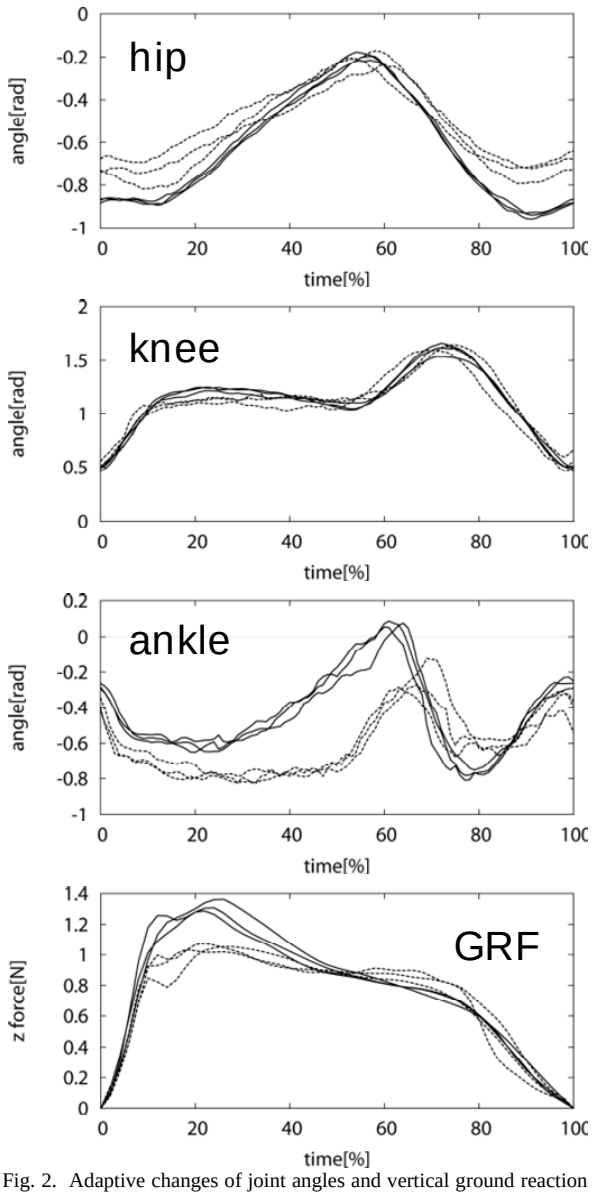

Fig. 2. Adaptive changes of joint angles and vertical ground reaction force (GRF) with increase in walking velocity. (solid line = 5km/h, dotted line = 3km./h). Angles are positive for hip extension, knee flexion and plantarflexion.

quasi-Newtonian method was used to solve this minimization problem. Figure 1B illustrates a result of matching, indicating that the whole-body kinematics of a Japanese monkey walking on a treadmill was successfully reconstructed using an anatomically based musculoskeletal model and the model-based matching technique. By introducing kinematc constraints defined by joint morphology, the present study yielded anatomically reasonable, natural skeletal motion from a limited number of external markers. Based on this estimated skeletal kinematics, hip, knee and ankle joint angles were calculated and changes in the joint angle profiles with increasing walking velocity were investigated. As illustrated in Figure 2, it was found that the hip and knee joints were relatively more flexed and plantarflexed, respectively, with increasing waking velocity and hence their ranges of joint motion increased, indicating that gait pattern is adaptively altered depending on velocity; the velocity was not controlled by simple tuning of step frequency of the locomotor rhythm generated by a neuronal network. The comparison of the

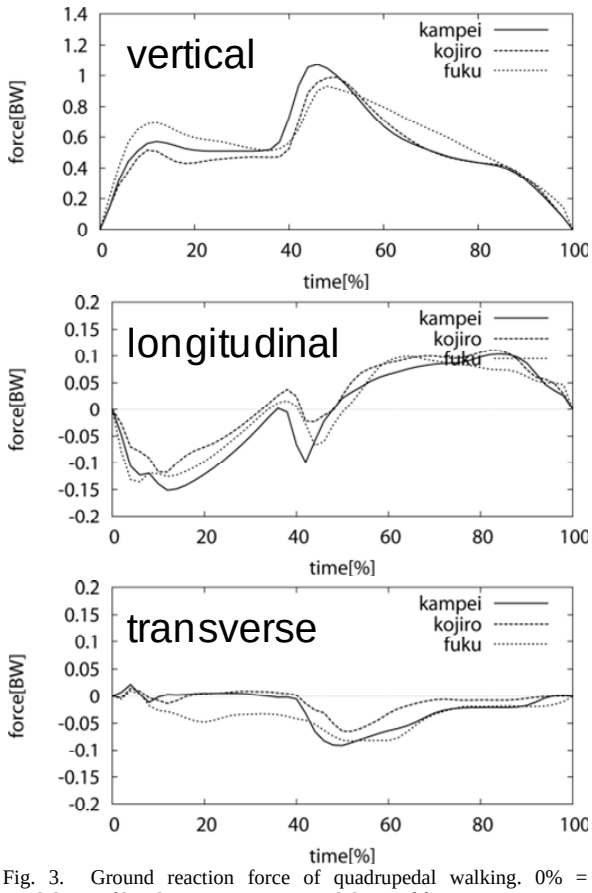

Fig. 3. Ground reaction force of quadrupedal walking. 0% = touchdown of hand, approx. 40% = touchdown of foot, approx. 60% = liftoff of hand, 100% = liftoff of foot. The lines are the average force profiles of 3 participants. Forces are positive for upward, forward, and lateral directions, respectively.

vertical ground reaction force profile (Figure 2) showed that the peak vertical force is also altered and gets larger if the velocity is higher.

2.2 Ground reaction force of quadrupedal walking

The quadrupedal walking gait in primates is different from that of other mammals in the use of diagonal sequence walking pattern, i.e., the footfall of a hindfoot (foot) is followed by that of the contralateral forefoot (hand); other mammals use only lateral sequence walking pattern, i.e., the footfall of a foot is followed by that of the ipsilateral hand. The reason why primates adopt such unusual gait pattern still remains unclear and this has been a controversial subject in the field of physical anthropology. To this end, ground reaction force (GRF) profiles of quadrupedal walking in Japanese monkeys were analyzed and the functional significance of the diagonal sequence walking pattern was considered. Three Japanese monkeys walked on a wooden walkway at a self-selected speed, and three components of the GRF vector were measured using a force platform. Because the footfall of a hand is followed by that of ipsilateral foot in the diagonal sequence walking and the positions of ground contact of the ipsilateral hand and foot are almost identical, it is almost impossible to measure the GRF vectors of the hand and foot independently. Hence the sum (resultant force) of the ipsilateral hand and foot GRF vectors was measured and analyzed. Our measurements revealed that 1) the vertical GRF reached its maximum value when the ipsilateral hand and foot are both in contact with the ground; 2)

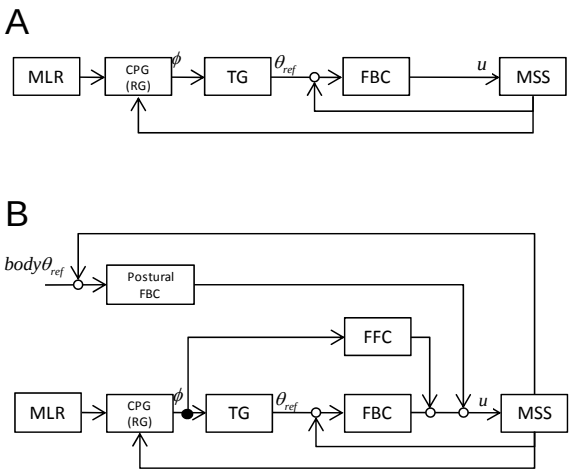

Fig. 4. Block diagram of locomotion control. A) Feedback control system. B) Present control system. MLR = Mesencephalic locomotor region, TG = Trajectory Generator, FBC = Feedback Controller, MSS = Musculoskeletal System, FFC = Feedforward Controller, CPG(RG)= Rhythm Generating layer of Central Pattern Generator. FFC corresponds to Pattern Generating layer (PG) of the CPG.

the propelling force generated by hand was largely countered by the breaking force generated by the ipsilateral foot and hence the forelimbs fundamentally generate net breaking force while the hindlimbs generate net propelling force; and 3) the transverse GRF are basically generated by the hindlimbs (Figure 3). We are now trying to figure out if such biomechanical characteristics of the quadrupedal walking in primates could be related to the energetic efficiency as well as the selection of the diagonal sequence walking pattern.

III. DYNAMIC SIMULATION OF LOCOMOTION

Animal locomotion, including that of primates, is generally accepted as being generated by a rhythm-generating neuronal network in the spinal cord known as the central pattern generator (CPG), with locomotion evoked by stimulus input from the mesencephalic locomotor region in the brainstem [1-2]. Such spinal rhythm-generating neuronal network also seems to exist in primates and is hypothesized to contribute to generation of actual locomotion [3-4]. On the other hand, recent neurophysiological studies have suggested that sensorimotor signals in the spinal circuitry encode global parameters of the limb kinematics, i.e., orientation and length of the axis connecting the most proximal joint and the distal position of a limb (limb axis) [5], suggesting such global representation of limb kinematics is used for sensorimotor integration and coordinated control of the limb musculoskeletal system. Up to last year, referring to these findings, we hypothesized that the CPG could be represented by a set of oscillators corresponding to each of the limbs and the trunk segment, and phase of the oscillator encoded the orientation and length of the limb axis, with the spinal circuitry generates muscle activation patterns using a PD feedback control law (Figure 4A). Based on this computational framework, three-dimensional dynamic locomotion of a Japanese monkey was emulated due to dynamic interactions among the body mechanical system, the nervous system consisting of the oscillators, and the environment.

However, in this simulation based on a feedback control low,

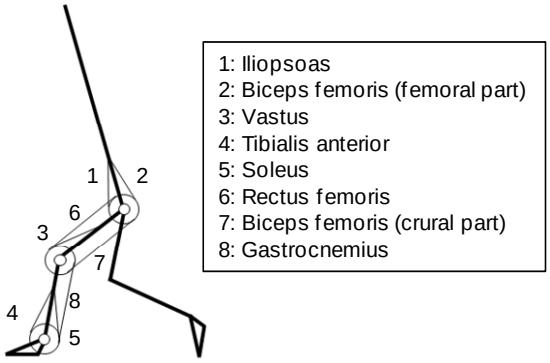

Fig. 5. Two-dimensional musculoskeletal model of Japanese monkey.

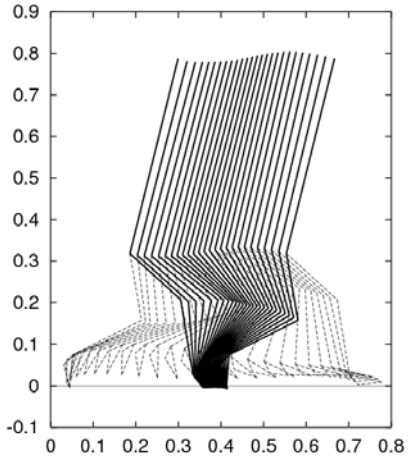

Fig. 6. Stick diagram of generated bipedal locomotion.

we must have assumed unrealistically high values for the gain of each joint to make it work. Furthermore, the system obviously destabilizes if we introduce transport delays in the nervous system. It was therefore anticipated that animals utilize some sort of feedforward control strategy to generate locomotion for adaptively coping with various changing environments.

Ivanenko et al. analyzed electromyographic activity patterns of muscles in human leg during walking using principal component analysis and found that activation patterns of muscles can be decomposed into a combination of five principal waveforms [6-7]. These invariant synergistic muscle activation patterns are considered to be created by a functional module located in the spinal cord, and control of this combination patterns alters muscle activity, and hence movement [8-9]. In this study, we assume that appropriate combinations of such basic muscle activation patterns are prescribed in the spinal cord level to form feedforward muscle activity for locomotion, and a new neuro-control model was constructed (Figure 4B). Specifically, each of the principal waveforms, represented by a Gaussian basis function, is assumed in the spinal module and each of the muscle activities is generated as a linear summation of the principal waveforms. The Gaussian function is represented as a function of phase of the corresponding CPG (oscillator), and motor commands are sent out to muscles in a feedforward manner based on this phase signal. Recent studies suggested that a CPG consists of two layers: a rhythm generator (RG) that generates oscillatory signal, and a pattern generator (PG) that generates muscle

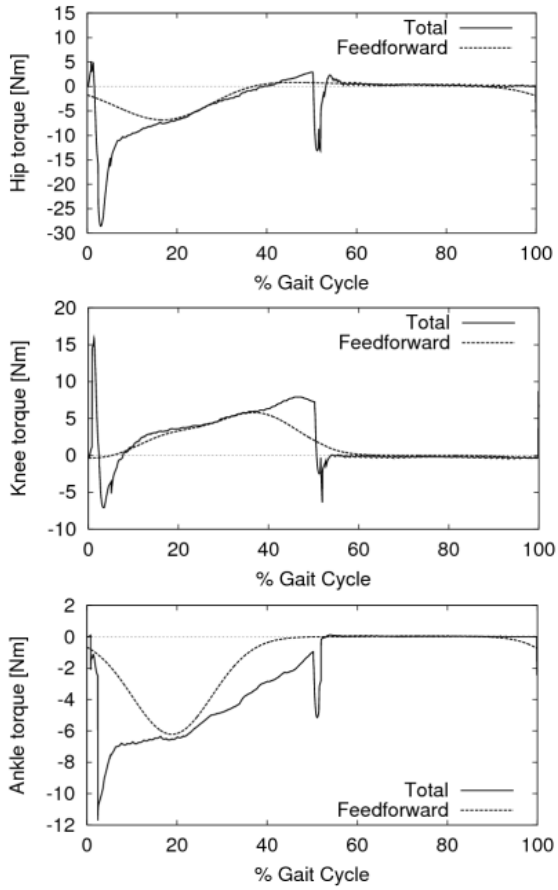

Fig. 7. Changes in joint moments over time (expressed as a % of gait cycle). Solid line = net joint moment, dotted line = feedforward component. Moment are positive for hip flexion, knee extension and foot dorsiflexion, respectively.

activity patterns based on the phase signal from the RG [10-11]. The feedforward controller here corresponds to this PG (Figure 4B). In addition to this feedforward controller, a PD feedback controller is incorporated that realizes desired locomotory trajectories of limb joints. To maintain the posture of a trunk segment, a postural feedback controller is also modeled.

Based on this control system, bipedal locomotion of a Japanese monkey was emulated. For the sake of simplicity, the musculoskeletal system was constructed as seven rigid links in a sagittal plane, with a total of 8 principal muscles (Figure 5). The inertial and muscular parameters were determined based on CT scans and dissection data. Locomotion was achieved by the following method. First, desired joint trajectories were reconstructed based on the measured kinematic data of locomotion (Figure 2), and locomotion was realized solely by the PD feedback controller. Subsequently, the muscle activation patterns of the model were roughly reconstructed by manually adjusting the timing, shape and combination of the Gaussian functions. These reconstructed waveforms were assumed to make up the feedforward commands sent to muscles for generation of locomotion. Figure 6 illustrates the generated bipedal locomotion pattern, indicating that the locomotion was successfully emulated based on the measured joint kinematics. Figure 7 displays the net and feedforward joint torques applied around the joints. The results show that the musculoskeletal model was actuated by combined signals from the feedforward and feedback controllers. We will investigate how such Gaussian-like feedforward commands should be acquired and controlled for generation of robust locomotion adaptable to changes in the neuromusculoskeletal systems and environments.

IV. CONCLUSION

Herein we report our system biomechanics studies of bipedal/quadrupedal locomotion in the Japanese monkey based on an anatomically based whole-body musculoskeletal model. The final goal of our project is to understand the dynamic principles underlying the emergence of adaptive locomotor phenomena to the extent that we can quantitatively reproduce them in a computer using the anatomical musculoskeletal model and biologically plausible neuro-control systems. To this end, we further investigate adaptive strategies of locomotion in Japanese monkeys by biomechanically analyzing adjustments of locomotion in response to perturbations such as weighted locomotion and locomotion on a split-belt treadmill. Furthermore, it is vitally important for the simulation to become capable of reproducing such elaborated adaptive behaviors observed in the Japanese monkey. We must improve our locomotor neuro-control model with the collaboration of neurophysiologists to achieve biologically plausible simulations.

REFERENCES

[1] S. Grillner, "Locomotion in vertebrates: central mechanisms and reflex interaction", Physiological Reviews, vol. 55, pp.274-304, 1975.

[2] M.L. Shik and G.N. Orlovsky, "Neurophysiology of locomotor automatism", Physiological Reviews, vol. 56, pp.465-501, 1976.

[3] E. Eidelberg, J.G. Walden and L.H. Nguyen, "Locomotor control in macaque monkeys", Brain, vol. 104, pp.647-663, 1981.

[4] B. Calancie, B. Needhamshropshire, P. Jacobs, K. Willer, G. Zych and B.A. Green, "Involuntary stepping after chronic spinal-cord injury - evidence for a central rhythm generator for locomotion in man", Brain, vol. 117, pp.1143-1159, 1994.

[5] R. Poppele and G. Bosco, "Sophisticated spinal contributions to motor control", Trends in Neurosciences, vol. 26, pp.269-276, 2003.

[6] Y.P. Ivanenko, R.E. Poppele and F. Lacquaniti, "Motor control programs and walking", *Neuroscientist*, vol. 12, pp.339-348, 2006.

[7] Y.P. Ivanenko, R.E. Poppele and E. Lacquaniti, "Five basic muscle activation patterns account for muscle activity during human locomotion", Journal of Physiology, vol. 556, pp.267-282, 2004.

[8] A. d'Avella, P. Saltiel and E. Bizzi, "Combinations of muscle synergies in the construction of a natural motor behavior", Nature Neuroscience, vol. 6, pp.300-308, 2003.

[9] M. Lafreniere-Roula and D.A. McCrea, "Deletions of rhythmic motoneuron activity during fictive locomotion and scratch provide clues to the organization of the mammalian central pattern generator", Journal of Neurophysiology, vol. 94, pp.1120-1132, 2005.

[10] I.A. Rybak, N.A. Shevtsova, M. Lafreniere-Roula and D.A. McCrea, "Modelling spinal circuitry involved in locomotor pattern generation: insights from deletions during fictive locomotion", Journal of Physiology, vol. 577, pp.617-639, 2006.

Group B--3: Realization of Adaptive Locomotion based on Dynamic Interaction between Body, Brain, and Environment

Koh Hosoda, Osaka University
Hiroshi Kimura, University of Electro-Communications
Katsuyoshi Tsujita, Osaka Institute of Technology
Kousuke Inoue, Ibaraki University

***Abstract*— Behavior of an agent is emerged from the interaction between body, control, and environmental dynamics. The research group B-3 aims to design body and control dynamics for emerging adaptive locomotion. We investigate three types of locomotion, biped, quadruped, and snake-like and developed robots. In 2007, we have developed (1) biped robots that have biarticular muscles and their dynamic locomotion, (2) a CPG network for a quadruped that enable gait generation as well as rhythm generation with feedback from the foot information, (3) a quadruped robot driven by pneumatic artificial muscles, and (4) a 3D dynamic simulator of a snake-like robot.**

I. Introduction

The research program entitled Emergence of Adaptive Motor Function through Interaction between Body, Brain, and Environment - Understanding of Mobiligence by Constructive Approach - started in 2005, as a MEXT Grant-in-Aid for Scientific Research on Priority Areas. One of the main goals of the project is to find a principle of emergence of adaptive locomotion. To approach the issue from the constructivist viewpoint, our research group B-3 aims to develop locomotive agents with various modalities based on dynamic interaction between body, control and environment. In 2007, we have developed (1) biped robots that have biarticular muscles and their dynamic locomotion, (2) a CPG network for a quadruped that enable gait generation as well as rhythm generation with feedback from the foot information, (3) a quadruped robot driven by pneumatic artificial muscles, and (4) a 3D dynamic simulator of a snake-like robot.

II. Biped Robots that have Biarticular Muscles and their Dynamic Locomotion

A. Overview

We developed several biped robots that are driven by antagonistic pneumatic artificial muscles, and showed that walking behavior can be changed by regulating muscle tonus [1]. We also realized walking, jumping and running by utilizing variable compliance provided by antagonistic drive mechanism [2]. These robots were, however, equipped only with monoarticular muscles. Biarticular muscles play important roles for realizing synergistic movement of humans and animals. Redundancy provided by these muscles is also important to realize robust and adaptive motion. The redundancy may play an important role for the interaction between body, brain, and environment. In 2007, we develop biped robots that have biarticular muscles and conduct experiments to realize dynamic locomotion such as jumping and 3D bipedal walking.

B. 2D monopod with biarticular muscles

A 2D monopod with biarticular muscles is developed to investigate their roles on dynamic locomotion (Figure 1).

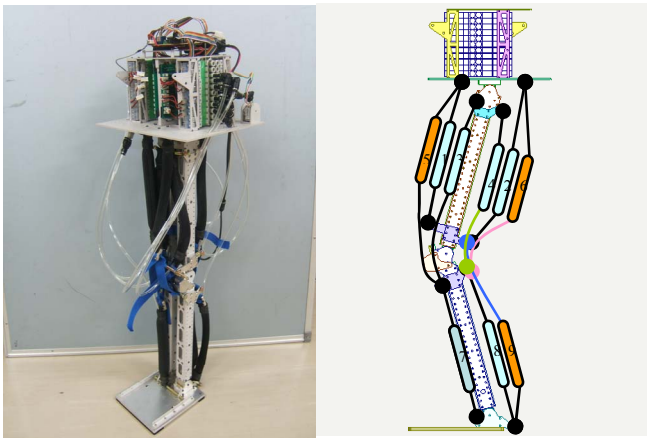

Figure 1: A 2D monopod with biarticular muscles

The robot consists of a body, a thigh, a shank and a foot. Three joints are driven by 6 (3 pairs) monoarticular and 3 biarticular McKibben artificial pneumatic muscles. These muscles are controlled based on the information observed by pressure sensors equipped in the artificial muscles and gyro sensor on the body. We conducted (1) jumping experiment from standstill, (2) landing experiment, and (3) bouncing experiment to investigate the role of the biarticular muscles. In this report, we show an experimental result on the jumping experiment.

C. Jumping from standstill

Biarticular muscles play important roles for realizing synergistic movement. Jumping experiments from standstill are conducted to investigate the roles. A sequence of operating valves is shown in Figure 2. In the figure, T_2 and T_8 denote time lag until the hip monoarticular muscle and the ankle monoarticular muscle are driven. These muscles are antigravity muscles to supply power for jumping.

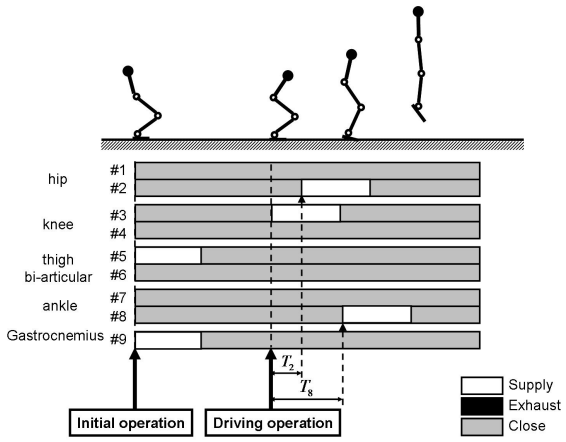

Figure 2: valve operation for jumping from standstill

To investigate the effectiveness of activation of the biarticular muscles, we conducted four experiments, with and without activation of the "gastrocnemius" #9, with two variations of T_2 and T_8. Experimental results are shown in Figure 3. If we do not activate the biarticular muscle, we have to control the other muscles precisely so that the robot can jump up without rotation [2]. On the other hand, if it is activated, activation of other muscles does not affect so much on the rotation. In the case (d) of the experiment, we confirm that the longer we supply air to the muscle #9, the less the rotation of the body becomes (Figure 4).

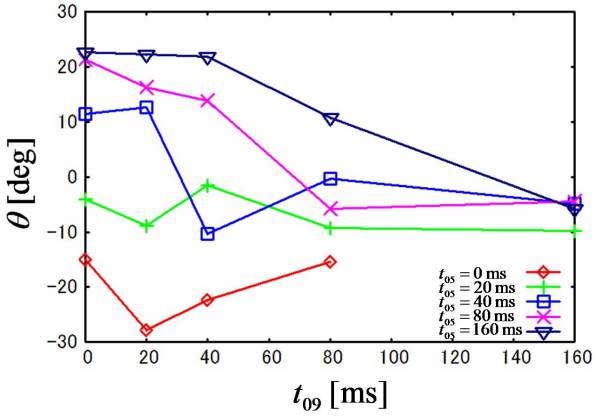

Figure 4: the longer we supply air to the muscle #9, the less the rotation of the body becomes.

(a) without biarticular muscle activation $T_2 = 0, T_8 = 0$

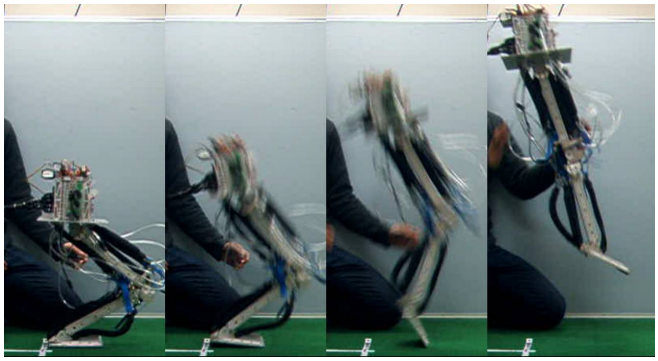

(b) without biarticular muscle activation $T_2 = 25[ms], T_8 = 50[ms]$

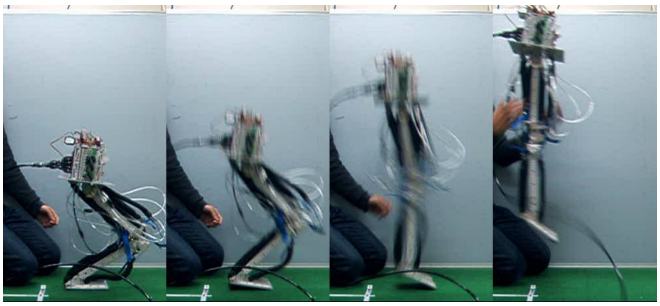

(c) with biarticular muscle activation $T_2 = 0, T_8 = 0$

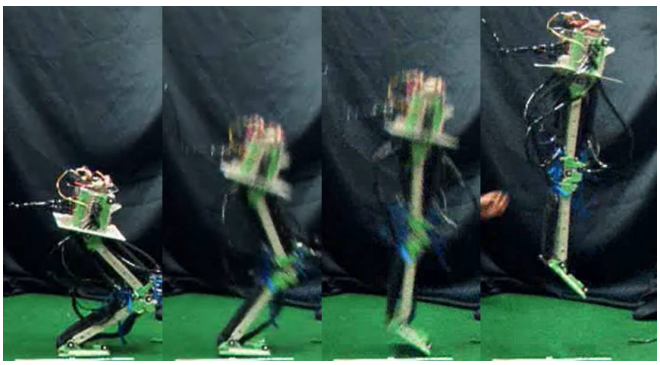

(d) with biarticular muscle activation $T_2 = 25[ms], T_8 = 50[ms]$

Figure 3: jumping experiments from standstill

D. 3D biped robot with biarticular muscles

We also develop a 3D biped robot whose leg structure is the same as the jumping robot shown in the last section. (see Figure 4), and conducted preliminary experiments on walking, jumping, and running separately. It is shown that the robot is capable for dynamic locomotion such as walking and jumping. We will conduct experiments to show that it is capable for the transition among locomotion modes.

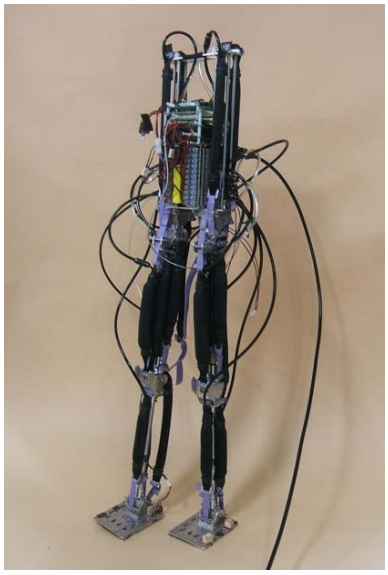

Figure 4: 3D biped robot with biarticular muscles

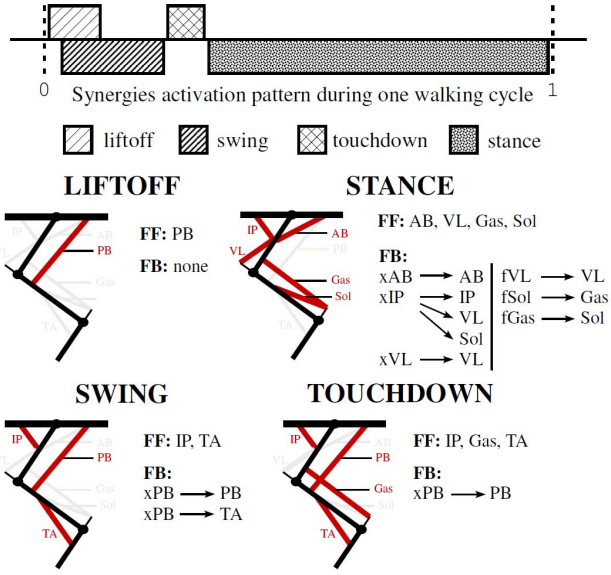

Figure 6: Example of synergies activation pattern during one stepping cycle and active muscles for each synergy.

III. Neural Controller for Quadrupedal Locomotion

A. Overview

In the former studies, we realized adaptive walking on irregular terrain using a mammal-like quadruped robot. However, adopted neural controller is mainly devoted for rhythm generation for irregular terrain, and its ability to adapt the gait is relatively week, for example, adaptation against the decrease of velocity. Therefore, we started to design a new CPG network that enable not only rhythm generation but also gait adaptation by utilizing feedback based on sensor signal of the legs. Preliminary simulation is conducted to show the effectiveness of the network.

B. Leg Controller (LC)

Our Leg Controller (Figure 5) is made of three parts: the Neural Phase Generator (NPG), the Motor Output Shaping Stage (MOSS) and the Propulsive Force Control Module (PFCM).

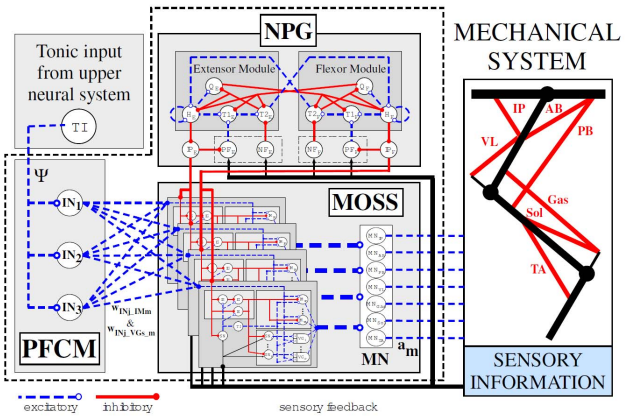

Figure 5: Overview of the Leg Controller

1) Neural Phase Generator (NPG)

The NPG activity characterizes the current phase of the leg. The functional units of the NPG layer are called ``modules." Transition of activity from one module to another is under heavy sensory control, and all the modules are activated in sequence during one locomotion cycle. Our NPG is made of two modules, the extensor and flexor modules (Figure 5). Each module is made of seven neurons (all the following neurons are interneurons, except PF and NF which are sensory neurons).

We used the same kinds of sensory information as Ekeberg et al. (2005) for the sensory feedback to the NPG, those are, Anterior Extreme Position (AEP), Posterior Extreme Position (PEP) and Leg Loading (LL).

2) Motor Output Shaping Stage (Moss)

Associated to each NPG module is a set of so-called ``synergies" in the MOSS layer. Initiation and termination of the activity of one synergy obey to a given timing or can be triggered on the basis of sensory information. Each synergy has a feed-forward and a feedback component. The outputs of such components are summed by the motor neurons (MN), which output the muscular activation levels a_m for the muscular system.

The MOSS is under inhibitory influences from the NPG, coming from the IP neurons of each module (Figure 5). These signals are used to select the synergies during the active period of the corresponding NPG module.

Currently, two synergies are implemented for each module: liftoff (LO) and swing (SW) synergies for the flexor module, and touchdown (TD) and stance (ST) synergies for the extensor module. These four synergies are the same as the ones used in Wadden et al. (1998) and Ekeberg et al. (2005) (Figure 6). Each synergy is responsible for the simultaneous feed-forward activation of a certain number of

muscles and the opening of specific feedback paths in order to fulfill a given motor function.

3) Propulsive Force Control Module (PFCM)

The PFCM is the part of the LC responsible for adjusting the propulsive force according to the intensity of the tonic input from upper neural system.

C. Simulation Results

In order to validate our Leg Controller (LC) architecture, we tested it on the two hind legs model shown in Figure 7. First, we confirmed that the results of Ekeberg et al. (2005) could be reproduced. Using the biped simulation model, we were able to generate stable alternative stepping at various speeds. As there is no explicit interaction between two LCs, the coordination of the legs is an emergent property of the system, induced by the way the LC are interacting with the environment through the sensory feedback. This was, however, a predictable result since the LC uses the information about the load supported by the leg as the main sensory signal to trigger the transition between the extensor and the flexor modules.

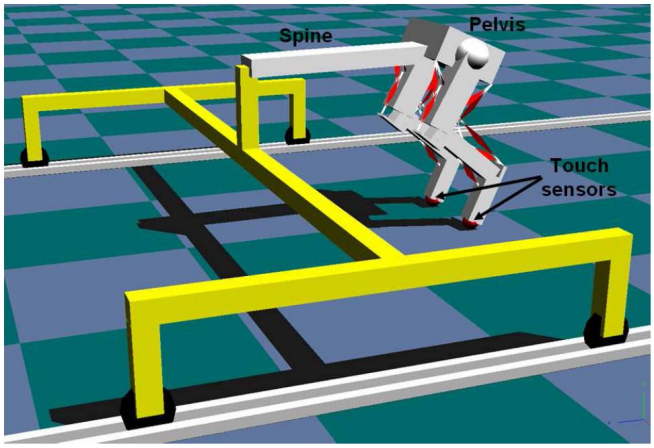

Figure 7: Simulation model. The spine can rotate around the pich axis

IV. Development of a Quadruped Driven by Pneumatic Artificial Muscles

We develop a quadruped robot whose joints are driven by pneumatic artificial muscles (Figure 8) to investigate the hypothesis that the tonus control modifies the lower rhythmic control, and the resultant behavior changes according to the interaction between the body and the environment.

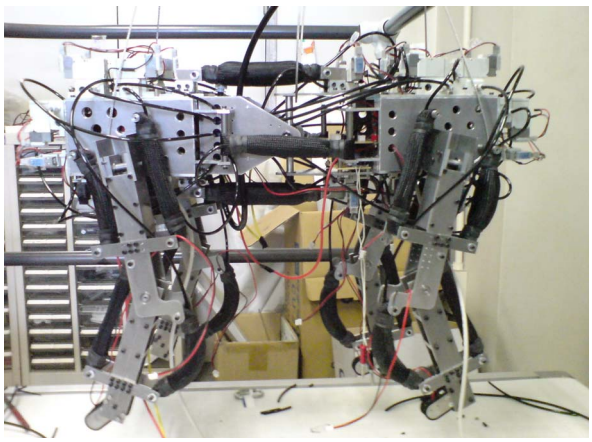

Figure 8: A quadruped robot driven by artificial muscles

V. Construction of a Snake-like Robot Mimicking Musclo-skeletro System of Snake

To understand the locomotion mechanism of a snake, we developed a 3D dynamic simulator, and investigate the behavior together with a neural network model. We confirmed that feedback signal from the force sensors that sense the reaction force against the ground enables adaptive snake-like locomotion by the simulator.

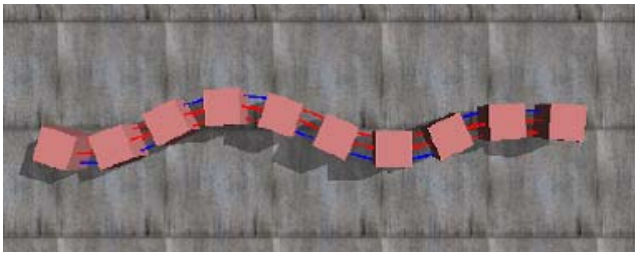

Figure 9: 3D simulation model of a snake-like robot

References

[1] Takashi Takuma and *Koh Hosoda*, "Controlling the Walking Period of a Pneumatic Muscle Walker", International Journal of Robotics Research, Vol.25, No.9, pp.861-866, 2006.

[2] Koh Hosoda, Takashi Takuma, Atsushi Nakamoto, and Shinji Hayashi, "Biped robot design powered by antagonistic pneumatic actuators for multi-modal locomotion", Robotics and Autonomous Systems, Vol.56, No.1, pp.46-53, January 2008.

Neural afferents to the muscular tonus regulating system in the brainstem

Yoshimasa Koyama, Kazumi Takahashi and Tohru Kodama

Abstract—**To understand the brainstem mechanisms for regulation of muscular tonus effects of several kinds of neurotransmitters on the tonus related neurons in the brainstem. In the mesopontine area, the cholinergic neurons in the pedunculopontine tegmental nucleus (PPN) and the glutamatergic neurons in the nucleus pontis oralis (NRPo) have a crucial role in generation of muscular atonia. On the PPN neurons carbachol (cholinergic agonist) and serotonin affected inhibitory, while glutamate and bicuculline ($GABA_A$ receptor antagonist) have excitatory effect. On the NRPo neurons, carbachol had excitatory effect as well as glutamate and bicuculline, while noradorenaline had inhibitory effect. Based upon these findings, the mechanisms in the brainstem for regulation of muscular tonus is discussed.**

1. INTRODUCTION

VARIOUS kinds of motor behavior are based upon appropriate level of muscular tonus which is regulated mainly by the brainstem muscular tonus regulating system. As is shown in Figure 1, the muscular tonus is maintained or facilitated by the noradrenergic (NA) neurons in the locus coeruleus (LC), serotonergic (5HT) neurons in the raphe magnus (RM) and is suppressed by the cholinergic neurons in the pedunculopontine tegmental nucleus (PPN). The cholinergic PPN neurons project to the rostral pons (nucleus reticulalis pontis oralis, NRPo) which through activating the gigantocellular nucleus of medulla (Gc) , suppress the spinal motoneurons, resulting in muscular atonia. On the other hand, the glutamatergic neurons in the midbrain locomotion inducing region (MLR) have a crucial role in inducing locomotion pattern [1].

Yoshimasa Koyama is with Department of Science and Technology, Fukushima University. 1 kanaya-gawa, Fukushima 960-1296, Japan (Phone: 81-24-548-8440; Fax: 81-24-548-2571; e-mail, koyamay@sss.fukushima-u.ac.jp).

Kazumi Takahashi is with Department of Physiology, Fukushima Medical University. 1 hikari-ga-oka, Fukushima 960-1295, Japan (e-mail, takahasi@fmu.ac.jp).

Tohru Kodama is with[1]Department of Psychology, Tokyo Metropolitan Institute for Neuroscience, 2-6 Musashidai, Fuchu, Tokyo 183-8526, Japan (e-mail, hiro@tmin.ac.jp).

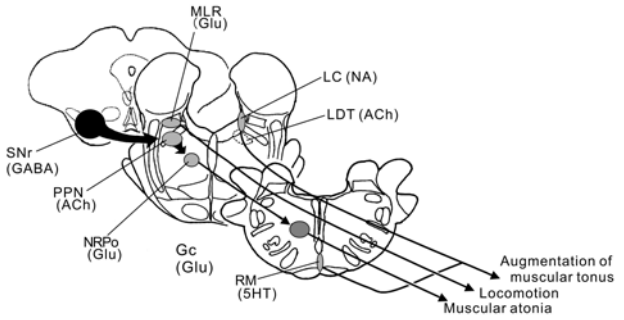

Figure 1 Muscular tonus regulating system in the brainstem

Although the role of the neural groups in the regulation of muscular tonus has been elucidated, the neural inputs to the atonia regulating system are scarcely known. In the present study, we examined the effects of various kinds of neurotransmitters on the cholinergic neurons in the PPN and the glutamatergic neurons in the NRPo which were deeply involved in muscular atonia.

2. METHODS

Since the muscular atonia appears during REM sleep, the neurons are considered to be muscular atonia generating neurons when they are specifically active during REM sleep (muscular atonia period) and send the descending projections to the medulla. So, in the present experiment, single neuronal activity was recorded during sleep-waking cycles in unanesthetized head-restrained cats paying attentions to correlation with REM sleep. Under pentobarbital anesthesia (50 mg/kg), cats received operation for implanting electrodes for electroencephalogram (EEG) and neck muscle activity (EMG) and for embedding acrylate plate to fix the animals to the stereotaxic apparatus. To check the projection of the neurons, stimulation electrodes were implanted to the medulla (Gc) and the thalamus (centromedian nucleus; CM). After more than one week for recovery, cats were fixed to the stereotaxic apparatus (Fig. 2A). Under this condition, cats show normal sleep-waking cycles. Single neuronal activity was recorded through the stainless electrode of 32 μ m in diameter. To apply drugs to the recorded neurons, multibarreled glass pipette with the recording electrode glued to it was used (Fig. 2B). Drugs applied were noradrenaline,

serotonin, cholinergic receptor agonist (carbachol), glutamate, glutamatergic receptor antagonists (5AP, GAMS), GABA and $GABA_A$ receptor antagonists (bicuculline). Drugs were applied iontophoretically to the vicinity of the recording neurons.

The cholinergic newurons in the brainstem are discriminated by a broad action potential**[2]** and by an inhibitory response to acetylcholine itself through the autoreceptors which appear on the soma on all the cholinergic neurons [3, 4].

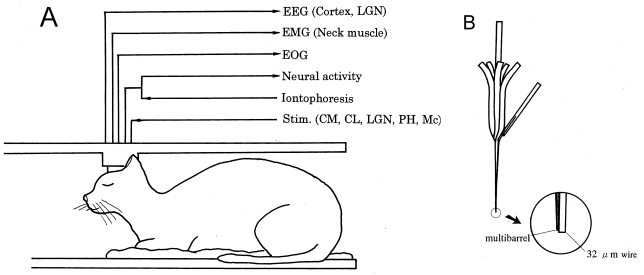

Figure 2 Experimental set up and electrode
A,Fixation of the cat to the stereotaxic apparatus.
B, Assembly of wire electrode for recording and multi-barreled glass pipette for drug application.

3. RESULTS

Figure 3 shows an example of the neurons that increased the activity during REM sleep or atonia period. This neuron was almost silent during waking and slow wave sleep (SWS), then increased the activity more than 30 seconds prior to the initiation of REM sleep and maintained the elevated activity during REM sleep. This kind of neurons are named PS-on neurons (REM sleep is also called paradoxical sleep (PS)). The neuron in Figure 3A was recorded from the PPN and had a broad action potential indicating it to be cholinergic (Fig. 3A upper). Since the stimulations to the thalamus (CM) induced the responses with constant latency, this neurons was judged to send projection to the CM (superimposed traces in Fig 3A lower). The neuron in Figure 3B, which was recorded from the NRPo, had a brief action potential and was considered to be non-cholinergic (probably glutamatergic) (Fig. 3B upper). The superimposed responses to the stimulation to the medulla (Gc) (constant latency) indicate the projection of this neuron to the Gc (Fig. 3B lower).

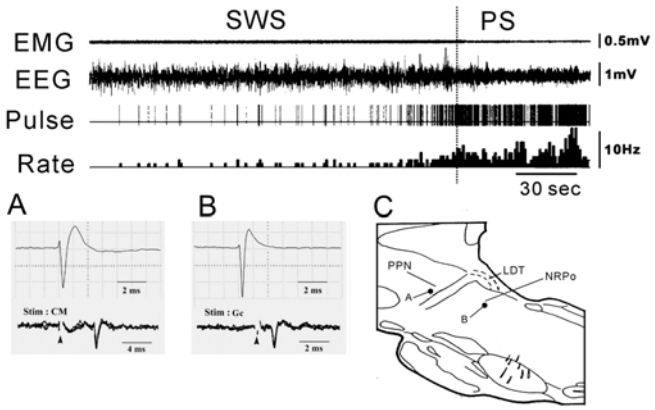

Figure 3 Activity of PS-on neuron during sleep
The neuron increased activity at the transition from slow wave sleep (SWS) to REM sleep (PS) more than 30 seconds prior to the onset of REM sleep (broken line). EMG, electromyogram from the neck muscle. EEG, electroencephalogram. Pulse, transformed action potential. Rate, firing rate of the neuron. A, PS-on neuron recorded from the PPN. Constant latency of the response indicates the projection of this neuron to the CM. B, PS-on neuron recorded from the NRPo. Constant latency of the response indicates the projection of this neuron to the Gc. C, recording sires of neuron A and neuron B.

Figure 4 indicates the effect of neurotransmitters on PS-on neuron in the PPN. With broad action potentials (not shown) and inhibitory response to carbachol (Cb), this neuron was considered to be cholinergic. Activity of this neuron during REM sleep was slightly inhibited by serotonin (5HT), while during waking or silent period (W), glutamate induced discharge.

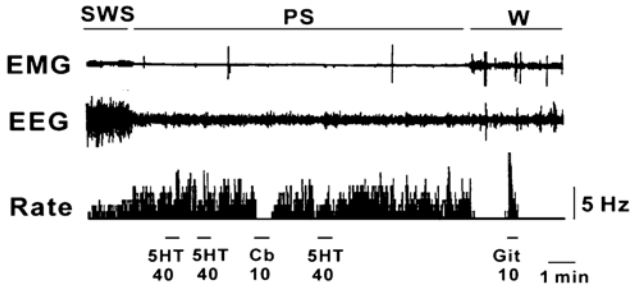

Figure 4 Effect of neurotransmitters on the PPN PS-on neuron
Cb, carbachol. Glt, glutamate. 5HT, serotonin. Numbers indicate the current used for drug application (nA).

Figure 5 shows the effects of glutamatergic receptor antagonists on the elevated activity of the PPN PS-on neuron during REM sleep. When applied during REM sleep, both NMDA receptor antagonist (AP5) and kainate receptor antagonist (GAMS) suppressed the activity of the neuron, indicating that, during REM sleep, the neuron receives the excitatory input from the glutamatergic neurons.

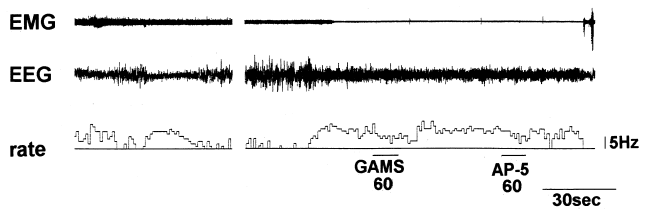

Figure 5 Effect of glutamatergic receptor antagonits on the PPN PS-on neuron
AP-5, NMDA receptor antagonist. GAMS, kainate receptor antagonist

Effect of bicuculline (Bic) on the PPN PS-on neuron is shown in Figure 6. When Bic is applied during silent period (SWS), it caused remarkable excitation in this neuron. The result suggests that this type of neuron receives GABAergic inhibition during waking.

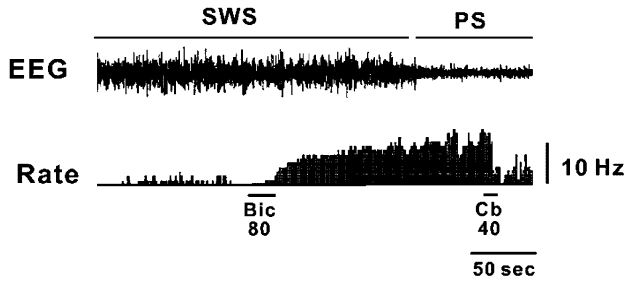

Figure 6 Effect of bicuculline (Bic) and carbachol (Cb) on the PPN PS-on neuron

In contrast to the PPN PS-on neurons, the PS-on neuron in the NRPo that projects to the medulla (Gc) showed excitatory response to Carbachol (Cb), indicating that the neuron was non-cholinergic and receives cholinergic excitation (Fig. 7). This neuron was excited by glutamate (not shown) and was suppressed by noradrenaline (NA), while no response was induced by serotonin (5HT) and histamine (HA).

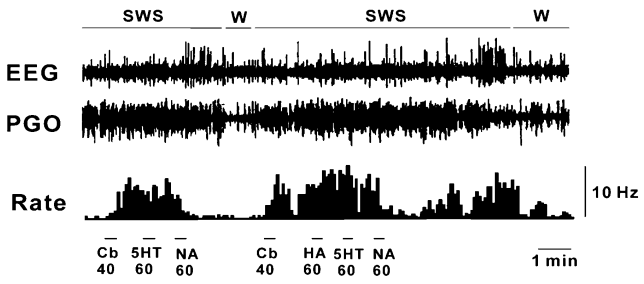

Figure 7 Effect of several neurotransmitters on the NRPo PS-on neuron
Cb, carbachol. HA, histamine. NA, noradrenaline. 5HT, serotonin.

4. SUMMARY

Based upon these findings, the neural mechanisms in the mesopontine area for the regulation of muscular atonia is discussed (Fig. 8).

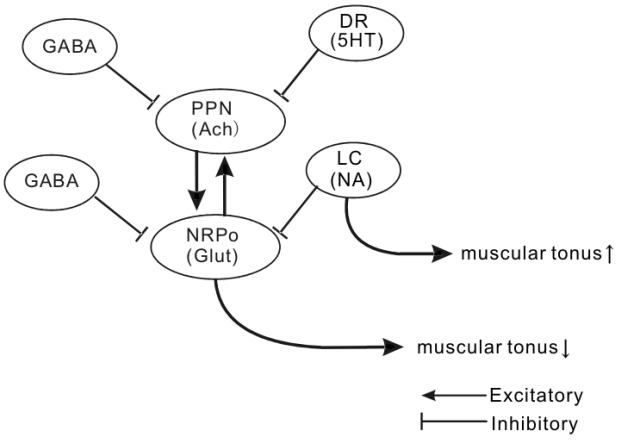

Figure 8 Muscular tonus regulating system in the mesopontine area

The cholinergic neurons in the PPN have the property of PS-on neuron which become specifically active during REM sleep and activating the cholinoceptive NRPo neurons, induce muscular atonia during REM sleep. The PPN cholinergic neurons receive glutamatergic excitation to maintain the elevated activity during REM sleep. Although the origin of the glutamatergic PS-on neurons is not known, it is possible that some of the NRPo PS-on neurons send ascending projection to the PPN to form a reciprocal excitatory loop with the PPN PS-on neurons.

The atonia mediating PS-on neurons are inhibited by the monoaminergic neurons including serotonergic and noradrenergic neurons. The monoaminergic neurons are the most active during waking, decrease the activity during slow wave sleep and become almost silent during REM sleep. They are therefore called waking on (or PS-off) neurons[5]. So, the inhibition of the monoaminergic neurons would work during waking on the atonia mediating neurons to suppress no desirable atonia during waking. Among them, the noradrenergic neurons would be originated from the locus coeruleus (LC), while the serotonergic neurons would be from the dorsal raphe (DR). The atonia mediating neurons would also receive inhibition from the GABAergic neurons. One of the possible candidates of the GABAergic origin is the substantia nigra pars reticulata (SNr) [6]. Similar to the monoaminergic neurons, this kind of GABAergic neurons would be Waking-on type. However, Waking–on type GABAergic neurons have not been identified not only from

the SNr, but also from other GABAergic neuron areas. It is a required future work to identify the Waking–on GABAergic neurons that suppress the atonia mediating neurons during waking.

The orexinergic neurons exert excitatory influences on the monoaminergic neurons (and probably on the GABAergic ones), resulting in suppression of the atonia mediating neurons. In addition to the orexinergic neurons, several kinds of afferents descend from the hypothalamus. So, for the future work, influences of the autonomic nervous system or motivation system on this atonia mediating system would be examined.

REFERENCES

[1] K. Takakusaki, T. Habaguchi, J. Ohtinata-Sugimoto, K. Saitoh and T. Sakamoto. "Basal ganglia efferents to the brainstem centers controlling postural muscle tone and locomotion: a new concept for understanding motor disorders in basal ganglia dysfunction," *Neuroscience*, vol.119, pp.293-308, 2003.

[2] Y. Koyama, T. Honda, M. Kusakabe, Y. Kayama and Y. Sugiura. "In vivo electrophysiological distinction of histochemically-identified cholinergic neurons using extracellular recording and labelling in rat laterodorsal tegmental nucleus," *Neuroscience*, vol.83, pp.1105-1112, 1998.

[3] Y. Koyama and Y. Kayama. "Mutual interactions among cholinergic, noradrenergic and serotonergic neurons studied by ionophoresis of these transmitters in rat brainstem nuclei," *Neuroscience*, vol.55, pp.1117-1126, 1993.

[4] C.S. Leonard and R. Llinas. "Serotonergic and cholinergic inhibition of mesopontine cholinergic neurons controlling REM sleep: an in vitro electrophysiological study," *Neuroscience*, vol.59, pp.309-330, 1994.

[5] B.L. Jacobs. "Overview of the activity brain monoaminergic neurons across the sleep-wake cycle," In: Wauquier A, editor. Sleep: Neurotransmitters and Neuromodurators. New York: Raven Press; 1985.pp.1

[6] K. Takakusaki, K. Takahashi, K. Saitoh, H. Harada, T. Okumura, Y. Kayama and Y. Koyama. "Orexinergic projections to the cat midbrain mediate alternation of emotional behavioural states from locomotion to cataplexy," *J Physiol*, vol.568, pp.1003-1020, 2005.

Study on brain adaptation in rat-machine fusion systems

Takafumi Suzuki*, Kunihiko Mabuchi*

Abstract— **The goal of this research project is to elucidate the brain adaptation function in rat-machine fusion systems. To achieve this goal, we have developed fundamental techniques. These techniques include A) a method for improving the accuracy of walking parameters estimated using neural signals measured in the primary motor cortexes of rats, and B) elemental techniques for long-term stable neural recording using devices such as B-1) an electrode array, B-2) a flexible neural probe with micro fluidic channels for injecting medicines and B-3) an electrode array with a hydraulic positioning system.**

I. Introduction

THE goal of this research project is to elucidate the ability of the brain (specifically the motor center) to adapt to a variable body environment by using a rat-machine fusion system in which the body's environmental conditions are changeable integrated with multi functional neural probes. We plan to construct a "rat car" vehicle system in which the car is controlled by neural signals in the motor cortexes of rats. The system allows us to change the relationship between the motor command signals and the effectors (muscles or the vehicle) arbitrarily. By using multi-recordings of neural signals together with injection and recording of certain medicines into the system, we plan to elucidate the brain property mentioned above.

We have been engaged in developing fundamental techniques to achieve this goal. The techniques includes A) a method for improving the accuracy of walking parameters, such as speed, estimated using the neural signals measured in the primary motor cortexes of rats, and B) elemental techniques for long-term stable neural recording such as a tungsten multi-electrode array, and a flexible neural probe integrated with micro fluidic channels for injecting medicines such as Neural Growth Facto.

II. Results

A) Rat-car system

In this section, the outline of the "RatCar system" will be explained, then the introduction and the potential of internal state model and Kalman filter-like algorithm will be showed.

We have developed a BMI in the form of a small vehicle, which we call the 'RatCar'. A unique point of our RatCar system is that a neural signal source (i.e., a rat) is mounted on the vehicle body and the two components move around as a unit. The rat is therefore provided with somatosensory feedback as the vehicle moves. This enables the rat to realize that its desire to move has been satisfied through the vehicle movement. We expect this condition to increase the ability of the rat to adapt to the system. Our ultimate goat is to illude the rat into recognizing the vehicle as corresponding to its own original limbs, and this will enable use of the RatCar as a platform for future neuroscience research. In addition, the movement of the vehicle system causes electromagnetic noise and artifacts in the recorded signals, an inevitable problem for real applications in hospitals and day to day society. The development of the RatCar system will help us investigate and solve these problems. Here, we focus on basic control of the vehicle movements. We previously built a linear model based on a least squares error approach to estimate the locomotion speed. We have expanded this model to estimate a more generalized locomotion state which includes the speed and changes of directions of a rat's movements. We compared these estimated values to the actual recorded ones, and attempted to control the vehicle.

A block diagram of the RatCar system is shown in Fig.1. First, neural signals are recorded by neural electrodes implanted in the motor cortices of the rat's brain. These are amplified, filtered, and transferred to the A/D converter. Next, neural spikes are detected from the raw signals. A simple template matching technique is used to reduce noises and artifacts. In principle, this part of the system corresponds to the neurons which generated the spike waveform. Finally, the locomotion speed and changes in direction are estimated from the firing rates of spikes in each category.

Signal Recording

We determined the coordinates of the recording sites according to a stereotaxic atlas of the rat brain and functional localization maps. The areas corresponding to the forelimbs and the trunk in the primary motor cortices and the nearby premotor cortices were selected to represent the body movement during locomotion. Next, we fabricated and implanted bundled electrodes consisting of tungsten wires to record signals in the areas described above. Each wire was 40um in diameter and coated with Parylene-C polymer. Its tip was cut off to gain 50 to 100 [k ohm] in impedance, which enabled us to simultaneously record the activities of several neurons around each electrode. The electrodes were tightly fixed on the skull using a resin adhesive and screws cut into the brain. Through the electrodes, the electrical potentials between any two wires were differentially recorded. The signals obtained from the electrodes were amplified by 10,000 times voltage, filtered through 500 Hz to 3kHz (Nihon Koden

*Department of Information Physics and Computing, Graduate School of Information Science and Technology, The University of Tokyo

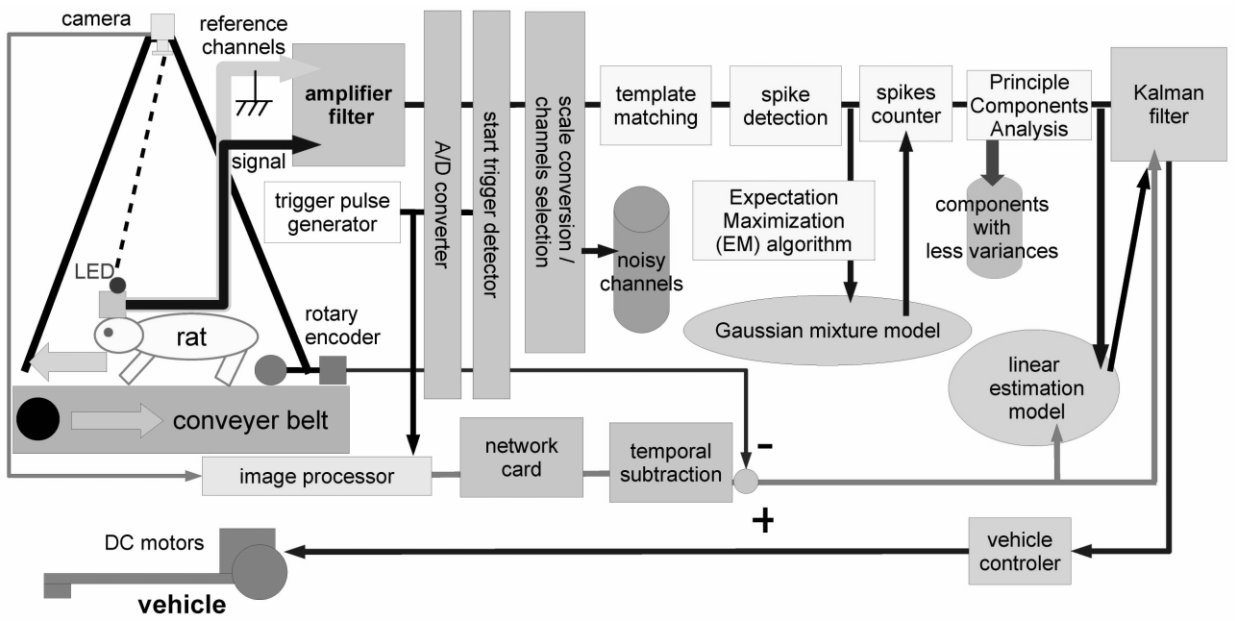

Fig. 1. Block diagram of the RatCar system 10)

MEG-6116), and transmitted to an A/D converter (National Instruments PCI-6071E) installed in a computer. The acquisition rate was 10 kHz for each channel.

Spikes Detection and Discrimination

We applied template matching to the signals acquired in the computer to reduce noise and artifacts. We then detected spike waveforms at the peak amplitudes (i.e., a relative maximum or minimum).

We applied a Gaussian-mixture model (GMM) to the distribution of spike heights, assuming that spikes having similar peak amplitudes originated from the same neuron. The parameters for the Gaussian-mixture were estimated by the expectation-maximization (EM) algorithm while a number of Gaussians were empirically determined. Linear Model for Locomotion Estimation

The muscle activity of the body is expected to change during locomotion. This suggests that variation in the neuronal firing rate will be either positively or negatively correlated to the walking speed. Consequently, we assumed a

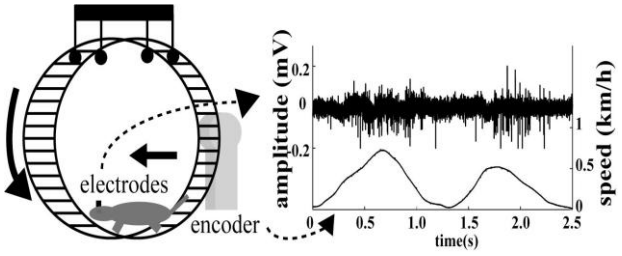

Fig. 2. Simultaneous recording of walking speed and neural signals. Rotation of wheel was recorded with encoder. 9)

model,

$$v(t) = \sum_{n=1}^{N} a_n x_n(t), \tag{1}$$

where the values of a_n are the contribution factors of neuron n having a firing rate of x_n at time t to the locomotion state v. This is the simplest representation describing the correspondence between neural activity and actual movements.

This linear model can be described in matrix form as,

$$X\vec{A} = \tilde{\vec{V}}, \tag{2}$$

where vector A = (a_1, a_2, . . . , a_i, . . . , a_n)T for the contribution factors, matrix X = ($x_{k,i}$) = ($x_i(t = t_k)$) representing the firing rate of each neuron at each time t, and estimated speed vector .V = (.v(t = t_1), . . . , .v(t = t_K))T at each time t. Therefore, vector A can be estimated by minimizing the square error of the actual walking speed V as follows:

$$\vec{A} = (X^{\mathrm{T}}X)^{-1}X^{\mathrm{T}}\vec{V}. \tag{3}$$

For all of these procedures, we used the same channels on the same rat for each trial, but the period of time for the estimation differed from that used to calculate weights (i.e., an open dataset).

1) Forward Speed: We used an animal exercising wheel (Fig. 2) to observe the locomotion speed of a rat as in our previous work . The rat walked without interruption inside the wheel and an encoder attached to the wheel recorded its rotation speed. Neural signals were simultaneously recorded and a firing rate for each neuron was calculated every 100 ms.

2) Changes in Direction: To find the correspondence between neural spikes and changes in direction during locomotion, we built a Y-branch passage for a rat to walk

through.

While a rat was guided to walk through one of the branches (left or right), neural signals were recorded for 1 s before the rat stepped on the detector at the start of each branch. We then assigned a value of -1 or 1 to the locomotion state to specify the weights for a rat walking into either the left or right passage.

We attempted to discriminate which side (left or right) that a rat went to and calculated the sequence of locomotion state values every 100 ms to investigate their variation.

Vehicle Control

According to the estimated locomotion speed and changes in direction, the vehicle was controlled to trace the actual movement of a rat. The vehicle had two DC motors connected to the driving wheels. These were controlled by pulse-width modulated (PWM) signals generated by a D/A converter (National Instruments PCI-6071E) attached to the personal computer.

State space model

This year we have updated the model for estimation of locomotion velocity and direction to an Kalman filter-like algorithm using an internal -state model.

In the discussion below, we used continual time period of 270 s for the test period and we have estimated and valuate the locomotion velocity at every bin of 100ms.

First, we have assume an time invariant model for the generation of neural firing.

$$x_{t+1} = Fx_t + w_t \quad \cdots\cdots (1)$$

$$y_t = Hx_t + v_t \quad \cdots\cdots (2)$$

$V(t)$ is the locomotion velocity vector at time t , $s_n(t)$ is the firing rate of unit n (n = 1,..., N),

$$x_t = (V(t), V(t-1), V(t-2))^{\mathrm{T}}$$

$$y_t = (s_1(t) \cdots s_N(t))$$

$$w_t = x_{t+1} - x_t$$

$$v_t = y_t - Hx_t$$

The state transition matrix F and the output matrix H will be identified using the measured value of x_t, y_t in the first time period 25 ms of the whole data,

$$F \text{ s.t. } \min_F \mathrm{E}\left\{|x_{t+1} - Fx_t|^2\right\}$$

$$H \text{ s.t. } \min_H \mathrm{E}\left\{|y_t - Hx_t|^2\right\}$$

(E{·} shows the expected value.)

Online estimation of the locomotion velocity

We developed an adaptive filter capable of estimate the locomotion velocity x_t from the measured firing rate y_t using a Kalman filter based on the model mentioned above. During the time period of 50 s following to the period for the identification of F and H, we use the measured value of the locomotion velocity as the true value of x_t, and updated the Kalman gain online. Then, we have validated the model by estimation by fixing the Kalman gain using the data of the remaining 190 s.

Result and Discussion

Figure 3 shows the estimated walking velocity of the freely moving rat on the conveyer belt during fixing the Kalman gain (190 s). And figure 4 shows the estimated walking trajectory. In figure 3, the accuracy of the walking velocity estimation is similar to that of our previous model.

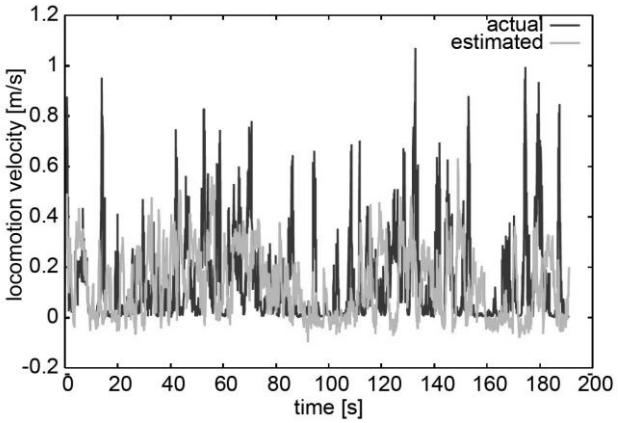

Fig.3 Actual(black) and estimated (gray) walking velocity of the freely moving rat.

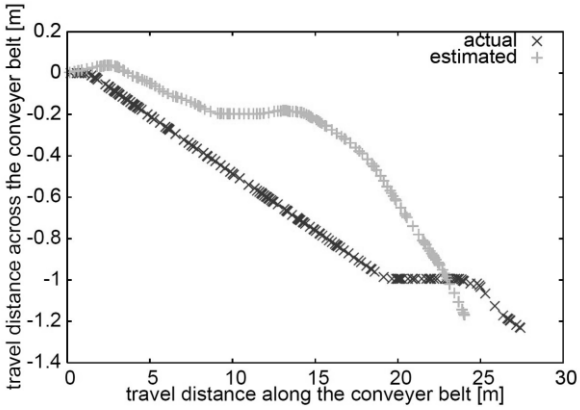

Fig. 4 Actual (black) and estimated (gray) walking trajectory of the freely moving rat.

In this state space model, the change of the parameter has a potential to represent the internal change of the brain itself.

B) Development of multi functional neural probes

We have focused on optimal electrode alignment for brain recording from various target area of the brain for Brain-Machine Interface (BMI) application. We fabricated multi-electrode arrays covering primary motor cortex. The

neural signal of the rat and its locomotion velocity were simultaneously recorded. Estimation of the walking speed was conducted from neural signals using four different recording sites and evaluated anterior electrodes group and posterior electrodes group provided a good estimation, on the other hand two electrode groups around the center gave a bad estimation however it was possible to record neural signals. These result therefore suggested improving estimation using the electrodes which concentrated on the both sides. We have also developed neural probes integrated with micro dialysis probes.

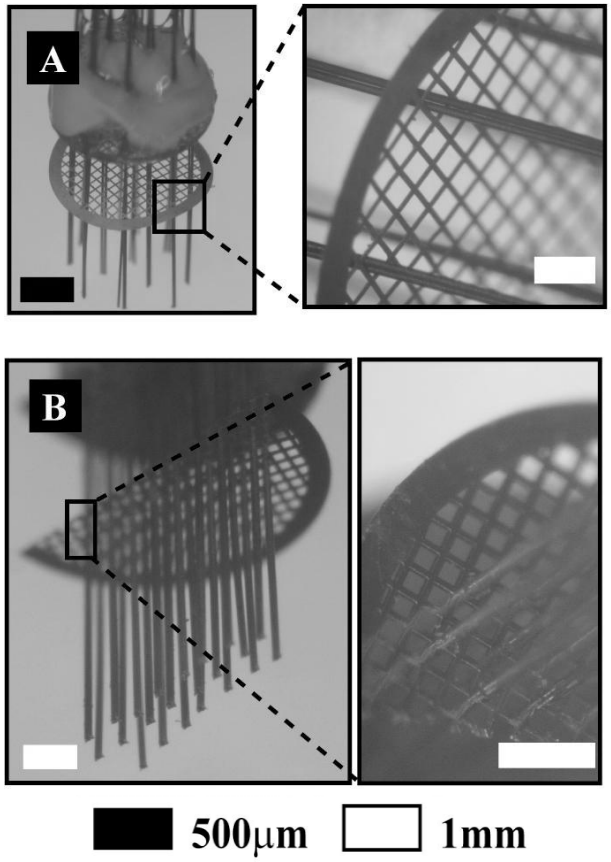

Fig. 5. Optical microscopic images of the multi-electrode array. A: wide, B: three-layer

III. Conclusion

We report the results of this project such as A) Development of RatCar system as a rat-machine fusion system to elucidate the ability of the brain to adapt to a variable body environment, and the introduction of an internal state model to improve the accuracy of walking parameters estimated from the neural signals measured in the primary motor cortex of rats using internal , and B) Development of multi functional neural probes such as an tungsten electrode array capable of easy design for variable targets and a flexible neural probe with micro fluidic channels for injecting and measuring medicines.

IV. References

1) Takafumi Suzuki, Naoki Kotake, Kunihiko Mabuchi, Shoji Takeuchi: Bundled Microfluidic Channels for Nerve Regeneration Electrodes, Proc of the 3rd International IEEE EMBS Conference on Neural Engineering, 17-18 (2007)
2) Takafumi Suzuki, Osamu Fukayama, Noriyuki Taniguchi, Shoji Takeuchi, Kunihiko Mabuchi: BMI system "Rat Car" as a tool for neuroscience, Proc. of the 2nd International Symposium on Mobiligence, 45-46 (2007)
3) Takafumi Suzuki, Osamu Fukayama, Noriyuki Taniguchi, Naoki Kotake, Shoji Takeuchi, Masanari Kunimoto, Kunihiko Mabuchi: Development of neural probes and their applications to neuroprostheses, Japan-Italy International Seminar, (2007)
4) Takashi Sato, Takafumi Suzuki, Kunihiko Mabuchi: Fast automatic template matching for spike sorting based on Davies-Bouldin validation indices, Proc. of 29th International Conference of the IEEE EMBS, 3200-3203 (2007)
5) Tatsuo Okubo, Noriyuki Taniguchi, Osamu Fukayama, Takafumi Suzuki, Kunihiko Mabuchi: Characterization of head pitch cells in rats, Neuroscience 2007, (2007)
6) Takashi Sato, Takafumi Suzuki, Kunihiko Mabuchi: Independent hydraulic positioning for an implantable multi-electrode array, Proc of the 3rd International IEEE EMBS Conference on Neural Engineering, 73-76 (2007)
7) Takashi Sato, Takafumi Suzuki, Kunihiko Mabuchi: A new multi-electrode array design for chronic neural recording, with independent and automatic hydraulic positioning, Journal of Neuroscience Methods, 160, 45-51 (2007)
8) Osamu Fukayama, Noriyuki Taniguchi, Saeri Saito, Takafumi Suzuki, Kunihiko Mabuchi: Control of a Vehicle-formed BMI system for Rats by Neural Signals Recorded in the Motor Cortex, Proc of the 3rd International IEEE EMBS Conference on Neural Engineering, 394-397 (2007)
9) Noriyuki Taniguchi, Takafumi Suzuki, Kunihiko Mabuchi: Biocompatibility of wire electrodes improved by MPC polymer coating, Proc of the 3rd International IEEE EMBS Conference on Neural Engineering, 122-125 (2007)
10) Noriyuki Taniguchi, Osamu Fukayama, Tatsuo Okubo, Takafumi Suzuki, Kunihiko Mabuchi: RatCar System: A vehicle-formed BMI system by neural signals recorded with implantable electrodes, International Symposium on Biological and Physiological Engineering, accepted (2008)

Detection with BMI methods how body movements are involved in neural coding in the brain

Yoshio Sakurai

Graduate School of Letters, Kyoto University

Abstract — The present study is detecting, with multineuronal recording and brain-machine interfaces (BMI), how body movements are involved in neural coding in the brain. In the present year, we have established behavioral learning tasks for rats and have developed a BMI system. As in the previous year, we report that neuronal activity was remarkably changing when the brain was working with the BMI and sharp synchrony of firing among closely neighboring neurons was valid for neuronal coding. We also examined spatial information coded by signals from the soma and dendrite of hippocampal pyramidal cells when the rats were moving in a familiar open environment. We conclude that a hippocampal pyramidal cell has the ability to code different information between its dendrites and the soma. This feature of coding can be applied to construct a new BMI system.

I. INTRODUCTION

Recognition and detection of valid information in the environments are must for animals to behave adaptively, that necessarily require neural coding in the brain. Recent neuroscience studies have suggested that the essential feature of neural coding is highly dynamic and distributed information processing by activity of functional neuron groups, as the famous psychologist D.O.Hebb suggested. However, as the other famous psychologist J.J.Gibson indicated, recognition and detection of valid information need action to and interaction with the environments of much information. This suggests that real features of neuronal coding could be experimentally uncovered by investigating how body movements are involved in neural activity of coding in the working brain of behaving animals.

Ⅱ. PURPOSE

As in the previous year, the present study is detecting, with multineuronal recording and brain-machine interfaces (BMI), how body movements are involved in neural coding in the brain. For that, we establish behavioral learning tasks for rats and develope a BMI system with long-term multineuronal recording. The main brain regions are hippocampal-cortical systems. We are also examining, this year, spatial information coded by signals from the soma and dendrite of hippocampal pyramidal cells when the rats were moving in an open environment.

Ⅲ. ORIGINALITY

The present study rejects the classical neuroscience framework, i.e., recognizing the brain as a simple device which passively percepts and processes incoming information in the environments. Instead, we focus on interactions between neural coding and body movements and aim to experimentally investigate them. To establish the BMI system for the present study, developing and integrating new hardwires and software and collaboration between psychological behavior experiments and neurophysiological recording experiments are required. That is surely a new multidisciplinary project among different fields of science.

Ⅳ. METHODS

We have already constructed a novel system consisting of automatic and real-time spike sorting with independent component analysis (ICA) in combination with a newly developed multi-electrodes for long-term recording from multi-sites of the brain. We are connecting the system with appropriate behavioral tasks for rats and look for valid neuronal activity and synchrony, which can be used as neuronal codes to work the BMI system. We especially focus on the firing

synchrony in the neuronal networks. This year we employ a place navigation task in which rats are moving around in a open field and detect neuronal codes representing information of places.

V. RESULTS

We have developed an unique multi-electrode (dodecatrode) with microdrive for recording of long-term multineuronal activity. This year we developed a specific method of surgery with PC micro screws implanted in the skull surfaces of rats (Fig. 1). This method guarantees stable recording of multi-neuronal activity for longer periods (more than half a year).

Fig. 1 : PC micro screws implanted in the skull surface by surgery. The PC screw has diameter of 1.5 mm and implanted into a hole tapped in the skull. Then microdrives with electrodes are fixed with dental cement.

As a simple behavioral task for rats, we developed approach-nose-poke task and BMI system to perform the task by neuronal activity instead of behavior (Fig.2). First the rats move to the wall in the opposite side of the box to do nose-poke responses to get reward. Then multi-neuronal activity connected to BMI moves the wall to the rats to do nose-poke responses.

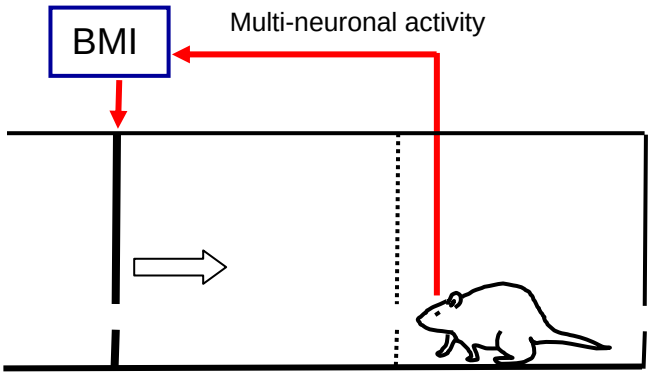

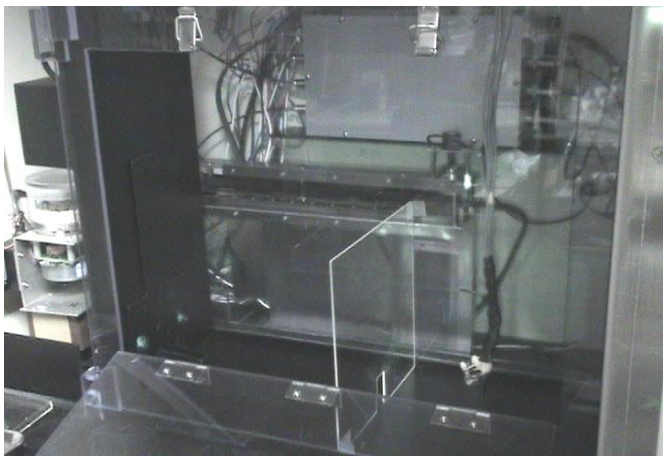

Fig. 2 : The above schema is the approach-nose-poke task and BMI system with multi-neuronal activity. The photo is the apparatus. The black wall on the left side moves to the right side with the pellet dispenser.

We have developed an unique multi-electrode (dodecatrode) with microdrive and a real-time spike sorting system RASICA (Real-time and Automatic Sorting with Independent Component Analysis) and are investigating how hippocampal neuronal activity change when the rat brain is connected to the BMI system based on RASICA (Fig. 3). Multi-neuronal activity was recorded from the hippocampal CA1 and 10 single neurons were automatically separated. The neuronal code instead of nose-poke behavior is a certain firing frequency in a 40 msec time window. The rat soon did not try to access the holes for nose-pokes and the neuronal code frequently appeared in short periods after the experiment started. This change of activity was maintained in the next day (Fig. 4).

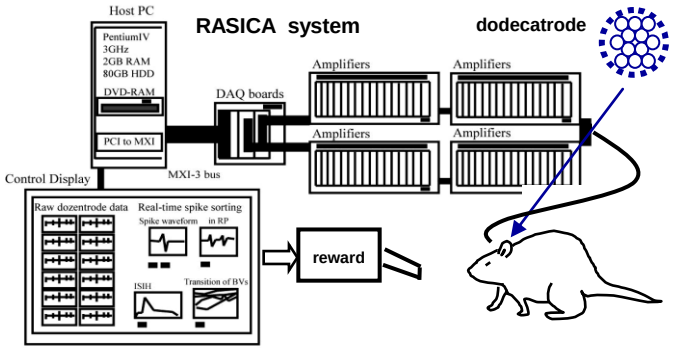

Fig. 3: BMI system with RASICA and dodecatrode. The rat can get reward pellets by generating specific activity of multi-neurons.

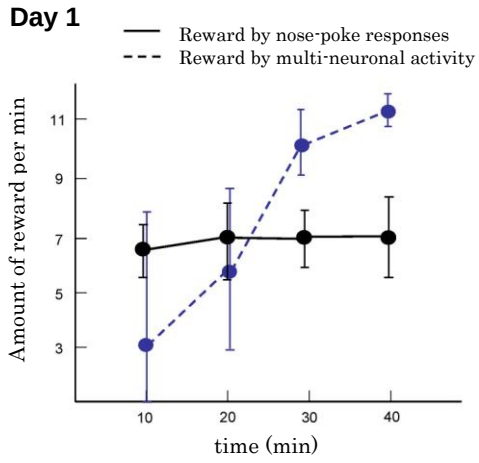

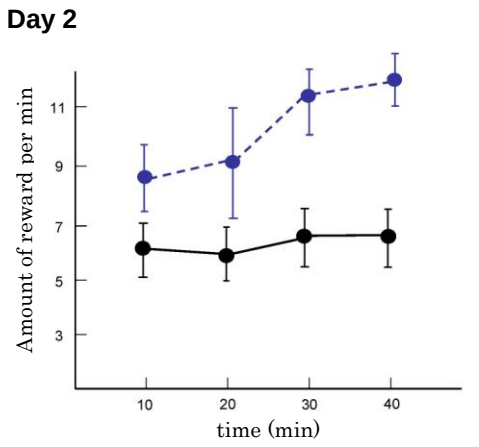

Fig. 4: The thick lines and dotted lines mean amount of reward by behavior (nose-poke) and CA1 neuronal activity respectively. The neuronal activity is a certain firing frequency in a 40 msec time window in 10 neurons.

We succeeded to separate extracellular signals from the soma and those from the dendrite of a single CA1 neuron by the unique method with the dodecatrodes and RASICA Then we examined spatial information coded by spikes from the soma and dendrite of CA1 neurons when the rats were moving in an open environment (Fig. 5). The results indicate that the somatic spikes had single place fields and showed higher spatial specificity than the dendritic spikes (Figs. 6 and 7). Therefore we conclude that a hippocampal pyramidal neuron has the ability to transform redundant spatial information received from upstream neurons via the dendrites into more place-specific information along the dendrosomatic axis.

Fig. 5: The open field for rats to move around. Size is 60cm x 55cm.

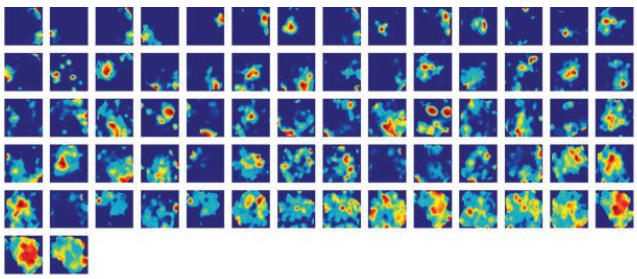

Fig. 6: Spatial firing maps of 72 CA1 neurons. Each panel represents the spatial distribution of the firing for one neuron in the open field. These firings are from dendrites of the neurons. See ref.(1) for detail.

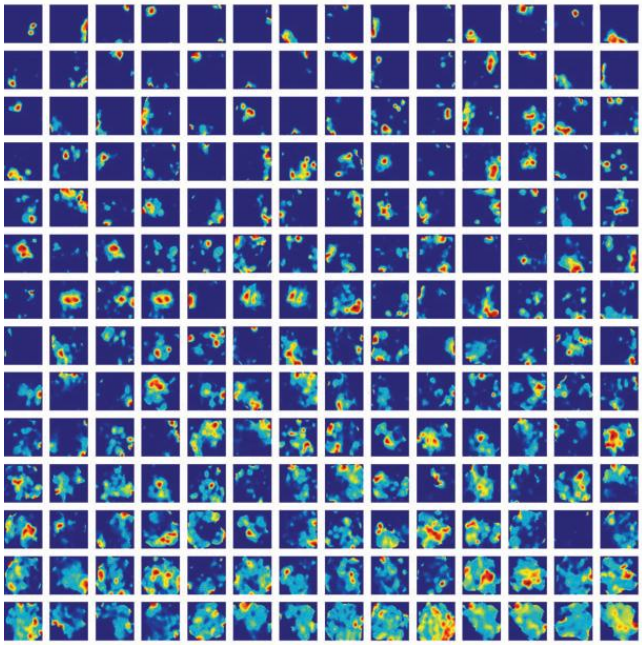

Fig. 7: Spatial firing maps of 196 CA1 neurons. Each panel represents the spatial distribution of the firing for one neuron in the open field. These firings are from somaes of the neurons. See ref.(1) for detail.

ACKNOWLEGEMENTS

The author thanks Dr. Susumu Takahashi, a post-doc researcher of Japan Science and Technology Agency, for collaborating for the present research project.

REFERENCES

(1) Takahashi, S., and Sakurai, Y. (2007) Coding of spatial information by soma and dendrite of pyramidal cells in the hippocampal CA1 of behaving rats. *European Journal of Neuroscience*, 26, 2033-2045.

(2) Nomura, M., Sakurai, Y. and Aoyagi, T.(2007) Analysis of multi-neuroral activities by means of a kernel method. *Journal of Robotics and Mechatronics,* 19, 364-368.

(3) Sakurai, Y. (2007) The present and future of brain-machine interfaces. *System, Control, and Information,* 51, 464-472. (In Japanese)

(4) Sakurai, Y. (2007) *Search for Representation in the Brain* · Kyoto University Press, Kyoto. (In Japanese)

(5) Sakurai, Y., Yagi, T., Koike, Y. and Suzuiki, T. (2007) *The frontiers of brain-machine interfaces.* Kogyo Chosa Kai (Tokyo). (In Japanese)

(6) Sakurai, Y. (2007) How can we detect ensemble coding by cell assembly. In Funahashi, S. (Ed.). *Representation and Brain*. pp.249-270, Springer, Tokyo.

(7) Sakurai, Y. (2007) Brain-machine interface to detect real dynamics of neuronal assemblies in the working brain. In Wu, J.L., Ito, K., Tobimatsu, S., Nishida, T. & Fukuyama, H. (Eds.). *Complex Medical Engineering*. pp.407-412, Springer, Tokyo.

A Multidisciplinary Study of Adjustment Mechanisms of Human Bipedal Gait: Annual Report 2007

Takashi Hanakawa, Kazumi Iseki, Hitoshi Shitara, Manabu Honda, and Hidenao Fukuyama

Abstract — **A hypothetical model of the functional neuroanatomy of human bipedal gait consists of both basal ganglia (BG)-thalamo-cortical and BG-brainstem pathways. It is important to test the validity of this model with various types of gait disorders and to clarify the interaction of this model with signals through sensory organs. First, we report a multi-disciplinary imaging study on patients with gait disorder secondary to age-related white matter changes (ARWMC), which typically reveal mixed hypokinetic and ataxic gait. Twenty elderly patients with ARWMC participated in the study. They were classified into the gait-disordered (GD) group and the intact group (non-GD). All the patients underwent a computerized gait analysis, blood flow activation study, and the assessment of white matter integrity by means of diffusion tensor imaging (DTI). The GD group showed greater double support time and step width, and slower walking velocity, than the non-GD group. Gait-induced blood flow changes were observed in the supplementary motor area (SMA), lateral premotor area (PM), primary motor and somatosensory areas, visual cortex, BG and cerebellum. The group comparison revealed underactivation of the SMA, thalamus, and basal ganglia in the GD group. Activity in these areas was correlated with variables from the gait analysis. A preliminary analysis of DTI indicated that the gait disturbed ARWMC patients had reduced integrity of the white matter neighboring the medial frontal areas and right thalamus/basal ganglia. These results consistently support abnormality in the BG-thalamo-cortical loops underlying gait disturbance in ARWMC patients. Second, to clarify contribution of signal from muscles to brain activity during movement, we performed a simultaneous recording of electromyography (EMG) and functional magnetic resonance imaging of evoked movement by means of transcranial magnetic stimulation. A preliminary result of correlation of motor area activity with EMG signals will be discussed.**

This work was supported by the Grant-in-Aid for the Priority Areas ("Emergence of adaptive motor function through interaction among body, brain and environment"; area 454) from the Ministry of Education, Science, Sports and Culture of Japan.

T. H. is with the Department of Cortical Function Disorders, National Institute of Neuroscience, National Center of Neurology and Psychiatry, Kodaira, Tokyo 187-8522, Japan (corresponding author, phone: 042-341-2711; fax: 042-346-1748; e-mail: hanakawa@ncnp.go.jp).

K. I. is with Human Brain Research Center, Kyoto University Graduate School of Medicine, Kyoto 606-8507, Japan (e-mail: iseki@kuhp.kyoto-u.ac.jp).

H. S. is with the Department of Cortical Function Disorders, National Institute of Neuroscience, National Center of Neurology and Psychiatry, Kodaira, Tokyo 187-8522, Japan (e-mail: h_shitara@nifty.com).

M. H. is with the Department of Cortical Function Disorders, National Institute of Neuroscience, National Center of Neurology and Psychiatry, Kodaira, Tokyo 187-8522, Japan (e-mail: honda@ncnp.go.jp).

H. F. is with Human Brain Research Center, Kyoto University Graduate School of Medicine, Kyoto 606-8507, Japan (e-mail: fukuyama@kuhp.kyoto-u.ac.jp).

I. Introduction

Gait disturbance and dementia are often comorbid in human elderly. These two health problems are a common yet great threat to well-being of the elderly. It is more than just a pity that the abilities that had been acquired through long-term leaning during the infancy and adolescence and flourished in the adulthood are gradually being lost. Especially in Japan where the unprecedented aging society is rapidly approaching, strategies must be developed to deal with the problems of gait and cognitive dysfunction in the elderly population. For this purpose, it is important to clarify the normal neural mechanisms of locomotor adjustment and how its dysfunction causes gait disorders in the elderly.

One of the currently ongoing projects to achieve that ultimate goal concerns multidisciplinary investigation of gait disorders in patients with ischemic white matter lesions prevalent in the elderly. Prevalence of gait disorders increases rapidly after the age of 65, and almost half of the elderly over 85 years old suffers from gait disorders for miscellaneous reasons. Multiple factors associated with senescence make it difficult to clarify the pathophysiology ageing-related gait disorders. Non-neurologic and peripheral factors such as orthopedic problems and neuropathies would partly be responsible for the aging-related gait disorders. However, it is of no doubt that factors of the central nervous system are also responsible. By means of computed tomography (CT) or magnetic resonance imaging (MRI), white matter lesions are highly prevalent in apparently normal elderly people. The term of age-related white matter changes (ARWMC) has been proposed to describe the neuroradiological state of excessive white matter lesions. As well as cognitive impairment, gait disturbance is one of the core symptoms in ARWMC. The pathophysiology of gait disorders in ARWMC patients is scarcely understood and, above all, the multiple and diffuse nature of the white matter lesions makes it difficult to determine the site of responsible lesions. Here we address this issue by combining multiple methods including a computed gait analysis, cerebral blood flow measurement by means of single photon emission computed tomography (SPECT), and the assessment of white matter integrity by means of diffusion tensor imaging (DTI). Results from a preliminary analysis will be discussed.

The second ongoing project concerns the development of methodology to evaluate the effects of peripheral afferents on brain activity during movement, by combining functional MRI, electromyography (EMG) and transcranial magnetic

stimulation (TMS). With neuroimaging technique, it has been difficult to discriminate signals associated with efferent motor commands and those associated with analysis of sensory afferents from the musculocutaneous system. The simultaneous measurement of functional MRI, EMG and TMS should allow us to have an objective measure of sensory afferent signals associated with movement induced by TMS. By examining both induced and voluntary movement, it may be possible to discriminate the motor commands and sensory signals, by varying movement size in both voluntary and induced fashions. Results from a preliminary analysis will be discussed.

II. Multidisciplinary Investigation of Gait Disorders Associated with Age-related White Matter Changes

A. Gait disorders in patients with ARWMC

A mixture of hypokinetic-rigid and ataxic gait is the most typical presentation of the gait disorders in patients with ARWMC. More generally, gait disturbance in patients with ARWMC is characterized by the loss of three gait functions of pivotal importance: locomotion, equilibrium and gait ignition. Failure in gait ignition or freezing may become evident at a later stage of the disease, and loss of postural control may evolve into disequilibrium, frequent falls and, eventually, immobility.

ARWMC patients may manifest prominent Parkinsonian symptoms, which could be evident only in the lower extremities. This peculiar condition may be termed as "lower-body parkinsonism". Such a similarity with Parkinson disease (PD) may help understand the pathophysiology of gait disturbance in ARWMC because mechanisms of gait disorders in PD have been clarified to some extent. Similarly to PD, gait disturbed patients in cerebrovascular disease may find easier to walk when guided by external cues than not. Overactivity in the lateral premotor cortex may be revealed during paradoxical improvement of gait guided by visual cues in PD. Moreover, dysfunction of the supplementary motor areas (SMA) has been indicated as one of the fundamental changes associated with gait disturbance in PD. The abnormality of the BG-thalamo-cortical loops has been proposed as underlying mechanisms of gait disturbance in PD [1], but no direct evidence has been accumulated thus far that gait-disturbed patients with ARWMC share the same pathophysiology.

Several structural MRI studies have produced conflicting results as for the site of lesions responsible for gait disorders in ARWMC. For example, Bazner et al. [2] examined gait disturbance in ARWMC patients by combining structural MRI and gait analyses. It was exemplified that some patients with severe white matter changes did not exhibit severe gait disturbance and patients with characteristic gait disturbance did not necessarily show severe MRI changes.

To clarify the mechanisms of gait disorder in patients with ARWMC, brain activity during walking was measured in patients presenting with various degrees of gait disturbance, by employing a split-dose tracer injection method with SPECT. Further, objective measures of gait disturbance from a computerized gait analysis were utilized for the assessment of the blood flow study.

B. Methods

1) Subjects: Twenty ARWMC patients with Fazekas' grade of 3 and above were recruited [3]. The exclusion criteria were: (i) a history of acute stroke episode in the past one month, (ii) pain in the back or knee, (iii) surgery of the vertebrae or knee in the past six months, (iv) severe brain atrophy, ventricular dilatation, or narrowing of the cerebrospinal fluid space in the superior convexity on MRI, (v) cortical infarction on MRI, and (vi) prescription of anti-Parkinsonian medication. Three neurologists evaluated the status of gait disturbance in each patient recorded on a video, and 11 and 9 patients were classified into the gait-disturbed group (GD) and the non-GD group, respectively. All the patients gave informed consent before participating in the study.

2) Computerized gait analysis: Both the GD and non-GD patients were assessed with a three-dimensional (3D) locomotion analysis system (GATAL-ITS-60, Sumitomo Metal Inc., Osaka, Japan) equipped with 2 force plates and foot switches (9090S, Bertec Inc., OH, USA) located on an 8-m walkway. Following parameters were computed: cadence, gait speed, step length, double support phase, single support phase, and step width.

3) Cerebral blood flow (CBF) measurement: A CBF measurement was conduced on a 3-head SPECT scanner (Prism3000, Picker, OH, USA). The measurement was performed during walking and resting. The half of the patients conducted the gait condition first, and the rest of them did the rest condition first. In the gait-rest order, the patients first walked on a treadmill under the supervision of a medical doctor. They were allowed to grip side bars of the treadmill gently for safety. When walking reached a stable state, a 300-MBq bolus of ^{99m}Tc-ethyl cysteinate dimer (ECD) was administered intravenously through a venous line fixated on the subject's forearm. The subjects kept walking for another 5 minutes after the tracer injection. Then they were moved onto a bed of the SPECT scanner, and were positioned for scanning in a supine position. Scanning lasted for 24 minutes after the first tracer injection. Five minutes after the completion of the first scan, the subjects received the second 500-MBq bolus of ^{99m}Tc-ECD while lying supine on the scanner bed. The second scanning also lasted for 24 minutes. Reconstructed CBF images were analyzed with SPM2. Images were motion corrected, were spatially normalized to fit into a standard stereotaxic space, and were smoothed with an isotropic Gaussian kernel (FWHM = 10 mm). A statistical analysis was performed voxel-by-voxel, which produced statistical parametric mapping of t-statistics.

4) DTI acquisition: DTIs (TR/TE =5200/77 ms, 1.7×1.7×3-mm voxel, 40 slices, 12 directions for motion probing gradients) were acquired for 13 ARWMC patients and 11 age-matched healthy volunteers on a 3-Tesla MRI

(Trio, Siemens, Erlangen, Germany). Fractional anisotropy (FA) images were calculated from the DTIs. The FA images were spatially normalized to fit into a standard stereotaxic space, and were smoothed with an isotropic Gaussian kernel (FWHM = 10 mm). A statistical analysis was performed voxel-by-voxel by SPM2, which produced statistical parametric mapping of t-statistics.

C. Results

1) Gait analysis: The computerized gait analysis showed reduction of walking speed (Fig. 1), reduction of step length, prolongation of double support phase, and wide step width in patients with GD than those without GD.

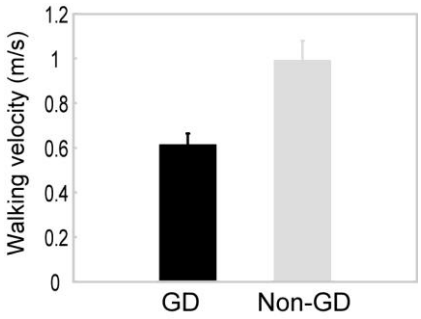

Fig. 1: Reduction of walking speed in patients with gait-disturbed group (ND) than non-GD group. The error bars represent standard error of mean.

2) Blood flow changes during gait: Averaged across all patients, the comparison of CBF changes during the walking condition with those during the rest condition showed activity in the medial fronto-parietal areas, the visual areas, and the cerebellum extending into the dorsal brainstem as previously reported [4]. The group comparison between the GD and non-GD group revealed differences in brain activity in the SMA, right thalamus and basal ganglia (Fig. 2).

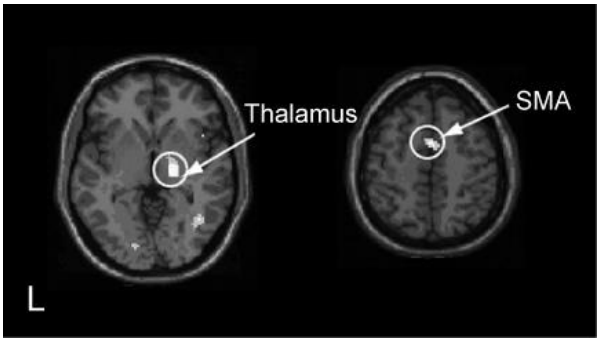

Fig. 2: Underactivity during gait in the GD group as compared with the non-GD group.

3) Correlation of blood flow changes with gait parameters: The double support time per gait cycle (DST/GC) was selected as a single representing parameter of gait disturbance in each patient. The DST/GC was negatively correlated with the gait-induced activity in the SMA ($P < 0.05$) and in the right thalamus ($P < 0.01$).

4) DTI analysis: When the FA images of the GD patients with ARWMC were compared with those of non-GD patients, the GD patient groups showed widespread areas with reduced FA, indicating reduced integrity of the white matter structures (Fig.3). Such areas were pronounced in the white matter neighboring the medial frontal lobe and right thalamus/basal ganglia.

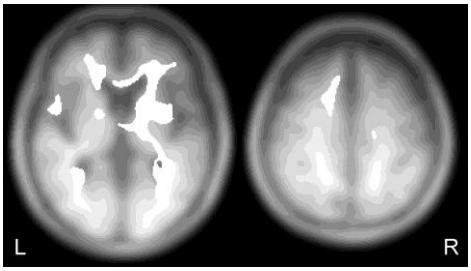

Fig. 3: A preliminary result showing reduced white matter integrity in the GD patients with ARWMC than non-GD elderly subjects.

D. Discussion

The decreased brain activity during gait in the SMA, thalamus, and basal ganglia for the GD group suggested that the dysfunction of the BG-thalamo-cortical loops might be responsible for gait disorders in ARWMC patients. The results from the gait analysis have indicated that the gait disorders in ARWMC are characterized by slow walking speed with shuffling steps and balance instability possibly compensated by wide step width. The negative correlation of DST/GC with brain activity in the thalamus and SMA support that brain activity in the SMA or thalamus reflected gait dysfunction of the ARWMC patients almost in a linear fashion. Overall, these finding are compatible with the idea that gait disorders in ARWMC patients share its pathophysiology, to some extent, with PD.

III. Electromyographic Correlates of Brain Activity during Voluntary and Induced Movements

A. Specific background

With the temporal resolution of currently available fMRI technique, it is virtually impossible to differentiate brain activity reflecting motor commands generating a movement from activity reflecting sensory signals as a result of the movement. In this regard, simultaneous recordings of EMG may provide useful information as a measure of movement size. In addition, the comparison of voluntary movement and induced movement by TMS under EMG monitoring may help discriminate sensory afferents from voluntary motor commands from the viewpoint of brain activity. However, recording and analysis methods still need to be optimized for removing imaging and stimulation artifacts from EMG recordings and for application of EMG-derived information to fMRI analysis. Here we applied a stepping stone sampling (SSS) scheme, originally developed for artifact-free electroencephalogram recording during fMRI [5], to a preliminary study of concurrent TMS-EMG-fMRI.

B. Methods

Participants were 5 right-handed healthy volunteers (mean 22 years old) with neither history of neuro-psychiatric illness nor regular medication. TMS was conducted with a non-ferromagnetic figure-of-eight coil connected to a Magstim Rapid stimulator (Magstim Company Ltd., Wales, UK). Surface EMGs were recorded with shielded Ag/AgCl surface electrodes connected to a SynAmp (NeuroScan Inc., Sterling, VA, USA). EMG data were recorded at a sampling rate of 1 kHz, without any filtering. During fMRI, motor evoked potentials (MEPs) were continuously monitored from the right abductor pollicis brevis (APB) and abductor digiti minimi (ADM) muscles. Individual resting and active motor thresholds (RMT and AMT) were determined with a standard method under EMG monitoring. fMRI was performed at 3 T (Siemens Trio) equipped with a standard head-coil. SSS imaging sequence based on a $T2^*$-weighted gradient-echo EPI (TR/TE= 998/25 ms, flip angle 60°, 3×3×4-mm voxel, 12 slices) was acquired with a nearly coronal slices. The SymAmp was externally driven by the MRI scanner clock. A single pulse TMS was applied to the left M1, with 120% RMT and 90% AMT at inter-stimulus frequency of 0.07-0.125Hz. fMRI data were motion-corrected, distortion-corrected, and pre-analyzed with a model-free independent component analysis tool (FSL) for de-noising, and spatially normalized. A statistical analysis was performed with an event-related design (SPM5), using integrated EMG values (iEMG) of MEP as a parametric modulator of the induced movement events by TMS.

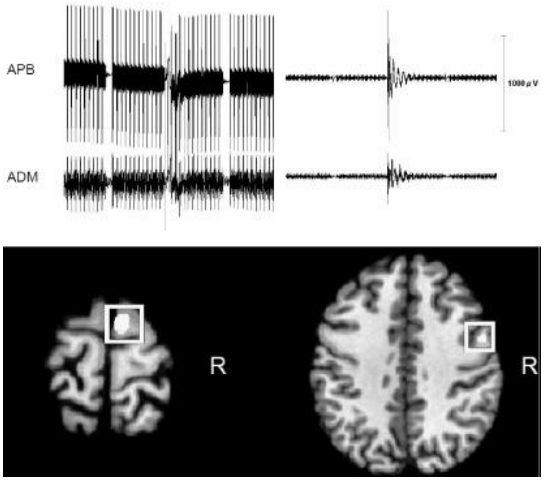

Fig. 4: Raw (left) and artifact-removed (right) EMG data from APB and ADM muscles acquired during fMRI (upper row). Brain activity correlated with iEMG was detected in the SMA and ventral premotor cortex (bottom).

C. Results

With the SSS method, artifact-attenuated surface EMG data were successfully obtained during the fMRI acquisition (Fig. 4). MEPs were clearly detected during TMS stimulation at 120% RMT while they did not at 90% AMT. Brain activity during TMS at 120% RMT included the M1, primary somatosensory cortex and dorsal premotor cortex, but little activation was observed in these areas during TMS at 90% AMT. In contrast, SMA activity was found in both conditions. Brain activity captured by the iEMG parametric modulator involved right SMA, thalamus, middle temporal gyrus, and ventral premotor cortex.

D. Discussion

The SSS scheme was proven useful for detecting MEPs during concurrent TMS- fMRI measurement. It is feasible to detect fMRI activity correlated parametrically with iEMG, but the question why these activities were mainly observed in motor-related areas on the contra-stimulated (contra-movement) side remains to be clarified.

IV. Conclusion

Multi-disciplinary imaging methods have produced consistent results suggesting that the disconnection of the BG-thalamo-cortical loops is responsible for gait disturbance in patients with ARWMC. This result is consistent with the idea that the BG-thalamo-cortical loops are important for human gait. On the other hand, continuing efforts would be needed to understand the contribution of sensory signals to interpret neuronal activity in the motor areas.

Acknowledgment

The authors thank Dr Manabu Nankaku at the Kyoto Universiy Hospital for his technical help for the gait analysis and Dr Hidekazu Tomimoto at Department of Neurology, Kyoto University Graduate School of Medicine for referring patients.

References

[1] T. Hanakawa. “Neuroimaging of standing and walking: Special emphasis on Parkinsonian gait”Parkinsonism Relat. Disord., vol. 12, suppl. 2, pp. S70-S75, October 2006.

[2] H. Bazner, M. Oster, M. Daffertshofer, M. Hennerici. “Assessment of gait in subcortical vascular encephalopathy by computerized analysis: a cross-sectional and longitudinal study” J .Neurol., vol. 247, no. 11, pp. 841-849, November 2000.

[3] F. Fazekas, J. B. Chawluk, A. Alavi, H. I. Hurtig, R. A. Zimmerman. “MR signal abnormalities at 1.5T in Alzheimer’s dementia and normal aging” AJR Am. J. Roentgenol vol. 149, no. 2, pp. 421-426, August 1987.

[4] T. Hanakawa, Y. Katsumi, H. Fukuyama, M. Honda, T. Hayashi, J. Kimura, H. Shibasaki. “Mechanisms underlying gait disturbance in Parkinson’s disease: a single photon emission computed tomography study,” Brain vol. 122, part 7, pp. 1271-1281, July 1999.

[5] T. Anami, T. Mori, F. Tanaka, Y. Kawagoe, J. Okamoto, M. Yarita, T. Ohnishi, M. Yumoto, H. Matsuda, O. Saitoh. ”Stepping stone sampling for retrieving artifact-free electroencephalogram during functional magnetic resonance imaging,” Neuroimage, vol. 19, no. 2, Jun 2003.

Neural subsystems involved in the control of hopping locomotion in rabbits: functional implications of descending locomotion driving pathways and peripheral sensory feedback

Kiyoji MATSUYAMA, Masanori ISHIGURO and Mamoru AOKI

Summary: Neural control of locomotion in vertebrates features continuous tripartite interactions between (1) locomotion command signals mediated by descending pathways; (2) spinal central pattern generators; and (3) sensory feedback from active body parts. In this study, we wanted to know how such neural subsystems interact in the control of locomotion in rabbits, of which locomotion is characterized by nonalternating, in phase movements of bilateral hindlimbs, viz. hopping. For this purpose, we investigated influences of 1) partial transection of descending pathways and 2) blocking of sensory feedback on the generation of hopping movements evoked by stimulation to the mesencephalic locomotor region in decerebrate rabbits, and then discussed their functional implications in the control of hopping locomotion.

I. Introduction

Locomotion in vertebrates is characterized by coordinated movements of varying parts of the body including all limbs and trunk. The neural control of such locomotion involves continuous interactions between various kinds of neural subsystems which are widely distributed throughout the central nervous system **[1,2]**. Among the subsystems, those in the brainstem and spinal cord are largely involved in the generation and coordination of basic locomotor patterns of the limbs. In the control of such basic locomotion, continuous tripartite interactions between (1) descending command signals mediated by largely reticulospinal (RS) pathways; (2) interneuronal spinal central pattern generators (CPGs); and (3) sensory feedback from the active body parts are necessitated **[1,2]**.

In the present study, we wanted to know functional implications of descending locomotion driving signals and peripheral feedback in the control of locomotion in rabbits. Unlike usual locomotor patterns in many quadrupeds such as cats and dogs, those in rabbits are characterized by nonalternating, in phase hopping movements of bilateral hindlimbs. To specify functional roles of descending locomotion driving signals and sensory feedback in the control of such locomotion, we investigated influences of 1) partial transection of descending pathways including RS pathways and 2) blocking of sensory feedback from active body parts on the generation of hopping movements evoked by stimulation to the mesencephalic locomotion (MLR) in decerebrate rabbits.

Kiyoji Matsuyama: Dept. of Physiology, Sapporo Medical University School of Medicine, South-1, West-17, Chuo-ku, Sapporo 060-8556, Japan. (TEL: +81-11-611-2111, FAX: +81-11-644-1020, e-mail: matsuk@sapmed.ac.jp)

Masanori Ishiguro: Dept. of Physiology, Sapporo Medical University School of Medicine. Address as above.

Mamoru Aoki: Dept. of Physical Therapy, Hokkaido Bunkyo University, Faculty of Human Science, Kogane-cho, Eniwa 061-1408, Japan.

II. Materials and Methods

A. *Surgical procedures*

Experiments were performed on 17 adult male rabbits (New Zealand White) weighing 2-2.5 kg. Under halothane gas anesthesia with oxygen, the animal was surgically decerebrated at the precollicular-post mammillary level. Immediately after the decerebration, gaseous anesthesia was discontinued. The head was then fixed in a stereotaxic apparatus, and the chest and abdominal parts were supported by rubber belts to set the body axis in a horizontal position (Fig 1A). The feet were placed on a smooth floor material (linoleum) matted on a still surface of a treadmill belt. To maintain the reflex standing posture of the hindlimbs, the forelimbs were kept hanging in midair because their lengths are short.

B. *Experimental procedures*

Experiment 1. Partial transection of descending pathways conveying locomotion driving signals

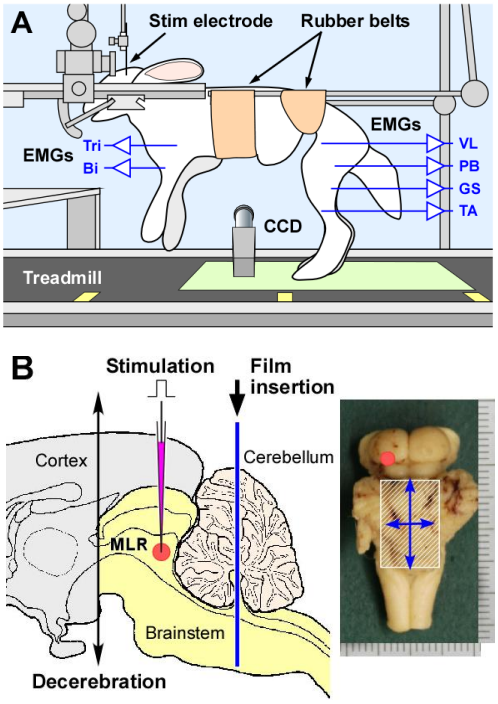

Fig 1. Experimental setup of decerebrate rabbit preparation (A) and midsagittal and dorsal views of the brainstem (B). **A:** Reflex standing posture of the decerebrate rabbit. To record extensor and flexor EMGs of all limbs, pairs of insulated copper wires were implanted into the biceps brachii (Bi) and triceps brachii (Tri) muscles in the forelimbs, and the vastus lateralis (VL), posterior biceps (PB), gastrocnemius-soleus (GS) and tibialis anterior (TA) muscles in the hindlimbs. **B:** Location of the mesencephalic locomotor region (MLR) and methods for partial transection of the brainstem. Arrows in the right photo indicate directions of midsagittal and transverse transection. A hatched area indicates an ablated portion of the cerebellum.

A Wood's metal-filled glass microelectrode with a tip replaced with a carbon fiber was inserted stereotaxically into the MLR of the animal (Fig 1B), and electrical stimuli (50 Hz, 10-110 μA, 0.2 ms duration) were delivered for 5-15 sec to evoke hopping locomotion. EMGs were recorded by implanting pairs of insulated copper wires (diameter 75 μm) into selected extensors and flexors of the four limbs (Fig 1A). Using a CCD camera and a videotape recorder, movements evoked by MLR stimulation were recorded at 60 frames/sec.

After observation of MLR-evoked locomotion, the animal was anesthetized again, and then hemisection of the spinal cord at the lower thoracic and/or upper cervical levels were made. In addition, in some cases, a central portion of the cerebellum including the vermis was ablated to expose the floor of the fourth ventricle. Then, partial transection of the brainstem was made by vertically inserting thin plastic films (width 4~8 mm) through the brainstem to the internal base of skull. After recovery from anesthesia, the MLR was stimulated again, and EMG recordings were made during the evoked locomotion.

Experiment 2. Blocking of sensory feedback from active body parts

After decerebration, the animals were paralyzed with pancuronium bromide (0.2-0.4 mg), and artificially ventilated to maintain the expired CO_2 level at 3.5-5%. Rectal temperature was kept at 35-37 degree.

In the paralyzed animals, the MLR was stimulated (50 Hz, 50-150 μA, 0.2 ms duration, 10-15 sec) to evoke locomotor rhythm without muscle contractions, viz. fictive locomotion, which mostly corresponds to neural outputs of spinal locomotor circuits including CPGs. To monitor such fictive locomotor rhythm, cuff electrodes were placed around the nerves innervating hindlimb extensors and flexors, and then electroneurograms (ENGs) were recorded. In a few cases, hemisection of the lower thoracic cord was additionally made.

Based on findings from experiments 1 and 2, functional implications of descending locomotion driving pathways and peripheral sensory feedbacks in the control of hopping locomotion in rabbits were discussed.

III. Results and Discussions

A. Partial transection of descending pathways conveying locomotion driving signals

In decerebrate rabbits, stimulation to the MLR on one side of the brainstem evokes coordinated hopping movements of bilateral hindlimbs **[3]** (see Fig 2Aa). To diminish descending routes by which locomotion driving signals arising from the MLR are mediated, we made partial transection into the brainstem and spinal cord in decerebrate rabbits, and then investigated their influences on patterns of hopping movements evoked by MLR stimulation.

In a decerebrate rabbit with the right hemisection at the lower thoracic cord of Th12, stimulation to the left MLR evoked hopping movements in the left hindlimb, contralateral to the hemisection, but not in the right hindlimb (Fig 2Ab). As shown in Fig 2B, in a decerebrate animal with the left hemisection at Th12, the left MLR stimulation evoked hopping movements in the right hindlimb, contralateral to the stimulation. Bilateral forelimbs, of which CPGs are located in the cervical cord, exhibited left-right alternating movements during the stimulation.

In an animal with the right hemisection of the upper cervical cord at C2 in addition to Th12, the left MLR stimulation evoked locomotor movements in the left fore- and hind-limbs, but not in the right limbs (Fig 3B). After additional hemisection at the caudal medulla on the left side, MLR stimulation could no longer evoke any locomotor movements in all limbs (Fig 3C).

These findings indicate that locomotion driving signals arising from a unilateral MLR are mediated bilaterally to the spinal cord. Among the signals, those mediated contralaterally would cross the midline at the

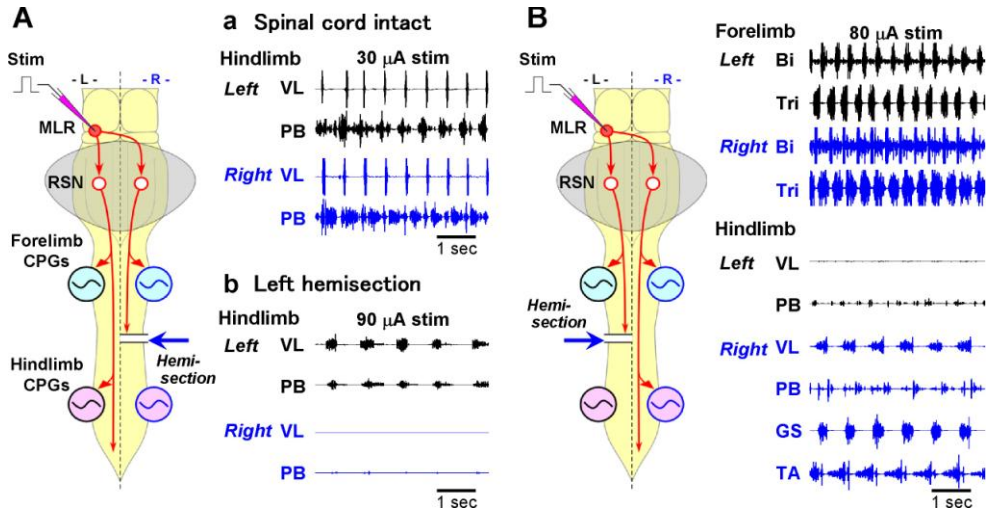

Fig 2. EMG recordings from fore- and hind-limb muscles during the left MLR stimulation in decerebrate rabbits with hemisection of the lower thoracic cord at Th12.

A: EMGs of bilateral hindlimbs before (a) and after (b) the right hemisection. **B:** EMGs of four limbs after the left hemisection. Schematic drawings in A and B illustrates dorsal views of the brainstem and spinal cord. On the drawings, CPGs for fore- and hind-limb locomotion and putative descending pathways that convey locomotor driving signals from the MLR to the spinal cord are superimposed. Thick transverse arrows indicate sides and levels of hemisection of the spinal cord. L, left side; R, right side; RSN, reticulospinal neuron.

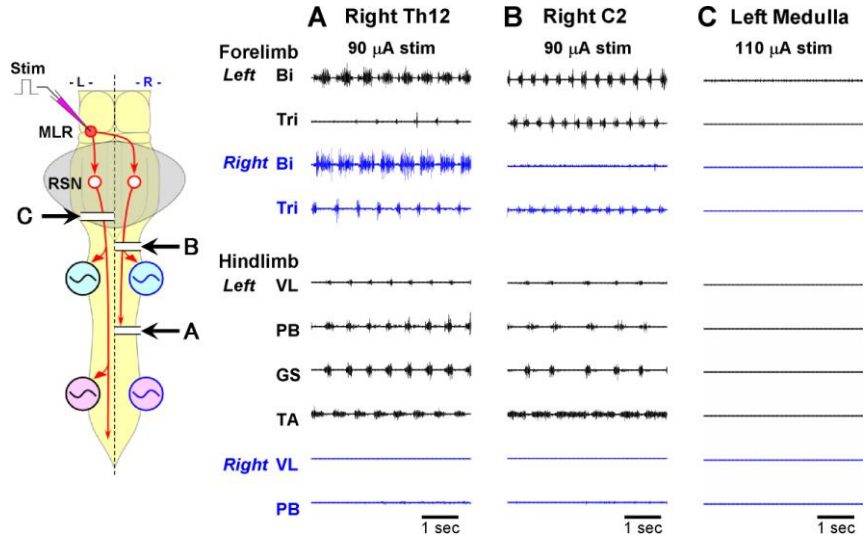

Fig 3. EMG recordings from fore- and hind-limb muscles during the left MLR stimulation after step-by-step hemisection on 3 sites within the spinal cord and brainstem in a decerebrate rabbit.
A: Right hemisection in the lower thoracic cord at Th12. **B:** Right hemisection in the upper cervical cord at C2. **C:** Left hemisection in the caudal medulla.

brainstem level and then descend caudally to the contralateral spinal cord.

To reveal brainstem levels at which locomotion driving signals from the MLR cross the midline, we made partial midsagittal sections into the brainstem, and investigated their influences on the generation of hopping locomotion in decerebrate rabbits. In a decerebrate rabbit with the left Th12 hemisection, as shown in Fig 4B~C, rhythmic EMG activities evoked by MLR stimulation decreased along with rostrocaudal extensions of midsagittal sections in the brainstem. After additional midsagittal section and left hemisection at the caudal medulla, the MLR stimulation could no longer evoke any locomotor movements of all limbs.

These findings indicate that locomotion driving signals from the MLR cross the midline at wide rostrocaudal levels in the brainstem, i.e. from the midbrain to the caudal medulla.

B. Blocking of sensory feedback from active body parts

In the experiments using decerebrate, paralyzed rabbit preparations, it was difficult to obtain reliable ENG recordings from hindlimb nerves, around which cuff electrodes were placed. This might be largely due to weakness of exposed peripheral nerves of rabbits, of which connective tissues including fat were stripped, such that stable ENG recordings would be gradually disturbed.

Fig 5A shows a representative example of ENG activities recorded successfully from extensor (GS) and flexor (PB) nerves of bilateral hindlimbs during MLR-evoked fictive locomotion in a decerebrate, paralyzed rabbit. In this example, GS- and PB-ENGs from identical limbs displayed in phase rhythmic bursts.

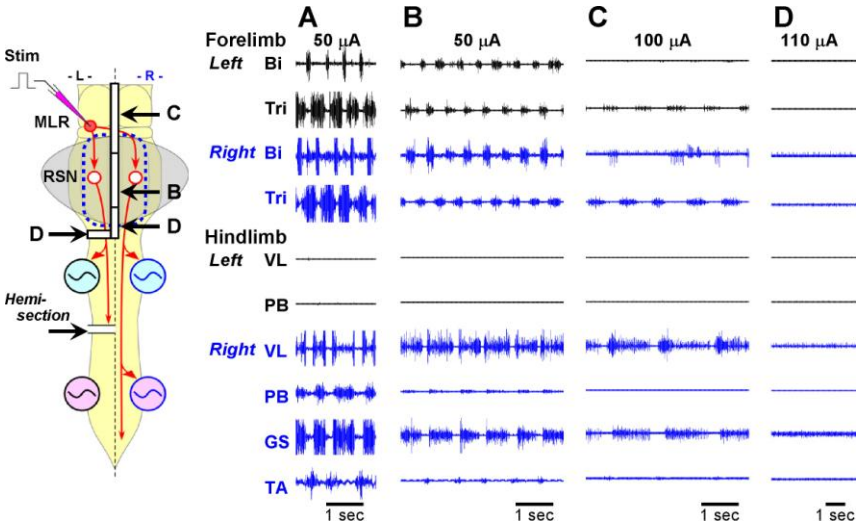

Fig 4. EMG recordings from fore- and hind-limb muscles during the left MLR stimulation after step-by-step brainstem sections in a decerebrate rabbit with the left hemisection at Th12.
A: Left hemisection at Th12. **B:** Midsagittal section in the caudal pons and rostral medulla. **C:** Midsagittal section in the midbrain and rostral pons. **D:** Midsagittal section and hemisection in the caudal medulla. In this animal, a central portion of the cerebellum was ablated to expose the floor of the fourth ventricle (see a region encircled by a dotted line in the drawing).

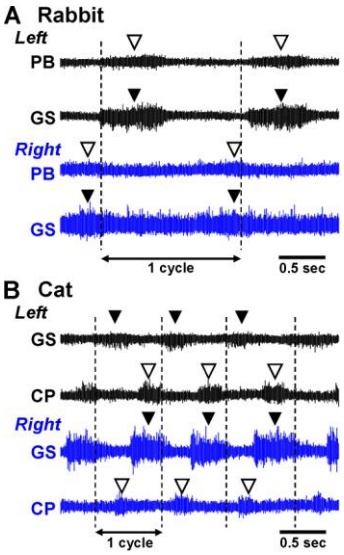

Fig 5. ENG recordings from hindlimb extensor and flexor nerves during MLR-evoked fictive locomotion. **A:** Recordings in a decerebrate, paralyzed rabbit at 90μA stimulation. **B:** Recordings in a decerebrate, paralyzed cat at 150μA stimulation. Dark and white arrow heads indicate bursts of extensor and flexor ENGs, respectively. CP, common peroneal nerve; GS, gastrocnemius-soleus muscles' nerves; PB, biceps femoris muscle nerves.

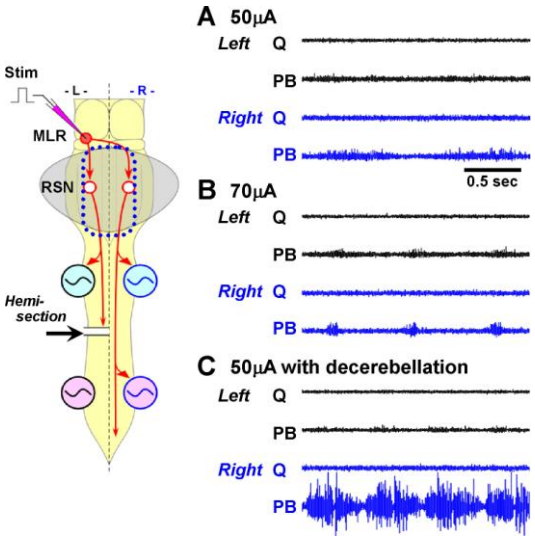

Fig 6. ENG recordings from hindlimb muscle nerves during MLR stimulation in a decerebrate, paralyzed rabbit with the left Th12 hemisection. **A-B:** Recordings during 50μA and 70μA stimulation. **C:** Recordings during 50μA stimulation after decerebellation. In this animal, ENG burst activities were recorded from bilateral PB nerves but not from nerves innervating quadriceps muscles (Q).

This burst pattern well corresponds to EMG activities of GS and PB muscles during MLR-evoked locomotion in decerebrate rabbits (see Figs 3A and 4B).

Fig 5B shows ENG activities of extensor (GS) and flexor (common peroneal, CP) nerves of the hindlimbs during MLR-evoked fictive locomotion in a decerebrate, paralyzed cat. In contrast to the rabbit described above, GS- and CP-ENGs of identical limbs exhibited antiphase rhythmic bursts like rhythmic activities of extensor and flexor EMGs during locomotion in decerebrate cats.

EMGs of homonymous muscles of left and right hindlimbs usually exhibit in phase rhythmic activities during hopping locomotion in decerebrate rabbits (see Fig 2A), while ENGs of left and right homonymous nerves in Fig 5A displayed rhythmic bursts with a phase shift during fictive locomotion (see arrow heads). In decerebrate, paralyzed cats, ENGs of left and right homonymous nerves usually show antiphase rhythmic activities during fictive locomotion (see Fig 5B).

These findings suggest that hindlimb CPGs of rabbits are constituted in a specific manner so as to meet neural substrates which are highly specialized in the generation of hopping movements. In addition to neural outputs of such CPGs, sensory feedback from active body parts should also be necessary to generate coordinated, in phase hopping movements of the hindlimbs. It is known that spinal commissural neuronal (CN) systems in cats are involved in the generation of left-right alternating movements of the limbs during locomotion **[4, 5]**.

In a decerebrate, paralyzed rabbit with the left hemisection at Th12, the left MLR was stimulated and its effects were investigated (Fig 6). During the stimulation, rhythmic ENG activities were recorded from PB nerve on the right side, ipsilateral to the intact spinal cord. At higher stimulus intensity and after decerebellation, the ENG activities became larger and their cycle frequencies remarkably increased (Fig 6B-C). Furthermore, in this animal, rhythmic ENG activities were recorded from the left PB nerve. Although the ENG activities were much weak, cycle frequencies and timing of the bursts were the same as those of the right PB-ENG.

These findings suggest that locomotion driving signals descending in one side of the spinal cord in rabbits would be possible to activate hindlimb CPGs in the opposite spinal cord although such crossed actions might be weak and supplementary. It is known that in cats, spinal CN systems could mediate descending RS actions to the opposite spinal cord **[6]**. In rabbits, in addition to crossed actions of spinal CN systems, synchronized locomotion driving signals descending through bilateral RS pathways together with sensory feedback from active body parts should also be necessary to coordinate and integrate activities of hindlimb CPGs on both sides and then generate a full pattern of hopping locomotion.

References

1. Grillner S (1981) Control of locomotion in bipeds, tetrapods, and fish. In: Handbook of Physiology, Section 1, The Nervous system, Vol.2 Motor Control, pp.1179-1236.
2. Stein PSG, Grillner S, Selverston AI, Stuart DG (eds) (1997) Neurons, Networks, and Motor Behavior. MIT Press.
3. Matsuyama K, Kobayashi S, Ishiguro M, Aoki M. (2007) Brainstem-spinal cord mechanisms involved in the generation of coordinated hopping locomotion in rabbits. Proceedings of The 2nd International Symposium on Mobiligence. p157-160.
4. Matsuyama K, Nakajima K, Mori F, Aoki M, Mori S (2004) Lumbar commissural interneurons with reticulospinal inputs in the cat: morphology and discharge patterns during fictive locomotion. J Comp Neurol 474:546-561.
5. Matsuyama K, Kobayashi S, Aoki M (2006) Projection patterns of lamina VIII commissural neurons in the lumbar spinal cord of the adult cat: an anterograde neural tracing study. Neuroscience 140:203-218.
6. Jankowska E, Hammar I, Slawinska U, Maleszak K, Edgley SA (2003) Neuronal basis of crossed actions from the reticular formation on feline hindlimb motoneurons. J Neurosci 23:1867-1878.

An Approach toward the Modeling of the Motion Control

Taishin Nomura (Osaka University), Ikuko Nishikawa (Ritsumeikan University)
and Yasuaki Kuroe (Kyoto Institute of Technology)

***Abstract*— Two approaches are reported for the modeling of the motion control The first one presents a control model of body sway in quiet standing, which aims at achieving bounded stability by means of an intermittent control mechanism. Control bursts are generated when the current state vector exits an area of uncertainty around the reference point in the phase plane. This area is determined by the limited resolution of proprioceptive signals and the burst generation mechanism is predictive in the sense that it incorporates a rough but working knowledge (internal model) of the biomechanics of the human inverted pendulum. We show that such a model, in spite of its simplicity and of the fact that it relies on very noisy measurements, is robust and can explain in a detailed way the measured sway patterns. The second is a neural network model of the lateral accessory lobe and ventral protocerebrum of Bombyx mori to generate the flip-flop activity.**

I. Bounded stability of the quiet standing posture: an intermittent control model

A. Background and research purpose

The human upright posture against gravity during quiet stance is maintained mostly by the ankle torque. In spite of the mechanical instability of the standing body, the posture is stable, but is it asymptotically stable? Asymptotic stability is indeed a very strong form of stability: it implies that the controller (including the actuators) can enforce a continuous, converging force field, attracting the body to an equilibrium state. Two possible implementation mechanisms of the attractive force field can be formulated: 1) actuator stiffness and 2) positional feedback (supplemented by derivative and/or integral components). The stiffness control hypothesis was proposed by Winter et al. (2001) but direct measurements of ankle stiffness (Loram and Lakie 2002, Casadio et al. 2005) failed to find sufficient levels of stiffness, which in fact ranges between 60% and 90% of the critical value determined by the destabilizing gravity torque. Moreover, EMG recordings of the ankle muscles during postural sway (Gatev et al. 1999, Loram et al. 2005, Nomura et al. 2007) do not provide any hint of a robust coactivation of muscles that, in theory, could induce a sufficient degree of stiffness and recent measurements of the contractile to series elastic stiffness ratio of the calf muscles (Loram et al 2007) rule out even this possible mechanism of stiffness control, because ankle stiffness appears to be mainly determined by the compliant tendon: as a consequence, coactivation of the stiffer muscles would only have a minor effect on the ankle stiffness. The alternative control mechanism for achieving asymptotic stability, either in the form of a PD (Proportional + Derivative) controller (Masani et al. 2006) or a PID (Proportional + Integral + Derivative) controller (Peterka 2000, 2002) runs into other types of difficulties: although feedback gain parameters can be identified that stabilize the system, the stability margin is quite narrow, if we consider the large delays induced by segmental and supra-segmental loops. Moreover, since the stability achieved by a PD or PID controller can only be asymptotic, the residual sway movements are totally noise-driven and must be attributed to neural noise sources, in the sensory and/or motor part of the system.

However, asymptotic stability is not the only form of stability. A weaker form is bounded stability, where the control actions confine the system state in a small neighbourhood of the equilibrium state, although are unable to keep it there. This kind of stability can be obtained by an intermittent controller, where stabilizing control actions occur in bursts and are eventdriven. The control scheme is robust but even in the absence of noise is unable to damp out sway movements that remain persistent within a confined area. Thus, in this framework persistent sway patterns are not noise-driven but are the result of a limited-resolution control mechanism.

The intermittent nature of the control actions has been suggested by the analysis of posturographic patterns , EMG signals , and the sway trajectories of the center of mass in the quasi-phase plane.

It is relatively easy and straightforward to formulate and simulate a continuous time postural control model based on linear feedback, driven by suitable noise sources; the model parameters can be tuned in such a way to reproduce many features of natural sway patterns, as shown by previous studies.

On the contrary, little effort has been put in the design and experimental validation of intermittent, non linear control models, with the exception of a recent paper by van der Kooij and de Vlugt (2007). In this paper we describe a candidate model that can stabilise a humanlike inverted pendulum without enforcing asymptotic stability either by means of a very high intrinsic ankle stiffness or a strong and precise continuous sway feedback. The model is very robust because it can operate successfully with large delays and very low resolution afferent signals. We analyse the sway movements generated by the model and we compare them with natural sway, by using a number of posturographic indicators. It appears that the model captures the subtle structure of postural oscillations, including features that cannot be reproduced by continuous time, linear control, namely the bimodal distribution of sway patterns and the on-off structure of the gravity-related diagram, which displays the time course of the instantaneous correlation between sway

and fall. The parameters of the proposed model were derived from the analysis of experimental sway patterns not from an optimisation method. The comparison with PD-like models is carried out in qualitative and quantitative terms. In the latter case, we consider a specific PD model: the model proposed by Masani et al (2006), who carried out a thorough sensitivity analysis and identified regions of stability in parametric space. In order to have a fair comparison we chose a set of parameters that fall in the middle of the region of stability1.

We wish to emphasize the fact that our analysis is restricted to quiet standing. Postural stabilization in response to external or self-generated disturbances (anticipatory postural adjustments) as well as voluntary sway shifts require additional control levels. The proposed intermittent stabilization mechanism is intended to be only the innermost control layer.

B. Discussion

We have shown that a simple intermittent control model can explain the variability and, at the same time, the bounded stability of sway patterns in quiet standing.

This is not the only example of biological intermittent feedback control. Another well known case, for instance, is the control mechanism of saccadic eye movements. In both cases, in our opinion, the evolutionary pressure to choose the intermittent design instead of the apparently more straightforward continuous time feedback design comes from the need to overcome the potential instability due to the propagation delays in the control loop. In the saccadic system, in which the mechanical plan t is stable although quite laggish, stability of the feedback control could be achieved easily by means of suitably low values of the loop gain, but this would reduce the speed of the movements by at least an order of magnitude with respect to the observed values. The saccadic intermittent control, on the contrary, closes the loop only at specific time instants and at those instants triggers maximal bursts modulated in time (phasic commands) on top of the eye position-dependent tonic activity. Propagation delays do not affect stability but only determine a delay in the response delivery. In posture control the mechanical plant is unstable, to start with, and keeping the loop closed all the time makes the overall stability a real challenge. It is also worth mentioning that performing saccadic eye movements improves postural control (Rougier and Garin 2007) as regards a reduction of the amplitude of the CoP and CoP-CoM signals, whereas simple blinking does not: considering that the average frequency of saccadic eye movements is quite similar to the estimated frequency of posturographic bursts in the intermittent control model, one might envisage some form of mutually beneficial entraining among the two control mechanisms, to be tested in suitable experimental paradigms.

II. A Neural network model of the premotor center of Bombyx mori

The lateral accessory lobe (LAL) and the ventral protocerebrum (VPC) are known to form a premotor center of brain in insects. The present report focuses on the neural network of the LAL-VPC of Bombyx mori, which is known, from the neuroethological experiments, to generate the pheromone oriented behavior composed of a sequential activity of surge, zigzag-turn and loop. The physiological experiments partly elucidate the information pathway which is evoked by a pheromone stimulus given to antennal lobe (AL) and finally projected to LAL-VPC to generate a motor command to thoracic motor systems. The LAL-VPC regions have been characteristically considered to be similar to the electric flip-flop circuit by the records of response from the descending neurons (DN). Moreover, electrophysiological and immunohistochemical studies enable the morphological and physiological classification of each LAL-VPC neuron, and show possible anatomical connection among the neurons.

We propose a neural network model in which a connection between a pair of neurons is intermediated by a region, which is call a neuropile. This is based on the experimental finding that both LAL and VPC in each hemisphere consist of two compartments. Therefore, our model assumes four regions (or additional fifth region according to the new report), and each neuron possesses input branches from one or more regions and output branches to one or more regions. The temporal activity of each region is given by the weighted summation of the inputs from the corresponding neurons, and it gives the outputs to the corresponding neurons. In other words, a kind of mean field coupling through the neuropile region is assumed, and thus the connection from i-th neuron to j-th neuron is decomposed into two connections from i-th neuron to the region, and from the region to j-th neuron.

The goal of this study is to estimate the weights of the anatomically observed connections to elucidate the main pathway of the information processing to generate the characteristic flip-flop activity in LAL-VPC, under the constraints that the stimulus-evoked activities of all regions and all LAL-VPC neurons are consistent with the physiologically observed response activities of all neurons. At the first step, the possible connection weight patterns are searched by the optimization of an evaluation function, which measures and evaluates the degree of the above consistency using a static model. Then, a neural network simulator is applied to verify whether the obtained connection is able to reproduce the temporal activity with alternating flip-flop patterns between both hemispheres. All of experimentally observed LAL-VPC neurons with a physiological classification is considered in our simulator, and the dynamics of each model neuron is given by a simple integrate-and-fire model.

The search of the connection patterns with high evaluation scores are executed, and some characteristic patterns are obtained from the statistics of the highest groups. On the other hand, the simulator shows an alternating firing between both hemispheres when the post inhibitory rebound firing (PIR) is taken into the consideration. The details of the obtained connection patterns and the verification by the simulator will be reported in a conference paper.

Coherent activities between spinal cord and muscles in monkeys performing a precision grip task

Tomohiko Takei & Kazuhiko SEKI

***Summary*—In this study, we recorded local field potentials (LFPs) from cervical spinal cord (C5-C8) in monkeys performing a precision grip task, and examined their coherence with electromyographic activities (EMGs) (spinomuscular coherence) recorded from hand and arm muscles. Among 168 LFP-EMG pairs, significant coherence was found in 68 pairs (40%). We classified the coherence into two groups based on its frequency range, narrowband coherence and broadband coherence. The narrowband coherence was restricted to between 10-40 Hz and was widespread throughout the superficial and deep gray matter. In contrast, the broadband coherence distributed between 10-95 Hz and was found only in the ventral half of the spinal cord. The narrowband coherence suggests that oscillations, which have been described in many motor control areas of the brain, could also pass though spinal interneurons to affect motor output and sensorimotor integration. On the other hand, the broadband coherence could be a unique feature of spinal motoneuron - muscle physiology.**

I. Introduction

Rhythmic oscillatory activity has commonly been observed in the mammalian central nervous systems (CNS) and elucidating its significance in regulating behavior is an important question in neuroscience (MacKay 1997). This oscillatory activity may have a role in controlling volitional movement since it has been found in various key motor control areas. Oscillatory activity in the primary motor cortex (M1) seems to be involved in controlling finger movements. For example, M1 local field potentials (LFPs) exhibit oscillations around 15-35 Hz (beta-band) during precision grip performance in monkeys (Baker et al. 1997), as originally found in human subjects performing isometric finger contractions (Conway et al. 1995), which are dynamically coherent with electromyographic activities (EMGs) (corticomuscular coherence) (Baker et al. 1997).

Sensory input from peripheral afferent neurons is also known to affect the beta-band oscillations in the motor system. Digital nerve anesthesia (Fisher et al. 2002) or deafferentation (Kilner et al. 2004) reduces the coherence between different agonist muscle EMGs during precision grip. Coherence between sensorimotor EEG and EMG of hand and arm muscles is also affected by arm cooling suggesting peripheral afferent and/or efferent pathways contribute to the generation of beta-band coherence (Riddle and Baker 2005). Finally, the direct recording of single-unit activity from the C8/T1 dorsal root ganglia (DRG) in behaving monkeys showed that afferent neurons and muscles exhibit coherent oscillations during wrist movements (Baker et al. 2006). These data strongly implicate afferent input to the central nervous system in the genesis of coherent beta-band oscillations in motor system during voluntary movement.

The spinal cord is the first relay of both afferent and descending pathways and it is well known that spinal interneurons receive highly convergent input from a number of motor centers as well as peripheral afferents (Baldissela et al. 1981). It is reasonable to postulate therefore that oscillatory activity in the descending and afferent pathways is relayed through spinal interneurons, and that spinal interneurons can affect, and can be affected by this oscillatory activity. Therefore it is important to know if coherent oscillations exist in spinal interneurons during movement. However, no previous reports have examined this question in awake, behaving animals. The aims of this study were to determine if the oscillations are present in areas of spinal cord containing spinal interneurons and, if so, are they coherent with similar activity in forelimb muscles during voluntary movement. To this end, we have recorded cervical spinal cord LFPs and forelimb muscle EMGs in monkeys performing a precision grip task.

II. Methods

The data presented here were taken from two male macaca fuscata monkeys (monkey A: 6.8kg and monkey U: 8.5kg). The experiments were performed in accordance with the National Institutes of Health Guidelines for the Care and Use of Laboratory Animals and were approved by the Animal Research Committee at National Institute for Physiological Sciences.

Behavioral task

A monkey was trained to sit in a chair with its right and left elbow restrained whilst it performed a precision grip task using a custom-made manipulandum (Fig.1A,B). Thumb and index finger positions were continuously presented to the monkey via the positions of two rectangle cursors displayed on a screen in front of monkey (Fig.1C). Two target boxes were also displayed and the monkey was required to keep each cursor inside its target box during a trial.

Each trial began with the presentation of two target boxes positioned so that the thumb and index finger were 3.0 cm apart ('Trial Start', Fig.1C). After 1.0-2.0 sec, the "out"

This work was supported in part by the Ministry of Education, Culture, Sports, Science, and Technology, Grant-in-Aid for Scientific Research on Priority Areas (No.454).

K. SEKI and T.Takei are with Department of developmental physiology, the National Institute for physiological sciences, Okazaki, Aichi 444-8585 JAPAN (phone: 0564-55-7757; fax: 0564-55-7766; e-mail: kazuseki@nips.ac.jp).

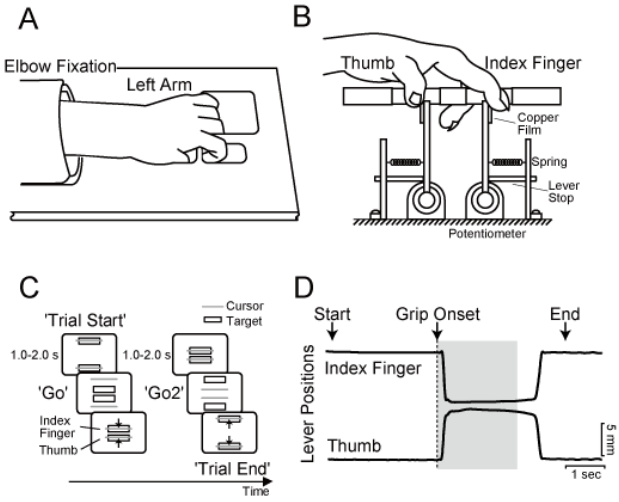

Figure 1.

Experimental setup. A,B: diagrams of the custom-made manipulandum for the precision grip task in top view (A) and lateral view (B). C: Sequence of a trial. Lever positions were reported to the monkey as two visual cursor signals on the computer display (gray bars). Two target boxes were also displayed (black rectangles). D: Example of finger movements during a single trial. Upper arrows indicate the time point of each task event. Two traces show lever positions (upper: index finger, lower: thumb). Shaded area indicates the time range where frequency analyses were performed (from 0 to 2.048 sec after 'Grip Onset').

targets disappeared and two "center" targets appeared simultaneously, signaling monkey to flex its thumb and index finger ('GO') to bring the cursors into the center targets. The required displacement of both fingers was 0.7-1.3 cm (monkey A) and 0.3-0.8 cm (monkey U), which corresponded to a force of 0.9-1.1 N and 0.4-0.6 N, respectively. The monkey was required to maintain the lever positions within the center targets for 1.0-2.0 sec then release them back into the out targets once the center targets disappeared ('GO2'). Successful completion of a trial was rewarded with a drop of applesauce. On average, ca 1500 successful trials/recording session with the success rate of ca 80% were performed by both monkeys.

Surgical operations

After behavioral training was complete, three separate surgeries were performed to implant a head restraint, a recording chamber over the cervical spinal cord, and EMG wire electrodes into multiple forelimb muscles. Two head restraints (plastic tubes) were fixed to the skull with titanium screws and dental acrylic. An oval-shaped spinal recording chamber (Perlmutter et al. 1998) was implanted over the lower cervical spinal cord. For recording EMGs, pairs of stainless steel wires (AS632, Cooner wire) were implanted subcutaneously in 19 muscles.

Recording procedure

During each recording session, a glass-insulated tungsten microelectrode (impedance 1 to 2 MΩ at 1 kHz) was inserted into cervical spinal cord. The signal from the microelectrode was amplified (x1000) and filtered (0.1 Hz – 10 kHz) using a differential amplifier (A-M Systems Model1800) for LFPs. LFPs were digitized at 20 kHz. EMGs were amplified and filtered using a multichannel differential amplifier (SS-6110, Nihon Kohden, x3000-25000, 5 Hz - 3 kHz) and digitized at 5 kHz. Signals from potentiometers, strain gages, and touch sensors were digitized at 1 kHz. All subsequent analyses were performed offline using MATLAB (Mathworks Inc.).

III. Results

LFPs were recorded from 22 sites in the cervical spinal cord (C5-C8, 15 from monkey A and 7 from monkey U). From 299 LFP-EMG pairs recorded, 131 pairs were eliminated because of significant EMG-EMG cross-talk. Consequently, further analysis was performed on 168 LFP-EMG pairs (154 and 14 pairs from monkey A and U, respectively).

Fig.2A and B show LFP power spectra recorded from two separate intraspinal sites. In these spectra, there were peaks at around 15 Hz (A) or 30 Hz (B). Among the LFP power spectra recorded from 22 intraspinal sites, 14 (64%) LFPs showed similar peaks between 10 and 40 Hz. Fig.2C and D show the corresponding power spectra of rectified EMGs recorded from the FDI muscle. Broad peaks around 30 Hz were dominant in both spectra. From the LFP-EMG pairs shown in A-C and B-D, the coherence spectra between LFP and EMG were calculated (E and F, respectively). Although the LFP and EMG power spectra showed similar characteristics in both cases, the coherence spectra were clearly different. The first example (E) shows significant coherence only within a very restricted frequency range between 19.0 and 24.9 Hz (peak width=5.9 Hz, see shaded area in E). In contrast, the second example (F) shows

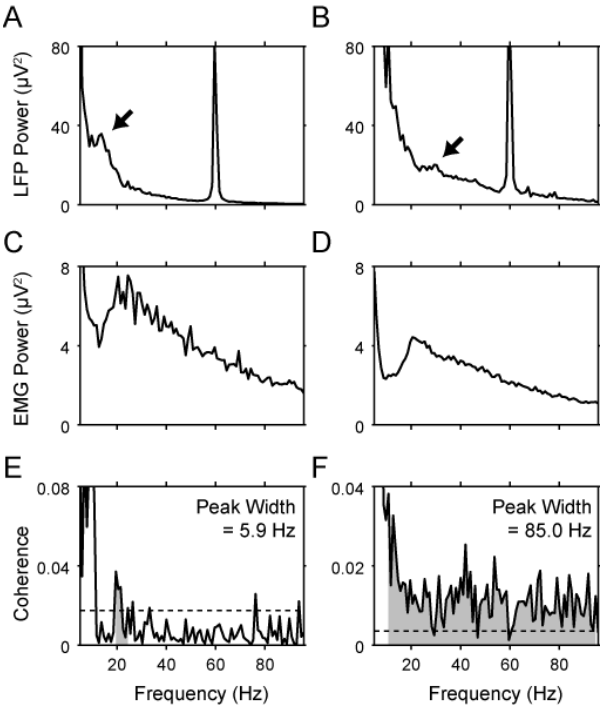

Figure 2.

Two examples of frequency and coherence analyses for LFP and EMG pairs. A,B: power spectra for LFPs recorded from two different intraspinal sites (Monkey A, both from C8 spinal segment). Resolution= 0.98 Hz. Note that peak around 15 Hz (A) or 30 Hz (B) was visible in each spectrum (arrows). C,D: power spectra of rectified EMGs from the first dorsal interosseous (FDI) muscle recorded simultaneously with the LFPs in A,B. E,F: coherence spectra between the LFP and EMG pairs shown in A,B and C,D. Dashed line indicates significance limit ($P < 0.05$) and the shaded area indicates significant coherence peak.

significant coherence over the entire frequency range examined (10.3 to 95.2 Hz, peak width=85.0 Hz, see the shaded area in F).

Among the 168 LFP-EMG pairs, 68 pairs (40%) showed at least one significant peak in their coherent spectrum (60/154 and 8/14 from monkey A and U, respectively). Quantitative comparison amongst these coherence spectra were made by measuring the width of the significant peak in each spectrum (see Fig.2 E and F). Fig.3A shows the distribution of the peak width in the 60 coherent LFP-EMG pairs from monkey A. The width of coherent peak was broadly distributed from about 3 to 85 Hz. For subsequent analysis, LFP-EMG pairs were categorized into two groups: the pairs with a "narrow" coherent peak (<25 Hz, n=50) and the pairs with a "broad" coherent peak (>25 Hz, n=10). Fig.3B-C show the percentage of LFP-EMG pairs with significant coherence peak at a given frequency in the "narrow" group (B) and the "broad" group (C). The dashed

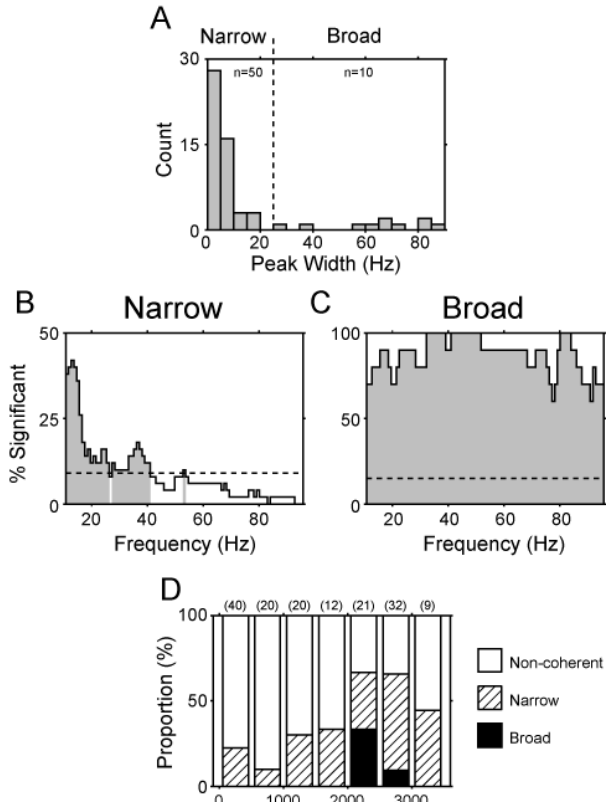

Figure 3.
A: distribution of the width of significant coherence peaks (n=60). LFP-EMG pairs were categorized into two groups: LFP-EMG pairs with narrow coherence peak ("narrow", n=50) and the pairs with broad coherence peak ("broad", n=10), using a criterion of 25 Hz peak width (interrupted line). B, C: percentage of LFP-EMG pairs showing significant coherence peak at each frequency. B: narrowband pairs, C: broadband pairs. Dashed line indicates the significance limit (P < 0.05, binomial test) and the shaded area indicates the significant coherence peaks. D: distribution of broad- and narrow band coherence according to the depth of recording site. The depth of recording site is expressed relative to the depth where unit activity was first recorded in each penetration. Black, hatched and white bars indicate the proportion of broadband, narrowband and non-coherent pairs, respectively. Parenthetic numbers indicate number of pairs classified into each category.

lines indicate the significance limit based on binomial test (P < 0.05). The bins that exceeded this significance limit were restricted to 10-40 Hz in the "narrow" group. On the other hand, these significant bins were distributed almost all frequency range in the "broad" group. From these results, we have concluded that the spinomuscular coherence occurred in two different modes, narrowband coherence (NB) and broadband coherence (BB). The dominant coherence frequency was restricted to 10-40 Hz in NB and occurred at all frequencies examined (10-95 Hz) in BB.

To further characterize these two modes of coherence, they were analyzed with respect to depth of the recording sites in the spinal cord (Fig.3D). The proportion of LFP-EMG pairs with significant coherence (NB or BB) was not uniformly distributed with depth in the spinal cord, rather it was unimodal with a peak at 2500 μm. Interestingly, the NB (hatched) was present at every depth while the BB (filled) was restricted to depths between 2000-3000 μm. This difference indicates that the BB is restricted to the ventral portion of spinal cord whereas the NB can be found throughout dorsal and ventral spinal cord. A part of these observations has been confirmed in the second monkey (monkey U). In monkey U, 8 (out of 14) significant pairs could be assigned to NB, their coherent frequencies were within the range of 10.3-18.1 Hz, and their sites were widely distributed throughout the spinal gray matter, similar to the distribution of "narrow" group in Fig.3D.

IV. Discussion

Oscillation of spinal LFP

As shown in Fig.2A-B, a majority (63%) of spinal LFPs exhibited a peak between 10-40 Hz in their power spectrum. These results suggest that spinal interneurons could exhibit oscillatory activity around beta-band frequencies, a phenomenon that has been widely reported in many other motor control areas (Baker et al. 1997, 2003; Marsden et al. 2000; Murthy and Fetz 1992; Ohara et al. 2001; Pellerin and Lamarre 1997). To our knowledge, this is the first report to show that spinal LFPs exhibit oscillation around beta-band frequency in awake, behaving animals.

Coherence between spinal LFP and EMG

Forty% of LFP-EMG pairs showed significant coherence peaks, and this spinomuscular coherence was of two different types, narrowband coherence (NB) and broadband coherence (BB).

Narrowband coherence

NB was distributed widely throughout the spinal gray matter (Fig.3D) and two potential mechanisms for the genesis of NB would be suggested from this result, oscillatory output from- and oscillatory input to the spinal interneurons.

Some of spinal segmental interneurons are known to have direct and indirect projections to motoneurons, and their locations are distributed widely throughout the dorsolateral extent of the spinal gray matter (Perlmutter et al. 1998). If these premotor spinal INs show the oscillatory activity as shown in Fig.2A-B, therefore, their oscillatory outputs may drive oscillations in target motoneurons and muscles during voluntary movement. Similar mechanism has already been proposed in the primary motor cortex (M1) and corticomuscular coherence. In M1, the oscillatory activity of corticospinal cells, which have direct and indirect connections to

motoneurons, is proposed to be a source of corticomuscular coherence during voluntary movement (Baker et al. 1997).

On the other hand, abundant afferent fibers are known to terminate within the spinal gray matter, and the location of these terminals also distributed widely throughout the dorsolateral extent of the spinal gray matter (Brown 1981). Therefore, if the oscillatory muscle activity (Piper 1912) induces oscillatory afferent activity, it could also drive oscillation in spinal neurons and LFPs. In fact, group Ia and cutaneous primary afferents, both of which are known to have highly divergent intraspinal projections (Brown 1981), show oscillatory firing and coherence with EMGs during precision grip (Baker et al. 2006).

Broadband coherence (BB)

Another type of spinomuscular coherence described in the present study exhibited a much wider range of coherent frequencies (10-95 Hz) suggesting synchronous activity of LFPs and EMGs in a wider frequency band. In contrast to the NB, the BB was recorded only from the ventral portion of the spinal cord (Fig.3D). The most likely source of this BB coherence is therefore the activity of motoneurons projecting muscles active during precision grip. It is well known that the neuromuscular junction has a high safety margin that minimizes transmission failure from motoneurons to motor units (Trontelj et al. 2002) so motoneuronal activity could be directly represented in muscle activity. In fact, the firing pattern of every recorded motoneuron was closely correlated to the EMG profiles of target muscles in walking cats (Hoffer et al. 1987). Therefore, it is likely that spinal LFPs with BB reflect the activity of motoneurons that can drive motor units at a wide range of different frequencies. Furthermore, the fact that BB has never been described in sensorimotor cortex indicates that BB is a unique feature of the spinal cord.

In conclusion, we found the oscillatory LFPs in the spinal grey matter of monkeys performing a precision grip task which was coherent with forelimb muscle activity in either a restricted or broad frequency range. Spinomuscular coherence could reflect oscillatory input from descending and/or peripheral afferents. Elucidating mechanisms underlying spinomuscular coherence will be important for understanding the role of motor system oscillatory activity in controlling voluntary movements.

REFERENCES

[1] Baker S, Chiu M, and Fetz E. Afferent encoding of central oscillations in the monkey arm. J Neurophysiol 95: 3904-3910, 2006.

[2] Baker S, Olivier E, and Lemon R. Coherent oscillations in monkey motor cortex and hand muscle EMG show task-dependent modulation. J Physiol 501: 225-241, 1997.

[3] Baldissela F, Hultborn H, and Illert M. Integration in spinal neuronal systems. In: Handbook of physiology. The nervous system, Bethesda, MD: Am. Physiol. Soc., 1981, sect. 1, vol II, chapt 12, p. 509-595.

[4] Brown A. Organization in the spinal cord. Berlin, Germany: Springer, 1981.

[5] Conway B, Halliday D, Farmer S, Shahani U, Maas P, Weir A, and Rosenberg J. Synchronization between motor cortex and spinal motoneuronal pool during the performance of a maintained motor task in man. J Physiol 489: 917-924, 1995.

[6] Fisher RJ, Galea MP, Brown P, and Lemon RN. Digital nerve anaesthesia decreases EMG-EMG coherence in a human precision grip task. Exp Brain Res 145: 207-214, 2002.

[7] Hoffer J, Sugano N, Loeb G, Marks W, O'Donovan M, and Pratt C. Cat hindlimb motoneurons during locomotion. II. Normal activity patterns. J Neurophysiol 57: 530-553, 1987.

[8] Kilner JM, Fisher RJ, and Lemon RN. Coupling of oscillatory activity between muscles is strikingly reduced in a deafferented subject compared with normal controls. J Neurophysiol 92: 790-796, 2004.

[9] MacKay W. Synchronized neuronal oscillations and their role in motor processes. Trends Cogn Sci 1: 176-183, 1997.

[10] Marsden JF, Ashby P, Limousin-Dowsey P, Rothwell JC, and Brown P. Coherence between cerebellar thalamus, cortex and muscle in man: cerebellar thalamus interactions. Brain 123: 1459-1470, 2000.

[11] Murthy V, and Fetz E. Coherent 25- to 35-Hz oscillations in the sensorimotor cortex of awake behaving monkeys. Proc Natl Acad Sci USA 89: 5670-5674, 1992.

[12] Ohara S, Mima T, Baba K, Ikeda A, Kunieda T, Matsumoto R, Yamamoto J, Matsuhashi M, Nagamine T, Hirasawa K, Hori T, Mihara T, Hashimoto N, Salenius S, and Shibasaki H. Increased synchronization of cortical oscillatory activities between human supplementary motor and primary sensorimotor areas during voluntary movements. J Neurosci 21: 9377-9386, 2001.

[13] Pellerin JP, and Lamarre Y. Local field potential oscillations in primate cerebellar cortex during voluntary movement. J Neurophysiol 78: 3502-3507, 1997.

[14] Perlmutter S, Maier M, and Fetz E. Activity of spinal interneurons and their effects on forearm muscles during voluntary wrist movements in the monkey. J Neurophysiol 80: 2475-2494, 1998.

[15] Piper H. Electrophysiologie Menschliche Muskeln. Berlin, Germany: Springer, 1912.

[16] Riddle CN, and Baker SN. Manipulation of peripheral neural feedback loops alters human corticomuscular coherence. J Physiol 566: 625-639, 2005.

[17] Trontelj J, Mihelin M, and Khuraibet A. Safety margin at single neuromuscular junctions. Muscle Nerve Suppl 11: S21-27, 2002.

Group C: Social Adaptation

Hitoshi Aonuma, Research Institute for Electronic Science, Hokkaido University

I. Introduction

The main subject of group C is social adaptation, especially the mechanisms underlying social adaptive behavior and social structure formation. There are various organisms living on the earth, and they have succeeded to survive in the ever-changing environment. As the result of long history of evolution, the organisms have diverged into such a huge number of species. In their process of evolution, animals have acquired a nervous system to exhibit adaptive behavior as the environment changes. It is important to understand the mechanism of adaptive behavior to get an insight how the organisms have evolved. In addition, it is also important to elucidate the information processing system and the design principle of the network, and to apply them to engineering. Social adaptation is one of the most fundamental features of animals to survive. And thus, it has been studied in broad sense, i.e. from interactions between individuals (short-term) to evolutional adaptation (long-term). We consider a society, which is a population of individuals, as one of the environmental factors and try to elucidate the mechanisms of social adaptation in various animals and derive a common principle from them.

II. Contents and Overviews

Simple mechanisms of social adaptation are investigating using insects as model animals, both solitary insects, such as crickets or silkworm moths, and social insects, such as honeybees, ants or termites. An insect brain consists of only 10^5 neurons, which is less than 10^{-6} compared with those of mammals. In spite of such a small number of neurons, insects have very sophisticated adaptive capability, e.g. higher brain function including learning and sociality. On the other hand, any present robots still do not have such a capability. We believe that the elucidation of the brain mechanism underlying insect adaptive behavior is quite useful for construction of adaptive system such as a distributed automonous system. Complex mechanisms of social formation, such as inter-individual communication, affect or others understanding, are investigating using vertebrates including humans. For example, birds are used for studies on acquisition mechanisms of social adaptive behavior by vocal communication, Japanese macaques for studies on brain mechanisms underlying the formation of social hierarchy and behavioral decision based on the hierarchy, and humans and machines for studies on others understanding.

So far, throughout these studies, two methodologies have been established, in which traditional biological and engineering studies could be organically combined each other. We named each of them "Synthetic Neuroethology" and "Brain-Machine Fusion System".

1) Synthetic Neuroethology

A research approach in which a multi-leveled system model is constructed by integrating fragmentary physiological data sets and then performance and validity of the model is ethologically evaluated (Fig. 1).

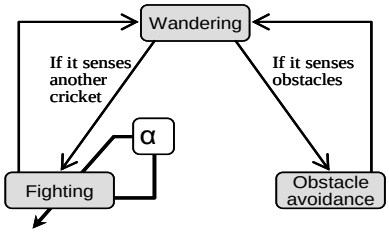

Fig. 1. Behavior model of artificial cricket.

2) Brain-Machine Fusion System

A research approach to clarify biological functions by constructing an integrative system as a combination of biological and artificial elements (Fig. 2).

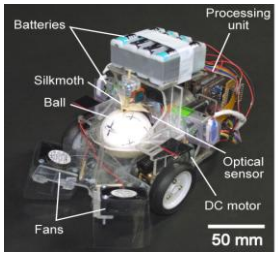

Fig. 2. Insect-controlled robot.

In addition to the research activity of the individual groups, several collaborative activity between planned and subscribed research groups, and/or biological and engineering groups are in progress.

Aonuma's group, a planned research group, and Nagao's group, a subscribed research group, are investigating the neural mechanisms of fighting behavior in crickets, and the contribution of social experience, especially the environmental social factor during their developmental processes, to the crickets' behavioral patterns to others. These biological researches are linked to the collaboration with another planned research group, Ota, Kawabata, Asama and others, who simulate a dynamical behavioral model of the

population of the male crickets and investigate the behavioral modulation of individuals in the population. In addition, a neural network model of the brain, in which the functions of nitric oxide and biogenic amines are involved, is also constructed to understand the social experience-based adaptive mechanism in insect. The mechanism of 'population-dependent behavioral modulation' in crickets was validated by the behavioral and internal state (neurophysiological) model, and the possible technological application of this mechanism to forging task of multiple mobile robots was suggested. These studies are an example of 'Symthetic Neuroethology'.

Studies on adaptability of pheromone-induced behavior in moths by Kanzaki, Kurabayash and others, a planned research group, are an example of 'Brain-Machine Fusion System'. They have developed a two-wheel insect-controlled robot and evaluate the adaptability of moths to change in the motor gain of the robot. They are also trying to develop a fusion system of a robot body and a moth brain and understand the brain mechanism.

Social insects, including ants, honeybees and termites, organize a colony based on division of labor, trophallaxis and formation of caste. Tsuji's group, Miura's group and Ito's group try to elucidate the mechanism of colony formation from the aspects of recognition of nestmates, maintenance of the caste and learning of the social environment.

Tsuji, Yamaoka Sugawara and others have discussed the ingenuity of the rules underlying the local decision-making system function well as a whole group. They study the 'patrol behavior' of the ant *Diacamma sp.* queen as an example of global behavior based on local information and found a common point between the colony maintenance mechanism in ants and multirobot control system.

Ito, Ikeno, Okada and others are attempting to reveal the effects of the waggle dance as a good model of the 'propagation and sharing of knowledge'. A honeybee informs her nestmates of the location of a flower she has visited by a unique behavior called a 'waggle dance.' They found that the information of the waggle dance contains a substantial margin of error. In spite of this they showed effective foraging behavior. They discussed a novel system for transfering informaiton through constructing a mathematical model that descibes a manner of maintenance of society (bee colony) using such an amibiguous inforamtion.

Miura, Ikemoto, Asama and others have studied the caste differentiation and the maintenance of the caste in the termite. They tried to clarify the social behavior between castes by constructing a mathematical model for caste differentiation. They included the growth inhibitory function of the juvenile hormone, which is important for the caste differentiation, into the model. The eusocial insects, such as termites, are good model to discuss the mechanism of self-organization in the animals' society, and their mathematical model gave an idea to discuss the animals' evolution.

Oka *et al.* have studied the information processing mechanism of the males' tweet, which is important communication behavior for mating, in the female brain. They have investigated expression patterns of genes and behavior of the neural circuit, and found that the females responded to the complexity of the tweet. They are now attempting to understand systematically how the complexity of the tweet is represented in the brain.

Fujii has studied the switching mechanism of behavior based on the social situation in the Japanese macaque. They found that the adaptive behavior of the Japanese macaque could be easily observed by overlapping the working spaces of two animals. Under such a situation, they recorded their brain activities and the motion of their body simultaneously using the multi-channel recording method and the motion-capture technique, and found that the neurons in the lobus parietalis could adaptively change their response patterns depending on the spatial change of the social structure.

To reveal the neural mechanism underlying others understanding is important for elucidation of the mechanism of social adaptive behavior in humans. The schizophrenic disorder, which is one of the social problems presently, is considered as a functional deficit of the brain mechanism for others understanding.

Kato, Ohtake and others are attempting to prove the importance of understanding the others' gaze and faces for recognition of the social signal. They have applied the studies on the patients with schizophrenic disorder to construct a agents and interface with the social adaptability. They adapt characteristics of cognition behavior to artificial agents that has ability of social cognition. They constructed cognition models to explain the interaction of an attention and its disease. Then they proposed forward model to elucidate how we recognize a behavior that is by oneself or by others.

Sawaragi's group has constructed a model for the process of understanding others intention, including agents, and systematically discussed understanding others. In the communication of human being, it is known that a tacit understanding and assignment of work help cooperation. Considering this adaptive mechanism, they proposed modeling of the ability of communizing cognition of a situation.

That is the brief description of the contents of the project. Detailed results of each research group are summarized by each group leader in the following chapter, respectively.

Systematic understanding of neuronal mechanisms for adaptive behavior in changing environment

Hitoshi AONUMA, Hokkaido University. Ryohei KANZAKI, The University of Tokyo

Abstract: **We have investigated the design principle of neuronal mechanisms of social adaptation in animals, by focusing on how animals select their behavior depending on social interactions. Insect communication behaviors such as pheromone behaviors provide a good model system to elucidate the mechanisms of social adaptation. We have focused on cricket agonistic behavior and silkworm moth orientation behavior that are both released by pheromones. Our biologist group mainly concentrated on revealing behavioral and physiological aspects of socially adaptive behaviors. Based on our results, we collaborate with engineering groups to establish dynamic models. We established 2 methodology, they are Synthetic Neuroethology and Brain-Machine Hybrid System. In Synthetic Neuroethology, we contribute dynamical multi-system model using biological achievements and then the validity of the model is examined by biological experiments. Using Brain-Machine Hybrid System, we can analyze neuronal mechanisms underlying adaptive behaviors by changing external factor of environmental signals.**

I. Introduction

Adaptive behavior in animals can be classified fast adaptive behavior and evolutionally adaptive behavior. Animals perceive many kinds of signals in changing environments and they quickly select and adjust their behaviors to the changed environment by choosing and switching behavior program in the central nervous system. Animals have evolved nervous systems as an adaptive function through long evolutional history of the organisms. Animals do not always respond the same way to the same stimuli, which indicates that the state of the central nervous system must be modified depending on their experiences as well as internal and/or external conditions. Social environment is one of the important factors of animals' adaptive functions.

Insects have rather simple and identical nervous systems. Mammalian brain has about 10^{12} neurons. On the other hand, an insect nervous system has about 10^{6} neurons. Such insect brains allow us to access each neuron easily, which accelerate us to investigate how animals show socially adaptive behavior from cellular level to behavioral level analysis. We have here investigated the neuronal mechanisms underlying socially adaptive behaviors that are emerged from individual interactions among animals.

Our goals is to understand how nervous systems adjust animal behaviors to changing external environments including society. We will combine neuroethological approaches and system engineering approaches to understand how animals form social communities, how they learn and retain previous experiences and how they alter their behavior depending on dynamic environments, which will help us to unravel the universal design of central nervous systems.

II. Aims

The aim of our project is to elucidate the neuronal mechanism of socially adaptive behavior. To understand mobiligence of social adaptation, we have focused on neuronal mechanisms that animals alter their behaviors in order to respond to the demands of changing circumstances in particular social environment.

Insects provide us a good model system to investigate neuronal mechanisms of adaptive behavior, since they have rather simple and identical nervous systems. Communication behavior using pheromones in insects must be one of the greatest model systems to investigate neuronal mechanisms of animal adaptive behavior. Most of pheromone induced behaviors in insects have been thought to be hard-wired: a behavior that could be turn on and off but with no plasticity. However, some of pheromone behaviors are revealed to be modified by their previous experiences. Cricket aggressive behavior is an example of such pheromone induced behaviors. The response of males to the pheromone can be modified by the previous fighting experiences [(1)]. The behavior of insects has been understood that internal factor and external environments drastically mediate threshold of releasing a behavior or behavioral pattern. Previous social interaction such as mating and agonistic interaction mediates following behavior. In this study, we have focused on insect communication behavior using silkworm moths and crickets.

III. Achievements

Insects can adapt to various environments and perform adaptive behaviors with their simple nervous system. We have investigated neuronal mechanisms of agonistic behavior of the cricket. In order to carry out synthetic neuronethological research, we performed behavioral work to elucidate functional role of contact-chemo receptive information from antennae, performed biochemical analysis to elucidate functional role of neuro-activators such as NO and biogenic amines, and performed neuro- anatomical research to elucidate information processing pathway in the cricket brain.

We used silkmoth for our research of Brain-machine hybrid system. We developed a two-wheeled insect-controlled robot for analyzing adaptability of pheromone searching behavior of a male silkmoth on board. By operating motor parameters of the robot, we could evaluate adaptability of the silkmoth. We analyzed whether the silkmoth could compensate its own motor output for unintentional movements during its instinctive pheromone orientation, and we showed that visual feedback had important role for correcting course deviation. We developed a brain-machine fusion system that enables us to evaluate functions of the brain itself. In this study concerned

with pheromone orientation in male silkmoths, we investigated the feasibility of using a nervous system as command generator for simulated and real devices. Our hardware implementation consisted in a robot equipped with a physiological data acquisition system.

3-1 Social experience-induced behavior in crickets

Male crickets *Gryllus bimaculatus* show intensive aggressive behaviors when they come across another male and start to fight each other (Fig. 1). However, once a male loses, he does not fight any more in his second encounter with another male, but shows avoidance behavior. We have focused on loser cricket (subordinate) behavior to understand how animals alter their behavior dependent on social interaction [(1)].

Fig. 1. Agonistic behavior between male crickets.

3-1-1 Role of the antennae in the fighting behavior

The aggressive and avoidance behaviors have been studied for many years. It is considered that, the aggressive and avoidance behavior is released when males detect cuticular substances on the surface of another male body by the antennae. But the neural mechanism of the fighting behavior is still unknown. To test if the antennae are necessary to elicit the aggressive behavior of male crickets, the behavior to another male were observed 1 hr after antennal legions. Over 90 % of intact crickets showed aggressive behavior, such as antennal fencing and/or threat posture, and start to fight with the other male (Fig. 2). On the other hand, the percentage of aggressive crickets was significantly reduced when the whole antennae were cut (Fig. 2). The crickets, whose maxillary palpi were removed as a sham operation, showed aggressive behavior to the other male as well as intact crickets (Fig. 2). These results suggest that the male crickets use the sensory information from the antennae to perform correctly to other crickets, i.e. the aggressive behavior to males or the courtship behavior to females [(2)].

Although the males without the antennae did not show clear aggressiveness to another male with the same operation, they could fight against another intact male. When they faced to the intact male, the percentage of the aggressive males became significantly higher than that to the males without the antennae (Fig. 2). The level of the fighting between the intact male and the male without the antennae was not significantly different compared with those between intact males and males without the maxillary palpi (Fig. 2). These results indicate that the input from the antennae is necessary to start fighting to another male but not to fight against an aggressive male. The fact that the males without the antennae could fight against the intact males under the dark conditions (data not shown) suggests that there are at least two parallel pathways to elicit the male aggressive behavior, 1) one mediated by the sensory input from the antennae, and 2) the other one mediated by the mechanical input from the body surface.

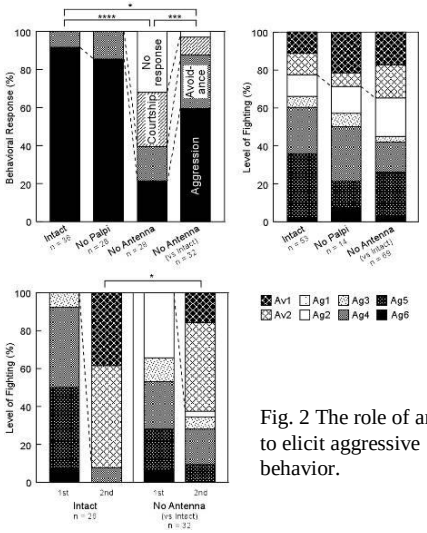

Fig. 2 The role of antennae to elicit aggressive behavior.

3-1-2 Role of the antennae in the experience-induced modulation of the fighting behavior

To test the effect of antennal removal to the behavioral change in losers from aggression to avoidance (see above), the behavior of intact losers and losers without antennae in their second encounter were compared. The second encounter was held 15 minutes after the first fight. In the case of fighting behavior between intact males, over 90% of losers showed avoidance behavior in their second encounters (Fig. 2). When the male without antennae lost the first fight between the intact male and the male without antennae, they show significantly higher aggressive behavior in their second fight compared to intact losers (Fig. 2). This result suggests that the participation of the antennal neural pathway to the behavioral change in losers. It has been reported that the blockade of NO/cGMP signaling cascade also impaired the behavioral change in losers, and thus it is suggested that the NO/cGMP signaling cascade plays a crucial role to the behavioral change in losers.

3-1-3 Regulation of biogenic amine system in the cricket brain

We have demonstrated that biogenic amine in particular octopamine (OA) level in the brain decrease just after the agonistic behavior. Our behavior experiments showed that loser crickets wouldn't elicit agonistic behavior to conspecific males for 1 hour after the fighting. Nitric oxide (NO) system is shown to regulate agonistic behavior and also it also regulates biogenic amine system in the brain [(3)]. Since NO is free radical substance in the tissue, it must be oxidized quickly. Therefore biogenic amines can be one of the candidates to regulate behavior for 1 hour after agonistic interactions. We examined the changes of biogenic amine levels in the brain after agonistic behavior. We found

decreased OA level gradually restored to the original level after the agonistic behavior. It took about 1 hour. Now we are planning to inhibit OA receptor and action of transporter of OA to understand functional role of NO signal and OA in the brain during agonistic behavior.

3-1-4 Neuroanatomical research of the cricket brain.

In order to develop neurophysiological research of the cricket agonistic behavior, as a first step, we have performed Neuroanatomical research of the cricket brain. The agonistic behavior of the cricket is released by the cuticular substances as a tactile chemical stimulus. Therefore, the processing pathway for tactile chemical signals from antennae was investigated. The antennal lobe is the primary center for the chemical processing. It is composed of 49 glomeruli. The tactile signals, on the other hand, are processed at ventral area of flagellar afferents (VFA) (Fig. 3). Innervating pathway of the projection neurons from AL and VFA was examined. Ten tracts were originated from the AL, whereas eight tracts from the VFA. Several projection tracts were shared by the tracts from the AL and the VFA, but their termination areas were segregated in the lateral protocererbrum [4].

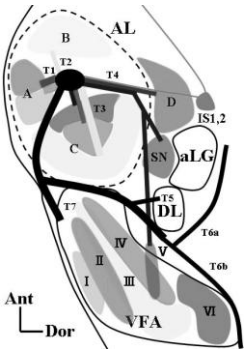

Fig. 3. Projection of sensory afferent neurons through antennal nerve. The primary center for chemical information processing is AL and that for tactile information processing is VAF.

3-2 Research for adaptability in insect using Brain-Machine Hybrid System

Silkworm moth (*Bombyx mori*) shows stereo-typed behavior. However it's behavior can be modified by external environment information, internal factor of individuals and different modality of stimuli etc.

3-2-1 Adaptability of pheromone tracking behavior of the silkmoth evaluated by the insect-controlled robot

Insects have adaptability: they can perform appropriate adaptive behaviors in various environments with their small bodies and brains. On the other hands, adaptability is one of the most important topics in robotics; therefore, we can propose novel control systems for robotics by understanding the mechanisms underlying these adaptive behaviors. For analyzing adaptive behaviors, we should consider experiments under closed-loop condition, because adaptive behaviors are elicited by interaction between insects and environments. We have developed a two wheeled insect- controlled robot (Fig. 4) [5]. This robot was controlled by a silkmoth on board, and we could evaluate the adaptability of the silkmoth by inducing unintentional movements of the robot. We adopted pheromone searching behavior of a male silkmoth as a model adaptive behavior. In this study, we analyzed compensation of the silkmoth for unintentional movements induced by motor gain operations.

We manipulated motor gain of the robot asymmetrically (Fig. 5). The robot was put in a windtunnel (1800 (L) x 900 (W) x 300 mm (H)) where a plume of a principle component of the female sex pheromone (bombykol) was flowing. We observed all 10 trials (N = 5) succeeded in orientation to the pheromone source. To confirm a role of visual information (optic flow) for this compensation for the asymmetrical gain setting, we surrounded visual field of the pilot with a transparent sheet (with optic flow) or a white sheet (without optic flow) which did not disturb air intake from fans.

The results indicated that 11of 14 trials (N = 7) with optic flow succeeded in orientation, however, only 4 of 14 trials (N = 7) without optic flow succeeded (Fig. 6). Further experiments indicated that the silkmoth could respond to different gain setting within 1 second. From these results, we concluded that the silkmoth used visual feedback for correcting course deviation instantaneously during its instinct pheromone searching behavior. We could also show that the insect-controlled robot could induce adaptability of the silkmoth by the motor operation, which was useful for evaluation of adaptability of the insects.

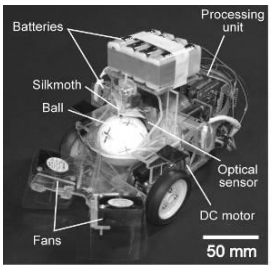

Fig. 4. Insect-controlled robot.

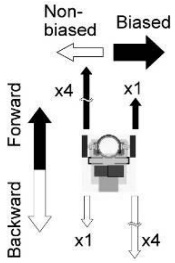

Fig. 5. Gain setting

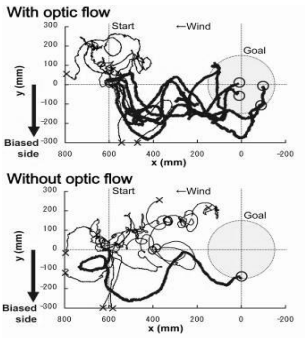

Fig. 6. Trajectories of orientation with/without optic flow.

3-2-2 Construction of a Brain-Machine Fusion System to Evaluate Adaptability of an Insect

Insects perform adaptive behavior according to changing environmental conditions using a small brain. There are two classes of

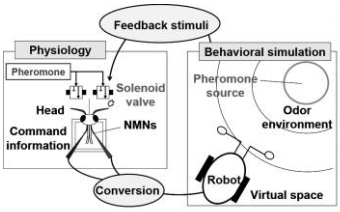

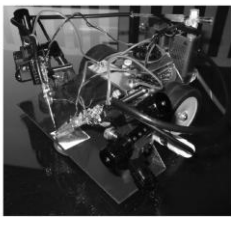

approaches to understand such adaptive behavior and small brains. One route is using a bottom-up approach that aims at gathering information about the system's components (neurons) which will eventually be merged to understand the generation of behavior by the brain. Alternatively, top-down strategies investigate the system at a high level being concerned with its input/output relationships rather than its internal organization. Using the former approach, a vast body of data has been piled up in different biological disciplines, but there is no method to integrate and evaluate the findings and related models. In the present study, we employed a brain-machine fusion system as a new method of evaluation. A brain-machine fusion system essentially replaces a robot's controller by a wet neural system. Using this strategy enabled us to investigate brain function under closed-loop conditions comparing behavioral performance of the animal model and hybrid systems. In this study, we examined methods to construct brain-machine fusion system subjecting male silkmoths' odor searching behavior. Male moths orient towards conspecific females displaying a programmed behavioral pattern (straight-line walking, zigzagging turns and looping) upon detection of sex pheromone by their antennae [1]. The programmed behavioral pattern is repeated each time a pheromone plume is encountered resulting in localization of the goal.

In the class of brain-machine fusion systems, we call a system that connects electrophysiological recording with simulation experiments a brain-virtual machine fusion system. We measured command signals derived from a moth's brain physiologically, and translated this information into behavior generated by the virtual moth. Virtual moths were designed to be able to orient towards a pheromone source in the simulated environment. Depending on the simulated behavior, pheromone stimuli were fed back to the real moth in the experimental setup creating a closed-loop situation (Fig. 7).

In the behavioral simulation, elements of the moth's programmed behavioral patterns (zigzagging turns and looping) were observed, and 10 of 29 trials (N=5) succeeded in reaching the odor source (Fig. 8). From these results, we concluded that the nervous system could be suitable for use as a robot controller.

It is difficult to reproduce realistic pheromone distributions in simulations because diffusion occurs in turbulent flow. Experiments in a real odor environment are necessary. Therefore, we developed a brain-real machine fusion system consisting of the e-puck mobile robot platform equipped with the physiological measurement system (Fig. 9). In order to transfer a physiological recording system that is normally rigidly installed to a mobile robot, circuitry must be minimized and electrical interference as well as vibrations has to be kept at bay.

The brain-machine system was tested in a wind tunnel. Although we could observe turning movements induced by pheromone and visual stimuli, the programmed behavioral pattern and orientation behavior could not be observed so far. The main reasons were technical in nature and are currently being resolved.

Fig. 7. Brain-virtual machine system.

Fig. 8. Brain-real machine system.

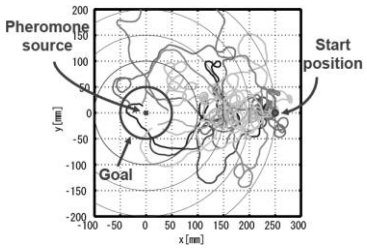

Fig. 9. Results of behavior simulation environment

IV. Conclusion and future plan

We have established methodology to investigate neuronal mechanisms underlying adaptive behaviors. Synthetic Neuroethology will help us to understand systematically how animals select behavior program using central nervous systems under the changing environment. Brain-Machine Hybrid System will also help us to understand the adaptability of animals by evaluating responses of animals to external environment signals.

The approaches using cricket demonstrat neuronal mechanisms of behavior program selection under social environment. Focusing on subordinate animals, we have been investigated how neuroactivators such as NO and biogenic amines mediate commands of behavior program in the brain. The approaches using silkmoth demonstrate how internal and external factors of environment modulate animal behaviors.

For the next plan, we will carry on investigate the detail of neuronal function of behavior selection in cellular level and neuronal circuit level and carry on collaboration with engineering research group to understand systematically by constructing dynamic models.

REFERENCES

1. Delago A and Aonuma H (2006). Experience based agonistic behavior in female crickets, *Gryllus bimaculatus. Zool. Sci.* 23: 775-783.
2. Sakura M, Yoritsune A, and Aonuma H (2007) Fighting experiences modulate aggressive and avoidance behaviors in crickets against male cuticular substances. Proc. International Symp. Mobiligence, 2: 243-246
3. Aonuma H, Nagao T, Ota J, Kawabata K, Asama H (2007) Modeling of socially adaptive behavior and its application – Lesson from agonistic behavior in the cricket–. J. Socie. Instr. Contr. Engin. 46: 903-909.
4. Yoritsune A and Aonuma H (2007) 3-D atras of the cricket antennal lobe. Proc. International Symp. Mobiligence, 2: 187-190
5. Emoto S, Ando N, Takahashi H, Kanzaki R (2007) Insect-controlled robot –Evaluation of adaptability-, *J. Robotics and Mechatronics*, 19: 436-443.

Modeling of Fighting Behavior in Crickets

Jun OTA, Hajime ASAMA, The Univ. of Tokyo, Kuniaki KAWABATA, RIKEN

Abstract: Individual interaction among crickets was simulated by constructing an artificial cricket model. Using simulations of artificial cricket models with multi-layers, we investigated the principle mechanism underlying social interaction.

Keywords: multi-agent robot systems, crickets, adaptive behavior

1. Introduction

Our group studies adaptation mechanisms of crickets to other individuals and environments, through analyzing fighting behaviors among crickets and the effect of social population.

Our aim is to clarify the mechanisms embedded in animates to adapt to other animates and environments. In our study, we apply a system engineering approach with mathematical models focusing on the crickets to clarify its mechanisms of adaptation. This can be basis of the social adaptive mechanism of animates. The cricket models are created with multiple layers such as a neuronal structure level, an individual behavior level, and group behavior level.

In Chapter 2, behavior modeling of crickets is presented connecting cricket individual fighting behavior and the effect of social population. In Chapter 3, it is discussed that simulated swarm behavior based on proposed neuronal circuit model of the cricket and advanced modeling approaches. In Chapter 4, growth modeling of cricket is described considering growing environment. We conclude the paper in Chapter 5.

2. Behavior modeling of crickets

2. 1 Approach in modeling

In the former study [1], we only focused on the aggressive behaviors of crickets, and propose the behavior model with only one internal state variable. In this year, based on the observation result of cricket group behaviors, we newly introduce a state variable expressing the activity of crickets.

2. 2 Behavior model of crickets

We skip to explain the biological background of cricket's behaviors such as fighting behavior among two male crickets and the effect of social population [1].

Parameters utilized in this paper

The artificial crickets are modeled of the mechanisms underlying the socially adaptive behavior of crickets. Here, the artificial crickets are described as having two internal states α and β. Internal state α expresses the level of passivity and has a value of 0.01 through 1. On the other hand, internal state β expresses the level of activity and has a value of 0.01 through 1. The artificial crickets select behaviors using internal states α and β and information from their sensors.

Behavior of artificial crickets

The artificial crickets have four basic behaviors, namely, (i) Wandering, (ii) Stopping, (iii) Fighting, and (iv) Obstacle avoidance. The selection depends on a finite-state machine model.

(i) Wandering

The artificial crickets walk randomly while going straight and turn ±90 degrees instantaneously. Thus, the artificial crickets walk randomly.

(ii) Stopping

The artificial crickets do not walk and remain in the same position. They select wandering and stopping behaviors using their internal state β, which means activity. In reality, the artificial crickets change from the wandering to the stopping behavior at a probability of 1/1000. On the other hand, the artificial crickets change from the stopping to the wandering behavior at probability Q.

$$Q = 1 - \beta \qquad (1)$$

Thus, the artificial crickets select stopping and wandering behaviors using their activity.

(iii) Fighting

If an artificial cricket senses other crickets in its personal field, it will select a behavior compatible with fighting in male crickets. This behavior will stop when one cricket loses a fight. The probability P of losing a fight is defined in

$$P = \alpha \qquad (2)$$

Thus, the artificial cricket loses at probability P and continues fighting at probability (1-P). This behavior continues until one cricket loses. The above process is made within one sampling time 0.1 (sec).

When one loses, the loser turns to the opposite directions to outside of winner's personal field. After that, the winner takes the wandering behavior, while the loser takes the stopping behavior. Please be careful there is possibility that both crickets lose the fight when they determine to give up fighting at the same time.

(iv) Obstacle avoidance

If an artificial cricket senses obstacles with its right-hand antenna, it will turn right. If an artificial cricket senses an obstacle with its left-hand antenna, it will turn left. If an artificial cricket senses obstacles with both antennae simultaneously, it will turn randomly right or left. This behavior stops when the artificial cricket no longer senses obstacles.

How to update the internal states α and β

The artificial crickets update the internal states α and β when they interact with other crickets.

$$\alpha_{t+1} = (1-\omega)\alpha_t + \varepsilon_{lose}\eta_{lose} + \varepsilon_{win}\eta_{win} \quad (3)$$

$$\beta_{t+1} = (1-\omega')\beta_t + \varepsilon_{\text{int}}\eta_{\text{int}} \quad (4)$$

Here, α_t and β_t are the values of the internal states α and β at time t. ω and ω' are the forgetting coefficient. ε_{lose} and ε_{win} are the coefficient effects of fighting with other crickets. ε_{int} is the coefficient effect of contact with other crickets. These coefficients are set by trial and error, $\omega = 10^{-4}$, $\omega' = 10^{-4}$, $\varepsilon_{lose} = 0.3$, $\varepsilon_{win} = -0.1$, and $\varepsilon_{\text{int}} = 0.1$. Then, η_{lose}, η_{win}, and η_{int} are the functions of (5), (6), and (7), respectively.

$$\eta_{lose} = \begin{cases} 1 & \text{:If it loses} \\ 0 & \text{:Other} \end{cases} \quad (5)$$

$$\eta_{win} = \begin{cases} 1 & \text{:If it wins} \\ 0 & \text{:Other} \end{cases} \quad (6)$$

$$\eta_{\text{int}} = \begin{cases} 1 & \text{:If it contacts other crickets} \\ 0 & \text{:Other} \end{cases} \quad (7)$$

2. 3 Simulation results

The proposed model is evaluated through computer simulations. All the simulations are made with the time length of 60 minutes. The field size is set as 150[mm] × 200[mm]. The number of the artificial crickets is set as 2 and 6. Here, the case of two crickets is assumed as low density, and the case of six crickets is assumed as high density.

Figure 1 shows the time transition of α in the low density case and high density case. In the low density case (Fig. 1(a)), one cricket has low α value and the other has high α value. In the high density case (Fig. 1(b)), α values are divided into two: a low value for one cricket and high values for five other crickets. In this case, the cricket with a low α value becomes aggressive when it contacts with others. On the other hand,

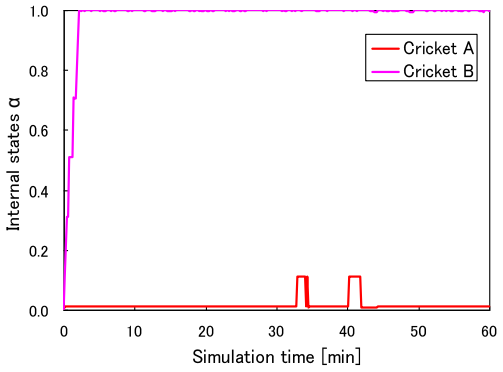

(a) Low density

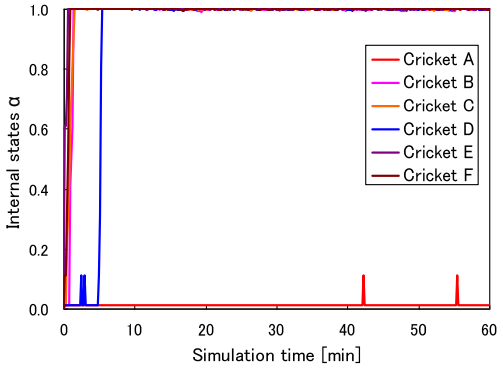

(b) High density

Fig. 1 Time transition of α values of each crickets

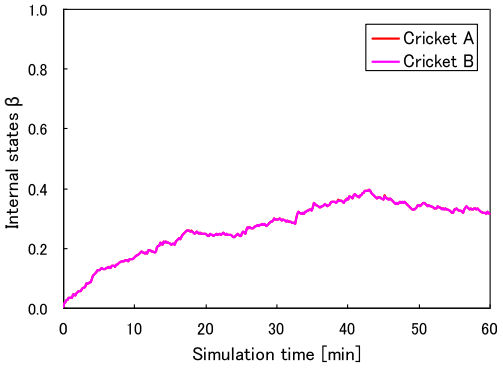

(a) Low density

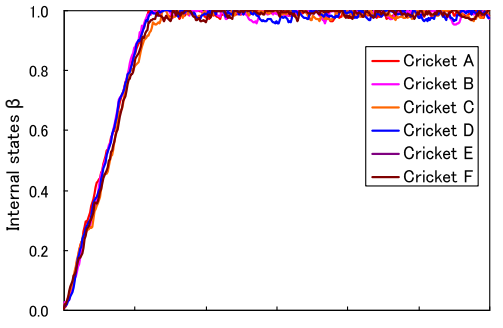

crickets with high α values tend to avoid others from others. The first cricket corresponds to the winner, other crickets correspond to the losers. This result shows the similar situation with crickets in the real world.

Time transition of β value is shown in Figure 2. In the low density case (Fig. 2(a)), β value increases in the beginning and converges to about 0.3 in the end. In the high density case (Fig. 2(b)), β value increases drastically and converges to 1, maximal value at about 12 minutes. From these results, we can say that the proposed cricket model can emerge the effect of social population.

3. Neuronal Circuit Modeling of Cricket

In our former study [1], we proposed a neuronal circuit model of cricket based on the biological knowledge related to NO/cGMP and OA. In this year, we run multi-agent simulations where the agent with our proposed model interacts with the other ones, and observe the emerging swarm behaviors and introduce antennal sensitivity concept to our previous neuronal model.

Simulation in Multi-individual Environment

There are four artificial cricket agents with our proposed internal model in a square simulation field, on a side. An agent's movement is selected randomly from 3 behaviors (go straight, turn around, and stop). If any other agent is found within one's sensing area, antennal sensory input is brought to the agent and changes its state to fighting behavior or avoidance behavior according to its internal state. This fighting behavior continues until one agent selects avoidance behavior. The escaped agent is the loser, and the other agent recognizes its victory.

Agents' density is changed by moving x in the range of $2^7 \le x \le 2^{13}$. A trial is terminated after 1000[sec], and the simulation is run for 50 times in each conditions. We utilized the number of aggressive agents when a simulation ended as an index of the characteristics of the population. Here, an aggressive agent means the agent which shows aggressive behavior against another agent, in other word, the agent whose OA level is over 0.5. Figure 3 shows the rate in 50 simulations in each x.

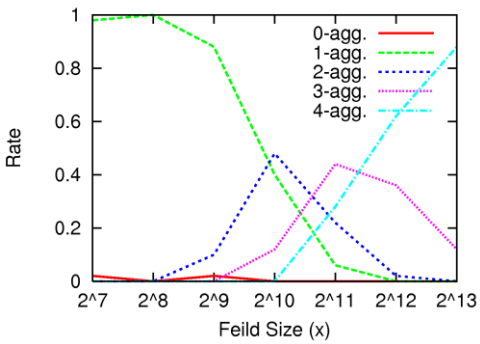

Fig.3 Rate of aggressive individuals

There is a tendency to increase the number of aggressive agents as the agents' density decline. This tendency can be found in real crickets with exception of next two points. Firstly, result doesn't change dramatically in every density environment, so that the rate of 4-agg. should be dominant in those areas. Secondly, the rate of 0-agg. is always low in every conditions, contrary to the real crickets don't show aggressive behaviors in high-density environment.

The simulation shows only the influence of the encountering frequency and doesn't take agents' perception in to account, which seems to be the cause of this difference. It is important to introduce such factors to our model

Introducing Antennal Sensitivity Factor

In real crickets, there is a tendency not to switch to fighting behavior under many contacts condition with other crickets. Also, in other insect, it was reported that biogenic amine level affects to the process to antennal stimuli in the other insect. Therefore, we introduce antennal sensitivity factor based on contact frequency and internal parameter related to one's biogenic amine level to our proposed neuronal model.

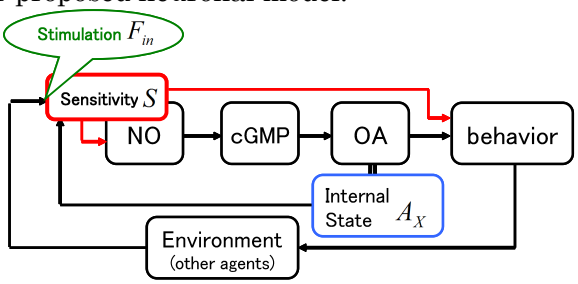

Fig. 4 Schematic View of Advanced Neural Model

Figure 4 shows the schematic view of our advanced model and Equation (8) indicates dynamics for antennal sensitivity. By introducing this dynamics to our previous model, we can confirm the

possibility of that fighting behavior is depressed under many contacts condition if OA level is high.

$$\frac{dS}{dt} = -\rho S + f(A_x) - g(F_{in}) \quad (8)$$

Here, $S, f(A_x), g(F_{in}), \rho$ indicate antennal sensitivity, internal state function, contact frequency function and a positive coefficient. In our future works, we attempt to swarm behavior simulations based on this advanced model and also confirm such functions and substances by biological experiments.

4. Growth Modeling of Cricket

Iba[2] reported that isolated-breeding crickets become more black-colored, bigger and more aggressive than collective-breeding ones. This means that the breeding environment make one's growth state change. Therefore, we attempt to model cricket's growth based on breeding parameters.

By our investigation, cricket's mass development varied like Logistic-shape function. Equation (9) indicates differential equation for mass development.

$$\frac{dm}{dt} = r_0\left(1 - \frac{m}{M}\right)m \quad (9)$$

Here, r, m means relative growth rate and cricket's mass. M >0 is maximum value of the mass and m converges to M. The equation of relative growth rate r is as follows;

$$\frac{dr}{dt} = r_0\left(\frac{r}{r} - 1\right)r \quad (10)$$

We can model basic cricket's growth by adding environmental effects to these equations. As the environmental effects, the duration of the growth period and the growth rate are introduced. The former one is regulated by $\phi(T,p)$:relationship between optimal temperature effect and feeding condition. The latter one is regulated by $\phi(T,p)$: relationship between accumulated temperature effect and feeding condition. Thus following equations are derived.

$$\frac{dm}{dt} = \phi(T,p)r_0\left(1 - \frac{m}{M}\right)m \quad (11)$$

$$\frac{dr}{dt} = \varphi(T,p)r_0\left(\frac{r}{r_0} - 1\right)r \quad (12)$$

Here, p , T indicates feeding condition and temperature. By solving these equations, mass development is expressed as follows;

$$m = m_0\left(\frac{1+\exp(\varphi r_0 \tau_0)}{1+\exp(\varphi r_0(\tau_0 - t))}\right)^{\phi/\varphi} \quad (13)$$

Merkel[3] reported the relationship between final mass and the growth rate like Figure 5. Our proposed model derives the result like Figure 6. Our result shows differences in high protein level of Merkel's result but consists with Iba's result.

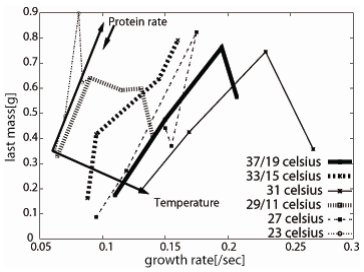

Fig.5 Merkel's data

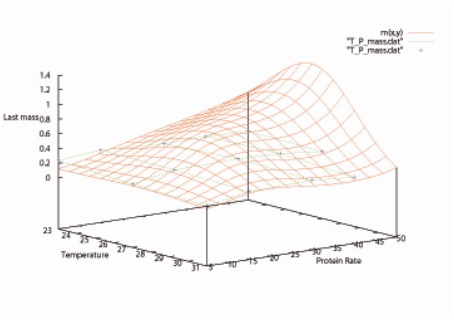

Fig.6 Result of Proposed Model

5. Conclusion

Cricket models are created with various layers. Simulation results indicate the effectiveness of the proposed models. Future studies will deal with collaboration with biological studies and improvement of the mathematical models.

References

[1] J. Ota, H. Asama and K. Kawabata, Modeling Neuronal Mechanism of Fighting Behavior in Crickets, Grant-in-Aid for Scientific Research on Priority Area from the Japanese Ministry of Education, Culture, Sports, Science and Technology "Emergence of Adaptive Motor Function through Interaction among the Body, Brain and Environment - A Constructive Approach to the Understanding of Mobiligence –," 2006 Annual Report, 99/102 (2007).

[2] M. Iba, T. Nagao and A. Urano:Effects of population density on growth, behavior and levels of biogenic amines in the cricket, Gryllus bimaculatus. Zool. Sci. 12 695-702 (1995).

[3] Merkel,G.:The Effects of Temperature and Food Quality on the Larval Development of Gryllus bimaculatus (Orthoptera, Gryllidae), Oecologia (Berl.) 30, 129-140 (1977).

Analysis of adaptive behaviors emerged by functional structures in intearction networks

C01-03 Daisuke Kurabayashi

Abstract– Insects have only a little brain but the behavior is highly adaptive. We consider that physical structure of the interaction network works on the creation of the brain function and model the behavioral processor that controlled by its structural disposition. In this research, we investigate mechanisms for intelligent behaviors from the viewpoint of network property. In this report, we investigate bodies to interact with an environment. We focus on (i) modeling of behavior-switching by nonlinear oscillator network, (ii) direct feedback system employing actual brain of silkworm.

Key Words: Network, oscillator, odor-source searching

1 Introduction

In this study, we investigate adaptive behavior switching mechanism. A moving individual obtains many types of information through interactions with other individuals and environments. Creatures can adaptively feed back conditions around it to adaptive behaviors. Robots, artificial products can work perfectly only in limited environment. Insects have high adaptability with limited resources. So, we have focused on the aspect of network property in some levels observed in creatures.

In this research, we investigate mechanisms for intelligent behaviors from the viewpoint of network property. Especially, we focus on the effects of embodiment that mediates interactions between brains and environments. In this manuscript, we report (i) effect of behavior-switching by nonlinear oscillator network, (ii) direct feedback system employing actual brain of silkworm.

2 Adaptation through behavior selection by oscillator-network model

Crickets have a fixed-habit to avoid fighting for a certain minutes after their defeat[1]. If the fighting opportunity is too frequent, some crickets cannot recover the militancy, which limits the number of fighting crickets depending on the density[2]. This phenomenon shows the property of crickets as an autonomous system that adapts to the density variation only by a local communication. In this section, a behavior selector is modeled based on the brain function, and the model is equipped to a robot[3]. Through implementation by analog circuit and simulations, we investigate an essential factor to induce the environmental effect into the individual robot behavior.

2.1 oscillator-network model

The pheromone that induces the fighting behavior is processed in the organ called antennal lobe and nitric oxide(NO) is secreted there during behavior transition[4], which affects the connection among neurons where NO is spread. We consider a model of the neural network that changes the attribute depending on the structure in this subsection.

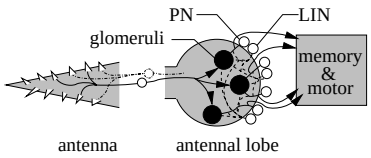

Fig. 1: Configuration of pheromone processor

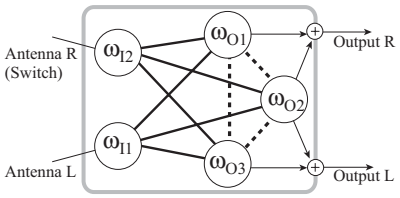

Fig. 2: Oscillator Network Model

We focus on the biological knowledge that an odor information, like pheromone, is coded by the synchrony of neural oscillations[5]. We have also mathematical knowledge that the synchrony of an oscillator network depends on its structure[6].Therefore we adopt an oscillator network for the network modeling.

Based on the pheromone processing unit (Fig.1), we construct a network as in Fig. 2 where the gromeruli of the antennal lobe are modeled with the oscillators and the LINs are modeled with the connection between the oscillators. In the figure, ω_* indicates an oscillator. When an external input is given, corresponding ω_{I1} or ω_{I2} starts oscillating. We extract outputs of the network as summation of $\omega_{O1}, \omega_{O2}, \omega_{O3}$ as shown in the figure. We assume that the oscillators, connected by lines, have different eigen values by which they cannot synchronize without external input. Then, we can control synchronization of the oscillators by adding or removing connections indicated by broken lines in the figure[3]. Thus, this network alternates the output depending on the structure.

We implemented the behavior-switching system with the simplest body, as an analog circuit, indicated in Fig.3. We employ van der Pol(VDP) oscillators that we can easily realize.

By the nature of oscillators, they enforce each other if only they act in the same timing. We directly con-

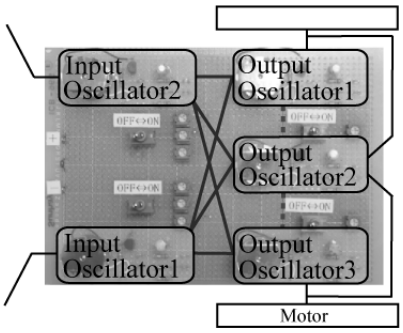

Fig. 3: The developed robot circuit

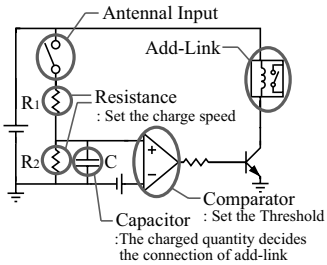

Fig. 4: Delay circuit for connection switching

nect motor driver to the output oscillators. The motors are actuated if the two oscillators are synchronized.

When the dotted line (additonal link) in Fig.3 is vaild, all output oscillators synchronize each other. If not, only two of them synchronize. Thus, the motion of robot becomes meaningful action such as the avoidance and the aggressive behavior.

Figure 4 illustrates a delay circuit that changes the additional links automatically. In this circuit, the capacitor is charged during a fight. Because the additional links are not valid at the initial state, the robot towards to an object (Fig. 5a). When the chaged level exceeds 70%, the additional links become valid. Then, the robot run away (Fig. 5b).

2.2 Adaptation to group density

Aonuma, et al.[2] have reported the variation in number of winner cricket depending on its group density. When the density is so high (or low), all crickets loose (or keep) aggressive. When the density is medium, only one cricket suppresses others. We carried out simulations with the analog circuit model to

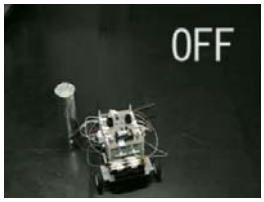

After 10 sec.: the robot was fighting against the metal cylinder.

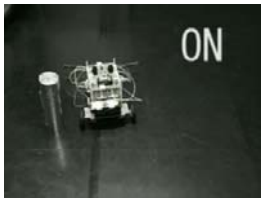

After 25 sec.: it gave up fighting and got away.

Fig. 5: Behavior switching by the oscillator network.

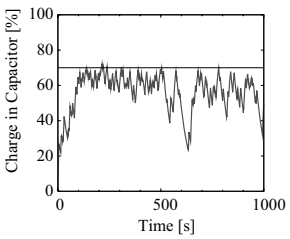

(a) Charge level of capacitance

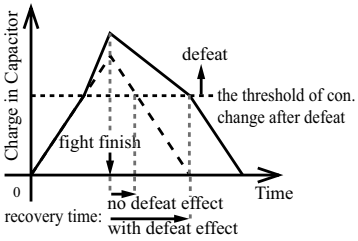

(b) Memory of defeated experience

Fig. 6: The charge of capacitance

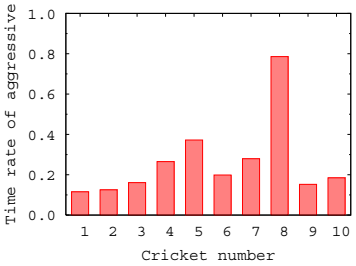

Fig. 7: Fraction of aggressive state

reproduce the adaptive phenomena.

However, the simulation result does not show any differentiation of behaviors. Figure 6a illustrates the transition of the charge of a robot. The horizontal line in the middle show the threshold to change behaviors. The charge level hardly exceeds the threshold. This result implies that the behavior change suppresses the reduction of aggression afterwards, which enables the cricket to recover within a short time and remove the difference between winner and loser. In order to avoid this saturation, we enforce the memory of defeat experience. For this purpose, we accelerate the charge speed and reduce the discharge speed after showing defeat behavior as Fig. 6b. As is read from the same figure, the recovery time is postponed by this operation.

In order to confirm the effect of the defeat memory, a simulation with 10 robots under the same condition was conducted. Figure 7 shows the rate of aggressive time in the simulation. Only the 8th robot fights in the most of the simulation time and the others continuously avoid from it. This results the differentiation among robots can be realized like real cricket group by enforcing the defeat memory.

Furthermore, by expanding the field size, every robot continuously fight in most of the simulation time, and by reducing the field size, no robot continuously fight. Thus, we had demonstrated that the adaptation to the density change can be achieved by using a defeat memory on the proposed oscillator network robot.

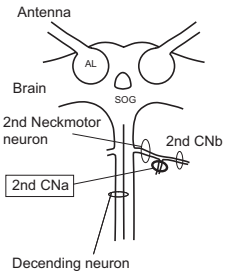

(a) Brain and 2nd CNa.

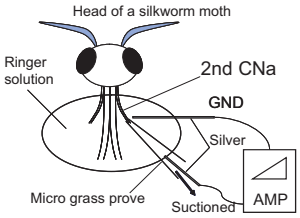

(b) Sensing by glass microelectrodes.

Fig. 8: Sensing of motion commands

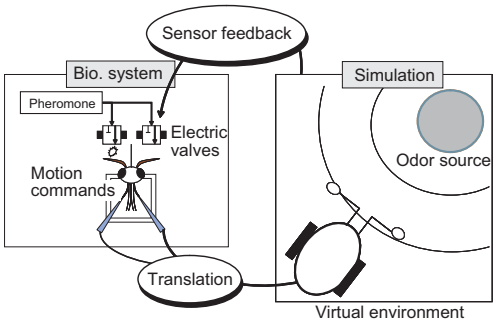

Fig. 9: Feedback through virtual environment.

3 Direct brain-controlled robot

3.1 Cyborg: robot with living brain

We are investigating the mechanism and the performance of insect brain. We build direct control system of robotic/simulated body by neural system of silkworm in order to emulate feedback of behavioral outputs. By the system, we can operate interactions between a brain and an environment, therefore, we can make clear the difference between artificial intelligence and ability of living brain. This will make possible to build novel network model to exhibit adaptability like a silkworm moth does.

Figure 8a illustrates schematic view of neural fibers, in which two thick lines bring motion commands to the legs[7,8]. Thus, we can measure behaviors of the brain. However, extracting motion commands from a thick line is quite difficult because it contains more than 200 neurofibers. So, we measure activity of the neck motor neurons (NMNs) that has high correspondence with motion commands to legs[9]. We remove all legs, wings, and an abdomen, then mount the moth on a wax chamber ventral-side up. Left and right 2nd CNas of exposed NMNs are suctioned into the glass microelectrodes (Fig. 8).

3.2 Adaptation to a virtual environment

At first, we connect a brain of a silkworm to a virtual body in a virtual environment to observe adaptability to replacement of a body. We assume a 2D free space in which one pheromone source is located. A silkworm moth moves with a virtual body in this workspace. The virtual body, shown in Fig. 10, is a nonholonomic vehicle with two driving wheels. Its

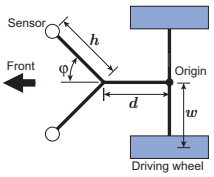

Fig. 10: Virtual mechanical body

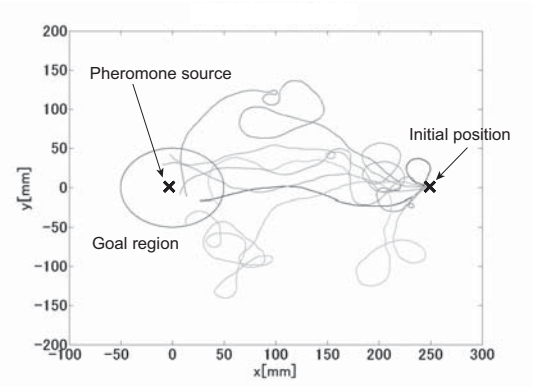

Fig. 11: Trajectories in the virtual environment

dimensions are $w = d = 5$[mm], $h = 2.5$[mm], and $\psi = \pi/4$.

We count number of spikes in a certain sampling period, since biological observation shows the spiking ratio corresponds to the travel distance. Let n_L and n_R be counts of spikes in the left and the right side NMN, respectively. We directly translate them into travel distances of the wheels, $x_L = Kn_R$ and $x_R = Kn_L$, where K represents a constant gain.

We assume that shape of a pheromone plume is a circle, and a virtual body senses a plume only coming from heading direction. When an antenna hits a plume, an electric valve injects pheromone to corresponding antenna of the insect (Fig. 9).

We have carried out experiments by using the bio-machine system with virtual body and environment. Figure 11 indicates the virtual environment and examples of trajectories. We suppose that the initial position is (250, 0) [mm], and set pheromone source at (0,0). Because the silkworm moth cannot obtain any visual information, we regard that it reaches at the pheromone source when it enters the goal region where the distance form the pheromone source is smaller than 50[mm]. During 29 trials, we observed 10 reaching at the goal region.

Figure 12 shows a transition of heading direction. The figure represents that the bio-machine agent exhibited typical set of motions, straight walking, zigzag, and turn around.

3.3 Brain-controlled mobile robot

The virtual environment is easy to implement, but it has many limitations, e.g. representation of wind, turbulence, visual information, etc. Thus, we realize brain-controlled mobile robot that can act in real environment. We employ EPFL e-puck mobile robot as

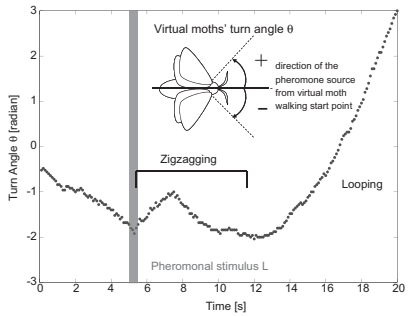

Fig. 12: Transition of the headings of the body axis

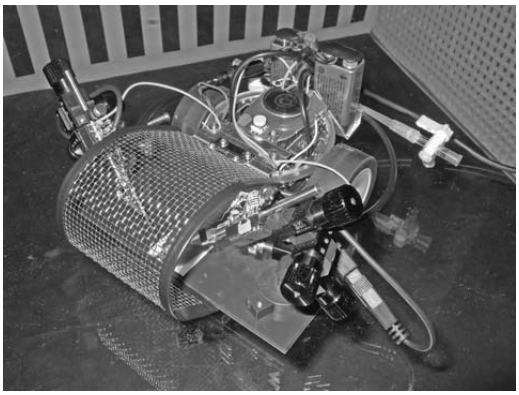

Fig. 13: Mobile robot controlled by a brain

a platform. We implement the sensing module that usually needs electro-magnetic shield.

We have to measure the spiking voltage of neurons that is $-90\sim30[mV]$. The spectrum has a peek at $1[kHz]$, and it distributes $DC\sim100[kHz]$. A grass electrode outputs $100[\mu V]$ order voltage.

The impedance of a grass electrode is about $1\sim100[M\Omega]$ order, and it is easily disturbed by noise. It also works as a capacitance that causes voltage drift. So, we combine RFI filter, passive HPF, and high-impedance amplifier (Fig. 13). We fix the head of the silkworm moth by agarose, which supports stable measurement and long-life of the brain.

3.4 Test run

We carried out experiments with the brain-controlled robot. It exhibits reactions by pheromone and visual stimuli. In some conditions, it reaches a pheromone source about 0.5 [m] away from its initial position. However, we are still improving the experimental system in order to observe typical behavior, zigzag-turn. Currently, the robot cannot exhibit the behavior. We consider that external noise prevents precise measurement. We are introducing new filter and algorithms to extract correct spikes from observed signal contains noise.

4 Conclusions

In this research, we investigate mechanisms for intelligent behaviors through bodies that mediate interactions between brains and environments. We consider that physical structure of the interaction system works on the creation of the brain function and model the behavioral processor that controlled by its structural disposition. We formulate behavior-switching by nonlinear oscillator network and build direct feedback system employing actual brain of silkworm. We are also building actual robotic bodies for experiments in the real world.

Acknowledgement

The authors thank researchers in group C01-01, C01-02, and C01-12 very much for their kindly providing biological data, experimental system, and comments to the authors.

References

[1] S. A. Adamo and R. R. Hoy: Agonistic behaviour in male and female field crickets, gryllus bimaculatus, and how behavioural context influences its expression, *Animal Behaviour*, 49, 1491/1501, 1995.

[2] H. Aonuma, et al.: Social experience dependent behavior selection in the cricket – from neuroethological approaches to modeling. In *The 2nd Int. Symp. on Mobiligence*, 2007.

[3] T. Funato, et al.: Development of structure-mediated behaviour selector using oscillator network. In *IEEE Int. Conf. on Robotics and Biomimetics*, 1206/1211, 2007.

[4] H. Aonuma and K. Niwa: Nitric oxide regulates the levels of cgmp accumulation in the cricket brain. *Acta Biologica Hungarica*, 55(1-4), 65/70, 2004.

[5] G. Laurent, et al.: Temporal representations of odors in an olfactory network. *J. Neuroscience*, 16(12), 3837/3847, 1996.

[6] T. Funato and D. Kurabayashi: Network structure for control of coupled multiple non-linear oscillators. *to be published in IEEE Trans. Systems, Man and Cybernetics - Part B*, 2008.

[7] T. Mishima and R. Kanzaki: Coordination of flipflopping neural signals and head turning during pheromone-mediated walking in a make silkworm moth *Bombyx mori*, *J. Comp. Physiol. A*, 183, 273/282, 1998.

[8] R. Kanzaki, et al.: Self-generated zigzag turning of *Bombyx mori* males during pheromone-mediated upwind walking, *Zool. Sci.*, 9, 515/527, 1992.

[9] S. Wada, R. Kanzaki: Neural control mechanisms of the pheromone-triggered programmed behavior in male silkmoths revealed by double-labeling of descending interneurons and the motor neuron, *J. Neurol.*, 484, 168/182, 2005.

Analysis on the brain differentiation that regulates the cooperative behaviors in social insects

Toru Miura[1], Hideaki Takeuchi[2], Mamiko Ozaki[3]

[1]Graduate School of Environmental Science, Hokkaido University, [2]Graduate School of Science, University of Tokyo, [3]Graduate School of Science, Kobe University

***Abstract*—In colonies of social insects, there are various castes, among which tasks are allocated. As the results, we can see the elaborate social behavior in those insects. Furthermore, the complicated communication system is also required for the integration of such behavior. Through various approaches, we are investigating the molecular and neurophysiological basis of organized behavior in social insects, to understand the mechanism and evolution of insect society, and to find out new concepts in relation to the autonomous decentralized systems.**

I. INTRODUCTION

Termites (Order Isoptera), ants, wasps and bees (Orde Hymenoptera) organize colonies, live together with their related individuals, and perform elaborate social behavior [1]. In the colonies, there are reproductive and sterile individuals, and those sterile ones are helpers that are engaged in altruistic tasks such as foraging, defense, etc. Those types of individuals that specialize in certain tasks are called 'castes'. Although there are diverse research subjects in the studies of social insects, one of the fundamental questions is that what mechanisms underlie the caste differentiation, and how they communicate with each other. In this article, we summarize the recent progresses in our studies on the mechanisms regulating social behavior in termites, honeybee, and ants. We are mainly applying molecular, neurophysiological and behavioral techniques to analyze the social systems such as caste differentiation, learning and nestmate recognition.

II. REGULATIONS OF TASK ALLOCATION IN THE DAMP-WOOD TERMITE

As mentioned above, the termite social behavior is organized elaborately by task allocation and cooperation. In order to accomplish the social behavior, there must be at least two intrinsic mechanisms in termites. The first mechanism is that all individuals possess a set of genes (a genome) that enable them to differentiate into any castes. Similar mechanism is seen in the cell differentiation of multicellular organisms, in which all of the cells include the genomic information that is required for any cells constituting the organismal body. The second mechanism is to regulate the caste ratio in a colony. If all of the individuals differentiate into soldiers, the colony should be destroyed because they lack reproductive options. For this reason, they have flexible options that can change the caste fate during their developmental processes. Namely, each individual can change the physiological status in response to the environmental factors, followed by the change of developmental pathways. Thus, by means of mechanism of "polyphenism" and "feedback", termites can realize the appropriate caste ratio under a certain environment [2].

As the study material to investigate caste-specific gene expressions, we chose the Japanese damp-wood termite *Hodotermopsis sjostedti*. In this species, soldiers are differentiated from pseudergates, which function as workers, via presoldiers.

2-1. Neural modifications in relation to the soldier differentiation

The division of labor is crucial mechanism of social insects, and it is founded on behavioral differentiation among castes. The behavioral differentiation should be the key component to discuss on the social evolution. Although previous studies have focused only on limited social hymenopterans, termites have evolved sophisticated sociality independent of social hymenopterans. One of the most remarkable features of termites is the presence of distinctive “soldier” caste. In contrast to workers, soldiers attack aggressively against invaders. In spite of the evident behavioral differences between soldier and worker, its neural basis was almost unknown so far. Here we focused on the difference of termite nervous systems between soldier and worker, and discovered neural modifications of motor and sensory systems involved with the soldier defensive behavior.

In the motor systems of soldiers, the mandibular motor neurons (MdMNs), that are located in subesophageal ganglion (SOG) and control the mandibles, were found to be enlarged (Fig. 1). The analysis of the developmental processes revealed that the enlargement of the MdMNs occurred prior to the presoldier molt. Later, the MdMNs were slightly diminished in size, then reached the maximum size in the mature soldiers. Based on these results, two functions of the enlargement of MdMNs can be suggested; the behavioral function that causes fast and strong mandibular motion, and the developmental function that contributes to the morphogenesis of mandibular muscles. Moreover, it was revealed that the enlargement was seen in all examined termite families, suggesting the functional importance of the enlargement of MdMNs in soldier defensive behavior. In the

sensory systems, the mechanosensory hairs were elongated in soldiers [3]. The degrees of elongation of these hairs varied with body parts. The mechanosensory hairs on headcapsule and pronotum were especially elongated. On the other hand, the chemosensory sensilla showed no caste difference in length. The mechanosensory hairs should receive the physical stimuli like mechanical vibration associated with the destruction of nests. Therefore, the elongated sensilla are suggested to have an important role in detection of enemy invasion, leading to the initiation of defensive behavior. These observations showed that the soldier-specific neural modifications of sensory and motor system should be closely associated with the soldier defensive behavior. In the future studies, the analyses of integration system will reveal the more crucial mechanisms of defensive behavior.

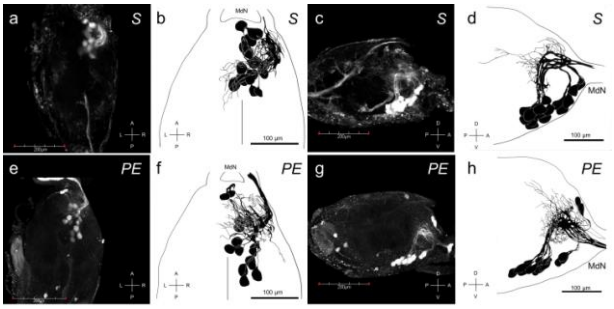

Fig. 1. The mandibular motor neurons (MdMNs) stained by the retrograde tracing from mandibular closer muscles of soldier (a-d) and pseudergate (e-h). Horisontal (a,b,e,f) and lateral views (c,d,g,h) were shown.

2-2. Hormonal controls in the caste differentiation

The developmental processes underlying caste differentiation in termites are mainly controlled by juvenile hormone (JH). Although many fragmentary data did support this fact, there was no comparative work on JH titers during the caste differentiation processes. In this experiment, JH titer variation was investigated using LC-MS quantification method in all castes of *H. sjostedti*, especially focusing on the soldier caste differentiation pathway, which was induced by treatment with a JH analog. Hemolymphatic JH titers fluctuated between 20 pg/µl and 720 pg/µl. A peak of JH was observed during molting events for pseudergate stationary molt and presoldier differentiation, but this peak was absent prior to imaginal molt. Soldier caste differentiation was generally associated with high JH titers and nymph to alate differentiation with low JH titers (Fig. 2). However, JH titer rose in females during alate maturation, probably in relation to vitellogenesis. In comparison, JH titer was surprisingly low in neotenics. On the basis of these results in both natural and artificial conditions, the current model for JH action on termite caste differentiation was discussed.

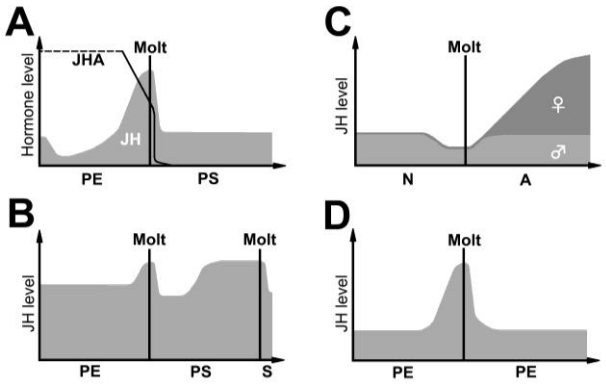

Fig. 2. The transitions of JH titer during intermolt periods, predicted based on the quantification of JH by LC-MS.

2-3. Expression analysis on the soldier-specific lipocalin SOL1

The gene termed '*SOL1'* that were identified in mature soldiers, was shown to express extensively in the mandibular gland, which is known as an exocrine gland [4]. Recent experimental analyses showed that the product of this gene was a secretory protein, which is secreted externally in a large amount from the mandibular glands. In addition, based on the prediction of tertiary protein structure, it has been revealed that the SOL1 protein belongs to the lipocalin family, suggesting that this protein is transferred between colony members. Interestingly, SOL1 protein is extensively secreted at the time of attack against predators (Fig. 3). From these results, we predict that the SOL1 protein may be involved in the communication among individuals and/or the regulation of caste ratio in termite colonies.

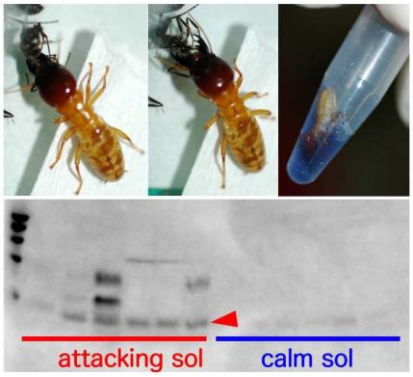

Fig. 3. The SOL1 protein is secreted from the mandibular glands at the time of attack against predators.

2-4. Mathematical model of caste differentiation in termites

Self-organization of hierarchy of system has been focused in task allocation of distributed autonomous systems and network analysis. It is important to realize the mechanism of hierarchy generation for implementation to artificial systems. In order to know the principle, we try to model caste differentiations control of termite. Equations of evolution are created, using both of biological data and some assumptions obtained by mathematical analysis. In addition, the model is

validated by computer simulations (Fig. 4). In this study, we propose that probability migration of individuals and modulations of fluctuation are operated as a differentiation control strategy.

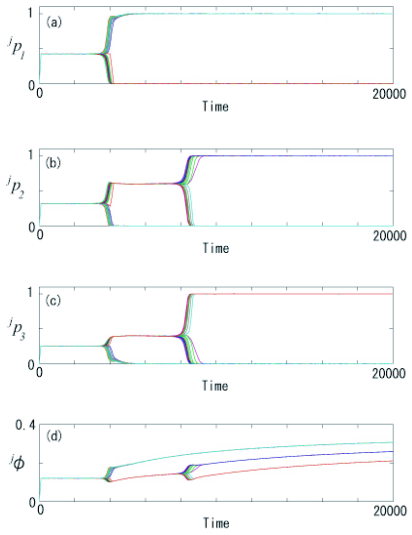

Fig.4. The resultant simulations of mathematical model on the caste differentiation in termites. The evolution of phenotypes $^{j}p_1$, $^{j}p_2$ and $^{j}p_3$ are shown (a, b, c). $^{j}\phi$ (d) provides a limiting factor. The differentiation processes are actually realized by this model.

III. Associative visual learning in the harnessed honeybee *Apis mellifera* L

The honeybee (*Apis mellifera* L.) is a social insect and colony members can interact with each other, which are mediated by division of labour and/or communication. Especially the workers can recruit their nestmates to food sources using the dance communication. They represent the "waggle dance", which shows the direction and distance of the food source. Considering that visual memory (spatial information) can be converted into the dance (mechano-sensory information) and vice versa, analysis of the neural basis involved in both visual and mechanosensory learning could lead us to clarify neural basis related to dance communication (Fig. 5).

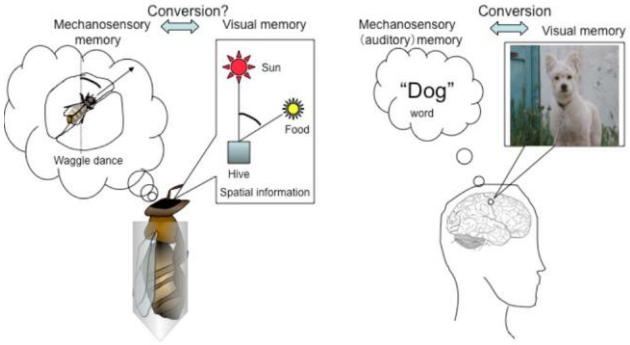

Fig. 5. Symbolic communication in human and honeybee. Both of them can convert visual memory into auditory (mechonosensory) information and vice versa.

In honeybee, neural mechanism involved in visual learning or mechano-sensory learning, however, remain totally unknown. So far, the honeybee's visual learning had been demonstrated using free-flying bees. Therefore it was difficult to analyze brain function underling visual capacity of honeybee under laboratory condition. To overcome this problem, we recently developed a visual conditioning paradigm to associate the proboscis extension reflex (PER) and a visual stimulus *via* feeding with sucrose solution using the honeybee harnessed in a plastic tube. Using the harnessed honeybees, we can use many experimental techniques, such as electrophysiology, calcium imaging, pharmacology, and double-stranded RNA-directed RNA interference.

First we established a conditioning paradigm to associate the PER and monochromatic light (Fig. 6). After a total of 20 conditioning trials, over 40% of the trained bees exhibited a conditioned response [6]. We also found that antennae deprivation significantly increased the memory acquisition. It suggests that sensory information (olfactory and/or mechano sensory information) from the antennae interfere with visual learning. Moreover, we demonstrated that bees can discriminate between 540 nm (green) and 439 nm (blue) light stimulus in this paradigm [6]. Finally, bees conditioned with a 540 nm (green) light stimulus exhibited PER immediately after the 439 nm (blue) light was turned off, suggesting that the bees reacted to an afterimage induced by prior adaptation to the blue light, which might be similar to green light [6].

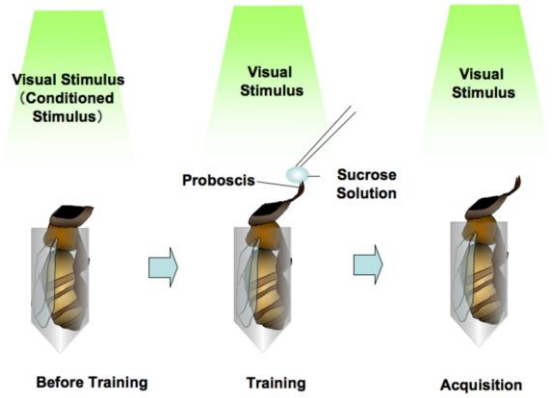

Fig. 6. A visual conditioning paradigm to associate the proboscis extension reflex (PER) and a visual stimulus *via* feeding with sucrose solution using the harnessed bee.

The free-flying honeybees use optic flow to gauge their flight distance, which is reflected to the dance. Thus, the dances convey "distance image" using information on the total amount of image motion en route to the food source. Next, to clarify the honeybee's visual capacity related to the optic flow, we use optic flow as a conditioned stimulus (Fig. 8). Optic flow was presented using liquid crystal projector on a translucent circular cone as a screen, which largely covers visual field of the harnessed bee. The memory acquisition level reached a plateau at approximately 40% after 7 trials. [7]. The bees can also discriminate two directions in this paradigm [7].

To clarify neural and/or molecular basis that underlie dance communication, we will examine whether the harnessed bee can memorize amount of image motion in this paradigm. Furthermore it is important to search neural basis involved in both mechono-sensory and visual learning.

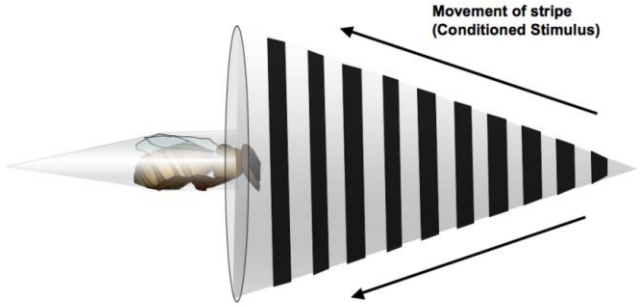

Fig. 7. Associative learning using optic flow as a conditioned stimulus.

IV. CAST POLYMORPHISM IN THE SOCIAL AGGRESSIVE CENTER IN THE ANTENNAL LOBE OF THE ANT, *CAMPONOTUS JAPONICUS*

It is important for ants to recognize the congeneric encounterers as nestmates or non-nestmates. In *Camponotus japonicus* 18 cuticular hydrocarbons (CHCs) were identified and the CHC blend pattern is colony-specific to act as nestmate recognition factor. CHC sensilla recently found on the antennae respond only to non-nestmate CHCs but not to nestmate CHCs, so that the ants aggressively reject non-nestmate. Thus, the projection region of sensory neurons in the CHC sensilla is considered to be primary center of the nestmate recognition and social aggressive behavior.

We conducted the anterograde staining from antenna, and counted 433 glomeruli in an antennal lobe stained. We construct the topological map of all the glomeruli in an antennal lobe in the worker ants of *C. japonicus* and compare that in the queen and the drone [8]. When we followed the sensory nerves in a single CHC sensillum, about 130 glomeruli in the ventro-median (VM) region in the antennal lobe were stained. Thus, previously we estimated that this VM region should be the primary center of the nestmate recognition and social aggressive behavior.

We also investigated the localization of nitric oxide (NO) synthase with a histochemical staining of NADPH diaphorase activity (Fig. 8). Almost all antennal lobe region were stained except for the VM region [9]. Consequently, we suggested that VM region identified as the primary center of aggressiveneass does not use NO as the signal transmitter to higher brain. In comparison with the NADPH diaphorase staining among workers, queens and drones, we found that the drones have no such an aggressiveness center in the antennal lobe and that they exhibits aggressive behavior towards non-nestmate worker ants.

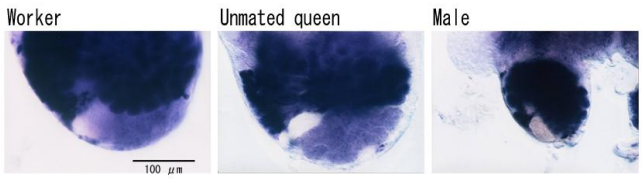

	Worker	Unmated queen	Male
CHC sensilla	+	+	-
VM region	+	+	-
Aggressiveness	++	+	-

Fig. 8. Localization of NO synthase revealed by the histochemical staining of NADPH diaphorase activity. The VM region was found to be different among castes.

V. PERSPECTIVES

In this article, we introduced our studies on the mechanical basis underlying elaborate social life in termites, honeybee, and ants. This year, the lots of experimental results were obtained on the physiological regulations, molecular evolution of pheromone-like proteins in termites, in addition to the establishment of experimental systems on the learning and memory in the honeybee, and the identification of social aggressive center in the ant.

Based on these studies on social regulation in these insects, we will understand the elaborate systems of social organization in insects, and will obtain some clues to find out new concepts of autonomous decentralized systems that can be applied to the area of robotics.

REFERENCES

[1]Wilson EO (1971) Insect Societies. Harvard.

[2] Miura T (2005) Developmental regulation of caste-specific characters in social-insect polyphenism. *Evol Dev* 7: 122-129.

[3] Ishikawa Y, Koshikawa S, Miura T (2007) Differences in mechanosensory hairs among castes of the damp-wood termite Hodotermopsis sjostedti (Isoptera: Termopsidae). Sociobiol 50: 895-907.

[4] Miura T, Kamikouchi A, Sawata M, Takeuchi H, Natori S, Kubo T, Matsumoto T (1999) Soldier caste-specific gene expression in the mandibular glands of *Hodotermopsis japonica* (Isoptera: Termopsidae). PNAS 96: 13874-13879.

[5] Ikemoto Y, Kawabata K, Miura T, Asama H (2007) Mathematical model of proportion control and fluctuation characteristics in termite caste differentiation. J Robotics Mechatronics 19: 1-7.

[6] Hori S, Takeuchi H, Kubo T (2006) Associative visual learning, color discrimination, and chromatic adaptation in the harnessed honeybee *Apis mellifera* L. *J Comp Physiol 192:* 691-700.

[7] Hori S, Takeuchi H, Kubo T (2007) Associative learning and discrimination of motion cues in the harnessed honeybee *Apis mellifera* L. *J Comp Physiol* 193: 825-833.

[8] Nishikawa M, Nishino H, Misaka Y, Kubita M, Tsuji E, Satoji Y, Ozaki M, Yokohari F (2008) Sexual dimorphism in the antennal lobe structure of the ant, *Camponotus japonicus*. Zool Sci: in press.

[9] Ishiura K, Satoji Y, Aonuma H, Ozaki M (2007) Morphological investigation of aggressive center in the antennal lobe of *Camponotus japonicus*. Proc 4th Asia-Pacific Conf Chem Eco: 143.

Brain mechanisms in insects for social adaptation

Etsuro Ito[1], Hidetoshi Ikeno[2] and Ryuichi Okada[1]

[1]Tokushima Bunri University and [2]University of Hyogo

Abstract—A honeybee informs her nestmates of the location of a flower she has visited by a unique behavior called a "waggle dance." We regard the waggle dance as a good model of the "propagation and sharing of knowledge" that maintains a society, and thus we are attempting to reveal the effects of the waggle dance in terms of the colony's benefit using mathematical models and computer simulation based on parameters from observations of the bee behavior. This past year, we improved our mathematical model and observed honeybee behavior in the field to obtain detailed biological parameters of the waggle dance. Video analysis showed that the information of the waggle dance contains a substantial margin of error. Angle and duration of waggle runs varied from run to run, with the range of ± 15° and ± 15%, respectively, even in a series of waggle dances of a single individual. We also found that most dance followers that listen to the waggle dance left the dancer after one or two sessions of listening. Furthermore, we found most bees in the hive do not walk for long distance. We are also developing to automatic measurements of necessary behavioral parameters for our model. Additionally, for construction of a better model, we have started the experiments in a dome to control feeding place. They will bring us better understanding of the effects of the waggle dance on the colony.

I. Introduction

HIGHLY developed societies such as those of human beings require communication between individuals. The honeybee (*Apis mellifera*), one of the social insect species, is well known to have the ability to communicate with its nestmates, using the so-called "waggle dance" to inform them of the location of a food source (Fig. 1, [1]-[4]). In the waggle dance, the dancer moves in a straight line with her wings beating (waggle run), then circles back to the starting point without wing-beating (the return run). On a vertical comb, the direction of the waggle run (during which the dancer wags her body from side to side and emits sounds) relative to gravity indicates the direction to the food source relative to the sun's azimuth in the field. The duration of the waggle run depends on the distance to the food source. A few follower bees keep close contact with the dancer, and these bees may be recruited to visit the flower the dancer is locating for her nestmates.

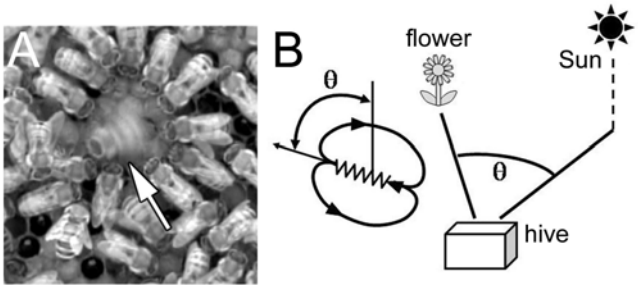

Fig. 1 Waggle dance (left panel) and the relationship between the dance orientation and food source (right panel).

We regard the waggle dance as a good model of the "propagation and sharing of knowledge" that maintains a society, and are attempting to reveal the effect of the waggle dance in terms of its benefits to the colony using mathematical models and computer simulation based on parameters from observations of the bee behavior [5, 6]. Last year, we (1) constructed a mathematical model and simulated foraging behavior, (2) found the locations where waggle runs observed appears to be "clusters", and (3) found qualitatively behavioral patterns about dancers and followers.

Here, we will report that we (1) improved our mathematical model, (2) obtained biological parameters for dance and locomotion behaviors after quantitative analysis, and (3) started experiments in a dome to control the location of the food source.

II. Results

2-1 Results of observation of dance behavior

Behavioral studies were done in the campus of Hokkaido University (Sapporo, Japan) from 8:30 am to 4 pm on several days in between August and October, 2006 and 2007 (temperature: 25-36 ˚C in most experiments). Honeybees, *Apis mellifera*, were kept in the beekeeping box with a queen. Bee behavior on the vertical comb was monitored by a video camera (JVC, GR-HD1), stored on a digital video tape (30 frames/sec), and then analyzed off-line frame by frame.

2-1-1 Precision of waggle dance in orientation

One waggle dance behavior consists of one or more

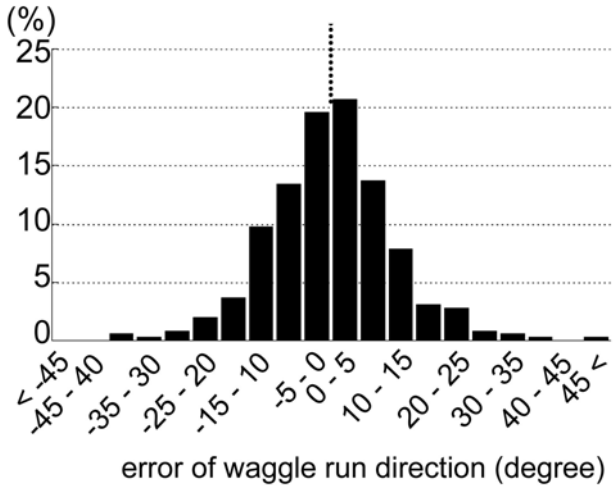

Fig. 2 Distribution of error of run angles. Angles of 84.9% of waggle runs differed from the mean orientation by ±15˚.

waggle runs. We measured the angles of all 358 waggle runs (20 dancing bees) relative to the perpendicular orientation (gravity) and found that the orientation of the run varied from run to run even in a series of waggle runs performed by same the individual. Calculating means of waggle agles for each dancer, it is found that angles of 84.9% of waggle runs differed from the mean orientation by ± 15° (Fig. 2). This suggests that the difference between two waggle runs could be up to 30°. This error range is too huge for foragers to ignore because they often fly more than 1 km for forage.

2-1-2 Precision of waggle dance in duration

The durations of 140 waggle runs of 9 bees that performed more than 10 runs (max, 26 runs; min, 14 runs) were measured. Waggle run duration varied considerably from run to run, even in a series of waggle runs by the same individual. In Bee 12, the difference in the duration was at most 0.87 sec (1.47 sec in the 4th run and 0.6 sec in the 3rd run) although the mean duration was 1.08 sec. Bee 3 and Bee 6 exhibited long runs (averaging 8.37 sec in Bee 3 and 11.81 sec in Bee 6). In 16 out of 21 runs for Bee 3 and 9 out of 14 runs for Bee 6, the difference of each run from the mean duration was larger than 1 sec; when translated into the distance the bee was representing, the difference was more than 200m. Dividing the duration of each single waggle run by the mean duration of a corresponding series of waggle runs, we found that 56.1% of waggle runs ranged within a mean duration ± 15%, and 81.3% of them were within ± 30% (Fig. 3). This means that the distance information of 80% of waggle runs covers 700-1300 m for a food source 1000 m away from the nest (the error range is 600 m). If the error range is reduced within 100 m, only 20 % of waggle run is reliable (Fig. 3).

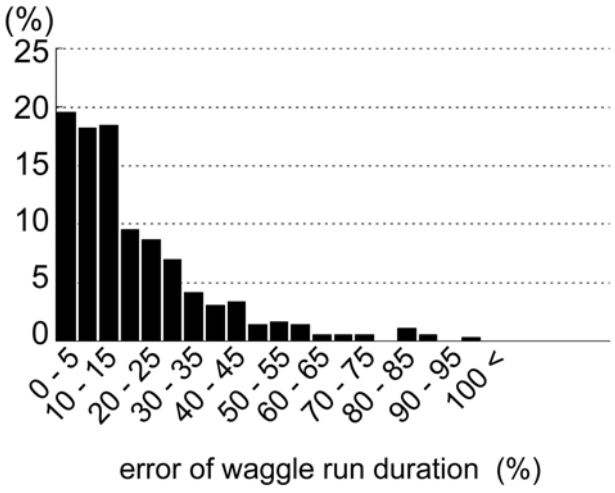

Fig. 3 Distribution of error of run durations..56.1% of waggle runs ranged within a mean duration ±15%, and 81.3% of them were within ±30%

Followers may, as mentioned above, receive "ambiguous" information about the location of the food source, which entails a non-negligible error for foraging (Fig. 4), since followers do not listen to all of the waggle runs performed by a dancer (see the next section).

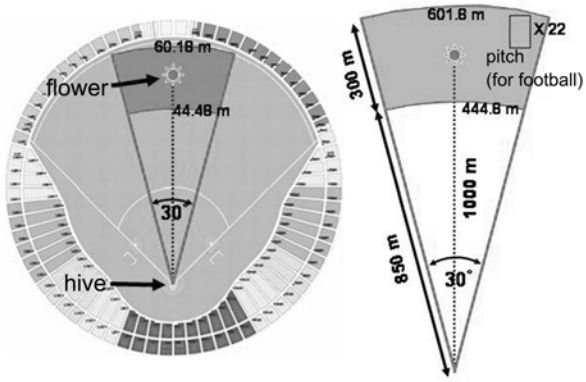

Fig. 4 Dance information covers huge area. When the hive is on the "home plate" and a flower is 100 m away from it, dance indicates the grey area. In the case of 1000-m away, dance indication covers 22-fold football pitch area.

2-1-3 Behavioral patterns of dance followers

Followers go out to forage after listening to several sessions of waggle runs. Some followers left the dancer after listening to only one waggle run, while others followed the dancing bee more than 10 times. Behavior of 62 follower bees for 5 corresponding dancers were individually traced and it was found that about 80% of followers observed left dancers after one or two waggle runs (Fig. 5). Only 5 bees listened to more than 6 consecutive waggle runs. Even in a series of waggle runs by the same individual, some waggle runs attracted no followers while others attracted up to 10 bees. We observed a positive correlation between the duration of waggle run and the number of followers. When waggle runs lasted longer than 10 seconds, at least 6 followers were

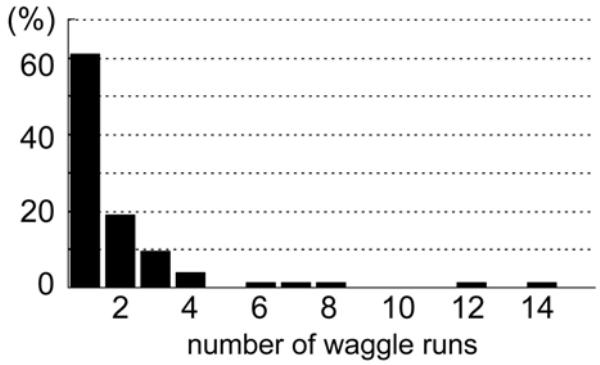

Fig. 5 The number of bees that followed waggle runs from observation of 62 followers. Most of followers used to listen to dance one or two times.

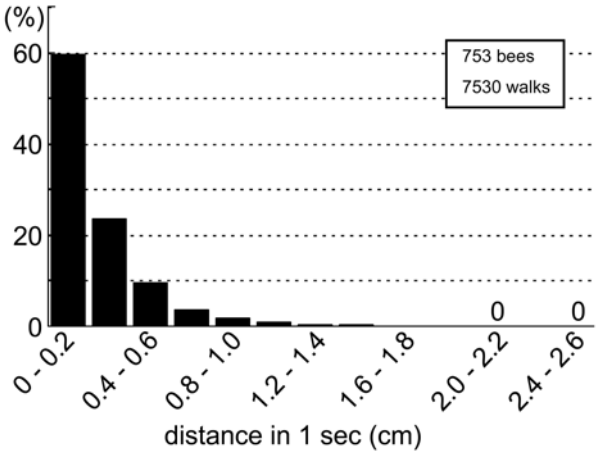

Fig. 6 Distribution of walk distances of bee in 1 sec. Not so many bees walk in the hive.

usually attracted. In short runs (shorter than 2 sec), wider ranges in the number of followers were observed, from 0 to 9. This suggests another factor in the dance behavior for attracting bees except for waggle duration.

2-1-4 Locomotion of bees in the hive

We analyzed the locomotor patterns of bees in the hive, which is necessary for modeling basic bee behaviors. Tracing trajectories of locomotion for 10 sec from all analyzable 753 bees on a side of a comb (sampling rate = 1 Hz), we found that walk distance for 1-sec is less than 0.4 cm in about 80% of 7530 walks (Fig. 6). The longest distance among non-dancers was about 2 cm. Figure 7 shows the relative positions of bees after 10 sec to the initial bee position. The bee's forward direction is 0°. The longest distance was about 13 cm. Out of 753 bees, 113 bees moved over 2 cm and only 48 (6.4%) bees over 3 cm. Although there was a weak tendency that bees move forward in a short time (1 sec), no clear preference for the position after long time (10 sec) locomotion was found. We will continue analysis and incorporate this paremeter into our model.

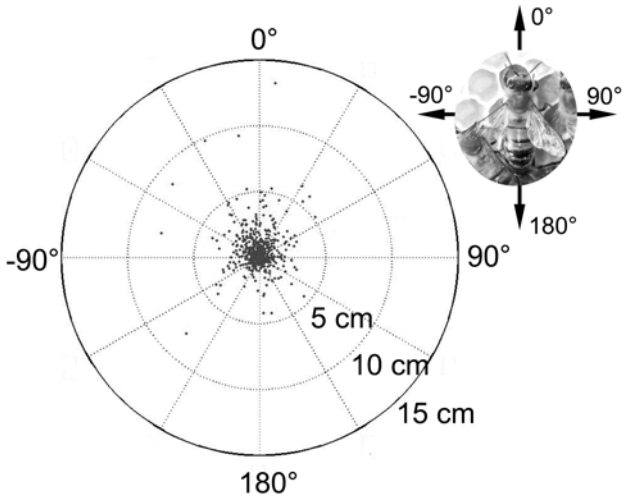

Fig. 7 Relative bee positions with the polar plot. Bees do not move long distance neither have preference in orientation for moving. The inset picture shows orientation.

2-2 Model and simulations

In order to construct a mathematical model and simulation that evaluate the effects of information sharing on foraging behavior, it is required to evaluate the total activity of the whole hive, i.e., CO_2 concentration, temperature, and humidity both inside and outside of the hive for an estimation of a bees activity, the temporal changes in the number of bees entering and exiting the hive, and the temporal change in the weight of the hive which could be a good indication for amount of collected nectar. Presently, we are developing to automatic measurement system to obtain these parameters necessary for our modeling and simulation. Some of them were already completed. Detection of dance sound enable tracking a dancer, therefore we are now analyzing detail of dance sound (Fig. 8). On the other hand, other bees including followers cannot be tracked in this manner because they are essentially silent. Hence, we are making a program as a first step of extracting the spatial pattern of the total activity of the hive. Last year, to evaluate the effect of the waggle dance, we constructed a foraging model by assuming that honeybee foraging behavior is the result of decision-making after a transition through 3 states: 1) resting, 2) wandering in the hive, and 3) foraging. And we showed importance of dance for the efficient foraging [6]. This year we improved our model by re-classifying behavioral states into more detail (Fig. 9). We will continue to make behavioral experiments and video analysis for obtaining of additional parameters that could not be measured by our developing automaton system.

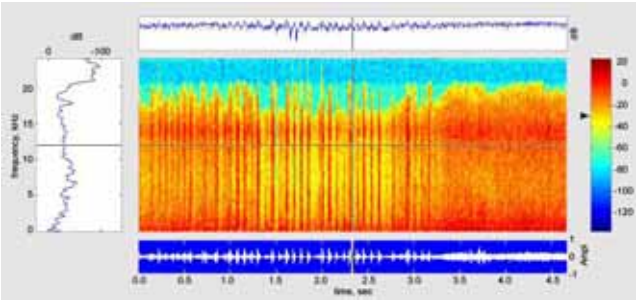

Fig. 8 An example of spectra analysis of dance sound. During waggle run, periodic oscillations are observed in the wide band component including 250 Hz which is main carrier frequency for dance information.

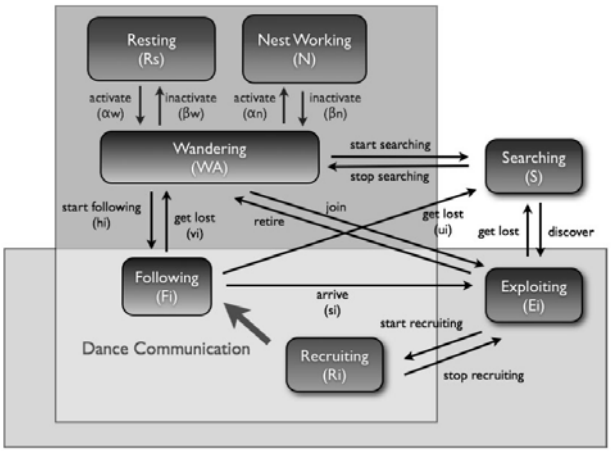

Fig. 9 Our developing model. Individual behavior was classified into 7 behavioral categories possibly relating to dance communication or foraging. We are now attempting to obtain all parameters. Our old model has only three states (resting, wandering, exploiting)

III. Future Plan

We found that 1) the locations where waggle runs appear to be "clusters" [5], 2) dance information entails a non-negligible error for foraging, and 3) most of followers left dancers after one or two waggle runs. It is expected that the probability of the failure foraging is high because of the small number of chance to listen to such dance information as "ambiguous" information about the location of the food source. However, even if the number of listening of each individual is small, the colony itself would obtain averaged information, if the number of honeybees that fly out for foraging is large. Bee colonies may overcome this problem caused from impression information in this manner. This possibility is an opposite direction of the design for engineering products that are never allowed to fail.

Since our experiments were done in the field under full natural conditions, dance information may reflect the distributions of more than one feeding place or merely spatial range of the location of a food source. We need, as a next step, to control the location of the food source and also trace all of the behavior of the recruited bee from following the dancer to foraging. To do this, we have already started the experiments in a dome (Tajima dome, Toyooka, Hyogo) to control feeding place (Fig. 10).

This coming year, we will improve our model to reflect natural phenomena more precisely by continuing behavioral experiments, for example, experiments on the condition that control feeder number and position. After then, it will be examined how well the new mathematical model predicts biological phenomena in nature by behavioral experiments. Finally we hope to obtain a better understanding of the effect of the waggle dance on maintenance of the colony.

We believe that our research is not merely a topic for biology, and that the mechanisms for maintaining a society by the sharing of information will have useful applications to practical utility, such as, optimization and control of robots under a multi-agent environment.

Fig. 10 Experiment in Tajima dome.

IV. References

[1] K. von Fricsh, *The dance language and orientation of bee.* Harvard University Press, Cambridge, Massachusetts, London, 1993

[2] J. M. Gould and C. G. Gould, *The honey bee.* Scientific American Library, New York, 1988

[3] A. Michelsen, "The transfer of information in the dance language of honeybees: progress and problems", *J Comp Physiol* vol. 173, pp. 135-141, 1993

[4] A. Michelsen, "Signals and flexibility in the dance communication of honeybees", *J Comp Physiol* vol. 189, pp. 165-174, 2003

[5] R. Okada, H. Ikeno, N. Sasayama, H. Aonuma, D. Kurabayashi, and E. Ito "The dance of the honeybee: how do honeybees dance to transfer food information effectively?", *Acta Biol Hung*, in press, 2008.

[6] H. Ikeno, N. Sasayama, R. Okada, E. Ito, "Behavioral analysis of honeybee waggle dance and its effect on foraging", 2nd International Symposium on Mobiligence in Awaji, 223-226.

Constructive Approach to Interface Design by Modeling Human-Automation Interactions Based on Social Communication Model:
Modeling User's Recognition of Complex Mechanical Systems Having Multiple Modes

Tetsuo Sawaragi*, Yukio Horiguchi*, Hiroaki Nakanishi* and Tadahiro Taniguchi**

*Graduate School of Engineering, Kyoto University. **Graduate School of Informatics, Kyoto University

Abstract— **For the purpose of designing a human-automation collaborative system, it is of great importance to clarify how a human gets to grasp the behaviors of the automation when he/she uses that. Many of the current advanced automation are apt to have multiple modes, whose complex transitions are not always transparent to a human user. We regard this mode-recognition problem as analogous to a problem on how a human can recognize the others, one of the key issues for clarifying a human ability of sociality. By introducing a technique of module learning, we implement a computational model of a human mode-recognition process, and the simulation results are discussed. Finally, the methodology for analyzing the safe usability of the designed artifact is presented that can detect the error-prone logics of the automation inducing the human user's wrong mode-recognition in use.**

I. Introduction

Human and computer subsystems should be structured and designed to work in mutually cooperating ways guaranteeing a user's usability. For this purpose, progressive system redesigns are needed with respect to human computer interactions to increase system reliability and transparency by increasing human-system interactions and especially a human user's proactive participation. Such a *socially-centered view* on the human-machine system design regards a human and an automated agent as equivalent partners, and through their mixed-initiative interactions some novel relations of mutual dependency and reciprocity would emerge. Sharing the recognition on their common task between those partners is an essentially important issue, but the complexity of automation's behaviors embedded by the designer is preventing a human user from correctly grasping the working status and predicting the future behaviors of the automation. This is because the automation is apt to have multiple modes and their output behaviors shown to a human user are quite different according to its active mode. A human user has to learn what transitions among modes are embedded within the automation in order to grasp how the automation behaves and to adapt to that through experiencing the interactions with that. This is actually a process of acquiring an ability of *sociality*.

To many of the biological beings, complexities of the environments they encounter are quite varied depending upon what embodied interactions are allowed and upon the quality of coordination they need for their survival. For instance, the significance environment to insects are quite simple as compared to human, since it is genetically determined what external stimuli to perceive and how to react to that [1]. On the other hand, more social primate beings have to recognize the other's intentions reflected within the environment in order to make efficient cooperation with their partners; they learn a variety of powerful social rules which minimize interference and maximize their benefit.

What distinguishes a human ability from other lower biological beings is that a human can build up structures by interacting with the unstructured. Through interactions with the surrounding environment he/she can selectively find some cues that are meaningful to their survivals and structurize them into some ordered internal constructs. This is realized by adaptively rebuilding their internal constructs (i.e., representations) on the objects in use as they accumulate the experiences. Wherein, the objects that a human has to use are becoming more complex and dynamical, thus their behaviors are getting less predictive especially for the novice users.

In this report, we focus on human-automation collaboration, where a human driver has to correctly recognize a working status of modes that are embedded within an automated vehicle. A computational model of a process of recognizing multiple modes is build up based upon the findings obtained in the fields of brain neurology. Then, the methodology for analyzing the safe usability of the designed artifact is presented that can detect the error-prone logics of the automation inducing the human user's wrong mode-recognition in use. The final goal of our work is to find out the fundamental design principles of artifacts that can socially behave and collaborate with a human.

II. Constructive Model of User's Developing Multiple Internal Models of Automated System

Introduction of some automated device does not always improve a human user's task performance, but it may sometimes interfere that. Especially, it is likely that so many functions are installed within a single advanced automated system, thus the design strategy for this requirement is to adopt different control *modes*. The complexity of control logics embedded within those multiple modes would make a human user bothered from a risk of *mode-recognition errors*; misunderstanding the status of the current active mode, a human user would make a wrong prediction on how the automated system behaves reacting to his/her operation and/or to the environmental changes. Modes are regarded as

internal states of the automation system, among which an automation system dynamically transits, but are usually hidden to a user. In this sense, this mode-recognition process is containing a general aspect of *social intelligence* (i.e., how to recognize the others). In the followings of this section, we present a constructive approach to this by developing a computational model of human's mode recognition [5].

During a human uses an automated tool having multiple modes, he/she interacts with that, accumulates the experiences of bodily interactions, and then gets to acquire an internal model on how the tool behaves in each of the modes. Having acquired that, in facing with a behavior of the system, he/she attempts to match that with the model and recognize what mode is currently active. In a field of computational neuroscience and/or machine learning, an idea of *module learning* was proposed, and we attempt to model a human mode recognition process by extending that computational model [3,4,5]. Our model is built to represent two concurrent processes of the users. One is a process through which they develop multiple internal models corresponding to system's multiple control modes through interactions with their facing systems and with the external environments. The other is a process that the users recognize current mode by using prediction errors calculated by their developing internal models.

First, experiments of observing human user's mode awareness using a driving simulator with ACC (adaptive cruise control) system embedded. Then, the simulation results using our proposing model are presented. Comparative analysis between those will suggest us what and how the model should be improved, thus we can investigate our understanding on how the human recognize the others having multiple modes and switching them in a constructive fashion.

An automated system with multiple control modes embedded can be modeled as shown in the right of Fig.2. Individual mode is defined as a discrete subsystem that does transit from and to different modes, while each mode has different continuous input-output dynamics. Transitions are made either by a user's intentional operation or in reply to the occurrence of particular events in the environment. A user of the above system may grasp its behaviors as shown in the left of Fig.2, where the dynamics and transition rules among the modes are not always identical with the right one. These two models are referred to as a *user model* and *machine model*, respectively. As mentioned in the above, users grasp the current active mode either by referring to his pre-existing knowledge on mode-transitions or to a display presented to them in the interface, but most of time they do that by referring to the *input-output relations*, i.e., the relationships between input operations by a user and observed responses in the environment where an operation by an automated system is reflected [6]. Each mode is characterized as this input-output relation uniquely.

We denote the dynamics embedded in each control mode as $\boldsymbol{y} = \boldsymbol{f}_m(\boldsymbol{x}, \boldsymbol{u})$, where $\boldsymbol{u}$, $\boldsymbol{x}$ and $\boldsymbol{y}$ represent a user's inputs, states of the environment, and responses observed in the next time step, respectively. For simplicity, all $\boldsymbol{f}$'s are assumed linear, and superscripts m denote the *m*-th mode of

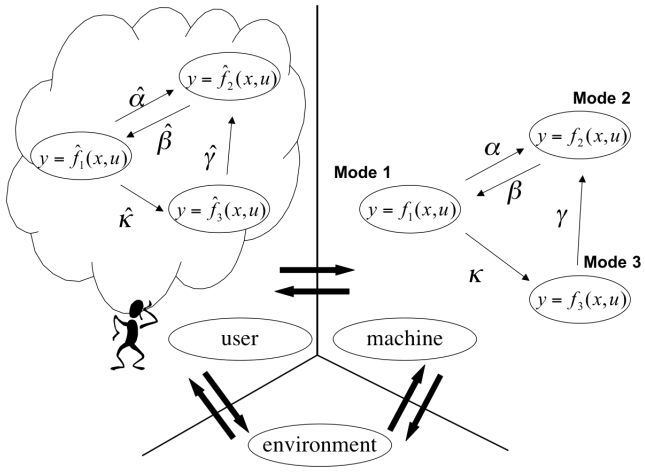

Fig.1 User model grasping actual machine states

the multiple modes. Dynamics in the user model are denoted with ^ attached.

We assume that a user acquires a user model by accumulating interactions with the target system whose dynamic responses are changed depending upon the hidden states (i.e., the active modes) of the automated system.

At first, a series of experiments using a driving simulator are done and drivers' recognitions of the operating mode of ACC while driving with it are examined. Within the ACC, dynamics of the machine model are installed. In these experiments, a number of mode- recognition errors are observed actually, so they are *error-prone* behaviors. Then, the same data of the driving situation with the above are input to our implemented user model and it is analyzed what mode the model recognizes and when the recognition is switched. The result shows that most of user's error-prone behaviors is replayed by our model although they were not identical. The detailed analysis on how each mode of a user's model is acquired by the model is investigated. Although the model initially has a rough definition of the mode, the model is improved further by accumulating the experiences of interactions. Since our model attempts to interpret the new situation as behaviors generated under the previous mode, the prediction errors are detected when a mode shifts into the current one. Being aware of these misrecognitions, learning continues excluding a latest part of the memory and its quality is recovered to the state before such transitions.

III. A Model of Hybrid Dynamical System

Our model mentioned in the above can predict the current mode state based upon the input-output relations, but does not learn any relations on mode transitions, i.e., individual modes are learned independently. On the other hand, human mode recognition is partially attributed to such regular relations; recognition of the current mode is mostly helped by observed transition events that bridges between the previous mode and the current mode. That is, a user has acquired knowledge on transitions among the multiple nodes.

In order to implement this, the above model is extended to another compound computational model that consists of two layers. A role of the bottom layer is the same with the one of the previous model (i.e., to recognize the current mode based upon input-output relations), and the other upper layer deals with learning the transition events among modes as well as with predicting the following mode when the observations of the transition events are input. Those two layers are connected with each other via sharing the recognized status of current mode. The model, called Transitional Mixture of Experts (TME) model, is shown in Fig.2.

The transition events can be generally represented in a form of "if-then rules", whose antecedent part is defined by the variables of $\boldsymbol{z} = (z_1, z_2, \ldots)$; we define a set of transition events from j-th mode to i-th mode as $S_{i \leftarrow j}(\boldsymbol{z})$. A user of a machine with multiple modes can predict the next mode (i.e., i-th mode) by recognizing the events of $S_{i \leftarrow j}(\boldsymbol{z})$ when he/she is recognizing the current mode as the j-th mode. Since it is difficult to exhaustively learn a set of deterministic rules of $S_{i \leftarrow j}(\boldsymbol{z})$, we regard individual transitional rules as stochastic with transition probabilities of $g_{i \leftarrow j}(\boldsymbol{z})$. More generally, the entire set of transition rules is represented as a mode transition matrix $\boldsymbol{G}(\boldsymbol{z})$.

In the following, we mention the details of the proposed model of Fig.2. As for a mechanical system having m different modes, we define posterior probabilities of the belief that it is in the i–th mode at a particular time t; $\boldsymbol{\theta}_t = (\theta_{t,1}, \theta_{t,2}, \ldots, \theta_{t,m})^T$. The mode having the highest probability among $\theta_{t,m}$ is regarded as a mode that is recognized by a human user at this time t. This belief of $\boldsymbol{\theta}_t$ is calculated both by the likelihood of $\boldsymbol{L}_t = (L_{t,1}, \cdots, L_{t,\mathrm{m}})$, that is derived from the lower layer based upon the input-output relations of the modes, and by the prior probability of $\boldsymbol{P}_t = (P_{t,1}, \cdots, P_{t,\mathrm{m}})$, that is derived by mode transition matrix $\boldsymbol{G}(\boldsymbol{z})$:

$$\theta_{t,u} = \frac{L_{t,u} P_{t,u}}{\sum_{s=1}^{k} L_{t,s} P_{t,s}} \qquad (u = 1, \cdots, m)$$

Likelihood of $\boldsymbol{P}_t$ at time t can be defined using posterior probability $\boldsymbol{\theta}_{t-1}$ at the previous time step and mode transition matrix $\boldsymbol{G}$:

$$\boldsymbol{P}_t = \boldsymbol{G}\, \boldsymbol{\theta}_{t-1}$$

The details of the process of acquiring multiple internal models and the derivations of $\boldsymbol{L}_t$ and $\boldsymbol{G}$ are omitted herein and are given in the reference [7].

We verified that this extended model more correctly replays what a human user actually grasps on the complex mode transitions embedded within the automated system. In this sense, our model can be regarded as a model of recognizing the others' hidden internal states both from input-output relations particular to the individual modes and from the recognition of the events that trigger the mode transition.

Using the above-mentioned driver's mode-recognition model, we make a comparative analysis between the model's recognitions and the driver's actual recognitions during the experiments using a driving simulator.

Within the driving simulator used in the experiments, an extended ACC is embedded, which has the following six different driving modes;

IDLE mode: ACC is inactive

ARMED mode: Transferable from IDLE mode by turning on the switch resulting in ACC on standby

CONSTANT SPEED mode: Automatic driving mode with a specified speed

CAR FOLLOWING mode: Automatic driving mode in inter-vehicle gap keeping

OVER-RIDE mode: Transferable from CONSTANT SPEED mode or CAR FOLLOWING mode by a driver's pressing down the gas pedal resulting in the control of the vehicle transferred to human a driver from ACC

CANCELED mode: Transferable from either of CONSTANT SPEED mode, CAR FOLLOWING mode, or OVER-RIDE mode by a driver's pressing down the breaking pedal resulting in a standby mode.

A trial of the experiments lasts for seven minutes, and during the trial the simulator is paused every 30 seconds and the display is hidden to the subject for five seconds, when the subject is forced to answer the current active mode he/she guesses. The experimental data are gathered from 13 subjects and 217 answers of the modes are obtained from them in total. 26 answers out of those were wrong answers showing mode-recognition errors. The causes of those errors are classified into the following five types:

1 Errors induced by the lack of drivers' attentions (about 10 %)
2 Errors occurred at the driving situations in which the boundary conditions between modes are quite vague and noisy
3 Errors caused by the similarities of input-output relations of the mode
4 Errors caused by the immature learning of mode-transitions
5 Errors caused by being tied to the past mode

Based upon the above classification of errors, we attempt to replay those errors in the simulations of our proposing model by investigating into the mappings between the parameters of the model and the causes of the above errors.

The first class of the errors is out of the scope of the model, so this is excluded from the following discussions. As for the second class of errors, the causes are divided into two types; boundary conditions between the modes determined by particular threshold values of continuous variables and by the occurrence of some discrete events. Both cases can be reflected in the model, and the similar errors can be replayed. As for the third class of errors, we analyzed in details by investigating into a particular mode-recognition error of mistaking CONSTANT SPEED mode for CANCELED mode. Although these two modes have different dynamical properties, they may be confused for particular driving situations and mode-recognition errors are occurring at this time. We input the data of the driving situations in which a human subject errs into our model, and it was found that the model also replays the recognition errors.

A more complex error in which multiple causes are combined to induce the recognition error is shown in Fig.3. In this case, the mode is changed by a driver's unconscious

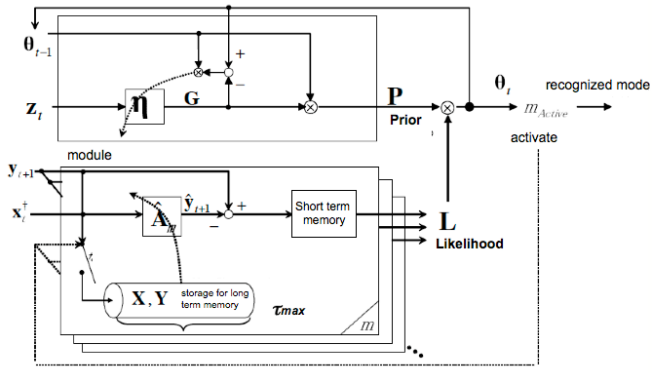

Fig.2 Transitional Mixture of Experts

action of pressing the breaking pedal, which caused the actual mode status changed into CANCELED mode, while a driver fails in recognizing that and continues to believe that the mode still remains in CONSTANT SPEED mode. Furthermore, due to the similarities of the input-output relations the subject confuses in distinguishing between CONSTANT SPEED mode and Over-ride mode, which prevented the subject from returning to the correct recognition on the current mode. Fig.3 replays this situations showing how the beliefs on the six modes are changing as the time passes. The modes with the most confirmed beliefs are the ones that our model outputs at the individual time steps. The upper and lower bars in the bottom part show the subject's recognitions obtained in the experiment and the actual mode in the driving simulator, respectively.

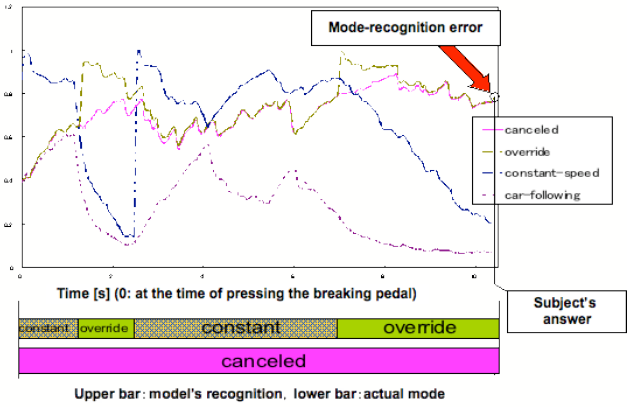

Fig.3 Comparative analysis of recognitions by the proposed model and a human subject

IV. USAGE FOR PREDICTIVE ANALYSIS OF LATENT HUMAN ERRORS

It would be possible to analyze the probable human errors exhaustively by inputting a variety of driving situations into the model and evaluating the recognition outputs of the model. Through such analysis, we can evaluate the safety usability of the newly designed mechanical system with multiple modes without making time-consuming experiments using the human subjects. Moreover, by changing and adjusting the parameters of the model, we assume a variety of the human drivers with different driving skills, so our model could be used as a digital human model having a capability of dynamical recognition [8].

Another usage of our proposed model is to identify the boundary of safety-guaranteed usage of the designed artifact. As shown in the experiment shown in Fig.3, mode-recognition errors between particular pairs of modes are observed in the human subject. In order to analyze why such errors occurs, we changed the input data on inter-vehicular distances, difference of speeds between the speed of a preceding vehicle and a specified speed for constant speed mode, amounts of pressing gas pedals and the vehicle speed, etc. and it would be possible to evaluate how the outputs of the recognition is changed according to those.

V. CONCLUSIONS

Major difference in sociality between insects and humans is an ability to recognize the others and to adapt to them by constructing their representations within them. It is not a simple pattern recognition problem, but is more close to an activity of *interpretation*; what is signified on the provided object is not solely determined by the properties of the objects but also depends upon the internal states of the *interpretant*. It would be of importance to develop a human recognition model on complex artifact systems like multi-mode machines for designing and analyzing the complex behaviors emerging out of interactions within the human-in-the-loop systems.

REFERENCES

[1] M. Ashikaga, T. Hiraguchi, M. Sakura, H. Aonuma and J. Ota: Modeling of adaptive behaviors in crockets, in Reprints of SICE 18th Symposium on Autonomous Distributed Systems, Fukui, pp.189—194, 2006. (in Japanese).

[2] T. Taniguchi and T. Sawaragi. Dynamic process of a user 's development of multiple internal models of automation behavior including mode transitions. In *2nd International Symposium on Mobiligence in Awaji*, 2007.

[3] D.M. Wolpert, K. Doya, and M. Kawato. A unifying comuputational framework for motor control and social interaction. *Phil Trans R Soc Lond B*, Vol. 358, pp. 593–602, 2003.

[4] D.M. Wolpert and M. Kawato. Multiple paired forward and inverse models for motor control. *Neural Networks*, Vol. 11, pp. 1317–1329, 1998.

[5] R. A. Jacobs, M. I. Jordan, et al: Adaptive mixtures of local experts, *Neural Computation*, Vol.3(1), pp. 79/87, 1997.

[6] Y. Horiguchi, R. Fukuju, T. Sawaragi: Effects of Similarity in Response Behaviors of Automated Mechanical System on User's Awareness of Operation Modes, in *Preprints of HIS2006*, pp.109-114, 2006. (in Japanese).

[7] T. Taniguchi, Y. Tanaka, Y. Horiguchi and T. Sawaragi: Acquisition of multiple internal models including mode transition events during driving, in *Preprints of HIS 2007*, pp.189-194, 2007. (in Japanese).

[8] H. Hattori, T. Taniguchi, Y. Tanaka, Y. Horiguchi, H. Nakanishi and T. Sawaragi: A method of predictive analysis for preventing mode recognition errors, in *Preprints of the 52-nd SCI Conference*, 2008 (to be appeared). (in Japanese).

Regulatory dynamics of colony-level adaptive behavior in social insects and its underlying individual-level interaction

Kazuki TSUJI（University of the Ryukyus）, Ryohei YAMAOKA（Kyoto Institute of Technology）,
Ken SUGAWARA（Tohoku Gakuin University）

Summary: We investigated decentralized control and self-regulated dynamics of adaptive behavior in social insect colonies. We focused mainly on colony-size dependent regulation of the social systems in ants. In *Diacamma* sp. reproductive division of labor is regulated by information transmission via physical contacts and movements of individual ants. The underlying density-dependent feed back system was investigated both experimentally and by computer simulation. We are also going to test the efficiency of the dynamics using real robots. We also screened chemical substances that bear the key information in the hypothetical regulatory dynamics by the GC analysis and a bioassay. Related topics, such as policing, fractal geometry of individual behavior, key chemicals for the caste differentiation in this ant were also investigated

Unlike human societies colonies of social insects are regulated by a decentralized control. Individual colony members respond to local information that they encounter according to simple rules. Nevertheless, the colony as a whole can behave adaptively. In this study we focus the social regulation related to the intra-nest density and the proportion of individuals. An ant colony changes its behavior depending on the number and the proportion of workers. For example, in small colonies workers are usually timid, whereas in large colonies workers behave more aggressively. For another example an ant colony switches the production of castes related to colony size; sexual castes (queens and males) are usually produced when the colony size exceeds a certain threshold. However, its underlying proximate regulatory mechanisms, though they seem to be general in social insects, are largely unknown. Living in the dark, it is unlikely for individual earth-bounded ants directly to obtain global information on the colony size and the individual proportion. We assumed that there could be a self-organized and decentralized feedback mechanism mediated by physical contacts between individual colony members. This study consists of three parts. First, we will experimentally show the presence of such regulatory mechanisms in real ants. Second, we identify chemical substances that bear the key information in the hypothetical regulatory dynamics. Last, we constructed mathematical models that can simulate the regulatory dynamics. The validity the hypothetical feedback mechanism is also going to be tested using real robots. The goal of this study is in the biological sense to understand a general mechanism that regulates animal societies, and in technological sense to accumulate basic information that will be used to develop a control program for decentralized controlled robots.

Density sensing

We used *Diacamma* sp.from Japan throughout this study of this year. This is the only *Diacamma* species found in Japan. Recently, as a new model organism, its biology has been extensively studied (e.g. Nakata and Tsuji 1996). The gamergate (functional queen) of *Diacamma* sp. transfers information of her presence to nestmate workers through direct physical contacts (Tsuji et al. 1999). The gamergate regularly walk around in the nest touching workers with her antennae. We defined this active information transmission behavior as the patrol. It is predicted that in a large colony the gamergate has to invest more efforts in this patrol. In fact, our detailed observation revealed that as colony grows the gamergate increased the number of patrol bouts per unit time, the proportion of time spent on patrol and the mean duration of patrol (Figure 1).

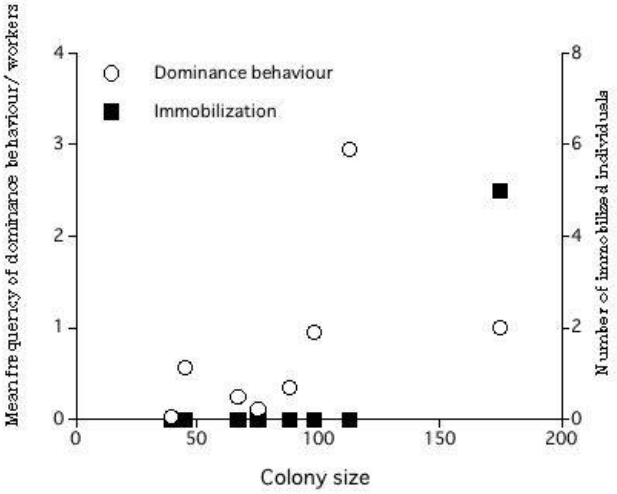

Figure 1. The relationship between the frequency of aggressive interaction among workers and colony size.

This colony size related behavioral change in the gamergate was also confirmed experimentally (Figure 2). The above results suggest that gamergates can adaptively change behavior, as if they can recognize the colony size. But how they can do so? The frequency of the gamergate's contact per worker per time was almost constant regardless of the colony size, whereas there were more workers that had by chance no contact for a long time in larger colonies. Simultaneously, the frequency of aggressive dominance interaction and that of immobilization (a worker policing behavior directed to ovary-developed workers) has increased as the colony size increased (Figure 1). These behaviors are characteristics of orphaned workers. From these results we set out a hypothetical self-organized feedback system that can control the adaptive shift of the patrolling

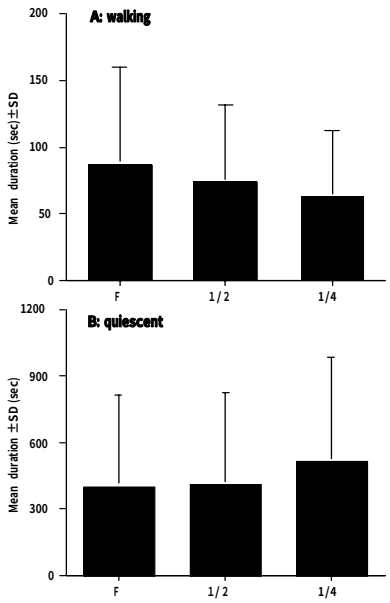

Figure 2. Behavioral changes of gamergates in response to the colony size manipulation. F, 1/2 and 1/4 represent full, half and quarter of natural colony size, respectively.

behavior. The hypothesis assumes that the gamergate invests more efforts in patrolling, when she encounters physiologically "orphaned" workers during patrolling. We conducted an experiment that varied the proportion of physiologically orphaned workers under a constant colony size. The gamergates actually respond to the presence of orphaned workers and prolonged the average patrol duration (Tsuji K. and Kikuchi, T. et al., unpublished data), qualitatively supporting the working hypothesis.

Information of gamargate presence

Queens of social insects are considered to produce a queen substance that inhibits self-reproduction of workers. However, in ants such a queen substance has been unidentified yet. Recently, cuticler hydrocarbons (CHCs) are suspected to be the queen substance. In *Diacamma* sp. from Japan queen information is transferred to workers only through direct contact, suggesting that hardly volatile chemicals can bear the information. Our careful bioassay indicates that among gamergate extracts only CHCs inhibit dominance behavior of orphan workers (Y. Fujito et al. unpublished data). This is the first empirical demonstration for the CHCs-queen substance hypothesis. As the next step, we have conducted a more sophisticated bioassay separating gameragate's CHCs into long-chained gamergate specific components (B peaks) and short-chained non-specific components (A peaks). After separating A and B using HPLC, we did a bioassay by exposing those extracts to workers. Workers responded only to A peaks with extensive antennations. This indicatesthat A peaks CHCs are likely the gamergate presence information.

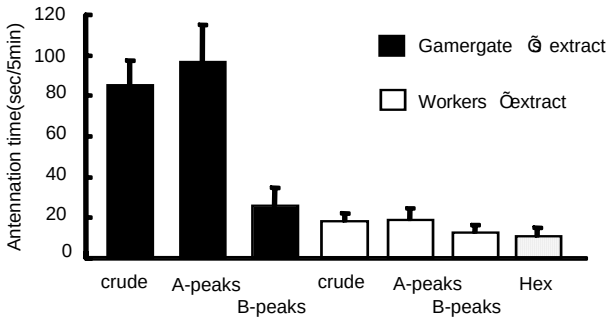

Figure 3. Workers response to each category of extract. Hex means hexiane as a control treatment.

Gemmae substances that regulate functional castes differentiation in *D.* sp.

The caste differentiation into gamergates and workers is regulated by mutilation of gemmae, a pair of thoracic appendages in *Diacamma.* Minute pores exist on the surface of gemmae, which are connected to secretary glands that fully fill gemmae. GC and GC/MS analyses showed that the major components of the gemmae secretion are lauric acid and other fatty acids. We extracted these chemical components from gemmae that are used to a bioassay. Workers sowed statistically significantly more interest to this extract than control.

Modeling of the patrol behavior of *Diacamma's* gamergate

We propose a simple simulation model of the colony-size dependent gamerate's patrolling behavior. We assume the gamergate and the workers have their

$$\begin{cases} \dot{I}_{gam} = -\gamma \cdot I_{gam} + \alpha \cdot (I_j - I_{th}) \cdot \delta(\vec{r}_{gam} - \vec{r}_j) \\ \dot{I}_j = c - \varepsilon \cdot I_j \cdot \delta(\vec{r}_{gam} - \vec{r}_j) \end{cases}$$

own internal states which change depending on their bodily contacts. The internal state of the gamergate reflects the patroling-time, and that of workers reflects the degree of ovarian development. By numerical simulations, we confirm that the patrol time depends on the size of colony (Figure 4). Now we are trying to construct the universal model that contains the diffusion term.

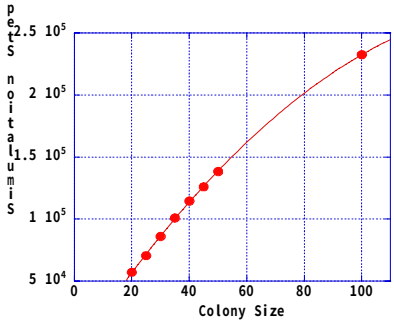

Figure 4. The outputs of the simulation model of colony

size dependent the gamergate's patrolling behavior.

Analysis of multi-body behavior

We have analyzed and discussed the behavior of a single ant that has a power law relation between the velocity and the fluctuation of velocity. Now we are investigating the effect of the interaction among individuals. As ants prefer to move the edges of the field and narrow spaces, we introduce an acrylic hemisphere field to decrease the edge effect (Figure 5). We treat 2-4 ants and measure their trail, velocity, distance etc. We obtained some qualitative results, such that they tend to make a contact positively, and contact state with two bodies is a basic state even when the group size is more than two. Quantitative analyses are now under going.

Figure 5. The acrylic hemisphere for the behavioural observation.

Division of labor in multi-robot system based on chemical communication

(1) Simulation

Division of labor is one of the most important aspects of multi-robot system. For effective performance, the groups need to exhibit proportion regulation of the population. It is also needed to regulate the system against external disturbances without aid from a special individual. Focusing on the application for multi-robot system, we discuss the simple dynamics for homogenous multi-robot system. We propose a dynamic probability model focusing on the transition rates between the internal states in each robot. We introduced a foraging task in a plain field, and discussed their performance mainly focusing on the size effect of the system (Figure 6).

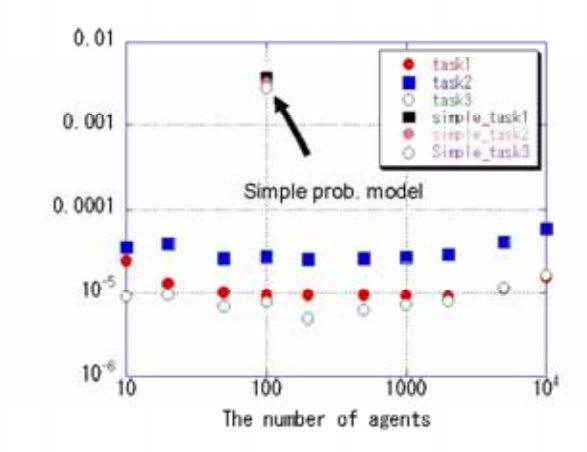

Figure 6. An output of the simulation for multi robots

(2) Development of prototype robot

To execute a preliminary experiment, we made a prototype robot which enables to communicate by chemical signals. We treat a few alcohols as a communication media and tried to make a fundamental experiment to switch two tasks.

References

Nakata K, Tsuji K.1996. The effect of colony size on conflict over male-production between gamergate and dominant workers in the ponerine ant *Diacamma* sp. Ethol. Ecol. Evol. 8: 147-156.

Tsuji, K., Egashira, K., Hölldober, B. (1999) Regulation of worker reproduction by direct physical contact in the ant Diacamma sp. from Japan. Animal Behaviour 58 (2): 337-343.

Construction of Quantitative Neural Model for Discrimination of Bird Songs in Zebra Finch

Kotaro Oka, Takuro Sakuratani, Akira Fujimura, Mai Iwasaki and Masafumi Hagiwara

***Abstract*— To construct the quantitative model for information processing in song birds, we investigated the neural activity in hippocampal formation (HF) in female zebra finches. We applied neutral red, a fluorescent pH indicator that is sensitive at neutral pH region and shows large fluorescent change (~ 20 % ΔF/F), for visualizing the neural activity. The light stimulation to the eyes induced the pH decrease in the huge area of HF. From the recent anatomical study, the HF receives neuronal input from the visual cortex in the bird brains, this neuronal response is reasonable. Then, we applied two types of male bird songs: song A and song B. No eminent response was observed by these typical bird songs. This result is not consistent with our previous study by visualization of neuronal activity with immediate early genes expression of *Arc* or *c-fos*: the several neurons of HF responded by male songs, and some of these neurons responded to both of songs. And finally, we applied song A and B simultaneously (song A & B simulation). This simultaneous presentation of two songs induced the neuronal activity in the anterior part of the HF. This result suggest that the HF of the bird response not to simple or typical songs but also to complex or modulated song, and provide us the hint of information processing for song discrimination in female zebra finches.**

I. Introduction

Zebra finches communicate with their songs. Male finches have several kinds of their own songs and female finches choose the male for mating by his song. For understanding the song communication, information processing in the female brains is crucial. However, the neural network for the information processing in female brains has been poorly understood.

There are a few numbers of studies for female brains [1, 2]. In our laboratory, we are interested in the bird song recognition and discrimination in female birds. We focused on the hippocampal formation (HF, Fig.1), and investigated the neuronal activity with electrophysiological and molecular biological approaches.

The HF of bird brains can be identical to the HF of the mammals from the developmental, anatomical, and their functions including spatial memory and imprinting [3. 4]. From our previous study using retrograde labeling by fluorescent dye, we found the neural connection between HF and auditory cortices; caudomedial nidopallium (NCM), caudomedial mesopallium (CMM), robust nucleus of the arcopallimu (RA) cup (unpublished data). We also found the neuronal activity propagation form the posterior to the anterior of HF, and this observation is recent anatomical findings [11].

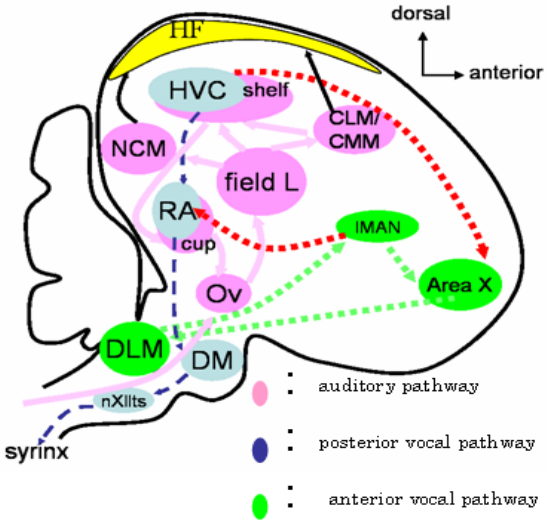

Fig. 1 Brain architecture of male zebra finch

Recently we used catFISH (cellular compartment analysis of temporal activity by fluorescence in situ hybridization) technique for *Arc* (activity-regulated cytoskeletal-associated protein) mRNA to visualize the active neurons [5]. *Arc* is one of effector immediate early genes, and expression of *Arc* is synaptic-activity dependent. *Arc* mRNA is not translated at the cell bodies but transferred to the peripheral of the neurons and translated locally. Because this process is time-dependent, two populations of neurons that are activated at different timings can be discriminated with *Arc* mRNA expression by FISH. Therefore, we provided two different male songs sequentially with 50 min interval as auditory stimulations and found that CMM and HF were candidates for song discrimination. This finding is useful for understanding the

Kotaro Oka is with Department of Biosciences and Informatics, Keio University, 3-14-1 Hiyoshi, Kohoku-ku, Yokohama, Kanagawa 223-8522, Japan (phone: 045-566-1728; fax: 045-564-5095; e-mail: oka@bio.keio.ac.jp).

Takuro Sakuratani is with Department of Biosciences and Informatics, Keio University, 3-14-1 Hiyoshi, Kohoku-ku, Yokohama, Kanagawa 223-8522, Japan.

Akira Fujimura is with Department of Biosciences and Informatics, Keio University, 3-14-1 Hiyoshi, Kohoku-ku, Yokohama, Kanagawa 223-8522, Japan.

Mai Iwasaki is with Department of Biosciences and Informatics, Keio University, 3-14-1 Hiyoshi, Kohoku-ku, Yokohama, Kanagawa 223-8522, Japan.

Masafumi Hagaiwara is with Department of Information Engineering, Keio University, 3-14-1 Hiyoshi, Kohoku-ku, Yokohama, Kanagawa 223-8522, Japan

neural coding in female brains.

The catFISH technique is effective for investigating the neuronal populations but maximum number of stimulation categories is two. We, therefore, have to develop the new technique to study the neuronal information processing. One of the interesting differences of HF location between bird and mammal brains; bird HF is located on the surface of the brain. This indicates that we can use the several imaging techniques for neuronal activity. By using imaging techniques, we can apply several numbers of stimulation sequentially, and found the functional areas of the bird brain. We can select several imaging techniques: membrane potential imaging, intrinsic fluorescence from mitochondria, and pH imaging with pH sensitive dyes.

In this study, we choose pH imaging with a fluorescent dye, neutral red (Fig.2). Neutral red is sensitive at neutral pH region and shows large fluorescent change (~ 20 % ΔF/F), for visualizing the neural activity. Neurons lower their intracellular pH by their metabolism, and its pH recovers by Na^+/H^+ pumps located on cell membrane. In mouse brain neurons, it takes about 60 seconds to recover to the initial pH [6]. Neural activity change was observed in rat cerebellum cortex by the stimulation *in vivo* [7]. Tactile stimulation induced climbing fibers and parasagaital fluorescent bands were observed on the cortex. Another application of this dye was for visualization of long-tem depression in cerebellum cortex by the simultaneous simulation of parallel fibers and climbing fibers in mouse [8].

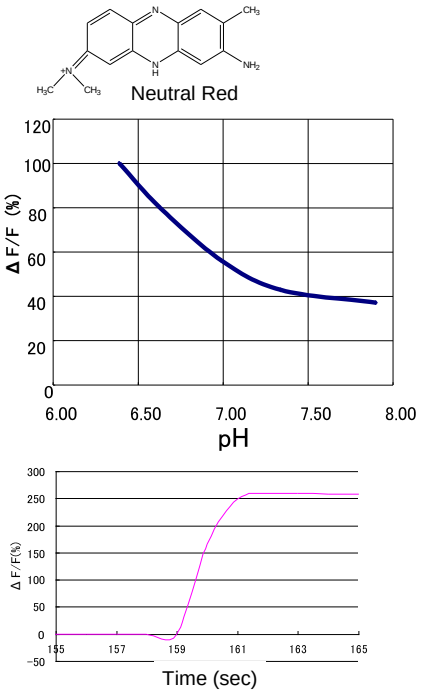

Fig. 2 Characteristics of neutral red. Structure of neutral red (upper), relative fluorescent change as the function of pH (middle) and response to transient change of pH (lower).

II. Experimental Method

A. Animal Preparation

Experiments were performed on adult female zebra finches (> 90 days old) that were housed in groups of 5 to 10 individuals and maintained on a 12:12 hrs light/dark cycle in a temperature-controlled room (26℃). All subjects were treated under Keio University's Animal Use Guidelines.

The bird was anesthetized intramuscularly with a mixture of ketamine (40 mg/kg; SIGMA) / xylazine (8 mg/kg; SIGMA). Supplemental doses were administered as necessary. The bird was placed on a platform attached to a stereotaxic head holder (David Kopf Instruments, USA). Under local anesthesia with a 0.4% lidocaine (SIGMA), the cranium and the dura were removed. We made the small window for observation of HF.

B. Optical imaging with pH sensitive dye, neutral red

After anesthesia, the cranium and the dura were removed and a handmade plastic chamber was bonded on the skull with dental cement (GC Unifast II, GC, Japan). The brains were stained for 30-40 min by neutral red (10 mM, Sigma) in artificial cerebrospinal fluid (ACSF, in mM: NaCl 119.0, KCl 2.5, $MgCl_2$ 1.3, $CaCl_2$ 2.5, NaH_2PO_4 1.0, $NaHCO_3$ 26.2, glucose 11.0). Following wash the brain with ACSF, the surface was covered with ACSF. The camber was then held on with a handmade head positioner under an epifluorescent microscope (MZ-6, Leica, Japan) on a vibration isolator (AET0806-NC, Meiritsu, Japan).

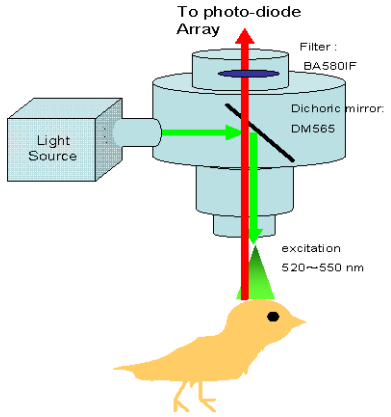

Fig. 3 Experimental setup for optical recording from female zebra finches

The MiCAM01 optical imaging system (Brainvision, Japan) consists of an area sensor with 96 × 64 photodiodes and a data processing unit. The epifluorescent optics, consisting of two lenses, ×1.0 objective lens, ×0.63 light focusing lens (PLANAPO, Leica) and a dichroic mirror (575 nm) with absorption (590 nm) and excitation (530 nm) filters, were mounted above the brain. Each photodiode received signal from a 20 × 20μm^2 sample area, thus creating a 2.0 × 1.3mm^2 entire imaging field. The experimental setup was shown in Fig.3. The data was collected 2730 sequential

images (0.75 ms/frame). The ratio of the fractional change in fluorescence of voltage sensitive dye to the fluorescence of the background ($\Delta F/F_0$) was calculated and used as the optical signal.

III. Results

A. Neural response to white noise and optical stimulation

First of all, we applied white noise and observed the neuronal responses in HF (Fig.4, upper panel). We selected 7 areas that covered whole areas of HF. No responses were observed by white noise application. Small deviation of fluorescent response depends on heart beat of the bird. This result confused us because previous our work shows that HF responds to bird songs. We, therefore, tried to demonstrate the validity of optical imaging system.

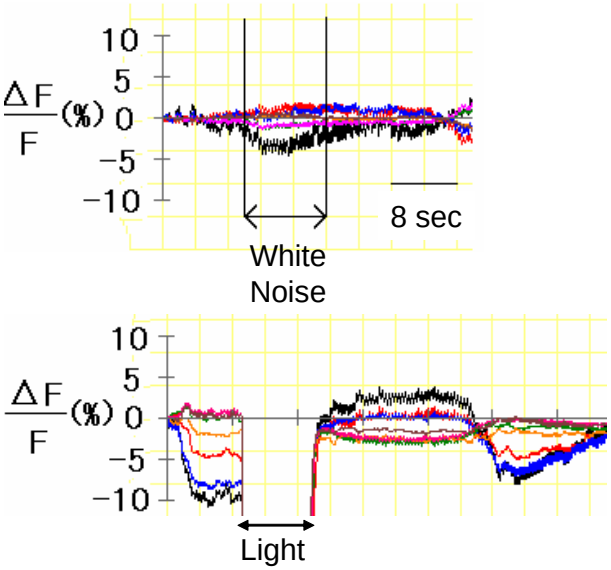

Fig. 4 Neural responses to white noise (upper panel) or light (lower panel) in HF region in female zebra finch.

We tried to visualize the neuronal response to the light stimuli to the eyes. From previous anatomical study [11], HF receives neuronal input from visual cortices, and the visual stimuli will be induced the neuronal response in HF. We applied the light with a flashlight and observed the fluorescent response in HF (Fig.4 lower panel). Basal levels of the fluorescent intensities were different in 7 areas before the light stimulation, and the light stimulation induced huge increase of fluorescent intensities (during the light stimulation, fluorescent responses were saturated). The amplitude of relative fluorescent responses are almost same as previously reported [6, 7, 8], and time course of fluorescent intensities to return to the initial level is also same. This result confirms us that neuronal activity recordings with the pH-sensitive fluorescent dye, neutral red, is applicable for investigating the bird brains.

B. Response to bird songs

Two types of bird songs (song A & song B) were applied to the birds and neuronal responses in HF were visualized (Fig.5). These two songs were used previously in the catFISH study [5], and induced neuronal responses in different populations of neurons in CMM and HF. Interestingly, no neuronal response was observed by application of song A and also song B. However, simultaneous presentation of song A and B (song A&B, Fig. 4, lower panel) induced huge responses in HF. The areas of response are mainly located at the anterior of the HF. Because the intensities of sound is adjusted among white noise, song A, song B and song A&B, this specific responses to song A&B is not due to sound intensities.

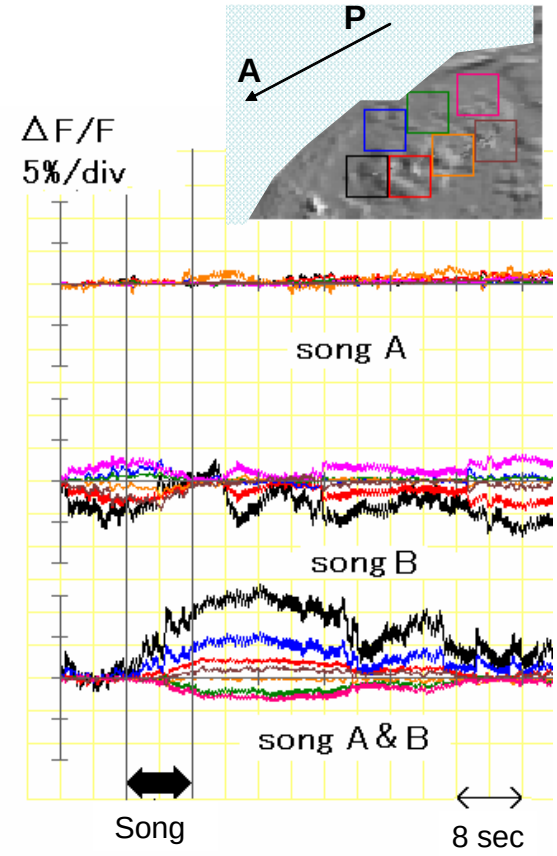

Fig. 5 Neural activity changes to several types of bird songs. Upper panel indicates the location for measurement from anterior (black) to posterior (pink) areas in HF. Typical bird songs A and B induced no eminent responses in HF (two middle panels), but simultaneous presentation of two songs (song A & B) induced huge responses, especially, at the anterior areas in HF.

IV. Discussion

A. catFISH results vs. pH imaging responses

The signal of *Arc* mRNA is observed in the several regions

of the brain, especially CMM and HF [5]. This finding indicates a possibility that theses regions are used for the information processing of the discrimination of songs. One of our unlooked-for results is the response in HF because no relation has been reported in auditory systems and HF. In this study, we shows that HF responds to sound (white noise, Fig. 4), and also typical bird songs (Fig. 5). This result seems to conflict to our previous catFISH results. One possibility is sensitivity of pH imaging. The detection limit of catFISH is high compared to pH imaging, and single bird song is not detected by pH imaging but combination of song A and B induced responses from enough numbers of neurons for pH detection. Another explanation is the location of responded neurons; single song responded neurons located the depths of HF. We further check the methodology of pH imaging to the bird brain.

B. How dose HF process the information of male songs?

In mammals, the function of HF is demonstrated: working memory and spatial recognition [9]. One of the fascinating findings is place cells in HF [10]. These neurons are rapidly constructed in HF when mice are located in the novel place, and place cells code the location in this novel place. In bird brains, the function of HF is related to the spatial recognition, sexual behaviors, social behaviors, and imprinting. However, no relationship was described in song learning because of no responses to songs in immediate early gene studies. Recently, detailed anatomical study has been reported [11], and inter HF neuronal connections and neuronal projections from and/or to another cortices are demonstrated. Combination of experimental results and these anatomical results will illustrate the function of HF in bird brains.

V. CONCLUSION

We applied neutral red, a fluorescent pH indicator that is sensitive at neutral pH region and shows large fluorescent change, for visualizing the neural activity. We applied two types of male bird songs; song A and song B. No eminent response was observed by these typical bird songs. This result is not consistent with our previous study by visualization of neuronal activity by immediate early genes expression of *Arc* or *c-fos*: the several neurons of HF responded by male songs, and some of these neurons responded to both of songs. And finally, we applied song A and B simultaneously (song A & B simulation). This simultaneous presentation of two songs induced the neuronal activity in the anterior part of the HF. This result suggest that the HF of the bird response not to simple or typical songs but also to complex or modulated song, and provide us the hint of information processing for song discrimination in female zebra finches.

ACKNOWLEDGMENT

We thank Dr. Koji Hotta for his helpful suggestion and discussion of optical imaging.

REFERENCES

[1] Terpstra NJ, Bolhuis JJ, Riebel K, van der Burg JM, den Boer-Visser AM. 2006. Localized brain activation specific to auditory memory in a female songbird. J Comp Neurol 494:784-791.

[2] Riebel K. 2000. Early exposure leads to repeatable preferences for male song in female zebra finches. Proc Biol Sci 267:2553-2558.

[3] Watanabe S, Bischof HJ. 2004. Effects of hippocampal lesions on acquisition and retention of spatial learning in zebra finches. Behav Brain Res 155:147-152.

[4] Sandananda M BH. 2004. *C-fos* is induced in the hippocampus during consolidation of sexual imprinting in the zebra finches. Hippocampus 14:19-27.

[5] Fujimura A, Hotta K, Oka K. 2007. Proceedings of the 2nd international symposium on mobiligensce 215-218.

[6] Chen G, Hanson CL, Ebner TJ. 1998. Optical responses evoked by cerebellar surface stimulation in vivo using neutral red. Neuroscience 84:645-668.

[7] Chen G, Hanson CL, Ebner TJ. 1996. Functional parasagittal compartments in the rat cerebellar cortex: an in vivo optical imaging study using neutral red. J Neurophysiol 76:4169-4174.

[8] Gao W, Dunbar RL, Chen G, Reinert KC, Oberdick J, Ebner TJ. 2003. Optical imaging of long-term depression in the mouse cerebellar cortex in vivo. J Neurosci 23:1859-1866.

[9] Squire LR, Kandel ER. 1999. Memory from mind to molecules. 106-127, Scientific American Library .

[10] O'Keefe J, Dostrovsky J . 1971. The hippocampus as a spatial map. Preliminary evidence from unit activity in the freely-moving rat. Brain Res. 34, 171-175.

[11] Atoji Y, Wild MJ. 2007 Limbic systems in birds: morphological basis. Watanabe S, Hofman MA (eds.) Integration of comparative neuroanatomy and cognitive. 97-123, Keio Univ.

Extended Multiple Forward Models on Attribution of Own Actions to the Intention of Self or Others

Motoichiro Kato*, Mihoko Otake**, Kohei Arai**, Takaki Maeda*,
Yusuke Ikemoto**, Kuniaki Kawabata***, Toshihisa Takagi**, and Hajime Asama**

Abstract—**Human cognitive mechanisms on voluntary action and intention have been studied for design in user-friendly interface. One of the key issues on cognitive science of self-consciousness is sense of agency, or the attribution of own actions to the intention of self or others. The patients with schizophrenia often show mis-attribution of their own actions to the intentions of others, that is, the disorder of sense of agency. In this study, we administered the experiments of sense of agency to normal subjects. We also conducted computational simulations through extending the multiple forward models, which successfully described the experimental results.**

I. Sense of Agency, Schizophrenia and Information System

The sense of agency has been studied in schizophrenia research, because several psychotic symptoms with schizophrenia could result from dysfunction of the awareness of one's own action as well as recognition of actions performed by others. Paranoid schizophrenia has a variety of delusions or hallucinations. Delusions and hallucinations could be described as dysfunction of the sense of agency. The patients with auditory hallucinations misattribute self-generated internal speech to external others' voice. Frank et al. investigated the possibility that delusions of influence could be related to abnormal recognition of one's own actions in individuals with schizophrenia [5]. Subjects executed discrete movements in different directions holding joystick. The image of a virtual handholding a joystick was presented on a screen with angular biases and time delays. Patients with schizophrenia made significantly more recognition errors in trials with time delays, compared with normal subjects. In the experiment by Daprati et al., hallucinating and deluded patients with schizophrenia tended to over-attribute the alien hand to themselves [2]. The two brain areas, the inferior part of the parietal lobe and the insula, appeared to be modulated by the degree of discrepancy, which has been investigated through brain imaging studies [3, 4]. Diverse models such as Forward model [1] and Who system [6] have been proposed which describe the mechanism of the sense of agency. In this study, we focus on normal subjects rather than patients with schizophrenia in order to understand the sense of agency characteristics of normal subjects for designing efficient human-machine interface, because previous studies have been focusing on patients with schizophrenia, and the performances of normal subjects were not tested in detail.

Information systems are ubiquitous in the modern information society. People spend a long time in front of the personal computer using the typical input and output devices: keyboard, mouse, and display. It is very important to analyze how we adopt to this human-machine interface in order to understand cognitive mechanism of human, because such a mechanism provides us design principle of daily used human-machine interface. In general, people become comfortable using machines when they feel the machines as if they are part of their bodies. To date, usability of typical human-machine interface with key board, mouse, and display have not been analyzed in terms of the sense of agency. In this study, we experimentally analyze the sense of agency and the experimental results are simulated by the multiple forward models. We conduct a research whether our model is validated through computational simulation.

II. Forward Model

Forward model could qualitatively describe the sense of agency. Forward model contains a dynamic model which predicts the consequences of motor commands and an output model which makes a prediction of the sensory consequences of motor commands, which is compared with the actual consequences of movement from sensory system. Blakemore et al. [1] proposed that an underlying dysfunction in the forward model may lead to the lack of the sense of agency, and consequently the development of delusions of control in patients with schizophrenia (Fig. 1). It was not clear, however, how the forward model predicts the consequences of actions which are necessary for attribution of actions to the intention of self or others. A purpose of this study is to propose a quantitative forward model which can simulate the experimental results of sense of agency, in order to understand its mechanism. In this paper, the characteristics of the attribution of actions to self or others are explored, and the novel forward models are developed whose simulation results are comparable to experimental results.

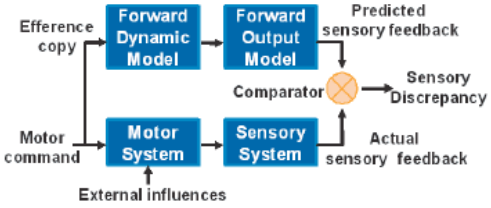

Fig. 1. The forward model of motor control: forward model contains a forward dynamic model which predicts the consequences of motor commands and a forward output model which makes a prediction of the sensory consequences of motor commands, which is compared with the actual consequences of movement from sensory system [1].

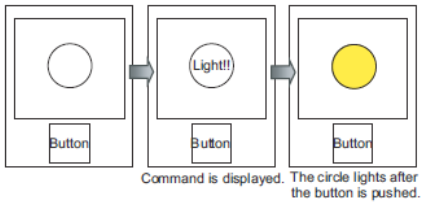

Fig. 2. A graphical user interface for the sense of agency experiment.

III. Behavioral Experiments

A. Subjects

Eight normal subjects (6 men and 2 women; mean age=22.9 years, SD=16.8) participated in the study. Subjects were naive about the purpose of the study procedure.

B. Materials

During the study, the image of a circle and a button were presented to the subjects on a computer screen with a high refresh rate. After the button is pushed by the subjects, the circle lights and the color of the circle turn yellow (Fig.2). Time delays could be introduced in this representation.

C. Procedure

Subjects held the mouse button with a hand. The task consisted of executing a series of simple movements with the mouse button. Each trial started with a white screen with a white circle and a white button. The instruction "Light!" is displayed at the center of the circle. The subjects push the button and the color of the circle become yellow with delays. Immediately after the trial, the subjects had to answer the following question with a yes or-no response: "Who did switch on the light you saw on the screen?" The buttons with the term "self" or "computer" appear on the screen and the subjects select each of them. Trials with time delays were used, in which the lighting of the circle were delayed by a given time (0, 40, 80, 120, 160, 200, 240, 280, 320, 360, and 400 [ms]). Thus, we prepared eleven kinds of time delays in total. Each trial was run four times for each of the 11 kinds of time delay. Each subject executed a total of 44 trials. The order of presentation of the 44 trials was randomized for each subject. Identical trials could not be presented one after the other.

D. Data Analysis

The numbers of "self" responses of subjects were counted by time delay of lighting on the screen. The percentage of "self" responses from the first 22 trials (1 - 22 trials) to the last 22 trials (23 - 44 trials) for every successive 22 trials was calculated by time delay. The percentages of "self" responses of every successive 22 trials were analyzed by logistic regression analysis. The gradients of logistic regressions of the percentage of "self" responses were calculated.

IV. Results

A. Descriptive Analysis

Figure 3 shows the number of "self" responses or "self-attribution" by subjects, who switched on the light they saw on the screen, as a function of time delay. There were total of 8 subjects and 4 trials for each time delay. Therefore, 32 responses was maximum number of "self" responses while 0 was minimum number. Subjects gave "self" responses in nearly all trials without time delay and small delay (40 ms). Subjects gave "computer" responses in nearly all trials with large delay (360 - 400 ms). The number of "self" responses was higher for the smaller time delay and decreased as the delay increased. Subjects showed a clear and sharp reduction in "self" responses for a relatively small bias (120 - 160 ms).

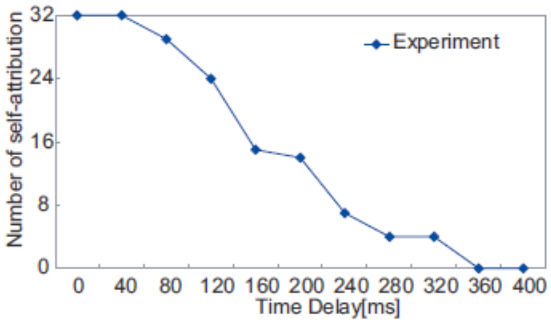

Fig. 3. Relationship between the number of self attribution and time delay: sum of 8 subjects.

B. Time Series Analysis

Time series of attribution of one representative subject on each trial is shown in Fig. 4. X-coordinate is a number of trial and Y-coordinate is a time delay. Circle dot is plotted with the time delay when the subject answered "self". Triangle dot is plotted with the time delay when the subject answered "computer", which means other-attribution. The time delay which discriminates self- or other-attribution is around from 200 to 240 ms in the early stage of total trials (0 to 16 trials). The time delay which discriminates self or other gradually decreases in time. It is about 80 to 120 ms in the end stage (28 to 44 trials). The discrimination criterion changes as the trial proceeds. This characteristic is observed for every subject. Then, temporal change of the percentage of self-attribution was analyzed in the course of trials for the average of 8 subjects. The percentage of self-attribution was calculated by dividing the number of self-attribution by total number of trials for each time delay. The percentage of self-attribution for each time delay in the first 22 trials (plotted in dotted line) and the last 22 trials (plotted in line) are shown in Fig. 5. The percentage of the first 22 trials showed smooth decrease in "self" responses while that of the last 22 trials showed sharp decrease in "self" responses.

C. Logistic Regression Analysis

The percentages of self-attribution in every successive 22 trials which were sampled by turns in 44 trials, were calculated by bringing out the percentages from *i*-th trial to (*i*+21)-th trial, and shifted the number *i* from 1 to 23 recursively. They were analyzed by logistic regression analysis. The curves of the percentages were hypothesized as logit curves. They were converted with the following equation:

$$\mathrm{logit}(p) = \log\left(\frac{p}{1-p}\right) \quad (1)$$

The percentages of every 22 trials were substituted to the variable p. First-order approximations were calculated for each curve of every 22 trials. The gradient of the first order approximation of every 22 trials obtained by logistic regression is plotted in Fig. 6. X-coordinate is a number of the first 22 series of trials and Y-coordinate is a gradient of the first-order approximation of the 22 trials. The absolutes of the gradient of the first-order approximation increase in the course of trials. The discrimination criterion of self-attribution becomes clear in the course of trials.

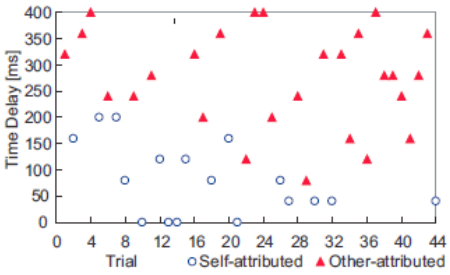

Fig. 4. Attribution of one subject on each trial: x-coordinate is a number of trials; y-coordinate is time delay. Circle dots are self-attributions while the triangle dots are others-attributions.

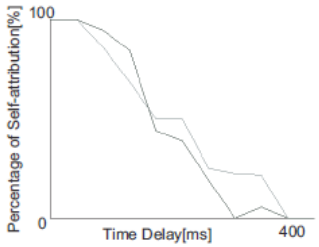

Fig. 5. The percentage of self-attribution on each time delay in the first 22 trials and the last 22 trials (sum of 8 subjects: the first 22 in gray, the last 22 in black).

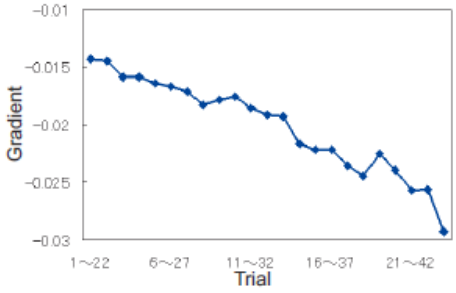

Fig. 6. The gradient of the line which is produced by logistic regression analysis on every 22 trials.

V. Computer Simulation

A. Multiple Forward Models

Next, we focus on multiple forward models. The models proposed for context estimations [7]. Multiple paired forward and inverse models were proposed for motor control in order to generate accurate and appropriate motor behavior under many different and often uncertain environmental conditions [8]. The condition which was presented by Wolpert et al. [7] could be applied to the attribution problem. The example condition in

Wolpert's model is in which a teapot to be lifted is either full or empty. If we replace full for self and empty for others, our condition is modeled as almost the same. In our case, the multiple forward models contain two forward models, one predicts the stochastic distribution of time delay of self and another predicts that of other. The multiple forward models that we use contain only predictors, in other words, forward models. Originally, each prediction is pared with controller, in other words, inverse models. We removed the controller from the models because output behavior, button press does not change by the consequences of action in this study. Original unit that accumulates the output of predictors was also removed because which was only used for motor control. States of each predictor change by the errors of prediction and realfeedback from the sensory system at each state (Fig. 7).

B. Simulated Time Delays of Self and Other Attribution

The estimated delay of each forward model was simulated by using the experimental data. Initial average time delay of self-attribution was 200 ms, and that of others-attribution was 250 ms. Variance of each predictor, σ_1 was 5122 for self-attribution and σ_2 was 6796 for others-attribution based on the experimental data of all delays for each decision. Fig. 8 shows the transition of predicted time delay. X-coordinate is a number of trial and y-coordinate is a time delay. $x_1(t)$ is the average time delay of the first forward model, self predictor. $x_2(t)$ is the average time delay of the second forward model, others predictor. The difference between the average time delay of the first and the second forward model presents clarity of the discrimination of self and others. Discrimination is clear when the difference is large. Discrimination is ambiguous when the difference is small. We can see that the discrimination criterion changes in time and the criterion of self-attribution becomes clear in the course of trials. These characteristics are observed in the experimental results. Simulation results were well correspondent to the characteristics of the experimental results. Therefore, multiple forward models mechanisms were suggested to be valuable to explain the problems of the self- and others-attribution on the sense of agency, through the comparison of simulation and experimental results.

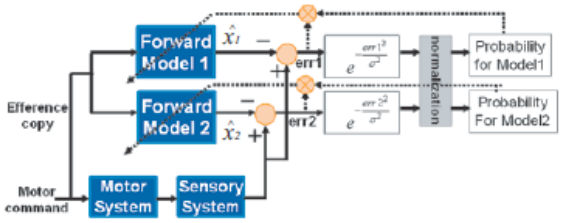

Fig. 7. Multiple forward models for sense of agency based on those for motor control [8].

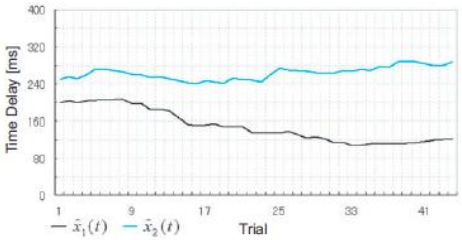

Fig. 8. Transition of predicted time delay: $\hat{x}_1(t)$ is the average time delay of the first forward model, self predictor. $\hat{x}_2(t)$ is the average time delay of the second forward model, others predictor.

REFERENCES

[1] S. J. Blakemore, D. A. Oakley, and C. D. Frith, "Delusions of alien control in the normal brain," Neuropsychologia, Vol.41, pp. 1058-1067, 2003.

[2] E. Dapratia, N. Francka, N. Georgieffa, J. Proustc, E. Pacheriec,J. Daleryd, and M. Jeanneroda, "Looking for the agent: an investigation into consciousness of action and self-consciousness in schizophrenic patients," Cognition, Vol.65, pp. 71-86, 1997.

[3] C. Farrer, N. Franck, N. Georgieff, C. D. Frith, J. Decety, and M. Jeannerod, "Modulating the experience of agency: a positron emission tomography study," Neuroimage, Vol.18, pp. 324-333, 2003.

[4] C. Farrer and C. D. Frith, "Experiencing oneself vs another person as being the cause of an action : the neural correlates of the experience of agency," Neuroimage, Vol.15, pp. 596-603, 2002.

[5] N. Frank, C. Farrer, N. Georgieff, M. Marie-Cardine, J. Dalery, T. d. Amato, and M. Jeannerod, "Defective recognition of one's own actions in patients with schizophrenia," American Journal of Psychiatry, Vol.158, pp. 454-459, 2001.

[6] M. Jeannerod and N. Georgieff, "Consciousness of external reality: a "who" system for consciousness of action and self consciousness," Consciousness and Cognition, pp. 465-477, 1998.

[7] D. M. Wolpert, K. Doya, and M. Kawato, "A unifying computational framework for motor control and social interaction," Philosophical Transactions of the Royal Society of London B, Vol.358, pp. 593-602, 2003.

[8] D. M. Wolpert and M. Kawato, "Multiple paired forward and inverse models for motor control," Neural Networks, Vol.11, pp. 1317-1329, 1998.

Reorganization of the central nervous system responding to changes in social environment in insects

T. Nagao and K. Sasaki

Abstract—**Phenotypic plasticity can enhance the survival probability or the reproductive success on an identical genetic background in the species. We investigate the neuro-endocrine systems for the transition of behavioral phenotype in response to changes in social environment in insects. We found the physiological dimorphisms in the brain between different phenotypes: the different levels of brain biogenic amines between the castes in honeybees. Workers can change their reproductive states in the absence of a queen. During the transition, the levels of tyramine and dopamine in the brains increased in reproductive workers. Oral application of these amines accelerated ovarian development in queenless workers. These biogenic amines in the brain can modulate the caste-specific behaviors and these have an important role of the behavioral transition. The process may lead to the formation of morphological caste-specific brain.**

I. Introduction

Phenotypic plasticity can enhance the survival probability or the reproductive success on an identical genetic background in the species. This involves a complex suite of characters, including behavior, color, morphology, endocrine physiology, reproductive development and fecundity. Phenotypic plasticity is known in broad taxa of animals [1], [2], [3], [4]. In social insects, the caste is a phenotypic plasticity with diverse morphological changes. The division of reproduction (reproductive caste) is a behavioral specialization to enhance the efficiency of individual behaviors, and the growth and reproductive success of the colony. Queens engage directly in reproduction, whereas workers perform other tasks, including care of the queen and brood, guarding the nest and foraging. Such a behavioral dimorphism may result from the physiological and morphological differences of the central nervous systems (CNSs) that formed through the developmental program during larval and pupal stages [2], [5]. There have been reported the morphological dimorphism of the CNSs between castes in social insects (Fig. 1) [5], [6], [7], [8], [9]. Adult individuals can not change their morphology of exoskeleton, but they can change the morphology and physiology of the CNSs. Workers can develop the reproductive organs with its motor systems in the absence of a queen and appear the queen-like behaviors. The behavioral transition of reproductive individuals can be a good model for studying the remodeling of CNSs in response to social environment.

Both authors are with Kanazawa Institute of Technology, 3-1 Yakkaho, Hakusan, Ishikawa 924-0838, Japan (corresponding author to provide phone: 076-274-8260; fax: 076-274-8251; e-mail: nagao@his.kanazawa-it.ac.jp).

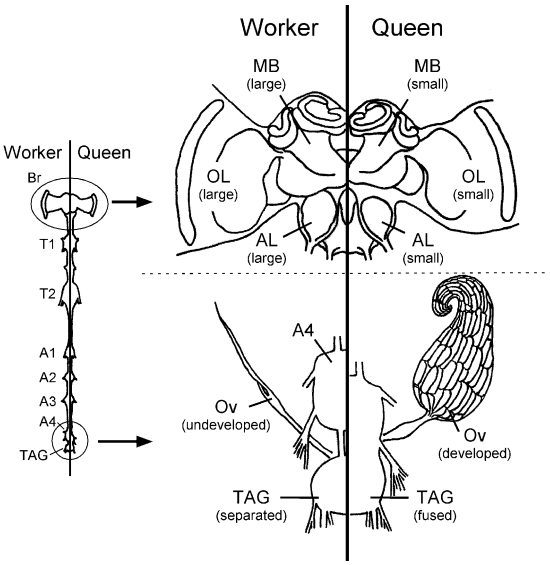

Fig. 1 Morphological dimorphism between castes in honeybees (Sasaki & Nagao, 2007) AL: Antennal lobe, MB: Mushroom body, OL: Optic lobe, Ov: Ovary, TAG: Terminal abdominal ganglion

II. Model

Brain transition from normal workers to reproductive workers seems to be composed of the steps at physiological, behavioral and morphological levels. First step of the caste transition in the brain may be the detection of changes of social environments by sensory systems (Fig. 2). The process follows the changes of endocrine valances within a brain (physiological transition), the appearance of queen-specific behaviors and disappearance of worker-specific behaviors (behavioral transition) and the feedback into the brain morphology by the repetitive queen-specific behaviors (morphological transition). We have the working hypothesis as a model of the remodeling of brains for caste transitions (Fig. 2) [9]. This model is partly supported by previous reports [10], [11], [12], [13], [14], [15], [16], but is not fully demonstrated and still controversial.

To test our working hypothesis and to explore the neural mechanisms underlying the caste transition, we would tackle the following topics:

(1) Physiological and morphological differences of the brain

between castes
(2) Physiological changes of brain during the caste transition
(3) Effects of biogenic amines on caste-specific behaviors
(4) Morphological changes of brain during the caste transition

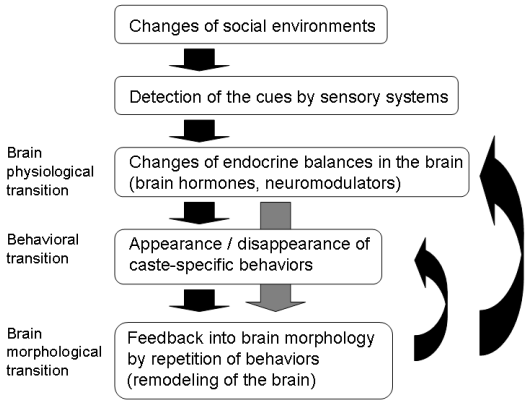

Fig. 2 Transition process of reproductive workers (Sasaki & Nagao, 2007).

III. EXPERIMENTS

A. *Physiological differences of the brain between castes*

To determine whether the brain endocrine condition differs between the caste in honeybees or not, we quantified the brain biogenic amines by HPLC-ECD system and compared the levels between queen and workers. Brain dopamine levels in newly emerged queens were remarkably higher than those in same aged workers (Fig. 3). The dopamine levels in queens were more than 5 times as large as those in workers. These higher dopamine levels were also detected in the haemolymph, suggesting that the higher dopamine levels in queens may affect not only the brain but also the other tissues. Although the behavioral roles of dopamine in the queens remain

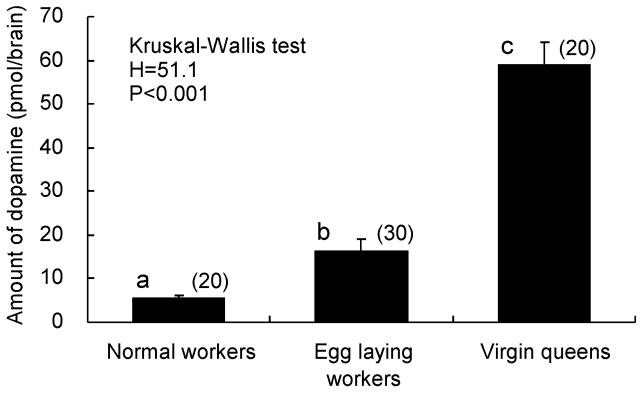

unknown, dopamine may be involved in the reproductive
Fig. 3 Brain dopamine levels in workers and queens in honeybees. Values above the bar indicate the sample size that we examined. Differences were examined by Mann-Whitney U-test.
states or queen-specific behaviors [17]. The distribution dopamine secretory cells in the brain of honeybees have been reported [18][19]. Since morphological differences of the cells between the castes were not found [20], the differences of dopamine levels may result from differences of activities for dopamine synthesis. Pupae of the queens had also the higher levels of brain dopamine. Therefore, the differences of brain dopamine levels between the castes were formed through the developmental program during larval or pupal stages. Dopamine may be a key substance to investigate the physiological dimorphism in the brain between the castes.

B. *Physiological changes of brain during the caste transition*

To induce the transition of reproductive states from normal workers to reproductive workers, two cohorts of newly emerged workers were kept under queenless condition. The other two cohorts of the same aged workers were kept under queenright condition as a control. Queenless workers could develop the ovaries with mature eggs and initiate to lay eggs until 15day-old, whereas queenright workers did not develop the ovaries. Both 17day-old normal and queenless workers were sampled and quantified the brain dopamine levels. Brain levels of dopamine in queenless workers were significantly higher than those in normal workers (Fig. 3).

Tyramine is also a candidate of substance for the transition from normal workers to egg-laying workers. Brain tyramine levels in queenless workers were significantly higher than those in normal workers at both 10days and 17days (Fig. 4).

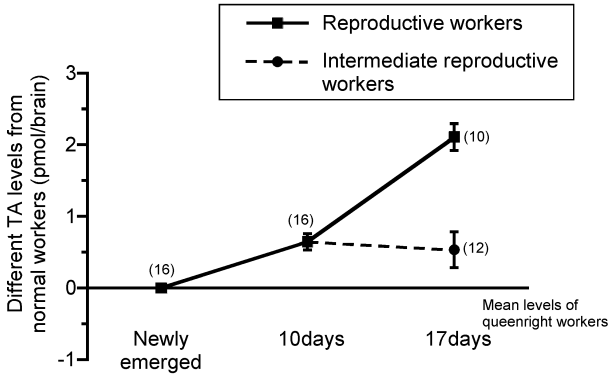

Fig. 4 Relative differences in brain levels of tyramine in reproductive and intermediate reproductive workers.

This results show the earlier increase of brain levels of tyramine than dopamine. To test whether tyramine levels can respond to the changes in social environment, we transferred the 10day-old queenless workers into the queenright cohort. These transferred individuals (17day-old) showed an intermediate ovarian development in comparison to reproductive workers. The intermediate reproductive workers had intermediate levels of tyramine in the brain (Fig. 4). Thus, brain levels of tyramine seem to be sensitive to changes in

social environment, which suggest that tyramine may be involved in a switching of the transition in reproductive workers.

C. Effects of dopamine or tyramine on the reproductive states

To explorer the functional roles of tyramine and dopamine in the transition in reproductive workers, we tried an oral application of tyramine or dopamine to the queenless workers. Oral treatment with biogenic amines serves as a non-invasive method of reliably elevating the levels of biogenic amines in the brain [21], [22]. For these treatments, newly emerged workers were transferred into plastic cups and given freely a tyramine or dopamine solution for 2 h. As a control, bees were given only 50% sucrose solution for 2 h in another cup. The set of feeding treatments was repeated on the same individuals 4 days old (3 days after the first introduction), 9 days old and 16 days old. Then10day-old and 17-day-old bees were collected and killed with liquid nitrogen, and used for HPLC analysis. The queenless workers fed tyramine solution had significantly larger levels of tyramine and dopamine than control queenless workers (Fig. 5a) [23]. The queenless workers fed dopamine solution had significantly larger levels of brain dopamine and its metabolites (NADA) than control queenless workers (Fig. 6a) [9]. These suggest that both tyramine and dopamine can be absorbed from the gut and transferred into the brain and that tyramine may have a role of enhancement of brain dopamine levels in queenless bees.

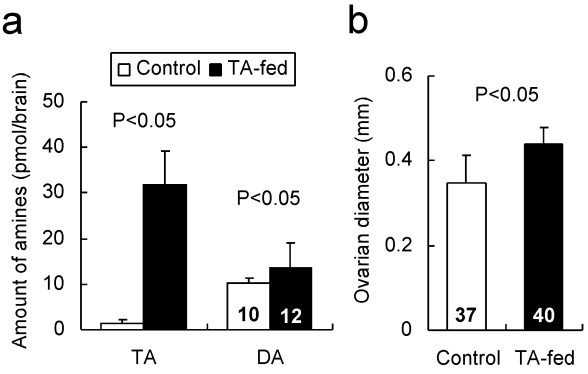

Fig. 5 Effects of tyramine application on the brain amine levels (a) and the ovarian development (b). Values in the bar indicate the sample size that we examined. Differences between groups were examined by Mann-Whitney U-test (Sasaki & Harano, 2007).

The treatment of tyramine or dopamine can accelerate the ovarian development (Fig. 5b and 6b) [9], [23]. Ovarian diameters in the workers given tyramine or dopamine were significantly larger than those in control workers. Since tyramine could cause the elevation of brain dopamine levels, the ovarian development by tyramine may be due to direct effects by tyramine or effects by dopamine.

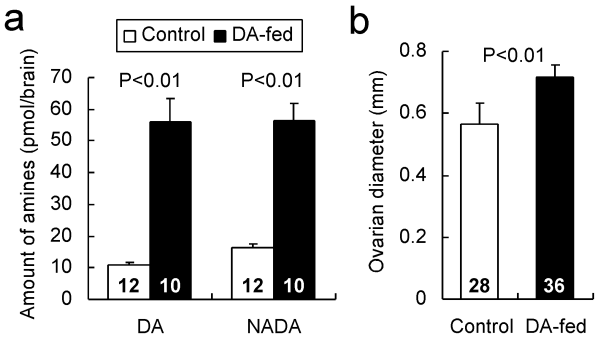

Fig. 6 Effects of dopamine application on the brain amine levels (a) and the ovarian development (b). Values in the bar indicate the sample size that we examined. Differences between groups were examined by Mann-Whitney U-test (Sasaki & Nagao, 2007).

D. Behavioral effects of dopamine or tyramine on worker's behaviors

There are several reports on behavioral effects of dopamine or tyramine on worker's behaviors. Dopamine reduces the percentage of bees responding to conditioned stimuli and inhibits information retrieval, but does not affect the storage processes [24], [25], [26]. Tyramine can inhibit the initiation of foraging behavior [22]. These effects seem to be consistent with behaviors of the queenless workers.

We tried to determine the other behavioral effects of tyramine by its oral application. Since honeybee workers respond sucrose solution by the taste sensilla on both the antennae and the tarsi, we examined the behavioral response to sucrose in queenless workers fed tyramine. The behavioral responses to sucrose by the tarsi were higher in workers fed tyramine than control workers (Fig. 7). The enhanced sucrose response may make the queenless workers intake more food for yolk formation in the ovaries.

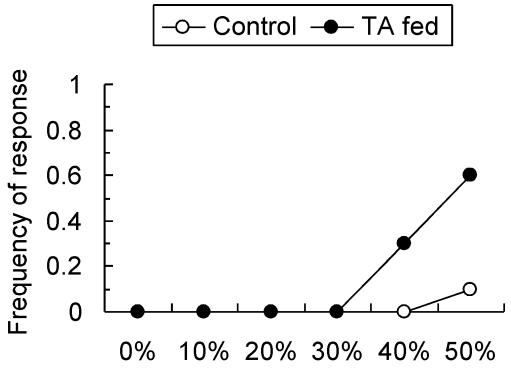

Fig. 7 Behavioral response to sucrose by the tarsi in both tyramine fed (n = 20) and control workers (n = 20).

E. Brain amine levels associated with reproductive states in other primitively eusocial insects

To determine the involvement of brain dopamine in reproductive states of workers in other eusocial hymenopteran,

we investigated the brain dopamine levels in workers of the paper wasps (*Polistes chinensis*). Since this wasp is a primitive eusocial species, some workers have well-developed ovaries. In two colonies of workers, brain dopamine levels were significantly correlated with ovarian width. Individuals showing oviposition behaviors had higher dopamine levels than other individuals with developed ovaries. Thus, the involvements of brain dopamine in reproductive states of workers may be generalized in eusocial hymenopteran [27].

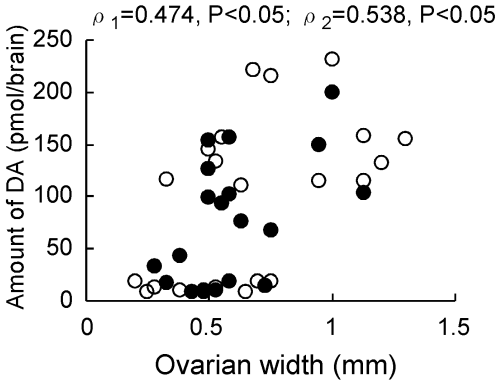

Fig. 8 Correlation of brain dopamine levels with ovarian widths in *P. chinensis*. Workers in two colonies were independently analyzed by Spearman's rank correlation test (Sasaki *et al.*, 2007).

IV. Conclusion and Future plan

A series of our experimental works reveals the neuro-endocrine process of the brain transition to reproductive workers. Biogenic amines, especially tyramine and dopamine may have important roles in the physiological and behavioral transition. Tyramine may be associated with a switching on the initial process of the physiological transition and with an increase the brain dopamine levels. Brain dopamine may be related with ovarian development. These biogenic amines may also affect the caste-specific behaviors. Behavioral effects of these amines still remain unknown. Further investigations of behavioral modulations by the biogenic amines at neural levels are needed. We also plan to determine the brain morphological changes by a repetition of the caste-specific behaviors. Since there have been reported the brain morphological dimorphism between queens and workers [5], [6], [7], [8], we would focus on the dimorphic brain region.

References

[1] Shapiro, A.M. 1976. Seasonal Polyphenism. In: Hecht, M.K., Steere, W.C. (eds) *Evolutionary Biology*, vol 9, Plenum, New York, pp259-333.

[2] Hölldobler, B., Wilson, E.O. 1990. *The ants*. The Belknap Press of Harvard University Press, Cambridge, Mass. 732 pp.

[3] Simpson, S.J., McCaffery, A.R., Hägele, B.F. 1999. A behavioural analysis of phase change in the desert locust. *Biol. Rev*. 74, 461-480

[4] Rogers, S.M., Matheson, T., Sasaki, K., Kendrick, K., Simpson, S.J., Burrows, M. 2004. Substantial changes in central nervous system neurotransmitters and neuromodulators accompany phase change in locust. *J. Exp. Biol.*, 207, 3603-3617.

[5] Winston, M.L. 1987. *The biology of the honeybee*. Harvard University Press, Cambridge, Mass. 281 pp.

[6] Snodgrass, R.E. 1956. *Anatomy of the Honey Bee*. Cornell Univ. Press, Ithaca, N.Y..

[7] Wilde, J.de., Beetsma, J. 1982. The physiology of caste development in social insects. *Adv. Insect Physiol.*, 16, 167-246.

[8] Arnold, G.C., Budharugsa, S., Masson, C. 1988. Organization of the antennal lobe in the queen honey bee, *Apis Mellifera* L. *Int. J. Insect Morphol. Embryol.*, 17, 185-195.

[9] Sasaki, K., Nagao, T. 2007. Reorganization of the central nervous systems in response to changes of social environment in insects *J. Robot. Mechatro.*, 19, 369-373.

[10] Withers, G.S., Fahrbach, S.E., Robinson, G.E. 1993. Selective neuroanatomical plasticity and division of labour in the honeybee. *Nature*, 364**,** 238-240.

[11] Fahrbach, S.E., Robinson, G.E. 1996. Juvenile hormone, behavioral maturation, and brain structure in the honey bee. *Dev. Neurosci*. 18, 102-114.

[12] Sigg, D., Thompson, C.M. and Mercer, A.R. 1997. Activity-dependent changes to the brain and behavior of the honey bee, *Apis mellifera* (L.). *J. Neurosci*. 17, 7148-7156.

[13] Morgan, S.M., Huryn, V.M.B., Downes, S.R., Mercer, A.R. 1998. The effects of queenlessness on the maturation of the honey bee olfactory system. *Behav. Brain Res*., 91, 115-126.

[14] Gronenberg, W., Liebig, J. 1999. Smaller brains and optic lobes in reproductive workers of the ant *Harpegnathos*. *Naturewissenschaften*, 89, 343-345.

[15] Sasaki, K., Nagao, T. 2001. Distribution and levels of dopamine and its metabolites in brains of reproductive workers in honeybees. *J. Insect Physiol.*, 47, 1205-1216.

[16] Sasaki, K., Nagao, T. 2002. Brain tyramine and reproductive states of workers in honeybees. *J. Insect Physiol.*, 48, 1075-1085.

[17] Harano, K. Sasaki, K., Nagao, T. 2004. Depression of brain dopamine and its metabolite after mating in European honeybee (*Apis mellifera*) queens. *Naturwissenschaften*, 92, 310-313.

[18] Schäfer, S., Rehder, V. 1989. Dopamine-like immunoreactivity in the brain and suboesophageal ganglion of the honeybee. *J. Comp. Neurol*., 280, 43-58.

[19] Schürmann, F. W., Elekes, K., Geffard, M. 1989. Dopamine-like immunoreactivity in the bee brain. *Cell Tissue Res*., 256, 399-410.

[20] Blenau, W., Schmidt, M., Faensen, D., Schurmann, F. 1999. Neurons with dopamine-like immunoreactivity target mushroom body Kenyon cell somata in the brain of some hymenopteran insects. *Int. J. Insect Morphol. Embryol.*, 28, 203-210.

[21] Harris, J.W., Woodring, J. 1999. Effects of dietary precursors to biogenic amines on the behavioural response from groups of caged worker honey bees (*Apis mellifera*) to the alarm pheromone component isopentyl acetate. *Physiol. Entomol.*, 24, 285–291.

[22] Schulz, D.J., Robinson, G. 2001. Octopamine influences division of labor in honey bee colonies. *J. Comp. Physiol. A*, 187, 53–61.

[23] Sasaki, K., Harano, K. 2007. Potential effects of tyramine on the transition of reproductive workers in honeybees (*Apis mellifera* L.). *Physiol. Entomol*., 32, 194-198.

[24] Mercer, A.R., Menzel, R. 1982. The effects of biogenic amines on conditioned and unconditioned responses to olfactory stimuli in the honeybee *Apis mellifera*. *J. Comp. Physiol.*, 145, 363-368.

[25] Michelsen, D.B. 1988. Catecholamines affect storage and retrieval of conditioned odour stimuli in honey bees. *Comp. Biochem. Physiol.*, 91C, 479-482.

[26] Menzel, R., Hammer, M., Braun, G., Mauelshagen, J., Sugawa, M. 1991. Neurobiology of learning and memory in honeybees. In: Goodman, L. J., Fisher, R. C. (Eds.), *The behaviour and physiology of bees*, C. A. B. International, Wallingford, pp. 323-353

[27] Sasaki, K., Yamasaki, K., Nagao, T. 2007. Neuro-endocrine correlates of ovarian development and egg-laying behaviors in the primitively eusocial wasp (*Polistes chinensis*). *J. Insect Physiol.*, 53, 940-949.

Social cognition in premotor and parietal cortex

Naotaka Fujii
RIKEN

Abstract

Socially correct behavior requires constant observation of the social environment. The brain keeps the eyes focused on the current social space and constantly updates its internal representation of the environment and social context. Monitoring the behavior of others is essential for this updating. The neural systems involved in perceiving the actions of others have been explored extensively, but the detailed, quantitative character of the system at the single-cell level remains poorly understood. To address this question, we used the new technique of multidimensional recording to record neuronal activity in monkeys simultaneously from ventral premotor cortex (PM) and parietal cortex in the left hemisphere while they performed a food grab task. 35% (52/148) of PM neurons and 54% (94/174) of parietal neurons showed motion-related (MR) response, meaning their activity increased in response to various combinations of arm motions made by self and/or other. Both areas showed robust lateralized preference to Self-Right action. When it came to recognizing the actions of the other monkey, PM-MR neurons showed the same kind of right-arm preference as self-action while parietal-MR neurons, in contrast, did not show arm preference. And while both areas discriminated self-action from other, a significantly larger proportion of PM-MR neurons did so. These results suggest that PM neurons provide information about an action's agent and effector as primitives of action cognition within the mirror neuron network, while parietal neurons represent social space and participate in the recognition of another agent's actions in relation to one's own actions within the parieto-prefrontal network.

● INTRODUCTION

The world is full of events, most of which we detect easily and respond to automatically. This suggests that our brains are continuously updating their models of the environment and preparing for likely or expected events. A major unresolved question in neuroscience is how the brain executes such functions. Since the environment changes continuously, this task must impose a heavy cognitive load on our brains. Among the hardest events to predict are the behaviors of others, because others' behaviors are driven by rules different from one's own. But despite the fact that social prediction is difficult, our brains are usually able to make them well enough to behave in a socially safe or advantageous manner.

Social brain function is what allows us to adapt our behavior and understand others' behavior in relation to social context. Social brain function guides our behaviors according to prevailing social rules in order to maximize the economical benefit as well as minimize the social risk our actions may engender. There are few studies of social brain function at the neural level. The most important aspect of social brain function is social cognition. To perform socially correct behavior we must stay vigilant and update our internal representation of the social environment continuously, because social situations are fluid and behavioral rules are often subtle.

The visual response of mirror neurons is thought to play an essential role in social brain function. Mirror neurons were first described in the primate premotor area in 1992 by di Pellegrino et al. and later found in PFG of parietal cortex. Mirror neurons tend to respond both to specific actions by the experimenter and to the same action made by monkey itself. Mirror neurons have been discussed in many contexts, including imitation learning. These studies revealed that the mirror neuron system not only generates a sensorimotor copy of intended actions but also contributes to action learning through imitation. Communication is a process in which the mirror neurons system may be involved in understanding the intentions of others through gestural messages between individuals. This aspect has been discussed in relation to speech communication, because human imaging studies have demonstrated the contribution of the mirror system in speech.

Previous experiments on social brain function were performed in highly controlled and artificial environments that were mostly detached from real

social contexts. The social and action stimuli were unidirectional, non-interactive and often rather predictable. Yet the essence of social communication is the bidirectional interaction between individuals and uncertainty in the environment. To study social cognitive brain function, reality, or at least a goodly degree of realism, must be introduced into the experimental environment. Such experiments require careful observation of social activity, which requires a certain amount of behavioral freedom for the animals being studied, which in turn renders conventional electrophysiological methods insufficient. To get around these limitations we developed multi-dimensional recording (MDR), a new technique that combines a motion capture system with a chronic multi-electrode recording system. With this technique, we aimed to reveal neural mechanisms of action cognition in the primate premotor and parietal cortices while monkeys were sharing the same social space.

●METHODS

Two male Japanese macaques (M1 and M2, 6.0 kg and 5.5 kg, respectively) were used for all recordings. All procedures used in the experiment were pre-approved by the RIKEN animal committee preceding the experiment. A recording chamber (30mm x 50mm) was surgically implanted in each monkey's skull over the left hemisphere. Neuronal activity was recorded from multiple tungsten electrodes that were chronically implanted during the following months. The electrodes were attached to a custom-made micromanipulator that was affixed to the recording grid inside the recording chamber, and were inserted into the brain through a stainless guiding tube that penetrated the dura mater. The depth of each electrode was independently adjusted to obtain the best signal-to-noise (S/N) ratio. A depth adjustment was performed daily for each electrode to compensate for changes in the S/N ratio. Neural activity was recorded using a Digital Lynx system (Neuralynx Tuscon AZ, USA). Recorded spikes were isolated using offline cluster-cutting software (Offline-Sort: Plexon, Dallas TX, USA) with manually set parameters. The isolated spikes were then used for further analyses. Neural activity was recorded from both monkeys simultaneously from the ventral premotor cortex (PM) and the parietal cortex as identified by MRI images taken before the experiment (Figure 1B).

The monkeys' behavior was monitored and recorded using a motion capture system (Vicon: Vicon-Peak, Oxford, UK) sampling at 120 Hz and conventional video cameras. Each monkey wore a custom-ordered motion capture suit. Ten reflective markers were attached to each suit at bilateral shoulder, elbow, wrist, and hand, and at forehead and back of head. Ten motion capture cameras were placed around the monkeys. Using all motion capture camera views together with calibration data containing the cameras' spatial distribution, the motion capture software reconstructed each marker's location in three-dimensional space (Figure 1A).

During the simultaneous recording of neural activity and motion data, the monkeys faced each other from either end of a square table (50 cm × 50 cm). They could see each other but could not touch each other. Each monkey sat in a primate chair with his waist, hips and legs restrained by a plastic cover, and his neck restrained by an aluminum collar attached to the chair. Although their waists, legs and necks were restrained, the monkeys could move their arms, torsos, and heads freely. Their task was a simple food grab task—that is, on each trial we placed a piece of food on the table, and the monkeys took the food if it was within reach. Since there was no overlap between their reachable spaces, there was no social conflict between them. No training was required for the performance of this task. However, recordings were not performed until after both monkeys had been exposed to the task situation for more than a month, which included chair training. This period was necessary for the monkeys to become familiar with experimental environment, so that they would feel more relaxed and behave naturally during recording.

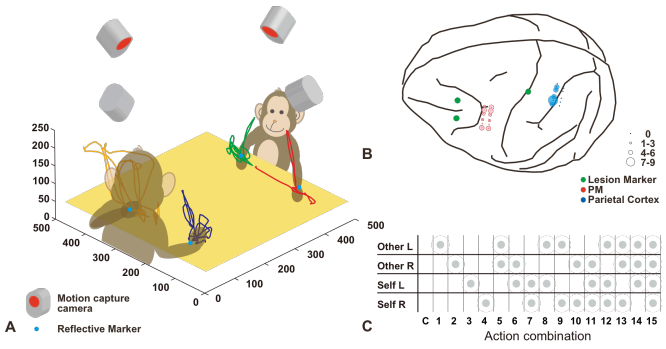

Figure 1

● RESULTS

The MDR technique was used to isolate and identify 148 neurons in premotor cortex and 174 neurons in parietal cortex (Figure 1B).

We analyzed our neural data using the action combination (AC) sequences, which eliminated concern about motion contamination. A second advantage of this method was that it provided a reliable control period during which no motion occurred. Using the AC sequences and the control period, neural activity was analyzed in response to 15 different combinations of actions made by Self-Left, Self-Right, Other-Left and Other-Right arms. After the analysis, each neuron had 15 statistical results that showed whether it had responded to each of these ACs or not. Ninety-four parietal and 52 PM neurons were identified as motion-related (MR) neurons. Again, MR neurons were defined as cells that showed significantly greater activity (Wilcoxon test; $p < 0.05$) during at least one AC epoch compared with the control period. MR neurons were found in the anterior wall of IPS but not in the posterior wall. In PM, in contrast, the MR neurons were found evenly throughout most of our recording tracks (Figure 1B). In general, most of the parietal and PM-MR neurons increased their firing rates and peaked during reaching movements or the onset of grasping. Head direction did not modulate the activity of MR neurons in either area.

Figures 2A and B show cell counts and proportions of MR neurons in parietal cortex and PM, respectively, that showed positive response in each AC epoch. There was robust representation of Self-Right arm motion in both areas (AC 4). However, the proportion of parietal-MR neurons in eight ACs (indicated by asterisks) was significantly larger than among the PM-MR neurons (Fisher's exact test, $p < 0.05$). The result suggested that parietal-MR neurons could respond to more ACs than PM-MR neurons. This might be because of parietal-MR neurons' robust preference for Self-Right arm action, which seems to persist even when other actions occur simultaneously. In contrast, PM-MR neurons had weaker Self-Right arm preference and seemed to be more specialized and segregated for the detection of specific ACs.

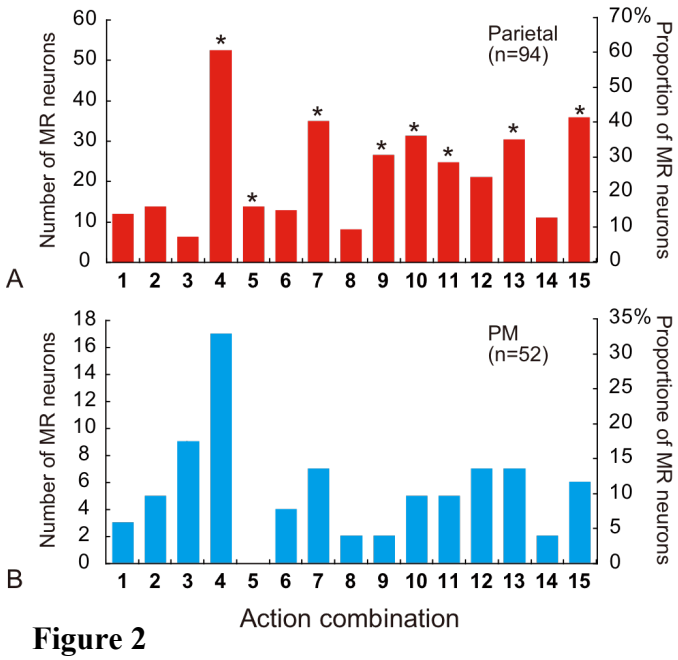

Figure 2

Although Figure 2 shows how parietal and PM neurons discriminated different combinations of actions that occurred in the task, it was not still clear how MR neurons were discriminating between the agents. To address the question, we divided ACs into two categories. One was Agent-specific ACs (ACs 1-5, 7) in which neurons segregated action of self and other. The other was Agent Non-specific ACs (ACs 6, 8-15) in which neurons showed positive responses to actions made by both monkeys and hence did not discriminate between the agents. These two categorical responses did not have to be mutually exclusive, and could be represented in the same neuron. However, only neurons that showed exclusive response to Agent-specific ACs (i.e. and no response to Agent Non-specific ACs) can identify a specific action agent. Figures 3A and B indicate how MR neurons showed positive responses in these AC categories. 77% of parietal-MR neurons (72/94) and 66% of PM-MR neurons (34/52) had MR response in Agent-specific ACs (blue circle). Meanwhile, in parietal cortex, 87% of MR neurons (82/94) showed MR response in Agent Non-specific AC and 72% (37/52) in PM-MR (green circle). The most striking difference between the two areas was the cross-representation ratio of Agent-specific and Non-specific ACs.

Parietal-MR neurons showed significantly larger cross-representation than PM neurons (middle column: Chi square test, $p < 0.05$), indicating that exclusive Agent-specific response (left column in Figures 3A and B) in PM was significantly larger than in parietal cortex. Exclusive Agent Non-specific response (right column) did not differ between the two areas. (Chi square test, $p < 0.05$) The results indicated that PM could discriminate action agent better than parietal cortex.

Hence we could find a difference in action agent cognition between the two areas. But one question still remained, which was laterality of response to actions of other. To address the question, two AC categories were selected: "Other-Left" (ACs 1, 8, 9 and 12) and "Other-Right" (ACs 2, 6, 10 and 11). Figures 3C and D indicate the proportion of MR neurons that responded in both categories (middle column), exclusively in the "Other-Left" category (left column) and exclusively in the "Other-Right" category (right column). Response laterality was not present in parietal-MR neurons, but in PM-MR neurons there was significant right-arm preference associated with cognition about the other monkey's actions.

●DISCUSSION

MR neurons responded to multiple ACs in a complex manner. In some neurons, response to self-action was modulated by the co-occurrence of action by the other monkey, as if there was interaction between the responses in different ACs. Similar observations were reported in human imaging studies in inferior frontal cortex and superior temporal cortex. The modulation was observed in both areas and seems to be a result of integration of different action properties. Parietal neurons showed more cross-representation of AC responses than PM neurons. This suggests that parietal neurons have broader response modalities and can integrate action information as well as other environmental parameters that are proposed to be represented in the area. If this is indeed the case, parietal cortex is able to represent internal subjective social space by integrating socially important issues. In contrast, the population of PM-MR neurons we found could discriminate action agents and action effectors precisely. Such information must be essential in action cognition, and is already proposed to be a function of PM. The results indicateFithat PM-MR neurons represent essential primitives of social cognition that might be used in the mirror neuron network for inferring the intentions of others.

PM and parietal MR neurons represent similar information in terms of action cognition at the single-cell level, but at the population level they are involved in different social-cognitive systems—the mirror neuron network and the parieto-frontal network respectively. These two networks perform different, but parallel and complementary, functions in social cognition.

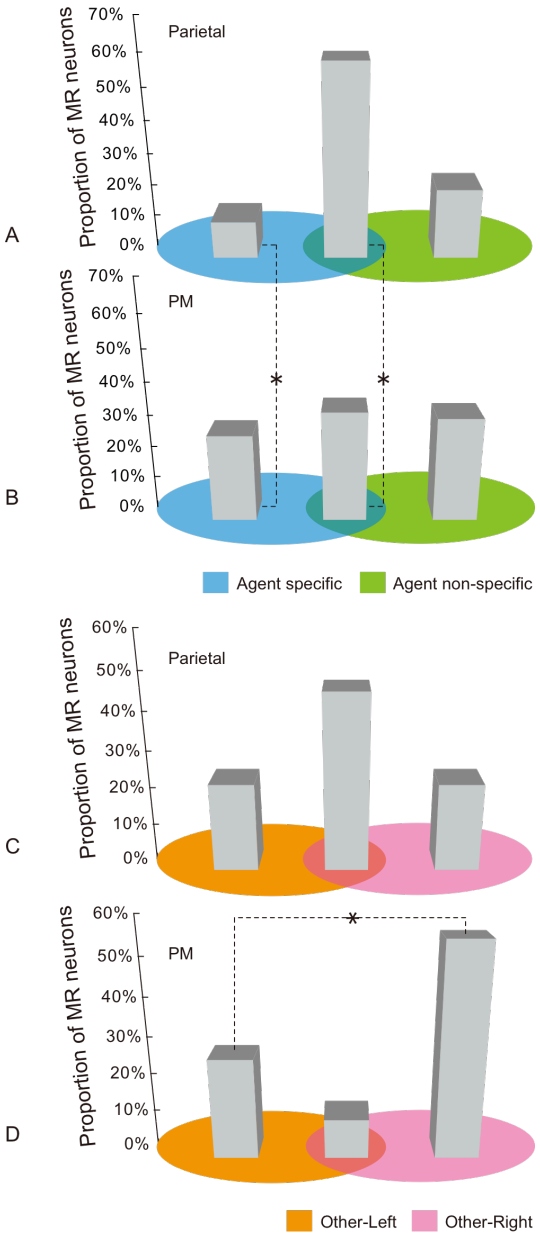

Figure 3

Group D: On Common Principle of Mobiligence

Koichi Osuka, Kobe University

1.Intruduction

A common principle of Mobiligence observed in various living things is considered in Group D. To do so, we should explain the principle as objective as possible. That is, we try to express various phenomena in living thing by mathematical or physical way. Now, some hypotheses are going to propose in Group D. Multi-Layer, Multi-Feedback, Multi-Optimality of Prediction Mechanism are the examples. We expect that one of the common principles of Mobiligence is understood if these are expressible unitedly in the word of the mathematic. In this note, we report the results in Group D in 2007.

2.Structure of Mobiligence Mechanism

First of all, considering the Mobiligence in the living thing, Hierarchy-multi layers is hit on. Then if we go down the layers, dynamics of the body can be recognized at the bottom of the layer. At that point Passivity seems very important feature. One of the most important examples is passive dynamic walking. That is, adaptive function in walking can be constructed by two layers. The lower layer is realized by passive adaptive function in passive dynamic walking. The upper layer is realized by active adaptive function using neural networks. Oppositely, if we go up the layers, the highest region of brain can be recognized at the top of the layer. At this point we think that the structure of this region is unstructured. Because, if the top of the brain is structured then any adaptive function against unlimited environment can not seems to be realized. We think that this unstructured part plays very important role in adaptive function.

From the above discussions, we claim the following hypothesis about the structure of mobiligence mechanism.

(1)The structure of mobiligence is multi-layered one.

(2)At each layer, the higher layer sees the lower layer as a passive mechanism.

(3)There are many feedback structure, that is multi-feedback structure, can be seen in the mobiligence mechanism.

(4) Concept of multi-optimal may be a common principle lays in mibiligence mechanism.

3. Structure of D-Group

In D group, each member considers the each layer of Fig.1 from dynamical aspect. We introduce the activities of the each group in the following.

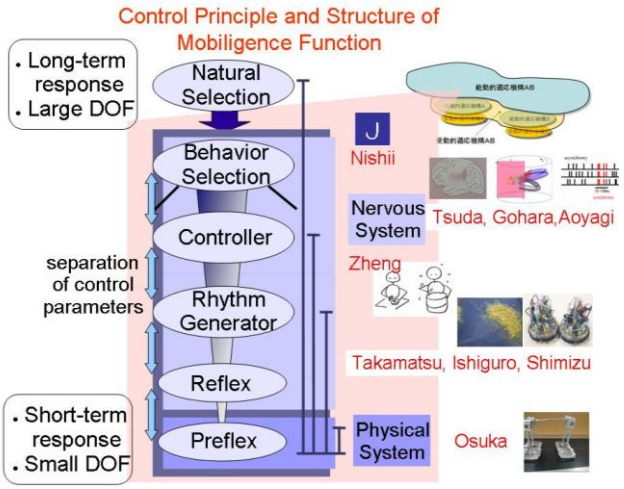

Fig.1 The image of the structure of Mobiligence

D01 : Discovery and development of dynamical common principle of mobiligence (Leader: Koichi Osuka, Professor, Kobe University)

We focused on the following two themes.

A.Analysis of adaptive mechanism in ultimately simplified system (passive dynamic walking) and expand the results to the multi- legged passive dynamic walking.

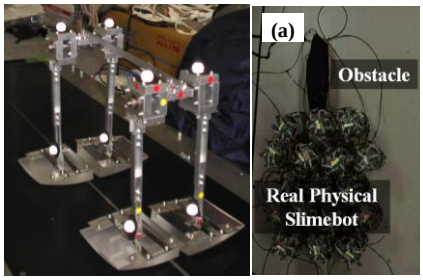

B.Development of real-time morphological control of ultimately complicated system (modular robot) and the real robots.

D01-11 : Spatiotemporal dynamical systems interacting with external world （Leader: Kazutoshi Gohara, Hokkaido University ）

Mobiligence is analyzed as one of the dynamical systems. As a result, it is revealed that the behavior of a mobiligence can be generally expressed as state transitions on a fractal set and can be characterized by the hierarchical spatiotemporal dynamics. Using the Sierpinski gasket as a one of well known fractal set, this figure shows a characteristic feature of dynamical systems excited by three external inputs. This is a triangle which consists of self-similar small clusters of triangle. Each cluster can be addressed such symbols as 1-2-3, 11-21-31, 12-22-32,

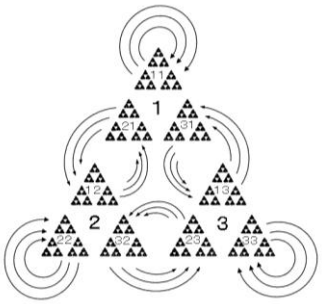

13-23-33, etc. This is a hierarchical structure. The behavior of a mobiligence, i.e. dynamics, can be expressed by the trajectory connected between two points on the fractal set. This implies that a spatiotemporal hierarchy emerges in the movement of the mobiligence.

D01-12：Roles of the limbic system for Mobiligence（Leader: Ichiro Tsuda, Hokkaido University）

Self-similar emergent clustering of sets of membrane potentials of CA1 model neurons for spatio-temporal input sequences. As a mathematical model, two-compartment model is used. The most upper figure is a clustering of membrane potentials for the input patterns (depth 1), the middle one indicates a clustering of membrane potentials for the input sequences of depth 2, and the lowest one for the depth 3 input time series. These self-embedding and almost self-similar sets organized in the networks appear, following the emergent rules which are described by affine transformations.

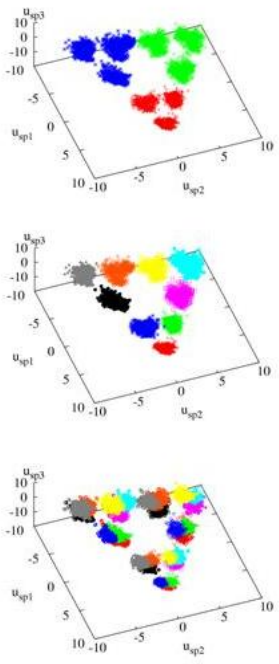

D01-13：Computational model of neural systems for learning causality of external events and performing actions（Leader: Toshio Aoyagi, Kyoto University）)

To realize high adaptability to the environment for the survival, the animal has to decide the optimal action, for example, to walk to the better environment. The central nervous system is an extremely efficient information processing device for this purpose. As underlying mechanisms, we found that a network organized under spike-timing dependent plasticity (STDP), not only is capable of memorizing the activity patterns of the external stimulus, but also exhibits a systematic transition behavior among the memorized patterns in response to uniform external synchronized spikes. Recurrent infomax provides a simple framework explaining for a wide range of phenomena observed in in vivo and in vitro neuronal networks. On the basis of these findings, using the novel experimental methods such as brain machine interface and cultured neural systems, we will explore the essential mechanisms of neuronal systems for emergence of adaptation through interaction among the body, brain and environment.

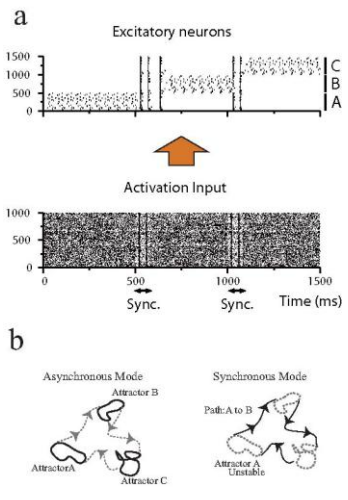

D01-14：Basic strategy for trajectory planning in human movements（Leader: Jun Nishii, Yamaguchi University）

During swing large variance of the trajectory is often observed. We have confirmed that the variance is distributed around the optimal trajectory which minimizes the energy cost with the condition of a retraction of the leg just before grounding. A control experiment of a biped robot also have shown that the retraction effectively reduces the variance of the joint angles at grounding and stabilizes the walking. These results suggest that human improves the success rate of movement tasks by suppressing the variance of movement in someeffective ways and acquires optimal movements which suppress the expected value of energy cost..

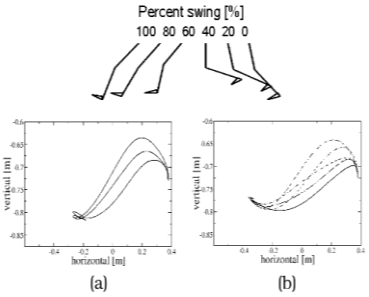

D01-15：Network geometry of plasmodial slime mold and emergence of biological function (Leader: Atsuko Takamatsu Waseda University)

The Physarum plasmodium, which is an amoeba-like giant unicellular organism, crawls on environment with cell thickness oscillation. The plasmodium consists of tubular network where nutrients and intracellular molecules are transported by protoplasmic streaming. The morphology of the tubular networks dramatically changes depending on environment. We analyze the environment dependent network morphology in synthetic and systematic way. Our goal is to abstract the algorithm for the adaptive behavior with the morphology by investigating the relation between the network morphology and the biological function in the Physarum plasmodium.

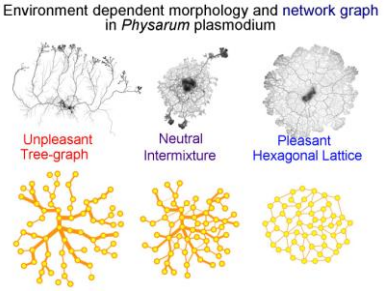

4. Conclusion

In this report, we described the image of the structure of Mobiligence which will be constructed in Group D. And we also showed the abstract of the results from the subgroup in Group D. The point of our policy is to describe the common principle of Mobiligence by using a kind of terminology of mathematics or physics.

Discovery and development of dynamical common principle of mobiligence

－ Common Understanding of Artificial Thing and Living Thing －

Koichi Osuka(Kobe Univ.), Akio Ishiguro, Masahiro Shimizu (Tohoku Univ.) and Xin-Zhi Zheng(ASTEM)

Abstract : In this note, we summarize the research results of Group D01 in 2007. This group is organized for considering a common principle of mobiligence. In 2007, we focused on the following two themes. A.Analysis of adaptive mechanism in ultimately simplified system (passive dynamic walking) and expand the results to the multi- legged passive dynamic walking. B.Development of real-time morphological control of ultimately complicated system (modular robot) and the real robots. From these case studies, we report a kind of common structure of mobiligence.

1. INTRODUCTION

Mobiligence is a dynamic form of intelligence that emerges through the tight interplay between brain-nervous system (control system), body (mechanical system) and environment (see Fig.1). Considering the fact that control and mechanical systems that are normally the direct targets to be designed for robotic agents are positioned at the source of this interplay, these two systems should be treated with an equal emphasis. Despite this fact, traditional robotics has often ignored this and has focused on either mechanical designs or control architectures in isolation. Generally speaking, system enhancement has been achieved normally by increasing the complexity of its control system. This, however, causes serious problems, particularly in terms of adaptivity, agility, versatility and energy efficiency.

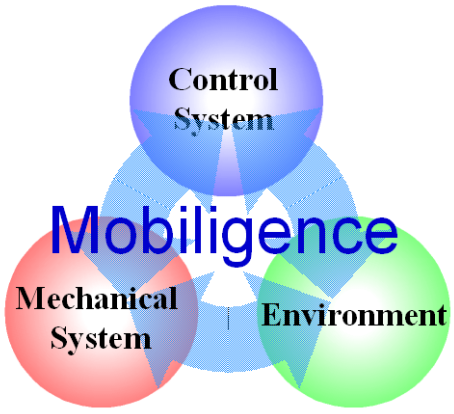

Fig.1 Image of Mobiligence

Group D has so far investigated the common principle for the generation of mobiligence focusing on the concept of “balance”. More specifically, one of the key concepts we have focused on is the balance -- or task distribution between control and mechanical systems. In this report, we particularly introduce the robotic case studies based on this view point.

2. WHAT IS THE EFFECTIVE APPROACH FOR FINDING A COMMON SENSE OF MOBILIGENCE？

Based on the standpoint of "Minimal design" is important to understand the appearance and the construction principle of mobiligence through synthetic approach. Here the "Minimal design" means a kind of research approach start from the simplest situation. In this case, the important thing is to set a start point appropriately.

In Group D01, up to now, it has been considering from "Minimal design" in two shown next meanings (See Fig.2):

(A) Analysis of adaptive mechanism in ultimately simplified system (passive dynamic walking) and expand the results to the multi- legged passive dynamic walking.

(B) Development of real-time morphological control of ultimately complicated system (modular robot) and the real robots.

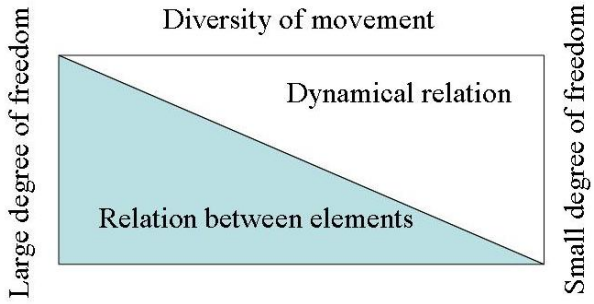

Fig.2 Tow approach for mobiligence

In the following, we introduce the result of the case study that has been advanced based on this two approaches, and the basic structure of mobiligence assumed there is

considered.

3. CASE STUDY FOCUED ON PASSIVE DYNAMIC WALKING

In this chapter, we introduce multi-legged passive dynamic walkers.

3.1 Multi-legged Passive Dynamic Walk

The reason why the human race selected two-legged walking by evolution is variously said. We が, We think about "self-stability of the passive dynamic walking" as the one grounds. Oppositely, it seems that the human race did not select two-legged walking if the passive dynamic walking phenomenon is unstable. Because, controlling the body for walking implies energy consumption, judging from the criterion of motion of the living thing, it might not be selected. When considering it from the above-mentioned, a lot of four-legged animals' existing in this world might also imply that four-legged passive dynamic walking exists.

Therefore, we would like to ensure the existence of multi-legged passive dynamic walking. To do so, consider the following situation. Firstly, we assume that there is a pair of two-legged passive dynamic walkers on a slight slope. Then, connect the two two-legged passive dynamic walkers each other by body. Then, connect the hip of the two two-legged passive dynamic walkers by a body. Here is a question. What happens in this four-legged passive dynamic walker?

If such a four-legged passive dynamic walker exist, and two or more walking patterns arise, it is likely to become one of the reasons why the quadraped walks by four legs. Moreover, it seems that there are strong relationship between 4-legged passive dynamic walking and a walking pattern of a decerebrated cat. Furthermore, we try to show the existence of 6-legged passive dynamic walking.

3.2 Quartet-4

Three sets of the two-legged PDW prototype mechanism are experimentally made to perform PDW experiments of 2-legged, 4-legged, and 6-legged cases.

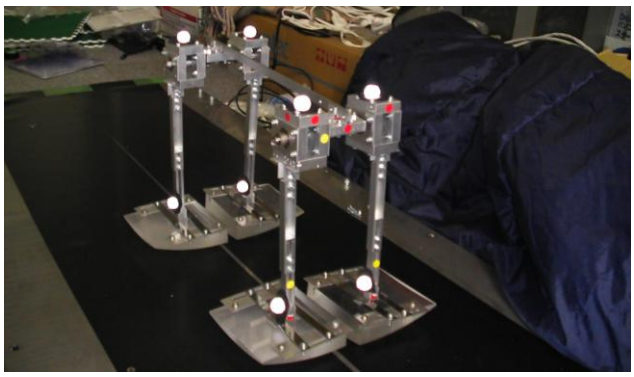

Fig.3 4-legged PDW

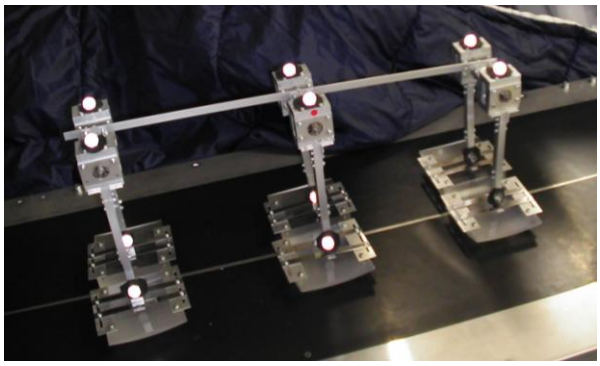

Fig.4 6-legged PDW

This mechanism has a joint at the upper end where two legs are connected with a shaft. The length of legs is 153mm, and the mass is 1100g for each. The length of legs is adjustable, and the sole of all feet is spheral-shaped. Connecting two sets of such mechanism forms a four-legged PDW system, and 3 sets build up a six-legged one.

3.3 Experiments on Multi-Legged PDW

The Quartet-4 was originally designed with potentiometers mounted at hip joint to measure its rotating angles. However, such directly attached sensors for motion measurement may affect the gait of the PDW because there are no actuators in PDW mechanisms. Therefore, in this research, a motion capture system is used to obtain the three-dimensional positions at each of the parts of this walking robot.

Some results of the Quartet-4 walking are depicted in Figures 5 and 6. Figure 5 is for a case where the angle of inclination is 3.9[rad], the trunk of the body is assumed to be rigid, and all the four legs are 153mm in length. Figure 6 is for a case where the angle of inclination is 3.9[rad], the trunk of the body is rotatable around the roll axis, and all the four legs are 153mm in length.

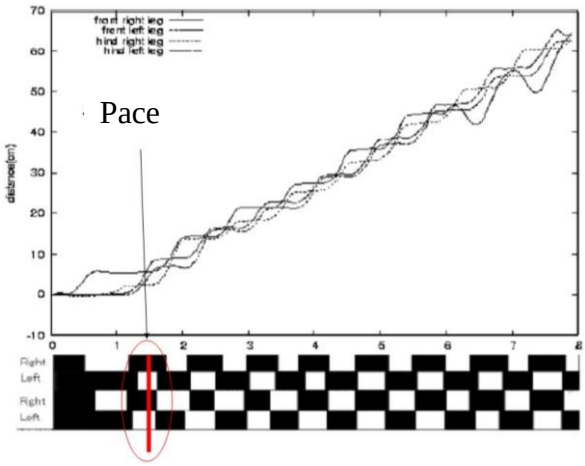

Fig.5 Pace walking

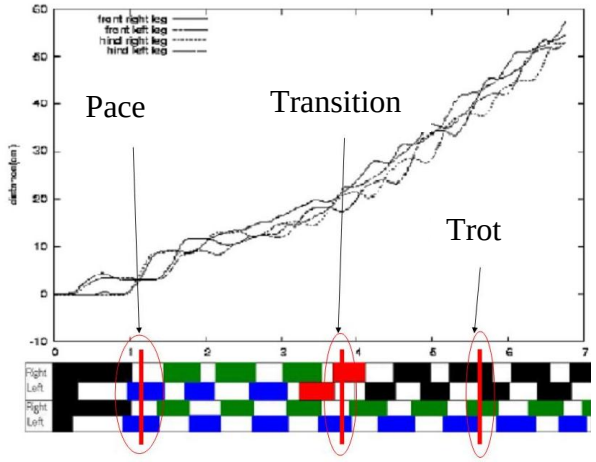

Fig.6 Trot walking

As seen in the above Figures, the existence of phenomena of the four-legged PDW is exhibited. Moreover, it is shown there that the gait may change upon the properties of trunk of the body. These results suggest the strong association among the embodiment and the motion patterns, which is considered to be possibly an underlying nature of the Mobiligence.

4. A Robotic Case Study: A Modular Robot That Exhibits Amoeboid Locomotion

In this section, we introduce a robotic case study with the use of coupled nonlinear oscillators with simple motile function.

4.1 Approach Employed

A significant feature of this case study is to model the behavior of true slime mold with the use of a reconfigurable modular robot in order to investigate the common principle of mobiligence. The reasons why we have employed this approach are treefold:

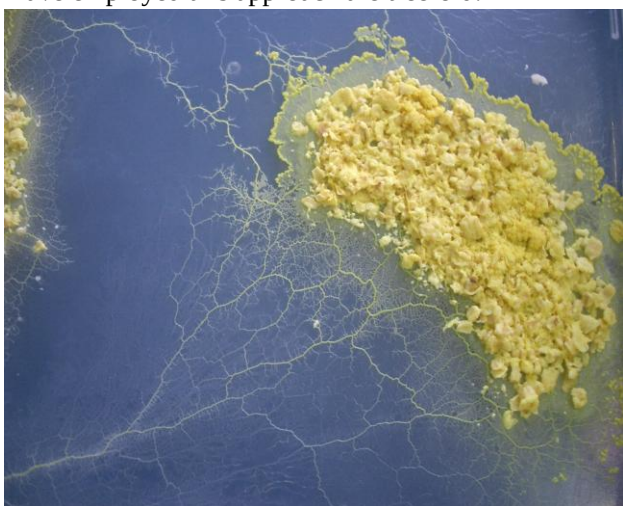

Fig.7 Physarum polycephalum

(1) True slime mold exhibits amazing collective intelligence without any centralized control mechanism.
(2) The control mechanism observed in true slime mold can be seen as a primitive form of brain function.
(3) Amoeboid locomotion is one of the most primitive form of locomotion. This allows us to effectively investigate the principle of mobiligence.

4.2 Amoeboid Robot: Slimebot

The Slimebot consits of many identical mechanical modules, each of which has simple motile function (see Fig.8). These modules are connected via a passive and spontaneous connectivity control mechanism exploiting a functional material. A significant feature of the Slimebot is focusing on emergent phenomena stemming from the interplay between the modules, and between the modules and the environments. In order to negotiate the environment encountered, the Slimebot has to alter its morphology without losing the coherency of the entire system. Furthermore, the control algorithm to be implemented should possess scalability: the Slimebot should exhibit adaptive amoeboid locomotion irrespective of the number of modules. In order to satisfy these requirements, we have focused on the mutual entrainment phenomena observed in coupled nonlinear oscillators. We have implemented a nonlinear oscillator into each module, by which we control the telescopic action of the arms and the ground friction mechanism. Fig.9 (a) and (b) show representative simulation results obtained under the condition of 100 and 500 modules, respectively. In these simulations, the task of the Slimebot is to move upward. The two thick circles in the figures denote obstacles. These snapshots are in the order of time evolution (view from left to right). As the figure illustrates, the Slimebot can successfully negotiate the environmental changes without losing the coherence. It should be noted that the passive/spontaneous connectivity control mechanism is fully exploited during the negotiation with the environment.

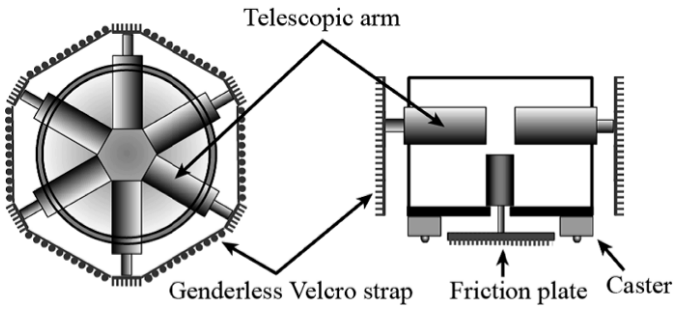

Fig.8 Mechanical structure of each module.
(Left) top view. (Right) cross-section of side view.

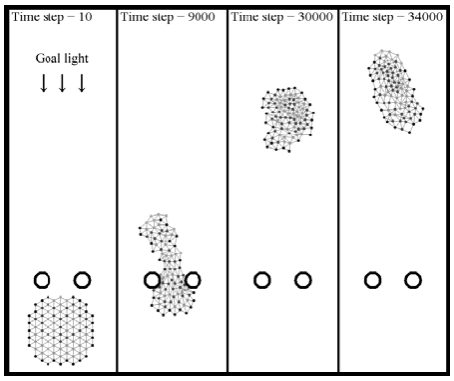

(a) Number of module : 100

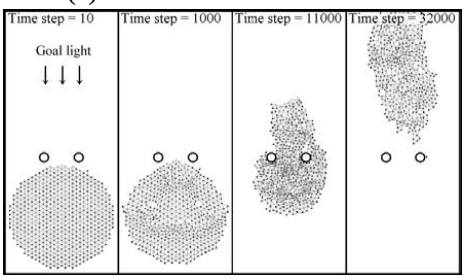

(b) Number of Module : 500

Fig.9 Simulated results of Slimebot

Fig.10 illustrates an experimental result using a real physical Slimebot. As the figure shows, the Slimebot exhibits adaptive locomotion against the obstacle. We are currently developing a new Slimebot which allows us to conduct experiments with several dozens of modules (see Fig.11).

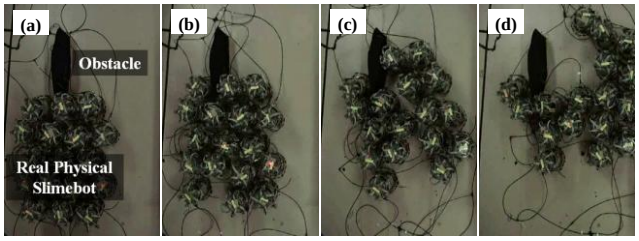

Fig.10 Experimental results using Slinebot

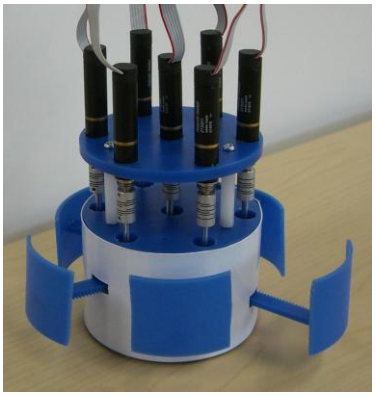

Fig.11 A developed newest module of the Slimebot.

5. SUMMARY

The two robotic case studies introduced above makes the following two novel contributions for understanding mobiligence:

1) In the case study taking the passive dynamic walking, we have found that the feature of body is very important. That is, increasing the slope angle, the walking pattern changes in spite of the same body. This results implies a kind of adaptive function is embedded in the dynamics of the body.

2) In the case study using the Slimebot, we have particularly focused on the deformability stemming from the passive and spontaneous connectivity control mechanism implemented for investigating how the control and mechanical systems should be coupled. A very interesting point we have found is that the degree of deformability that allows the Slimebot to adjust its morphology in ways favorable to the motion underway maximizes the adaptivity.

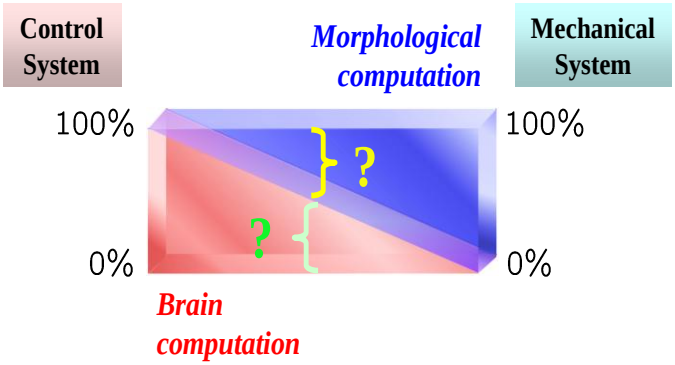

Fig.12 A graphical representation of the contribution of control and mechanical systems to resulting behavior

Fig.12 illustrates a graphical representation of possible task distribution between control and mechanical systems in generating behavior. From the two case studies, we have found that a certain amount of computation for generating the behavior should be offloaded from the control system to its mechanical system. Based on these results obtained, in the next two years, we intensively investigate the followings in terms of dynamical systems:

1) To what extent computational offloading should be achieved from the control system to its mechanical system so as to emerge useful functionalities such as adaptivity and agility?

2) Clarifying the structure of dynamical system observed under the well-balanced coupling between control and mechanical systems.

Spatiotemporal Dynamics in Dynamical Systems Interacted with Environment

Kazutoshi Gohara

Graduate School of Engineering, Department of Applied Physics,
Hokkaido University, Sapporo 060-8628, Japan

Abstract—We have presented a theory for dissipative continuous dynamical systems stochastically excited by external temporal inputs. The theory revealed that the dynamics is characterized by a set $\Gamma(C)$ of trajectories in hyper-cylindrical phase space, where C is a set of initial states on the Poincaré section. Two sets, $\Gamma(C)$ and C, are attractive and invariant fractal sets. In this paper, using nonlinear Duffing equation, we show numerically that the correlation dimension of the set C is approximately inverse proportional to the time length of inputs while the dimension is independent of amplitude of inputs. These obtained results might be general characteristics of dissipative continuous dynamical systems stochastically excited by temporal inputs.

1. Introduction

A theory has been presented in order to model complex systems that interact strongly with other systems. It has been revealed that these dynamics are generally characterized by fractals [1, 2] when the iterated functions are not the contractions [3]. The hierarchical structure of fractals and the noise effect of inputs have been investigated [4]. The fractals generated by switching vector fields have been observed in different domains such as a forced damped oscillator [5], an electronic circuit [6], artificial neural networks [7], and human behavior [8]. Closure of the fractals in both linear [9] and non-linear systems [10] has been also presented. A set of attractors obtained by periodic inputs can approximate trajectories of fractals [11]. These works show that fractals are indispensable for understanding of dynamics observed in the Mobiligence as a complex system[12].

2. Theory of dynamical systems stochastically excited by temporal inputs

In this section, we briefly summarize the theoretical framework for dissipative dynamical systems that interact with other systems through an input (see Fig. (1)). More precise descriptions are given in the reference [3]. We focus on dynamics expressed as dissipative non-autonomous dynamical systems defined by the following ordinary differential equations:

$$\dot{x} = f(x, I(t)), \qquad (1)$$
$$x, I \in R^N,$$

where, x, f, I, and t are state, vector field, input, and time, respectively. Equation (1) implies that a system is influenced by other systems through the input I. For the periodic input $I(t) = I(t + T)$ with period T, introducing the angular variable $\theta \equiv \frac{2\pi}{T} t \bmod 2\pi$ and the new state variable $y \equiv (x, \theta)$, we can transform the non-autonomous system expressed by Eq. (1) into the following autonomous system:

$$\dot{y} = f_I(y), \qquad (2)$$
$$y \in R^N \times S^1.$$

The vector field f_I is defined on a manifold $\mathcal{M} : R^N \times S^1$ that is a hyper-cylindrical space. In the space $\mathcal{M}$, we can globally define the Poincaré section, $\Sigma = \left\{(x, \theta) \in R^N \times S^1 | \theta = 2\pi\right\}$, where a trajectory starting from an initial state at $\theta = 0$ returns at $\theta = 2\pi$. On the section Σ, a mapping can be defined:

$$x_{\tau+1} = g_I(x_\tau), \qquad (3)$$
$$x_\tau \in R^N,$$

where, g_I is an iterated function that transforms a state x_τ to another state $x_{\tau+1}$ after interval T. We can summarize the dynamics with a periodic input as follows. The periodic input I defines two dynamical systems, one continuous and the other discrete, expressed by Eqs. (2) and (3), respectively. In the hyper-cylindrical phase space $\mathcal{M}$, a solution $\phi(t, x_0)$ starting from an initial state x_0 at $t = 0(\theta = 0)$ converges to an attractor at $t \to \infty$. For periodic driven systems, there are several kinds of attractors, including point,

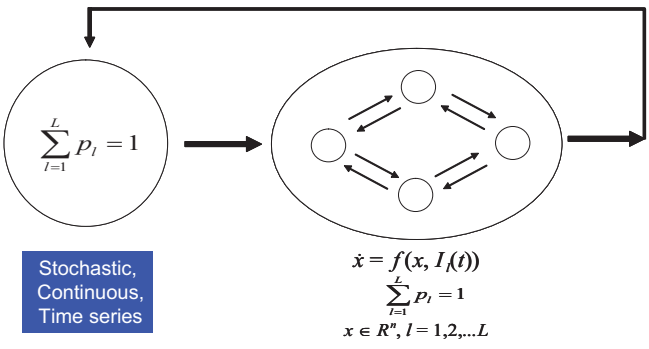

Figure 1: A Model of Interaction between Dynamical System and Environment

limit cycle, torus, and chaos. We call the attractor corresponding to a periodic input the *excited attractor* in order to emphasize that the attractor is excited by the external input.

Next, we consider a dynamics when plural input patterns are stochastically fed into a system one after another. Let us suppose that *each input is one period of a periodic function*. For example, we can define a parameterized periodic function by the finite Fourier series with the amplitude vector $A \in R^M$ for Fourier coefficients and with the period $T \in R^1$. The set of these parameters defines the *input space*:

$$\mathcal{I} = \mathcal{I}(A, T). \tag{4}$$

The input space $\mathcal{I} : R^{M+1}$ is a function space. Within this space, an arbitrary point represents an external temporal input. We consider the input as a set $\{I_l\}_{l=1}^{L}$ of time functions I_l sampled on the parameterized space $\mathcal{I}$. We sometimes abbreviate the subscripts and express individual sets as $\{\cdot\}$ for simplicity. In the same way as in the case of periodic input, we can define two sets of dynamical systems corresponding to the set $\{I_l\}$. One is the set of continuous dynamical systems that is defined by the set $\{f_l\}$ of vector fields on the hyper-cylindrical space $\mathcal{M}$. The other is the set of discrete dynamical systems that is defined by the set $\{g_l\}$ of iterated functions on the Poincaré section Σ. When the inputs I_l are stochastically fed into the system one after another, the vector fields f_l and the iterated functions g_l are also stochastically switched. To emphasize the relation among the set $\{I_l\}$, $\{f_l\}$ and, $\{g_l\}$, we use the following schematic expression:

$$\{I_l\} \rightarrow \{f_l\} \rightarrow \{g_l\}\,. \tag{5}$$

The set of iterated functions is designated as the *Iterated Function System* (IFS) by Barnsley [2]. Similarly, we call the set of vector fields the *Vector Field System* (VFS). Therefore, the two sets, $\{f_l\}$ and $\{g_l\}$, are examples of the VFS and the IFS, respectively. The discrete dynamics on the Poincaré section Σ correspond to the random iteration algorithm using the IFS with probabilities. When $Lip(g_l) < 1$, the map $g_l : x \rightarrow x$ is called the *contraction* or the *contraction map*, where, $Lip(g_l)$ is the Lipschitz constant for g_l. If all the iterated functions are contractions, the state x_τ on the Poincaré section approximately changes on the attractive and unique invariant set C after sufficient random iterations. The set C satisfies the following equation:

$$C = \bigcup_{l=1}^{L} g_l(C). \tag{6}$$

The property of set C of having a fractal-like structure affects the trajectory in the hyper-cylindrical space $\mathcal{M}$. In the space $\mathcal{M}$, the trajectory set $\Gamma(C)$ starting from the initial set C is obtained by the union of the trajectory set $\gamma_l(C)$ for each input I_l:

$$\Gamma(C) \;=\; \bigcup_{l=1}^{L} \gamma_l(C). \tag{7}$$

$\Gamma(C)$ is also the attractive and unique invariant set with a fractal-like structure. We have analytically proved Eqs. (6) and (7) when all the iterated functions $g_l (l = 1, 2, ..., L)$ are contractions. Even without this condition, we have shown numerically that these equations are valid [3]. C and $\Gamma(C)$ are also characterized by the hierarchy of a tree structure [4]. By introducing the interpolating system under some conditions, we can also show that the set $\Gamma(C)$ in the cylindrical phase space is enclosed by the tube structure whose initial set is the closure of the fractal set C on the Poincaré section [9].

The following expression of correlation dimension of the fractal set C has previously been derived for such a strictly self-similar set as the Sierpinski gasket constructed by a set of iterated functions that uniformly contract any two points on the Poincaré section [3]:

$$d = -\frac{\ln N}{\lambda T} \tag{8}$$

where, N, λ, and T are the number of the inputs, the real part of the eigenvalue of a matrix, and the input time length. Equation (8) holds to a self-affine set whose iterated functions are non-contractions that expand two points in some regions [6] . At this point, we have to notice that this equation does not include amplitude parameters of external inputs. This implies that correlation dimension of the fractal set C independent of details of temporal structure of input, except for time interval. It is interesting question that Eq. (8) holds or not to nonlinear equation stochastically excited by temporal inputs. In the following section, we numerically investigate this question.

3. Numerical Experiment

We use the following Duffing equation as an example of nonlinear equations:

$$\ddot{x} + k\dot{x} + x + \varepsilon x^3 = A_l \cos\frac{2\pi}{T_l}t, \tag{9}$$

where, $k(> 0)$, ε, A_l, and $T_l(> 0)$ are parameters for dissipation, nonlinearity, lth input amplitude, and lth input time length, respectively. k and ε are internal parameters while A_l and T_l are external ones. From dynamical systems viewpoint, this second order ordinary equation can be transformed into the following first order equations:

$$\begin{cases} \dot{x}_1 = x_2 \\ \dot{x}_2 = -x_1 - \varepsilon x_1^3 - k x_2 + A_l \cos x_3 \\ \dot{x}_3 = \frac{2\pi}{T_l}. \end{cases} \tag{10}$$

This is a dynamical system, $D = (\mathcal{M}, f_l)$, where $\mathcal{M} = R^2 \times S^1 = (x_1, x_2, x_3)$ and $f_l = (x_2, -x_1 - \varepsilon x_1^3 - k x_2 + A_l \cos x_3, \frac{2\pi}{T_l})$. D is a dissipative dynamical system:

$$div f_l = -k < 0. \tag{11}$$

Then, for periodic input, an initial state converges to an attractor after sufficient long time. Our main interesting is

the dynamics of switching inputs. In this paper, for simplicity, we limit description of numerical examples to equal switching probability using two inputs, i.e. I_1 and I_2, whose amplitudes are different each other, i.e. $A_1 \neq A_2$, while time intervals are the same, i.e. $T_1 = T_2 = T$.

Equation (9) with $\varepsilon = 0$ results in a linear equation driven by external force. In this case, the real part of the eigenvalue of the linear equation is k. Replacing λ with $-\frac{k}{2}$, Equation (8) for two input, i.e. $N = 2$, becomes as follows:

$$d = 2\frac{\ln 2}{kT} \tag{12}$$

This expression implies that correlation dimension does not depend on two parameters, i.e. ε and k. To verify this equation, we calculated correlation dimension for fractal set C constructed numerically by switching input. In the following simulations, $k = 0.2$ is used.

3.1. Dependence on Input Time-length

Figure 3 (below) shows T dependence of correlation dimension d using three different values of ε, i.e. 0, 0.01 and 1.0, respectively. Amplitudes of two inputs were $A_1 = 1$ and $A_2 = -1$, respectively. Ten thousand iterations of switching inputs were plotted after discarding the initial 100 iterations. The solid line is calculated by Eq. (12). At the longer interval the dimension is nearly zero, while at the shorter interval it is nearly two. These tendencies on both sides are easy to intuitively understand as follows. At the limit $T \to \infty$, a trajectory could reach excited attractors that are points in this example. At the limit $T \to 0$, a trajectory might be disordered around two attractors due to the rapid transitions between them. On the other hands, we could not intuitively imagine what happens in the middle range. However, not only for $\varepsilon = 0$ but also for $\varepsilon = 0.01$ and $\varepsilon = 1.0$, Equation (12) shows good agreement, except for short time length where the points overlap each other.

For reference, examples of fractal set C on the Poincaré section are shown in the above. Three rows and four column of panel correspond to three different values of ε and four different length of T, respectively. In each row of four panels, the points spread in every direction at $T = 1$ gradually cluster around to specific region as T becomes larger. At $T = 50$, two clusters around two excited attractors are observed at most. At both sides, i.e. $T = 1$ and $T = 50$, three panels in the same column are very similar in feature. However, in the middle range of $T = 5$ and $T = 10$, fractal pattern are quite different in feature each other in the same column. These observations means that feature of fractal pattern is very sensitive to nonlinearity while correlation dimension is almost the same.

3.2. Dependence on Input Amplitude

Figure 2 shows A_1 dependence corresponding to Fig. 3. Time length and the amplitude of second input are fixed on $T = 6$ and $A_2 = -1$, respectively. In the below, A_1?d graph plotted for three different values of ε. The solid line is $d = 1.16$ obtained by Eq. (12). Although slight deviation can be observed for $\varepsilon = 1.0$ and for 0.01, we can say that Eq. (12) shows good agreement. For reference, example of fractal set C are shown in the above. Three rows and four column of panels correspond to three different values of ε and four different amplitude of A_1, respectively. Fractal patterns in each row for $\varepsilon = 1.0$ and for $\varepsilon = 0.01$ are quite different in feature while they are almost the same for $\varepsilon = 0$, except their scales. In each column for the same amplitude A_1, they are completely different in feature. These observations imply that fractal pattern in their feature is very sensitive to nonlinearity and amplitude while the correlation dimension hardly depend on both parameters.

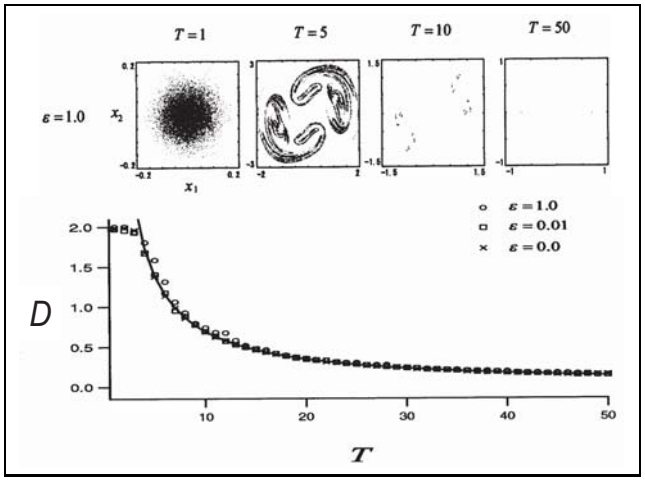

Figure 2: Dependence on Input Time-length

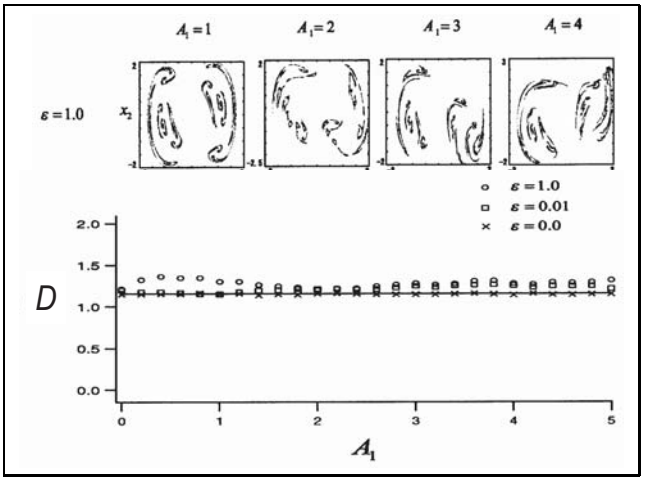

Figure 3: Dependence on Input Amplitude

4. Summary and Discussion

In this paper Eq. (8) of correlation dimension approximately holds to the support of the fractal set obtained by stochastically switching Duffing equation through external temporal inputs. The experimental results clearly show that the correlation dimension is approximately inverse proportional to the time length of inputs while the dimension is independent of amplitude of inputs.

We can calasify parameters into two categories, i.e. internal ones and external ones, respectively. Example presented in this paper includes two internal parameters, i.e. ε for nonlinearity and k for dissipation, and two external parameters A_l for amplitude and T_l for time length of inputs, respectively. Equation (8) and numerical experiment show that $k(= divf)$ and $T_l(= T)$ are essential for define the correlation dimension. Although correlation dimension is just one of generalized dimensions , our results suggest that statistical property of ODE stochastically switched by temporal inputs might be universally defined by dissipation and switching interval independently of details of switching mechanism. We expect that our results would be extended to a multifractal formalism [13, 14] for dissipative continuous dynamical systems stochastically excited by temporal inputs.

References

[1] J. Hutchinson, "Fractals and self-similarity", *Indiana Journal of Mathematics*, vol.30, pp.713-747, 1981.

[2] M. F. Barnsley, Fractals Everywhere, Academic Press, Boston, 1988.

[3] K. Gohara and A. Okuyama, "Dynamical Systems Excited by Temporal Inputs: Fractal Transition between Excited Attractors", *Fractals*, vol.7(2), pp.205-220, 1999.

[4] K. Gohara and A. Okuyama, "Fractal Transition - Hierarchical Structure and Noise Effect," *Fractals*, vol.7(3), pp.313-326, 1999.

[5] K. Gohara, H. Sakurai, and S. Sato, "Experimental Verification for Fractal Transition Using a Forced Damped Oscillator", *Fractals*, vol.8(1), pp.67-72, 2000

[6] J. Nishikawa and K. Gohara, "Fractals in an Electronic Circuit Driven by Switching Inputs", *Int. J. Bifurcation and Chaos*, vol.12(4), pp.827-834, 2002.

[7] S. Sato and K. Gohara, "Fractal Transition in Continuous Recurrent Neural Networks", *Int. J. Bifurcation and Chaos*, vol.11(2), pp.421-434, 2001.

[8] Y. Yamamoto and K. Gohara, "Continuous Hitting Movements Modeled from the Perspective of Dynamical Systems with Temporal Input", *Human Movement Science*, vol.19(3), pp.341-371, 2000.

[9] R. Wada and K. Gohara, "Fractals and Closures of Linear Dynamical Systems Stochastically Excited by Temporal Inputs", *Int. J. Bifurcation and Chaos*, vol.11(3), pp.755-779, 2001.

[10] R. Wada and K. Gohara, "Closures of Fractal Sets in Non-linear Dynamical Systems with Switched Inputs", *Int. J. Bifurcation and Chaos*, vol.11(8), pp.2205-2215, 2001.

[11] H. Oka and K. Gohara, "Approximation of the Fractal Transition Using Attractors Exited by Periodic Inputs ", *Int. J. Bifurcation and Chaos*, vol.13(4), pp.943-950, 2003.

[12] M. Shimizu, K. Gohara, and A. Ishiguro, "Adaptive Amoeboid Locomotion Induced from Embodied Coupled Oscillators," *Proc. of the 2nd International Symposium on Mobiligence*, pp.271-274, 2007.

[13] T.C. Halsey et al., *Phys. Rev. A.* **33**,1141, 1986.

[14] K. J. Falconer, *Techniques in Fractal Geometry*, John Wiley and Sons, 1997.

The Role of Limbic System for Mobiligence

Ichiro Tsuda* and Yutaka Yamaguti**
*Research Institute for Electronic Science, Hokkaido University, Sapporo, 060-0812, Japan
**Department of Mathematics, School of Science, Hokkaido University, Sapporo, 060-0810, Japan

Abstract— **Extending Freeman's theory on the creation of intentional intelligence which is represented by five specific loops of information flow, we developed the theory on the mechanism of creation and annihilation of mobiligence in terms of the modified loops of information called "mobiligence loop". In order to establish the embodiment, which is assumed to appear in the process of formation of the sense of "now" in the body, we introduced a concept, reafference copy, and describe its relation with efference copy of von Holst. Based on this theory, we developed a mathematical model for the hippocampus since the hippocampus plays a decisive role of the formation of episodic memory that is viewed as a remembering process of past experience and imagining process of future as well. We also propose a hypothesis that at least mammals can embody their experience and control to rapidly respond to an abrupt change of environment by copying episodic memory in peripheral receptors. Cantor coding will be effective for this compact coding method. In this fiscal year, we further investigated our model for CA1 and found the most appropriate time interval of input sequence and its dependence on the cell type and synaptic properties.**

I. Episodic copy hypothesis and mobiligence loop

The aim of this study is to obtain a new insight for the mechanism of creation and annihilation of intelligence by movements, that is, "mobiligence", taking into account the role of limbic system in that mechanism. Extending a theory constructed by Walter J. Freeman, we proposed a mobiligence loop (Fig. 1). Animals and men search the environment actively by using motor cortex, cerebellum cortex, or basal ganglia, and sense its response from environment via receptors. This information is sent to the entorhinal cortex as sensory information and back to the motor system. This is called a motor loop. Since the body is used for movement, a control loop must act to control the body via the motor system. Furthermore, a reafferent loop to the sensory systems from the body works as a proprioceptive loop. A spatio-temporal loop as an interaction system between the entorhinal cortex and the hippocampus participates in these processes.

In a mobiligence loop, we introduced efference copy as an internal image as for the response of the receptors to the body movement in the environment. This definition seems to be slightly different from the original definition of von Holst that the sensory systems utilize exactly negative image of the response in order to match the response with the anticipated one, but essentially the same in the following sense. An efference copy can be used not only for the judgment of the correctness of the present motor pattern, but also for extracting the difference of the effect to the body between in active and voluntary movements and in passive movements, by which the embodiment as harnessing of sensory-motor systems can be established.

There seems to be at least two roles of efference copy. One is to copy the response stemming from the existence of body in order to distinguish it from the response stemming purely from the environment. Other one is to find the difference between subjective embodiment and objective response of the body to stimulus. However, the latter seems to be difficult to be established only by efference copy in the above sense. Then, we need another concept, say called " reafference copy " as information for the control of body by interpreting efference copy. For the establishment of these loops, not only proprioceptive loop but interroceptive loop is necessary.

In addition to the above theory, we also introduced the following hypothesis. Episodic memory plays a role not only for a slow process of cognition but also for a fast process of sensing and embodiment, by embodying episodic memory and copying it into receptors. This fiscal year was devoted to study our model for CA1 in details and obtained several important dynamic features.

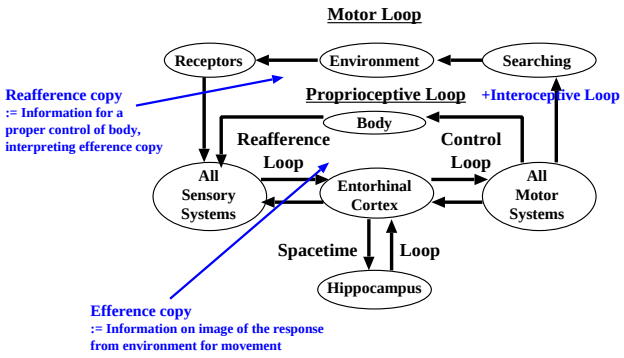

Fig. 1. The mobiligence loop.

II. Mathematical Model for the Hippocampal CA1

A. Network

Fig. 3(a) shows the CA1 network which receives the CA3 output. We assume that the input temporal series of firing patterns to CA1 is a temporal series of evoked attractors embedded in CA3, which may represent a series of events, that is, an episode. In the present model of CA3 which consists of N_{ca3} pyramidal cells, it is assumed that M firing patterns denoted by $X(0), ..., X(M-1)$ is stored in the networks via Hebbian learning algorithm as event memories. Each stored pattern can be represented by an attractor in the state space of neural activity.

The pyramidal cells of CA1 receive such activity via both AMPA- and NMDA- receptors. We also assume that the synaptic strengths from CA3 to CA1 is accomplished by Hebbian learning. More specifically, the synaptic strength, w_{ij} of j-th neuron of CA1 from the i-th neuron of CA3 is given by the following expression:

$$w_{ij} = S_{\max} \sum_{k=0}^{M-1} X_i(k) Y_j(k), \tag{1}$$

where $X_i(k)$ denotes the activity of i-th neuron in CA3, and $Y_j(k)$ the activity of j-th neuron in CA1 for both input pattern k, and $S_{\max}$ is an adjustable parameter for controlling the input strength. Here, we treat only the case that the network consists of only pyramidal cells and no explicit connections between CA1 neurons.

B. Neuron model

We used two-compartment model proposed by Pinsky and Rinzel[1]. This model can represent the electric properties of dendrite and cell body, each of which is assumed to be electrically uniform. The equations of

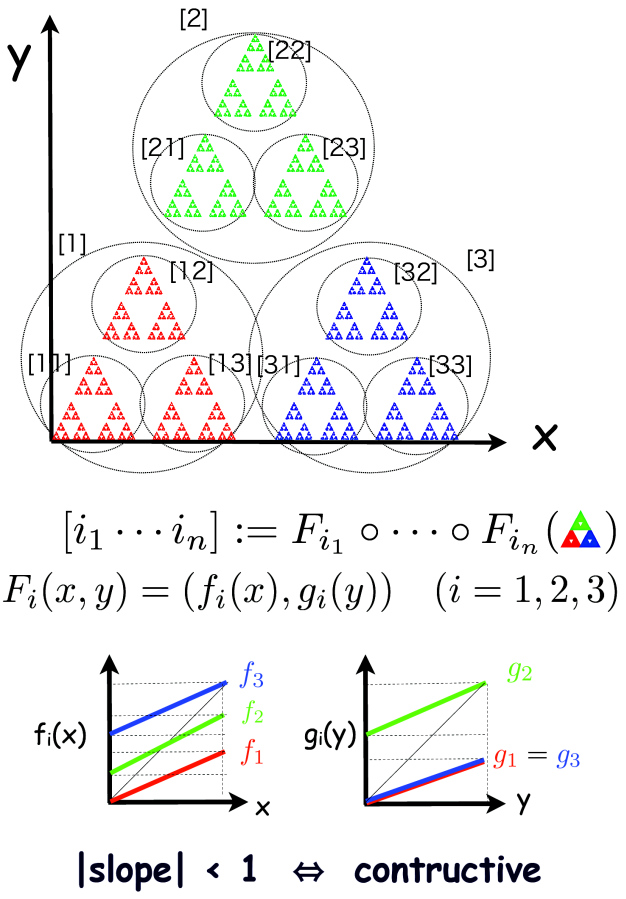

Fig. 2. Example of Cantor set.

model neuron are given as follows:

$$\begin{aligned} C_m V_s' = &- I_{Leak}(V_s) - I_{\mathrm{Na}}(V_s, h) - I_{\mathrm{K-DR}}(V_s, n) \\ &+ (g_c/p)(V_d - V_s) + I_s/p \end{aligned} \tag{2a}$$

$$\begin{aligned} C_m V_d' = &- I_{Leak}(V_d) - I_{\mathrm{Ca}}(V_d, s) - I_{\mathrm{K-AHP}}(V_d, q) \\ &- I_{\mathrm{K-C}}(V_d, Ca, c) - I_{\mathrm{Syn}}/(1-p) \\ &+ (g_c/(1-p))(V_s - V_d) + I_d/(1-p), \end{aligned} \tag{2b}$$

where V_s and V_d are the membrane potential of cell body and dendrite, respectively. C_m is conductance of membrane, each I_z is an ionic current associated with each kind of ionic channels, I_{Syn} is a synaptic current, g_c is a conductance, and p is a ratio of the surface area of cell body with the whole cell area.

C. Encoding of sequences

We investigated how the temporal sequences can be encoded in the membrane potential and/or spike events of CA1 neurons. It turns out that this system

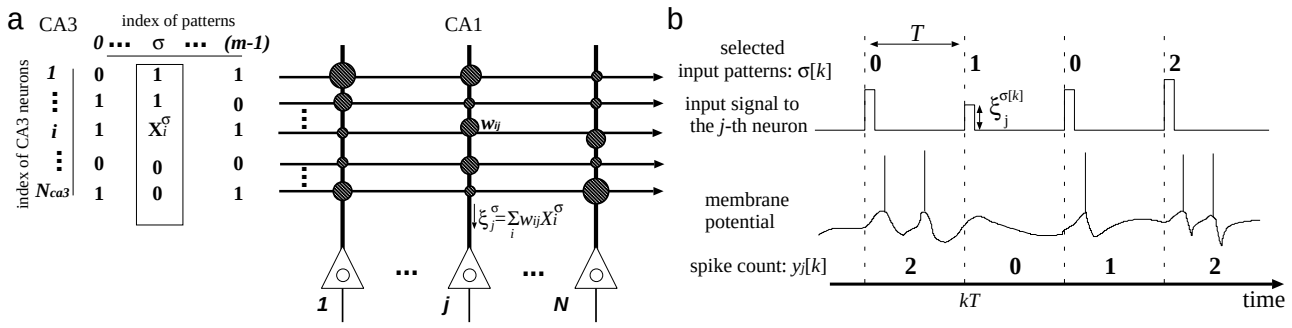

Fig. 3. The schematic representation of the CA1 model. (a) Network connections. (b)Inputs and responses of a CA1 neuron.

can be described by Iterated Function System (IFS)[2], because this CA1 neural network receives the input pattern series whose elementary pattern is selected with a certain probability.

III. Performance of Coding

Using Linear Discriminant Analysis (LDA), we investigated how much the Cantor coding obtained is effective(Fig.3). The error rate of the linear discrimination is regarded as an index of the coding. Using this index, we obtained good performance of coding for input sequences with the length of at least five spatial patterns. Furthermore, the best performance for the input interval was 80-200 msec, which is a characteristic time window of this system. The preferred interval for coding strongly depends on the cell type and the balance of synaptic strength of AMPA and NMDA. The bursting neuron preferred longer interval (θ range) than the non-bursting regular spiking neuron. The cell with NMDA synapses favors longer interval than the cell which has AMPA synapses only which may play better in γ range of activity (see Fig. 4).

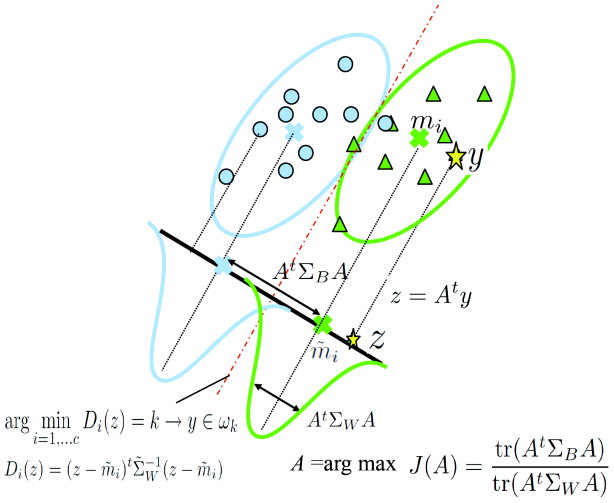

Fig. 4. Schematic diagram of Linear Discriminant Analysis.

References

[1] P. F. Pinsky and J. Rinzel, Intrinsic and Network Rhythmogenesis in a Reduced Traub Model for CA3 Neurons, *J. Comp. Neurosci.*, 1, 1994, pp39-60.

[2] M. F. Barnsley, *Fractals Everywhere*, Academic Press, 1988.

[3] I. Tsuda and S. Kuroda, "Cantor coding in the hippocampus," *Japan J. of Industrial and Appl. Math.*, 18, 2001, pp 249-258.

[4] I. Tsuda and S. Kuroda, "A Complex Systems Approach to an Interpretation of Dynamic Brain Activity II: Does Cantor coding provide a dynamic model for the formation of episodic memory?", *Lecture Notes in Computer Science*, 3146, pp. 109-128. (Springer-Verlag, 2004)

[5] I. Tsuda, "Toward an interpretation of dynamic neural activity in terms of chaotic dynamical systems", *Behavioral and Brain Sciences*, 24, 2001, pp. 793-847.

[6] Y.Fukushima, M. Tsukada, I. Tsuda, Y. Yamaguti and S. Kuroda, "Spatial clustering property and its self-similarity in membrane potentials of hippocampal CA1 pyramidal neurons for a spatio-temporal input sequence," *Cognitive Neurodynamics*, 1, 2007, pp 305-316.

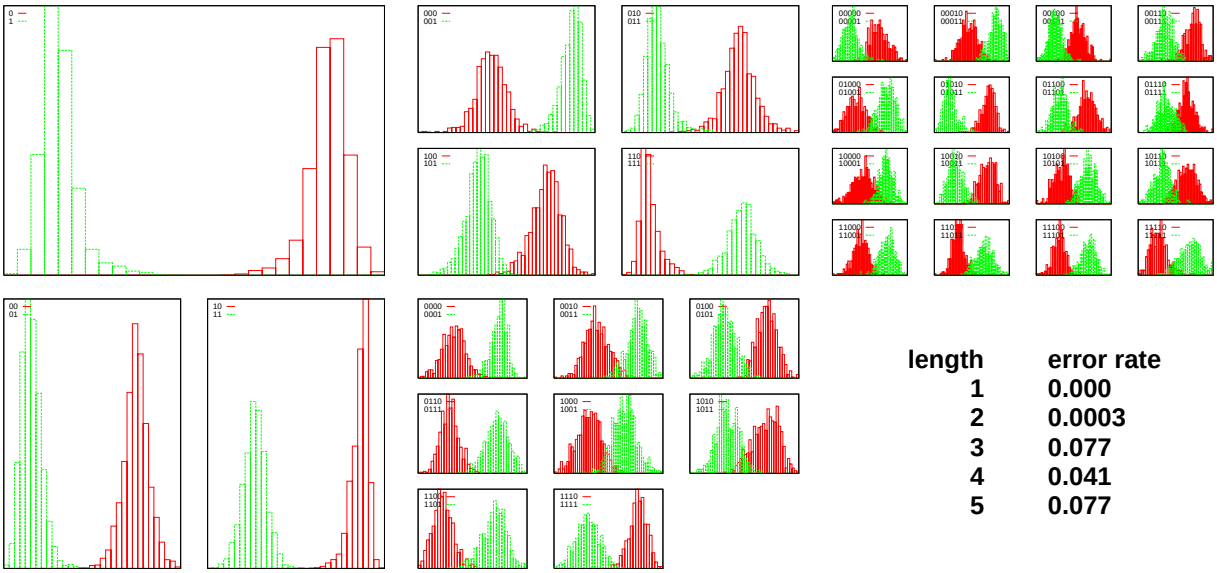

Fig. 5. An example of LDA.

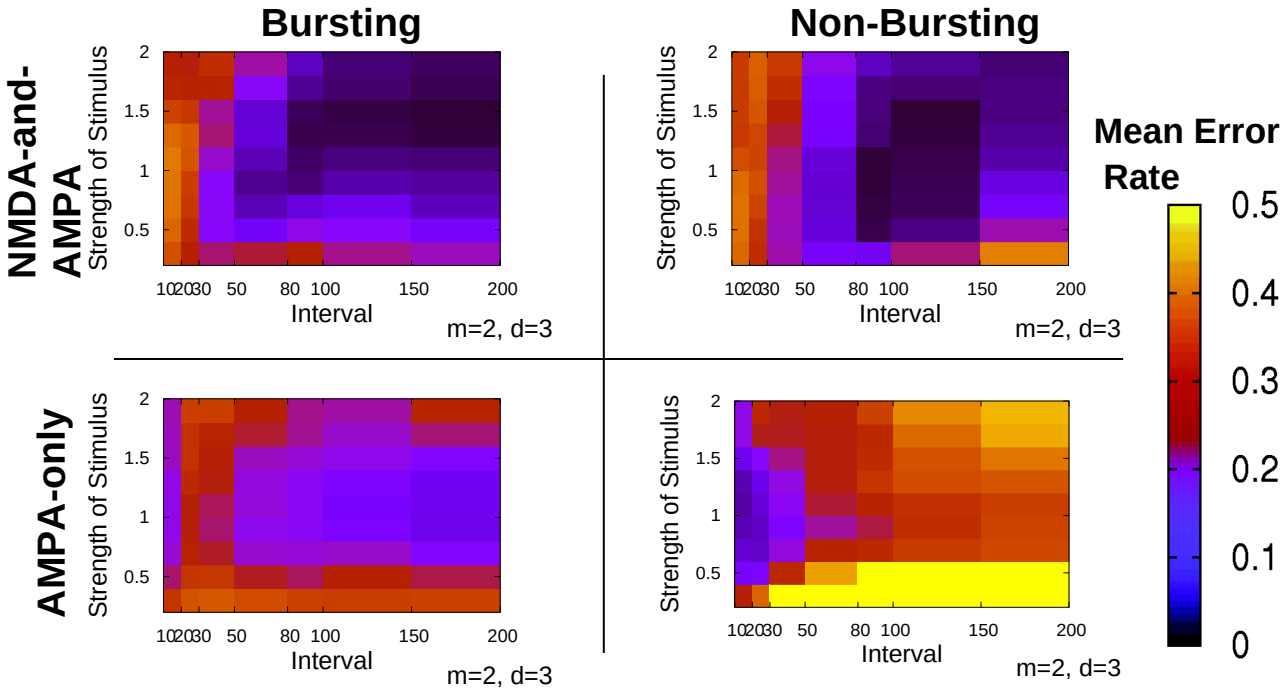

Fig. 6. Dependence of performance on cell and synaptic property

Computational model of neural systems for learning causality of external events and performing actions

Toshio Aoyagi

Department of Applied Analysis and Complex Dynamical Systems, Graduate School of Informatics, Kyoto University, Kyoto, Japan

Abstract

To realize high adaptability to the environment for the survival, the animal has to decide the optimal action, for example, to walk to the better environment. The central nervous system is an extremely efficient information processing device for this purpose. Among various neuronal activity patterns, synchronous activity associated with behavior and cognition has been observed in many neuronal systems. As underlying mechanisms, we first demonstrate that a network organized under spike-timing dependent plasticity (STDP), not only is capable of memorizing the activity patterns of the external stimulus, but also exhibits a systematic transition behavior among the memorized patterns in response to uniform external synchronized spikes. We next consider the recurrent infomax, which maximizes the information retention and thereby minimizes the information loss through time in the recurrent network. Numerical simulations demonstrate that recurrent infomax provides a simple framework explaining for a wide range of phenomena observed in in vivo and in vitro neuronal networks. On the basis of these findings, using the novel experimental methods such as brain machine interface and cultured neural systems, we will explore the essential mechanisms of neuronal systems for emergence of adaptation through interaction among the body, brain and environment.

I. INTRODUCTION

Recent advance in the multineuron recording techniques has initiated a new stage in the analysis of the neuronal mechanisms underlying the intelligence. For example, we can examine neuronal activity in behaving animals by directly measuring the multineuron activities. One of the most important challenges in neuroscience is to discover a way to decode the neuronal activity, for example, to predict the decisions, choices, behaviors. In particular, synchronous activity associated with behavior and cognition has been observed in many neuronal systems [1], [2]. However, its functional role remains unclear [3], [4]. It is reasonable to assume that such generated synchronous spikes drive certain cortical networks as input signals and thereby affect their functions. Another related phenomenon is spike-timing dependent plasticity (STDP) [5], which allows cortical networks to learn the causality of experienced events through the coding of the temporal structures of neuronal activity. Considering that both phenomena affect the functioning of cortical neurons, it is natural to ask what effect synchronous inputs have on a neural network organized under STDP learning. For this purpose, let us consider the specific situation in which a model network of spiking neurons, whose synaptic connections are modified through STDP, receives an activity pattern as an external stimulus as a result of the experiencing of some external events.

II. EXPLORING ROLE OF SYNCHRONY IN BRAIN SYSTEMS

A. A network of spiking neurons with STDP

Figure 1D presents a schematic illustration of the model network, in which the excitatory and inhibitory neurons are indicated by triangles and ellipses, respectively. Each mathematical model of neurons has been adopted in the previous studies and typical behaviors of membrane potentials are illustrated in Figure 1B. We assume that the excitatory synaptic strength are modified according to the STDP rule as shown in Figure 1A, whereas a globally uniform inhibition without modification of learning is included in an all-to-all manner.

We employ two types of controllable external inputs. One is a stimulus input, in which an initial stimulus-pattern and a training stimulus-pattern are presented

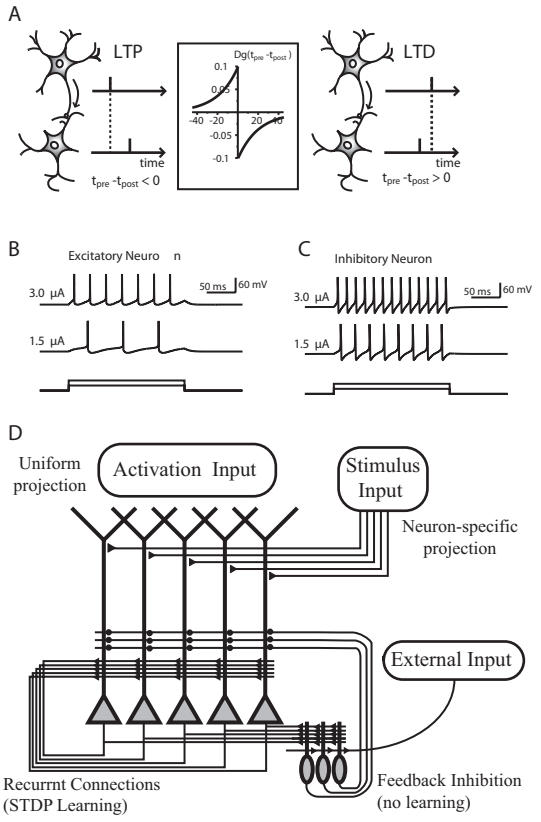

Fig. 1. A:Spike-timing dependent plasticity (STDP). In this synaptic plasticity as an elementary process of learning, LTP or LTD is evoked dependent on spike timing. When a post-synaptic neuron fires after a pre-synaptic neuron firing, the synaptic connection strength increases. In contrast, if a post-synaptic neuron firing proceeds pre-synaptic one, the synaptic connection strength decreases. B:Typical behavior of single excitatory pyramidal neuron model. C:Inhibitory fast-spiking neuron model. From bottom to top, input current time course, membrane potential with 1.5 μA input, and membrane potential with 3.0 μA input. D:Schematic illustration of synaptic connections of excitatory and inhibitory neurons. Triangles represent excitatory neurons, and ellipses inhibitory neurons.

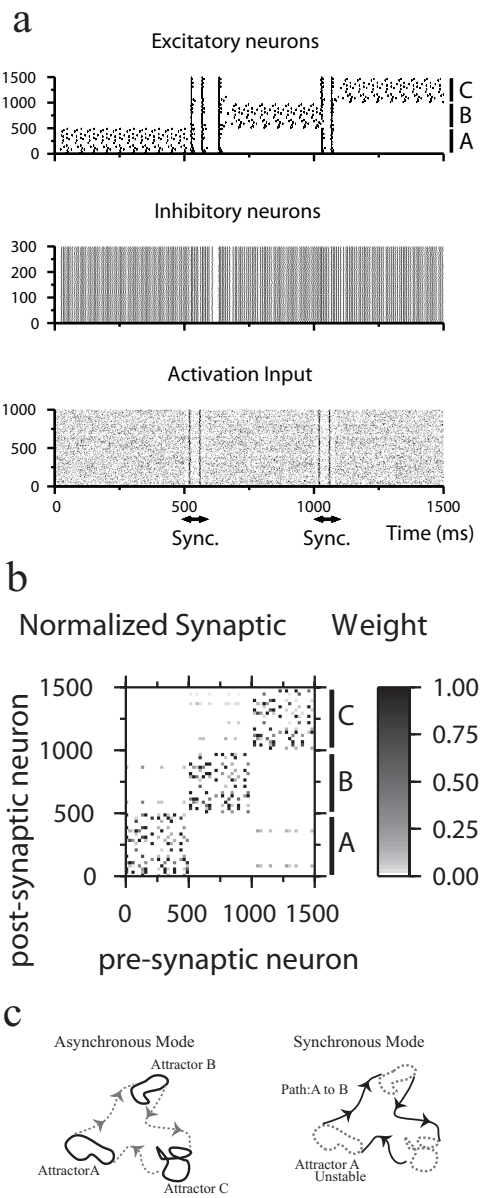

Fig. 2. Typical effect of a uniformly synchronized spike input on the network of spiking neurons organized under the STDP learning rule. a:Typical response of network activity to incoming synchronous spikes. A transition between spike patterns is induced by an transient synchronous spike input, in which next pattern realizing after the transition is determined systematically by the presentation sequence of the spike patterns in the learning period, owning to the causality of the STDP rule. b:The weight matrix of synaptic connection formed by the STDP learning, normalized by the maximum value. The major connections concentrated in three diagonal blocks, gives the feed-forward loops realizing the memories of the spike patterns (A, B and C). The weak connections in the off-diagonal blocks (A $\rightarrow$ B, B $\rightarrow$ C, and C $\rightarrow$ A) are formed reflecting the presentation sequence of the learned spike patterns. c.Interpretation of the synchrony-induced switching behavior from the point of view of dynamical systems.

during a trial and a learning session, respectively. For learning, we use a simple training stimulus-pattern, as depicted in Figure 2a. This pattern is divided into three parts consisting of firing patterns referred to as A, B and C, in which each composed of a particular set of active neurons. These neurons that are active for a given pattern fire periodically, and in each pattern, there are certain fixed phase relationships among the active neurons. During learning, these three patterns are presented as the stimulus input (Figure 1a) in the fixed order (A,B,C,A,B,C$\cdots$). This can be regarded as representing a certain external sequence of events that the network is to learn, in other words, the causality of certain external events.

The other type of controllable input is an activation

input, which projects to all neurons uniformly. This input is introduced to examine the effect of synchrony on the neuronal dynamics. This uniform background input serves to activate the entire network and to allow each neuron to be in a firing state under suitable conditions. There are two modes of neuronal activity for the activation input: asynchronous and synchronous modes. In the asynchronous mode, spike trains are randomly generated by a Poisson process. During learning, the activation input is always in the asynchronous mode. In the synchronous mode, some of the neurons fire synchronously, while the other neurons remain in the asynchronous firing state. The fraction of neurons firing synchronously represents the degree of synchrony. To remove the influence of firing rate modulation, in both modes, the average firing rate is set to the same constant value.

B. A role of uniformly synchronous inputs

The main question of interest in this study is the following: after the STDP learning process described above has been completed, what activity pattern does the resultant network exhibit? To answer this question, we first examine the case in which the activation input is initially set in the asynchronous mode, with the level of the total current such that the neurons are in an active state in response to an appropriate stimulus input and maintain an active state through recurrent excitatory synapses organized under the STDP. Figure 2a illustrates some typical activity patterns displayed by the network (top) and the activation input (bottom) as rasterplots. First, the network exhibits the pattern A, which is stable when the activation input is in the asynchronous mode. Thus, in this case, the network exhibits ordinary associative memory. In Figure2b, we can see clearly that three diagonal blocks of major synaptic connections, which are formed by the three basic stimulus patterns (A,B,C), enable the network to retrieve each pattern in an associative manner. In addition, there are three off-diagonal blocks of weak synaptic connections arising from the less frequent transitions among the stimulus patterns as shown in Figure 1c. Because the synaptic connections for transitions are relatively weak, under ordinary conditions, each individual pattern is sufficiently stable that no transition among patterns occurs.

Interestingly, Figure 2a demonstrates that a brief period of synchrony in the uniform activation input can enhance this weak effect embedded in the synaptic matrix and can thereby cause a transition from the

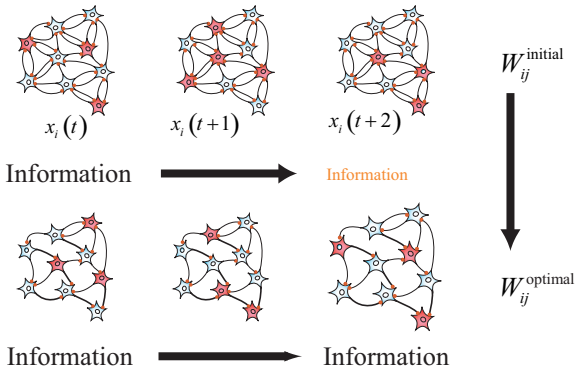

Fig. 3. Basic ideas of recurrent Infomax. Maximizing the mutual information between the state of the network at time t and t + 1 reduces the information loss through time.

one pattern to another. Therefore, when the activation input is switched for a brief time to the synchronous mode, a transition from the pattern A to the pattern B occurs. Hence, the retrieval of a learned sequence in the presented order can be triggered by globally uniform synchronous inputs. From the perspective of dynamical systems, when the network is activated by a uniformly asynchronous spike input, the system possesses some attractors formed by the STDP learning rule (Figure2c left). However, a brief uniformly synchronous input activates the paths between attractors, leading to a transition to the next pattern in the learned order (Figure2c right).

III. Infomax for recurrent neural networks

Under the unpredictable environments, a voluntary movement of animals plays an important role not only in taking action for adapting the given environments (for example, moving to the better place for survival.) but also in getting more useful information for the optimal action. For this purpose, an animal has evolved neuronal systems as an efficient information processing device to take better action for survival. However, the information coding in the brain is still a controversial issue, particularly, how does multiple neurons work in concert to realize specific brain functions? The principle of information maximization (Infomax) [6], which maximizes the information transmitted from the input to the output in the feedforward network, is effective for a learning mechanism the stimulus selectivity of the neuron to visual stimuli. Although Infomax is one of the plausible candidates for leaning mechanisms, no recurrent connection was taken into account. However, the existence of the recurrent connection is inevitably essential to realize the higher brain functions such as

adaptation and decision making. Therefore, we will try to theoretically extend Infomax to the case of recurrent networks and we named this extended theory Recurrent Infomax. Recurrent Infomax maximizes the information retention, thus, minimizes the information loss through time in the recurrent network as shown in Figure 3.

We found that, in response to visual stimuli of natural scenes, the Recurrent Infomax organized the initial random network into a feedforward network with simple cell-like output neurons [7]. More interestingly, in the case of spontaneous firing state without external input, the resultant network exhibits the cell assembly-like and synfire chain-like activities [8] and the critical neuronal avalanche [9]. Figure 4 shows the typical firing patterns of network after leaning and the frequency distribution of the burst size.

IV. CONCLUSIONS AND FUTURE WORKS

The first results suggest that synchronous spikes may act as a signal in biological systems, serving to link learned sequences of actions in response to some external stimuli. We believe that some experimental results can be more clearly reinterpreted using our results. Second, we demonstrated that the emergent of the simple cell-like stimulus selectivity, the spontaneous synfire chain-like activity and neuronal avalanche were explained in by the Recurrent Infomax in a unified way. On the basis of the above findings, using the novel experimental methods such as brain machine interface and cultured neural systems, we will study the adaptation mechanism through the interaction between environments and neuronal systems in the near future.

V. ACKNOWLEDGMENTS

I thank T. Tanaka, M. Nomura and T. Aoki who participated in this study.

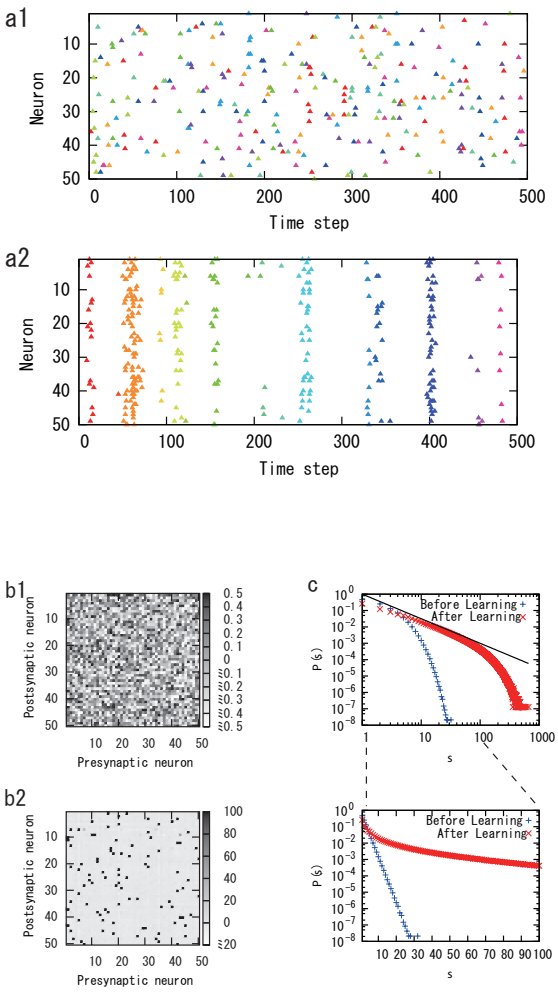

Fig. 4. Spontaneous activity of the recurrent network with $p_{\max} = 0.5$. (a1,2) Individual bursts in the spontaneous activities before (a1) and after learning (a2) are indicated by different colours. The bursts before learning were short and frequently interrupted by the steps without firing, whereas the bursts after learning had much longer duration. (b1,2) Initial W_{ij} with random weights changed to a matrix with relatively few strong weights. (c) Frequency distribution $P(s)$ of the burst size is plotted against size s. The black line shows the slope of -1.5.

REFERENCES

[1] C. M. Gray, P. Konig, A. K. Engel, and W. Singer, "Oscillatory responses in cat visual cortex exhibit inter-columnar synchronization which reflects global stimulus properties." *Nature*, vol. 338, pp. 334–337, 1989.

[2] A. Riehle, S. Grun, M. Diesmann, and A. Aertsen, "Spike synchronization and rate modulation differentially involved in motor cortical function." *Science*, vol. 278, pp. 1950–1953, 1997.

[3] A. K. Engel, P. Fries, and W. Singer, "Dynamic predictions: oscillations and synchrony in top-down processing." *Nat. Rev. Neurosci.*, vol. 2, pp. 704–716, 2001.

[4] E. Salinas and T. J. Sejnowski, "Correlated neuronal activity and the flow of neural information." *Nat. Rev. Neurosci.*, vol. 2, pp. 539–550, 2001.

[5] G. Q. Bi and M. M. Poo, "Synaptic modifications in cultured hippocampal neurons: dependence on spike timing, synaptic strength, and postsynaptic cell type." *J. Neurosci.*, vol. 18, pp. 10 464–10 472, 1998.

[6] R. Linsker, "Self-organization in a perceptual network," *Computer*, vol. 21, no. 3, pp. 105–117, 1988.

[7] A. J. Bell and T. J. Sejnowski, "An information-maximization approach to blind separation and blind deconvolution." *Neural Comput.*, vol. 7, no. 6, pp. 1129–1159, 1995.

[8] M. Abeles, *Corticonics*. Cambridge: Cambridge. Univ. Press, 1991.

[9] J. M. Beggs and D. Plenz, "Neuronal avalanches in neocortical circuits," *J. Neurosci.*, vol. 23, no. 35, pp. 11 167–11 177, Dec 2003.

Basic strategy for trajectory planning in human movements

Jun NISHII
Yamaguchi University

I. INTRODUCTION

Living bodies show various kinds of movements in order to acquire energy, and the profit which is given by the balance of the energy cost of the movements and obtained energy determines the probability of survival. Intelligence in movements and behaviors would be regarded as something which living bodies have acquired through natural selection or learning in order to raise the profit.

To understand the intelligence in movements of living bodies which realize adaptive movements under various environments, it would be necessary to understand the movement itself, in other words, to understand the basic strategy of living bodies to determine a movement from redundant solutions. If living bodies have accomplished some optimization through natural selection, the minimization of energy cost would be a candidate of the basic strategy. In this paper, we introduce our studies to evaluate this hypothesis on arm reaching movements and leg swing trajectories during walking, and show that living bodies might minimize the expected value of energy cost by increasing adaptability. We also show some results to consider how living bodies coordinate the rhythm generator and reflex systems to realize adaptive locomotion.

II. OPTIMALITY OF REACHING MOVEMENT

It has been reported that arm trajectories during reaching movements are slightly curved and their speed profiles take bell-shaped curve (Fig.1(a)). As computational models to explain why our nervous system select such a trajectory, the minimum jerk model [1] and the minimum torque change model [2] which respect the smoothness of reaching trajectories, and the minimum end-point variance model [3] which respects the noise effect on nervous system, were proposed and have been reported to express many characteristics of reaching trajectories. Although the minimum energy cost model was also investigated as a criterion which determines the reaching trajectory [4], [5], it has been reported that the trajectory which minimizes the energy cost differs from actual one in some aspects, e.g., the speed profile does not take a bell shape [5]. Does this result mean that reaching trajectories are determined by the factor of the smoothness or the noise, and independent of the energy cost?

We investigated which model, the minimum end-point variance, the minimum energy cost or the minimum torque change model, have an advantage in the total energy cost when we consider signal-dependent noise and corrective submovements so as to compensate for the positional error (Fig. 2) [6]. The result showed that the trajectories which minimize the end-point variance and the torque change are less sensitive to noise than the minimum energy cost trajectories, therefore, they require smaller amount of energy cost on average to reach a target area. Furthermore, we have computed the optimal reaching trajectory which minimizes the expected value of energy cost to reach a target area under noise effect [7]. The speed profile of the optimal trajectory showed a bell-shaped curve like human data when movement duration is short and showed a collapsed shape when the du-

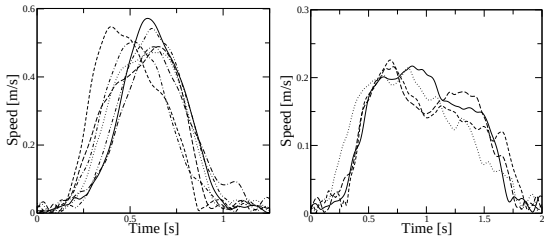

Fig. 1. Hand speed during arm reaching between two points with (a) short duration (b) and long duration.

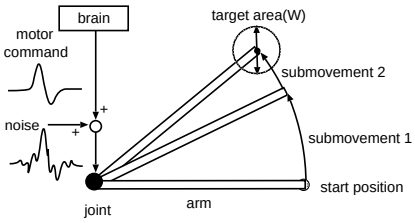

Fig. 2. Schematic view of an arm reaching movement.

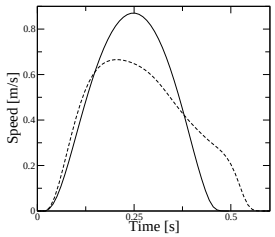

Fig. 3. Hand speed profile which minimizes the expected energy cost under noise effect for the duration of 0.5 [s] (solid) and 0.6 [s] (dotted). The noise was assumed to be $N(0, \sigma)$ where the variance σ is proportional to the amplitude of motor command u ($\sigma = ku^2$, $k = 0.015$).

The graduate school of science and engineering, Yamaguchi University, 1677-1 Yoshida, 753-8512 Yamaguchi, JAPAN, nishii@sci.yamaguchi-u.ac.jp

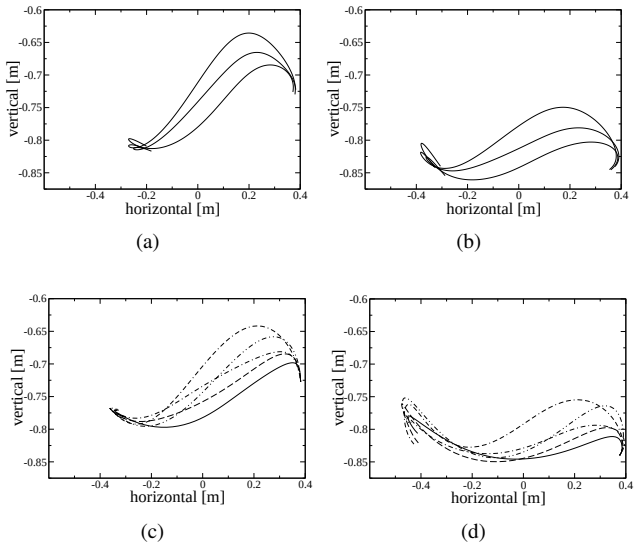

Fig. 4. Horizontal view of leg swing trajectories. (a) and (b) show the ankle and toe position relative to the hip position, respectively, in three walking cycles by a subject at walking speed of 4 km/h. (c) and (d) show the horizontal view of the ankle and toe position, respectively, for the computed swing trajectories of which energy cost are from the minimum value 12 (solid) to 48 [J].

ration is long (Fig.2). In fact speed profile of human reaching movements becomes collapsed shape when the movement duration is over about 1.5 s (Fig.1(b)). Therefore, the results suggest that the criteria of minimization of the expected value of energy cost explain not only the characteristics of usual reaching movements but also those for slow movements.

III. Optimality of leg swing trajectory during walking

The idea that the swing movement during walking is a kind of pendulum motion has attracted many researchers not only in biomechanics but also in robotics. On the other hand, especially in recent years many experimental and computational analysis for the swing phase have shown the counterarguments for the ballistic model, e.g., the large joint torque at the end of swing causes the retraction of the foot which has been suggested as an important feature to obtain a stable locomotion [8], [9]. Authors have shown that the optimal leg swing trajectory that minimizes the energy cost under the condition of the leg retraction for smooth grounding is in good agreement with measured trajectory in many aspects [10]. On the other hand, swing trajectories often fluctuate even in successive walking strides in a subject (Fig. 4(a)(b)). If the swing trajectories are planned so as to suppress the energy cost with leg retraction, the variance of the trajectories would distribute around the optimal trajectory. We verified this idea and examined the effect of leg retraction on the stability of walking by a robot experiment to confirm whether the retraction contributes to suppress the long-term energy cost or not.

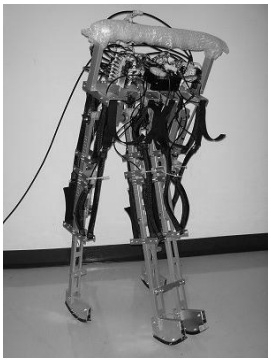

Fig. 5. The biped robot used in the evaluation of leg retraction in the end of swing.

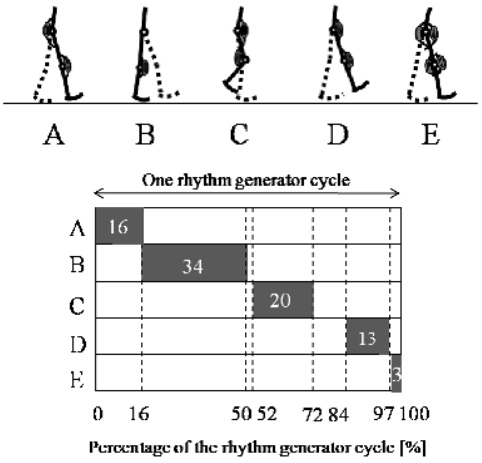

Fig. 6. Muscle synergies during walking. Five synergy patterns are prepared including the pattern for for leg retraction in the end of swing (E). These synergy patterns are activated at a fixed timing in a given stride period.

A. Variability of leg swing trajectories and their optimality

In this study, we modeled a leg as a simple three-link system and computed the optimal trajectory which minimizes the energy cost with the condition of smooth grounding, and then we examined possible trajectories by allowing a specific range of energy cost from the optimal one. In the computation, the energy cost was estimated by a model proposed by Alexander [4].

Fig. 4(c)(d) shows the results and indicates that computed trajectories well express the characteristics of actual ones qualitatively and quantitatively (Fig. 4(a)(b)). In other word, the basic design of swing trajectory would be to minimize energy cost with the condition of leg retraction in the end of swing, however, the trajectory sometimes fluctuate around the optimal one.

B. Stabilization of walking by swing-leg retraction

As mentioned above, the human walking seems to be stabilized by consuming energy for leg retraction in the end of swing. However, the effect of the retraction has been reported only in theoretical studies which used a simplified leg model [8], [9]. We examined whether the retraction stabilizes walking by using a biped robot (Fig. 5) [11]. Each

TABLE I

SUCCESS RATE OF WALKING WITH AND WITHOUT RETRACTION OF LEG IN THE END OF SWING PHASE.

	without retraction	with retraction
success of walking	30% (9/30)	70% (21/30)

leg of the robot has one-degree joints at the hip and the knee and are actuated periodically by Mckibben artificial muscles as shown in Fig. 6.

Table I shows the success rate of continuous walking from the initiation with and without swing-leg retraction (without synergy E in Fig. fig:matsuno-mt), and indicates that the retraction effectively improves the walking performance. The leg trajectory of the robot also showed the variance especially at the middle of swing like human walking (Fig. 4(a)(b)), however, it was confirmed that the swing-leg retraction reduces variance of joint angles at grounding. These results suggest that the control system in living bodies might not try to realize a target trajectory over movement duration but allows some variance and suppresses it in some effective ways to acquire adaptive movements which suppress the expected value of energy cost.

IV. CONTROL MECHANISM TO ACQUIRE ADAPTIVE MOVEMENT

The concept of the rhythm generator (RG) and reflex systems have been often discussed as control systems of locomotion. The RG are capable of sending control signals at specific phases of the oscillation with synchronizing with body movements. The effectiveness of the control by the RG for locomotion has been reported in many computer simulations and robot experiments. As mentioned in the previous section, the swing-leg retraction generated by even an open-loop rhythm generator effectively stabilizes the walking. On the other hand, some studies have suggested that legged animals might realize adaptive locomotion by reflex systems without the RG. Then, which is effective to acquire adaptive locomotion, reflex systems or the RG? If legged animals utilizes both, how are they combined?

First, we took a simulation experiment of controlling a one-dimensional hopping robot by the hierarchical learning model (Fig. 7) which we proposed based on physiological knowledge [12]. In this model, higher center (HC) sends control signal, excitatory signal and suspend signal, to the RG according to the states of the physical system and the RG, therefore, it works like a kind of reflex systems. The RG sends motor command to motor neuron periodically. The HC learns the control signal to make the robot hop at a target height by reinforcement learning, and the RG learns its intrinsic frequency and coupling weights of sensory inputs so as to decrease the control signal from the HC.

Fig. 8 shows typical activities of the HC during learning. As learning proceeds, the control signals from the HC became silent and desired hopping was realized only by the signal from the RG. However, if the robot was perturbed, the RG sent signals with synchronizing with the robot movement

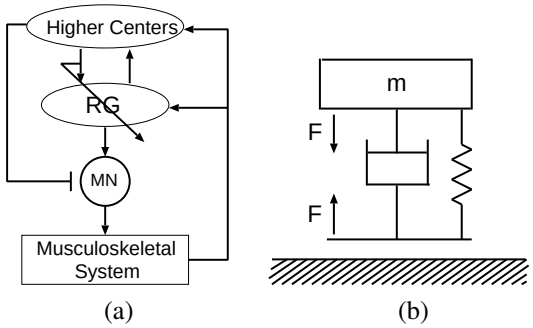

Fig. 7. A hierarchical control learning model by a higher center and a rhythm generator (RG). The higher center evaluates the result of movement and learns the control signal to the RG. The RG tunes its parameters so as to decrease the control signal from the higher center.

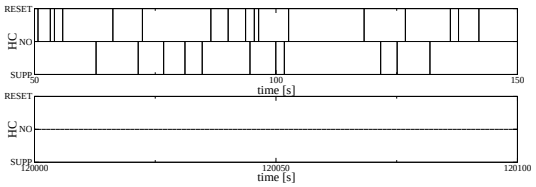

Fig. 8. The control signal from the HC to the RG. Upper and lower side of each graph shows the excitatory and inhibitory signals, respectively. In the beginning of the learning (upper) the HC searches an appropriate signal set. After a sufficient learning time (lower), the HC becomes almost silent because the RG learned appropriate control signal.

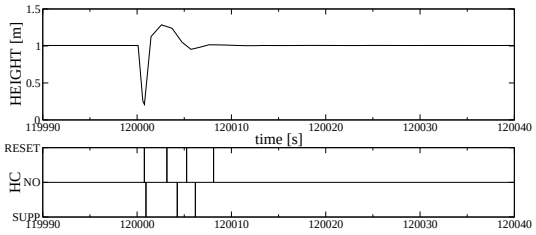

Fig. 9. Response to perturbation. Upper graph shows the height of robot and lower one shows the control signal from the HC to the RG.

and the HC sent control signal for recovery (Fig. 9). Table II shows the recovery time of hopping obtained by the control only by the RG, and by both of the RG and HC, and indicates that cooperative control results in better performance.

Second, we took an experiment to consider how the RG and a reflex system should work on locomotion control, by using a locomotion simulator of cat hindlimb developed by Maufroy et al. [13]. This simulator is designed to realize a locomotion by switching four synergies of muscles, swing, touchdown, stance, liftoff, as Ekeberg and Pearson proposed (Fig. 10) [14]. The state transition is regulated by a kind of a reflex system, the NPG (Neural Phase Generator), and is triggered by muscle length and tension. The resultant change of locomotor parameters, such as stride period and duty ratio, with locomotion speed is in good agreement with that observed in cats qualitatively. In this study we compared the walking performance obtained by the reflex system with

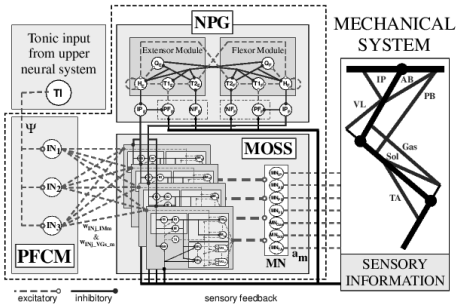

Fig. 10. Neural controller of a hindlimb musculo-skeletal model of a cat by Maufroy et al.[13].

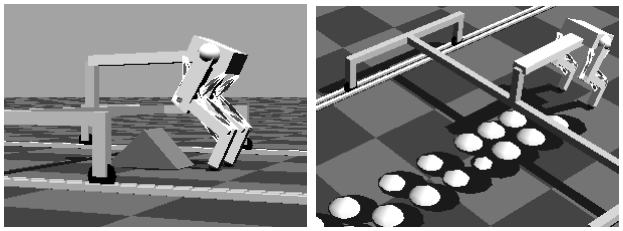

(a) (b)

Fig. 11. Walking against an obstacle (a) and on an irregular terrain (b).

that by a modified version of the NPG so as to work as a RG which autonomously changes its state periodically. The control signals sent from the RG were tuned so as to be the same as those from the reflex system during walking on a flat surface. In this simulation weak sensory signals were added to the RG so as to synchronize the activity of the RG with the leg movement. The performance was evaluated by the success rate of walking against a collision into an obstacle and on an irregular terrain (Fig. 11).

Table III shows the result and indicates that the reflex system worked well for the obstacle and the RG did for the irregular terrain. Furthermore, when a sensory signal to the RG was strong enough to suspend the state transition from stance to swing until the ground reaction force to the leg becomes small, and when the intrinsic frequency of the RG is a little lower than the stride frequency, best performance was obtained.

Although if we prepare many reflexes against many kinds of perturbations, the walking performance might become better than the above simulation, the simulation results show that the autonomous oscillation in nervous system can effectively improve the locomotion performance.

V. Conclusion

In this paper we have reported our current studies about the problems; (1) what is the basic strategy for living bodies to design movements, and (2) how living bodies realize adaptive locomotion. Concerning (1), we analyzed the arm reaching and leg swing movements and have shown that the basic strategy in trajectory planning is to minimize the expected value of energy cost. This result shows that living bodies optimize movements based on long-term experiences. It was also suggested that living bodies allow variance in some part of movement trajectories and suppress it in some effective ways, such as a swing-leg retraction, in order to acquire adaptive movements which suppress the expected value of energy cost. Concerning (2), we considered how reflex systems and the RG should work on the control of locomotion and have shown that the combination would effectively improve the performance. The future work is to combine these two kinds of results and consider the learning control mechanism of legged locomotion.

TABLE II

The recovery time from a perturbation.

	RG	RG+HC
recovering time	28.1 [s]	14.9 [s]

TABLE III

The recovery rate from a perturbation.

	Reflex	RG	Reflex+RG
success rate of recovery	15%	1.5%	51%
success rate of walking	18%	22%	47%

References

[1] T. Flash, N. Hogan, "The coordination of arm movements: Anexperimentally confirmed mathematical model," *J. Neurosci.*, vol. 5, pp. 1688–1703, 1985.

[2] Y. Uno, M. Kawato, R. Suzuki, "Formation and control of optimal trajectory in human multijoint arm movement: minimum torque-change model," *Biol Cybern*, vol. 61, pp. 89–101, 1989.

[3] C. M. Harris, D. M. Wolpert, "Signal-dependent noise determines motor planning," *nature*, vol. 394, pp. 780–784, 1998.

[4] R. McN. Alexander, "A minimum energy cost hypothesis for human arm trajectories," *Biol Cybern*, vol. 76, pp. 97–105, 1997.

[5] J. Nishii, T. Murakami, "Energetic optimality of arm trajectory," *Proc Int Conf on Biomech of Man 2002*, pp. 30–33, 2002.

[6] Y. Taniai, J. Nishii, "Optimality of reaching movements based on energetic cost under the influence of signal-dependent noise," *Tech. Rep. of IEICE (in Japanese)*, vol. NC2006-153, pp. 1–5, 2007.

[7] Y. Taniai, J. Nishii, "Optimality of reaching movements based on energetic cost under the influence of signal-dependent noise," *Abstract of the ICONIP2007*, p. 226, 2007.

[8] A. Seyfarth, H. Geyer, H. Herr, "Swing-leg retraction: a simple control model for stable running," *J Exp Biol*, vol. 206, pp. 2547–2555, 2003.

[9] M. Wisse, C. G. Atkeson, D. K. Kloimwieder, "Dynamic stability of a simple biped walking system with swing leg retraction," *Lecture Notes in Control and Information Sciences*, vol. 340, pp. 427–443, 2006.

[10] A. Fujii, H. Suenaga, Y. Taniai, J. Nishii, "Optimality of leg swing trajectories during walking based on metabolic cost," *Proc of the 2nd International Symposium on Mobiligence*, pp. 291–294, 2007.

[11] Y. Matsuno, R. Ishida, D. Owki, J. Nishii, A. Ishiguro, "On the spatiotemporal activation of muscles for adaptive walking," *Proc of the 20th SICE symposium on decentralized autonomous systems (in Japanese)*, pp. 273–278, 2008.

[12] Y. Miyazaki, H. Maeda, T. Hioki, J. Nishii, "A hierarchical learning control model of locomotor patterns of legged animals," *Proc of the 2nd International Symposium on Mobiligence*, pp. 295–298, 2007.

[13] C. Maufroy, H. Kimura, K. Takase, "Towards a general neural controller for quadrupedal locomotion," *Neural Networks*, in press.

[14] Ö. Ekeberg, K. Pearson, "Comupter simulation of stepping in the hind legs of the cat: an examination of mechanisms regulating the stance-to-swing transition," *J. Neurophysiol.*, vol. 94, pp. 4256–4268, 2005.

Network Geometry of Plasmodial Slime Mold and Emergence of Biological Function

Atsuko Takamatsu*, Masateru Ito, and Yuki Kagawa
Department of Electrical Engineering and Bioscience, Waseda University,
3-4-1, Okubo, Shinjuku-ku, Tokyo, 168-8555, Japan

***Abstract*— An oscillating amoeba-like unicellular organism, plasmodium of true slime mold, *Physarum polycephalum*, shows dramatical change in morphology to adapt to environment. The plasmodium consists of tubular structures inside which protoplasm streams to transport inner substances and nutrient. We regard the plasmodium as a network of the tubes by defining the oscillating portions of the plasmodium as oscillators or nodes, and the tubes interconnecting the nodes as links. In this study, we focus on the environment dependent topology of the networks, and investigate the relation between the spatio-temporal patterns and the behavior. We proposed simple network models to compare with the experimental result in synthetic and systematic way. Our goal is to elucidate the mechanism of adaptation by morphology and to abstract its algorithm.**

I. INTRODUCTION

Plasmodium of true slime mold, *Physarum polycephalum*, is an oscillatory amoeba-like unicellular organism. The cell crawls on various environment oscillating the cell thickness, while the cell transforms its morphology to adapt to the environment. Although the organism is primitive and peculiar, it is one of the ideal biological model systems to investigate "mobiligence" with synthetic and systematic approach. In this study, we analyze the dynamical behavior of the plasmodium by focusing on the morphology of the tubular networks consisted in the plasmodia, and investigate the relation of the network geometry and the biological function.

The single cell size of the plasmodium is relatively large and ranges $10\ \mathrm{m} - 1\mathrm{m}$. To keep such a large body, the plasmodium developed multinucleated system, where a single cell contains numerous nuclei. Therefore, the cell can be cut and divided into multiple parts without losing the original biological functions. On the other hand, multiple cells can fuse into a single cell. So to speak, each divided unit is individually equipped with sensors, motors, and actuators, and can independently functions. The collective of the interacting units can autonomously generate adaptive behavior such as escaping from repellents or gathering to attractants [1] without commands from centeral-processing-units(CPU). Differently from the higher animals that have brains, i.e., CPU dependent systems, the plasmodia can sense and process the environment information using the whole body consisting of distributed units then emerge the adaptive behavior.

*Corresponding author, atsuko_ta@waseda.jp

Each unit in the plasmodium can be defined as an oscillator that exhibits oscillation phenomena, e.g., periodical changes in concentrations of intracellular chemicals such as ATP and Ca^{2+}, and contraction and relaxation rhythms that drive the cell thickness oscillation [2]. By defining the minimum unit as an oscillator, plasmodia can be treated as a collective of oscillators [3], [4].

The partial bodies of the plasmodium are interconnected by tubular structures as shown in Fig.1(a). The cell thickness oscillation generates the pressure difference among the partial bodies in the plasmodium, which results in the protoplasmic streaming inside the tubes [5]. The plasmodial oscillators interact through the protoplasmic streaming. We define the plasmodium as a network consisting of oscillators (nodes) and tubes (links) as shown in Fig.1(b) then perform network analysis.

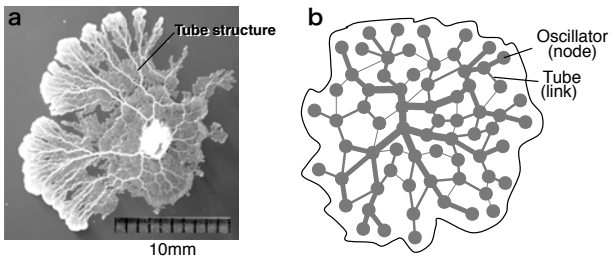

Fig. 1. Plasmodium of *Physarum polycephalum*. (a) Plasmodium as a tube network. (b) Schematic diagram of plasmodium consisting of oscillators (nodes) and tube structures (links) that connect the oscillators.

The plasmodium interestingly changes its shape, i.e. morphology of tubular network, and oscillation period depending on environmental condition. The environment dependent morphological change could correspond to adaptive behavior in the plasmodium. To know how the dynamical morphological change bring biological benefits, we analyzed the environment dependent morphology and its spatio-temporal structures quantitatively in this study. We focus on the tubular network topology and characterize them. Based on the experimental results, we constructed the coupled cell models to analyze the cooperative behavior in each network. Then we propose a very simple model for growing networks. Finally, by synthetic and systematic approach with the experiment and model analysis, we discuss the relation between the network morphology and the biological function to obtain a fundamental algorithm abstracting the adaptive behavior by morphology in collectives of simple units.

II. Adaptive behavior by environment dependent morphology

This section summarizes the experimental results for the adaptive behavior by environment dependent morphology.

A. Environment dependent morphology

The morphology of the plasmodium depend on environmental conditions such as species and concentration of chemical substances contained in the culture substratum, and stiffness of the substratum surface [6]. Fig.2 summarizes the environment dependent morphology against two parameters: One is concentration of chemical substances (oat flakes as an attractant and KCl as a repellent) and another is concentration of agar powder that controls the substrate stiffness.

The plasmodium show round shape in pleasant condition on nutrient rich and hard substratum. On the contrary, it show dendritic shape in unpleasant condition on harmful-chemicals-containing and soft substratum. We perform quantitative analysis of the morphology on spreading area size, move distance of centroid, maximum reaching distance, circularity, fractal dimension, flatness, and contact area.

We found that the contact area is large/small (the ratio is about 10) and the move distance is short/long (the ratio is about 1/10) in pleasant/unpleasant condition [6]. That is, the plasmodium can effectively uptake nutrient by maximizing the contact area and staying the place in pleasant condition. On the other hand, it can avoid exposure to harmful chemicals as small as possible, and escape from the place as fast as possible.

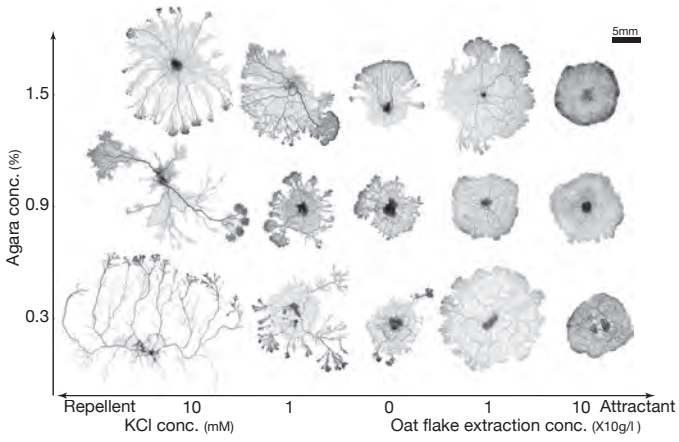

Fig. 2. Environment dependent morphology in plasmodium of *Physarum polycephalum* [6]. After 8 hours cultivation under constant temperature at 25° and humidity at RH85 %. Initial weight of plasmodia were 0.005 ± 0.001 (g).

B. Spatio-temporal patterns

Fig3 shows spatio-temporal patterns observed in each environment [7], [8]. Oscillation frequency is high and the dispersion is small in pleasant condition. The phases of oscillation is not so coherent and propagating distance is short as shown in Fig3(a). The cooperativity of the phase waves could generate the active streaming of the protoplasm. Then, the plasmodium with incoherent phase waves can not move, preferably, stay the place. This results in the short move distance found in the previous section.

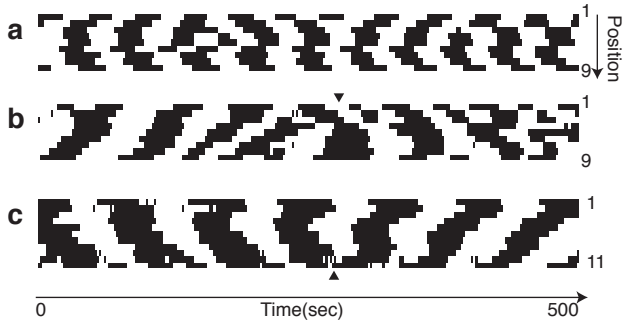

Fig. 3. Spatio-temporal patterns in each environment. (a) Pleasant; 1.5 % agar medium containing 100g/l oatmeal extraction. (b) Neutral; 1.5 % agar medium without nutrient. (c) Unpleasant; 1.5 % agar medium containing 10mM KCl. Black denotes increase of cell thickness and white denotes decrease in Figs. a-c. The position numbers are assigned in radial direction crossing the center in the plasmodia. The plasmodia were cultured for 7 hours under constant temperature at 25° and humidity at RH85 %.

In unpleasant condition, the frequency is low but the dispersion is small as same as in the pleasant condition. The phase waves propagate transversally from a tip portion to another tip potion as shown in Fig3(c) in contrast with the case of the pleasant condition. Then the protoplasm is effectively transported. That results in the long move distance as found in the previous section.

Fig3(b) shows the result for intermediate condition. The frequency distribution has two peaks: Higher and lower ones correspond to the frequency for the pleasant and unpleasant condition, respectively [7]. The spatial distribution of the frequencies has characteristics that peripheral part of the plasmodium shows higher frequency and inner part shows lower frequency. The phase waves originate from the peripheral parts with higher frequency, then transversally propagate. The propagation direction often changes at the peripheral parts. This observation suggests that the move direction fluctuates to seek for better condition into unknown environment, which could be one of adaptive behavior by moving fluctuation.

C. Analysis of network topology

Before proceeding synthetic and systematic approach, we should reconstruct the plasmodium as a system consisting of simple components. Here we define it as a network consisting of tubular structures then analyze the network topology [9], [10].

We defined nodes at branching points of the tubes and links at the tubes connecting branching points (Fig.1b) as discussed in the section I, then abstracted network topology by a image processing method [9]. We analyzed the network characteristics for each environment not only conventional indices such as number of nodes, mean link number, mean node-node distance and clustering coefficient [11]–[13], but also meshedness coefficient [14], whose results are partly shown in Fig.4.

In a typical sample of the pleasant condition (denoted with filled triangles), number of nodes increases fast and meshedness coefficient keeps at higher value s around 0.20 from the early stage, while hexagonal lattice shows $0.15 - 0.25$ in meshedness coefficient. This suggests that the plasmodium in pleasant condition forms a highly linked lattice network from the early state. In a typical sample of the unpleasant condition (denoted with filled circles), number of nodes increases slowly and meshedness coefficient keeps at lower values, while tree-graph shows 0 in meshedness coefficient. This suggests that the plasmodium in unpleasant condition forms a tree-like network.

Actually, the plasmodia in both the pleasant and unpleasant conditions frequently show intermediate network structure, where meshedness coefficient raise to the pleasant level then fall to the unpleasant level, which denoted with open triangles and open circles in Fig.4(b). This suggests that the basic mechanism of network formation is common in the both environment where the plasmodium forms a lattice network then transforms to a bifurcated structure like a tree network. The period to the bifurcation is earlier in pleasant condition than in unpleasant condition. This bifurcation mechanism could effectively perform for the network formation with limited resources of the protoplasm. Further analysis is needed to elucidate this hypothesis.

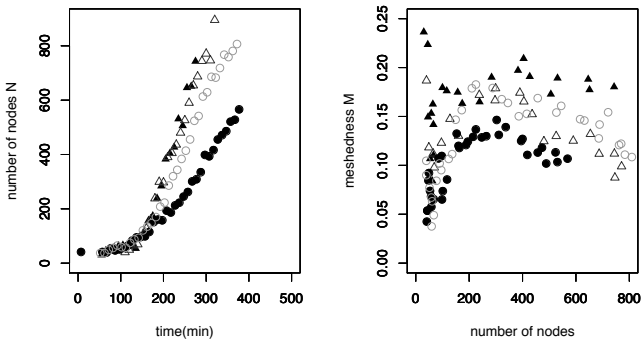

Fig. 4. Network analysis. (a) Number of nodes N, (b) Meshedness M. Triangles, circles are the data obtained from plasmodia on 1.5 %, 0.3 % agar media, which correspond to pleasant and unpleasant environment, respectively. Filled marks show typical data and open marks show the other data.

III. MODEL ANALYSIS

The experimental results can be summarized as follows: The plasmodium tends to form a lattice network in pleasant condition and a tree-like network in unpleasant condition. According to the observation, we analyze cooperativity of each network then propose a growing network model depending on environment.

A. Cooperativity in lattice and tree-like networks

To elucidate the effect of network topology on the spatio-temporal strucuture, we modeled the plasmodium as a coupled dynamical units on two-dimensional weighted networks and analyzed the spatio-temporal patterns in the system [15].

The two-dimensional weighted networks were constructed by assigning the nodes and links on a concentrical lattice, then the weights on the links were varied by parameter R and S. Finally tree-like networks, lattice-like networks, and intermixture of them are obtained as shown in Fig. 5. Here, the parameter R is the ratio of the link weights in radial directions: Small R generates center-concentrated networks. The parameter S is the ratio of the link weights in circumference directions: Small S generates tree-like networks with little circumferential connections. Note that the total weights in a single network is set to a certain fixed value, which resemble the constant total amount of protoplasm in the plasmodium.

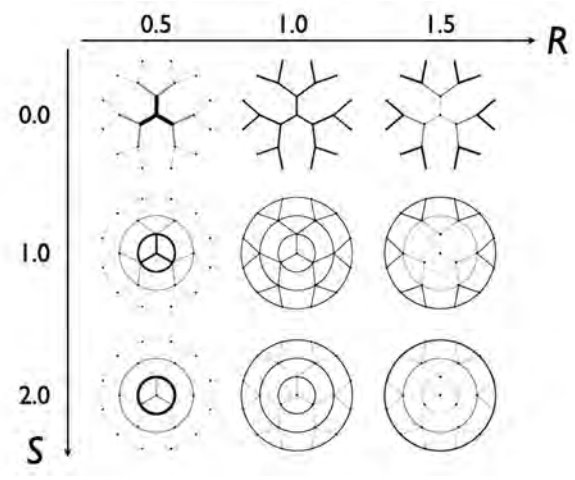

Fig. 5. Effect of the ratios R and S on the appearance of the weighted network.

Next, we considered the dynamics for each nodes on the networks to evaluate the cooperativity of the networks. Fig.6 shows the probability that the whole system shows phase synchronization [16], where logistic maps with the parameter that generates oscillation solutions were adopted as dynamics for each unit. This figure shows that the coupled maps on center-weighted lattice-like networks are easy to phase-synchronize.

It can be concluded that the network topology and weight distribution on links affect the cooperativity in the whole system. For further analysis, we are applying the continuous dynamical units such as phase equations to the nodes to compare with the observed phase wave propagations shown in the section II-B.

B. Growing network model

To study how the environment dependent networks emerges, we proposed a growing network model based on very simple rules [6], [10]. The plasmodium is considered to show the whole behavior as the result of local interaction of the simple minimal units. To verify this hypothesis, we demonstrate how complex patterns can be generated from local simple rules.

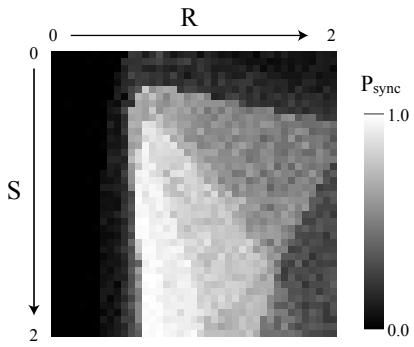

Fig. 6. Probability that the coupled maps on a weighted 2D network are phase synchronized (P_{sync}) calculated in $R-S$ space. $w_{tot}=2.0, b=2, d_{max}=3$ are used.

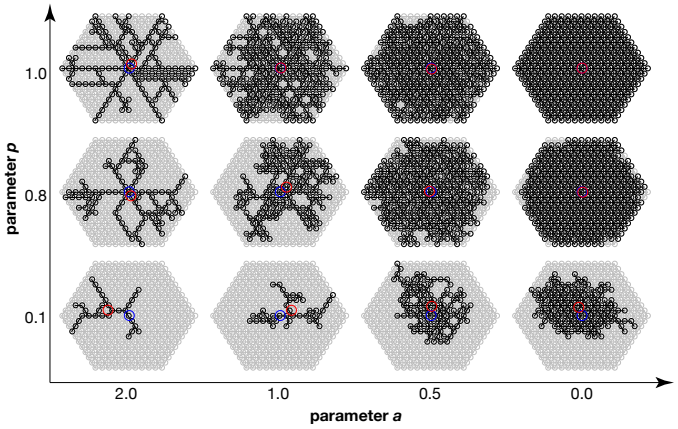

Fig. 7. Simulation results with the cellular automaton model.

We assumed only two rules on growing process of branches (links) in the plasmodial networks according to the experimental observation shown in the section II-A. The first rule is that directional preference a for the newly added links depends on chemical substances containing on the culture substrate: The links can be added toward any direction under pleasant condition where a is set to be smaller. On the contrary, under unpleasant condition, the direction for newly added links is kept to the one for the existed links where a is set to be larger. The second rule is that sprouting probability p is controlled by the substrate stiffness: The probability p is higher/lower on the hard/soft substratum. That is, small a and large p represent pleasant condition and vice versa.

Numerical results are shown in Fig.7 Networks consist of many nodes were formed in pleasant condition, where the nodes are highly linked. On the contrary, networks consist of less nodes were formed in unpleasant condition, where the nodes and the links is arranged to be tree-like branching structure. This result resemble to the experimental observation shown in Fig. 2 and agree with the network characteristics analyzed in the section II-C. It can be concluded that the local simple rules can emerges the complex networks as seen in the experimental systems.

For the further works, we will consider dynamics in the nodes and the links. In addition, by taking into account of conservation low of the protoplasm in the system, we will show how the simple plasmodial system exhibit adaptation to the environment in elegant way under constraint.

IV. CONCLUSIONS

The *Physarum* plasmodium could no more than passively generate the tubular network by receiving external information. However, it emerges effective behavior by generating spatio-temporal structure and sometimes fluctuating through the local interactions among the simple nodes. Although the plasmodium is simple and primitive, it can take smart and elegant strategy for adaptation by getting the best out of the limited resources. This could be natural consequence of that the system consists of simple units.

REFERENCES

[1] D. J. C. Knowles and M. J. Carlile, The chemotactic response of plasmodia of the myxomycete *Physarum polycephalum* to sugars and related compounds, J. Gen. Microbiol. 108 (1978) 17-25.

[2] Y. Yoshimoto and N. Kamiya, ATP- and calcium-controlled contraction in a saponin model of *Physarum polycephalum*, Cell Struct. Funct. 9 (1984) 135-41.

[3] A. Takamatsu and T. Fujii, Construction of a living coupled oscillator system of plasmodial slime mold by a microfabricated structure, in Sensors Update, Wiley-VCH, Weinheim (2002), Vol. 10, pp. 33.

[4] A. Takamatsu, T. Fujii, and I. Endo, Time delay effect in a living coupled oscillator system with the plasmodium of *Physarum polycephalum*, Phys. Rev. Lett. 85 (2000) 2026.

[5] N. Kamiya, The rate of protoplasmic flow in the myxomycete plasmodium. Cytologia 15 (1950)183-193.

[6] A. Takamatsu, E. Takaba, and G. Takizawa, Environment dependent morphology in plasmodium of true slime mold *Physarum polycephalum* and its minimal model, (2008) in preparation.

[7] A. Takamatsu, Morphology and biological function. -Spatio-temporal structure in an oscillating amoeboid unicellular organism of true slime mold-, Hyomen Kagaku, 28 (2007) 653-658. (in Japanese)

[8] A. Takamatsu, Mobiligence in an amoeboid cell, plasmodium of Physarum polycephalum, Proceedings in 2nd International Symposium on Mobiligence in Awaji (2007) 48-51.

[9] M. Ito and A. Takamatsu, Analysis on environmnet dependent topology of transportation networks in plsamodium of true slime mold. Proceedings of 20th SICE Symposium on Decentralized Autonomous Systems. (2008) 337-342 (in Japanese).

[10] A. Takamatsu, M. Ito, and Y. Kagawa, Network geometry analysis in plasmodial slime mold, Proceedings in 2nd International Symposium on Mobiligence in Awaji (2007) 275-278.

[11] M. E. J. Newman, The structure and function of complex networks., SIAM review 45 (2003) 167-256.

[12] S. Boccaletti, V. Latora, Y. Moreno, M. Chavez, D.-U. Hwang, Complex networks: Structure and dynamics., Physics Reports 424 (2006) 175-308.

[13] R. Albert and A.-L. Barabasi, Statistical mechanics of complex networks., Rev. Mod. Phys. 74 (2003) 47-97.

[14] J. Buhl, J. Gautrais, R. V. Solé, P. Kuntz, S. Valverde, J.L. Deneubourg, and G. Theraulaz, Efficiency and robustness in ant networks of galleries. Eur. Phys. J. B, 42, (2004) 123-129.

[15] Y. Kagawa, M. Ito, and A. Takamatsu, Collective behavior in coupled dynamical systems on two-dimensional weighted networks. Proceedings of 20th SICE Symposium on Decentralized Autonomous Systems. (2008) 353-358 (in Japanese).

[16] Jalan, S., Amritkar, R. E. and Hu, Chin-Kun, Synchronized clusters in coupled map networks. I. Numerical studies, *Phys. Rev. E* **72**, (2005) 016211.

Members

■=Director ■=Planned Research Groups ■=Subscribed Research Groups

	Name	Organization	
Director	Hajime Asama	The University of Tokyo	■
A01	Masafumi Yano	Tohoku University	■
A01	Kazuhiro Sakamoto	Tohoku University	■
A01	Yoshinari Makino	Tohoku University	■
A02	Koji Ito	Tokyo Institute of Technology	■
A02	Toshiyuki Kondo	Tokyo Institute of Technology	■
A02	Manabu Gouko	Tokyo Institute of Technology	■
B01	Kaoru Takakusaki	Asahikawa Medical College	■
B01	Masahiko Inase	Kinki University	■
B01	Shigeru Kitazawa	Juntendo University	■
B01	Taizo Nakazato	Juntendo University	■
B01	Kenji Yoshimi	Juntendo University	■
B01	Katsumi Nakajima	Kinki University	■
B01	Futoshi Mori	Yamaguchi University	■
B01	Dai Yanagihara	The University of Tokyo	■
B02	Naomichi Ogihara	Kyoto University	■
B02	Kazuo Tsuchiya	Kyoto University	■
B02	Yasuhiro Sugimoto	Kyoto University	■
B02	Shinya Aoi	Kyoto University	■
B02	Masato Nakatsukasa	Kyoto University	■
B03	Koh Hosoda	Osaka University	■
B03	Kousuke Inoue	Ibaraki University	■
B03	Hiroshi Kimura	Kyoto Institute of Technology	■
B03	Katsuyoshi Tsujita	Osaka Institute of Technology	■
C01	Hitoshi Aonuma	Hokkaido University	■
C01	Ryohei Kanzaki	The University of Tokyo	■
C02	Jun Ota	The University of Tokyo	■
C02	Hajime Asama	The University of Tokyo	■
C02	Kuniaki Kawabata	RIKEN	■
C03	Daisuke Kurabayashi	Tokyo Institute of Technology	■
D01	Koichi Osuka	Kobe University	■
D01	Akio Ishiguro	Tohoku University	■
D01	Xin-Zhi Zheng	ASTEM	■
D01	Masahiro Shimizu	Tohoku University	■
Evaluation	Shinzo Kitamura	Kobe University	■
Evaluation	Ryoji Suzuki	Kanazawa Institute of Technology	■
Evaluation	Shigemi Mori	National Institute for Physiological Sciences	■
Evaluation	Rolf Pfeifer	University of Zurich	■
Evaluation	Sten Grillner	Karolinska Institutet	■
Evaluation	Avis H. Cohen	University of Maryland	■

A01-11	Satoshi Shioiri	Tohoku University	
A01-12	Tetsunari Inamura	National Institute of Informatics	
A01-13	Yasuharu Koike	Tokyo Institute of Technology	
A01-14	Yusuke Maeda	Yokohama National University	
A01-15	Toshiya Matsushima	Hokkaido University	
A01-16	Yasuji Sawada	Tohoku Institute of Technology	
A01-17	Sumiaki Ichikawa	Tokyo University of Science, Suwa	
A01-18	Akira Murata	Kinki University	
A01-19	Jun Tani	RIKEN	
B01-11	Yoshimasa Koyama	Fukushima University	
B01-12	Takafumi Suzuki	The University of Tokyo	
B01-13	Yoshio Sakurai	Kyoto University	
B01-14	Takashi Hanakawa	National Center of Neurology and Psychiatry	
B01-15	Kiyoji Matsuyama	Sapporo Medical University	
B01-16	Ikuko Nishikawa	Ritsumeikan University	
B01-17	Kazuhiko Seki	National Institute for Physiological Sciences	
C01-11	Toru Miura	Hokkaido University	
C01-12	Etsuro Ito	Tokushima Bunri University	
C01-13	Tetsuo Sawaragi	Kyoto University	
C01-14	Kazuki Tsuji	University of Ryukyus	
C01-15	Kotaro Oka	Keio University	
C01-16	Motojiro Kato	Keio University	
C01-17	Takashi Nagao	Kanazawa Institute of Technology	
C01-18	Naotaka Fujii	RIKEN	
D01-11	Kazutoshi Gohara	Hokkaido University	
D01-12	Ichiro Tsuda	Hokkaido University	
D01-13	Toshio Aoyagi	Kyoto University	
D01-14	Jun Nishii	Yamaguchi University	
D01-15	Atsuko Takamatsu	Waseda University	

Publications, Awards

Publications

1. Ito, M.* and Yano, M.,Sinusoidal modeling for nonstationary voiced speech based on a local vector transform,The Journal of the Acoustical Society of America,121,3,1731-1741,2007
2. Nozomi Tomita*, Masafumi Yano,Bipedal Robot Controlled by the Basal Ganglia and Brainstem Systems
3. Adjusting to Indefinite Environment,Proc. of 2007 IEEE/ICME International Conference on Complex Medical Engineering,116-121,2007
4. Yuki Yoshihara*, Nozomi Tomita, Yoshinari Makino, and Masafumi Yano,Control of Voluntary Movement in Indefinite Environment- Real-time Optimization of Reaching Patterns by Constraints Emergence and Satisfaction - ,Proc. of 2007 IEEE/ICME International Conference on Complex Medical Engineering,107-110,2007
5. Tomita, N.*, Asano, T., Makino, Y. and Yano, M.,Real-time and Distributed Autonomous Control of 2-joints Arm with Biarticular Muscles,Proceedings of the 3rd International Symposium on Measurement, Analysis and Modeling of Human Functions,39-46,2007
6. Y. Yoshihara*, N. Tomita, Y. Makino, and M. Yano,Autonomous Control of Reaching Movement by 'Mobility Measure', International Journal of Robotics and Mechatronics,19,4,448-458,2007
7. Y. Yoshihara*, N. Tomita, Y. Makino, M. Yano,Autonomous Decentralized Control of Redundant Arm in 3D Space by Mobility Measure,2nd International Symposium on Mobiligence,81-84,2007
8. M. Yano*, Y. Yoshihara, N. Tomita, Y. Makino,Voluntary Movements Controlled by Mi-Nashi Created in the Motor Cortices,2nd International Symposium on Mobiligence,22-25,2007
9. Ito, M.* and Yano, M.,Articulatory feature estimation for nonstationary vowels based on a local vector coding,19th international congress on acoustics (Madrid), CAS-03-005,2007
10. Matsumoto, J., Makino, Y., Miura, H. and Yano, M.,Hippocampal model for spatial learning by using reward related cells,Proceedings of Neuro2007 (The 30th Annual Meeting of the Japan Neuroscience Society), ,01P-G02,2007
11. Makino Y, Yasuike M, Naka Y, Miura H, Yano M,Olfactory computation using spatiotemporal pattern of network activity for odor representation,NEUROSCIENCE RESEARCH(The 30th Annual Meeting of the Japan Neuroscience Society),58,S103-S103,2007
12. Masakatsu Tsukamoto, Toshiyuki Kondo and Koji Ito,A Prosthetic Hand Control based on Nonstationary EMG at the Start of Movement,Jr. of Robotics and Mechatronis,19,4,381-387,2007
13. Koji Ito, Makoto Doi, Toshiyuki Kondo,Feed-forward Adaptation to a Varying Dynamical Environment during Reaching Movements, Jr. of Robotics and Mechatronis,19,4,474-481 ,2007
14. Toshiyuki Kondo and Koji Ito,An Environment Cognition and Motor Adaptation Model by Eliciting Sensorimotor Constraints based on Time-series Observations,Jr. of Robotics and Mechatronis,19,4,395-401 ,2007
15. Toshiyuki Kondo,Evolutionary design and behavior analysis of neuromodulatory neural networks for mobile robots control,Applied Soft Computing,7,189-202,2007
16. Toshiyuki Kondo, Koji Ito,An Intrinsic Neuromodulation Model for Realizing Anticipatory Behavior in Reaching Movement under Unexperienced Force Fields,in M.V. Butz et al. (eds.): Anticipatory Behavior in Adaptive Learning Systems: Advances in Anticipatory Processing, Springer,4520,254-266,2007
17. J.L.Wu, K.Ito, S. Tobimatsu, T. Nishida, F. Fukuyama,Complex Medical Engineering,Springer,2007
18. Manabu Gouko, Naoki Tomi, Tomoaki Nagano and Koji Ito,Self-Organized Learning Model for behavior emergence and its application to mobile robot,Proceedings of The 3rd International Symposium on Communications, Control and Signal Processing (ISCCSP2008),in press,2008
19. Koji Ito, Masakatsu Tsukamoto and Toshiyuki Kondo,Discrimination of Intended Movements based on Nonstationary EMG for A Prosthetic Hand Control, Proceedings of The 3rd International Symposium on Communications, Control and Signal Processing (ISCCSP2008),in press,2008
20. Tomoaki Nagano, Manabu Gouko and Koji Ito, Distributed Motor Control System With Transmission Time Delay,Proceedings of The 3rd International Symposium on Communications, Control and Signal Processing (ISCCSP2008),in press,2008
21. Manabu Gouko, Naoki Tomi, Tomoaki Nagano and Koji Ito,Behavior emergence model for performing multiple tasks,Proceedings of 2008 IEEE International Conference on Distributed Human-Machine Systems (DHMS2008),in press,2008
22. Tomoaki Nagano, Manabu Gouko and Koji Ito,A 3-dimensional Distributed Motor Control System With Transmission Time Delay,Proceedings of 2008 IEEE International Conference on Distributed Human-Machine Systems (DHMS2008),in press,2008
23. Takeshi Sakurada, Hiroaki Gomi, Kojj Ito,Implicit interaction between bimanual cyclic finger movements examined by kinematic and force field adaptation tasks,SfN Final Program,56,2007
24. Takayuki Nozawa, Toshiyuki Kondo,Lattice Molecular Automata with Reversibility,2nd International Workshop on Natural Computing,2007
25. Manabu Gouko, Koji Ito,An Action Generation Model Using Time Series Prediction,Proceedings of International Joint Conferences on Neural Networks 2007,602-607,2007
26. Naoki Tomi, Manabu Gouko, Koji Ito, Toshiyuki Kondo,Decomposition of Internal Models in Arm Movements under Mixed Force,Proceedings of The second International Symposium on Mobiligence,69-72,2007
27. Manabu Gouko, Koji Ito,A predictive modules selection model for an action generation,Proceedings of The second International Symposium on Mobiligence,65-68,2007
28. Koji Ito, Toshiyuki Kondo,Feedforward Adaptation to a varying dynamical environment in arm movements,Proceedings of The second International Symposium on Mobiligence,26-29,2007
29. Toshiyuki Kondo, Yuya Kobayashi,Simultaneous Learning of a Mouse Operation with Conflicting Rotational Transformations,Proceedings of 2nd International Symposium on Mobiligence,73-76,2007
30. Naoki Tomi, Manabu Gouko, Koji Ito, Toshiyuki Kondo,Decomposition of Internal Models in Arm Reaching Motions under Mixed Dynamic Environments,Proceedings of The 3rd International Symposium on Measurement, Analysis, and Modeling of Human Functions (ISHF2007),55-60,2007
31. Takeshi Sakurada, Hiroaki Gomi, Jun Izawa, Koji Ito,Bimanual finger control mechanism related to the force field and visual

adaptation,Proceedings of The 3rd International Symposium on Measurement, Analysis, and Modeling of Human Functions (ISHF2007),47-54,2007
32. Mitsuru Takahashi, Manabu Gouko, Koji Ito, Toshiyuki Kondo,Reconstruction of Motor Function by Combining Electroencephalogram (EEG) with Functional Electrical Stimulation (FES),Proceedings of The 3rd International Symposium on Measurement, Analysis, and Modeling of Human Functions (ISHF2007),67-73,2007
33. Koji Ito,Mobiligence: Adaptive Motor Behaviors in Dynamic Environments,Proceedings of The 3rd International Symposium on Measurement, Analysis, and Modeling of Human Functions (ISHF2007),11-16,2007
34. *Toshiyuki Kondo, Yuya Kobayashi,Simultaneous Learning of Computer Mouse Operation with Conflicting Rotational Transformations, The Third International Symposium on Measurement,Proceedngs of 3rd International Symposium on Measurement Analysis and Modeling of Human Functions (ISHF2007),55-60,2007
35. Koji Ito, Makoto Doi, Toshiyuki Kondo,Feedforward Adaptation to Stable and Unstable Dynamics in Arm Movements,Proceedings of 15th Meditierrranean Conference on Control and Automation (MED2007),1-6,2007
36. K. Takakusaki, R. Ohta, H. Harada.,Modulation of the excitability of hindlimb motoneurons by the basal ganglia efferents to the brainstem in decerebrate cats. ,2nd Mobiligence International Symposium in Awaji, 2007,161-165,2007
37. R. Ohta R, K. Takakusaki, H. Harada, S. Nonaka, Y. Harabuchi.,Contribution of GABAergic receptors on neurons in the lateral lemniscus to the control of swallowing in decerebrate cats.,2nd Mobiligence International Symposium in Awaji, 2007,170-174,2007
38. Y. Koyama, K. Takahashi, T. Kodama, K. Takakusaki,Hypothalamic regulation of muscular tonus -Involvement of orexinergic and GABAergic neurons,2nd Mobiligence International Symposium in Awaji, 2007,166-169,2007
39. K. Takakusaki, R. Ohta, H. Harada.,Modulation of the excitability of hindlimb motoneurons during fictive locomotion by the basal ganglia efferents to the brainstem in decerebrate cats.,37th Annual Meeting of Society for Neuroscience, San-Diego, CA, USA, 2007.,2007
40. R. Ohta R, K. Takakusaki, H. Harada, S. Nonaka, Y. Harabuchi.,Contribution of GABAergic receptors on neurons in the lateral lemniscus to the control of swallowing in decerebrate cats. ,37th Annual Meeting of Society for Neuroscience, San-Diego, CA, USA, 2007.,2007
41. K. Takakusaki,Forebrain control of locomotion,Japan _ Italy International Seminar Scientific Program "Motor Adaptation / Learning Analysis and Its Application to Neuro-Rehabilitation", Tokyo, JAPAN,2007
42. K. Takakusaki,Role of cholinergic projections from the pedunculopontine tegmental nucleus (PPN),International NSCC workshop, Tokyo, JAPAN,2007
43. K. Yoshimi, A. Suzuki, G. Oyama, M. Kagohashi, N. Hattori, T. Nakazato, Y. Einaga, S. Kitazawa.,Diamond microelectrodes for in vivo dopamine detection,37th Annual Meeting of Society for Neuroscience (SFN) San Diego,2007
44. A. Suzuki, T. Ivandini A, K. Yoshimi,A. Fujishima, G. Oyama, T. Nakazato, N. Hattori, S. Kitazawa, Y. Eianga. ,Fabrication of Boron-Doped Diamond Microelectrodes for in vivo Analysis of Dopamine,Material Research Society (Boston, MA),2007
45. B. Bloem, I. Toni, F. Mori and J. Nielsen,Functional imaging of axial motor control,International Society of Posture and Gait Research,2007
46. F. Mori and K. Nakajima,Adaptive locomotor control in bipedal walking monkey,SICE Annual Conference,2007
47. K. Nakajima, F. Mori, A. Murata, M. Inase,Neuronal Activity in Cortical Motor Areas of an Unrestrained Japanese Monkey Walking on a Treadmill, The 2nd International Symposium on Mobiligence,35-38,2007
48. K. Nakajima, F. Mori, A. Murata, M. Inase,Neuronal Activity in Cortical Motor Areas of an Unrestrained Japanese Monkey Walking on a Treadmill, The 2nd International Symposium on Mobiligence,35-38,2007
49. K. Takakusaki,What are substrates for normal and abnormal gait?,16th International Parkinson Diease Treatment Symposium, Tokyo, JAPAN, 2007,2007
50. K. Takakusaki,Forebrain control of locomotor behaviors,Brain Research Review,57,192-198,2008
51. H.Yamada, S. Tanno, K. Takakusaki, T.Okumura.,Intracisternal injection of orexin-A prevents ethanol-induced gastric mucosal damage in rats,Journal of Gastroenterology,42,336-341,2007
52. K. Takakusaki,What are substrates for normal and abnormal gait?,Journal of Neurology (in press),
53. M. Adachi, S. Nonaka, A. Katada, T. Arakawa, R. Ota, H. Harada, K. Takakusaki, Y. Harabuchi,Carbachol injection into the pontine reticular formation depresses laryngeal muscle activity and airway reflexes in decerebrate cats,Neuroscience Research (in press),
54. K. Takakusaki,Basal ganglia modulation of fictive locomotion in decerebrate cats,Neuroscience Research (Suppl),58,S34,2007
55. N. Kamiyama, H. Matsui, K. Takakusaki, M. Kashiwayanagi.,Insulin-like grouth factor-1 and 2-aminoethoxydiphenyl borate induce extracellular calcium influx in mouse olfactory sensory neurons,Journal of Physiological Science (Suppl),57,S98,2007
56. M. Kagohashi, T. Nakazato, K. Yoshimi, S. Moizumi, N. Hattori, S. Kitazawa,Wireless voltammetry recording in unanesthetised behaving rats,Neuroscience Research ,60,1,120-127,2008
57. T. Nakazato, M. Kagohashi, K. Yoshimi,Influence of pH on voltammetric measurement of dopamine,Biogenic Amines,20,1-2,23-30,2006
58. A. Suzuki, A. T. Ivandini, K. Yoshimi, A. Fujishima, G. Oyama, T. Nakazato, N. Hattori, S. Kitazawa, Y. Einaga,Fabrication, Characterization, and Application of Boron-Doped Diamond Microelectrodes for in Vivo Dopamine Detection ,Analytical Chemistry,79,22,8608-8615,2007
59. S. Ohmae, X. Lu, Y. Uchida, T. Takahashi, S. Kitazawa S,Neuronal activity related to anticipated and elapsed time in macaque supplementary eye field. ,Experimental Brain Research, 184(4):593-8, 2008
60. Y. Uchida, X. Lu, S. Ohmae, T. Takahashi, S Kitazawa.,Neural activity related to reward size and rewarded target position in primate supplementary eye field.,Journal of Neuroscience,27,50,13750-13755,2007
61. S. Kitazawa, S. Moizumi, A. Okuzumi, F. Saito, S. Shibuya, T. Takahashi, M. Wada, S. Yamamoto. ,Reversal of subjective temporal order due to sensory and motor integrations,In: Attention Perform edited by Haggard P, Kawato M, and Rossetti Y. Oxford Univ Press,73-97,2007
62. S. Moizumi, S. Yamamoto, S. Kitazawa.,Referral of tactile stimuli to action points in virtual reality with reaction force. ,Neuroscience Research ,59,1,60-67,2007
63. K. Yamamoto, M. Kawato, S. Kotosaka, S. Kitazawa.,Encoding of movement dynamics by Purkinje cell simple spike activity during fast arm movements under resistive and assistive force fields.,Journal of Neurophysiology,97,2,1588-1599,2007

64. S. Shibuya, T. Takahashi, S. Kitazawa.,Effects of visual stimuli on temporal order judgments of unimanual finger stimuli. ,Experimental Brain Research ,179,701-709,2007
65. Shinya Aoi, Yuuki Sato, Kazuo Tsuchiya,Investigation of the Effects on Stability of Foot Rolling Motion Based on a Simple Walking Model,IEEE/RSJ International Conference on Intelligent Robots and Systems (IROS2007),2987-2992,2007
66. Ogihara, N., Aoi, S., Sugimoto, Y., Nakatsukasa, M., Tsuchiya, K,System biomechanics study of locomotion in the Japanese monkey,The 2nd International Symposium on Mobiligence,41-44,2007
67. Ogihara, N., Aoi, S., Sugimoto, Y., Nakatsukasa, M., Tsuchiya, K,A constructive simulation study of locomotion in the Japanese moneky based on a neuro-musucloskeletal model,International Workshop on Mobiligence,2007
68. S. Aoi, K. Tsuchiya,Adaptive Behavior in Turning of an Oscillator-driven Biped Robot,Autonomous Robots,23,1,37-57,2007
69. N. Ogihara, E. Hirasaki, H. Kumakura, M. Nakatsukasa,Ground-reaction-force profiles of bipedal walking in bipedally trained Japanese monkeys,Journal of Human Evolution,53,302-308,2007
70. Kagaya, M., Ogihara, N., Nakatsukasa, M,Morphological study of the anthropoid thoracic cage: scaling of thoracic width and analysis of rib curvature,Primates,in press
71. Y. Sugimoto, S. Aoi, N. Ogihara, K. Tsuchiya,The Stabilizing Function of Musculoskeltal System for Periodic Motion,2nd International Symposium on Mobiligence,2007
72. Y. Sugimoto, K. Osuka,Hierarchical Implicit Feedback Structure in Passive Dynamic Walking,2007 IEEE/RSJ International Conference on Intelligent Robots and Systems,2007
73. Takashi Takuma and Koh Hosoda,Utilizing Joint Compliance for Controlling Walking Velocity of the Passive Dynamic Walker,2nd International Symposium on Mobiligence,2007
74. Takashi Takuma and Koh Hosoda,Controlling Walking Behavior of Passive Dynamic Walker utilizing Passive Joint Compliance,IEEE/RSJ 2007 International Conference on Intelligent Robots and Systems,2975-2980,2007
75. Zu Guang Zhang, Toshiki Masuda, Hiroshi Kimura and Kunikatsu Takase,Towards Realization of Adaptive Running of a Quadruped Robot Using Delayed Feedback Control,IEEE Robotics and Automation,4325-4330,2007
76. Christophe Maufroy, Hiroshi Kimura and Kunikatsu Takase,Biologically Inspired Neural Controller for Quadruped,IEEE Robotics and Biomimetics,1212-1217,2007
77. K.Inoue, T.Sumi, S.Ma,CPG-based Control of a Simulated Snake-like Robot,IEEE/RSJ Int. Conf. on Intelligent Robots and Systems,1957-1962,2007
78. K.Inoue, T.Sumi, N.Sato, S.Ma,CPG-based Adaptable Control of a Snake-like Robot,SICE Annual Conference 2007,2161-2164,2007
79. Takashi Takuma and Koh Hosoda,Terrain Negotiation of a Compliant Biped Robot Driven by Antagonistic Artificial Muscles,Journal of Robotics and mechatronics,19,4,423-428,2007
80. Koh Hosoda and Takashi Takuma and Atsushi Nakamoto and Shinji Hayashi,Biped Robot Design Powered by Antagonistic Pneumatic Actuators for Multi-Modal Locomotion,Robotics and Autonomous Systems,56,1,46-53,2008
81. Hiroshi Kimura, Chris Maufroy and Toshiki Masuda,Emergence of Quadrupedal Gaits as Interaction among the Brain, Body and Environment,2nd International Symposium on Mobiligence,113-116,2007
82. Chris Maufroy and Hiroshi Kimura,Towards a General Neural Controller for Quadrupedal Locomotion,2nd International Symposium on Mobiligence,117-120,2007
83. Yuji Otoda and Hiroshi Kimura,Bipedal Walking Using Natural Dynamics and Delayed Stepping Reflex,2nd International Symposium on Mobiligence,121-124,2007
84. Toshiki Masuda and Hiroshi Kimura,Realization of Adaptive Running of a Quadruped Robot Using Delayed Feedback Control and Phase Resetting,2nd International Symposium on Mobiligence,125-128,2007
85. Yuji Otoda, Hiroshi Kimura and Kunikatsu Takase,Efficient Bipedal Walking Using Delayed Stepping Reflex,SICE Annual Conference 2007,2170-2174,2007
86. K.Tsujita, T.Inoura and T.Masuda,Development of Oscillator-controlled Biped Walker with Pneumatic Actuator,Proc. of Int. Symp. on Mobiligence,129-132,2007
87. K.Tsujita, T.Inoura and T.Masuda,Oscillator-controlled Bipedal Walker with Pneumatic Actuators,Proc. of SICE Annual Conference 2007,2165-2169,2007
88. K.Tsujita, T.Inoura, T.Kobayashi and T.Masuda,daptive locomotion control of a legged robot with pneumatic actuators,Proc. of Int.Conf. on Robotics and Biomimetics 2007,1218-1223,2007
89. Hiroshi Kimura, Yasuhiro Fukuoka and Avis H. Cohen,Adaptive Dynamic Walking of a Quadruped Robot on Natural Ground Based on Biological Concepts,Int. Journal of Robotics Research,26,5,475-490,2007
90. K.Tsujita and T.Masuda,Simulation Study on Acquisition Process of Locomotion by using an Infant Robot,International Journal of Advanced Robotic Systems,409-422,2007
91. K.Tsujita, A.Morioka, K.Nakatani, K.Suzuki and T.Masuda,Oscillator-controlled Bipedal Walk with Pneumatic Actuators,International Journal of Mechanical Science and Technology,21,976-980,2007
92. M. Sakura, A. Yoritsune, M. Ashikaga and H. Aonuma,Fighting experiences modulate aggressive and avoidance behaviors in crickets against male cuticular substances,Proceeding of the 2nd International Symposium on Mobiligence,2,243-246,2007
93. M. Ashikaga, M. Kikuchi, T. Hiraguchi, M. Sakura, H. Aonuma and J. Ota ,Modeling of socially adaptive behavior in crickets,Proceeding of the 2nd International Symposium on Mobiligence,2,2007
94. H. Aonuma, M. Sakura, M. Kikuchi, T. Hiraguchi, M. Ashikaga, J. Ota, K. Kawabata, T. Fujiki, Y. Ikemoto and H. Asama,Social experience dependent behavior selection in the cricket - from neuroethological approach to modeling -,Proceeding of the 2nd International Symposium on Mobiligence,2,2007
95. M. Kikuchi and H. Aonuma ,Distributions of aminergic and nitric oxidergic neurons,Proceeding of the 2nd International Symposium on Mobiligence,2,2007
96. A.Yoritsune and H. Aonuma,3-D atras of the cricket antennal lobe,Proceeding of the 2nd International Symposium on Mobiligence,2,2007
97. K. Kawabata, T. Fujiki, M. Ashikaga, J. Ota, H. Aonuma and H. Asama,A study on neural circuit model of insects for adaptive behavior

selection - Verification of action selection model in multi-individual environments -, Proceeding of the 2nd International Symposium on Mobiligence, 2, 2007
98. E. Tsuji, H. Aonuma, F. Yokohari and M. Nishikawa , Serotonin-immunoreactive Neurons in the Antennal Sensory System of the Brain in the Carpenter Ant, Camponotus japonicus, Zool. Sci., 24, 836-849, 2007
99. D. Hatakeyama, H. Aonuma, E. Ito and K. Elekes , Localization of glutamate-like immunoreactive neurons in the central and peripheral nervous system, The Biological Bulletin, 213, 172-186, 2007
100. M. Iwasaki , H. Nishino, D. Antonia and H. Aonuma, Effects of NO/cGMP signaling on the behavioral change in subordinate male crickets, Gryllus bimaculatus, Zool. Sci., 24, 860-868, 2007
101. M. Ashikaga, M. Kikuchi, T. Hiraguchi, M. Sakura, H. Aonuma and J. Ota, Foraging task of multiple mobile robots in a dynamic environment using adaptive behavior in crickets, Journal of Robotics and Mechatronics, 19, 4, 446-473, 2007
102. K. Kawabata, T. Fujiki, Y. Ikemoto, H. Aonuma and H. Asama, A neuromodulation model for adaptive behavior selection of the cricket, Journal of Robotics and Mechatronics, 19, 4, 388-394, 2007
103. M. Sakura, T. Hiraguchi, K. Ohkawara and H. Aonuma, The compartment stuctures of the antennal lobe in the ant Aphaenogaster smythiesi japonica, Acta Biol Hungarica, accepted, 2008
104. R. Okada, H. Ikeno, N. Sasayama, H. Aonuma, D. Kurabayashi and E. Ito :, The dance of the honeybee: how do honeybees dance to transfer food information effectively?, Acta Biol Hungarica, accepted, 2008
105. D. Kurabayashi, H. Aonuma, T. Funato, T. Fujiki, M. Ashikaga, J. Ota and H. Asama, Artificial model for behavior switching by using network transition through neuromodulation effect, Comp. Biochem. Physiol., 148A, S32, 2007
106. H. Aonuma , NO/cGMP system and biogenic amine system in antagonistic behavior in the cricket, Comp. Biochem. Physiol., 148A, S33, 2007
107. Kanzaki R, Insect-machine hybrid systems -novel neuroethological approaches for analyzing adaptive behaviors-, The 4th Asia-Pacific Conference on Chemical Ecology, 2007
108. Kanzaki R, Insect-Machine Hybrid System for Evaluating an Adaptive Behavior, Comparative Biochemistry and Physiology, 148A, Suppl. 1, S32, 2007
109. Sakurai T, Uchino K, Sezutsu H, Tamura T and Kanzaki R, Molecular and neural bases of pheromone discrimination in the silkmoth, Bombyx mori., Comparative Biochemistry and Physiology, 148A, Suppl. 1, S80, 2007
110. Kanzaki R, How does the Insect-Microbrain Generate Adaptive Behavior?, The 3rd Yamada Symposium on From Chaos to Cosmos: Integration in Biological Systems , 2007
111. Kanzaki R, Insect-Machine Hybrid System for Evaluating and Understanding an Adaptive Behavior., IEEE International Conference Robotics and Biomimetics , 2007
112. Wang H, Ando N and Kanzaki R, The steering control of free flight maneuvers in Agrius, Comparative Biochemistry and Physiology, 146, 4 Suppl. 1, S114-S115, 2007
113. Ando N, Yamashita A, Matsuura W, Takahashi H and Kanzaki R, Visual and odor integration for high efficacy of odor searching tasks based on the silkmoth, Proceedings of the 2nd International Symposium on Mobiligence , 227-230, 2007
114. Minegishi R, Toriihara S, Kurabayashi D and Kanzaki R, Construction of a bio-machine fusion system using brain information that commands an insect's behavior., Proceedings of the 2nd International Symposium on Mobiligence , 235-238, 2007
115. Emoto S, Ando N, Takahashi H and Kanzaki R, Behavioral responses to unintentional body movements in insects analyzed by an insect-controlled robot., Proceedings of the 2nd International Symposium on Mobiligence , 231-234, 2007
116. Kanzaki R, Emoto S, Minegishi R, Toriihara S, Kurabayashi D and Takahashi H, Insect-machine hybrid systems -novel neuroethological approaches for analyzing adaptive behaviors-, Abstract of the 8th Congress of the International Society for Neuroethology, 253, 2007
117. Fukushima R and Kanzaki R, Anatomical organization of Kenyon cells in the mushroom body of the silkworm moth, Bombyx mori., Abstract of the 8th Congress of the International Society for Neuroethology, 70, 2007
118. Ando N, Wang H, Kanzkai R, Flight control of a freely flying hawkmoth: flight muscle activities and wing kinematics, Abstract of the 8th Congress of the International Society for Neuroethology, 167, 2007
119. Sakurai T, Yamagata T, Uchino K, Sezutsu H, Tamura T and Kanzaki R, Molecular cloning and expression pattern of elav-like genes from silkmoth, Bombyx mori., Comparative Biochemistry and Physiology, 148A, Suppl. 1, S10, 2007
120. Sakurai T, Uchino K, Sezutsu H, Tamura T and Kanzaki R, Axonal projections of pheromone receptor neurons to the antennal lobe macroglomerular complex in the silkmoth, Bombyx mori., The 4th Asia-Pacific Conference on Chemical Ecology, 2007
121. Shuzo M, Okada K, Kanzaki R and Shimoyama I, Fluorescence detection system using matal-coated glass micropipette. , 20th International Conference on Micro Electro Mechanical Systems , 207-210, 2007
122. K. Ishiura, Y. Satoji, H. Aonuma and O. Mamiko, The 4th Asia-Pacific Conference on Chemical Ecology, 2007
123. M. Sakura, T. Hiraguchi, K. Ohkawara and H. Aonuma, Distribution of neuromodulators in the olfactory center of the ant Aphaenogaster smythiesi japonica, The 11th ISIN Symposium on the Neurobiology of Invertebrates, 2007
124. R. Okada, H. Ikeno, N. Sasayama, H. Aonuma, D. Kurabayashi and E. Ito, he dance of the honeybee: how do they dance to transfer the food information effectively?, The 11th ISIN Symposium on the Neurobiology of Invertebrates, 2007
125. Ikeno H, Nishioka T, Hachida T, Kanzaki, Seki Y, Ohzawa I and Usui S, Development and application of CMS based database modules for neuroinformatics., Neurocomputing, 70, 2122-2128, 2007
126. Emoto S, Ando N, Takahashi H and Kanzaki R, Insect-Controlled Robot - Evaluation of Adaptation Ability -, Journal of Robotics and Mechatronics , 19, 4, 436-443, 2007
127. Seki Y and Kanzaki R, Morphological classification of antennal lobe local interneurons in Bombyx mori by the intracellular staining under visual control method., Jornal of Comparative Neurology, 506, 93-107, 2007
128. Iwano M, Hill E, Mori A, Mishima T, Kumagai T, Ito K and Kanzaki R, Generation mechanism of flip-flop activity in the lateral accessory lobe and ventral protocerebrum of the insect brain., Jornal of Comparative Neurology, Accepted, 2007
129. Kanzaki R, How does a microbrain generate adaptive behavior?, Congress Series 1301 Brain-Inspired IT III, 2007
130. Wang H, Ando N and Kanzaki R, Active control of free flight manoeuvres in a hawkmoth, Agrius convolvuli, Journal of Experimental Biology, 211, 409-422, 2008

131. K. Kawabata, T. Fujiki, Y. Ikemoto, H. Aonuma, H. Asama, A Neuromodulation Model for Adaptive Behavior Selection by the Cricket -Nitric Oxide(NO)/Cyclic Guanoise MonoPhosphate(cGMP) Cascade Model-, Journal of Robotics and Mechatronics, 19, 4, 388-394, 2007
132. Y. Ikemoto, K. Kawabata, T. Miura, H. Asama, Mathematical Model of Proportion Control and Fluctuation Characteristic in Termite Caste, Journal of Robotics and Mechatronics, 19, 4, 429-435, 2007
133. M. Otake, K. Arai, M. Kato, T. Maeda, Y. Ikemoto, K. Kawabata, T. Takagi, H. Asama, Experimental Analysis of the Attbirution of Own Actions to the Intention of Self or Others by the Multiple Forward Models, Journal of Robotics and Mechatronics, 19, 4, 482-488, 2007
134. Masatoshi Ashikaga, Mika Kikuchi, Tetsutaro Hiraguchi, Midori Sakura, Hitoshi Aonuma and Jun Ota, Foraging Task of Multiple Mobile Robots in a Dynamic Environment Using Adaptive Behavior in Crickets, Journal of Robotics and Mechatronics, 19, 4, 466-473, 2007
135. K. Kawabata, T. Fujiki, M. Ashikaga, J. Ota, H. Aonuma, H. Asama, A Study on Neural Circuit Model of Insects for Apactive Behavior Selection -Verification of Action Selection Model in Multi-individual Environments -, Proceedings of The 2nd International Symposium on Mobiligence, 187-190, 2007
136. H. Aonuma, M. Sakura, M. Kikuchi, T. Hiraguchi, M. Ashikaga, J. Ota, K. Kawabata, T. Fujiki, Y. Ikemoto, H. Asama, Social Experience Dependent Behavior Selection in the Cricket -from neuroethological approaches to modeling -, Proceedings of The 2nd International Symposium on Mobiligence, 16-19, 2007
137. Y. Ikemoto, T. Fujiki, K. Kawabata, H. Aonuma, T. Miura, H. Asama, Neural Modeling of Social Adaptive Behaviors of Insects, Japan-Korea Joint Seminar on Information, Communications and Robotics Technologies for Dependable and Secure Societies, 2007
138. Y. Ikemoto, K. Kawabata, T. Miura, H. Asama, Mathematical Model of Proportion Control in Termite Caste Differentiation, Proceedings of The 2nd International Symposium on Mobiligence, 195-198, 2007
139. Masatoshi Ashikaga, Mika Kikuchi, Tetsutaro Hiraguchi, Midori Sakura, Hitoshi Aonuma and Jun Ota, Modeling of Socially Adaptive Behavior in Crickets, Proceedings of The 2nd International Symposium on Mobiligence, 191-194, 2007
140. Yusuke Tamura, Masao Sugi, Jun Ota and Tamio Arai, Estimation of User's Intention Inherent in the Movements of Hand and Eyes for the Deskwork Support System, Proceedings of the 2007 IEEE/RSJ International Conference on Intelligent Robots and Systems, 3709/3714, 2007
141. Kenji Terabayashi, Natsuki Miyata, Makiko Kouchi, Masaaki Mochimaru and Jun Ota, Experience of Variously Sized Hands: Visual Delay Effect, Proceedings and Posters of 12th Int. Conf. HCI International 2007, 1009/1013, 2007
142. Kenji Terabayashi, Natsuki Miyata and Jun Ota, Grasp Strategy when Experiencing Hands of Various Size, Proceedings of the 2007 IEEE International Conference on Robotics and Biomimetics, 1422/1427, 2007
143. Tetsuro Funato, Daisuke Kurabayashi, Masahito Nara, Hitoshi Aonuma, Development o Structure-mediated Behavior Selector Using Oscillator Network, Proc. IEEE Int. Conf. Robotics and Biomimetics, 1206-1211, 2007
144. Takaaki Shimone, Daisuke Kurabayashi, Kunio Okita, Tetsuro Funato, Implementation of Formation Transition System using synchronization among a Mobile Robot Group, 6th International Conference on Field and Service Robotics, 303/312, 2007
145. Daisuke Kurabayashi, Hitoshi Aonuma, Tetsuro Funato, Tomohisa Fujiki, Masatoshi Ashikaga, Jun Ota, Hajime Asama, Artificial model for behavior switching by using network transition through neuro modulation effect, 7th Int. Congress of Comparative Physiology and Boichemistry, 2007
146. Tetsuro Funato, Daisuke Kurabayashi, Network Structure for Control of Coupled Multiple Non-Linear Oscillators, IEEE Transactions on Systems, Man and Cybernetics - Part B, in print, 2008
147. Daisuke Kurabayashi, Tomohiro Inoue, Akira Yajima, Tetsuro Funato, Emergence of a small-world like communication network by local ad hoc negotiations, Journal of Robotics and Mechatronics, 194, 4, 459-465, 2007
148. Daisuke Kurabayashi, Katsunori Urano, Tetsuro Funato, Emergent Transportation Networks by Considering Interactions between Agents and their Environment, Advanced Robotics, 21, 12, 1339-1349, 2007
149. M. Iribe, *K. Osuka, Design of the Passive Dynamic Walking Robot by Applying its Dynamic Properties, Journal of Robotics and Mechatronics, 19, 4, 402-408, 2007
150. M. Iribe, *K. Osuka, A Designing Method of the Passive Dynamic Walking Robot via Analogy with the Phase Locked Loop Circuits, Bioinspiration and Robotics - Walking and Climbing Robots-, Eds.: M. K. Habib, 79-94, 2007
151. *K. Osuka, M. Iribe, Y. Sugimoto, On Passive Adaptive Mechanism in Passive Dynamic Walking, Proceedings of the International Conference on Morphological Computation, session27-2, 2007
152. *K. Osuka, M. Iribe, Y. Sugimoto, Adaptive Function Embedded in Passive Dynamic Walking, Proceedings of the International WORKSHOP on MOBILIGENCE, 2007
153. *K. Osuka, On Passive Adaptive Mechanism in Passive Dynamic Walking, Proceedings of the International Conference on Control, Automation and Systems 2007, 2683-2686, 2007
154. D. Owaki, *A. Ishiguro, Mechanical Dynamics That Enables Stable Passive Dynamic Bipedal Running - Enhancing Self-stability by Exploiting Nonlinearity in the Leg -, Journal of Robotics and Mechatronics, 19, 4, 374-380, 2007
155. D. Owaki and *A. Ishiguro, Mechanical Dynamics That Enables Stable Passive Dynamic Bipedal Running - Enhancing Self-stability by Exploiting Nonlinearity in the Leg -, Journal of Robotics and Mechatronics, 19, 4, 374-380, 2007
156. T. Umedachi, *A. Ishiguro, Amoeboid Locomotion That Exploits Real-time Tunable Springs and Law of Conservation of Protoplasmic Mass, Proc. of the 2nd International Symposium on Mobiligence, 263-266, 2007
157. D. Owaki, K. Osuka, *A. Ishiguro, Stable Passive Dynamic Bipedal Running by Exploiting the Body Dynamics Properties, Proc. of the 2nd International Symposium on Mobiligence, 259-262, 2007
158. W. Watanabe, *A. Ishiguro, Cheap Learning That Exploits Multiarticular Muscles: A Case Study with a 2D Serpentine Robot, Proc. of the 2nd International Symposium on Mobiligence, 267-270, 2007
159. M. Shimizu, K. Gohara, *A. Ishiguro, Adaptive Amoeboid Locomotion Induced from Embodied Coupled Oscillators, Proc. of the 2nd International Symposium on Mobiligence, 271-274, 2007
160. *A. Ishiguro, M. Shimizu, Amoeboid Locomotion Tells Us a Lot!: A Collective Behavioral Approach to Mobiligence, Proc. of the 2nd International Symposium on Mobiligence, 52-55, 2007
161. W. Watanabe, *A. Ishiguro, Improvement of Learning Efficiency by Exploiting Multiarticular Muscles ── A Case Study with a 2D

Serpentine Robot ―, SICE 2007 PROCEEDINGS, 2155-2160, 2007
162. T. Umedachi, *A. Ishiguro, Adaptive Amoeboid Locomotion That Exploits Law of Conservation of Protoplasmic Mass, SICE 2007 PROCEEDINGS, 2150-2154, 2007
163. Y. Yokokohji, T. Tsubouchi, A. Tanaka, T. Yoshida, E. Koyanagi, F. Matsuno, S. Hirose, H. Kuwahara, F. Takemura, T. Ino, K. Takita, N. Shiroma, T. Kamegawa, Y. Hada, *X. Zheng, K. Osuka, T. Watasue, T. Kimura, H. Nakanishi, Y. Horiguchi, S. Tadokoro, and K. Ohno, Guidelines of Human Interface Design for Rescue Robots, Proc. IEEE/RSJ International Conference on Intelligent Robots and Systems (IROS), 2007
164. D. Owaki, Y. Matsuno, *A. Ishiguro, Efficient and Adaptive Control of Walking Biped by Exploiting a Pulsed-CPG, 2007 IEEE/ICME International Conference on Complex Medical Engineering-CME2007, 111-115, 2007
165. M. Shimizu, *A. Ishiguro, A Self-reconfigurable Robotic System That Exhibits Amoebic Locomotion, Proc. of the 2007 IEEE/ICME International Conference on Complex Medical Engineering-CME2007, 101-106, 2007
166. Mano, T., Fujita, K, Shioiri, S., Matsumiya, K. & Kuriki, I., Implicit and explicit learning in visual search_the influence of eye movements, KEER2007 CD-ROM Proceedings, A17. 1- A17. 4, 2007
167. Nagata, H., Matsumiya, K., Shioiri, S. & Kuriki, I., Investigating the differences between explicit and implicit learning in a visuo-motor task, KEER2007 CD-ROM Proceedings, A14. 1- A14. 4, 2007
168. Shioiri, S, Iwaida, Y., Tamai, N., Matsumiya, K., Yaguchi, H, The effect of attention on perception of facial expression, Proceedings of the 2nd International Symposium on Mobiligence in Awaji, 105-108, 2007
169. Matsumiya, K., Sugiyama, H., Shioiri, S, Kuriki, I, Effects of auditory information reading, Proceedings of the 2nd International Symposium on Mobiligence in Awaji, 97-100, 2007
170. Lee, S., *Shioiri, S. & Yaguchi H., , Stereo channels with different temporal frequency tunings, Vision Research , 47, 3, 258-297, 2007
171. Kuriki I., Aftereffect of adaptation to chromatic notched-noise stimulus., Journal of the Optical Society of America A, 24, 7, 1858-1872, 2007
172. Tetsunari Inamura, Tomohiro Shibata, Interpolation and Extrapolation of Motion Patterns in the Proto-symbol Space, International Conference on Neural Information Processing, 2007
173. Jean C. Quinton, Tetsunari Inamura, Human-Robot Interaction Based Learning for Task-Independent Dynamics Prediction, Proc. of the Seventh International Conference on Epigenetic Robotics, 133-140, 2007
174. Tetsunari Inamura, Behavior Adaptation and Induction in Unknown Situation based on Multimodal Mimesis Model, 2nd International Symposium on Mobiligence, 85―88, 2007
175. Tetsunari Inamura, Behavior Imitation and Induction for Humanoid robots based on mimesis model, IMEKO/SICE/IEEE International Symposium on Measurement, Analysis and Modeling of Human Functions (ISHF2007), 211―218, 2007
176. T. Inamura, T. Kawaji, T. Sonoda, K. Okada and M. Inaba, Cooperative Task Achievement System between Humans and Robots based on Stochastic Memory Model of Spatial Environment, Lecture Notes in Artificial Intelligence, 4384, 77, 87
177. Kawase, T, Shin, D, Koike, Y., Visuomanual coordination In ball catching task, The 3rd International Symposium on M odeling of Human Functions, 129-134, 2007
178. Kambara Hiroyuki, Kim Kyoungsik, Shin Duk, Sato Makoto, & Koike Yuharu, Motor control-learning model for arm's reaching movement without desired trajectory, The 3rd International Symposium on M odeling of Human Functions, 181-187, 2007
179. DaSalla, Charles S., Sato, Mkoto, and Koike Yasuharu, EMG Vowel Recognition using a Support Vector Machine, The 3rd International Symposium on M odeling of Human Functions, 227-232, 2007
180. N. P. UTAMA, A. TAKEMOTO, Y. KOIKE, K. NAKAMURA, Serial Processing of information from facial emotion:evidence from an ERP study, Neuroscience 2007, 2007
181. Toshihiro Kawase, Duk Shin, Yasuharu Koike, Unrealistic condition between visual and haptic stimuli in ball catching task, The 2nd International Symposium on Mobiligence, 89-92, 2007
182. Nugraha P. Utama, Atsuhi Takemoto, Yasuharu Koike, Katsuki Nakamura, Serial Processing of Emotional Type and Intensity:evidence from an ERP stuy, 14th International Conference on Neural Information Processing, 119, 2007
183. Kyuwan Choi, Hideaki Hirose, Yoshio Sakurai, Toshio Iijima, Yasuharu Koike, Prediction of arm trajectory from the neural activities of the primary motor cortex using a modular artificial neural network model, 14th International Conference on Neural Information Processing, 122, 2007
184. Yusuke Maeda, Tatsuya Ushioda, Analysis of Human Pivoting Operations Using Hidden Markov Models, Proc. of 2nd Int. Symp. on Mobiligence, 93-96, 2007
185. Yusuke Maeda, Tatsuya Ushioda, Hidden Markov Modeling of Human Pivoting, J. of Robotics and Mechatronics, 19, 4, 444-447, 2007
186. Toshiya Matsushima, Neuro-economics in chicks., IBRO (International Brain Research Organization) satellite meeting on "Brain mechanisms, cognition and behaviour in birds," July 19-23, Heron Island, Queensland, Australia, 2007
187. Ai Kawamori, Toshiya Matsushima, Are chicks optimal foragers? Discounting food value by distance and risk., The 30th International Ethological Conference (IEC2007), August 15-23, Halifax, Nova Scotia, Canada, 2007
188. Matsushima, T., Economical decision making in chicks: brain mechanisms meet foraging ecology, The 39th Annual Genral Meeting of European Bain and Behaviour Society, September 15-19, Trieste, Italy, 2007
189. Yamaguchi, S., Katagiri, S., Hirose, N., Fujimoto, Y., Mori, M., Fujii-Taira, I., Takano, T., Matsushima, T., and Homma, K., In-vivo gene transfer into newly hatched chick brain by electroporation, NeuroReport, 18, 735-739, 2007
190. Matsushima, T., Kawamori, A., and Bem-Sojka T., Neuro-economics in chicks: foraging choices based on delay, cost and risk, Brain Research Bulletin, in press,
191. Yamaguchi, S., Fujii-Taira, I., Katagiri, S., Izawa, E.-I., Fujimoto, Y., Takeuchi, H., Takano, T., Matsushima, T., and Homma, K. J., Gene expression profile in cerebrum in the filial imprinting of domestic chicks (Gallus gallus domesticus), Brain Research Bulletin, in press,
192. Yamaguchi, S., Fujii-Taira, I., Murakami, A., Hirose, N., Aoki, N., Izawa, E.-I., Fujimoto, Y., Takano, T., Matsushima, T., and Homma, K. J., Upregulation of microtubule-associated protein 2 accompanied by the filial imprinting of domestic chicks (Gallus gallus

domesticus), Brain Research Bulletin, in press,
193. Takachi, Y., *Ishida, F. and Sawada, Y. , Enhancement of proactivity in hand tracking by the discretization of visual information, Proc. of 3rd International Symposium on Measurement, Analysis and Modeling of Human Functions, 219-225, 2007, 219-225, 2007
194. F. Ishida and Y. Sawada, Semi-analytical transient solution of a delayed differential equation and its application to the tracking motion in the sensory-motor system, Physical ReviewE, 75, 9, 12901, 2007
195. *Akira Murata, Hiroaki Ishida , Representation of bodily self in the multimodal parieto-premotor network, In: Representation and Brain, edited by Shintaro Funahashi, Springer Verlag, 151-176, 2007
196. Akira Murata, Self based on the body, 2nd annual symposium on Japanese-French frontier of Science, 2007
197. *Akira Muratra and Hiroaki Ishida , Bodily self and others representation in the brain, 2nd International symposium on the Mobiligencei in Awaji 2007 June Awaji, 30-33, 2007
198. Hiroaki Ishida and Akira Murata, Representation of others' body parts by visuo-tactile bimodal neuron in area VIP, 2nd International symposium on the Mobiligencei in Awaji 2007 June Awaji, 109-112, 2007
199. Elena Borra, Abdelouahed Belmalih, Roberta Calzavara, Marzio Gerbella, Akira Murata, Stefano Rozzi and *Giuseppe Luppino, Cortical connections of the macaque anterior intraparietal (AIP) area, Cerebral cortex[Epub ahead of print], 2007
200. R. Yokoya, T. Ogata, J. Tani, K. Komatani, and H. G. Okuno, Discovery of other individuals by projecting a self-model through imitation, Proc. of IEEE/RSJ Int. Conf. on Intelligent Robots and Systems (IROS2007), 1009-1014, 2007
201. T. Ogata, M. Murase, J. Tani, K. Komatani, and H. G. Okuno, Two-way translation of compound sentences and arm motions by recurrent neural networks, Proc. of IEEE/RSJ Int. Conf. on Intelligent Robots and Systems (IROS2007), 1858-1863, 2007
202. H. Arie, S. Sugano, and J. Tani, Constructive Approach to Understanding the Active Learning Process of Adaptation within a Given Task Environment, Proc. of 2nd Int. Symp. on Mobiligence, 77-80, 2007
203. Y. Yamashita, T. Okumura, K. Okanoya, and J. Tani, Function of the sensori-motor nucleus NIf in generation of complex syntactical song in the Bengalese Finch, Proc. of 2nd Int. Symp. on Mobiligence, 101-104, 2007
204. S. Nishide, T. Ogata, J. Tani, K. Komatani, and H.G. Okuno, Predicting Object Dynamics from Visual Images through Active Sensing Experiences, Proc. of IEEE Int. Conf. on Robots and Automation (ICRA2007), 2501-2506, 2007
205. T. Ogata, S. Matsumoto, J. Tani, K. Komatani, and H.G. Okuno, Human-Robot Cooperation using Quasi-symbols Generated by RNNPB Model, Proc. of IEEE Int. Conf. on Robots and Automation (ICRA2007), 2156-2161, 2007
206. R. Yokoya, T. Ogata, J. Tani, K. Komatani, and H. G. Okuno, Experience Based Imitation Using RNNPB, Proc. of IEEE/RSJ Int. Conf. on Intelligent Robots and Systems (IROS2006), 3669-3674, 2006
207. I. Igari, C. Hirata, and J. Tani, Computational Model for Sequence Learning: Generalization and Differentiation Dynamics of Learning Modules, Proc. of 5th Int. Conf. on Development and Learning (ICDL2006), 45-1~45-6, 2006
208. R. Yokoya, T. Ogata, J. Tani, K. Komatani, and H. G. Okuno, Robot Imitation from Active-Sensing Experiences, Proc. of 5th Int. Conf. on Development and Learning (ICDL2007), 27-1~27-6, 2006
209. J. Tani, On the interactions between top-down anticipation and bottom-up regression, Frontiers in Neurorobotics, 1, 2007
210. R. Yokoya, T. Ogata, J. Tani, K. Komatani, and H. G. Okuno, Experience-based imitation using RNNPB, Advanced Robotics, 21, 12, 1351-1367, 2007
211. H. Arie, T. Ogata, J. Tani, and S. Sugano, Reinforcement learning of a continuous motor sequence with hidden states, Advanced Robotics, Special Issue on Robotic Platforms for Research in Neuroscience, 21, 10, 1215-1229, 2007
212. Yoshimasa Koyama, Regulation of muscular tonus through hypocretinergic and GABAergic systems, 5th congress of the World Federation of Sleep Research and Sleep Medicine Societies, Cairns , 2007
213. Kodama, T, Honda, Y. , Hsieh, KC. , Siegel, JM. Lai, YY. , GABA Related To The Differential Effect Of Nuclei Gigantocellularis And Magnocellularis Stimulation On Muscular Activity Under The Absence Of Pontine Regulation, 5th congress of the World Federation of Sleep Research and Sleep Medicine Societies, Cairns , 2007
214. Y Koyama, K Takahashi, T Kodama and K Takakusaki, Hypothalamic regulation of muscular tonus -involvement of orexinergic and GABAergic neurons, 2nd Mobiligence International Symposium in Awaji, 2007, 166-169, 2007
215. Soya, A, Song, Y., Kodama, T., Honda, Y., Fujiki, N., Nishino, S. , Cerebrospinal fluid histamine levels in rats across 24 hours and after various behavioral and pharmacological manipulations., , Sleep 2007 APSS meeting, Minneapolis, 2007
216. Kodama, T., Honda, Y. Siegel, JM., Lai Y.Y., Changes in inhibitory amino acids release onto the ventral horn during nucleus gigantocellularis stimulation - the role of medial pons, 37th Annual Meeting of Society for Neuroscience, San-Diego, CA, USA, 2007., 2007
217. Hsieh, KC., Nguyen, D., Kodama, T., Siegel, JM., Lai, YY. , Histamine release in substantia nigra is correlated with wakefulness., 37th Annual Meeting of Society for Neuroscience, San-Diego, CA, USA, 2007., 2007
218. Hui Wang, Yoshiyuki Tanaka, Eiich Jodo, Yukihiko Kayama, Akihiro Kawauchi, Tsuneharu Miki , Manabu Otsuki, Yoshimasa Koyama. , Acupuncture stimulation to the sacral segment affects the state of vigilance in rats. , Neuroscience Research, 57, 531-537, 2007
219. Juan Carlos Toledo Salas, Hiroshi Iwasaki, Eiichi Jodo, Markus H. Schmidt, Akihiro Kawauchi, Tsuneharu Miki, Yukihiko Kayama, Manabu Otsuki, Yoshimasa Koyama, Penile erection and micturition events triggered by electrical stimulation of the mesopontine tegmental area, Americal Journal of Physiology, 292, R102-R111, 2008
220. Lapierre, JL., Kosenko, PO., Lyamin, OI., Kodama, T., Mukhametov, LM., Siegel, JM., Cortical Acetylcholine Release Is Lateralized during Asymmetrical Slow-Wave Sleep in Northern Fur Seals, Journal of Neuroscience, 27, 44, 11999-12006, 2007
221. Imai, Y. , Inoue, H. , Kataoka, A. , Hua Qin, W. , Masuda, M. , Ikeda, T. , Tsukita, K. , Soda, M. , Kodama, T. , Fuwa, T. , Honda, Y. , Kaneko, S. , Matsumoto, S. , Wakamatsu, K. , Ito, S. , Miura, M. , Aosaki, T. , Itohara. S. , Takahashi, R, Pael receptor is involved in dopamine metabolism in the nigrostriatal system, Neuroscience Research, 59, 413-425, 2007
222. Soya A., Song, Y-H., Kodama, T., Honda, Y., Fujii, N., Nishino, S., CSF histamine levels in rats reflect the central histamine neurotransmittion, Neuroscience Letter (in press) ,
223. K Takahashi, Y Koyama, Y Kayama, J-S Lin, K Sakai, A temporal sequence of activity changes among wake- and sleep-promoting neurons in the brainstem and posterior hypothalamus in mice, 5th congress of the World Federation of Sleep Research and Sleep Medicine Societies,

Cairns , 2007

224. Noriyuki Taniguchi, Osamu Fukayama, Tatsuo Okubo, Takafumi Suzuki, Kunihiko Mabuchi, RatCar System: A vehicle-formed BMI system by neural signals recorded with implantable electrodes, International Symposium on Biological and Physiological Engineering, accepted, 2008
225. Takashi Sato, Takafumi Suzuki, Kunihiko Mabuchi, Independent hydraulic positioning for an implantable multi-electrode array, Proc of the 3rd International IEEE EMBS Conference on Neural Engineering, 73-76, 2007
226. Noriyuki Taniguchi, Takafumi Suzuki, Kunihiko Mabuchi, Biocompatibility of wire electrodes improved by MPC polymer coating, Proc of the 3rd International IEEE EMBS Conference on Neural Engineering, 122-125, 2007
227. Osamu Fukayama, Noriyuki Taniguchi, Saeri Saito, Takafumi Suzuki, Kunihiko Mabuchi, Control of a Vehicle-formed BMI system for Rats by Neural Signals Recorded in the Motor Cortex, Proc of the 3rd International IEEE EMBS Conference on Neural Engineering, 394-397, 2007
228. Takafumi Suzuki, Osamu Fukayama, Noriyuki Taniguchi, Naoki Kotake, Shoji Takeuchi, Masanari Kunimoto, Kunihiko Mabuchi, Development of neural probes and their applications to neuroprostheses, Japan-Italy International Seminar, 2007
229. Takashi Sato, Takafumi Suzuki, Kunihiko Mabuchi, Fast automatic template matching for spike sorting based on Davies-Bouldin validation indices, Proc. of 29th International Conference of the IEEE EMBS, 3200-3203, 2007
230. Tatsuo Okubo, Noriyuki Taniguchi, Osamu Fukayama, Takafumi Suzuki, Kunihiko Mabuchi, Characterization of head pitch cells in rats, Neuroscience 2007, 2007
231. Takafumi Suzuki, Osamu Fukayama, Noriyuki Taniguchi, Shoji Takeuchi, Kunihiko Mabuchi, BMI system Rat Car as a tool for neuroscience, Proc. of the 2nd International Symposium on Mobiligence, 45-46, 2007
232. Osamu Fukayama, Noriyuki Taniguchi, Takafumi Suzuki, Kunihiko Mabuchi, Estimation of Locomotion Speed and Directions Changes to Control a Vehicle Using Neural Signals from the Motor Cortex of Rat, Proceedings of the 28th IEEE EMBS Annual International Conference, 1138-1141, 2006
233. Yasuhiro Kato, Itsuro Saito, Takayuki Hoshino, Takafumi Suzuki, Kunihiko Mabuchi, Preliminary Study of Multichannel Flexible Neural Probes Coated with Hybrid Biodegradable Polymer, Proceedings of the 28th IEEE EMBS Annual International Conference, 660-663, 2006
234. Takashi Sato, Takafumi Suzuki, Kunihiko Mabuchi, A new multi-electrode array design for chronic neural recording, with independent and automatic hydraulic positioning, Journal of Neuroscience Methods, 160, 45-51, 2007
235. Takafumi Suzuki, Naoki Kotake, Kunihiko Mabuchi, Shoji Takeuchi, Bundled Microfluidic Channels for Nerve Regeneration Electrodes, Proc of the 3rd International IEEE EMBS Conference on Neural Engineering, 17-18, 2007
236. Takahashi, S., Sakurai, Y. , Coding of spatial information by soma and dendrite of pyramidal cells in the hippocampal CA1 of behaving rats. , European Journal of Neuroscience, 26, 2033-2045, 2007
237. Nomura, M., Sakurai, Y., Aoyagi, T., , Analysis of multi-neuronal activities by means of a kernel method. , Journal of Robotics and Mechatronics, 19, 364-368, 2007
238. Sakurai, Y., How can we detect ensemble coding by cell assembly., Representation and Brain (Springer), 249-270, 2007
239. Sakurai, Y., Brain-machine interface to detect real dynamics of neuronal assemblies in the working brain., Complex Medical Engineering, Springer, 407-412, 2007
240. Takahashi, S., Sakurai, Y. , Spatial information coded by the soma and dendrite of pyramidal cells in the hippocampus of behaving rats, , 37th Society for Neuroscience Annual Meeting, , 2007
241. Hara, K., Takahashi, S., Sakurai, Y. , Hippocampal and prefrontal multi-neuronal activities during acquisition, reversal, and reacquisition of a conditional association task in rats , 37th Society for Neuroscience Annual Meeting. 米国. (2007年11月) , 2007
242. Takahashi, M., Lauwereyns, J., Sakurai, Y., Tsukada, M., Sequential coding of spatial response bias in rat hippocampal CA1 neurons., 37th Society for Neuroscience Annual Meeting., 2007
243. Takahashi, M., Lauwereyns, J., Sakurai, Y., Tsukada, M., Hippocampal code for alternation sequence during fixation period., 7th International Neural Coding Workshop, , 2007
244. Sakurai, Y., Takahashi, S., Brain-machine interface can detect dynamic neuronal activity and synchrony in the working brain. , 2nd Internaional Symposium on Mobiligence., 2007
245. Nomura, M., Sakurai, Y., Aoyagi, T., Kernel Analysis of Multi-neural Spike Trains. , IEEE/ICME International Conference on Complex Medical Engineering., 2007
246. Hanakawa T, The role of the basal ganglia-thalamo-cortical circuits for controlling human gait: Neuroimaging Evidence, 2nd Internatinal Symposium of Mobiligence, 39-40, 2007
247. Iseki K, Hanakawa T, Shinozaki J, Nankaku M, Fukuyama H, Activation of bilateral premotor areas during both observation and imagery of gait movement , 2nd Internatinal Symposium of Mobiligence, 145-148, 2007
248. Mikuni N, Okada T, Enatsu R, Miki Y, Hanakawa T, Urayama S, Kikuta K, Takahashi JA, Nozaki K, Fukuyama H, Hashimoto N, Clinical impact of integrated functional neuronavigation and subcortical electrical stimulation to preserve motor function during resection of brain tumors., Journal of Neurosurgery, 106, 4, 593-598, 2007
249. Lerner A, Bagic A, Boudreau EA, Hanakawa T, Pagan F, Mari Z, Bara-Jimenez W, Aksu M, Garraux G, Simmons JM, Sato S, Murphy DL, Hallett M., Neuroimaging of neuronal circuits involved in tic generation in patients with Tourette syndrome., Neurology, 68, 23, 1979-1987, 2007
250. Shinozaki J, Hanakawa T, Fukuyama H., Heterospecific and conspecific social cognition encoded in the anterior cingulate cortex., Neuroreport, 18, 10, 993-998, 2007
251. Fushimi Y, Miki Y, Urayama SI, Okada T, Mori N, Hanakawa T, Fukuyama H, Togashi K., Gray matter-white matter contrast on spin-echo T1-weighted images at 3 T and 1.5 T: a quantitative comparison study., European Radiology, 17, 11, 2921-2925, 2007
252. Namiki C, Hirao K, Yamada M, Hanakawa T, Fukuyama H, Hayashi T, Murai T, Impaired facial emotion recognition and reduced amygdale volume in schizophrenia., Psychiatry Research, 156, 1, 23-32, 2007
253. Fushimi Y, Miki Y, Okada T, Yamamoto A, Mori N, Hanakawa T, Urayama SI, Aso T, Fukuyama H, Kikuta KI, Togashi K., Fractional anisotropy and mean diffusivity: comparison between 3.0-T and 1.5-Tdiffusion tensor imaging with parallel imaging using histogram and region of interest analysis., NMR in Biomedicine, 20, 8, 743-748, 2007
254. Hanakawa T, Dimyan MA, Hallett M., The representation of blinking movement in cingulate motor areas: a functional magnetic resonance

imaging study.,Cerebral Cortex, in press,
255. Aso T, Hanakawa T, Matsuo K, Toma K, Shibasaki H, Fukuyama H, Nakai T.,Subregions of human parietal cortex selectively encoding object orientation.,Neuroscience Letters, 415, 3, 225-230, 2007
256. Sawamoto N, Honda M, Hanakawa T, Aso T, Inoue M, Toyoda H, Ishizu K, Fukuyama H, Shibasaki H. ,Role of the striatum in cognitive slowing in Parkinson's disease. ,Neurology, 68, 13, 1062-1068, 2007
257. Yamada M, Namiki C, Hirao K, Hanakawa T, Fukuyama H, Hayashi T, Murai T,Social cognition and frontal lobe pathology in schizophrenia: A voxel-based morphometric study. ,Neuroimage, 35, 1, 292-298, 2007
258. Abe M, Hanakawa T, Takayama Y, Kuroki C, Ogawa S, Fukuyama H,Functional coupling of human prefrontal and premotor areas during cognitive manipulation, Journal of Neuroscience, 27, 13, 3429-3438, 2007
259. HanakawaT, Hosoda C, Shindo S, Honda M.,Mental rotation of hands and feet involves somatotopically organized brain regions,Neuroscience Research, 58, suppl 1, S60, 2007
260. Shinozaki J, Sawamoto N, Murai T, Hanakawa T, Fukuyama H.,Neural basis of emotional facial recognition between parents and children,Neuroscience Research, 58, suppl 1, S64, 2007
261. Ban H, Yamamoto H, Hanakawa T, Urayama SI, Aso T, Fukuyama H, Ejima Y,Spatial specificity of V1/V2 responses to an occluded surface,Neuroscience Research, 58, suppl 1, S153, 2007
262. Yamamoto T, Takahashi S, Hanakawa T, Urayama SI, Aso T, Fukuyama H, Ejima Y,Different roles of the parietal and lateral occipito-temporal cortex for 3D perception from motion,Neuroscience Research, 58, suppl 1, S214, 2007
263. Hanakawa T, Dimyan MA, Hallett M. Motor planning, imagery and execution: a time-course study with functional MRI. Cereb Cortex (in press)
264. Matsuyama K, Ishiguro M, Aoki M.,Descending routes of locomotor driving signals involved in the generation of coordinated quadrupedal locomotion in decerebrate rabbits.,Abstract for 37th Annual Meeting of Society for Neuroscience, 924.11, 2007
265. Matsuyama K, Kobayashi S, Ishiguro M, Aoki M.,Brainstem-spinal cord mechanisms involved in the generation of coordinated hopping locomotion in rabbits.,Proceedings of The 2nd International Symposium on Mobiligence, 157-160, 2007
266. Matsuyama K, Ishiguro M, Aoki M,Hindlimb locomotor pattern evoked by the midbrain stimulation in decerebrate, paralyzed rabbits,Neuroscience Research, 58, Suppl, S92, 2007
267. Matsuyama K, Ishiguro M, Aoki M,Characteristics of interlimb coordination in quadrupedal locomotion of rabbits,Journal of Physiological Sciences ,57, Suppl, S158, 2007
268. Ishiguro M, Maeda Y, Matsuyama K,The relationship between electrical stimulus intensity and inhibitory postsynaptic currents in CA1 pyramidal cells and dentate gyrus granule cells of rat hippocampal slices, Journal of Physiological Sciences ,57, Suppl, S148, 2007
269. Fujito Y, Cao Y, Matsuyama K, Aoki M,Involvement of medullary GABAergic and serotonergic raphe neurons in respiratory control in rats, Journal of Physiological Sciences ,57, Suppl, S238, 2007
270. H. Sakamoto, I. Nouno, K. Sakakibara, M. Ito and I. Nishikawa,Prediction of Mucin-type O-glycosylation using Structure Information by Support Vector Machines,Proceedings of the 18th International Conference on Genome Informatics, 55-56, 2007
271. Yang X.M., Chen Y.W., Ito M. and Nishikawa I.,Principal Component Analysis of O-linked Glycosylation Sites in Protein Sequence,Proceedings of the 3rd International Conference on Intelligent Information Hiding and Multimedia Signal, 2007
272. Nishikawa I., Sakamoto H., Nouno I., Sakakibara K. and Ito M.,Prediction of the O-Glycosylation with Secondary Structure Information by Support Vector Machines, Lecture Notes in Artificial Intelligence 4693, 335-343, 2007
273. Chen Y. W., Yang X.M.,Ito M. and Nishikawa, I.,Pattern analysis and prediction of O-linked glycolsylated sites in protein by principal component subspace analysis, Lecture Notes in Artificial Intelligence 4693, 326-334, 2007
274. Nishikawa I., Hayashi K. and Sakakibara K.,Complex-valued Neuron to Describe the Dynamics After Hopf Bifurcation: an Example of CPG Model for a Biped Locomotion,Proceedings of 2007 International Joint Conference on Neural Networks, #1097, 2007
275. Nishikawa and K. Sakakibara,A CPG Model for Multiped Gaits based on Phase Dynamics,Proceedings of the 2nd International Symposium on Mobiligence, 137-140, 2007
276. Nishikawa I., Sakamoto H., Nouno I., Sakakibara K. and Ito M.,Prediction of Mutin-type O-glycosylation by Support Vector Machines, Proc. 2007 IEEE/ICME International Conference on Complex Medical Engineeting, 1901-1905, 2007
277. Khoa N.L.D., Noishiki M., Sakakibara K., and Nishikawa I.,Stock Price Forecasting using Neural Networks with Inputs selected by Genetic Algorithm,Proceedings of the 5th International Conference on Research, Innovation and Vision for the Future, Addendum Contributions, 95-100, 2007
278. Yasuaki Kuroe and Hajimu Kawakami,Vector Field Approximation by Model Inclusive Learning of Neural Networks, Lecture Notes in Computer Science, 4668, 717-727, 2007
279. Yasuaki Kuroe and Yuriko Taniguchi,Models of Orthogonal Type Complex-Valued Dynamic Associative Memories and Their Performance Comparison, Lecture Notes in Computer Science, 4668, 838-84, 2007
280. Yoshihiro Mori, Takashi Kadowaki, Yasuaki Kuroe and Takehiro Mori,A Synthesis Method of Gene Networks Based on Gene Expression by Network Learing -Realization of Separatrix, Proc. of SICE Annual Conference 2007, 1951-1957, 2007
281. Hitoshi Iima and Yasuaki Kuroe, Swarm Reinforcement Learing Algorithms -Exchange of Information among Multiple Agents, Proc. of SICE Annual Conference 200, 1951-1957, 2007
282. Yasuaki Kuroe and Yoshihiro Mori,Neural Network Models for Identification and Realization of a Class of Discrete Events Systems, Proc. of IEEE International Conference on Systems, Man, and Cybernetics, 1363-1369, 2007
283. T. Nomura, T. Nakamura, K. Fukada, S. Sakoda,Characterizing postural sway during quiet stance based on the intermittent control hypothesis.,AIP Proceeding Series, Proceed. 19th Intl Conf on Noise and Fluctuations, Tokyo, sept 9-14, 2007, 922, 553-556, 2007
284. A. Bottaro, Y. Yasutake, T. Nomura, M. Casadio, P. Morasso,Bounded stability of the quiet standing posture:An intermittent control model,Human Movement Science, in press, 2008
285. K. Sakakibara, H. Tamaki and I. Nishikawa,Autonomous Distributed Approaches for Pickup and Delivery Problems with TimeWindows,Proceedings of SICE Annual Conference 2007, #3B15-2, 2007
286. Takei T, Seki K,Control of primate grasping movement by spinal cord,Proceedings of 2nd International symposium on

Mobiligence. , , , 153-157, 2007

287. Takei T, Seki K, Spinomusclar coherence in monkeys performing a precision grip task, Journal of Neurophysiology (in press), 2008
288. Seki K, Kizuka T, Yamada H, Reduction in maximal firing rate of motoneurons after 1-week immobilization of finger muscle in human subjects., Journal of Electromyography and Kinesiology., 17, 2, 113-120, 2007
289. Seki K, Takei T, Modulation of spinal unit resposes evoked from muscle afferents in a monkey performing an instructed delay task, Proceedings of the 30th annual meeting of the Japan neuroscience society, 58, S1, S33, 2007
290. Takei T, Seki K, Spinomusclar coherence in monkeys performing a precision grip task, Proceedings of the 30th annual meeting of the Japan neuroscience society, 58, S1, S151, 2007
291. Seki K, Takei T, Primary afferent depolarization evoked in monkey cervical spinal cord by natural tactile stimulation of cutaneous afferent, Proceedings of the 84th annual meeting of the physiological society of Japan, 57, suppl, S68, 2007
292. Miua T*, Molecular basis underlying Daphnia polyphenism, Daphnia Genome Consortium Meeting, 2007
293. Suehiro Y, Imada H, Okuyama T, Kubo T, and Takeuchi H*, Analysis of adaptive behaviors of small fishes by using combination of mathematical modeling and molecular biological approach, Proceeding of the Second International Symposium on Mobiligence, 219-222, 2007
294. M. Ozaki and T. Nakamura, Roles of NO cascade and G proteins in transduction and adaptation of the sugar receptor cell in the blowfly, Phormia regina, SEB Annual General Meeting, 2007
295. M. Ozaki, Comparative study of nestmate recognition of ant species, International Congress of Comparative Physiology and Biochemistry, 2007
296. Hanai and M. Ozaki, Scale free dynamics in the locomotor activity of ant, International Congress of Comparative Physiology and Biochemistry, 2007
297. M. Ozaki, Chemical input and neuronal system for aggressiveness in a Japanese carpenter ant, 4th Asian-Pacific Conference of Chemical Ecology, 2007
298. M. Kobayashi-Kidokoro, M. Iwakura, S. Dujiwara, S. Higashi and M. Ozaki, The nestmate recognition aggressiveness in unicolonial ant Formica yessensis., 4th Asian-Pacific Conference of Chemical Ecology, 2007
299. K. Ishiura, Y. Satoji, H. Aonuma and M. Ozaki, Morphological investigation of aggressive center in the antennal lobe of Camponotus japonicus, 4th Asian-Pacific Conference of Chemical Ecology, 2007
300. K. Nishida, T. Maeda and M. Ozaki, Appetite change by odor experience in the blowfly, Phormia regina., 4th Asian-Pacific Conference of Chemical Ecology, 2007
301. H. Okamoto, A. Nishimura Masanobu Ito, Toshiyuki Takano and M. Ozaki, Study on appetite regulation mechanism in a novel Drosophila melanogaster mutant , 4th Asian-Pacific Conference of Chemical Ecology, 2007
302. M. Hojo, A. Wada-Katsumata, T. Akino, S. Yamaguchi, M. Ozaki and R. Yamaoka , Intracolonial Chemical Mimicry in ant parasitic inquiline Niphanda fusca , 4th Asian-Pacific Conference of Chemical Ecology, 2007
303. A. Wada-Katsumata, M. Ozaki and R. Nishida, Female's specific gustatory perception of the nuptial gift in the german cockroach, 4th Asian-Pacific Conference of Chemical Ecology, 2007
304. S. Yui, A. Wada-Katsumata, M. Ozaki, R. Kanzaki, S. Niki, N. Mori and R. Nishida , Electrophysiological analysis of oviposition stimulants on tarsal chemosensilla in a citrus swallowtail Papilio xuthus, 4th Asian-Pacific Conference of Chemical Ecology, 2007
305. Y. Murata, A. Wada-Katsumata, S. Matsumoto, M. Ozaki, and R. Nishida, Behavioral and electrophysiology analyses of larval feeding stimulants for a primitive swallowtail butterfly, Sericinus montela, in the host plant, Aristolochia debilis., 4th Asian-Pacific Conference of Chemical Ecology, 2007
306. M. Ozaki, Ant nestmate and non-nestmate discrimination by a novel contact chemosensory sensillum, 5th International Symposium on Molecular and Neural Mechanism of Taste and Olfaction, 2007
307. Miura T*, Imai M, Predator-induced polyphenism in Daphnia pulex, Evolution2007, 2007
308. Miura T*, Cornette R, Juvenile hormone action during soldier differentiation in the damp-wood termtie, JH9, 2007
309. Koshikawa S*, Miura T, JHA-induced soldier differentiation and gene expression in the damp-wood termite, Hodotermopsis sjostedti, JH9, 2007
310. Miura T*, Molecular basis for social behavior and caste differentiation in termites, Neuro2007, 2007
311. Michiko Nishikawa, Hiroshi Nishino, Yuko Misaka, Maiko Kubita, Eriko Tsuji, Yuji Satoji, Mamiko Ozaki and Fumio Yokohari, Sexual dimorphism in the antennal lobe structure of the ant, Camponotus japonicus. , Zool. Sci., in press, 2008
312. Fabien Lacaille, Makoto Hiroi, Robert Twele, Tsuyoshi Inoshita, Daisuke Umemoto, Gerard Maniere, Frederic Marion-poll, Mamiko Ozaki, Wittko Franke, Matthew Cobb, Claude Zeveraerts, Teiichi Tanimura and Jean-Francois Ferveur , An inhibitory sex pheromone tastes bitter for Drosophola males., PLoS ONE, 2, 7, e661, 2007
313. Ishikawa Y, Koshikawa S, Miura T *, Differences in mechanosensory hairs among castes of the damp-wood termite Hodotermopsis sjostedti (Isoptera: Termitidae)., Sociobiology, 50, 3, 895-907, 2007
314. Ishikawa A, Miura T *, Morphological differences between wing morphs of two Macrosiphini aphid species, Acyrthosiphon pisum and Megoura crassicauda (Hemiptera, Aphididae)., Sociobiology, 50, 3, 881-893, 2007
315. Lo N*, Engel MS, Cameron S, Nalepa CA, Tokuda G, Grimaldi D, Kitade O, Krishna K, Klass K-D, Maekawa K, Miura T, Thompson GJ, Save Isoptera. A comment on Inward et al., Biolgoy Lett, 3, 5, 562-563, 2007
316. Cornette R, Matsumoto T, Miura T*, Histological analysis on fat body development and molting events during soldier differentiation in the damp-wood termite Hodotermopsis sjostedti (Isoptera, Termopsidae). , Zool Sci, 24, 11, 1066-1074, 2007
317. Ikemoto Y*, Kawabata K, Miura T, Asama H , Mathematical model of population ratio control and fluctuation characteristic in termite caste differentiation., J Robotics Mechatronics, 19, 4, 2007
318. Brandl R*, Hyodo F, von Korff-Schmising M, Maekawa K, Miura T, Takematsu Y, Matsumoto T, Abe T, Bagine R, Kaib M, Divergence times in the termite genus Macrotermes (Isoptera: Termitidae)., Mol Phylogen Evol, 45, 239-250, 2007
319. Fujita A, Miura T*, Matsumoto T, Differences in cellulose digestive systems among castes in two termite lineages, Physiol Entomol, in press, 2008
320. Ishikawa A, Hongo S, Miura T*, Morphological and histological examination of polyphenic wing formation in the pea aphid Acyrthosiphon

pisum (Hemiptera, Hexapoda), Zoomorphology, in press, 2008
321. M. Ozaki and T. Nakamura , Chemosensory regulation of feeding in the blowfly: Several studies after The Hungry Fly., Taste, Elsevier, 24, 11, in press, 2008
322. Hideaki Takeuchi, Establishment of behavior assays using adult Medaka fish , The 54th NIBB Conference New Frontiers for the Medaka Model Genome, Bioresources and Biology, in press, 2007
323. Hori S, Takeuchi H*, and Kubo T, Associative learning and discrimination of motion cues in the harnessed honeybee Apis mellifera L., J. Comp. Physiol. A, 193, 825-833, 2007
324. Hidetoshi Ikeno, Noriko Sasayama, Ryuichi Okada, Etsuro Ito, Behavioral analysis of honeybee waggle dance and its effect on foraging., 2nd International Symposium on Mobiligence in Awaji, 223-226, 2007
325. Hidetoshi Ikeno, Ryohei Kanzaki, Hitoshi Aonuma, Masakazu Takahata, Makoto Mizunami, Koji Yasuyama, Nobuyuki Matsui, Fumio Yokohari, Shiro Usui, Development of Inverterate Brain Platform: Management of research resources for invertebrate neuroscience and neuroethology, 14th International Conference on Neural Information Processing, 2007
326. Ryuichi Okada, Hidetoshi Ikeno, Noriko Sasayama, Hitoshi Aonuma, Daisuke Kurabayashi, Etsuro Ito, The dance of the honeybee: how do honeybees dnace to transfer food information effectively?, Acta Biologica Hungarica, in press, 2008
327. Hidetoshi Ikeno, Takuto Nishioka, Takuya Hachida, Ryohei Kanzaki, Youichi Seki, Izumi Ohzawa, Shiro Usui, Development and application of CMS-based database modules for neuroinformatics, Neurocomputing, 70, 2122-2128, 2007
328. Hidetoshi Ikeno, Ryohei Kanzaki, Youichi Seki, Tomoki Kazawa, Teijiro Isokawa, Nobuyuki Matusi, Chapter 9 - Web Based Resource Management and Its Application in the Laboratory, Neurocomputing Research Developments (Editors: Hugo A. Svensson), 223-239, 2008
329. Tadahiro Taniguchi, Kenji Ogawa, and Tetsuo Sawaragi, Implicit estimation of other's intention without direct observation of actions in a collaborative task: Situation-Sensitive Reinforcement Learning, SICE Annual Conference 2007, in CD-ROM, 2007
330. Tadahiro Taniguchi, Tetsuo Sawaragi, Dynamic Process of a User's Development of Multiple Internal Models of Automation Behavior Including Mode Transitions, 2nd International Symposium on Mobiligence in Awaji , in CD-ROM, 2007
331. Tadahiro Taniguchi, Tetsuo Sawaragi, ncremental Acquisition of Behaviors and Signs based on Reinforcement Learning Schema Model and STDP, Advanced Robotics, 21, 10, 1177-1199, 2007
332. Tadahiro Taniguchi, Tetsuo Sawaragi, Incremental acquisition of multiple nonlinear forward models based on differentiation process of schema model, Neural Networks (in press),
333. Yukio Horiguchi, Ryuichi Fukuju and Tetsuo Sawaragi, Differentiation of Input-Output Relations to Facilitate User's Correct Awareness of Operating Mode of Automated Control System, Proc. of 2007 IEEE International Conference on Systems, Man and Cybernetics, 2570-2575, 2007
334. Kazuki Tsuji, Hisashi Ohtsuki, Reproductive allocation conflict causes worker policing in hymenopteran societies, XV IUSSI Congress Proceedings, 131, 2006
335. Sugawara, Collective Motions and Formations of Multi-robots Based on Simple Dynamics, Proc. of 2007 IEEE/ICME Int. Conf. on Complex Medical Engineering, 2007
336. Sugawara, Proportion Regulation in Division of Labor for Multi-agent System, Proc. of 2nd Int. Symp on Mobiligence, 199-202, 2007
337. Y. Hayashi, K. Sugawara, T. Uchikawa, Y. Hayakawa, T. Kikuchi, K. Tsuji, Analysis and Modeling of Ants' Behavior from Single to Multi-body, Proc. of 13th Int. Symp. on Artificial Life and Robotics, 2008
338. Nakamaru, M., Beppu, Y., Tsuji, K., Does disturbance favor dispersal? An analysis of ant migration using the colony-based lattice model, Journal of Theoretical Biology , 248, 2, 288-300, 2007
339. Le Breton, J. Takaku, G., Tsuji、K, Brood parasitism in an invasive population of the pest ant Pheidole megacephala., Insectes Sociaux, 53, 2, 168-171, 2006
340. Kikuchi, T., Tsuji, K., Ohnishi, H., Le Breton, J., Caste-biased acceptance of non-nestmates in a polygynous ponerine ant, Animal Behaviour, 73, 4, 559-565, 2007
341. Tomonori Kikuchi, T, Miuazaki, S., Tsuji, K., Ohnishi, S., Takahashi, J., Nakajima, Y. , Small queens and big headed workers in a monomorphic ponerine ant, Naturwissenschaften, in press, 2008
342. Hayashi, R., Tsuji, K. , Spatial distribution of turtle barnacles on the green sea turtle, Chelonia mydas. Ecological Research , Ecological Research , 23, 1, 123-125, 2008
343. Suwabe, M., Ohnishi, H., Kikuchi, T., Tsuji, K. , Nestmate discrimination in the queenless ponerine ant Diacamma sp. from Japan., Entomological Science, 10, 1, 7--10, 2007
344. A. Fujimura, K. Hotta and K. Oka, Visualization of neuronal activity patterns in female of zebra finches for discrimination of song birds., mobiligence symposium , 2007
345. A. Fujimura, H. Ogawa, K. Hotta and K. Oka, Analysis of Arc mRNA expression in female zebra finch brain for song discrimination, Society for Neuroscience 2007 (San Diego, USA), Poster:646.5/KKK10, 2007
346. *Hidehiko Takahashi, Motoichiro Kato, Mika Hayashi, Yoshiro Okubo, Akihiro Takano, Hiroshi Ito, Tetsuya Suhara, Memory and frontal lobe functions; possible relations with dopamine D2 receptors in the hippocampus, Neuroimage, 34, 1643-1649, 2007
347. *Tatsuro Oda, Kuniaki Tsuchiya, Tetsuaki Arai, Takashi Togo, Hirotake Uchikado, Rohan de Silva, Andrew Lees, Haruhiko Akiyama, Chie Haga, Kenji Ikeda, Motoichiro Kato, Yuji Kato, Tsunekatsu Hara, Mitsumoto Onaya, Koji Hori, Hiroshi Teramoto, Itaru Tominaga, Pick's disease with Pick bodies: An unusual autopsy case showing degeneration of the pontine nucleus, dentate nucleus, Clarke's column, and lowermotor neuron, Neuropathology, 27, 81-89, 2007
348. *Yoshiyuki Shibukawa, Tatsuya Ishikawa, Yutaka Kato, Zhen-Kang Zhang, Ting Jiang, Masuro Shintani, Masaki Shimono, Toshifumi Kumai, Takashi Suzuki, Motoichiro Kato, Yoshio Nakamura, Cerebral Cortical Dysfunction in Patients with Temporomandibular Disorders in Association with Jaw Movement Observation, Pain, 128, 180-188, 2007
349. *Toshiyuki Kurihara, Motoichiro Kato, Accessibility and utilization of mental health care in Bali, Psychiatry and Clinical Neurosciences, 61, 205, 2007
350. Yoko Tanaka, *Motoichiro Kato, Taro Muramatsu, Fumie Saito, Seiji Sato, Haruo Shintaku, Yoshiyuki Okano, Hiroshi Kondo, Tatsushi Nukazawa, Early initiation of l-dopa therapy enables stable development of executive function in tetrahydrobiopterin

deficiency, Developmental Medicine and Child Neurology, 49, 372-376, 2007

351. *Yutaka Kato, Taro Muramatsu, Motoichiro Kato, Masuro Shintani, Haruo Kashima, Activation of right insular cortex during imaginary speech articulation, Neuroreport, 18, 5, 505-509, 2007
352. Mihoko Otake, Kohei Arai, Motoichiro Kato, Takaki Maeda, Yusuke Ikemoto, Kuniaki Kawabata, ToshihisaTakagi and Hajime Asama, Experimental analysis of the attribution of own actions to the intention of self or others by the multiple forward models. , Journal of Robotics and Mechatronics, 19, 4, 482-488, 2007
353. Yoshihide Akine, *Motoichiro Kato, Taro Muramatsu, Satoshi Umeda, Masaru Mimura, Yoshiyuki Asai, Shuji Tanada, Takayuki Obata, Hiroo Ikehira, Haruo Kashima, Tetsuya Suhara, Altered brain activation by a false recognition task in young abstinent alcoholic patients., Alcoholism: Clinical and Experimental Research , 31, 9, 1589-1597, 2007
354. *Ryoko Nakachi, Taro Muramatsu, Motoichiro Kato, Tomoko Akiyama, Fumie Saito, Fumihiro Yoshino, Masaru Mimura, Haruo Kashima, Progressive prosopagnosia at a very early stage of frontotemporal lobar degeneration, Psychogeriatrics , 7, 155-162, 2007
355. *Tomoko Akiyama, Motoichiro Kato, Taro Muramatsu, Satoshi Umeda, Fumie Saito, Haruo Kashima, Unilateral amygdala lesions hamper attentional orienting triggered by gaze direction, Cerebral Cortex , 17, 2593-2600, 2007
356. Yasushi Moriyma, Taro Muramatsu, Motoichiro Kato, Masaru Mimura, Tomoko Akiyama, Haruo Kashima, Fr_goli syndrome accompanied with prosopagnosia in a woman with a 40-year history of schizophrenia., The Keio Journal of Medicine, 56, 130-134, 2007
357. *Tomoko Akiyama, Motoichiro Kato, Taro Muramatsu, Takaki Maeda, Tsunekatsu Hara, Haruo Kashima, Gaze-triggered orienting is reduced in chronic schizophrenia, Psychiatry Research (in press),
358. *Hidehiko Takahashi, Masato Matsuura, Michihiko Koeda, Noriaki Yahata, Tetsuya Suhara, Motoichiro Kato, Yoshiro Okubo, Brain activations during judgments of positive self-conscious emotion and positive basic emotion: pride and joy, Cerebral Cortex (in press),
359. *Hidehiko Takahashi, Yota Fujimura, Mika Hayashi, Harumasa Takano, Motoichiro Kato, Hiroshi Ito, Tetsuya Suhara, Enhanced dopamine release by nicotine in cigarette smokers: a double-blind randomized, placebo-controlled pilot study, The International Journal of Neuropsychopharmacology (in press),
360. *Mihoko Otake, Kohei Arai, Motoichiro Kato, Takaki Maeda, Yusuke Ikemoto, Kuniaki Kawabata, ToshihisaTakagi and Hajime Asama, Experimental analysis of the attribution of own actions to the intention of self or others by the multiple forward models, Journal of Robotics and Mechatronics, 19, 4, 482-488, 2007
361. *Yasushi Moriyma, Taro Muramatsu, Motoichiro Kato, Masaru Mimura, Tomoko Akiyama, Haruo Kashima, Fr_goli syndrome accompanied with prosopagnosia in a woman with a 40-year history of schizophrenia, The Keio Journal of Medicine (in press), 56, 130-134, 2007
362. *Ryosuke Arakawa, Hiroshi Ito, Akihiro Takano, Hidehiko Takahashi, Takuya Morimoto, Takeshi Sassa, Katsuya Ohta, Motoichiro Kato, Yoshiro Okubo, Tetsuya Suhara, Striatal and extrastriatal dopamine D2 receptor occupancy by paliperidone ER, Journal of Clinical Psychopharmacology (in press),
363. *Hidehiko Takahashi, Tomohisa Shibuya, Motoichiro Kato, Masato Matsuura, Michihiko Koeda, Noriaki Yahata, Tetsuya Suhara, Yoshiro Okubo, Enhanced activation in the extrastriate body area by goal-directed actions., Psychiatry and Clinical Neurosciences (in press),
364. Hidehiko Takahashi, Motoichiro Kato, Masato Matsuura, Michihiko Koeda, Noriaki Yahata, Tetsuya Suhara, Yoshiro Okubo, Neural correlates of human virtue judgment., Cerebral Cortex (in press),
365. Mika Hayashi, Motoichiro Kato, Kazue Igarashi, Haruo Kashima, Superior fluid intelligence in children with Asperger's disorder., Brain and Cognition (in press),
366. Susumu Higuchi, Takefumi Yuzuriha, Yoshiro Kochi, Sachio Matsushita, Tomohiro Miyakawa, Motoichiro Kato and Hiroshi Suwaki , Clinical characteristics and treatment outcome of inpatients with alcohol dependence: results from a nationwide survey of specialized treatment hospitals, World Psychiatry Association International Congress, 2007
367. Mika Hayashi, Teruo Hashimoto, Motoichiro Kato, Satoshi Umeda, Masaru Mimura, Seiji Ogawa, Top-down Processing in Face Perception Detected by Seeing-as-face Task in fMRI Study, International Neuropsychological Society, 2007 Joint Mid-Year Meeting, 2007
368. Hidehiko Takahashi, Takashi Ideno, Shigetaka Okubo, Hiroshi Matsui, Kazuhisa Takemura, Eisuke Matsushima, Masato Matsuura, Motoichiro Kato, Kunihiko Asai, Yoshiro Okubo, THE IMPACT OF CHANGING THE TERM FOR SCHIZOPHRENIA ON THE IMPLICIT ATTITUDE AMONG THE GENERAL PUBLIC IN JAPAN., World Psychiatry Association International Congress, 2007
369. Mihoko Otake, Kohei Arai, Motoichiro Kato, Takaki Maeda, Yusuke Ikemoto, Kuniaki Kawabata, Toshihisa Takagi and Hajime Asama, Experimental Analysis and Computational Simulation of the Attribution of Own Actions by the Multiple Forward Models. , ROBIO 2007, IEEE International Conference on Robotics and Biomimetics, 2007
370. Toshiyuki Kurihara、Motoichiro Kato, Delays in seeking psychiatric care among patients with schizophrenia in Bali, Health Knowledge, Attitudes and Practices, eds by , Nova Biomedical Books, Nova Science Publishers, Inc, New York, 2007 (in press) , 2007
371. Yoshi Tamori, Noriyuki Tomita, Implicit activities in auditory magnetoencephalograpy (MEG) , Quantum Mind 2007, 107-108, 2007
372. K. Sasaki, Reorganization of the central nervous system responding to changes in social environment in insects, ESB Special Seminar, 2, 2007
373. K. Sasaki and K. Harano, Potential effects of tyramine on the transition of reproductive workers in honeybees (Apis mellifera L.), Physiological Entomology, 32, 194-198, 2007
374. K. Harano, M. Sasaki and K. Sasaki, Effects of reproductive state on rhythmicity, locomotor activity and body weight in European honeybee, Apis mellifera (Apidae: Hymenoptera) queens, Sociobiology, 49, 189-200, 2007
375. K. Sasaki, K. Yamasaki and T. Nagao, Neuro-endocrine correlates of ovarian development and egg-laying behaviors in the primitively eusocial wasp (Polistes chinensis), Journal of Insect Physiology, 53, 940-949, 2007
376. K. Sasaki and T. Nagao, Reorganization of the central nervous systems in response to changes of social environment in insects, Journal of Robotics and Mechatronics, 19, 369-373, 2007
377. T. Miyatake, K. Tabuchi, K. Sasaki, K. Okada, Y. Nishi, K. Katayama and S. Moriya, Pleiotropic anti-predator strategies, fleeing and feigning death, correlated with dopamine levels in Tribolium castaneum, Animal Behaviour, 75, 113-121, 2007
378. Yoshi Tamori, Noriyuki Tomita, Effect of implicit response in Auditory MEG measurement, Neuro2007, 151, 2007
379. Nagasaka Y., Hihara S., Iriki A. and Fujii N., Social context modulates motion-related neurons in primate parietal cortex, Society for Neuroscience, 748.6, 2007

380. Fujii N., Hihara S. and Iriki A, Actor and action recognition in premotor and parietal cortex, Society for Neuroscience, 558.12, 2007
381. Fujii N, Revealing adaptive social brain functions in primates, 2nd International Symposium on Mobiligence in Awaji, 2007
382. Fujii N., Hihara S., Iriki A, Dynamic Social Adaptation of Motion Related Neurons in Primate Parietal Cortex, PLoS ONE, 25, e397, 2007
383. Fujii N., Hihara S., Iriki A, Social cognition in premotor and parietal cortex, Social Neuroscience, in press, 2007
384. Fujii N., Abla D., Kudo N., Hihara S., Okanoya K. and Iriki A, Prefrontal activity during incense discrimination, Neuroscience Research, 59, 3, 257-264, 2007
385. Takenaka K. Nagasaka Y., Hihara S., Nakahara H. Iriki A. Kuniyoshi Y. Fujii N., Linear discrimination analysis of monkey's behavior in alternative free choice task , Journal of Robotics and Mechatronics, 19, 4, 416-422, 2007
386. Fujii, N,, Social Context Dependent Modulation in Primate Parietal Cortex, Vision, 19, 3, 143-146, 2007
387. D. Ito, H. Adaniya, M. Nagayama, T. Uchida, and K. Gohara, Long-term measurement for spatiotemporal dynamics of cultured neural networks, 37th Annual Meeting of the society for Neuroscience Abs. (Neuroscience 2007), San Diego, USA, 36.22, 2007
388. M. Uchida, Y. Maehara and H. Shioya, Design of an Unsupervised Weight Parameter Estimation Method in Ensemble Learning, 14th International Conference on Neural Information Processing (ICONIP 2007) , 253, 2007
389. M. Nagayama, T. Uchida, and K. Gohara, Temporal and Spatial variations of Lipid Droplets during Adipocyte Division and Differentiation, J. Lipid Res., 48, 1, 9-18, 2007
390. J. Motomura, T. Uchida, M. Nagayama, K. Gohara, T. Taira, K. Shimizu and M. Sakai, Effects of additives and cooling rates on cryo-preservation process of rat cortical cells, Physics and Chemsitry of Ice (ed. by W.F. Kuhs), Royal Soc. Chemistry, 409-416, 2007
391. *Kazuhiro Matsumoto, Ichiro Tsuda and Yuki Hosoi, Controlling Engine System: a Low-Dimensional Dynamics in a Spark Ignition Engine of Motorcycle , Z. Naturforsch A, 62a, 587-595, 2007
392. *I. Tsuda and H. Fujii, Chaos Reality in the Brain, J. of Integrative Neuroscience, 6 (2007), 6, 309-326, 2007
393. *Y. Fukushima, M. Tsukada, I. Tsuda, Y. Yamaguti and S. Kuroda, Spatial clustering property and its self-similarity in membrane potentials of hippocampal CA1 pyramidal neurons for a spatio-temporal input sequence. , Cogn. Neurodyn. , 1, 305-316, 2007
394. Takaaki Aoki , Kaiichiro Ota , Koji Kurata , Toshio Aoyagi, Ordering Process of Self-Organizing Maps Improved by Asymmetric Neighborhood Function, Proceedings of ICONIP 2007, in press
395. Takaaki Aoki, Toshio Aoyagi, ynchrony-Induced switching behavior of attractors in neural network organized by spike-timing dependent plasticity, Proceedings of 2nd International Symposium on Mobiligence in Awaji, 283-286, 2007
396. *Takaaki Aoki, Toshio Aoyagi, A cooperative dynamics of network of neural oscillators between the neuronal activity and the synatptic weight, Neuroscience Research, 58, S112, 2007
397. *Takaaki Aoki, Toshio aoyagi, Synchrony-induced switching behavior of spike-pattern attractors created by spike-timing dependent plasticity, Neural Computation, 19, 10, 2720-2738, 2007
398. *Takaaki Aoki, Toshio aoyagi, Self-Organizing maps with Asymmetric Neighborhood function, Neural Computation, 19, 8, 2525-2535, 2007
399. *Takashi Takekawa, Toshio Aoyagi, Tomoki Fukai, Synchronous and asynchronous bursting states: role of intrinsic neural dynamics, Journal of Computational Neuroscience, 23, 2, 189-200, 2007
400. *Takuma Tanaka, Toshio Aoyagi, Weighted scale-free networks with variable power-law exponents, Physica D, in press
401. *Takuma Tanaka, Fumino Fujiyama, Masaki Nomura, Toshio Aoyagi, Takeshi Kaneko, Presynaptic AMPA receptors on the corticostriatal terminals enhance the release probability of the synaptic vesicles, Neuroscience Research, 58, S211, 2007
402. *Yoshiyuki Kubota, Fuyuki Karube, Masaki Nomura, Toshio Aoyagi, Atsushi Mochizuki, Yasuo Kawaguchi, Dendritic dimensions of cortical nonpyramidal cells, Neuroscience Research, 58, S73, 2007
403. *Masaki Nomura, Yoshio Sakurai, Toshio Aoyagi, Behavioral inference based on hippocampal multi-neuronal activities of rats, Neuroscience Research, 58, S160, 2007
404. *Toshio Aoyagi, Yoshihiro Yoshii, Yukito Iba, Tsuyoshi Chawanya, Optimal weighted networks of phase oscillators maximizing frequency and phase orders, STATPHYS 23, the 23rd International Conference on Statistical Physics of the International Union for Pure and Applied Physics (IUPAP), 225, 2007
405. *Masaki Nomura, Yoshio Sakurai, Toshio Aoyagi, Analysis of multi-neuronal activities by means of a kernel method, Journal of Robotics and Mechatronics, 19, 4, 364-368, 2007
406. *Takaaki Aoki, Toshio Aoyagi, Synchrony-induced attractor transition in cortical neural networks organized by spike-timing dependent plasticity, Journal of Robotics and Mechatronics, 19, 4, 409-415, 2007
407. Y. Taniai, J. Nishii, Optimality of reaching movements based on energetic cost under the influence of signal-dependent noise, Lecture notes in computer science, Springer-Verlag, in press
408. Y. Taniai, J. Nishii, Optimality of reaching movements based on energetic cost under the influence of signal-dependent noise, Abstract of the 14th International Conference on Neural Information Processing, 226, 2007
409. J. Nishii, Basic strategy for the selection of locomotor patterns and movement trajectories in living bodies, Proceeding of the 2nd International Symposium on Mobiligence, 56-59, 2007
410. Y. Hashizume, J. Nishii, Emergence of altruistic behavior with common words through natural selection, Proceeding of the 2nd International Symposium on Mobiligence, 287-290, 2007
411. A. Fujii, H. Suenaga, Y. Taniai, J. Nishii, Optimality of leg swing trajectories during walking based on metabolic cost, Proceeding of the 2nd International Symposium on Mobiligence, 291-294, 2007
412. Y. Miyazaki, H. Maeda, T. Hioki, J. Nishii, A hierarchical learning control model of locomotor patterns of legged animals, Proceeding of the 2nd International Symposium on Mobiligence, 295-298, 2007
413. J. Nishii, T. Hioki, Basic concepts of the control and learning mechanism of locomotion by the central pattern generator, Bioinspiration and Robotics: Walking and Climbing Robots, 247-260, 2007
414. Takamatsu, A. and Gomi, T., 2/3-allimetric scaling law in a tw-dimmensional organism, European Conference on Complex Systems '07, Dresden, 2007
415. Yuki Kagawa, Masateru Ito and Atsuko Takamatsu, Synchronization in two-dimentional organism modeled with coupled maps on weighted trees, European Conference on Complex Systems '07, Dresden, 2007

416. Takamatsu, A. ,Mobiligence in an amoeboid cell, plasmodium of Physarum polycephalum,Proceedings in 2nd International Symposium on Mobiligence in Awaji,48-51,2007
417. Takamatsu, A., Ito, M and Kagawa, Y.,Network geometry analysis in plasmodial slime mold,Proceedings in 2nd International Symposium on Mobiligence in Awaji,275-278,2007

Awards

1. Masashi Ito and Masafumi Yano, 19th international congress on acoustics, 2-7 September 2007, Madrid, SpainYoung Scientist Conference Attendance Grant in 19th international congress on acoustics" Articulatory feature estimation for nonstationary vowels based on a local vector coding,"
2. Sakurai T, Uchino K, Sezutsu H, Tamura T and Kanzaki R: 4th Asia-Pacific Conference on Chemical Ecology Best Poster Award "Axonal projections of pheromone receptor neurons to the antennal lobe macroglomerular complex in the silkmoth, *Bombyx mori*." (Epocal Tsukuba, Tsukuba, Japan, Sep 10-14)
3. Tadahiro Taniguchi, Kenji Ogawa, and Tetsuo Sawaragi,``Implicit estimation of other' s intention without direct observation of actions in a collaborative task: Situation-Sensitive Reinforcement Learning'', SICE Annual Conference 2007, in CD-ROM, (2007) SICE Annual Conference 2007 International Award Finalist

Activity Records

1.	Date	March 13-14th, 2007
	Place	Dept. of Biomechatronics, TU-Ilmenau
	Name	B group meeting
2.	Date	March 15th, 2007
	Place	Locomotion Laboratory, Jena Univ.
	Name	B group meeting
3.	Date	March 16th, 2007
	Place	Institute of Sport Science, Jena Univ.
	Name	B group meeting
4	Date	April 4-6th, 2007
	Place	University of Padova, Padova campu and Vicenza campus, Italy
	Name	International Workshop on Mobiligence
	Schedule	April 4: Discussion in Padova campus 16:00-17:00 Visit to SIGNET Lab. 17:00-18:00 Visit to LTTM Lab. 18:00-19:00 Visit to IAS Lab. April 5: Oral sessions in Vicenza campus 9:45-10:00 Welcome and Opening Remarks 10:00-10:45 Koji Ito (Tokyo Institute of Technology) 11:15 -11:45 Toshiyuki Kondo (Tokyo University of Agriculture and Technology) 11:45-12:15 Naomichi Ogihara (Kyoto University) 13:45-14:15 Emanuele Menegatti (University of Padua) 14:15-14:45 Hitoshi Aonuma (Hokkaido University) and Jun Ota (University of Tokyo) 15:15-15:45 Koichi Osuka (Kobe University) 15:45-16:15 Luca Iocchi (University of Rome LaSapienza) 16:15-17:00 Discussion and Conclusion April 6: Special sessions in Padova campus 10:00-10:30 Koji Ito (Tokyo Institute of Technology, Japan) 10:30-11.00 Daisuke Kurabayashi (Tokyo Institute of Technology), Hitoshi Aonuma (Hokkaido University) 11:00-11:30 Koichi Osuka (Kobe University)

		12.00-12:30 Alessandro Farinelli (University of Rome LaSapienza) 12:30-12:55 Massimo Sartori (University of Padua), Enrico Pagello (University of Padua and ISIB-CNR) 12:55-13.00 Closing Remarks
5.	Date	April 10th, 2007
	Place	University of Zurich
	Name	D group discussion
6.	Date	June 14-17th, 2007, 9:00-18:00
	Place	Universidate Tecnica di Lisboa, Portugal
	Name	The 3rd International Symposium on Measurement, Analysis and Modeling of Human Functions (ISHF2007)
	Schedule	“Mobiligence: adaptive motor behaviors in dynamic environments”, K. Ito (Tokyo Institute of Technology) “Real time and distributed autonomous control of 2-joints arm with biarticular muscles”, N. Tomita (Tohoku University) “Bimanual finger control mechanism related to the force field and visual adaptation”, T. Sakurada (Tokyo Institute of Technology) “Decomposition of internal models in arm reaching motions under mixed dynamic environments”, N. Tomi (Tokyo Institute of Technology) “Reconstruction of motor function by combining electroencephalogram (EEG) with functional electrical stimulation (FES)”, M. Takahashi “Simultaneous learning of computer mouse operation with conflicting rotational transformations”, T. Kondo (Tokyo University of Agriculture and Technology) “Visuomanual coordination in ball catching task”, Y. Koike (Tokyo Institute of Technology) “Motor control-learning model for arm’s reaching movement without desired trajectory”, H. Kambara (Tokyo Institute of Technology) “Joint torque optimization for grasp/graspless manipulation”, Y. Maeda (Yokohama National University) “Behavior imitation and induction for humanoid robots based on mimesis model”, T. Inamura (NII) “Enhancement of proactivity in hand tracking by the discretization of visual information”, F.Ishida (University of Electro-Communications) “EMG vowel recognition using a support vector machine”, C. S. DaSalla (Tokyo Institute of Technology)

7.	Date	July 13th, 2007, 14:00～16:00
	Place	Salvador, Brazil
	Name	Organized Session: Multidisciplinary approaches for understanding the adaptive behavior in insects (Chairs: H. Aonuma, R. Kanzaki) Artificial model for behavior switching by using network transition through neuro modulation effect. Kurabayashi, D. (Tokyo Institute of Technology) Insect-machine hybrid systems for analyzing adaptive behaviors, Kanzaki, R. (University of Tokyo) Brain NOS activity regulates reproductive state-related behaviors in grasshoppers. Heinrich R. (University Goettingen, Germany NO/cGMP system and biogenic amine system in agonistic behavior in the cricket. Aonuma H., Hokkaido University, Japan. A neuroanatomical guide of the cercal scape system of the wood cricket. Insausti, T. Universiteacute Franccedil;ois Rabelais, France.
8.	Date	July 16-20th, 2007, 8:45～17:00
	Place	ETH Zurich, University of Zurich
	Name	ICIAM07 (6th International Congress on Industrial and Applied Mathematics)
9.	Date	July 18-20th, 2007, 13:30～12:00
	Place	Awaji, Hyogo, Japan
	Name	The second International Symposium on Mobiligence
10.	Date	November 7-12th, 2007, 14:00～11:00
	Place	University of Montevideo, Uruguay
	Name	NEURAL CODING 2007
11.	Date	November 17-21th, 2007, 8:30-12:30
	Place	East China University of Science & Technology Convention Center, Shanghai, China
	Name	ICCN'07 & SICPB'07